frontiers | Research Topics

Preventing and treating liver diseases: medicinal and food plants, their metabolites as potential options

Edited by
Qinge Ma, Rongrui Wei, Zhipei Sang, Chunsu Yuan and Chunlei Zhang

Published in
Frontiers in Pharmacology

ISSN 1664-8714
ISBN 978-2-8325-6190-4
DOI 10.3389/978-2-8325-6190-4

About Frontiers

Frontiers is more than just an open access publisher of scholarly articles: it is a pioneering approach to the world of academia, radically improving the way scholarly research is managed. The grand vision of Frontiers is a world where all people have an equal opportunity to seek, share and generate knowledge. Frontiers provides immediate and permanent online open access to all its publications, but this alone is not enough to realize our grand goals.

Frontiers journal series

The Frontiers journal series is a multi-tier and interdisciplinary set of open-access, online journals, promising a paradigm shift from the current review, selection and dissemination processes in academic publishing. All Frontiers journals are driven by researchers for researchers; therefore, they constitute a service to the scholarly community. At the same time, the *Frontiers journal series* operates on a revolutionary invention, the tiered publishing system, initially addressing specific communities of scholars, and gradually climbing up to broader public understanding, thus serving the interests of the lay society, too.

Dedication to quality

Each Frontiers article is a landmark of the highest quality, thanks to genuinely collaborative interactions between authors and review editors, who include some of the world's best academicians. Research must be certified by peers before entering a stream of knowledge that may eventually reach the public - and shape society; therefore, Frontiers only applies the most rigorous and unbiased reviews. Frontiers revolutionizes research publishing by freely delivering the most outstanding research, evaluated with no bias from both the academic and social point of view. By applying the most advanced information technologies, Frontiers is catapulting scholarly publishing into a new generation.

What are Frontiers Research Topics?

Frontiers Research Topics are very popular trademarks of the *Frontiers journals series*: they are collections of at least ten articles, all centered on a particular subject. With their unique mix of varied contributions from Original Research to Review Articles, Frontiers Research Topics unify the most influential researchers, the latest key findings and historical advances in a hot research area.

Find out more on how to host your own Frontiers Research Topic or contribute to one as an author by contacting the Frontiers editorial office: frontiersin.org/about/contact

Preventing and treating liver diseases: medicinal and food plants, their metabolites as potential options

Topic editors

Qinge Ma — Jiangxi University of Traditional Chinese Medicine, China
Rongrui Wei — Jiangxi University of Traditional Chinese Medicine, China
Zhipei Sang — Hainan University, China
Chunsu Yuan — The University of Chicago, United States
Chunlei Zhang — China Pharmaceutical University, China

Citation

Ma, Q., Wei, R., Sang, Z., Yuan, C., Zhang, C., eds. (2025). *Preventing and treating liver diseases: medicinal and food plants, their metabolites as potential options*. Lausanne: Frontiers Media SA. doi: 10.3389/978-2-8325-6190-4

Table of contents

frontiers | Frontiers in Pharmacology

TYPE Editorial
PUBLISHED 18 March 2025
DOI 10.3389/fphar.2025.1577547

OPEN ACCESS

EDITED BY
Javier Echeverria,
University of Santiago, Chile

REVIEWED BY
Luca Rastrelli,
University of Salerno, Italy

*CORRESPONDENCE
Wenmin Liu,
liuwm1969@163.com
Qinge Ma,
maqinge2006@163.com

RECEIVED 16 February 2025
ACCEPTED 03 March 2025
PUBLISHED 18 March 2025

CITATION
Wei R, Liu W, Yuan C, Zhang C, Sang Z and Ma Q (2025) Editorial: Preventing and treating liver diseases: medicinal and food plants, their metabolites as potential options.
Front. Pharmacol. 16:1577547.
doi: 10.3389/fphar.2025.1577547

Editorial: Preventing and treating liver diseases: medicinal and food plants, their metabolites as potential options

Rongrui Wei[1], Wenmin Liu[2]*, Chunsu Yuan[3], Chunlei Zhang[4], Zhipei Sang[5] and Qinge Ma[1]*

[1]College of Medicine and Health Science & School of Life Science and Technology, Wuhan Polytechnic University, Wuhan, China, [2]College of Chemistry and Pharmaceutical Engineering, Nanyang Normal University, Nanchang, China, [3]Tang Center for Herbal Medicine Research, Department of Anesthesia and Critical Care, Committee On Clinical Pharmacology and Pharmacogenomics, Pritzker School of Medicine, The University of Chicago, Chicago, IL, United States, [4]School of Traditional Chinese Pharmacy, China Pharmaceutical University, Nanjing, China, [5]School of Pharmaceutical Sciences, Hainan University, Haikou, China

KEYWORDS

hepatoprotective, bioactive natural products, pharmacological target, molecular mechanisms, liver disease

Editorial on the Research Topic
Preventing and treating liver diseases: medicinal and food plants, their metabolites as potential options

Liver disease is seriously endangering human health in the world. It has become the leading cause of death in the word (Israelsen et al., 2024). The presence and progression of liver fibrosis led by hepatic inflammation is the main predictor of liver-related death across the entire spectrum of steatotic liver diseases (Taru et al., 2024). A combination of recent advancements of widely available biomarkers for early detection of liver fibrosis together with considerable advancements in therapeutic interventions offer the possibility to reduce morbidity and mortality in patients with liver disease (Dabrowska et al., 2024). Thus, it is necessary to discover new hepatoprotective drugs to prevent and treat liver diseases. The medicinal and food plants have unique advantages in terms of safety and compliance, which have always been an important source for finding new hepatoprotective drugs (Xu et al., 2024). Therefore, medicinal and edible plants are the important sources for researching and developing new hepatoprotective drugs, which has the advantages of safety, multi-targets, and multi-pathways. We are honored to serve as topic editor of Frontiers in Pharmacology, and compile "*preventing and treating liver diseases: medicinal and food plants, their metabolites as potential options*".

The study by Han et al. discussed about the anti-cholestatic mechanism of zhuyu pill on rat model, which was induced by naphthyl isothiocyanate. In this study, some important methods were used to evaluate anti-cholestatic activity, including histopathology, serum biochemistry, mRNA-Seq, and qRT-PCR. As a result, zhuyu pill could obviously enhance the indexes of biochemical blood and liver histopathology of rats, regulate lipid metabolism pathway, and alleviate symptom of inflammation, and so on. Some important genes were verified by qRT-PCR, including Acox2, Cyp2a1, Cyp1a2, Cyp2c11, and Ephx2. In a word,

zhuyu pill displays significant anti-cholestatic effect, which indicates that zhuyu pill is a promising drug to treat cholestasis in the future.

Li et al. made a review on bioactivities of Rutaecarpine derivatives by consulting related references. Rutaecarpine is an important alkaloid, belonging to pentacyclic indolopyridoquinazolinone type, which is isolated from *Evodia rutaecarpa* for the first time. Rutaecarpine possesses multiple therapeutic functions in clinical practice. In this review, the structures of Rutaecarpine derivatives were modified to seek better properties and potency. This review summarized diverse bioactivities and mechanisms of Rutaecarpine derivatives, including anti-tumor, anti-inflammatory, anti-Alzheimer, anti-fungal, anti-atherogenic activities. These compounds inhibited acetylcholine, cyclooxygenase-2, phosphodiesterase 4B, phosphodiesterase 5, and topoisomerases (Li et al., 2023).

Nawaz et al. made a review on approaches for treating chronic hepatitis C. In this review, the treatment progress of hepatitis C virus was summarized and assessed. A comparison was made between traditional interferon/ribavirin treatment and herbal methods rooted in traditional medicine. This review made an updated summary of diverse hepatitis C virus genome, along with pathogenesis, natural variations, and the impacts of economic, social, dietary, environmental factors. In summary, this review summarized the complexity of the hepatitis C virus genome and explored the potential and advantages of medicinal plants to treat hepatitis C virus infection.

Feng et al. evaluated the hepatotoxic and hepatoprotective effects of matrine by meta-analysis. The radar charts and 3D maps were used to analysize the related data from multiple databases. It was found that matrine possessed bidirectional effects by measuring AST, TG, ALT, TC, MDA, CAT, TNF-α, and SOD levels. The effective dosage (10–69.1 mg/kg) of matrine for bidirectional effect was determined by three-dimensional analysis. Moreover, the high liver protection and low toxicity dosage (20–30 mg/kg/d) of matrine was summarized in this review. The molecular docking and multiple pathways of hepatotoxic and hepatoprotective effects of matrine were summarized and assessed in this paper.

Liu et al. evaluated hepatoprotective activities of total cucurbitacins from *H. pedunculosum* in this review. Cucurbitacin B (70.3%), isocucurbitacin B (26.1%), and cucurbitacin E (3.6%) were regarded as the main components of total cucurbitacins from *H. pedunculosum* by UHPLC-MS/MS and RP-HPLC. Total cucurbitacins could reverse CCl_4-induced metabolic changes with a dose-dependent manner, and impact energy and phenylalaninet pathways. The LD_{50} value (36.21 mg/kg) and NOAEL value (15 mg/kg) of total cucurbitacins were assayed in this study, respectively. In summary, total cucurbitacins of *H. pedunculosum* are promising potential hepatoprotective drugs in the future.

Kim et al. assayed additive activities of herbal medicines to treat non-alcoholic fatty liver disease with meta-analysis. In this review, eight trials with 603 participants were contained in this study. As a result, it was found that ultrasoundbased liver steatosis of herbal medicine group displayed a significant improvement, and the aspartate transferase levels of herbal medicine group decreased. In a word, herbal medicines displayed additive activities on lifestyle modification to treat non-alcoholic fatty liver disease, it established an important research foundation for the treatment of non-alcoholic fatty liver disease.

Zhou et al. studied *F. suspensa* (Thunb.) Vahl for the treatment of inflammation-associated diseases, and evaluated the signaling pathways of inflammation. In this study, forest plots, risk-of-bias summaries, funnel plots, and flow diagrams were applied to analyze the related data according to references. As a result, it was found that *Forsythia suspensa* (Thunb.) Vahl could alleviate inflammatory cytokine levels and improve anti-oxidant enzyme superoxide dismutase. Therefore, it is suggested that *F. suspensa* (Thunb.) Vahl will be a good potential drug for treating inflammatory diseases (Zhou et al., 2024).

Chang et al. evaluated the mechanism of Xie Zhuo Tiao Zhi for ameliorating chronic alcohol-induced liver injury in this paper. In this study, biochemical parameters and examinations were applied to seek mechanism of Xie Zhuo Tiao Zhi to alleviate alcohol-induced liver dysfunction. As a result, hepatic oxidative stress was ameliorated and Nrf2/Keap1 expression was enhanced by Xie Zhuo Tiao Zhi. Some pro-inflammatory factors were rescued by Xie Zhuo Tiao Zhi. Thus, it is concluded Xie Zhuo Tiao Zhi will be a potential drug in treating chronic alcohol-induced liver injury diseases in the future.

Elshaer et al. found that *S. costus* root ethanolic extract could alleviate $NaNO_2$-induced hepatorenal toxicity by means of regulating apoptosis, inflammation, and metabolism. The study displayed that the $NaNO_2$-treated group improved the expressions of TNF-α and P53, and reduced expressions of IL-4 and BCL-2. It was found that *Saussurea costus* root ethanolic extract could alleviate the toxic effects of $NaNO_2$ and improve liver function by assaying hematological parameters and modulating histopathological architecture. In a word, *S. costus* root ethanolic extract could alleviate $NaNO_2$-induced hepatorenal toxicity, which will serve as a promising detoxifying additive in the future.

Mounanga et al. made a survey with 97 participants in this study, and analyzed data by One-way ANOVA and *t*-test. The survey mainly selected 63 plants, which were belonging to 35 families. The common symptoms summarized in this survey included cough, fever, cold, and fatigue. The study data emphasized that male subjects (31–44 years) had university education level. It was found that some plants displayed the highest UV, RI, and, RFC values, including *Alstonia congensis*, *Annickia chlorantha*, *Carica papaya,* and *Zingiber officinale*. Therefore, this survey revealed that traditional medicines could alleviate COVID-19 symptoms, which suggested some traditional medicines were useful for preventing coronavirus infections.

Chu et al. assayed therapeutic activities on NASH with salidroside and clarified mechanism on C57BL/6J mice with methionine- and choline-deficient diet. The study revealed that salidroside possessed preventive and therapeutic effects for NASH *in vivo*, including alleviating inflammation, downregulating apoptosis, upregulating autophagy, and rebalancing immunity. It was found that salidroside might exert its multiple therapeutic effects by activating PPARα. In a word, this research exhibited that salidroside possessed anti-NASH effect by regulating autophagy, apoptosis, and immunity, and alleviating inflammation via activating PPAR pathway.

Chen et al. Established C57BL/6J mouse model of NASH by feeding high-fat diet for 12 weeks, which was used to reveal

mechanism of *P. cyrtonema* ethanol extract against non-alcoholic steatohepatitis. In this study, 211 metabolites were identified by UHPLC-MS/MS. The study showed *Polygonatum cyrtonema* ethanol extract could improve hepatocellular degeneration and steatosis. *Polygonatum cyrtonema* ethanol extract also could restore the expressions of SREBP1, AMPK, PPAR-α, SIRT1, and regulate and upstream molecules and canonical pathways by analyzing RNA-seq data. Thus, *P. cyrtonema* ethanol extract could alleviate NASH and activate AMPK/SIRT1 pathway to prevent and treat the non-alcoholic fatty liver disease.

Jiang et al. performed a systematic review to assay hepatoprotective and hepatotoxic effects with 2,3,5,4′-tetrahydroxystilbene-2-O-β-D-glucoside. In this review, 24 studies encompassing 564 rodents were selected and analyzed. It was found that 2,3,5,4′-tetrahydroxystilbene-2-O-β-D-glucoside showed certain bidirectional activity by measuring ALT and AST levels. Moreover, some important biochemical indicators had been tested to evaluate hepatoprotective and hepatotoxic effects, including MDA, TNF-α, TC, TG, IL-6, SOD, and IFN-γ. It was found that the toxic dosage (51.93–76.07 mg/kg/d) and the protective dosage (27.27–38.81 mg/kg/d) were summarized in this review. Furthermore, 2,3,5,4′-tetrahydroxystilbene-2-O-β-D-glucoside could generate bidirectional effects on liver injury by PPAR, NF-κB, JAK/STAT, TGF-β, PI3K/Akt pathways.

Author contributions

RW: Data curation, Writing–original draft. WL: Formal Analysis, Writing–original draft. CY: Methodology, Writing–review and editing. CZ: Investigation, Writing–review and editing. ZS: Conceptualization, Writing–review and editing. QM: Funding acquisition, Writing–review and editing.

Funding

The author(s) declare that financial support was received for the research, authorship, and/or publication of this article. This study was supported by National Natural Science Foundation of China (82360682, 82360825), Jiangxi Provincial Natural Science Foundation (20242BAB26172, 20224BAB206104, 20224BAB206112), "Chunhui Plan" Collaborative Research Project of Ministry of Education of the People's Republic of China (HZKY20220385, 202200200), and Training Project of Ganpo Juncai Support Plan for High Level and High Skilled Leading Talent in 2023.

Conflict of interest

The authors declare that the research was conducted in the absence of any commercial or financial relationships that could be construed as a potential conflict of interest.

Generative AI statement

The author(s) declare that no Generative AI was used in the creation of this manuscript.

Publisher's note

References

Dabrowska, A., Wilczynski, B., Mastalerz, J., Kucharczyk, J., Kulbacka, J., Szewczyk, A., et al. (2024). The impact of liver failure on the immune system. *Int. J. Mol. Sci.* 25, 9522. doi:10.3390/ijms25179522

Israelsen, M., Francque, S., Tsochatzis, E. A., and Krag, A. (2024). Steatotic liver disease. *Lancet* 404, 1761–1778. doi:10.1016/S0140-6736(24)01811-7

Li, D. P., Huang, Z. Q., Xu, X. J., and Li, Y. (2023). Promising derivatives of rutaecarpine with diverse pharmacological activities. *Front. Chem.* 11, 1199799. doi:10.3389/fchem.2023.1199799

Taru, V., Szabo, G., Mehal, W., and Reiberger, T. (2024). Inflammasomes in chronic liver disease: hepatic injury, fibrosis progression and systemic inflammation. *J. Hepatol.* 81, 895–910. doi:10.1016/j.jhep.2024.06.016

Xu, X. M., Liu, X. F., Yu, S. F., Wang, T., Li, R., Zhang, Y., et al. (2024). Medicinal and edible polysaccharides from ancient plants: extraction, isolation, purification, structure, biological activity and market trends of sea buckthorn polysaccharides. *Food Funct.* 15, 4703–4723. doi:10.1039/d3fo04140a

Zhou, C. Y., Xia, Q., Hamezah, H. S., Fan, Z., Tong, X. H., and Han, R. C. (2024). Efficacy of *Forsythia suspensa* (Thunb.) Vahl on mouse and rat models of inflammation-related diseases: a meta-analysis. *Front. Pharmacol.* 15, 1288584. doi:10.3389/fphar.2024.1288584

frontiers | Frontiers in Pharmacology

TYPE Original Research
PUBLISHED 10 October 2023
DOI 10.3389/fphar.2023.1280864

OPEN ACCESS

EDITED BY
Rongrui Wei,
Jiangxi University of Traditional Chinese Medicine, China

REVIEWED BY
Yang Xie,
Brigham and Women's Hospital and Harvard Medical School, United States
Xianggen Zhong,
Beijing University of Chinese Medicine, China

*CORRESPONDENCE
Tao Shen,
st@cdutcm.edu.cn
Xiaofeng Chen,
xiaofengchen@cdutcm.edu.cn
Han Yu,
yuhan@cdutcm.edu.cn

†These authors have contributed equally to this work and share first authorship

RECEIVED 21 August 2023
ACCEPTED 29 September 2023
PUBLISHED 10 October 2023

CITATION
Han J, Wu P, Wen Y, Liu C, Liu X, Tao H, Zhang F, Zhang X, Ye Q, Shen T, Chen X and Yu H (2023), The zhuyu pill relieves rat cholestasis by regulating the mRNA expression of lipid and bile metabolism associated genes.
Front. Pharmacol. 14:1280864.
doi: 10.3389/fphar.2023.1280864

The zhuyu pill relieves rat cholestasis by regulating the mRNA expression of lipid and bile metabolism associated genes

Jun Han[1†], Peijie Wu[1†], Yueqiang Wen[1,2†], Chao Liu[1], Xinglong Liu[1], Huan Tao[3], Fenghua Zhang[1], Xiaodan Zhang[1], Qiaobo Ye[1], Tao Shen[1*], Xiaofeng Chen[1*] and Han Yu[1*]

[1]School of Basic Medicine, Chengdu University of Traditional Chinese Medicine, Chengdu, China, [2]Department of Pediatrics, Guang'an Traditional Chinese Medicine Hospital, Guang'an, China, [3]Department of Dermatology, Cangxi Traditional Chinese Medicine Hospital, Guangyuan, China

Background: The Zhuyu pill (ZYP), composed of *Coptis chinensis* Franch. and *Tetradium ruticarpum* (A. Jussieu) T. G. Hartley, is an effective traditional Chinese medicine with potential anti-cholestatic effects. However, the underlying mechanisms of ZYP remain unknown.

Objective: To investigate the mechanism underlying the interventional effect of ZYP on mRNA-seq analysis in cholestasis rat models.

Materials and methods: This study tested the effects of a low-dose (0.6 g/kg) and high-dose (1.2 g/kg) of ZYP on a cholestasis rat model induced by α-naphthyl-isothiocyanate (ANIT, 50 mg/kg). Serum biochemistry and histopathology results were used to evaluate the therapeutic effect of ZYP, and mRNA-Seq analysis was performed and verified using real-time fluorescence quantitative PCR (qRT-PCR). GO, KEGG, and GSEA analyses were integrated to identify the mechanism by which ZYP impacted cholestatic rats.

Results: ZYP was shown to significantly improve abnormal changes in the biochemical blood indexes and liver histopathology of cholestasis rats and regulate pathways related to bile and lipid metabolism, including fatty acid metabolism, retinol metabolism, and steroid hormone biosynthesis, to alleviate inflammation, cholestasis, and lipid metabolism disorders. Relative expression of the essential genes Cyp2a1, Ephx2, Acox2, Cyp1a2, Cyp2c11, and Sult2a1 was verified by qRT-PCR and showed the same trend as mRNA-seq analysis.

Conclusion: ZYP has a significant anti-cholestatic effect by regulating bile metabolism and lipid metabolism related pathways. These findings indicate that ZYP is a novel and promising prospect for treating cholestasis.

KEYWORDS

cholestasis, interventional mechanism, bile metabolism, lipid metabolism, zhuyu pill

Abbreviations: ANIT, α-naphthylisothiocyanate; GO, Gene ontology; HE, Hematoxylin-eosin; HPLC, High-performance liquid chromatography; KEGG, Kyoto Encyclopedia of Genes and Genomes; qRT-PCR, Real-time fluorescence quantitative PCR; UDCA, Ursodeoxycholic acid; ALT, Alanine aminotransferase; γ-GT, γ-glutamyl transpeptidase; TC, Total cholesterol; TBATotal bile acid.

Introduction

In cholestasis, bile production, secretion, and excretion are blocked. Bile can no longer flow into the duodenum and enters the bloodstream instead. When the disease progresses, hyperbilirubinemia can occur, which, in severe cases, leads to cirrhosis, liver failure, or even death (Wu et al., 2021). Primary biliary cirrhosis (PBC) and primary sclerosing cholangitis (PSC) are the most acute cholestatic liver diseases. 882 (35%) of 2,520 patients with initially diagnosed chronic liver disease had cholestasis, which was more prevalent in PBC and PSC (Bortolini et al., 1992). A study of 1,000 patients with chronic viral hepatitis showed that 56% were discharged with ALP or GGT above the upper limit of normal (ULN), for whom disease severity and the risk of liver fibrosis and cirrhosis were significantly increased (Xie et al., 2017). Ursodeoxycholic acid (UDCA) is the most common drug used to treat PBC. However, some PBC patients do not respond well to UDCA, and no effective treatment has been developed for PSC (Lu, 2022). Cholestasis has become a public health problem of general concern to medical researchers due to its adverse outcomes and the absence of reliable treatment options. The design of effective drugs is urgently needed in clinical practice.

Traditional Chinese medicine (TCM) has a unique understanding of the pathogenesis and treatment of cholestasis. From the TCM perspective, cholestasis is primarily related to poor liver function and biliary *qi*, which are accompanied by the accumulation of pathological products. Based on this concept, *Coptis Chinensis* Franch. and *Tetradium ruticarpum* (A. Jussieu) T. G. Hartley, which can regulate the movement of *qi* in the liver and bile, are still widely used in the clinical treatment of digestive diseases.

Previous studies (Ma and Ma, 2013; Wang, 2016; Liu et al., 2017) have shown that *Coptis Chinensis* Franch. has anti-inflammatory, anti-hepatic steatosis, anti-oxidant, anti-tumor, anti-diabetic, anti-arrhythmic, and anti-hypertensive effects while *T. ruticarpum* (A. Jussieu) T. G. Hartley has analgesic, anti-inflammatory, anti-tumor, and anti-oxidant effects on the cardiovascular, central nervous, digestive, reproductive, and other biological systems (Yang et al., 2011; Du and Yao, 2013; Liu et al., 2016; Wu and Chen, 2019; Zhu et al., 2019; Xu et al., 2021). The combination of these botanical drugs (commonly known as the Coptis-Evodia botanical drug couple, CEBC) is effective against various digestive disorders by reducing the accumulation of fat in the liver and protecting liver function through various pathways, including reducing FGF21 secretion, upregulating ABCA1 mRNA expression, promoting reverse cholesterol transport, and upregulating GATA-2 and GATA-3 gene and protein expression (Shen, 2007; Hu et al., 2010; Zhang et al., 2022b). In addition, these botanical drugs have been shown to have significant lipid-lowering effects. (Shen, 2007; Shen et al., 2011).

Zhuyu pill (ZYP, representative formulae of CEHC, usually mixed at a 1:1 g/g ratio) was first documented in the official medical dictionary "*Tai Ping Sheng Hui Fang*" of the Song Dynasty and is now included in the "Prescription Dictionary of Chinese Medicine" (Peng, 1993), an officially recognized work in China. In traditional Chinese medicine theory, liver and biliary *qi* is a generalization of the liver and gallbladder functions, and liver and biliary *qi* dysfunction often contributes to digestive system disease. Zhuyu pill was traditionally used to treat hepatobiliary and gastrointestinal diseases for its prominent effect of improving the liver and biliary *qi* (Li, 2002). Previous studies (Yu et al., 2022) have shown that ZYP has a significant anti-cholestasis effect achieved through the dual effects of regulating fecal metabolic homeostasis and fecal microbial abundance, as well as regulating the expression of miRNAs such as miR-147 and its target genes in the liver. However, the mechanism by which ZYP treats cholestasis has not yet been fully characterized. Messenger RNA (mRNA) is a class of single-stranded ribonucleic acid transcribed from DNA and direct protein synthesis. In cholestasis, abnormal expression of transporters associated with bile acid metabolism and mRNA associated with lipogenesis and oxidative lipid metabolism in bile stasis (Qiu et al., 2021). This suggests that ZYP may play an anti-cholestasis role by modulating mRNA expression reverse these conditions. To confirm this hypothesis, cholestatic rats were treated with ZYP. The efficacy of this drug was evaluated by quantifying the levels of serum biochemical markers and assessing liver tissue pathology. Relevant metabolic pathways and differentially expressed mRNAs were screened by transcriptome sequencing based on a pharmacodynamic evaluation. This study sought to define further the mechanism for ZYP treatment of cholestasis using modern biological techniques, providing a biological basis for treating cholestasis using TCM.

Materials and methods

Reagent preparation

All the Chinese botanical drugs used in this experiment were purchased from Beijing Tongrentang Co., Ltd. (Beijing, China). Pentobarbital sodium, UDCA, and α-naphthylisothiocyanate (ANIT) were purchased from Sigma-Aldrich Co. (St. Louis, MO, United States). Olive oil was chosen from Shanghai Yi En Chemical Technology Co., Ltd. (Shanghai, China). The chemical reagents used in this experiment were all of high-performance liquid chromatography (HPLC) analytical grade.

Preparation of ZYP and high performance liquid chromatography (HPLC) analysis

In Table 1, the characteristics of the two constituent botanical drugs are listed. ZYP Preparation adheres to the Science of Prescription guidelines as outlined in the Ministry of Education's General Higher Education "13th Five Year Plan" national planning materials, using the traditional method of boiling Chinese herbal medicines, the dried botanical drugs, including *Coptis Chinensis* Franch. and *T. ruticarpum* (A. Jussieu) T. G. Hartley at the ratio of 1:1 (w/w), were immersed in purified water of 20 - fold volumes of botanical drugs (v/w) for 30 min and then were heated to boiling and were kept 30 min. The liquid was then filtered and collected. The decoction was boiled again as described above, and the liquid was collected, mixed with the initial liquid, concentrated to 120 mL. After filtration, the solution was evaporated under reduced pressure to a suspension with a final density of 0.1 g/mL, and stored at −20°C for backup (Li and Lian, 2016).

TABLE 1 Characteristics of the two constituent botanical drugs in Zhuyu pill.

Chinese name	Botanical name[a]	Genus family	Batch number	Medicinal parts	Origin	Weight (g)
Huanglian	*Coptis chinensis* Franch	Ranunculaceae	220701	Dried root	Chongqing, China	6
Wuzhuyu	*Tetradium ruticarpum* (A. Jussieu) T. G. Hartley	Rutaceae	220416008	Dried mature seed	Guizhou, China	6

[a]The plant name was verified using http://www.theplantlist.org.

The aforementioned solution was subjected to reflux extraction twice, each time for a duration of 1 h, and this process was repeated three times. Subsequently, the extraction solution was concentrated under reduced pressure and freeze-dried. The extraction rate was determined to be 10.6% using acid dye colorimetry, indicating a drug extract ratio of 10.6 g per 100 g. To determine the main metabolites, four alkaloids (berberine, coptisine, evodiamine, and rutecarpine) in ZYP were analyzed via HPLC using an Agilent 1,260 Infinity II (Agilent Technologies Inc., California, United States). Chromatographic separation was performed with a Welch Ultimate XB-C18 Column (4.6 mm × 250 mm, 5 μm, Maryland, California, United States) at a column temperature of 30°C. The linear-gradient mobile phase consisted of mobile phase A (50 mM monopotassium phosphate +0.4% sodium heptane sulfonate, pH = 4) and mobile phase B (pure methanol). A mobile phase gradient was used (0–15 min, 95% A, 5% B; 15–40 min, 50% A, 50% B; 40–55 min, 30% A, 70% B; 55–60 min, 95% A, 5% B), with a 1.0 mL/min flow rate and 10ul injection volume. The detection wavelength was set as (0–44 min, 345 nm; 44–48 min, 226 nm; 48–60 min, 345 nm) (Yu et al., 2022). ZYP was found to contain 36.8 mg/g berberine, 14.9 mg/g coptisine, 0.78 mg/g evodiamine, and 0.33 mg/g rutecarpine (Yu et al., 2022) **(Supplementary Material 1)**.

Animals and treatments

The experiments were conducted according to the internationally recognized Guiding Principles for the Care and Use of Laboratory Animals and the study received approval from the Animal Ethics Committee at the Chengdu University of Traditional Chinese Medicine. The ethics approval number for the use of animals in this study was 2019-15.

A total of 30 healthy male Sprague Dawley (SD) rats weighing 160–180 g were purchased from Beijing Harvest Biotechnology Co., Ltd. (Beijing, China; certification number: SCXK-JING, 2019-0008). After 4 days of acclimatization feeding, we randomly divided all rats into five groups: Control group (Control), Model group (Model), ZYP low-dose group (ZYP_L), ZYP high-dose group (ZYP_H), and Ursodeoxycholic acid group (UDCA), six rats in each group. The animal administration dosage of ZYP was determined to be 1.2 g/kg, taking into account the pre-experiment data and conversion based on body surface area. This dosage corresponds to the typical clinical dose of 12 g/60 kg. Beginning on day 5, rats in the ZYP_L, ZYP_H, and UDCA groups received daily administrations of 0.6 g/kg, 1.2 g/kg ZYP, and 60 mg/kg UDCA, respectively, by oral gavage until day 10. Meanwhile, rats in the Model and Control groups were given an equal volume of purified water. On day 11, the experimental groups were administered 50 mg/kg ANIT solution dissolved in olive oil. The Control rats were given the corresponding dose of olive oil, referring to the modeling method described previously (Xu and Miao, 2021). On days 12–14, rats in the ZYP_L, ZYP_H, and UDCA groups were given 0.6 g/kg, 1.2 g/kg of ZYP, and 60 mg/kg UDCA by gavage, respectively, while those in the Model and Control groups were given an equal volume of purified water. On day 15, all rats were sacrificed with 150 mg/kg sodium pentobarbital anesthesia, and blood and liver tissues were collected from each group for testing.

Liver function assays

After fasting for 12 h, the rats were anesthetized using an intraperitoneal injection of sodium pentobarbital solution, blood was removed from the inferior vena cava, and the livers were harvested. Serum samples were obtained by centrifugation of blood samples at 3,500 × g for 15 min at 4°C. The relevant biochemical parameters, including ALT, AST, ALP, γ-GT, DBIL, TBIL, TBA, TC, and TG, were detected by a fully automated biochemical analyzer (BS-240VET). Liver tissues from each group of rats were fixed in 4% paraformaldehyde, rinsed with running water, dehydrated, embedded, sectioned, and HE stained. The stained tissues were examined microscopically, and images were acquired for analysis.

RNA extraction and library construction

In each group, three liver tissue samples were randomly selected for mRNA sequencing. Total RNA was extracted using the mir Vana miRNA Isolation Kit (Ambion) according to the manufacturer's protocol. RNA integrity was evaluated using the Agilent 2,100 Bioanalyzer (Agilent Technologies, Santa Clara, CA, United States). Samples with RNA Integrity Number (RIN) ≥7 were used for subsequent analysis. The libraries were constructed using TruSeq Stranded Total RNA with Ribo-Zero Gold according to the manufacturer's instructions. The libraries were then sequenced on an Illumina sequencing platform, and 150/125 bp paired-end reads were generated.

Bioinformatic analysis

Raw reads generated during high-throughput sequencing were fastq format sequences that required further quality filtering to

TABLE 2 qRT-PCR primers used in this study.

Gene symbol	Forward primer (5′–3′)	Reverse primer (5′–3′)	Product length (bp)	Tm (°C)
ACTB	GCGAGTACAACCTTCTTGC	TATCGTCATCCATGGCGAAC	72	60
Alox15	CAACTGGAAGGATGGCTCA	TCCTCTCGAAATCGTTGGT	81	60
Cyp2a1	ATGGCAATTCAGAGTTCCAC	GAGCTGACTGTCTCAGACC	82	60
Ephx2	GCTGGACGACAGTGACAA	CGACCTGACAGGACTCTAT	92	60
Acox2	TGCCATGAATGCTATCCGA	TGTCTGGGCGTATGTTGT	100	60
Sult2a1	CAGATGAGCTGGATTTGGTC	CATGAGGCCAATTCCAGTAA	116	60
Cyp1a2	TGTCACCTCAGGGAATGCT	GACCACCGTTGTCTTTGTAG	212	60
Cyp2c11	ACGTGGATGTCACAGCTAAAGTCC	GGCTCCGGTTTCTGCCAATTAC	63	60

obtain high-quality reads for later analysis. Trimmomatic software was used for adapter removal, and the low-quality bases and N-bases or low-quality reads were filtered out to get high-quality clean reads. Using hisat2 to align the clean reads to the reference genome of the experimental species, the sample was assessed by genomic and gene alignment. The alignment result with the reference genome was stored in a binary bam file, and the new transcript was spliced using Stringtie software to assemble the reads. The mRNA transcript sequences were aligned with the sequencing reads of each sample and eXpress was used to obtain the fragments per kilobase of transcript per million (FPKM) and count values (the number of reads per gene in each sample).

The estimateSizeFactors function of the DESeq (2012) R package was used to normalize the counts, and the nbinomTest function was used to calculate the *p*-value and fold change values for the difference comparison. Differential transcripts with *p*-values ≤0.05 and fold change ≥2 were selected, and differential mRNA GO and KEGG enrichment values were assessed using the Hypergeometric Distribution Test. mRNA sequencing and analysis were conducted using OE Biotech Co., Ltd. (Shanghai, China).

mRNA validation using real-time quantitative qRT-PCR

The qRT-PCR verification of mRNA is generally divided into three steps: mRNA extraction, reverse transcription, and PCR quantification. The details of the specific experimental process in this part can be checked in **(Supplementary Material 2)**. The qRT-PCR primers (Table 2) used in this study were designed according to the mRNA sequences from the NCBI database and synthesized by TsingKe Biotech.

Statistical analysis

GraphPad Prism version 8 was used to assess the differences in serum biochemical indicators. One-way ANOVA was used for intergroup comparison. Statistical differences between the groups were assessed using the mean ± standard deviation, and $p < 0.05$ indicated that the differences were statistically significant.

Results

Impact of ZYP on liver function

As shown in Figures 1A–I, the serum levels of ALT, AST, ALP, γ-GT, DBIL, TBIL, TBA, TC, and TG in the rats in the cholestasis Model group were significantly higher than those in the Control group, while both ZYP_L and ZYP_H could significantly reduce the above indexes, showing a similar trend of action with UDCA. Moreover, the effect of ZYP in the treatment of cholestasis was a dose-effect relationship. While the liver tissue in the Control group showed a clear structure, tightly arranged cells with clear boundaries, abundant cytoplasm, uniform color, round nuclei, regular size, and an intact and normal venous endothelium, liver tissue in the Model group showed focal necrosis of hepatocytes and inflammatory cell infiltration. In the ZYP_L and ZYP_H groups, these pathological changes were improved to different degrees (Figure 1K). Combined with Ishak score analysis (Figure 1J), ZYP_H achieved a similar intervention effect as UDCA. These results indicate that ZYP has a positive therapeutic effect on cholestasis, especially when given at a higher dose. Therefore, the potential mechanism of ZYP_H for treating cholestasis is more valuable to investigate.

Screening and quantitative statistics of differentially expressed mRNAs

DESeq software was used to normalize the counts of each sample mRNA (Base Mean value was used to estimate the expression), calculate the difference ploidy, test the different significance of counts by negative binomial (NB) distribution, and screen for differences in gene expression based on the ploidy and significance test results.

The screening criteria for significantly differentially expressed mRNAs were $p < 0.05$ and FC > 2. Figure 2 shows that 3,053 genes were significantly altered (1,653 upregulated and 1,400 downregulated) after ANIT induction, indicating that ANIT significantly altered gene expression in rat liver tissues. In contrast, both low-doses (93 upregulated and 153 downregulated) and high-doses (62 upregulated and 158 downregulated) of ZYP

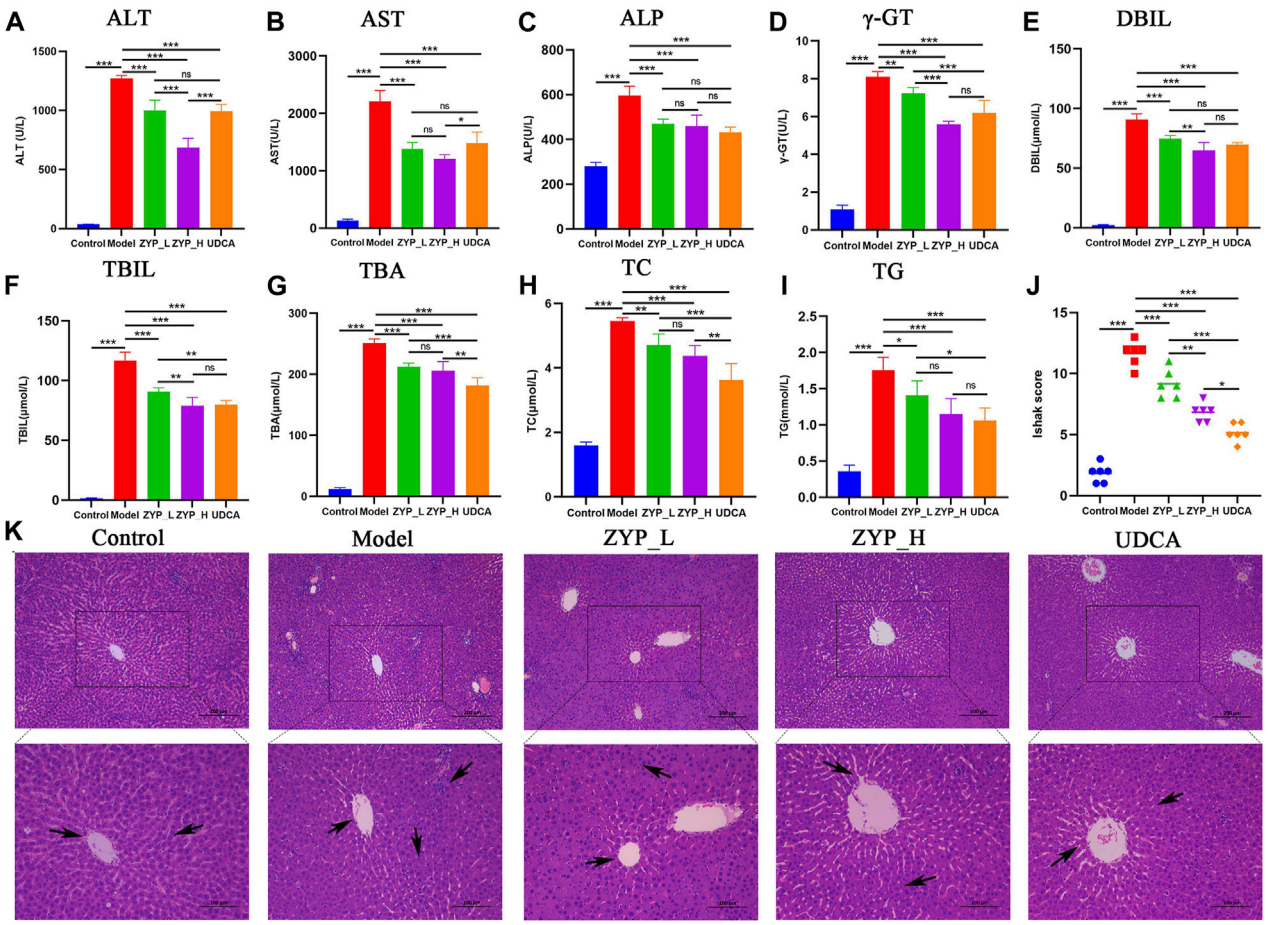

FIGURE 1
Serum biochemical tests and histopathological alterations of the liver in each group. **(A)** ALT, **(B)** AST, **(C)** ALP, **(D)** γ-GT, **(E)** DBIL, **(F)** TBIL, **(G)** TBA, **(H)** TC, **(I)** TG, **(J)** Ishak score of hepatic inflammation and necrosis, $n = 6$, ***, $p < 0.001$, **, $p < 0.01$, *, $p < 0.05$, ns, not significant. **(K)** Histopathological examination of each group at 100x and 200x.

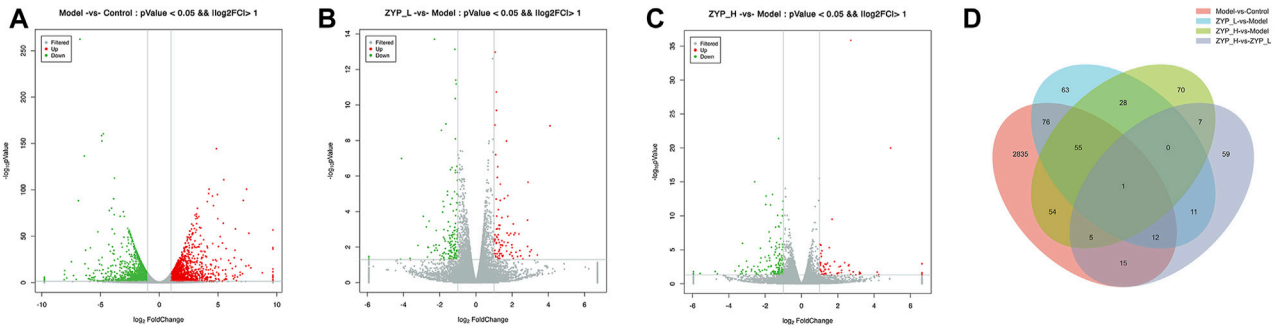

FIGURE 2
Differential gene expression analysis of the mRNA-Seq. **(A–C)** Volcano plot reflecting differences in gene expression. Genes with non-significant differences are gray, and genes with significant differences are red and green; **(D)** Numbers of the overlapping genes in different comparisons.

significantly changed the gene expression in the liver of cholestatic rats. These results indicated that ZYP treatment could reverse this expression trend, and these differentially expressed genes may be the regulatory targets of ZYP_H in treating cholestasis.

To further elucidate the mode of action of ZYP in cholestasis, we focused on the target genes in treating cholestasis with ZYP_H. These target genes were divided into upregulated target genes and downregulated target genes. Compared to controls, genes that are

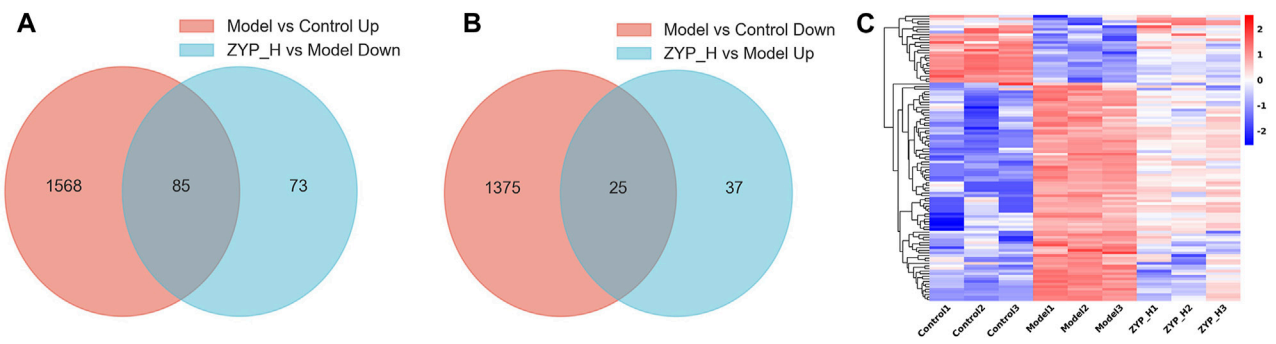

FIGURE 3
Target genes regulated by ZYP_H for the treatment of cholestasis. **(A)** Downregulated target genes of ZYP_H; **(B)** Upregulated target genes of ZYP_H; **(C)** Heatmap for hierarchical cluster analysis of different express genes between Control, Model, and ZYP_H.

downregulated in the cholestasis model and upregulated after ZYP_H treatment are upregulated target genes. Compared to the Control group, genes that were upregulated in the cholestasis model and downregulated after ZYP_H treatment were downregulated target genes. The present study showed 85 downregulated target genes and 25 upregulated target genes in ZYP_H treating cholestasis (Figures 3A, B). The expression of these target genes significantly differed between groups. More notably, the ANIT-induced cholestasis model, which had abnormal gene expression, showed a similar gene expression trend to the Control group after the ZYP_H intervention (Figure 3C). This indicates that ZYP_H may reverse-regulate the abnormal expression of genes caused by ANIT.

Functional description and pathway analysis of differentially expressed mRNAs

To determine the function of target genes regulated by ZHP_H during the treatment of cholestasis, GO and KEGG analyses were performed on differentially expressed mRNAs (Figures 4A–D). Compared to the Control group, biological processes and signaling pathways inhibited in the Model group and promoted after ZYP_H treatment, and those promoted in the Model group and inhibited after ZYP_H treatment were the therapeutic targets of ZYP_H in cholestasis.

GO enrichment analysis showed that the biological processes upregulated by ZYP_H were mainly involved in the steroid metabolic process, fatty acid metabolic process, lipid metabolic process, epoxygenase P450 pathway, and retinol metabolism. In contrast, the biological processes downregulated by the ZYP_H group included inflammatory response, neutrophil chemotaxis, cellular response to interleukin-1, etc. Combined with KEGG analysis, ZYP_H upregulated signaling pathways involved retinol metabolism, fatty acid degradation, arachidonic acid metabolism, steroid hormone biosynthesis, PPAR signaling pathway, and bile secretion. ZYP_H downregulated signaling pathways included cytokine-cytokine receptor interaction, IL-17 signaling pathway, Chemokine signaling pathway, etc. This was consistent with the results of the GO analysis. In general, the biological processes and signaling pathways promoted by ZYP_H in the treatment of cholestasis were mainly related to lipid metabolism and bile metabolism, while the biological processes and signaling pathways inhibited by ZYP_H were mainly related to inflammatory response and immune response. Considering the pathological process of bile secretion and excretion disorders caused by cholestasis, the bile metabolism and lipid metabolism-related pathways regulated by ZYP_H have become the focus of our research.

In addition, Gene Set Enrichment analysis (GSEA) was performed on all differentially expressed genes to avoid screening out essential genes with weak changes resulting from the fixed threshold screening method (Figures 4E–J). The results likewise indicated that fatty acid metabolism, retinol metabolism, and steroid hormone biosynthesis were upregulated target pathways of ZYP _H. These data suggested that ZYP has a therapeutic effect on cholestasis by regulating the expression of genes involved in lipid and bile metabolism.

Regulatory mechanism of ZYP in treating cholestasis

A regulatory network map was created using the above results to elaborate in more detail on the biological mechanisms underlying the therapeutic effects of ZYP on cholestasis. As shown in Figure 5, the pathways were inhibited to different degrees in the cholestasis model, and ZYP acted distinctly on each one. The genes regulated in all pathways, Cyp1a1, Cyp1a2, Cyp2a1, Cyp2b1, Cyp4a8, Cyp2c11, Rdh16, Alox15, Ephx2, Sult2a1, and Acox2, were the potential targets for ZYP treatment of cholestasis.

qRT-PCR validation of mRNA-Seq and correlation analysis between core genes and serum biochemistry

To determine the accuracy and reliability of mRNA-seq, several core genes, Alox15, Cyp2a1, Ephx2, Acox2, Sult2a1, Cyp1a2, and Cyp2c11 were validated by qRT-PCR (Figure 6). The expression trends of all genes except Alox15 were consistent with mRNA-seq, indicating that the findings were reliable. Spearman's calculation method analyzed the correlation of core gene expression differences

10.3389/fphar.2023.1280864

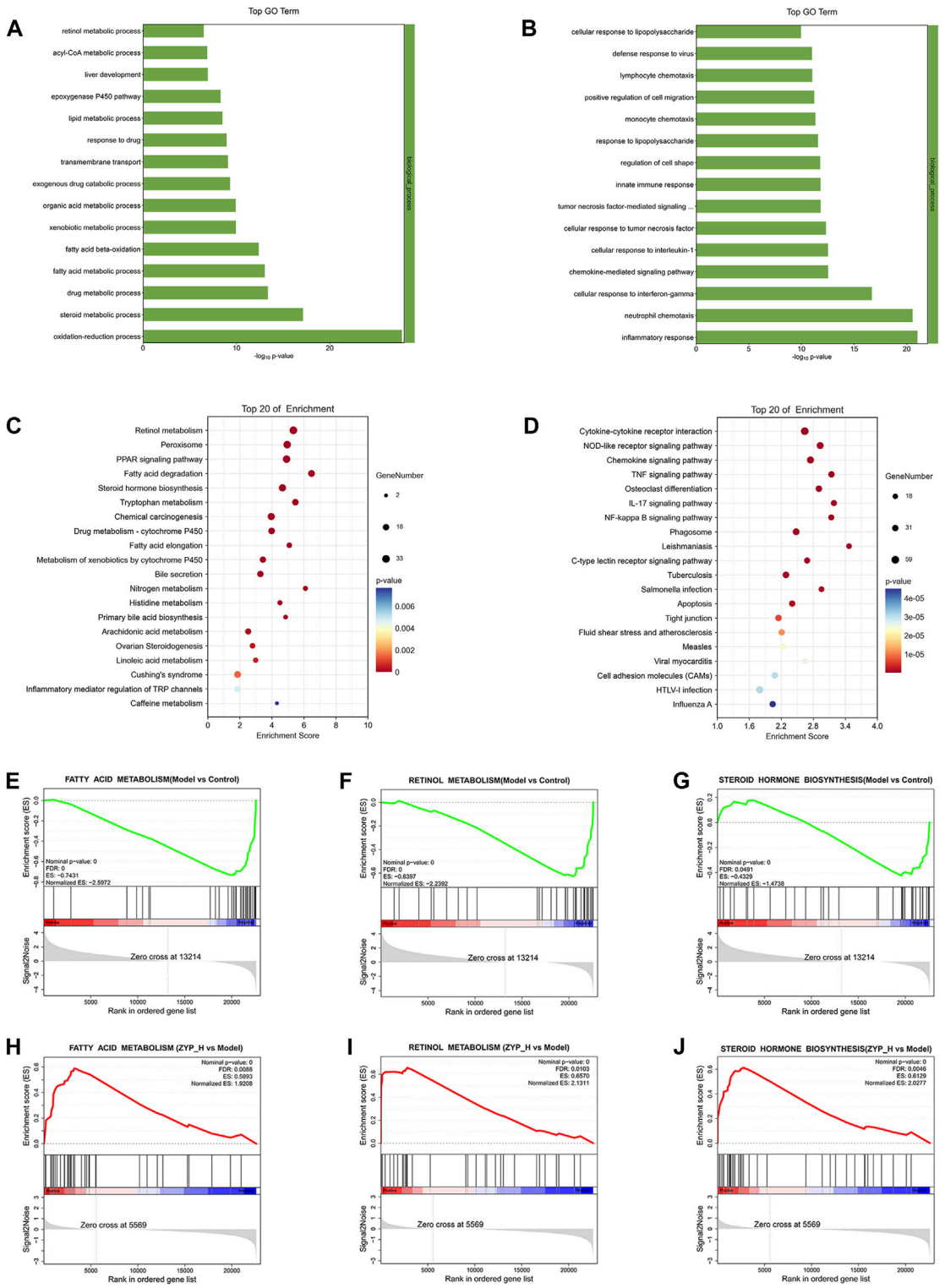

FIGURE 4
Functional analysis of differentially expressed mRNAs. **(A, C)** Biological processes and signaling pathways inhibited in the Model group and promoted after ZYP_H treatment; **(B, D)** Biological processes and signaling pathways promoted in the Model group and inhibited after ZYP_H treatment. **(E–J)**, GSEA analysis of the differentially expressed mRNAs between Model vs Control-down and ZYP_H vs Model-up, **(E, H)** fatty acid metabolism; **(F, I)** retinol metabolism; **(G, J)** steroid hormone biosynthesis.

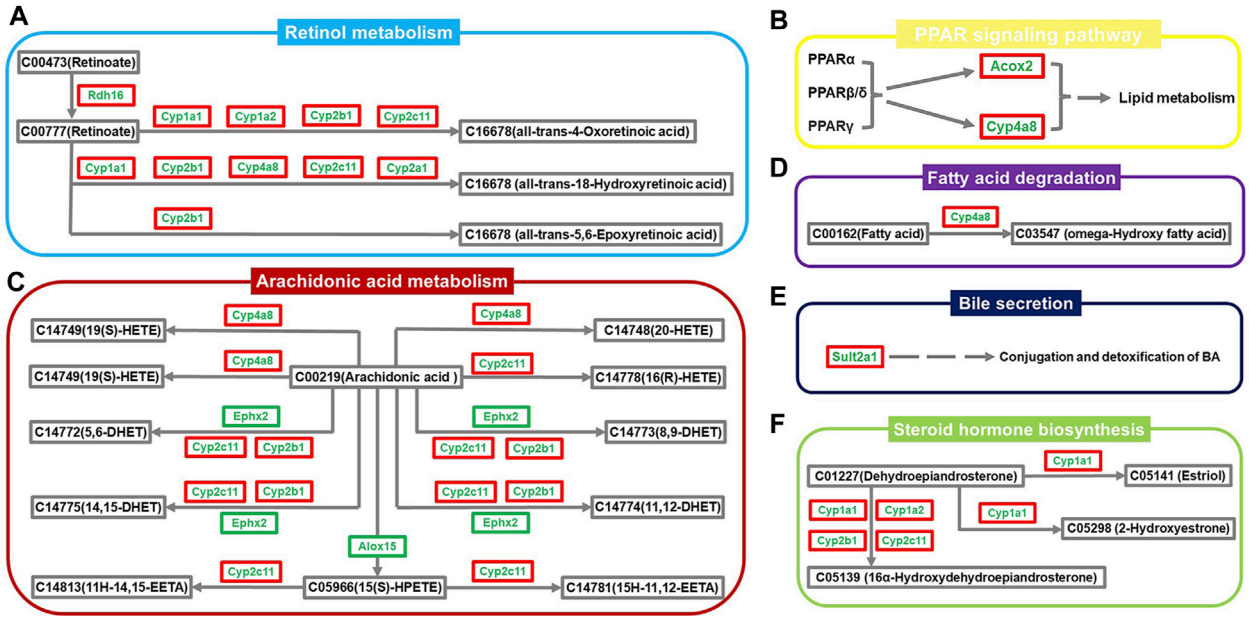

FIGURE 5
Network diagram of the regulatory mechanism of ZYP for cholestasis. **(A)** Retinol metabolism, **(B)** PPAR signaling pathway, **(C)** Arachidonic acid metabolism, **(D)** Fatty acid degradation, **(E)** Bile secretion, **(F)** Steroid hormone biosynthesis. Green names indicate that the gene is downregulated in the Model group compared to the Control group. The red outer box indicates that the gene is upregulated in the ZYP_H group compared to the Model group. The green outer box indicates that the gene is downregulated in the ZYP_H group compared to the Model group.

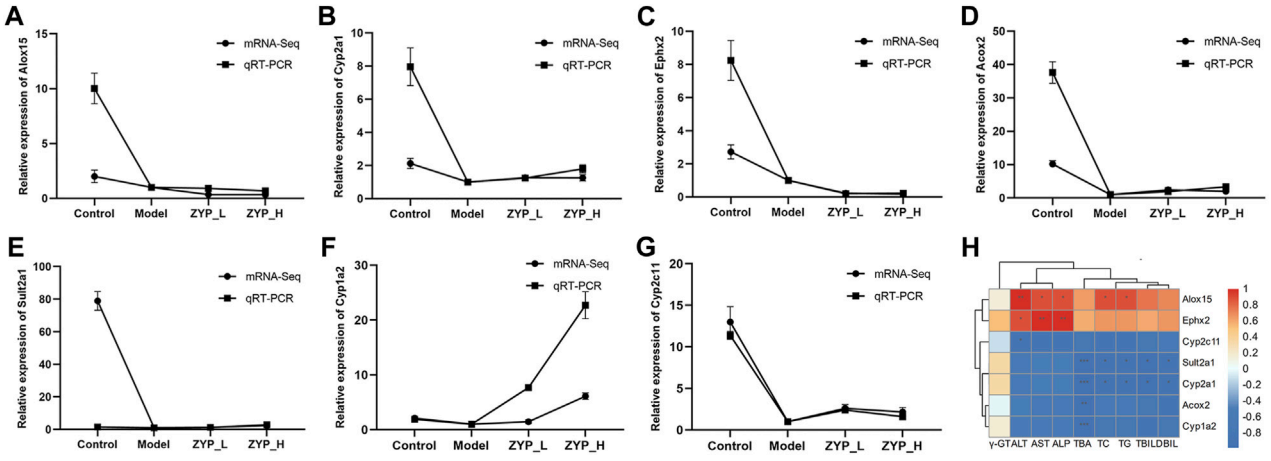

FIGURE 6
qRT-PCR validation of mRNA-Seq and correlation analysis between core genes and serum biochemistry. The genes selected for qRT-PCR validation were enriched in the regulatory network diagram in Figure 5. **(A)** Alox15, **(B)** Cyp2a1, **(C)** Ephx2, **(D)** Acox2, **(E)** Sult2a1, **(F)** Cyp1a2, **(G)** Cyp2c11. Data are expressed as the means ± sd (n = 3). **(H)** Correlation analysis between core genes and serum biochemistry: Orange-red is positive, blue is negative, and darker color indicates stronger correlation. *, $p < 0.05$, **, $p < 0.01$, ***, $p < 0.001$ (This result was done with Oebiotech cloud platform tools at the following website: https://cloud.oebiotech.cn/task/).

with ZYP_H for cholestasis. The findings of this study indicate that the expression levels of Sult2a1 and Cyp2a1 were found to have a significant negative correlation with TC, TG, TBA, TBIL, and DBIL. Acox2 and Cyp1a2 were significantly and negatively correlated with TBA, and Cyp2c11 negatively correlated with ALT. Conversely, the expression of Alox15 was significantly and positively correlated with ALT, AST, ALP, TC, and TG. Furthermore, the expression of Ephx2 was significantly and positively correlated with AST, ALT, and ALP. These results suggest that ZYP_H may have the potential to ameliorate cholestasis and enhance lipid metabolism by modulating the expressions of Alox15, Acox2, Cyp2a1, and Sult2a1, while also improving liver function.

Discussion

ANIT is an indirect hepatotoxic agent that damages intrahepatic bile duct epithelial cells, causing capillary hyperplasia and inflammation around the interlobular bile ducts, eventually leading to bile duct epithelial necrosis and obstruction by shedding. This results in evident bile excretion disorder accompanied by parenchymal cell damage through punctate necrosis, producing biliary stasis (Labiano et al., 2022). TCM theory considers that cholestasis requires the pungent-opening and bitter-subduing method to improve the movement of *qi*, and ZYP is a classic formula for this therapy. Serum biochemistry and pathological observations are the fundamental indicators of cholestasis, liver injury, and efficacy evaluation. ALT, AST, ALP, γ-GT, TBA, DBIL, TBIL, TG and TC levels can objectively and effectively reflect liver function, cholestasis, and lipid metabolism (Fickert et al., 2017; Nong et al., 2020). Pathological observation is the gold standard for diagnosis and is essential for determining the extent of liver damage. This study confirmed that ZYP had a dose-dependent therapeutic effect on cholestasis by pathological observations and serum biochemical indexes, which is consistent with our previous work (Yu et al., 2022). mRNA transcriptome sequencing and the ZYP gene regulation map identified six pathways and five differential genes that may be involved in ZYP's mechanism of action against cholestasis.

Cholestasis is usually associated with impaired fatty acid metabolism in the liver, and cholestatic and non-alcoholic fatty liver disease share several fundamental pathophysiological mechanisms (Trauner and Fuchs, 2022). Inflammation is also a critical pathological factor in cholestasis. The glucocorticoids in steroids inhibit the release of inflammatory factors, promote bile excretion, and reduce impaired liver function (Yan et al., 2016).

Steroid hormone biosynthesis also promotes cholesterol conversion and bile acid synthesis, increasing cholesterol excretion from the liver (Sun et al., 2021). The current study found that retinol metabolism was significantly inhibited in the livers of rats in the cholestasis model, which supports previous studies (Cai et al., 2014; Takitani et al., 2018; Yuan et al., 2018). Retinoic acid may improve lipid deposition. Retinoic acid upregulates peroxisome proliferator-activated receptor alpha (PPAR-α) and retinoic acid-like receptor alpha (RXR-α) to promote fatty acid oxidation and inhibits fatty acid synthesis via SREBP-1c and fatty acid synthase (Senoo et al., 2017; Cassim Bawa et al., 2022). Lipotoxicity caused by fatty acid accumulation can induce stress in hepatocytes and bile duct cells (Natarajan et al., 2017). Thus, increasing fatty acid metabolism and degradation can help to prevent lipid metabolism disorder and cholestasis.

Bile secretion, steroid hormone biosynthesis, and the PPAR signaling pathway play an essential role in regulating cholesterol and bile acid homeostasis by affecting biliary secretion and reducing the inflammatory response. Acox2 and Sult2a1 are essential genes in PPAR signaling and bile secretion, and studies have revealed a correlation between the expression of these genes and cholestasis. Acox2 is involved in bile acid biosynthesis, particularly in regulating bile acid intermediate metabolism and branched-chain fatty acid oxidation (Zhang et al., 2022a). Acox2 deficiency is characterized by the accumulation of bile acids and intermediates (Monte et al., 2017), bile acid synthesis, and elevated transaminase production (Alonso-Peña et al., 2022). PPARα regulates bile acid detoxification by upregulating Sult2a1 (Ghonem et al., 2015), which plays an essential role in catalyzing the sulfation of bile acids and promoting the elimination of toxic secondary bile acids (Kong et al., 2021), thereby alleviating bile stasis. ZYP upregulates the expression of Acox2 and Sult2a1 to induce bile metabolism and reduce liver injury.

Arachidonic acid is a critical inflammatory mediator that regulates oxidative stress and mediates hepatocyte injury. Alox15 and Ephx2 are potential hub genes in bile acid metabolism, which correlates with liver function. The downregulation of these genes is shown to improve liver injury, inflammation, and steatosis (Martínez-Clemente et al., 2010; Mello et al., 2021) and promote drug and fatty acid metabolism, thereby reducing liver toxicity (Zhang et al., 2017; Almansour et al., 2018). The current study showed that Alox15 and Ephx2 expression were downregulated by ZYP, suggesting that this drug may inhibit inflammation and improve liver function. However, it is worth noting that these two genes were also downregulated in the Model and Control groups, suggesting that they are not the anti-cholestasis targets of ZYP. Further research is required to determine their precise mechanisms of action.

Cyp enzymes also play a pivotal role in the biotransformation of steroids, fatty acids, and bile acids. Surprisingly, almost all cholestasis-specific pathways regulated by ZYP involve Cyp enzymes. Prior studies indicate that Cyp1a1, Cyp1a2, and Cyp2b1 are potential targets for treating of cholestasis (Ding et al., 2014; Ibrahim, 2015; Wang et al., 2022). Cyp2c11 exhibits significant catalytic activity in the metabolism of arachidonic acid, but its activity is diminished in various inflammation models, leading to lipid accumulation and liver injury (Sugatani et al., 2006; Zordoky et al., 2011). The expression and function of Cyp1a2 are diminished in cases of inflammation and cholestasis, which are both linked to the development of steatosis and cholestasis. (Klein et al., 2010; Deng et al., 2023). Our experiments showed that ZYP has a significant inverse regulatory effect on the expression of these genes. Cyp2a1 was confirmed as a critical enzyme in melatonin metabolism, helping to protect the bromoamide derivatives of melatonin from metabolic effects (Sangchart et al., 2021). Interestingly, both endogenous and exogenous melatonin can ameliorate liver injury by reducing oxidative stress, inflammatory response, and biliary senescence (Hu et al., 2009; Wu et al., 2017; Yu et al., 2018). The current study found that ZYP significantly increased the expression of Cyp2a1 in the liver of cholestatic rats, suggesting that promoting endogenous melatonin secretion is a potential mechanism for the anti-cholestatic effect of ZYP.

Finally, analysis of core gene expression and serum biochemistry results indicated that the promotion of bile acid and lipid catabolism and detoxification by ZYP was primarily associated with the upregulation of Sult2a1, Cyp2a1, Cyp1a2, and Acox2. In contrast, the improvement in liver function was mainly achieved through the downregulation of Cyp2c11, Alox15 and Ephx2. However, γ-GT levels were not significantly correlated with serum biochemistry results, which is consistent with our previous results (Yu et al., 2021). Future experiments are needed to further investigate this finding.

Conclusion

ZYP was found to have a significant dose-response effect on cholestasis, related to its regulation of the expression of mRNAs related to bile and lipid metabolism. The findings from this study contribute to the "TCM wisdom" used to diagnose and treat this disease.

Data availability statement

The datasets presented in this study can be found in online repositories. The names of the repository/repositories and accession number(s) can be found below: NCBI BioProject (https://www.ncbi.nlm.nih.gov/bioproject/), PRJNA908063

Ethics statement

The animal study was approved by the Animal Ethics Committee of Chengdu University of Traditional Chinese Medicine. The study was conducted in accordance with the local legislation and institutional requirements.

Author contributions

JH: Writing–original draft. PW: Methodology, Resources, Writing–review and editing. YW: Methodology, Resources, Writing–review and editing. CL: Data curation, Validation, Writing–review and editing. XL: Data curation, Validation, Writing–review and editing. HT: Data curation, Validation, Writing–review and editing. FZ: Data curation, Validation, Writing–review and editing. XZ: Data curation, Validation, Writing–review and editing. QY: Investigation, Visualization, Writing–review and editing. TS: Conceptualization, Supervision, Writing–review and editing. XC: Conceptualization, Funding acquisition, Writing–review and editing. HY: Conceptualization, Funding acquisition, Writing–review and editing.

Funding

The author(s) declare financial support was received for the research, authorship, and/or publication of this article. The Sichuan Provincial Science and Technology Program (Nos. 2023NSFSC1793, 2023YFQ0016, 2023YFS0476) and the Foundation for the Heritage and Development of Basic Medical Schools (No. CCCXYB202208) provided funding for this work.

Acknowledgments

We are very appreciated the experimental platform and resources provided by Research Innovation Center of Basic Medical College, Chengdu University of Traditional Chinese Medicine for this study. Thanks for HY patient guidance in writing this thesis. In addition, JH especially thanks HT for her care and attention in life.

Conflict of interest

The authors declare that the research was conducted in the absence of any commercial or financial relationships that could be construed as a potential conflict of interest.

Publisher's note

All claims expressed in this article are solely those of the authors and do not necessarily represent those of their affiliated organizations, or those of the publisher, the editors and the reviewers. Any product that may be evaluated in this article, or claim that may be made by its manufacturer, is not guaranteed or endorsed by the publisher.

Supplementary material

The Supplementary Material for this article can be found online at: https://www.frontiersin.org/articles/10.3389/fphar.2023.1280864/full#supplementary-material

References

Almansour, M. I., Jarrar, Y. B., and Jarrar, B. M. (2018). *In vivo* investigation on the chronic hepatotoxicity induced by sertraline. *Environ. Toxicol. Pharmacol.* 61, 107–115. doi:10.1016/j.etap.2018.05.021

Alonso-Peña, M., Espinosa-Escudero, R., Herraez, E., Briz, O., Cagigal, M. L., Gonzalez-Santiago, J. M., et al. (2022). Beneficial effect of ursodeoxycholic acid in patients with acyl-CoA oxidase 2 (ACOX2) deficiency-associated hypertransaminasemia. *Hepatology* 76 (5), 1259–1274. doi:10.1002/hep.32517

Bortolini, M., Almasio, P., Bray, G., Budillon, G., Coltorti, M., Frezza, M., et al. (1992). Multicentre Survey of the Prevalence of Intrahepatic Cholestasis in 2520 Consecutive Patients with Newly Diagnosed Chronic Liver Disease. *Drug Investig.* 4 (4), 83–89. doi:10.1007/BF03258368

Cai, S. Y., Mennone, A., Soroka, C. J., and Boyer, J. L. (2014). All-trans-retinoic acid improves cholestasis in α-naphthylisothiocyanate-treated rats and Mdr2-/- mice. *J. Pharmacol. Exp. Ther.* 349 (1), 94–98. doi:10.1124/jpet.113.209353

Cassim Bawa, F. N., Xu, Y., Gopoju, R., Plonski, N. M., Shiyab, A., Hu, S., et al. (2022). Hepatic retinoic acid receptor alpha mediates all-trans retinoic acid's effect on diet-induced hepatosteatosis. *Hepatol. Commun.* 6 (10), 2665–2675. doi:10.1002/hep4.2049

Deng, F., Qin, G., Chen, Y., Zhang, X., Zhu, M., Hou, M., et al. (2023). Multi-omics reveals 2-bromo-4,6-dinitroaniline (BDNA)-induced hepatotoxicity and the role of the gut-liver axis in rats. *J. Hazard Mater* 457, 131760. doi:10.1016/j.jhazmat.2023.131760

Ding, L., Zhang, B., Zhan, C., Yang, L., and Wang, Z. (2014). Danning tablets attenuates α-naphthylisothiocyanate-induced cholestasis by modulating the expression of transporters and metabolic enzymes. *BMC Complement. Altern. Med.* 14, 249. doi:10.1186/1472-6882-14-249

Du, F., and Yao, Z. W. (2013). Effect of evodiamine on polycystic ovary syndrome rat. *Laser J.* 34 (2), 86–88.

Fickert, P., Hirschfield, G. M., Denk, G., Marschall, H. U., Altorjay, I., Färkkilä, M., et al. (2017). norUrsodeoxycholic acid improves cholestasis in primary sclerosing cholangitis. *J. Hepatol.* 67 (3), 549–558. doi:10.1016/j.jhep.2017.05.009

Ghonem, N. S., Assis, D. N., and Boyer, J. L. (2015). Fibrates and cholestasis. *Hepatology* 62 (2), 635–643. doi:10.1002/hep.27744

Hu, S., Yin, S., Jiang, X., Huang, D., and Shen, G. (2009). Melatonin protects against alcoholic liver injury by attenuating oxidative stress, inflammatory response, and apoptosis. *Eur. J. Pharmacol.* 616 (1-3), 287–292. doi:10.1016/j.ejphar.2009.06.044

Hu, Y., Fahmy, H., Zjawiony, J. K., and Davies, G. E. (2010). Inhibitory effect and transcriptional impact of berberine and evodiamine on human white preadipocyte differentiation. *Fitoterapia* 81 (4), 259–268. doi:10.1016/j.fitote.2009.09.012

Ibrahim, Z. S. (2015). Chenodeoxycholic acid increases the induction of CYP1A1 in HepG2 and H4IIE cells. *Exp. Ther. Med.* 10 (5), 1976–1982. doi:10.3892/etm.2015.2719

Klein, K., Winter, S., Turpeinen, M., Schwab, M., and Zanger, U. M. (2010). Pathway-Targeted Pharmacogenomics of CYP1A2 in Human Liver. *Front. Pharmacol.* 1, 129. doi:10.3389/fphar.2010.00129

Kong, L., Dong, R., Huang, K., Wang, X., Wang, D., Yue, N., et al. (2021). Yangonin modulates lipid homeostasis, ameliorates cholestasis and cellular senescence in alcoholic liver disease via activating nuclear receptor FXR. *Phytomedicine* 90, 153629. doi:10.1016/j.phymed.2021.153629

Labiano, I., Agirre-Lizaso, A., Olaizola, P., Echebarria, A., Huici-Izagirre, M., Olaizola, I., et al. (2022). TREM-2 plays a protective role in cholestasis by acting as a negative regulator of inflammation. *J. Hepatol.* 77 (4), 991–1004. doi:10.1016/j.jhep.2022.05.044

Li, F. (2002). *Science of herbal formulas*. People's Medical Publishing House.

Li, J., and Lian, J. (2016). *Formulaology*. China Press of Traditional Chinese Medicine.

Liu, D., Cao, G., Si, X., Chen, Q., and Sun, H. (2017). Overview of antiarrhythmic studies on alkaloids in Coptis chinensis. *Shandong J. Traditional Chin.* 36 (2), 164–166. doi:10.16295/j.cnki.0257-358x.2017.02.024

Liu, Y., Fu, Y. Q., Peng, W. J., Yu, Y. R., Wu, Y. S., Yan, H., et al. (2016). Rutaecarpine Reverses the Altered Connexin Expression Pattern Induced by Oxidized Low-density Lipoprotein in Monocytes. *J. Cardiovasc Pharmacol.* 67 (6), 519–525. doi:10.1097/fjc.0000000000000372

Lu, L., and Chinese Society of Hepatology and Chinese Medical Association (2022). Guidelines for the Management of Cholestatic Liver Diseases (2021). *J. Clin. Transl. Hepatol.* 10 (4), 757–769. doi:10.14218/jcth.2022.00147

Ma, B. L., and Ma, Y. M. (2013). Pharmacokinetic properties, potential herb-drug interactions and acute toxicity of oral Rhizoma coptidis alkaloids. *Expert Opin. Drug Metab. Toxicol.* 9 (1), 51–61. doi:10.1517/17425255.2012.722995

Martínez-Clemente, M., Ferré, N., Titos, E., Horrillo, R., González-Périz, A., Morán-Salvador, E., et al. (2010). Disruption of the 12/15-lipoxygenase gene (Alox15) protects hyperlipidemic mice from nonalcoholic fatty liver disease. *Hepatology* 52 (6), 1980–1991. doi:10.1002/hep.23928

Mello, A., Hsu, M. F., Koike, S., Chu, B., Cheng, J., Yang, J., et al. (2021). Soluble Epoxide Hydrolase Hepatic Deficiency Ameliorates Alcohol-Associated Liver Disease. *Cell Mol. Gastroenterol. Hepatol.* 11 (3), 815–830. doi:10.1016/j.jcmgh.2020.10.002

Monte, M. J., Alonso-Peña, M., Briz, O., Herraez, E., Berasain, C., Argemi, J., et al. (2017). ACOX2 deficiency: An inborn error of bile acid synthesis identified in an adolescent with persistent hypertransaminasemia. *J. Hepatol.* 66 (3), 581–588. doi:10.1016/j.jhep.2016.11.005

Natarajan, S. K., Stringham, B. A., Mohr, A. M., Wehrkamp, C. J., Lu, S., Phillippi, M. A., et al. (2017). FoxO3 increases miR-34a to cause palmitate-induced cholangiocyte lipoapoptosis. *J. Lipid Res.* 58 (5), 866–875. doi:10.1194/jlr.M071357

Nong, C., Zou, M., Xue, R., Bai, L., Liu, L., Jiang, Z., et al. (2020). The role of invariant natural killer T cells in experimental xenobiotic-induced cholestatic hepatotoxicity. *Biomed. Pharmacother.* 122, 109579. doi:10.1016/j.biopha.2019.109579

Peng, H. (1993). *Prescription dictionary of Chinese medicine*. People's Medical Publishing House.

Qiu, J., Yan, J., Liu, W., Liu, X., Lin, J., Du, Z., et al. (2021). Metabolomics analysis delineates the therapeutic effects of Huangqi decoction and astragalosides on α-naphthylisothiocyanate (ANIT) -induced cholestasis in rats. *J. Ethnopharmacol.* 268, 113658. doi:10.1016/j.jep.2020.113658

Sangchart, P., Panyatip, P., Damrongrungruang, T., Priprem, A., Mahakunakorn, P., and Puthongking, P. (2021). Anti-Inflammatory Comparison of Melatonin and Its Bromobenzoylamide Derivatives in Lipopolysaccharide (LPS)-Induced RAW 264.7 Cells and Croton Oil-Induced Mice Ear Edema. *Molecules* 26 (14), 4285. doi:10.3390/molecules26144285

Senoo, H., Mezaki, Y., and Fujiwara, M. (2017). The stellate cell system (vitamin A-storing cell system). *Anat. Sci. Int.* 92 (4), 387–455. doi:10.1007/s12565-017-0395-9

Shen, T. (2007). Experimental study on the lipid-lowering effect of HuangLian and Wuzhuyu formula in experimental high-fat model mice. *J. Chengdu Univ. Traditional Chin. Med.* 30 (1), 18–19. doi:10.13593/j.cnki.51-1501/r.2007.01.009

Shen, T., Jia, B., Guo, L., and Xu, S. (2011). Effects of Huang Lian Wu Zhi Zhu on liver tissue in a rat hyperlipidemia model ABCA 1 gene expression. *J. Chengdu Univ. Traditional Chin. Med.* 34 (1), 49–51. doi:10.13593/j.cnki.51-1501/r.2011.01.018

Sugatani, J., Wada, T., Osabe, M., Yamakawa, K., Yoshinari, K., and Miwa, M. (2006). Dietary inulin alleviates hepatic steatosis and xenobiotics-induced liver injury in rats fed a high-fat and high-sucrose diet: association with the suppression of hepatic cytochrome P450 and hepatocyte nuclear factor 4alpha expression. *Drug Metab. Dispos.* 34 (10), 1677–1687. doi:10.1124/dmd.106.010645

Sun, C., Liu, W., Lu, Z., Li, Y., Liu, S., Tang, Z., et al. (2021). Hepatic miR-378 modulates serum cholesterol levels by regulating hepatic bile acid synthesis. *Theranostics* 11 (9), 4363–4380. doi:10.7150/thno.53624

Takitani, K., Kishi, K., Miyazaki, H., Koh, M., Tamaki, H., Inoue, A., et al. (2018). Altered Expression of Retinol Metabolism-Related Genes in an ANIT-Induced Cholestasis Rat Model. *Int. J. Mol. Sci.* 19 (11), 3337. doi:10.3390/ijms19113337

Trauner, M., and Fuchs, C. D. (2022). Novel therapeutic targets for cholestatic and fatty liver disease. *Gut* 71 (1), 194–209. doi:10.1136/gutjnl-2021-324305

Wang, W. (2016). A review on pharmacologic effects of effective ingredients in huanglian. *Clin. J. Chin. Med.* (8), 147–148. doi:10.3969j/issn.1674-7860.2016.26.080

Wang, W., Jiang, S., Xu, C., Tang, L., Liang, Y., Zhao, Y., et al. (2022). Transcriptome and Gut Microbiota Profiling Analysis of ANIT-Induced Cholestasis and the Effects of Da-Huang-Xiao-Shi Decoction Intervention. *Microbiol. Spectr.* 10 (6), e0324222. doi:10.1128/spectrum.03242-22

Wu, H., Chen, C., Ziani, S., Nelson, L. J., Ávila, M. A., Nevzorova, Y. A., et al. (2021). Fibrotic Events in the Progression of Cholestatic Liver Disease. *Cells* 10 (5), 1107. doi:10.3390/cells10051107

Wu, N., Meng, F., Zhou, T., Han, Y., Kennedy, L., Venter, J., et al. (2017). Prolonged darkness reduces liver fibrosis in a mouse model of primary sclerosing cholangitis by miR-200b down-regulation. *Faseb J.* 31 (10), 4305–4324. doi:10.1096/fj.201700097R

Wu, P., and Chen, Y. (2019). Evodiamine ameliorates paclitaxel-induced neuropathic pain by inhibiting inflammation and maintaining mitochondrial anti-oxidant functions. *Hum. Cell* 32 (3), 251–259. doi:10.1007/s13577-019-00238-4

Xie, W., Cao, Y., Xu, M., Wang, J., Zhou, C., Yang, X., et al. (2017). Prognostic Significance of Elevated Cholestatic Enzymes for Fibrosis and Hepatocellular Carcinoma in Hospital Discharged Chronic Viral Hepatitis Patients. *Sci. Rep.* 7 (1), 10289. doi:10.1038/s41598-017-11111-5

Xu, D., Qiu, C., Wang, Y., Qiao, T., and Cui, Y. L. (2021). Intranasal co-delivery of berberine and evodiamine by self-assembled thermosensitive *in-situ* hydrogels for improving depressive disorder. *Int. J. Pharm.* 603, 120667. doi:10.1016/j.ijpharm.2021.120667

Xu, W., and Miao, m. (2021). Application Analysis of Cholestasis Animal Models Based on Data Mining. *Pharmacol. Clin. Chin. Materia Medica*. doi:10.13412/j.cnki.zyyl.20211206.005

Yan, L., Xianzhi, L., and Hua, X. (2016). Effect of adenosine methionine combined with glucocorticoid in the treatment of drug-induced cholestasis liver disease. *Chin. J. Difficult Complicat. Cases* 15 (2), 176–182. doi:10.3969/j.issn.1671-6450.2016.02.018

Yang, Z., Meng, Y., Wang, Q., Yang, B., and Kuang, H. (2011). Property and taste pharmacological evaluation of the chemically resolved fractions of Evodia officinalis. *Inf. Traditional Chin. Med.* 28 (6), 20–23. doi:10.19656/j.cnki.1002-2406.2011.05.006

Yu, H., Li, Y., Xu, Z., Wang, D., Shi, S., Deng, H., et al. (2018). Identification of potential biomarkers in cholestasis and the therapeutic effect of melatonin by metabolomics, multivariate data and pathway analyses. *Int. J. Mol. Med.* 42 (5), 2515–2526. doi:10.3892/ijmm.2018.3859

Yu, H., Liu, C., Wang, J. F., Han, J., Zhang, F. H., Zhou, X., et al. (2022). miRNA and miRNA target genes in intervention effect of Zhuyu pill on cholestatic rat model. *J. Ethnopharmacol.* 283, 114709. doi:10.1016/j.jep.2021.114709

Yu, H., Liu, C., Zhang, F., Wang, J., Han, J., Zhou, X., et al. (2021). Efficacy of Zhuyu Pill Intervention in a Cholestasis Rat Model: Mutual Effects on Fecal Metabolism and Microbial Diversity. *Front. Pharmacol.* 12, 695035. doi:10.3389/fphar.2021.695035

Yuan, Z., Wang, G., Qu, J., Wang, X., and Li, K. (2018). 9-cis-retinoic acid elevates MRP3 expression by inhibiting sumoylation of RXRα to alleviate cholestatic liver injury. *Biochem. Biophys. Res. Commun.* 503 (1), 188–194. doi:10.1016/j.bbrc.2018.06.001

Zhang, W., Zhong, W., Sun, Q., Sun, X., and Zhou, Z. (2017). Hepatic overproduction of 13-HODE due to ALOX15 upregulation contributes to alcohol-induced liver injury in mice. *Sci. Rep.* 7 (1), 8976. doi:10.1038/s41598-017-02759-0

Zhang, Y., Chen, Y., Zhang, Z., Tao, X., Xu, S., Zhang, X., et al. (2022a). Acox2 is a regulator of lysine crotonylation that mediates hepatic metabolic homeostasis in mice. *Cell Death Dis.* 13 (3), 279. doi:10.1038/s41419-022-04725-9

Zhang, Y., Luo, J. X., Li, Y. G., Fu, H. F., Yang, F., and Hu, X. Y. (2022b). An Open-Label Exploratory Clinical Trial Evaluating the Effects of GLS (Coptidis Rhizoma-Evodiae Fructus 2:1) on Fibroblast Growth Factor 21 in Patients with Nonalcoholic Fatty Liver Disease. *Evid. Based Complement. Altern. Med.* 2022, 4583645. doi:10.1155/2022/4583645

Zhu, B., Zhao, L., Liu, Y., Jin, Y., Feng, J., Zhao, F., et al. (2019). Induction of phosphatase shatterproof 2 by evodiamine suppresses the proliferation and invasion of human cholangiocarcinoma. *Int. J. Biochem. Cell Biol.* 108, 98–110. doi:10.1016/j.biocel.2019.01.012

Zordoky, B. N., Anwar-Mohamed, A., Aboutabl, M. E., and El-Kadi, A. O. (2011). Acute doxorubicin toxicity differentially alters cytochrome P450 expression and arachidonic acid metabolism in rat kidney and liver. *Drug Metab. Dispos.* 39 (8), 1440–1450. doi:10.1124/dmd.111.039123

frontiers | Frontiers in Pharmacology

TYPE Original Research
PUBLISHED 23 November 2023
DOI 10.3389/fphar.2023.1253013

OPEN ACCESS

EDITED BY
Zhipei Sang,
Hainan University, China

REVIEWED BY
Kapil Upadhyay,
University of Michigan, United States
Zhenpeng Qiu,
Hubei University of Chinese Medicine, China
Yong Rao,
Hainan University, China

*CORRESPONDENCE
Fu Peng,
fujing126@yeah.net
Xiaofang Xie,
xiexiaofang@cdutcm.edu.cn
Cheng Peng,
cdtcmpengcheng@126.com

RECEIVED 04 July 2023
ACCEPTED 10 November 2023
PUBLISHED 23 November 2023

CITATION
Wang S, Li W, Liu W, Yu L, Peng F, Qin J, Pu L, Tang Y, Xie X and Peng C (2023), Total flavonoids extracted from *Penthorum chinense* Pursh mitigates CCl_4-induced hepatic fibrosis in rats via inactivation of TLR4-MyD88-mediated NF-κB pathways and regulation of liver metabolism.
Front. Pharmacol. 14:1253013.
doi: 10.3389/fphar.2023.1253013

Total flavonoids extracted from *Penthorum chinense* Pursh mitigates CCl_4-induced hepatic fibrosis in rats via inactivation of TLR4-MyD88-mediated NF-κB pathways and regulation of liver metabolism

Sujuan Wang[1], Wenqing Li[1], Wenxiu Liu[1], Lei Yu[1], Fu Peng[2]*, Junyuan Qin[1], Lin Pu[1], Yunli Tang[1], Xiaofang Xie[1]* and Cheng Peng[1]*

[1]State Key Laboratory of Southwestern Chinese Medicine Resources, School of Pharmacy, Chengdu University of Traditional Chinese Medicine, Chengdu, China, [2]Key Laboratory of Drug-Targeting and Drug Delivery System of the Education Ministry and Sichuan Province, Sichuan Engineering Laboratory for Plant-Sourced Drug and Sichuan Research Center for Drug Precision Industrial Technology, West China School of Pharmacy, Sichuan University, Chengdu, China

Background: *Penthorum chinense* Pursh (PCP) is widely utilized in China to treat a variety of liver diseases. It has been shown that flavonoids inhibit inflammation and have the potential to attenuate tissue damage and fibrosis. However, the mechanisms underlying how total flavonoids isolated from PCP (TFPCP) exert their anti-fibrotic effects remain unclear.

Methods: The chemical composition of TFPCP was determined using UHPLC–Q-Orbitrap HRMS. Subsequently, rats were randomly assigned to a control group (Control), a carbon tetrachloride (CCl_4)-induced hepatic fibrosis model group (Model), a positive control group [0.2 mg/(kg·day)] of Colchicine), and three TFPCP treatment groups [50, 100, and 150 mg/(kg·day)]. All substances were administered by gavage and treatments lasted for 9 weeks. Simultaneously, rats were intraperitoneally injected with 10%–20% CCl_4 for 9 weeks to induce liver fibrosis. At the end of the experiment, the liver ultrasound, liver histomorphological, biochemical indicators, and inflammatory cytokine levels were tested respectively. The underlying mechanisms were assessed using Western blot, immunohistochemistry, immunofluorescence, RT-qPCR, and metabolomics.

Abbreviations: ALB, Albumin; ALP, Alkaline phosphatase; ALT, Alanine aminotransferase; AST, Aspartate aminotransferase; BSA, Bovine Serum Albumin; CCl4, carbon tetrachloride; COL4, Collagen Type Ⅳ; CYP, Cytochrome P450; ECM, extracellular matrix; GroPCho, glycerophosphocholine; GroPEtn, Sn-Glycerol 3-phosphoethanolamin; GPs, Glycerophospholipids; HA, Hyaluronidase; H&E, hematoxylin & eosin; HPLC high-performance liquid chromatography; HSCs, hepatic stellate cells; IL-1β, interleukin 1 Beta; LN, Laminin; MyD88, myeloid differentiation factor 88; OATPs, Organic anion transporting polypeptides; PCP, Penthorum chinense Pursh; PC III, Procollagen III; TBIL, Total bilirubin; TFPCP, Total flavonoids of Penthorum chinense Pursh; TNF-α, Tumor necrosis factor-alpha; TP, Total protein.

Results: Fourteen flavonoids were identified in TFPCP. Compared with control animals, CCl_4-treated rats demonstrated obvious liver injury and fibrosis, manifested as increases in gray values, distal diameter of portal vein (DDPV) and a decrease in blood flow velocity (VPV) in the ultrasound analysis; increased biochemical index values (serum levels of ALT, AST, TBIL, and ALP); marked increases in the contents of fibrotic markers (PC III, COL4, LN, HA) and inflammatory factors (serum TNF-α, IL-6, and IL-1β); and significant pathological changes. However, compared with the Model group, the ultrasound parameters were significantly improved and the serum levels of inflammatory cytokines were reduced in the TFPCP group. In contrast, the expression of TGF-β_1, TLR4, and MyD88, as well as the p-P65/P65 and p-IκBα/IκBα ratios, were considerably reduced following TFPCP treatment. In addition, we identified 32 metabolites exhibiting differential abundance in the Model group. Interestingly, TFPCP treatment resulted in the restoration of the levels of 20 of these metabolites.

Conclusion: Our findings indicated that TFPCP can ameliorate hepatic fibrosis by improving liver function and morphology via the inactivation of the TLR4/MyD88-mediated NF-κB pathway and the regulation of liver metabolism.

KEYWORDS

Penthorum chinense **Pursh, total flavonoids, hepatic fibrosis, inflammation, liver metabolomics, TLR4/MyD88/NF-κB pathways**

1 Introduction

Hepatic fibrosis, the primary pathological characteristic of prolonged liver disease, results from the continuous repair of liver injury and persistent inflammation. During hepatic fibrogenesis, there is a gradual buildup of fibrillar extracellular matrix (ECM) and the formation of nodules in the liver parenchyma (Bottcher and Pinzani, 2017). Without intervention, extensive fibrosis eventually progresses to cirrhosis and even liver cancer, both of which can be fatal (Berumen et al., 2021). Cirrhosis is associated with high morbidity and mortality and ranks as the 11th leading cause of death globally (Asrani et al., 2019; Wang et al., 2021). Nevertheless, liver fibrosis can be reversed before it progresses to cirrhosis (Yu et al., 2019), highlighting the importance of prevention and early treatment for this condition.

Tissue damage and inflammation are two key triggers for fibrosis and regeneration in the liver. Kupffer cells and hepatic stellate cells (HSCs) are the major sources of ECM in liver fibrosis, and both are essential components in hepatic fibrogenesis and targets of pro-inflammatory mediators (Seki et al., 2007). Carbon tetrachloride (CCl_4) is extensively used to generate animal models of liver fibrosis owing to the reproducibility and efficiency of its effects. Moreover, the pathological alterations observed in these models closely resemble those seen in chronic hepatitis and hepatic fibrosis in humans (Liedtke et al., 2013). First, the metabolism of CCl_4 mediated by the cytochrome P450-dependent mixed-function oxidase system generates active trichloromethyl radicals (CCl_3•) and chlorine radicals (Cl•) (Zhang et al., 2018). This leads to lipid peroxidation and the subsequent solubilization of cell membranes, which can result in liver cell injury or death and, consequently, liver tissue damage. Inflammation results in cell death and *vice versa*, a process that has been termed "necroinflammation" (Mack, 2018). Specifically speaking, CCl_4 direct damage to hepatocytes, when hepatic cells are injured, neighboring liver cells, including Kupffer cells, produce pro-inflammatory cytokines, such as tumor necrosis factor-alpha (TNF-α) and interleukin 6 (IL-6), which can activate HSCs in a paracrine manner; activated HSCs are subsequently stimulated by both autocrine and paracrine signals pathways thereby driving the development of fibrosis (Liu et al., 2021; Wang et al., 2021). Meanwhile, inflammation in the liver acts as a further trigger for the activation of HSCs and their differentiation from quiescent cells into myofibroblasts, whereby they acquire proliferative, pro-inflammatory, and contractile properties (Sato et al., 2014). Colchicine protects from CCl_4-induced liver damage based mostly on the stimulation of repair by its mitogenic activity (Weber et al., 2003). Secondly, the liver is a primary target of intestine-derived bacterial products, and the incidence of bacterial translocation has been shown to increase in several models of liver disease, and leading to an increase in the levels of profibrogenic Toll-like receptor 4 (TLR4) agonists, such as LPS, in hepatic fibrosis (Seki et al., 2007). Both *in vitro* and *in vivo* studies have shown that TGF-β is a key modulator of HSC activation. Kupffer cells can produce large amounts of TGF-β, thereby promoting HSC activation and fibrogenesis, while TLR4 facilitates HSC activation by exposing the cells to Kupffer cell-derived TGF-β, which renders them more sensitive to this cytokine (Seki et al., 2007). These observations suggest that the suppression of liver inflammation may slow or even prevent the progression of hepatic fibrosis.

The medicinal plant *Penthorum chinense* Pursh (PCP; family: Saxifragaceae) is a well-known traditional Chinese medicine (TCM) that has been used for the treatment of liver disease since the Ming era (1400s) (Zeng et al., 2013; Wang et al., 2020). In modern times, PCP has been commercially developed ("Gansu" granules, capsules, and pills) for the treatment of chronic active hepatitis, hepatitis B, and different forms of acute viral hepatitis (Yin et al., 2020). Flavonoids are a group of substances with a C6-C3-C6 backbone structure found widely in the plant kingdom (Serafini et al., 2010). Studies have shown that these chemicals can block regulatory enzymes or transcription factors that are crucial for regulating inflammatory mediators, and also have the potential to attenuate tissue damage or fibrosis via their potent anti-oxidative properties and their ability to inhibit stellate cell activation

(Serafini et al., 2010; Wang et al., 2020). Flavonoids are among the primary bioactive components of PCP; however, it is still unknown whether total flavonoids isolated from PCP (TFPCP) play a substantial role in the anti-inflammatory and anti-fibrotic effects of PCP.

Because of the complexity of their components and their synergistic actions, it has proven extremely challenging to elucidate the mechanisms of action of TCMs (Beyoglu and Idle, 2020). Metabolomics represents a key approach for overcoming this difficulty and has shown great promise in bridging the gap between TCM and molecular pharmacology (Wang et al., 2005). Metabolomics is an emerging technique in systems biology for the identification of changes in holistic metabolic profiles in biological systems. Additionally, this technique represents a comprehensive quantitative and qualitative approach to investigating how metabolites interact with key environmental factors *in vivo* (Shu et al., 2020). Metabolomics has been utilized to describe the diverse physiological and pathological states of organisms in response to exogenous physical, chemical, and environmental stimuli (Chang et al., 2017). Over recent years, metabolomics has been widely employed in the evaluation and tracking of disease processes and has offered significant insights into the pathophysiology of a variety of conditions (Zhao et al., 2016). Importantly, several studies have reported shifts in host metabolism during the development of liver fibrosis, and have suggested that regulating the metabolism of the host may be one strategy for alleviating hepatic fibrosis (Zhang et al., 2018; Yang et al., 2021). For instance, compared with healthy controls, patients with hepatic fibrosis displayed significantly altered carbohydrate, lipid, and amino acid serum metabolism (Yoo et al., 2019). Given these observations, we postulated that TFPCP therapy may alter the metabolic profile and thus alleviate the systemic state of hepatic fibrosis. Accordingly, we performed a metabolomic analysis of liver tissue to identify which endogenous metabolites and biological processes are affected by TFPCP to regulate liver metabolism.

The objective of this study was to evaluate the therapeutic effect of TFPCP on hepatic fibrosis *in vivo* using a CCl_4-induced rat model of the disease, as well as clarify the potential underlying molecular processes employing pharmacodynamic and metabolomic approaches.

2 Materials and methods

2.1 Reagents and chemicals

CCl_4 (RH298281) was purchased from Luoen Chemical Reagent Co., Ltd. (Shanghai, China). Olive oil (J2122345) was purchased from Shanghai Aladdin Biochemical Technology Co., Ltd. (Shanghai, China). Colchicine (20200908) was bought from Yunnan Phytopharmaceutical Co., Ltd. (Yunnan, China). D101 macroporous adsorption resin (2020101901) was purchased from Chengdu Kelong Chemical Reagent Factory (Chengdu, China). The reagents for measuring aspartate aminotransferase (AST, 552616), alanine aminotransferase (ALT, 561236), alkaline phosphatase (ALP, 568781), total bilirubin (TBIL, 548537), serum albumin (ALB, 551772), and total protein (TP, 553813) levels were obtained from Roche (Basel, Switzerland). Rat procollagen III (PC III, R544UBAE9R), collagen type Ⅳ (COL4, RDTFJW7MYX), hyaluronidase (HA, 6E6UQPEADI), TNF-α (CHHNV14X86), IL-6 (2ULD7M9LKF), IL-1β (MKIMB94QHN), and transforming growth factor-beta 1 (TGF-β_1, AK03420T5560) ELISA Kits were purchased from Wuhan Elabscience Biotech Co., Ltd. (Wuhan, China). The anti-laminin antibody (LN, 031807CYF137370321) was obtained from Shanghai JONLN Reagent Co., Ltd. (Shanghai, China). Anti-TLR4 (AC220407057) and anti-P65 (AC220429001) antibodies were obtained from Wuhan Servicebio Technology Co., Ltd. (Wuhan, China). The anti-myeloid differentiation factor 88 antibody (MyD88, GR3356289-17) was obtained from Abcam, Inc. (Cambridge, United Kingdom). Anti-p-P65 (19u7497), anti-IκBα (80k0141), and anti-p-IκBα (47y8501) antibodies were purchased from Qingke Biotech Co., Ltd. (Jiangsu, China).

2.2 Preparation of the TFPCP extract and chemical component identification

PCP herbal slice was provided by Sichuan Gulin Gansu Pharmaceutical Co., Ltd. and was identified by Assoiate Professor Jihai Gao of Chengdu University of Traditional Chinese Medicine as *Penthorum chinense* Pursh of the genus *Penthorum Gronov. ex L* in the family Saxifragaceae. TFPCP were obtained as follows: Briefly, desiccated, above-ground portions of PCP were heated with distilled water under reflux for 2 h. After filtering, the residue was extracted a second time under identical conditions. The extracts were combined and condensed under reduced pressure to a concentration of 4 g/mL, applied to D101 macroporous resin, and eluted with 60% aqueous ethanol (aq. EtOH). The 60% aq. EtOH eluate was collected and concentrated *in vacuo* to yield a residue, with the final residue yield being the TFPCP. The percentage content of total flavonoids in PCP was determined by UV spectrophotometry at 510 nm, with rutin serving as the reference. The chemical components of TFPCP were identified using ultra-high performance liquid chromatography coupled with hybrid quadrupole-orbitrap high-resolution mass spectrometry (UHPLC–Q-Orbitrap HRMS). Separation was performed on an Accucore C18 column (3 mm × 100 mm, 2.6 μm; Thermo Scientific, Rockford, United States). The mobile phase was 0.1% formic acid (A) and 0.1% formic acid in acetonitrile (B). The elution gradient was 0–10 min, 6%–18% B; 10–20 min, 18%–35% B; 20–30 min, 35%–55% B; 30–40 min, 55%–85% B; 40–45 min, 85%–95% B; and 45–50 min, 95%–99% B; the flow rate was 0.3 mL/min.

2.3 Animals and treatments

Forty-eight male Sprague–Dawley rats, weighing 180–220 g, were procured from SPF (Beijing) Biotechnology Co., Ltd. (NO. SCXK 2019-0010) and maintained under controlled conditions (temperature: 20°C–25°C; relative humidity: 60% ± 5%; 12-h light/12-h dark photoperiod) and with free access to food and water. All animal experiments were approved by the Animal Ethics Committee of Chengdu University of Traditional Chinese

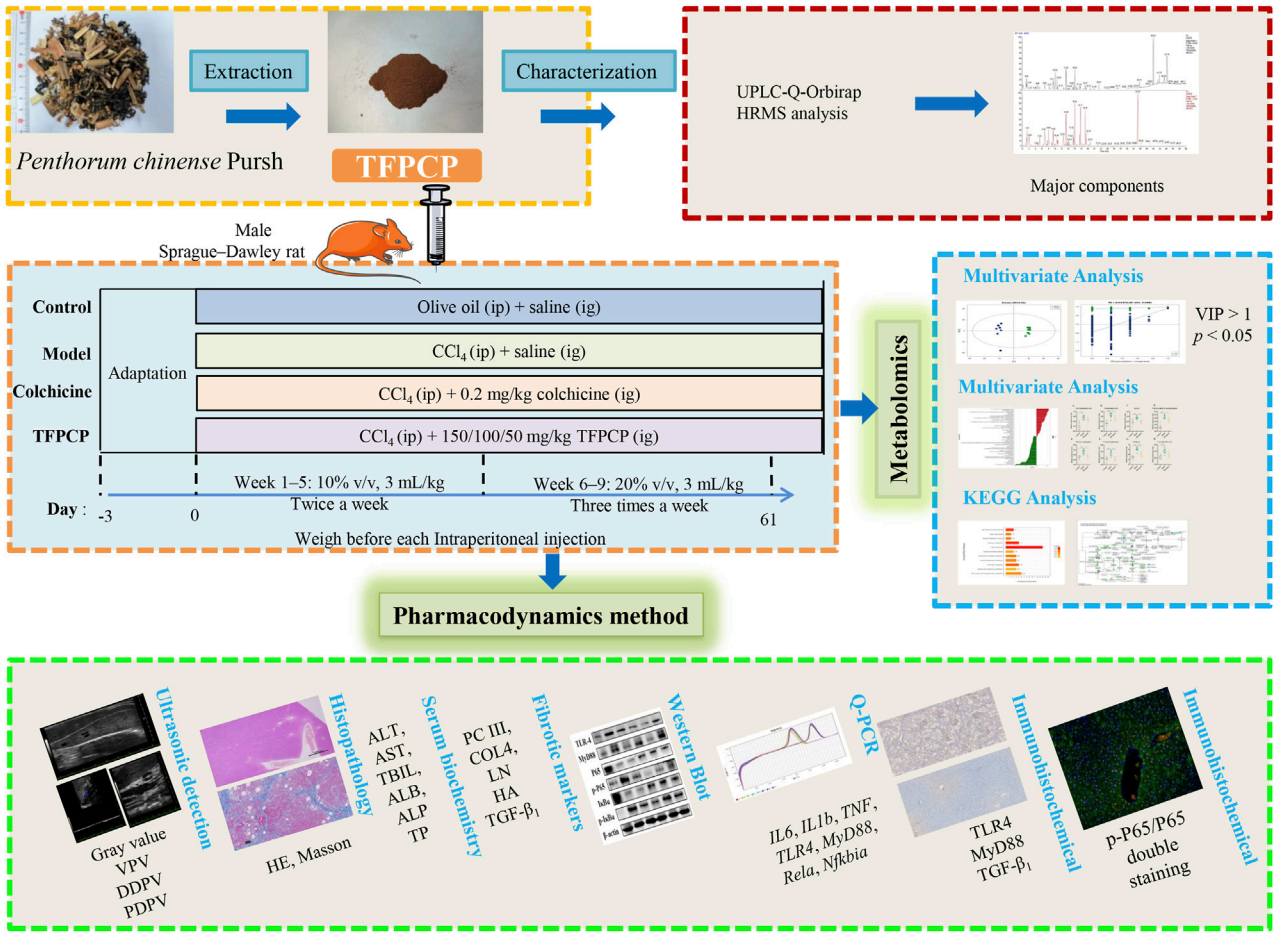

FIGURE 1
The schematic diagram of the animal and total experimental design.

Medicine (No. 2021-69). Following 3 days of acclimation, the rats were randomly divided into the following six groups (n = 8/group): A control group (Control); a CCl_4-induced hepatic fibrosis model group (Model); a CCl_4 + colchicine group (Colchicine, 0.2 mg/(kg·day) (Kershenobich et al., 1988; Zhang et al., 2016); and three CCl_4 + TFPCP groups [50, 100, and 150 mg/(kg·day), respectively]. Animals in both the Control and Model groups were administered saline intragastrically (10 mL/kg) for 9 weeks, while those in the Colchicine and CCl_4 + TFPCP groups were treated intragastrically with the same volume of saline containing the respective treatments continuously for 9 weeks. Meanwhile, olive oil was administered intraperitoneally to rats in the Control group (3 mL/kg), while rats in the other five groups received an intraperitoneal injection of olive oil containing CCl_4 (3 mL/kg) of differing concentrations (week 1 to week 5: 10% v/v, 3 mL/kg; week 6 to week 9: 20% v/v, 3 mL/kg). Olive oil or CCl_4 (to induce hepatic fibrosis) was given twice a week in the first 5 weeks and three times a week in the following 4 weeks. After 9 weeks of treatment, the rats were anesthetized with 40 mg/kg sodium pentobarbital, and serum and liver tissue were collected for further experiments. A schematic diagram of the animal and total experimental design is shown in Figure 1.

2.4 Liver ultrasound

On the last 3 days, to evaluate the status of the liver parenchyma and the lumen of the hepatic veins, rats were sedated through the inhalation of 4% isoflurane (RWD Life Science Co., Ltd., China) and subjected to ultrasonography. Liver ultrasound was conducted on a Vevo 3100 Preclinical Imaging System (FujiFilm VisualSonics, Canada) using a MX-250 probe (14–28 MHz). The gray value, the proximal diameter of portal vein (PDPV), the distal diameter of portal vein (DDPV), and the blood flow velocity (vein peak velocity [VPV]) were determined as an assessment of liver function.

2.5 Hepatic histopathological examination

After macroscopic examination, liver tissues were fixed in 4% paraformaldehyde, desiccated, embedded in paraffin wax, cut into 4-μm-thick sections, and subjected to hematoxylin and eosin (H&E) and Masson staining according to standard procedures. Images were captured using a digital slide scanner (NanoZoomer-S60, Hamamatsu, Japan). Three random fields were taken and

scoring by a blinded experimenter. The relative collagenous fiber areas were detected by Masson staining and quantified with the Image-Pro Plus 6.0 software. The fibrotic area (%) was calculated according to the following formula: DAB staining area/total image area × 100%.

2.6 Determination of serum biochemical indexes

To assess liver function, serum levels of ALT, AST, TBIL, ALB, ALP, and TP were measured using an automatic biochemical analyzer (Roche).

2.7 Measurement of serum inflammatory cytokine and fibrotic marker levels

At the end of 9 weeks, the serum levels of the inflammatory cytokines TGF-β_1, TNF-α, IL-6, and IL-1β and the fibrotic markers PC III, COL4, LN, and HA were assessed using the respective ELISA kits following the manufacturer's instructions.

2.8 Metabolomics analysis

Metabolomic analysis was carried out using the Agilent 1290 Infinity LC System (Agilent, United States) and the AB Triple TOF 6600 system (AB SCIEX, United States). Separation was performed on an ACQUITY UPLC BEH C18 column (2.1 mm × 100 mm, 1.7 μm) (Waters, Ireland). The mobile phase was 25 mM ammonium acetate and 25 mM ammonium hydroxide [v/v] in water (A) and acetonitrile (B) and the separation program was as follows: 0–1 min, 15:85, v/v; 1–11 min, gradient increase from 15:85 to 35:65, v/v; 11–11.1 min, gradient increase from 35:65 to 60:40, v/v; 11.1–15.1 min, 60:40, v/v; 15.1–15.2 min, gradient decrease from 60:40 to 15:85, v/v; 15.2–20.2 min, 15:85, v/v. The flow rate was 0.4 mL/min and *the* autosampler temperature was 5°C. Sample analysis was performed in both negative and positive ionization modes. For electrospray ionization (ESI), the source temperature was 600°C and the IonSpray Voltage Floating (ISVF) was ±5500 V.

2.9 Western blot

For protein extraction, liver tissue was homogenized in RIPA lysis buffer. Protein concentrations were determined using BCA Protein Assay Kits (Thermo Scientific, Rockford, United States). Protein samples were mixed with SDS sample buffer and heated to 100°C for 10 min. Subsequently, equal amounts of protein were separated by 8%–10% SDS–polyacrylamide gel electrophoresis, electro-blotted onto PVDF membranes, blocked with bovine serum albumin (BSA) for 2 h, and then incubated first with primary antibodies against TLR4, MyD88, P65, IκBα (1:1,000), p-P65, and p-IκBα (1:800) overnight at 4°C and, after washing, with the respective secondary antibodies (1:10,000). The immunoreactive bands were developed using chemiluminescence and the gray values were evaluated using ImageJ software.

2.10 RNA isolation and RT-qPCR analysis

Total RNA was extracted from liver tissue using Trizol reagent (Beyotime, Shanghai, China) according to the manufacturer's instructions. The extracted RNA was dissolved in RNase-free water and the RNA concentration was measured by spectrophotometry. Total RNA (1 μg) was reverse transcribed into cDNA (Thermo Scientific, Rockford, United States), following which qPCR was performed using standard TB Green Premix Ex Taq (Takara, Osaka, Japan) on a real-time PCR detection system from Rocgene (Beijing, China). β-actin served as an internal reference. The sequences of the primers used are shown in Table 1 (Designed and synthesized by Beijing Tsingke Biotech Co., Ltd.). The primers are all designed on exons.

2.11 Immunohistochemistry

Paraffin-embedded sections were dewaxed, rehydrated, subjected to antigen retrieval, and incubated with primary antibodies targeting TLR4 (1:1,000) and MyD88 (1:1,200) at 4°C overnight. After washing, the samples were incubated with secondary antibody (1:200) at ambient temperature for 1 h, washed, stained with DAB, stained with hematoxylin, dehydrated through a graded ethanol series, cleared with xylene, and mounted with neutral rubber. Images were captured using a digital slide scanner (NanoZoomer-S60). Three random fields were taken and scoring by a blinded experimenter. The TGF-β_1, TLR4 and MyD88 relative IOD in liver were analyzed using ImageJ software. The relative IOD was calculated according to the following formula: lg (255/mean gray value).

2.12 Immunofluorescence staining

Sections were deparaffinized, rehydrated, subjected to antigen retrieval, blocked in blocking buffer containing 3% BSA for 30 min, and incubated with primary antibodies against P65 (1:200) and p-P65 (1:500) overnight at 4°C. After washing, the sections were incubated with secondary antibody for 1 h at ambient temperature, counterstained with DAPI. Photographs were blindly taken at three random fields under a fluorescence microscope (Nikon Eclipse C1, Tokyo, Japan), and scoring by a blinded experimenter.

2.13 Statistical analysis

Principal component analysis (PCA) and orthogonal partial least squares discriminant analysis (OPLS-DA) were used to analyze metabolic alterations. Variable importance in projection (VIP) values > 1 and p-values <0.05 were considered significant. In addition, association and pathway analyses of the differentially abundant metabolites were conducted using online databases such as MetaboAnalyst, HMDB, and KEGG.

The data were analyzed in GraphPad Prism 8.0 and the results are presented as means ± SD. One-way ANOVA with Tukey's *post*

TABLE 1 Primer sequences used in RT-qPCR analyses.

Primer	Primer sequence	Gene ID	Amplified product size
TNF	F:CATCCGTTCTCTACCCAGCC	24835	146bp
	R:AATTCTGAGCCCGGAGTTGG		
IL6	F:TCCTACCCCAACTTCCAATGC	24498	73bp
	R:GGTCTTGGTCCTTAGCCACT		
IL1b	F:GACTTCACCATGGAACCCGT	24494	200bp
	R:CAGGGAGGGAAACACACGTT		
TLR4	F:TCCAGAGCCGTTGGTGTATC	29260	198bp
	R:AGAAGATGTGCCTCCCCAGA		
MyD88	F:CTCGCAGTTTGTTGGATGCC	301059	119bp
	R:CTCGATGCGGTCCTTCAGTT		
Rela	F:TGTATTTCACGGGACCTGGC	309165	110bp
	R:CAGGCTAGGGTCAGCGTATG		
Nfkbia	F:CTCAAGAAGGAGCGGTTGGT	25493	184bp
	R:CCAAGTGCAGGAACGAGTCT		
ACTB	F:AGATCAAGATCATTGCTCCTCCT	81822	174bp
	R:ACGCAGCTCAGTAACAGTCC		

hoc test was used for comparisons among multiple groups. A p-value <0.05 was considered significant.

3 Results

3.1 Chemical analysis of TFPCP extracts

The percentage content of total flavonoids in the residue was found to be 53.8%. TFPCP extracts were analyzed using UHPLC–Q-Orbitrap HRMS. The acquired molecular masses and formulae were matched to the information contained in online databases (PubChem, MassBank Europe, MassBank of North America [MoNA], mzCloud Best Match, and mzVault Best Match) as well as to references. Then, a manual search and match was performed to determine which compounds belonged to which structural categories based on the precise MS/MS data. Finally, 14 flavonoids with various intensities were identified in TFPCP (Table 2; Supplementary Figure S1).

3.2 TFPCP improved ultrasound parameters in the livers of rats with CCl_4-induced hepatic fibrosis

Ultrasound was employed to examine the therapeutic effects of TFPCP on CCl_4-induced hepatic fibrosis. Due to the pathology of hepatic fibrosis, there is a large amount of fibrous connective tissue hyperplasia and abnormal deposition of hepatic extracellular matrix in the confluent area and hepatic lobules leads to increased echogenicity of liver parenchyma. And the fenestrated structure of liver sinusoidal endothelial cell was damaged, which leads to the increase of hepatic sinusoids' resistance to blood flow and the alteration of portal venous flow. This pathologic change in the hepatic sinusoids reduces the pressure gradient difference that maintains the normal blood supply to the portal vein, resulting in a slowing of portal venous blood flow velocity (vein peak velocity [VPV]) (Afdhal and Nunes, 2004). Meanwhile, in order to maintain the blood flow of the portal vein, the body causes the hepatic portal vein obstructive congestion to persist. Due to the greater compliance of the hepatic portal vein, it can adapt to large blood flow changes while the hepatic portal vein pressure changes little, which can lead to the widening of the internal diameter of the portal vein, such as PDPV and DDPV (Albrecht et al., 1999; Afdhal and Nunes, 2004). As depicted in Figure 2, compared with the Control group, the gray scale values and the DPVD were markedly increased in the Model group, whereas the VPV values were significantly decreased ($p < 0.01$). After the administration of TFPCP or colchicine, the gray values and DPVD were significantly decreased, while the VPV values were significantly increased; no differences in PPVD values were observed among the groups. These results indicated that both TFPCP and colchicine improved CCl_4-induced liver fibrosis to some extent.

3.3 TFPCP ameliorated liver function and alleviated liver injury

Following 9 weeks of TFPCP administration, although the differences among the groups were not significant (Figure 3A), the body weight of rats in the Control, Colchicine, and CCl_4 + TFPCP groups increased with time. Meanwhile, compared with the

TABLE 2 Identification analysis of chemical component of TFPCP in ion mode of mass spectrometry.

No.	Identified compounds	Retention time (min)	Ionization Mode	Molecular formula	Detected (m/z)	Theoretical mass (m/z)	Error (ppm)	MS^2 data (m/z)	References/ Database ID
1	Quercetin-3β-D-glucoside	8.382	M-H	C21 H20 O12	463.08929	463.0882	−2.35376	301.03458,178.99768, 151.00310, 107.01246	Yang et al. (2021)
2	(+/−)-Taxifolin	8.638	M-H	C15 H12 O7	303.05157	303.05103	−1.78188	125.02362, 285.04053, 177.01894	MSBNK-RIKEN-PR309311[a]
3	Quercetin-3-O-pentoside	9.224	M-H	C20 H18 O11	433.07822	433.07763	−1.36234	433.07843	Amroun et al. (2021)
4	Quercetin	9.433	M-H	C15 H10 O7	301.03558	301.03538	−0.66437	178.99815, 151.00307, 107.01302	Yang et al. (2021)
5	Luteoloside	9.437	M-H	C21 H20 O11	447.09354	447.09329	−0.55917	151.00313, 107.01304	Yang et al. (2021)
6	Prunin	9.768	M-H	C21 H22 O10	433.11481	433.11402	−1.824	271.06146, 151.00299	Luo et al. (2021)
7	Kaempferol-3-O-arabinoside	10.26	M-H	C20 H18 O10	417.08353	417.08272	−1.94206	284.03284	Rescic et al. (2016)
8	Apigenin 7-O-glucoside	10.549	M-H	C21 H20 O10	431.09866	431.09837	−0.6727	151.00255, 107.01316	Yang et al. (2021)
9	Phloridzin	10.575	M-H	C21 H24 O10	435.13019	435.12967	−1.19505	273.07700, 123.04428, 119.04953	Chen et al. (2023)
10	Trilobatin	11.374	M-H	C21 H24 O10	435.13049	435.12967	−1.8845	273.07712	Xiao et al. (2017)
11	Pinocembrin	12.526	M + H	C15 H12 O4	257.08136	257.08084	−2.02271	153.01865	Simirgiotis et al. (2015)
12	Naringenin	14.192	M-H	C15 H12 O5	271.06171	271.0612	−1.88149	177.01903, 151.00305, 119.04947, 107.01301	Xiao et al. (2022)
13	Luteolin	14.56	M-H	C15 H10 O6	285.04086	285.04046	−1.40331	151.00316, 107.01313	Yang et al. (2021)
14	Cardamomin	24.522	M + H	C16 H14 O4	271.09723	271.09649	−2.72966	167.03436, 124.01624, 152.01097, 170.02182, 103.05477	CCMSLIB00000848351[b]

[a]MassBank Europe.

[b]MassBank of North America (MoNA).

10.3389/fphar.2023.1253013

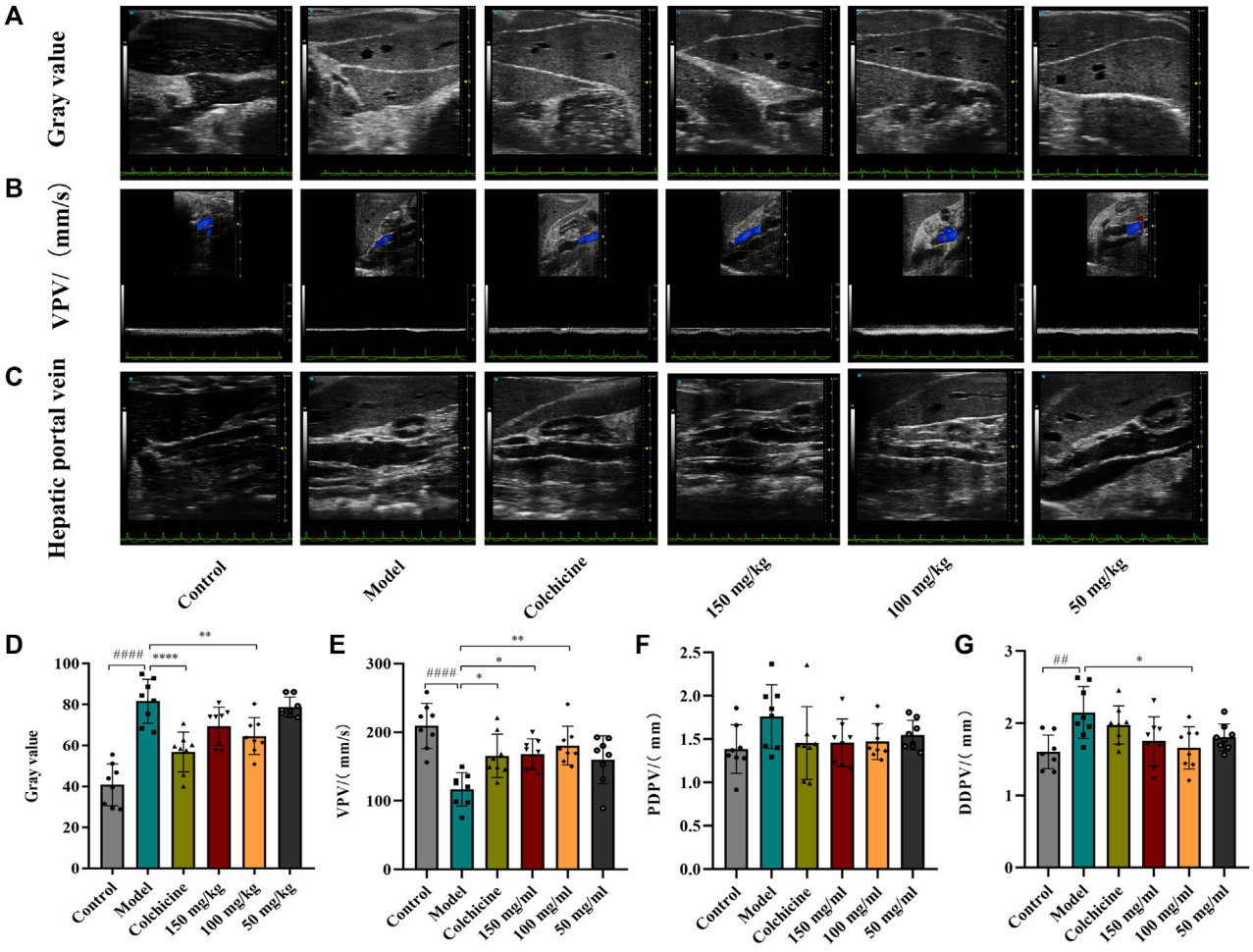

FIGURE 2
TFPCP improves ultrasonic Parameters of CCl_4-induced hepatic fibrosis in rats. The ultrasonic detection of **(A, D)** Gray value, **(B, E)** blood flow velocity (VPV), **(C, F, G)** proximal diameter of portal vein (PDPV) and distal diameter of portal vein (DDPV). Values are presented as the means ± SD (n = 6). $^{\#\#}p < 0.01$ and $^{\#\#\#\#}p < 0.0001$ vs. control group; $^{*}p < 0.05$, $^{**}p < 0.01$ and $^{****}p < 0.0001$ vs. model group.

Control group, the biochemical index values (Figure 3B) were markedly increased in the liver tissues of rats in the hepatic fibrosis Model group; however, these changes were greatly attenuated with TFPCP treatment. Regarding anatomy, the liver tissue presented evident granules on the surface, was light in color and coarse in texture, and exhibited large-scale, small-particle formation and tissue swelling in the model groups (Figure 3C). H&E staining results showed that the livers of rats in the control group possessed a normal lobular architecture, complete with distinct central veins and radiating hepatic cords. In contrast, the liver tissue of animals in the Model group displayed disordered hepatic lobules, irregular hepatocyte arrangement, extensive hepatocyte swelling, necrosis, cytoplasmic vacuolization, thin fibrous septa that surrounded the hepatocytes to form pseudobullets of different shapes, and massive hepatocyte steatosis, round vacuoles of different sizes in the cytoplasm. However, TFPCP alleviated liver damage and improved the pathology of the liver to varying degrees (Figure 3D).

The contents of ALT, AST, TBIL, ALP, ALB, and TP in serum are frequently utilized as indicators of liver function. As shown in Figures 3E–J, the levels of ALT, AST, TBIL, and ALP in rats were greatly elevated in the presence of CCl_4; however, the levels of these biochemical indices decreased considerably with TFPCP administration; no differences in TP and ALB concentrations were detected among the groups. Combined, these results demonstrated that although TFPCP treatment did not entirely prevent the development of liver injury, liver tissue morphology and transaminase levels were restored to varying degrees, indicating that TFPCP can alleviate liver damage.

3.4 TFPCP improved collagen deposition in the livers of rats with CCl_4-induced hepatic fibrosis

The results of the Masson staining revealed that collagen deposition was minimal in the Control group; in comparison, in the hepatic fibrosis Model group, there was a greater number of collagen fibers, dense collagen staining, and fibrotic scarring surrounding the central vein. Nevertheless, TFPCP treatment

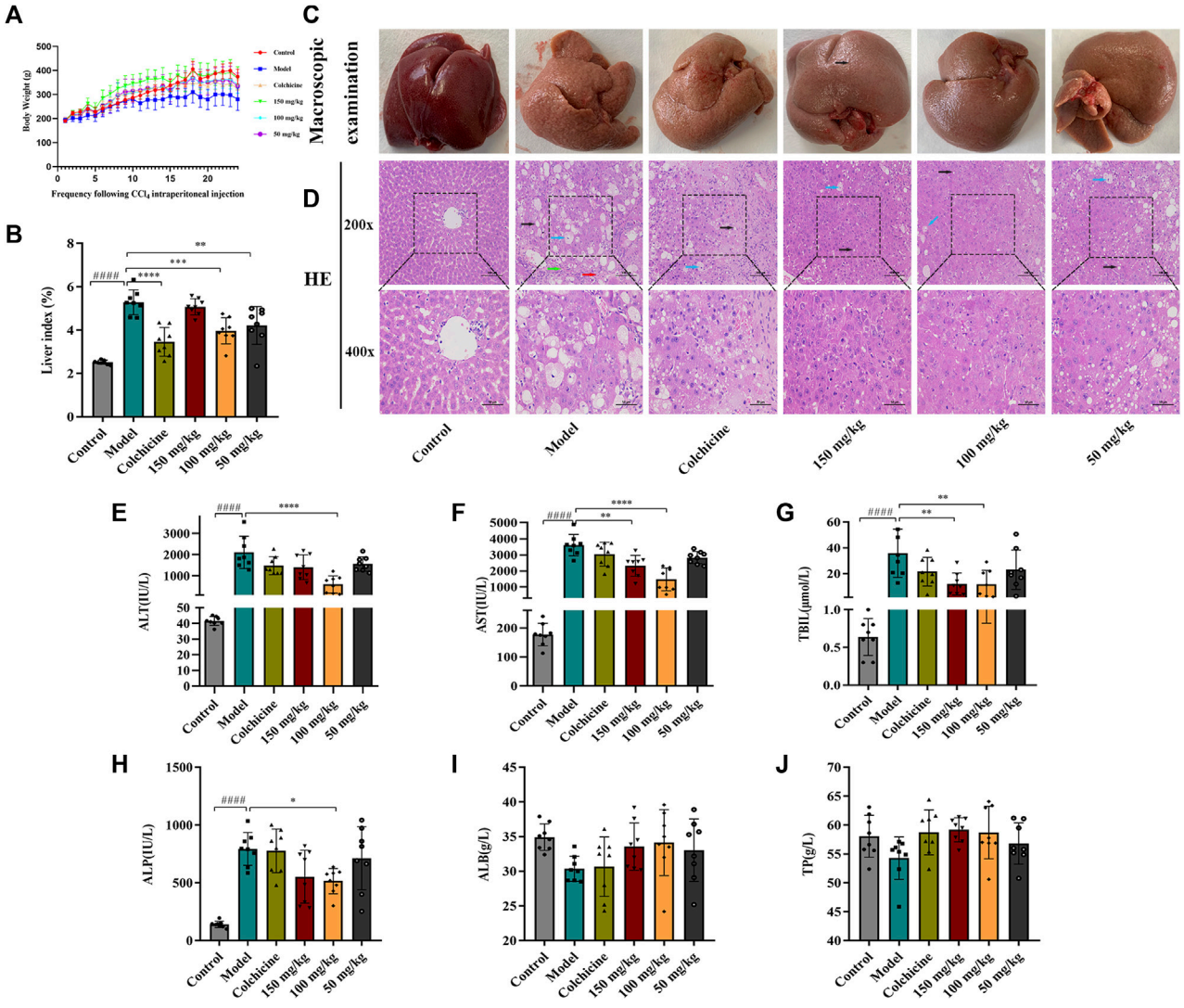

FIGURE 3
TFPCP can ameliorate liver function and alleviate liver injury. **(A)** Body weight (n = 8). **(B)** Liver index (n = 8). **(C)** Macroscopic examination of liver. **(D)** H&E staining (200×) and (400×) (n = 8). Black arrows indicate hepatocytes are steatosis, and circular vacuoles in cytoplasm. Blue arrows indicate hepatocyte swelling, necrosis, nuclear contraction, cytoplasmic vacuolation. Red arrows indicated infiltration of inflammatory cells. Green arrows indicate the thin fibrous septa that surrounded the hepatocytes to form pseudobullets of different shapes. **(E–J)** The ALT, AST, TBIL, ALP, ALB and TP levels in serum (n = 8). Values are presented as the means ± SD. $^{\#\#\#\#}p < 0.0001$ vs. control group; $^{*}p < 0.05$, $^{**}p < 0.01$ and $^{****}p < 0.0001$ vs. model group.

greatly attenuated collagen deposition and hepatic fibrosis induced by CCl_4; moreover, the effect of TFPCP was better than that of colchicine (Figures 4A, B). TGF-β is a key mediator of HSC activation both *in vitro* and *in vivo* (Seki et al., 2007), while the activation of quiescent HSCs into myofibroblast-like cells is a crucial stage in hepatic fibrogenesis. Consequently, to further determine whether the inhibitory impact of TFPCP on collagen deposition was connected to HSC activation, we compared the expression of TGF-β_1 among the groups. Immunohistochemical staining and serum ELISAs (Figures 4C–E) revealed that the level of TGF-β_1 was significantly higher in rats of the Model group than in those of the Control group. However, compared with that seen in the model condition, TFPCP administration reduced the TGF-β_1 staining intensity and serum TGF-β_1 levels. Meanwhile, serum PC III, COL4, LN, and HA concentrations are important markers in hepatic fibrosis diagnosis. As shown in Figures 4F–I, CCl_4 treatment substantially enhanced the serum concentrations of PC III, COL4, LN, and HA; however, the opposite effect was observed with TFPCP administration. These findings indicated that TFPCP can reduce collagen formation as well as prevent HSC activation.

3.5 The TLR4/MyD88/NF-κB signaling pathway was involved in the CCl_4-induced inflammatory response in hepatic fibrosis

Myofibroblast activation and fibrogenesis in the liver are both driven by TLR4. Furthermore, it has been demonstrated that the TLR4-dependent regulation of TGF-β signaling acts as a link between pro-inflammatory and profibrogenic signals (Seki et al., 2007).

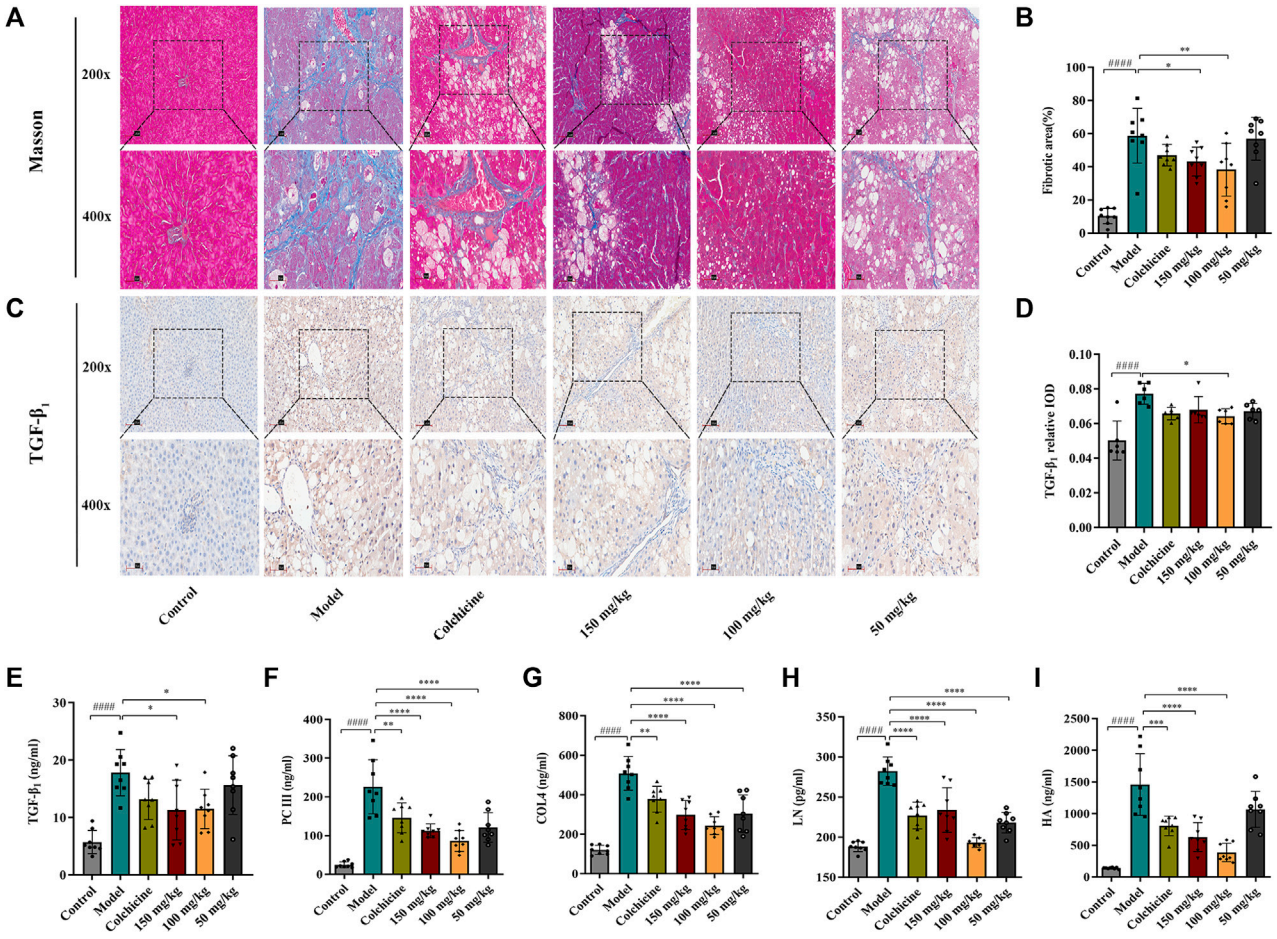

FIGURE 4
TFPCP improves the deposition of collagen. **(A, B)** Hepatic fibrosis assessed by masson staining (200×) and (400×) (n = 8). **(C, D)** TGF-β_1 assessed by immunohistochemical (200×) and (400×) (n = 6). **(E)** Analysis of the serum TGF-β_1 level (n = 8). **(F–I)** PC III, COL4, LN and HA fibrotic markers detection in serum (n = 8). Values were presented as the means ± SD. $^{\#\#\#\#}p < 0.0001$ vs. control group; $^{*}p < 0.05$, $^{**}p < 0.01$, $^{***}p < 0.001$ and $^{****}p < 0.0001$ vs. model group.

Consequently, we further investigated whether the anti-fibrotic effects of TFPCP involved the regulation of inflammation. Western blot analysis showed that the expression of TLR4 and MyD88 was markedly downregulated following TFPCP treatment, while the p-P65/P65 and p-IκBα/IκBα ratios were notably decreased relative to the Model group (Figures 5A–E). Simultaneously, immunohistochemical and qPCR assays further demonstrated that TFPCP inhibited the expression of TLR4 and MyD88 (Figures 6A–D; Figures 7A, B). The mRNA levels of *Rela* and *Nfkbia* were also markedly increased in the Model group (Figures 7C, D) compared with those in the Control group, whereas the opposite was seen with TFPCP treatment. In addition, we performed double immunofluorescence staining for P65 and p-P65 (Figure 6E) and found that the p-P65/P65 ratio (Figure 6F) was significantly decreased in the TFPCP treatment group relative to that in the Model group. Meanwhile, to explore the role of TFPCP in regulating fibrogenic responses in the liver, pro-inflammatory cytokine levels were evaluated by ELISA and RT-qPCR. As shown in Figures 6G–I; Figures 7E–G, CCl_4 treatment led to a noticeable increase in TNF-α, IL-6, and IL-1β contents in both serum and liver tissue compared with saline-only treatment (Control group). In contrast, the TNF-α, IL-6, and IL-1β level in serum were significantly lower in the TFPCP group than in the Model group. While, in addition to *TNF* mRNA, the expression of *IL6* and *IL1b* mRNA level was also lower in the TFPCP treatment groups than in the Model group, but the difference was not significant (Figures 7F, G). Taken together, these results suggested that TFPCP can limit the inflammatory response induced by CCl_4, thereby alleviating TLR4/MyD88/NF-κB signaling pathway-mediated hepatic fibrogenesis.

3.6 TFPCP regulated hepatic fibrosis-related metabolites

The PCA and OPLS-DA score diagrams for the positive and negative ion types are shown in Supplementary Figure S2. Significant clustering could be detected among the different groups. Metabolites meeting the VIP >1 and $p < 0.05$ criteria were considered to be differentially abundant. A total of 32 distinct metabolites were identified when the metabolomic analysis was performed in both positive and negative ion modes (Table 3). Nevertheless, after TFPCP administration, the levels of

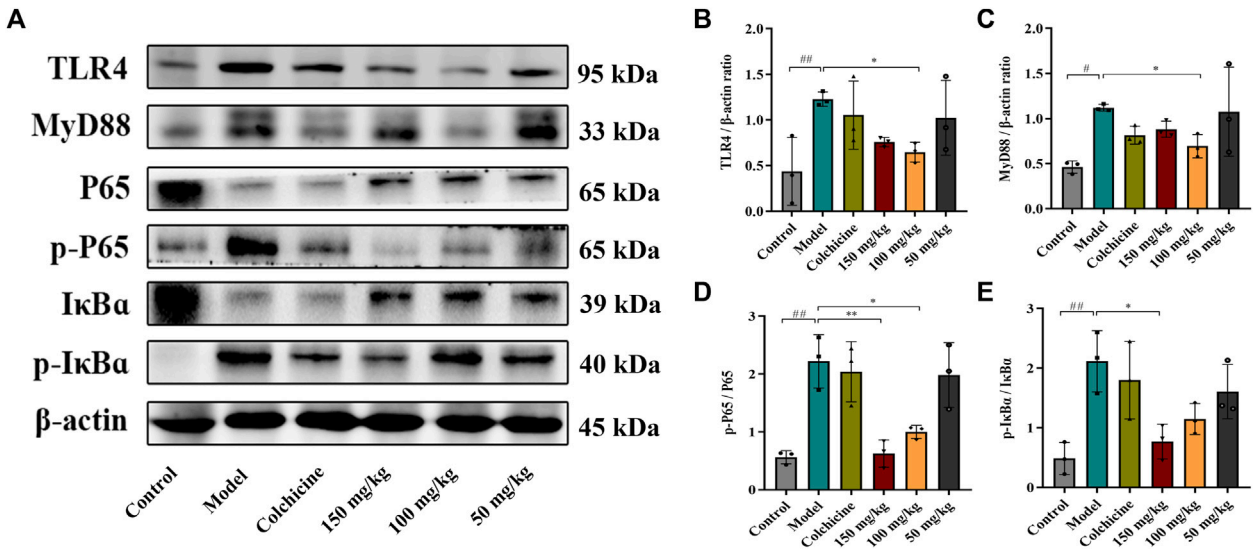

FIGURE 5
Western blotting photographs illustrating protein levels of TLR4/MyD88/NF-κB signaling pathway. **(A–E)** The expressions and quantitative analysis of TLR4, MyD88, p-P65/P65 and p-IκBα/IκBα proteins (n = 3). Values were presented as the means ± SD. $^{\#}p < 0.05$, $^{\#\#}p < 0.01$ vs. control group; $^{*}p < 0.05$, $^{**}p < 0.01$ vs. model group.

20 of the 32 distinct metabolites were significant restored (Figures 8A–F; Figure 9A). Meanwhile, the pathways that overlapped between the Control group and the Model group, and between the Model group and the TFPCP group, were regarded as relevant pathways. The differentially abundant metabolites were primarily involved in lipid, energy, nucleoside, and amino acid metabolism (Figure 9B), and could be categorized into the following six major metabolic pathways (Figure 9C): Thiamine metabolism, Ether lipid metabolism, Pantothenate and CoA biosynthesis, Amino sugar and nucleotide sugar metabolism, Glycerophospholipid metabolism, and Pyrimidine metabolism.

4 Discussion

Fibrosis, characterized by the net buildup of ECM and scarring, has been recognized for decades in patients with chronic liver illnesses. Throughout the majority of medical history, fibrosis was thought to be intractable (Lee et al., 2015). Despite extensive research into hepatic fibrosis (Kisseleva and Brenner, 2021), no anti-fibrotic medicines has yet been authorized for this condition. Natural products have gained substantial interest as novel anti-fibrotic medications given their rich diversity of chemical structure, biological activity, and drug-like characteristics. PCP has long been widely employed as an effective treatment for a variety of liver conditions in China. More recently, PCP has been shown to possess hepatoprotective properties in both *in vivo* and *in vitro* settings, effects that may be mediated by TFPCP. In this study, using pharmacodynamic analysis, we demonstrated that this herbal extract exerted preventive and alleviatory effects on hepatic fibrogenesis induced by CCl_4. Mechanistically, we found that TFPCP could mitigate inflammation, thus alleviating TLR4/MyD88/NF-κB signaling pathway-mediated hepatic fibrogenesis. The metabolomic analysis resulted in the identification of 32 distinct metabolites corresponding to 22 metabolic pathways. The levels of 20 of these metabolites were greatly restored with TFPCP treatment. These 32 metabolites were mainly involved in lipid, energy, nucleoside, and amino acid metabolism, and were likely to be associated with the occurrence of hepatic fibrosis.

The UHPLC–Q-Orbitrap HRMS analysis of TFPCP revealed the presence of 14 flavonoids, including quercetin, taxifolin, pinocembrin, and luteoloside, among others. Many of these flavonoids exhibit a wide range of pharmacological properties, such as antioxidant, anti-inflammatory, and antimicrobial effects (Chirumbolo and Bjorklund, 2018; Shang et al., 2021). In this study, we provided further evidence that TFPCP can ameliorate liver injury and fibrosis. In the clinic, ultrasound is widely used for diagnosing the staging of liver fibrosis and assessing therapeutical effects. Here, ultrasound analysis showed that CCl_4 treatment led to marked increases in gray values and the DDPV and a decrease in VPV values. Additionally, the liver tissue of animals in the Model group exhibited an irregular arrangement of hepatocytes, thin fibrous septa, and round vacuoles of varying sizes in the cytoplasm, as evidenced by the H&E staining results. The increases in the levels of ALT, AST, TBIL, ALB, ALP, and TP in serum provided more evidence that CCl_4 can cause liver impairment and dysfunction. However, the oral administration of TFPCP resulted in a substantial improvement in ultrasound parameters and pathological changes, as well as the downregulation of serum levels of biochemical indexes, indicating that TFPCP can ameliorate CCl_4-induced liver damage. During hepatic fibrogenesis, activated HSCs are the primary producers of excess ECM, including collagen (Li et al., 2018). Meanwhile, TGF-β_1 is regarded as the most potent profibrogenic cytokine and is also a key mediator of HSC activation *in vitro* and *in vivo* (Seki et al., 2007). Its effects include the stimulation of myofibroblasts, the induction of the synthesis of ECM components, and the suppression of collagen degradation. In this

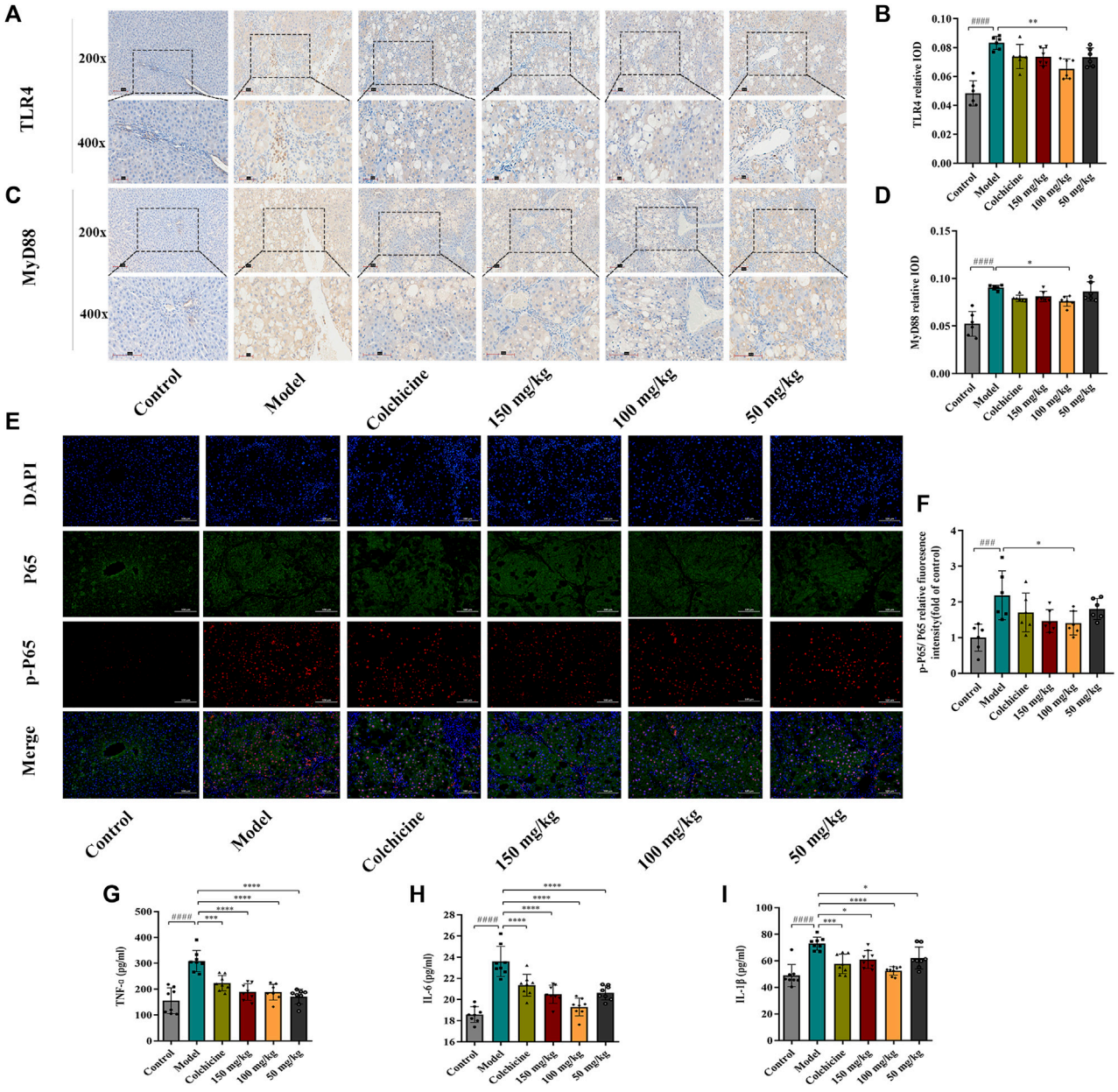

FIGURE 6
The expression of TLR4, MyD88, p-P65/P65 in liver tissue and the level of inflammatory cytokines in serum. **(A–D)** The expressions of TLR4 and MyD88 by immunohistochemical analysis (n = 6). **(E–F)** The expressions of p-P65/P65 by immunofluorescence staining analysis (n = 6). **(G–I)** The content of TNF-α, IL-6 and IL-1β in serum (n = 8). Values were presented as the means ± SD. $^{###}p < 0.001$, $^{####}p < 0.0001$ vs. control group; $^{*}p < 0.05$, $^{**}p < 0.01$, $^{***}p < 0.001$ and $^{****}p < 0.0001$ vs. model group.

study, we found that TFPCP reduced collagen deposition and HSC activation compared with the Model group, as evidenced by the results of Masson staining, tissue TGF-β_1 immunohistochemical analysis, and assessment of serum TGF-β_1 contents (Figure 4). Combined with the decrease in the levels of PC III, COL4, LN, and HA in serum, these findings support that TFPCP treatment can alleviate CCl_4-induced liver fibrosis.

In this study, the therapeutic effect of TFPCP on liver fibrosis did not show a dose-dependent relationship. The effect of the 150 mg/kg was not better than that of the 100 mg/kg. This phenomenon is quite common in TCM pharmacology due to the multiple ingredients and multiple targets as stated in the textbook (Peng, 2016). The drug TFPCP is a cluster of flavonoids from PCP, which includes more than 14 different compounds as detected by the UHPLC–Q-Orbitrap HRMS analysis in the study. Therefore, the absence of dose dependence here may be also caused by multiple components of TFPCP with different activities. In particular, we suspect it is because of the ingredients that can modulated the activity of drug metabolizing enzymes or transporters. P-glycoprotein is one of the main efflux transporters proteins in human body, which excretes exogenous substances such as poisons and drugs out of the cells and functions as a barrier for the body (Conseil et al., 1998).

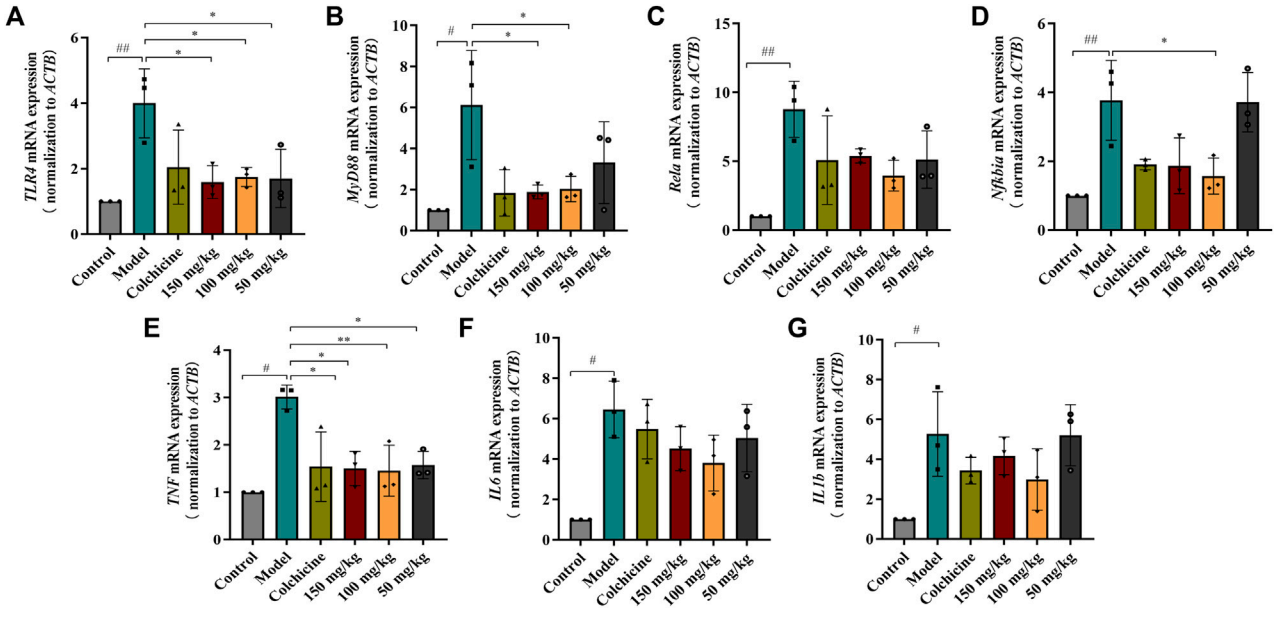

FIGURE 7
RT-qPCR analysis the mRNA expression of TLR4/MyD88/NF-κB signaling pathway. **(A–D)** The expressions of *TLR4*, *MyD88*, *Rela* and *Nfkbia* mRNA ($n = 3$). **(E–G)** The expressions of *TNF*, *IL6* and *IL1b* mRNA in tissue ($n = 3$). Values are presented as the means ± SD. $^{\#}p < 0.05$, $^{\#\#}p < 0.01$ vs. control group; $^{*}p < 0.05$, $^{**}p < 0.01$ vs. model group.

Cytochrome P450 (CYP) enzymes are involved in the oxidative biotransformation of most drug (Meunier et al., 2004). CYP3A4 takes part in the biotransformation of more than 50% of the orally administered medications, and some other CYP isoforms (Kaci et al., 2023). Organic anion transporting polypeptides (OATPs) are solute carrier-type membrane transporters, which are commonly involved in the tissue uptake of nutrients, drugs, and toxins (Mandery et al., 2012). The induce of CYP-catalyzed elimination and/or inhibition of OATP-mediated transport of drugs commonly lead to the development of pharmacokinetic interactions. For instance, It is found flavones (such as quercetin) were indeed shown to bind to purified P-glycoprotein and to efficiently inhibit its activity more strongly than flavanones (naringenin) (Conseil et al., 1998), and following it may reduce the excretion of other chemical components (naringenin). However, study reveals that the high intake of luteolin and naringenin can lead to the *in vivo* inhibition of hepatic and intestinal OATP2B1 and/or OATP1B1transporters mediated absorption of certain drugs (Kaci et al., 2023). In addition, quercetin can increase the expression of CYP3A4 in human hepatocytes, resulting in an induction effect (Raucy, 2003), thereby reducing drug bioavailability by increasing drug efflux and drug metabolism in the intestine and liver. Therefore, we speculate that in the high dose (150 mg/kg), there are more flavones in the drug induces strong influence on expression of CYP3A4 in liver, as well as binding to P-glycoprotein and OATP-mediated transport, which would finally reducing drug bioavailability for the active ingredients that protecting liver.

Tissue damage caused by toxins such as CCl_4 usually results in cell death. Necrotic cells and damaged tissues release inflammatory stimuli, many of which are categorized as danger-associated molecular patterns. The binding of these factors to their corresponding "pattern recognition receptors", such as TLRs, results in the release of pro-inflammatory factors such as TNF-α, IL-6, and IL-1β. This can lead to the activation of NF-κB, resulting in the continuous amplification of the initial inflammatory signals and the so-called inflammatory cascade effect. Meanwhile, the LPS/TLR4 signaling pathway is primarily responsible for mediating the inflammatory response and pro-fibrogenic activity in numerous liver diseases, and studies have established that this route contributes to liver damage and fibrosis (Nobili et al., 2015; Mack, 2018; Unsal et al., 2021). Consequently, we next focused on investigating one of the most common signal transduction pathways of the TLR4/NF-κB signaling system, that is, the MyD88-dependent pathway. We found that the expression of TLR4 and MyD88 and the p-P65/P65 and p-IκBα/IκBα ratios were noticeably downregulated in liver tissue after TFPCP intervention. Meanwhile, TGF-β can synergize with IL-6, TNF-α, or IL-1β to accelerate the development of hepatic fibrosis (Kisseleva and Brenner, 2021). In our study, the serum and tissue contents of TNF-α, IL-6, and IL-1β were lower in the TFPCP group than in the Model group as determined by ELISA and RT-qPCR (Figures 6G–I; Figures 7E–G). These results are compatible with the finding that treatment with TFPCP reduced the levels of the pro-inflammatory mediator TGF-β_1. Here, we provided evidence that TFPCP can mitigate the inflammatory response by regulating the TLR4/MyD88-mediated NF-κB signaling pathway, thereby ultimately inhibiting hepatic fibrogenesis (the putative signaling pathway is depicted in Figure 10).

Hepatic fibrosis is a metabolic disorder characterized by the presence of a multitude of aberrantly expressed endogenous metabolites. Thus, in this study, we used UHPLC-Triple TOF-MS/MS-based metabolomics to investigate the hepatic fibrosis-related liver tissue metabolite profile. The liver is an essential organ for lipid metabolism, and lipid metabolism is frequently impaired in

TABLE 3 Results of the discovery of putative biomarkers in rat tissue.

No.	Retention time (min)	m/z	Metabolite	Ionization Mode	*p*-value	VIP	HMDB ID	Trend Model/ Control	Trend Model/ Md
1	47.616	253.2135	Cis-9-palmitoleic acid	[M-H]-	2.17E-05	10.5792	HMDB0003229	↑	↓
2	414.004	160.0583	2-aminoadipic acid	[M-H]-	8.01E-05	1.08361	HMDB0000510	↑	↓
3	122.5085	227.0636	Ile-Pro	[M-H]-	0.000517	1.236435	HMDB0000012	↑	↓
4	92.049	307.0197	2′-deoxyuridine 5′-monophosphate	[M-H]-	0.00053	2.185498	HMDB0001409	↑	↓
5	406.521	241.0075	Glucose 1-phosphate	[M-H-H2O]-	0.000746	1.218041	HMDB0001586	↑	↓
6	396.295	188.0527	N-acetyl-l-glutamate	[M-H]-	0.000926	1.146512	HMDB0001138	↑	↓
7	305.832	128.0372	L-pyroglutamic acid	[M-H]-	0.002144	2.785282	HMDB0000267	↑	↓
8	57.0015	316.1298	Levofloxacin	[M-H-CO2]-	0.004883	1.142444	HMDB0001929	↑	↓
9	469.136	239.0124	L-Cystine	(M-H)-	0.01528	1.030341	HMDB0000192	↑	↓
10	397.191	76.07501	Trimethylamine n-oxide	[M + H]+	0.00022	1.344752	HMDB0000925	↑	↓
11	409.603	132.0769	Creatine	[M + H]+	0.003934	4.945975	HMDB0000064	↑	↓
12	409.411	90.05446	Alanine	[M + H]+	0.004155	1.061756	HMDB0000161	↑	↓
13	282.197	437.2081	Pantothenic acid	[2M-H]-	1.19E-06	3.079242	HMDB0000210	↓	↑
14	88.908	357.0956	Cyclohexanesulfamic acid	[2M-H]-	0.000132	1.52676	HMDB0031340	↓	↑
15	337.734	211.0781	Perseitol	[M-H]-	0.000134	2.244984	HMDB0033750	↓	↑
16	218.851	267.0694	Inosine	[M-H]-	0.000255	5.442514	HMDB0000195	↓	↑
17	301.6545	181.0671	D-mannitol	[M-H]-	0.000443	1.319364	HMDB0000765	↓	↑
18	307.886	359.1142	D-(+)-mannose	[2M-H]-	0.000554	2.015165	HMDB0062473	↓	↑
19	90.059	343.0805	Thiamine monophosphate	[M-H]-	0.001985	2.602537	HMDB0002666	↓	↑
20	394.124	214.0522	sn-Glycerol 3-phosphoethanolamine	[M-H]-	0.002616	4.907646	HMDB0000114	↓	↑
21	74.548	277.119	Pantetheine	(M-H)-	0.004156	1.455189	HMDB0003426	↓	↑
22	397.737	117.0217	Methylmalonic acid	[M-H]-	0.009969	1.349379	HMDB0000202	↓	↑
23	325.296	204.0852	N-Acetylmannosamine	(M + H-H2O)+	3.57E-05	1.068466	HMDB0001129	↓	↑
24	406.4905	265.1104	Thiamine	[M]+	0.000943	2.58757	HMDB0000235	↓	↑
25	341.853	144.1004	Stachydrine	[M + H]+	0.001233	1.418089	HMDB0004827	↓	↑
26	447.009	258.1107	Glycerophosphocholine	[M + H]+	0.007729	6.920794	HMDB0000086	↓	↑
27	390.619	230.0945	Ergothioneine	[M + H]+	0.044483	1.138287	HMDB0003045	↓	↑

↑: upregulated. ↓: downregulated.
↑: compared to the control group, the compound's level was elevated in the model group.
↓: compared to the model group, the compound's level was reduced in intervention group.

conditions that affect the liver (Weber et al., 2003). Specifically, CCl_4 is transformed into CCl_3• by the cytochrome P450-dependent mixed-function oxidase system. This radical can react with oxygen to produce the trichloromethylperoxy radical (CCl_3OO•), which then initiates a lipid peroxidation cascade, resulting in the destruction of polyunsaturated fatty acids, particularly those associated with phospholipids (Weber et al., 2003; Usami et al., 2013). Meanwhile, organic acids are known to exert a strong effect on lipid metabolism (Usami et al., 2013), and fatty acid production has been linked to energy metabolism, anti-inflammatory qualities, and antioxidant capabilities (Tang et al., 2022). Thus, metabolic disorders involving lipids and lipid-like molecules are extremely influential in the development of liver fibrosis.

Glycerophospholipids (GPs), as storage deposits for lipid mediators, function as integral membrane proteins, transporters, receptors and ion channels (Lieber et al., 1994). Therefore, dysfunction of the glycerophospholipid metabolism could negatively affect the energy metabolism in the liver (Mesens et al., 2012). Published data also reported CCl_4-treated rats can be subjected to perturbations of lipid metabolism to induce liver fibrosis (Chang et al.,

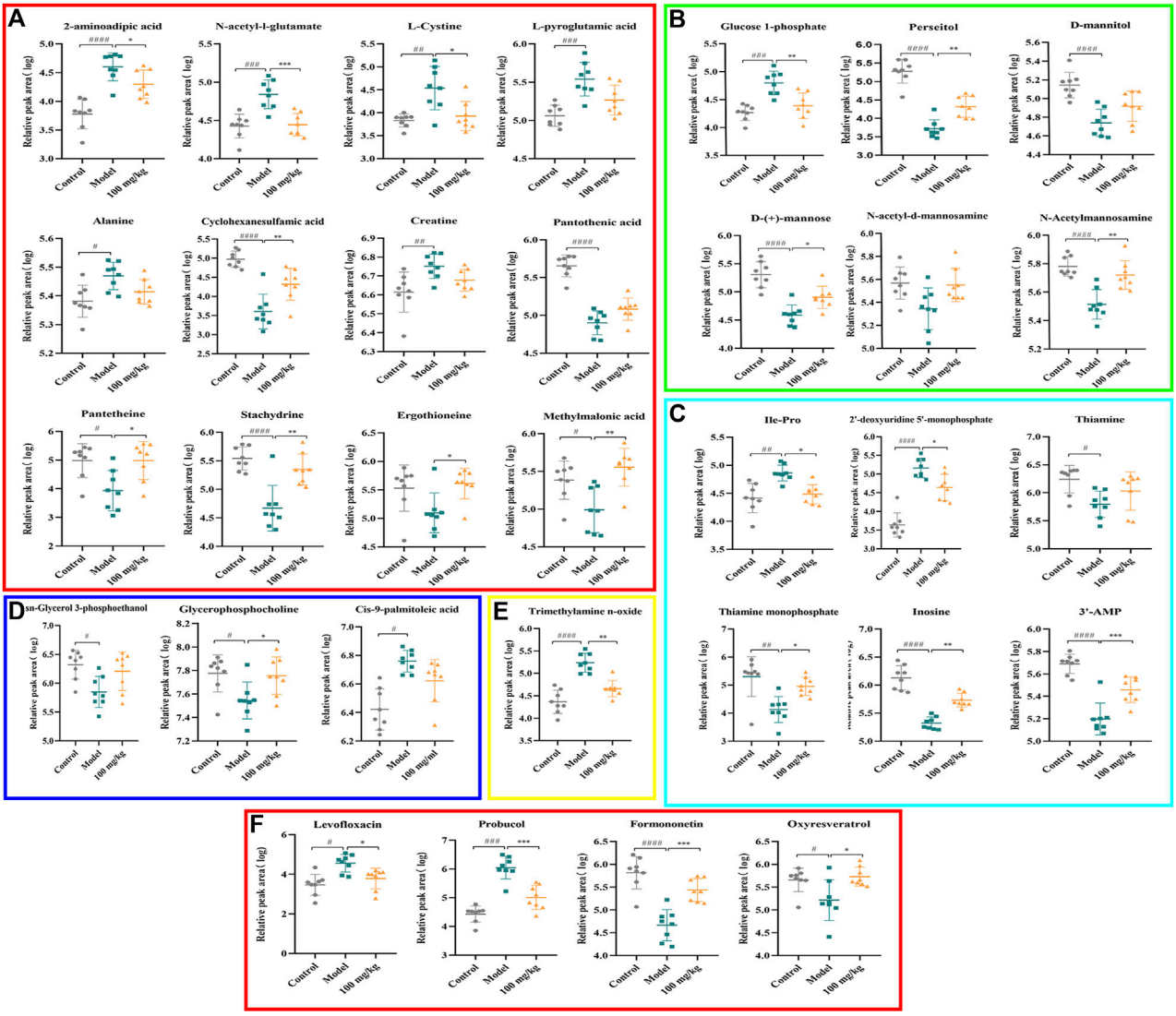

FIGURE 8
Effects of TFPCP on hepatic fibrosis related differential metabolites. **(A)** Effect of TFPCP-M (100 mg/mL) on amino acids metabolism (n = 8); **(B)** Effect of TFPCP-M (100 mg/mL) on carbohydrates metabolism (n = 8); **(C)** Effect of TFPCP-M (100 mg/mL) on nucleosides metabolism (n = 8); **(D)** Effect of TFPCP-M (100 mg/mL) on lipids metabolism (n = 8); **(E)** Effect of TFPCP-M (100 mg/mL) on trimethylamine n-oxide (TMAO) metabolism (n = 8); **(F)** Other metabolism (n = 8).

2017). In animal cells, glycerophosphocholine (GroPCho) is formed via the deacylation of the phospholipids Phosphatidylcholine (PC), which play a key role in the architecture of eukaryote membranes. Sn-Glycerol 3-phosphoethanolamin (GroPEtn) is a breakdown product of phosphatidylethanolamine (PE), and present in higher levels in normal liver relative to other organs (Tallan et al., 1954), which could stimulate the growth of hepatocytes and dropped significantly during liver regeneration (B Gowda et al., 2020). The decreased of PC to PE ratio impaired the cell membrane component and induced the permeability of the hepatocytes, which accelerated liver injury (Calzada et al., 2016). Also, altered PC/PE ratio has been shown to influence the dynamics and regulation of lipid droplets contributing towards steatosis (Mainali et al., 2021). Consistently, our results showed that the levels of GroPCho and GroPEtn decreased in the fibrosis rat model, and massive hepatocyte steatosis were found in the results of H&E pathological staining. On the contrary, TFPCP treatment increased the level of GroPCho and GroPEtn in liver tissue, alleviated liver damage and improved the pathology change, indicating that GPs metabolism was disturbanced in the process of liver fibrosis.

Thiamine is one of the carbohydrates metabolizing co-enzymes stored mainly in the liver (Hassan et al., 1991). Published research have shown that the cirrhotic liver may directly or indirectly affect phosphorylation, resulting in decreased levels of diphosphothiamine and, thus, hepatic thiamine storage (Hassan et al., 1991). Therefore, thiamine deficiency is likely to produce inadequate glucose utilization (Hassan et al., 1991). Meanwhile, research have shown animal models of thiamine deficiency have revealed increases in the levels of pro-inflammatory markers such as TNF-α (Karuppagounder et al., 2007). Similarly, our results showed that TFPCP could ameliorate the

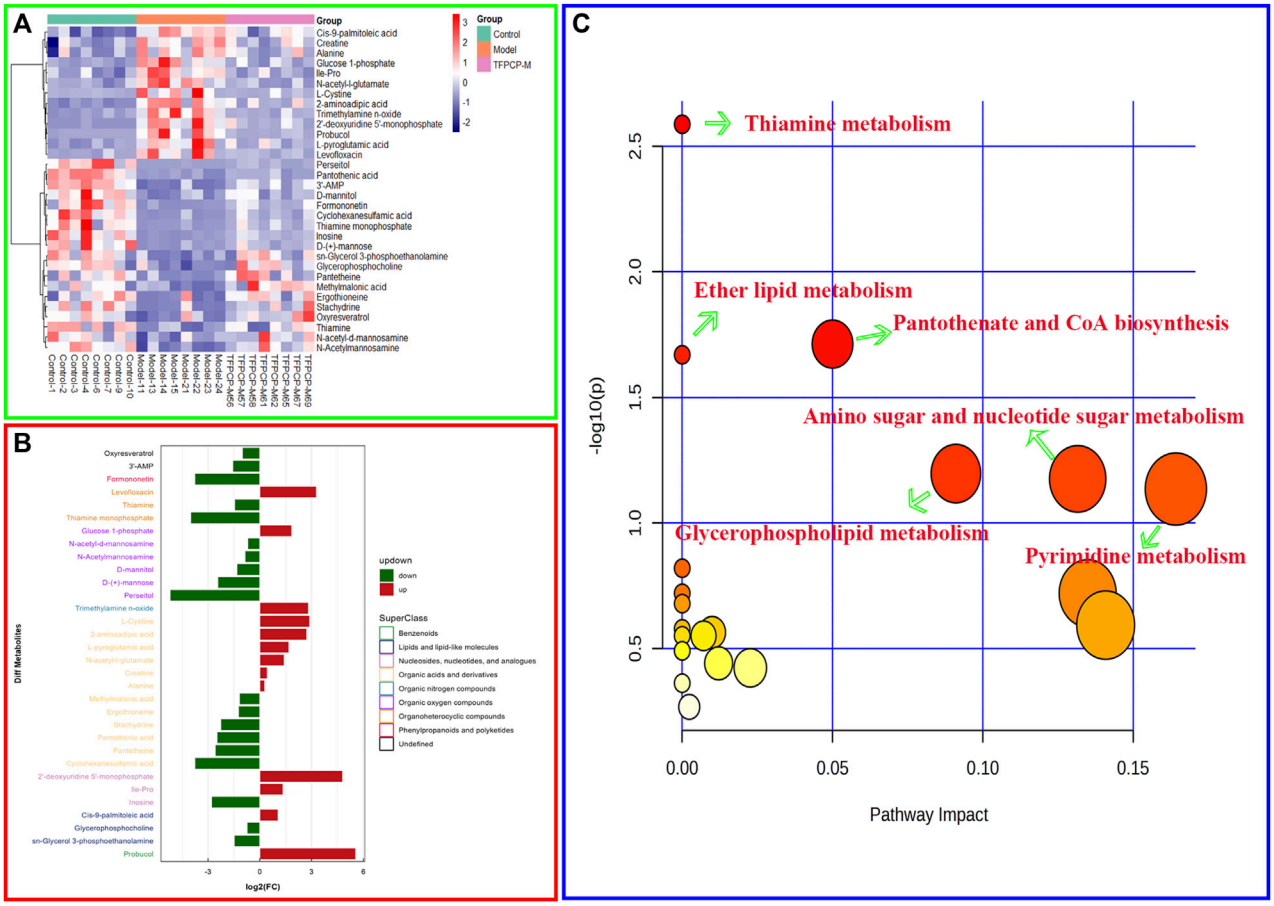

FIGURE 9
Effects of TFPCP on hepatic fibrosis related metabolic pathways. **(A)** Heatmap for the effect of TFPCP-M (100 mg/mL) supplementation on tissue metabolites in CCl_4-induced hepatic fibrosis rats (n = 8). **(B)** Multiple analysis of significant difference metabolite expression (n = 8). **(C)** The enrichment pathways result in the production of 32 metabolites.

inflammatory response (TNF-α, Il-6 and IL-1β) in a CCl_4-induced liver fibrosis rat model. Furthermore, the level of Thiamine, and its phosphate derivatives, thiamine monophosphate were decreased in the Model group, while TFPCP treatment increased these two biomarker levels.

In the Pantothenate and CoA biosynthesis pathway, the biomarker of pantothenic acid (vitamin B5), is the synthetic materials for coenzyme A. and pantetheine is the cysteamine amide analog of pantothenic acid which plays a central role in energy metabolism (Zhao et al., 2021). On the one hand, inflammation is energetically expensive (Zhang et al., 2022). Similarly, the level of pro-inflammatory markers TNF-α, IL-6 and IL-1β were correspondingly decrease in the TFPCP treatment groups than Model group. On the other hand, published research shown that pantothenic acid is a profibrotic agent that may increase and accelerate the wound-healing processes by recruiting migrating fibroblasts to the affected areas and promoting the proliferation and activation of fibroblasts, and collagen synthesis (Mariani and Roncucci, 2017). However, the changes in these two biomarkers in our experiments are not consistent with research reports, and we speculate that this may be the result of prolonged and not equilibrated succession of proliferation and death can lead to erosion of the liver cells, and thus to lack of function of the physical barrier.

Meanwhile, it is well established that metabolic processes involving galactose, nucleotide sugars, and amino sugars are also linked to chronic inflammation (Mir et al., 2022). Research reported that almost all glucosyl transfer reactions rely on glucose-1-phosphate (Glc-1-P) that either immediately acts as glucosyl donor or as substrate for the synthesis of the more widely used Glc dinucleotides, ADPglucose or UDPglucose (Fettke et al., 2011). Interestingly, in our research, 10 of the 32 metabolites that participate in amino and nucleotide sugar metabolism were restored after treatment with TFPCP (Figure 9A). This is in line with our finding that serum levels of pro-inflammatory factors were increased in hepatic fibrosis model rats. The results of the metabolomic analysis further confirmed that TFPCP inhibited the inflammatory response by regulating energy, lipid, nucleoside, and amino acid metabolism, thereby protecting against tissue damage and exerting anti-hepatic fibrosis effects (Figure 10).

In summary, employing a combination of molecular biology and metabolomic techniques, we elucidated the mechanism underlying the anti-hepatic fibrosis effects of TFPCP. We

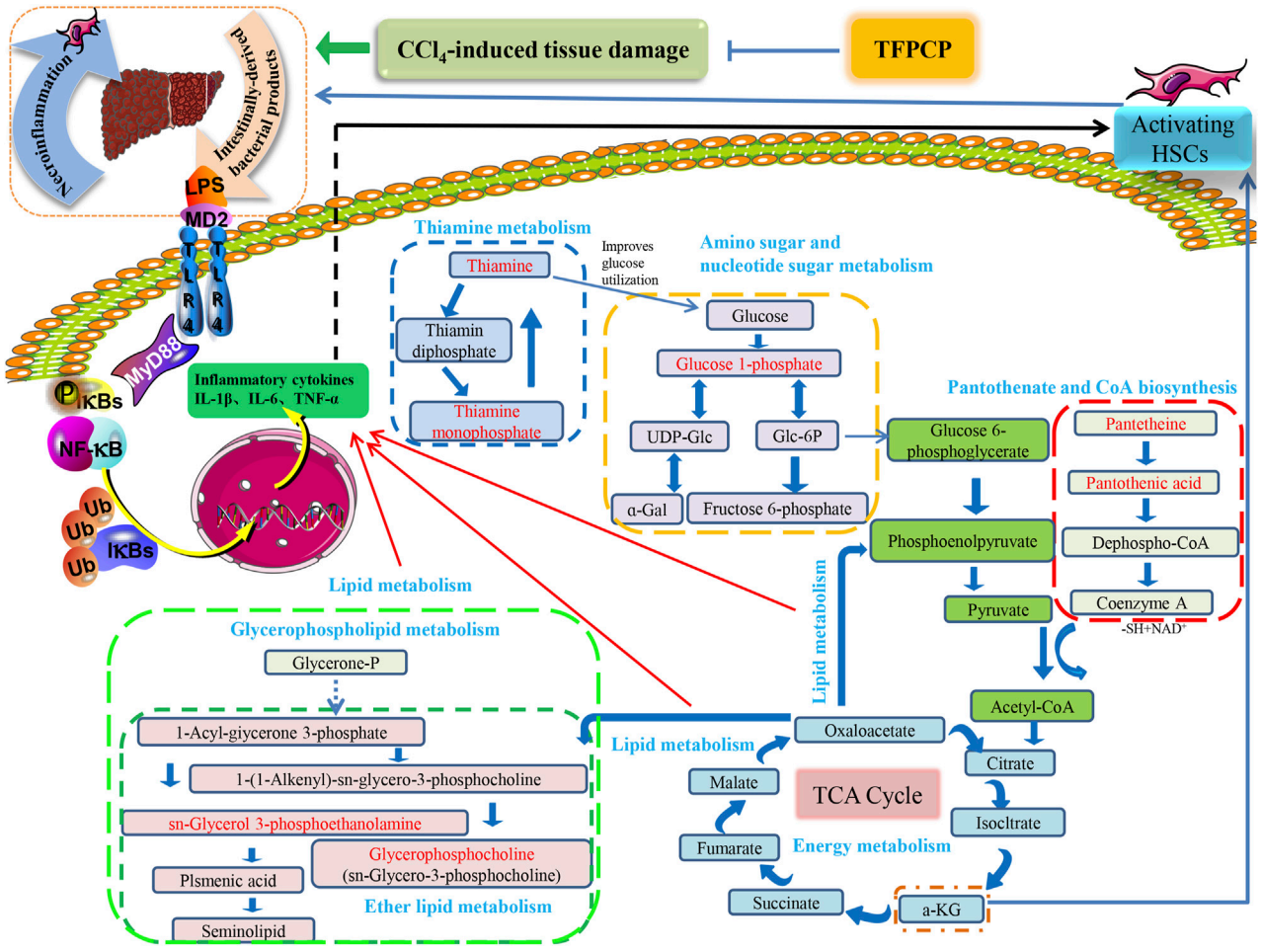

FIGURE 10
The relationship between differential metabolic pathways and the correlation analysis with the pharmacological effects of TFPCP on CCl_4-induced hepatic fibrosis rats, and the red portion represents the various metabolites studied in our investigation.

found that they are associated with the inactivation of the TLR4/MyD88/NF-κB signaling pathway and the regulation of lipid, energy, nucleoside, and amino acid metabolism. These findings suggest that TFPCP has potential as a natural therapy for hepatic fibrosis.

Data availability statement

The original contributions presented in the study are included in the article/Supplementary Material, further inquiries can be directed to the corresponding authors.

Ethics statement

The animal study was approved by the Animal Ethics Committee at Chengdu University of Traditional Chinese Medicine (No. 2021-69). The study was conducted in accordance with the local legislation and institutional requirements.

Author contributions

SW, CP, XX, and FP proposed the experimental scheme. SW, WQL, WXL, LY, and JQ carried out the experiments. LP and YT counted and analyzed the data. All authors revised the manuscript after it was completed by SW. All authors contributed to the article and approved the submitted version.

Funding

This work was supported by the Regional Joint Fund of the National Natural Science Foundation of China (No. U19A2010); National Natural Science Foundation of China (No. 81891012); National Natural Science Foundation of China (No. 82003879); National Inter disciplinary Innovation Team of Traditional Chinese Medicine (No. ZYYCXTD-D-202209); Sichuan provincial innovation team of Chinese medicine science and technology industry (No. 2022C001); Key Project of Science and Technology Department of Sichuan Province (No. 20ZDYF3092); National Scholarship Fund of China.

Conflict of interest

The authors declare that the research was conducted in the absence of any commercial or financial relationships that could be construed as a potential conflict of interest.

Publisher's note

All claims expressed in this article are solely those of the authors and do not necessarily represent those of their affiliated organizations, or those of the publisher, the editors and the reviewers. Any product that may be evaluated in this article, or claim that may be made by its manufacturer, is not guaranteed or endorsed by the publisher.

Supplementary material

The Supplementary Material for this article can be found online at: https://www.frontiersin.org/articles/10.3389/fphar.2023.1253013/full#supplementary-material

SUPPLEMENTARY FIGURE S1
Total ion chromatogram of TFPCP extract in positive-ion mode **(A)** and negative-ion mode **(B)**.

SUPPLEMENTARY FIGURE S2
Multivariate analysis of liver tissue metabolomics. **(A, B)** PCA score plot of liver tissue samples collected from different treatment groups of rats in positive and negative ion mode. **(C–F)** The difference distribution of tissue metabolites between control and model group by OPLS-DA and permutation tests score analysis in positive and negative ion mode. **(G–J)** The difference distribution of tissue metabolites between model and TFPCP-M (100 mg/mL) group by OPLS-DA and permutation tests score analysis in positive and negative ion mode.

References

Afdhal, N. H., and Nunes, D. (2004). Evaluation of liver fibrosis: a concise review. *Am. J. Gastroenterol.* 99 (6), 1160–1174. doi:10.1111/j.1572-0241.2004.30110.x

Albrecht, T., Blomley, M. J., Cosgrove, D. O., Taylor-Robinson, S. D., Jayaram, V., Eckersley, R., et al. (1999). Non-invasive diagnosis of hepatic cirrhosis by transit-time analysis of an ultrasound contrast agent. *Lancet* 353 (9164), 1579–1583. doi:10.1016/S0140-6736(98)06373-9

Amroun, D., Hamoudi, M., Khennouf, S., Boutefnouchet, S., Harzallah, D., Amrane, M., et al. (2021). In-vivo anti-inflammatory activity and safety assessment of the aqueous extract of Algerian Erica arborea L. (Ericaceae) aerial parts. *J. Ethnopharmacol.* 271, 113881. doi:10.1016/j.jep.2021.113881

Asrani, S. K., Devarbhavi, H., Eaton, J., and Kamath, P. S. (2019). Burden of liver diseases in the world. *J. Hepatol.* 70 (1), 151–171. doi:10.1016/j.jhep.2018.09.014

Berumen, J., Baglieri, J., Kisseleva, T., and Mekeel, K. (2021). Liver fibrosis: pathophysiology and clinical implications. *WIREs Mech. Dis.* 13 (1), e1499. doi:10.1002/wsbm.1499

Beyoglu, D., and Idle, J. R. (2020). Metabolomic insights into the mode of action of natural products in the treatment of liver disease. *Biochem. Pharmacol.* 180, 114171. doi:10.1016/j.bcp.2020.114171

B Gowda, G. S., Fuda, H., Yamamoto, Y., Chiba, H., and Hui, S. P. (2020). A simple and efficient method for synthesis of sn-glycero-phosphoethanolamine. *Lipids* 55 (4), 395–401. doi:10.1002/lipd.12243

Bottcher, K., and Pinzani, M. (2017). Pathophysiology of liver fibrosis and the methodological barriers to the development of anti-fibrogenic agents. *Adv. Drug Deliv. Rev.* 121, 3–8. doi:10.1016/j.addr.2017.05.016

Calzada, E., Onguka, O., and Claypool, S. M. (2016). Phosphatidylethanolamine metabolism in health and disease. *Int. Rev. Cell Mol. Biol.* 321, 29–88. doi:10.1016/bs.ircmb.2015.10.001

Chang, H., Meng, H. Y., Liu, S. M., Wang, Y., Yang, X. X., Lu, F., et al. (2017). Identification of key metabolic changes during liver fibrosis progression in rats using a urine and serum metabolomics approach. *Sci. Rep.* 7 (1), 11433. doi:10.1038/s41598-017-11759-z

Chen, M. Q., Zhu, W. F., Guan, Y. M., Feng, Y. L., Zhang, Y. L., Jing, X. C., et al. (2023). Analysis of chemical constituents in puerariae lobatae radix dispensing granules by UPLC-Q-TOFMS/MS. *Chin. J. Exp. Traditional Med. Formulae*, 1–13. doi:10.13422/j.cnki.syfjx.20230762

Chirumbolo, S., and Bjorklund, G. (2018). Quercetin in the experimental liver fibrosis induced by carbon tetrachloride (CCl(4)). *Int. Immunopharmacol.* 55, 254–256. doi:10.1016/j.intimp.2017.12.022

Conseil, G., Baubichon-Cortay, H., Dayan, G., Jault, J. M., Barron, D., and Di Pietro, A. (1998). Flavonoids: a class of modulators with bifunctional interactions at vicinal ATP-and steroid-binding sites on mouse P-glycoprotein. *Proc. Natl. Acad. Sci. U.S.A.* 95 (17), 9831–9836. doi:10.1073/pnas.95.17.9831

Fettke, J., Malinova, I., Albrecht, T., Hejazi, M., and Steup, M. (2011). Glucose-1-phosphate transport into protoplasts and chloroplasts from leaves of Arabidopsis. *Plant Physiol.* 155 (4), 1723–1734. doi:10.1104/pp.110.168716

Hassan, R., Qureshi, H., and Zuberi, S. J. (1991). Effect of thiamine on glucose utilization in hepatic cirrhosis. *J. Gastroenterol. Hepatol.* 6 (1), 59–60. doi:10.1111/j.1440-1746.1991.tb01146.x

Kaci, H., Bodnarova, S., Fliszar-Nyul, E., Lemli, B., Pelantova, H., Valentova, K., et al. (2023). Interaction of luteolin, naringenin, and their sulfate and glucuronide conjugates with human serum albumin, cytochrome P450 (CYP2C9, CYP2C19, and CYP3A4) enzymes and organic anion transporting polypeptide (OATP1B1 and OATP2B1) transporters. *Biomed. Pharmacother.* 157, 114078. doi:10.1016/j.biopha.2022.114078

Karuppagounder, S. S., Shi, Q., Xu, H., and Gibson, G. E. (2007). Changes in inflammatory processes associated with selective vulnerability following mild impairment of oxidative metabolism. *Neurobiol. Dis.* 26 (2), 353–362. doi:10.1016/j.nbd.2007.01.011

Kershenobich, D., Vargas, F., Garcia-Tsao, G., Perez, T. R., Gent, M., and Rojkind, M. (1988). Colchicine in the treatment of cirrhosis of the liver. *N. Engl. J. Med.* 318 (26), 1709–1713. doi:10.1056/NEJM198806303182602

Kisseleva, T., and Brenner, D. (2021). Molecular and cellular mechanisms of liver fibrosis and its regression. *Nat. Rev. Gastroenterol. Hepatol.* 18 (3), 151–166. doi:10.1038/s41575-020-00372-7

Lee, Y. A., Wallace, M. C., and Friedman, S. L. (2015). Pathobiology of liver fibrosis: a translational success story. *Gut* 64 (5), 830–841. doi:10.1136/gutjnl-2014-306842

Li, X., Jin, Q., Yao, Q., Xu, B., Li, L., Zhang, S., et al. (2018). The flavonoid quercetin ameliorates liver inflammation and fibrosis by regulating hepatic macrophages activation and polarization in mice. *Front. Pharmacol.* 9, 72. doi:10.3389/fphar.2018.00072

Lieber, C. S., Robins, S. J., Li, J., Decarli, L. M., Mak, K. M., Fasulo, J. M., et al. (1994). Phosphatidylcholine protects against fibrosis and cirrhosis in the baboon. *Gastroenterology* 106 (1), 152–159. doi:10.1016/s0016-5085(94)95023-7

Liedtke, C., Luedde, T., Sauerbruch, T., Scholten, D., Streetz, K., Tacke, F., et al. (2013). Experimental liver fibrosis research: update on animal models, legal issues and translational aspects. *Fibrogenes. Tissue Repair* 6 (1), 19. doi:10.1186/1755-1536-6-19

Liu, Y., Cavallaro, P. M., Kim, B. M., Liu, T., Wang, H., Kuhn, F., et al. (2021). A role for intestinal alkaline phosphatase in preventing liver fibrosis. *Theranostics* 11 (1), 14–26. doi:10.7150/thno.48468

Luo, S. N., Peng, Z. C., Fan, Q., Cai, S. K., Wei, M., Cheng, X. R., et al. (2021). Analysis on chemical constituents in xiao chengqitang by UPLC-Q-orbitrap-MS. *Chin. J. Exp. Traditional Med. Formulae* 27, 1–10. doi:10.13422/j.cnki.syfjx.20211450

Mack, M. (2018). Inflammation and fibrosis. *Matrix Biol.* 68-69, 106–121. doi:10.1016/j.matbio.2017.11.010

Mainali, R., Zabalawi, M., Long, D., Buechler, N., Quillen, E., Key, C. C., et al. (2021). Dichloroacetate reverses sepsis-induced hepatic metabolic dysfunction. *eLife* 10, e64611. doi:10.7554/eLife.64611

Mandery, K., Balk, B., Bujok, K., Schmidt, I., Fromm, M. F., and Glaeser, H. (2012). Inhibition of hepatic uptake transporters by flavonoids. *Eur. J. Pharm. Sci.* 46 (1-2), 79–85. doi:10.1016/j.ejps.2012.02.014

Mariani, F., and Roncucci, L. (2017). Role of the vanins-myeloperoxidase Axis in colorectal carcinogenesis. *Int. J. Mol. Sci.* 18 (5), 918. doi:10.3390/ijms18050918

Mesens, N., Desmidt, M., Verheyen, G. R., Starckx, S., Damsch, S., De Vries, R., et al. (2012). Phospholipidosis in rats treated with amiodarone: serum biochemistry and whole genome micro-array analysis supporting the lipid traffic jam hypothesis and the subsequent rise of the biomarker BMP. *Toxicol. Pathol.* 40 (3), 491–503. doi:10.1177/0192623311432290

Meunier, B., de Visser, S. P., and Shaik, S. (2004). Mechanism of oxidation reactions catalyzed by cytochrome p450 enzymes. *Chem. Rev.* 104 (9), 3947–3980. doi:10.1021/cr020443g

Mir, F. A., Ullah, E., Mall, R., Iskandarani, A., Samra, T. A., Cyprian, F., et al. (2022). Dysregulated metabolic pathways in subjects with obesity and metabolic syndrome. *Int. J. Mol. Sci.* 23 (17), 9821. doi:10.3390/ijms23179821

Nobili, V., Alisi, A., Cutrera, R., Carpino, G., De Stefanis, C., D'Oria, V., et al. (2015). Altered gut-liver axis and hepatic adiponectin expression in OSAS: novel mediators of liver injury in paediatric non-alcoholic fatty liver. *Thorax* 70 (8), 769–781. doi:10.1136/thoraxjnl-2015-206782

Peng, C. (2016). "Pharmacodynamics of Chinese medicine," in *The Pharmacology of Chinese medicine*. 4th edition (Beijing: China Press of Traditional Chinese Medicine), 35–36.

Raucy, J. L. (2003). Regulation of CYP3A4 expression in human hepatocytes by pharmaceuticals and natural products. *Drug Metab. Dispos.* 31 (5), 533–539. doi:10.1124/dmd.31.5.533

Rescic, J., Mikulic-Petkovsek, M., and Rusjan, D. (2016). The impact of canopy managements on grape and wine composition of cv. 'Istrian Malvasia' (Vitis vinifera L.). *J. Sci. Food Agric.* 96 (14), 4724–4735. doi:10.1002/jsfa.7778

Sato, A., Nakashima, H., Nakashima, M., Ikarashi, M., Nishiyama, K., Kinoshita, M., et al. (2014). Involvement of the TNF and FasL produced by CD11b Kupffer cells/macrophages in CCl_4-induced acute hepatic injury. *PLoS One* 9 (3), e92515. doi:10.1371/journal.pone.0092515

Seki, E., De Minicis, S., Osterreicher, C. H., Kluwe, J., Osawa, Y., Brenner, D. A., et al. (2007). TLR4 enhances TGF-beta signaling and hepatic fibrosis. *Nat. Med.* 13 (11), 1324–1332. doi:10.1038/nm1663

Serafini, M., Peluso, I., and Raguzzini, A. (2010). Flavonoids as anti-inflammatory agents. *Proc. Nutr. Soc.* 69 (3), 273–278. doi:10.1017/S002966511000162X

Shang, X., Yuan, H., Dai, L., Liu, Y., He, J., Chen, H., et al. (2021). Anti-liver fibrosis activity and the potential mode of action of ruangan granules: integrated network pharmacology and metabolomics. *Front. Pharmacol.* 12, 754807. doi:10.3389/fphar.2021.754807

Shu, Y., He, D., Li, W., Wang, M., Zhao, S., Liu, L., et al. (2020). Hepatoprotective effect of citrus aurantium L. Against APAP-induced liver injury by regulating liver lipid metabolism and apoptosis. *Int. J. Biol. Sci.* 16 (5), 752–765. doi:10.7150/ijbs.40612

Simirgiotis, M. J., Benites, J., Areche, C., and Sepulveda, B. (2015). Antioxidant capacities and analysis of phenolic compounds in three endemic nolana species by HPLC-PDA-ESI-MS. *Molecules* 20 (6), 11490–11507. doi:10.3390/molecules200611490

Tallan, H. H., Moore, S., and Stein, W. H. (1954). Studies on the free amino acids and related compounds in the tissues of the cat. *J. Biol. Chem.* 211 (2), 927–939. doi:10.1016/s0021-9258(18)71180-0

Tang, J., Song, X., Zhao, M., Chen, H., Wang, Y., Zhao, B., et al. (2022). Oral administration of live combined Bacillus subtilis and Enterococcus faecium alleviates colonic oxidative stress and inflammation in osteoarthritic rats by improving fecal microbiome metabolism and enhancing the colonic barrier. *Front. Microbiol.* 13, 1005842. doi:10.3389/fmicb.2022.1005842

Unsal, V., Cicek, M., and Sabancilar, I. (2021). Toxicity of carbon tetrachloride, free radicals and role of antioxidants. *Rev. Environ. Health.* 36 (2), 279–295. doi:10.1515/reveh-2020-0048

Usami, M., Miyoshi, M., Kanbara, Y., Aoyama, M., Sakaki, H., Shuno, K., et al. (2013). Analysis of fecal microbiota, organic acids and plasma lipids in hepatic cancer patients with or without liver cirrhosis. *Clin. Nutr.* 32 (3), 444–451. doi:10.1016/j.clnu.2012.09.010

Wang, A., Li, M., Huang, H., Xiao, Z., Shen, J., Zhao, Y., et al. (2020). A review of Penthorum chinense Pursh for hepatoprotection: traditional use, phytochemistry, pharmacology, toxicology and clinical trials. *J. Ethnopharmacol.* 251, 112569. doi:10.1016/j.jep.2020.112569

Wang, H., Che, J., Cui, K., Zhuang, W., Li, H., Sun, J., et al. (2021). Schisantherin A ameliorates liver fibrosis through TGF-β1mediated activation of TAK1/MAPK and NF-κB pathways *in vitro* and *in vivo*. *Phytomedicine* 88, 153609. doi:10.1016/j.phymed.2021.153609

Wang, M., Lamers, R. J., Korthout, H. A., van Nesselrooij, J. H., Witkamp, R. F., van der Heijden, R., et al. (2005). Metabolomics in the context of systems biology: bridging traditional Chinese medicine and molecular pharmacology. *Phytother. Res.* 19 (3), 173–182. doi:10.1002/ptr.1624

Weber, L. W., Boll, M., and Stampfl, A. (2003). Hepatotoxicity and mechanism of action of haloalkanes: carbon tetrachloride as a toxicological model. *Crit. Rev. Toxicol.* 33 (2), 105–136. doi:10.1080/713611034

Xiao, G. L., Chen, W. T., Zhong, H. X., Li, Y. X., and Bi, X. L. (2022). Analysis of chemical components in Bai Hu decoction based on UPLC-Q-TOF-MS/MS. *J. Chin. Med. Mater.*, 2656–2663. doi:10.13863/j.issn1001-4454.2022.11.022

Xiao, Z., Zhang, Y., Chen, X., Wang, Y., Chen, W., Xu, Q., et al. (2017). Extraction, identification, and antioxidant and anticancer tests of seven dihydrochalcones from Malus 'Red Splendor' fruit. *Food Chem.* 231, 324–331. doi:10.1016/j.foodchem.2017.03.111

Yang, D., Li, F. P., Liu, M., Song, F. Y., Ge, Y., Dai, Y. L., et al. (2021). Analysis of chemical components in Physalis Calyx seu Fructus using UPLC-Q-Orbitrap MS/MS. *J. Chin. Mass Spectrom. Soc.* 42, 253–260. doi:10.7538/zpxb.2020.0077

Yang, L., Bi, L., Jin, L., Wang, Y., Li, Y., Li, Z., et al. (2021). Geniposide ameliorates liver fibrosis through reducing oxidative stress and inflammatory respose, inhibiting apoptosis and modulating overall metabolism. *Front. Pharmacol.* 12, 772635. doi:10.3389/fphar.2021.772635

Yin, J., Ren, W., Wei, B., Huang, H., Li, M., Wu, X., et al. (2020). Characterization of chemical composition and prebiotic effect of a dietary medicinal plant Penthorum chinense Pursh. *Food Chem.* 319, 126568. doi:10.1016/j.foodchem.2020.126568

Yoo, H. J., Jung, K. J., Kim, M., Kim, M., Kang, M., Jee, S. H., et al. (2019). Liver cirrhosis patients who had normal liver function before liver cirrhosis development have the altered metabolic profiles before the disease occurrence compared to healthy controls. *Front. Physiol.* 10, 1421. doi:10.3389/fphys.2019.01421

Yu, J., He, J. Q., Chen, D. Y., Pan, Q. L., Yang, J. F., Cao, H. C., et al. (2019). Dynamic changes of key metabolites during liver fibrosis in rats. *World J. Gastroenterol.* 25 (8), 941–954. doi:10.3748/wjg.v25.i8.941

Zeng, Q. H., Zhang, X. W., Xu, X. L., Jiang, M. H., Xu, K. P., Piao, J. H., et al. (2013). Antioxidant and anticomplement functions of flavonoids extracted from Penthorum chinense Pursh. *Food Funct.* 4 (12), 1811–1818. doi:10.1039/c3fo60342c

Zhang, I. W., Curto, A., Lopez-Vicario, C., Casulleras, M., Duran-Guell, M., Flores-Costa, R., et al. (2022). Mitochondrial dysfunction governs immunometabolism in leukocytes of patients with acute-on-chronic liver failure. *J. Hepatol.* 76 (1), 93–106. doi:10.1016/j.jhep.2021.08.009

Zhang, K., Gao, Y., Zhong, M., Xu, Y., Li, J., Chen, Y., et al. (2016). Hepatoprotective effects of Dicliptera chinensis polysaccharides on dimethylnitrosamine-induced hepatic fibrosis rats and its underlying mechanism. *J. Ethnopharmacol.* 179, 38–44. doi:10.1016/j.jep.2015.12.053

Zhang, Y., Zhang, M., Li, H., Zhao, H., Wang, F., He, Q., et al. (2018). Serum metabonomics study of the hepatoprotective effect of amarogentin on CCl_4-induced liver fibrosis in mice by GC-TOF-MS analysis. *J. Pharm. Biomed. Anal.* 149, 120–127. doi:10.1016/j.jpba.2017.10.029

Zhao, L., Dong, M., Liao, S., Du, Y., Zhou, Q., Zheng, H., et al. (2016). Identification of key metabolic changes in renal interstitial fibrosis rats using metabonomics and pharmacology. *Sci. Rep.* 6, 27194. doi:10.1038/srep27194

Zhao, S., Schaub, A. J., Tsai, S. C., and Luo, R. (2021). Development of a pantetheine force field library for molecular modeling. *J. Chem. Inf. Model.* 61 (2), 856–868. doi:10.1021/acs.jcim.0c01384

frontiers | Frontiers in Pharmacology

TYPE Mini Review
PUBLISHED 12 January 2024
DOI 10.3389/fphar.2023.1334160

OPEN ACCESS

EDITED BY
Rongrui Wei,
Jiangxi University of Traditional Chinese Medicine, China

REVIEWED BY
Sidra Rehman,
COMSATS University, Islamabad Campus, Pakistan

*CORRESPONDENCE
Allah Nawaz,
allah.nawaz@joslin.harvard.edu
Ishtiaq Jeelani,
ijeelani@ucsd.edu

†PRESENT ADDRESS
Allah Nawaz, Joslin Diabetes Center, Harvard Medical School, Harvard University, Boston, MA, United States
Ishtiaq Jeelani, Department of Medicine, Division of Endocrinology and Metabolism, University of California, San Diego, CA, United States

RECEIVED 06 November 2023
ACCEPTED 18 December 2023
PUBLISHED 12 January 2024

CITATION
Nawaz A, Manzoor A, Ahmed S, Ahmed N, Abbas W, Mir MA, Bilal M, Sheikh A, Ahmad S, Jeelani I and Nakagawa T (2024), Therapeutic approaches for chronic hepatitis C: a concise review.
Front. Pharmacol. 14:1334160.
doi: 10.3389/fphar.2023.1334160

Therapeutic approaches for chronic hepatitis C: a concise review

Allah Nawaz[1,2*†], Azhar Manzoor[3], Saeed Ahmed[4], Naveed Ahmed[5], Waseem Abbas[2], Mushtaq Ahmad Mir[6], Muhammad Bilal[7], Alisha Sheikh[8], Saleem Ahmad[9], Ishtiaq Jeelani[2*†] and Takashi Nakagawa[2]

[1]Joslin Diabetes Center, Harvard Medical School, Harvard University, Boston, MA, United States, [2]Department of Molecular and Medical Pharmacology, Faculty of Medicine, University of Toyama, Toyama, Japan, [3]Department of Surgery, Bahawal Victoria Hospital, Bahawalpur, Pakistan, [4]Department of Medicine, and Surgery, Rawalpindi Medical University, Rawalpindi, Punjab, Pakistan, [5]Department of Pharmacy, University of Poonch Rawalakot, Rawalakot, Azad Jammu and Kashmir (AJ&K), Pakistan, [6]Department of Clinical Laboratory Sciences, College of Applied Medical Sciences, King Khalid University, Abha, Saudi Arabia, [7]First Department of Internal Medicine, Faculty of Medicine, University of Toyama, Toyama, Japan, [8]Jammu Institute of Ayurveda and Research, University of Jammu, Jammu, India, [9]Cardiovascular Center of Excellence, Louisiana State University Health Sciences Center, New Orleans, LA, United States

Hepatitis C virus (HCV) infection is a significant global health concern, prompting the need for effective treatment strategies. This in-depth review critically assesses the landscape of HCV treatment, drawing parallels between traditional interferon/ribavirin therapy historically pivotal in HCV management and herbal approaches rooted in traditional and complementary medicine. Advancements in therapeutic development and enhanced clinical outcomes axis on a comprehensive understanding of the diverse HCV genome, its natural variations, pathogenesis, and the impact of dietary, social, environmental, and economic factors. A thorough analysis was conducted through reputable sources such as Science Direct, PubMed, Scopus, Web of Science, books, and dissertations. This review primarily focuses on the intricate nature of HCV genomes and explores the potential of botanical drugs in both preventing and treating HCV infections.

KEYWORDS

hepatitis C virus, direct-acting antiviral agents (DAAs), botanical drugs, hepatitis C, hepatoprotective and antiviral properties of medicinal plants

Background

Hepatitis C virus (HCV) infection is a significant global health issue and is regarded as one of the primary causes of mortality worldwide. According to the World Health Organization (WHO), the worldwide prevalence of HCV infections is currently reported to be 58 million, with an estimated 1.5 million new HCV infections occurring each year. This high incidence results in approximately 290,000 deaths annually attributed to HCV infection (WHO, 2022). While most cases of HCV infection remain asymptomatic, the disease can advance to chronic conditions like liver fibrosis, liver cirrhosis, hepatocellular carcinoma or liver failure. Notably, liver cirrhosis emerges in around 20% of individuals with chronic hepatitis C. Chronic liver disease is mainly attributed to excessive alcohol consumption and persistent infections with hepatitis B and C viruses (Singh and Hoyert, 2000). Several factors contribute to an elevated risk of HCV infection,

including alcohol consumption, immunosuppression, and acquisition of HCV after the age of 40.

Recent research has elucidated that the impact of HCV extends beyond hepatocytes, leading to extrahepatic manifestations such as lymphoproliferative disorders, insulin resistance, type 2 diabetes, renal disease, and neurological disorders (Jacobson et al., 2010; Ito et al., 2011; Stanaway et al., 2016; Vanni et al., 2016; Drazilova et al., 2018; Moustafa et al., 2020). Consequently, there is an urgent need to identify new, and intensive treatment approaches capable of addressing both intra- and extrahepatic manifestations of HCV. The therapeutic approach for HCV is undergoing dynamic advancements aimed at attaining optimal responses and sustained viral eradication over the long term. The introduction of Interferon alpha-2b in 1986 marked an initial milestone in the pursuit of a curative approach for HCV (Tong et al., 1997; Hoofnagle et al., 1986). However, the sustained virologic response (SVR) rate with interferon monotherapy was limited to 10%–20% (Farrell et al., 1998; McHutchison et al., 1998). Subsequent research revealed that Ribavirin, an orally active synthetic guanosine analogue with antiviral and immunomodulatory properties, could enhance treatment outcomes when combined with interferon therapy (Bodenheimer et al., 1997; Davis et al., 1998). The administration of interferon and ribavirin therapy for the treatment of HCV can induce several adverse effects, including flu-like symptoms, nausea, vomiting, depression, insomnia, weight loss, anemia, and skin reactions. A significant advancement in HCV treatment has emerged with the introduction of various oral regimens that incorporate Direct-Acting Antivirals (DAAs), each characterized by distinct mechanisms of action (Asselah et al., 2018; Christensen et al., 2018). These treatments boast a favorable safety profile and are generally well-tolerated, resulting in a remarkable increase in SVR rates, often nearing 100%.

DAAs offer several advantages, including minimal side effects, short treatment durations (typically 8–12 weeks), and a low likelihood of viral resistance development. Targeting specific steps in the HCV life cycle, DAAs provide highly effective, well-tolerated, and curative treatment options. With cure rates often exceeding 95% across diverse patient populations and HCV genotypes, DAAs have a high barrier to the development of drug resistance. This approach has revolutionized HCV management, allowing healthcare providers to offer curative therapies to a broad range of patients, including those with co-infections (e.g., HIV) and special populations such as individuals with cirrhosis, transplant recipients, and people who inject drugs. While DAAs offer significant advantages, their high cost has raised concerns about access to treatment in some regions. Efforts are ongoing to make these medications more accessible globally.

In contrast, herbal treatments for HCV represent a traditional and alternative approach rooted in centuries-old natural remedies. Although some herbal products have been investigated for their hepatoprotective and potential antiviral properties, scientific evidence supporting their efficacy and safety in HCV management is limited and inconsistent. Herbs such as milk thistle, licorice root, and curcumin have been explored for potential benefits, but clinical study results are inconclusive. Moreover, the lack of standardization and quality control in herbal products raises concerns about consistency and safety.

Epidemiology of HCV worldwide

On a global scale, chronic liver disease and cirrhosis rank as the 10th leading cause of death. This condition affects both males and females disproportionately between the ages of 35 and 64, making it the 5th leading cause of mortality among individuals aged 45 to 64. Approximately 70% of individuals chronically infected with HCV develop progressive liver disease, and HCV infection accounts for the chronic liver disease in 40% of all affected patients (Nainan et al., 2006). According to the World Health Organization (WHO), approximately 200 million people are currently living with HCV, with an annual incidence of 3.5–4.0 million new infections. The prevalence of HCV varies globally, with notable regional distinctions. These insights into the global epidemiology of HCV underscore the importance of comprehensive strategies for prevention, diagnosis, and management on a worldwide scale.

HCV-induced tissue damage via activation of complement system

The liver, the largest solid organ in the body, plays a pivotal role in diverse physiological functions. Comprising various cell types, the liver includes hepatocytes as the predominant cell type, along with non-parenchymal cells, hepatic stellate cells, endothelial cells, and Kupffer cells. The latter are resident macrophages that mainly regulate liver homeostasis during liver inflammation (Kazankov et al., 2019; Sakai et al., 2019; Alharthi et al., 2020). Immune cells are key players in various metabolic diseases, including insulin resistance, fatty liver, and atherosclerosis. HCV, upon binding to extrahepatic peripheral B cells (CD81), triggers dysregulation within the immune system. This infection results in the chronic stimulation of lymphocytes, ultimately leading to the expansion of B-cell clones. This process then activates the complement system and antibody production to form immune complexes, resulting in tissue damage (Jacobson et al., 2010; Ito et al., 2011; Moustafa et al., 2020) (Figure 1A).

HCV and extrahepatic manifestations of metabolic disorders

HCV is involved in extrahepatic manifestations of metabolic disorders, particularly insulin resistance and type 2 diabetes, due to the aberrant activation of inflammatory cytokines. In the context of chronic HCV infections, there is a notable production of inflammatory cytokines, including interleukin-6 (IL-6) and tumor necrosis factor-alpha (TNF-α), within the liver. These cytokines, in turn, disrupt insulin signaling pathways, leading to the development of insulin resistance. Beyond the heightened risk of type 2 diabetes associated with HCV infections, individuals with chronic HCV infections also exhibit an elevated prevalence of cardiac-cerebrovascular disorders. This intricate relationship underscores the systemic impact of HCV beyond the liver and emphasizes the potential role of viral-induced inflammatory responses in contributing to broader metabolic and cardiovascular complications (Drazilova et al., 2018; Moustafa et al., 2020). HCV infection seems to accelerate the inflammatory response

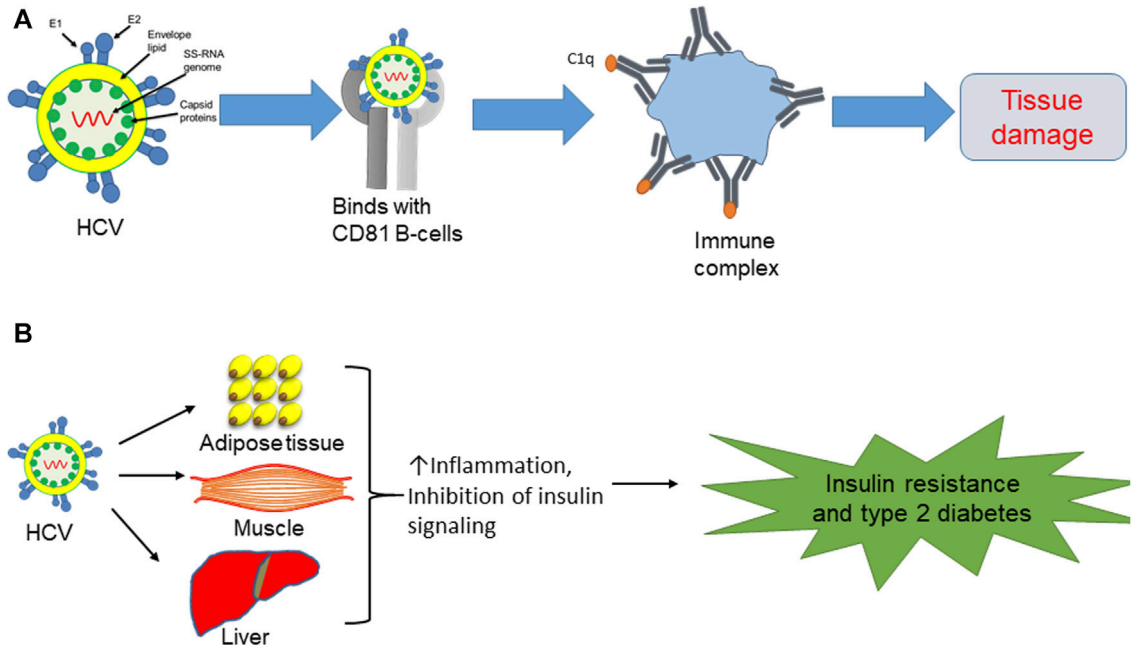

FIGURE 1
(A) HCV binds with CD81 B cells, leading to antibody production and formation of immune complexes, which then initiate tissue damage. **(B)** Direct effect of HCV on insulin resistance and type 2 diabetes via induction of proinflammatory cytokines in adipose tissue and liver, while also blocking insulin signaling in muscle.

and hinder insulin signaling in metabolically responsive tissues, including the liver, adipose tissue, and skeletal muscle (Figure 1B). The dysregulation of inflammatory pathways and interference with insulin signaling in these tissues contribute to the development of metabolic disturbances, including insulin resistance, highlighting the systemic effects of HCV infection beyond the liver (Fujisaka et al., 2009; Fujisaka et al., 2013; Fujisaka et al., 2016; Nawaz et al., 2017a; Nawaz et al., 2017b; Takikawa et al., 2019). Indeed, aging-induced inflammation plays a substantial role in the onset of diverse disorders, including diabetes, atherosclerosis, and mitochondrial dysfunction. The inflammatory milieu associated with aging can amplify the overall impact of HCV infection on the body's health, exacerbating its effects on metabolic and physiological processes (Zhang et al., 2016; Chia et al., 2018; Kazankov et al., 2019; Luo et al., 2019; Reidy et al., 2019). Consequently, HCV infection is correlated with metabolic complications due to the abnormal activation of inflammatory cytokines.

Contribution of botanical drugs in HCV management

The use of various medicinal plants for managing chronic hepatitis C infections has been a part of traditional medicine in different cultures for centuries. Many societies have relied on natural remedies derived from plants to address various health issues, including liver ailments. It is important to note that while traditional practices often involve the use of medicinal plants, the effectiveness and safety of these remedies can vary, and scientific research is essential to validate their therapeutic potential. Botanical drug(s), individually or in combination, are effective against HCV infection, blocking the virus's entry, translation, replication, and assembly (summarized in Table 1). Molecular studies have also demonstrated that medicinal plants can be used to develop anti-HCV drugs. Silymarin, derived from the seeds of the milk thistle plant (Silybum marianum: family Asteraceae), is known to inhibit inflammatory cytokines and other transcriptional factors, viral entry into hepatocytes, and viral replication (Polyak et al., 2007). Quercetin is reported to block HCV replication via a direct inhibitory effect on NS3 polymerase and IRES activity (Gonzalez et al., 2009; Bachmetov et al., 2012). *Ladanein* and *Limonium sinense* block viral entry through effects on post-attachment entry steps, including uncoating, fusion, and endocytosis (Haid et al., 2012; Hsu et al., 2015; Jardim et al., 2018). *Magnolia officinalis,* a member of *Magnoliaceae* family, blocks HCV translation (Lam et al., 2016). Furthermore, *glycyrrhizin,* an inherent compound present in the roots of the *Glycyrrhiza glabra* plant from the *Fabaceae* family, demonstrates anti-HCV activity. It acts specifically by impeding viral translation and replication, leading to a reduction in viral titer (Ashfaq et al., 2011; Matsumoto et al., 2013; Ashfaq and Idrees, 2014; Li et al., 2014; Li et al., 2019).

We previously found that a polyherbal formulation comprising five medicinal plants, including *Silymarin,* showed comparable results to interferon and ribavirin therapy in reducing viral loads in patients with HCV (Nawaz et al., 2015; Nawaz et al., 2016). In addition, polyherbal formulation has been found to have minimal or no side effects and was well-tolerated by patients, while also contributing to an improvement in quality of life. A recent cross-sectional study conducted on patients with HCV infection showed that herbal medicines are safe and effective against HCV (Nsibirwa et al., 2020). Complementary and alternative medicine therapies (CAM) may offer potential benefits in alleviating the chronic liver disease associated with HCV, even though they may not

TABLE 1 Compilation of medicinal plants and their metabolites, along with potential mechanisms of action against HCV.

Medicinal plants/ Metabolites	Effect on HCV	Properties	Mechanism	References
Milk Thistle (Silybum marianum): Asteraceae family	Viral entry, Viral replication	Hepatoprotective, anti-inflammatory	Inhibition of core protein and NS5 RNA-dependent RNA polymerase	Polyak et al. (2007), Polyak et al. (2010), Wagoner et al. (2010), Ahmed-Belkacem et al. (2010), Lovelace et al. (2015)
Diosgenin: A naturally occurring steroid sapogenin present in certain plants including Trigonella foenum-graecum (Family: Fabaceae), Costus speciosus (Family: Costaceae), Tribulus terrestris L (Family: Zygophyllaceae), Smilax china L. (Family: Smilacaceae), Rhizoma polgonation (Family: Asparagaceae)	Viral replication	Antiviral	Inhibition of transcription factor 3 and signal transducer	Wang et al. (2011), Jesus et al. (2016)
Embelia ribes: Primulaceae family	Viral replication	Antiviral	Inhibition of IRES activity and NS3 polymerase	Gonzalez et al. (2009), Bachmetov et al. (2012)
Iridoids: Secondary metabolites in species belonging to the Apocynaceae, Lamiaceae, Loganiaceae, Rubiaceae, Scrophulariaceae and Verbenaceae families	Viral entry	Antiviral	Blockage of E2 and CD81 contact	McGarvey et al. (1988), Zhang et al. (2009)
Luteolin, from the plant Reseda luteola: Resedaceae family	Viral replication	Antiviral	Inhibition of NS5B polymerase activity	Liu et al. (2012), Shibata et al. (2014), Zakaryan et al. (2017)
Naringenin: widely distributed in several Citrus fruits, bergamot, tomatoes and other fruits	Viral assembly	Antiviral	Suppression of core protein activity	Nahmias et al. (2008), Cheung et al. (1988)
Camellia sinensis: Theaceae	HCV replication and viral assembly	Antioxidant, anti-inflammatory, immunomodulatory	Direct antiviral effects against HCV are not well-established. May interfere with activity of NS3 and 4A proteases	Calland et al. (2012b), Calland et al. (2012a), Chen et al. (2012), Haid et al. (2012), Wang et al. (2016), Mekky et al. (2019)
Mangnolia grandiflora: Magnoliaceae family Swietenia macrophylla: Commonly known as mahogany, is a species of tropical hardwood tree belonging to the Meliaceae family. Phyllanthus amarus: Phyllanthus amarus, also known as "bhui amla" or "stonebreaker," is a tropical plant belonging to the Phyllanthaceae family. *Excoecaria agallocha*: Commonly known as the "Blinding Tree" or "Milky Mangrove," is a species of flowering plant in the Euphorbiaceae family	May block viral replication and viral assembly	Hepatoprotective, antiviral efficacy against HCV	-	Lan et al. (2012), Wu et al. (2012), Ravikumar et al. (2011), Bokesch et al. (2003), Takebe et al. (2013), Choi et al. (2014), Li et al. (2012)
Ladanein: is a metabolite found in certain plants, particularly in species belonging to the Labiatae (mint) family	Viral entry, Post attachment entry step	Hepatoprotective	Inhibition of receptor interactions, virus endocytosis, or membrane fusion	Haid et al. (2012), Hsu et al. (2015), Jardim et al. (2018)
Magnolia officinalis: Magnoliaceae family	HCV translation	Hepatoprotective, anti-inflammatory	-	Lam et al. (2016)
Glycyrrhizin: is a natural compound found in the root of the licorice plant (Glycyrrhiza glabra), which belongs to the legume family (Fabaceae)	Viral translation and replication	Antiviral, anti-inflammatory	-	Ashfaq et al. (2011), Ashfaq and Idrees, (2014), Li et al. (2014), Li et al. (2019), Matsumoto et al. (2013)

directly inhibit or eliminate the viral infection itself. Some CAM therapies have shown biological effects, including antioxidant, anti-fibrotic, or immune-modulating activities, which could contribute to the amelioration of the disease (Ferenci et al., 1989). Here are some host factors targeted by CAM therapies that have been studied in the context of viral infections: 1) Immune system modulation: CAM therapies such as herbal supplements, vitamins, and minerals are often used with the aim of modulating the immune system. For example, certain herbs like echinacea (Asteraceae family) and astragalus (Fabaceae family) are believed to have immune-enhancing properties. 2) Some CAM approaches involve the use of herbs and supplements with purported antiviral effects. Examples include elderberry, garlic, and licorice root, which have been studied for their potential to inhibit viral replication. 3) Stress can negatively impact the immune system, making the body more susceptible to infections. Mind-body practices such as meditation, yoga, and acupuncture, which fall under the CAM

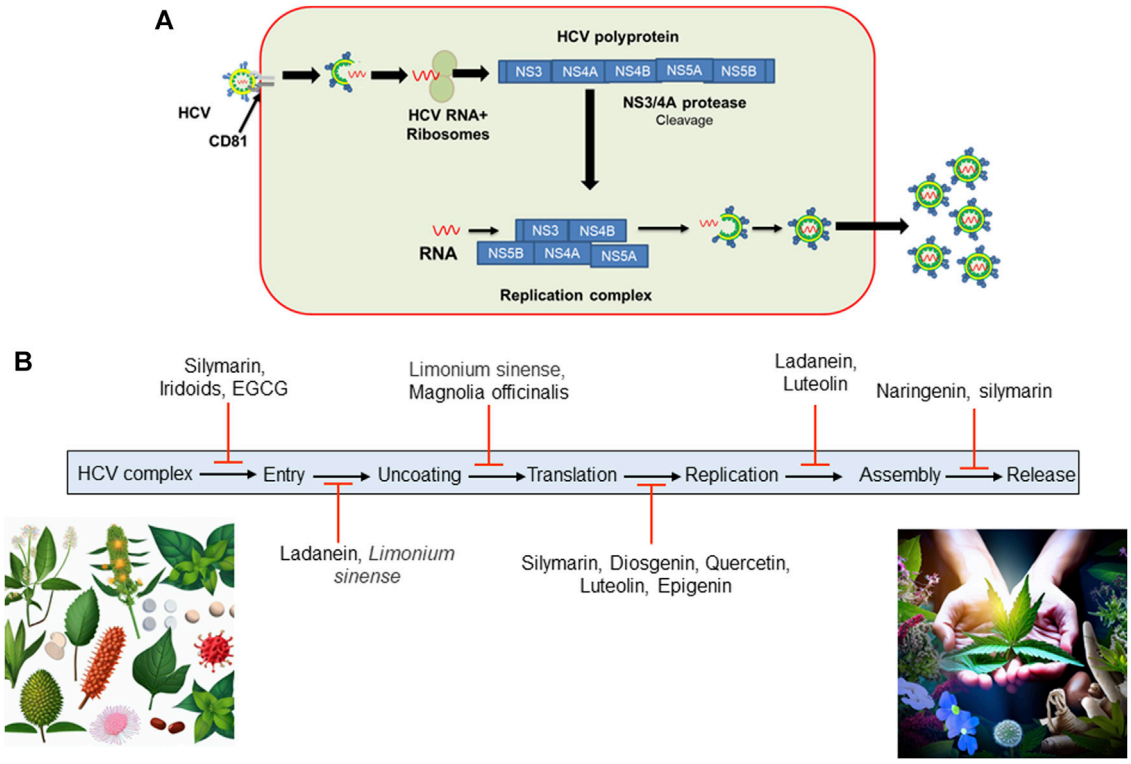

FIGURE 2
(A) HCV entry into hepatocytes. HCV complex enters into hepatocytes and uses a CD81 B-cell as a reservoir. After entry and fusion, the viral genome is released into the cytosol, accompanied by translation and replication. Once replication is complete, HCV assembles a new viral coat and is released from the host cell to infect other cells. **(B)** Certain botanical drugs have been documented to impede HCV activity by disrupting its replication cycle at various stages. (EGCG, Epigallocatechin-3-gallate found in green tea extract; HCV, Hepatitis C Virus).

umbrella, aim to reduce stress and promote overall wellbeing. 4) CAM often emphasizes the importance of a balanced and nutrient-rich diet to support overall health. Nutritional interventions, including dietary supplements and specific diets, may be recommended to enhance the host's nutritional status, potentially supporting the immune response. 5) Probiotics, considered as CAM intervention, focus on supporting a healthy balance of gut bacteria. Since the gut microbiome plays a role in immune function, some CAM practitioners recommend probiotics to enhance the body's defense mechanisms. It is important to note that the scientific evidence supporting these interventions can vary, and further research is often needed for validation.

In China, a combination of seven botanical drugs known as Sho-Sai-Ko or xiao-chai-hu-lang has been used to treat hepatitis C, leading to improvements in liver pathogenicity among selected hepatitis C patients who were not suitable candidates for interferon-based treatments (Deng et al., 2011). Hence, alternative herbal therapy presents a promising option for the treatment of hepatitis C (Nawaz et al., 2015). In Egypt, a year-long randomized double-blind trial was conducted with Silymarin on patients diagnosed with HCV. Despite the safe administration of Silymarin throughout the trial period, the study yielded discouraging outcomes with no significant improvements observed in terms of HCV viral load and serum ALT levels (Tanamly et al., 2004). On the contrary, Hepcinal, a formulation comprising Silymarin alongside four other drugs, exhibited enhanced clinical, biochemical, and serological responses (Nawaz et al., 2016). Shifting our focus to herbal treatments, we delve into their historical roots and significance in HCV management. Prominent herbs such as licorice root (*Glycyrrhiza glabra, Fabaceae family*), and curcumin (*Curcuma longa L. (turmeric)* of ginger family (*Zingiberaceae*)) have been subject to scientific scrutiny for their potential hepatoprotective and antiviral properties. Metabolites including flavonoids, alkaloids, and polyphenols present in *Phyllanthus niruri L. (Phyllanthaceae family)*, *Glycyrrhiza glabra* (licorice), and *Silybum marianum L.) Gaertn* (milk thistle) (Asteraceae family) have shown potential in inhibiting viral replication. Many medicinal plants including *Schisandra chinensis* (Schisandraceae family) and *Picrorhiza kurroa* (Plantaginaceae family), possess hepatoprotective properties, protecting liver from further damage. Some herbs, such as *Curcuma longa* (turmeric) (Zingiberaceae family), exhibit anti-inflammatory property that may help to mitigate the immune response and reduce liver inflammation. Overall, botanical drug(s), individually or in combination, are effective against HCV infection, blocking viral entry, translation, replication, and assembly. Furthermore, we acknowledge the challenges posed by the lack of standardization and quality control in herbal products. However, it is crucial to emphasize the need for further pharmacological investigations and large-scale clinical trials to validate the clinical safety and efficacy of these botanical drugs. We have summarized the effectiveness of selected botanical drugs and their ability to inhibit HCV activity in Figures 2A,B. In summary, while some botanical drugs may offer potential benefits for liver health, their use for HCV treatment should be approached with caution. Consultation with a healthcare provider and adherence to conventional medical treatments are

essential for managing HCV effectively. As far as our current knowledge extends, there are no large-scale cross-sectional studies available that comprehensively demonstrate the clinical and serological outcomes of botanical drugs in treating HCV. However, in smaller-scale studies, researchers have documented the potential benefits of medicinal plants in combating HCV infection and have elucidated some of the molecular mechanisms involved. Additional research is needed to further understand the mechanisms underlying these improvements resulting from herbal treatments, as well as to provide additional evidence regarding their effectiveness and safety.

Future perspectives and limitations

The emergence of new therapeutic approaches holds promise for curing a greater number of HCV patients. The availability of potent natural or botanical drugs for HCV infection is a positive development. Consequently, there should be a heightened focus on the screening and identification of potent medicinal plants for the management and treatment of both acute and chronic HCV infections. This exploration of botanical drugs may lead to more effective and accessible treatments for individuals affected by HCV.

Author contributions

AN: Conceptualization, Supervision, Writing–original draft, Writing–review and editing. AM: Writing–review and editing. SeA: Writing–original draft. NA: Writing–original draft. WA: Writing–review and editing. MAM: Writing–review and editing. MB: Writing–review and editing. AS: Writing–review and editing. SlA: Writing–review and editing. IJ: Writing–original draft. TN: Reviewing final draft.

Funding

The author(s) declare financial support was received for the research, authorship, and/or publication of this article from Japan Foundation for Applied Enzymology (a grant for Front Runner of Future Diabetes Research (to AN). This work was supported by the Young Research Grant from the Japan Diabetes Society (to AN) and Cell Science Foundation (to AN).

Acknowledgments

We would like to thank Editage (www.editage.com) for English language editing. The authors extend their appreciation to the all members of First Department of Internal Medicine and Department of Molecular and Medical Pharmacology, University of Toyama, Toyama, Japan.

Conflict of interest

The authors declare that the research was conducted in the absence of any commercial or financial relationships that could be construed as a potential conflict of interest.

Publisher's note

References

Ahmed-Belkacem, A., Ahnou, N., Barbotte, L., Wychowski, C., Pallier, C., Brillet, R., et al. (2010). Silibinin and related compounds are direct inhibitors of hepatitis C virus RNA-dependent RNA polymerase. *Gastroenterology* 138, 1112–1122. doi:10.1053/j.gastro.2009.11.053

Alharthi, J., Latchoumanin, O., George, J., and Eslam, M. (2020). Macrophages in metabolic associated fatty liver disease. *World J. Gastroenterol.* 26, 1861–1878. doi:10.3748/wjg.v26.i16.1861

Ashfaq, U. A., and Idrees, S. (2014). Medicinal plants against hepatitis C virus. *World J. Gastroenterol.* 20, 2941–2947. doi:10.3748/wjg.v20.i11.2941

Ashfaq, U. A., Masoud, M. S., Nawaz, Z., and Riazuddin, S. (2011). Glycyrrhizin as antiviral agent against hepatitis C virus. *J. Transl. Med.* 9, 112. doi:10.1186/1479-5876-9-112

Asselah, T., Marcellin, P., and Schinazi, R. F. (2018). Treatment of hepatitis C virus infection with direct-acting antiviral agents: 100% cure?. *Liver Int.* 38 (1), 7–13. doi:10.1111/liv.13673

Bachmetov, L., Gal-Tanamy, M., Shapira, A., Vorobeychik, M., Giterman-Galam, T., Sathiyamoorthy, P., et al. (2012). Suppression of hepatitis C virus by the flavonoid quercetin is mediated by inhibition of NS3 protease activity. *J. Viral Hepat.* 19, e81–e88. doi:10.1111/j.1365-2893.2011.01507.x

Bodenheimer, H. C., JR., Lindsay, K. L., Davis, G. L., Lewis, J. H., Thung, S. N., and Seeff, L. B. (1997). Tolerance and efficacy of oral ribavirin treatment of chronic hepatitis C: a multicenter trial. *Hepatology* 26, 473–477. doi:10.1002/hep.510260231

Bokesch, H. R., O'Keefe, B. R., Mckee, T. C., Pannell, L. K., Patterson, G. M., Gardella, R. S., et al. (2003). A potent novel anti-HIV protein from the cultured cyanobacterium Scytonema varium. *Biochemistry* 42, 2578–2584. doi:10.1021/bi0205698

Calland, N., Albecka, A., Belouzard, S., Wychowski, C., Duverlie, G., Descamps, V., et al. (2012a). (-)-Epigallocatechin-3-gallate is a new inhibitor of hepatitis C virus entry. *Hepatology* 55, 720–729. doi:10.1002/hep.24803

Calland, N., Dubuisson, J., Rouillé, Y., and Séron, K. (2012b). Hepatitis C virus and natural compounds: a new antiviral approach? *Viruses* 4, 2197–2217. doi:10.3390/v4102197

Chen, C., Qiu, H., Gong, J., Liu, Q., Xiao, H., Chen, X. W., et al. (2012). (-)-Epigallocatechin-3-gallate inhibits the replication cycle of hepatitis C virus. *Arch. Virol.* 157, 1301–1312. doi:10.1007/s00705-012-1304-0

Cheung, R., Dickins, J., Nicholson, P. W., Thomas, A. S., Smith, H. H., Larson, H. E., et al. (1988). Compliance with anti-tuberculous therapy: a field trial of a pill-box with a concealed electronic recording device. *Eur. J. Clin. Pharmacol.* 35, 401–407. doi:10.1007/BF00561372

Chia, C. W., Egan, J. M., and Ferrucci, L. (2018). Age-related changes in glucose metabolism, hyperglycemia, and cardiovascular risk. *Circulation Res.* 123, 886–904. doi:10.1161/CIRCRESAHA.118.312806

Choi, M., Kim, Y. M., Lee, S., Chin, Y. W., and Lee, C. (2014). Mangosteen xanthones suppress hepatitis C virus genome replication. *Virus Genes* 49, 208–222. doi:10.1007/s11262-014-1098-0

Christensen, S., Buggisch, P., Mauss, S., Böker, K. H. W., Schott, E., Klinker, H., et al. (2018). Direct-acting antiviral treatment of chronic HCV-infected patients on opioid substitution therapy: still a concern in clinical practice? *Addiction* 113, 868–882. doi:10.1111/add.14128

Davis, G. L., Esteban-Mur, R., Rustgi, V., Hoefs, J., Gordon, S. C., Trepo, C., et al. (1998). Interferon alfa-2b alone or in combination with ribavirin for the treatment of relapse of chronic hepatitis C. International Hepatitis Interventional Therapy Group. *N. Engl. J. Med.* 339, 1493–1499. doi:10.1056/NEJM199811193392102

Deng, G., Kurtz, R. C., Vickers, A., Lau, N., Yeung, K. S., Shia, J., et al. (2011). A single arm phase II study of a Far-Eastern traditional herbal formulation (sho-sai-ko-to or xiao-chai-hu-tang) in chronic hepatitis C patients. *J. Ethnopharmacol.* 136, 83–87. doi:10.1016/j.jep.2011.04.008

Drazilova, S., Gazda, J., Janicko, M., and Jarcuska, P. (2018). Chronic hepatitis C association with diabetes mellitus and cardiovascular risk in the era of DAA therapy. *Can. J. Gastroenterology Hepatology* 2018, 6150861. doi:10.1155/2018/6150861

Farrell, G. C., Bacon, B. R., and Goldin, R. D. (1998). Lymphoblastoid interferon alfa-n1 improves the long-term response to a 6-month course of treatment in chronic hepatitis C compared with recombinant interferon alfa-2b: results of an international randomized controlled trial. Clinical Advisory Group for the Hepatitis C Comparative Study. *Hepatology* 27, 1121–1127. doi:10.1002/hep.510270429

Ferenci, P., Dragosics, B., Dittrich, H., Frank, H., Benda, L., Lochs, H., et al. (1989). Randomized controlled trial of silymarin treatment in patients with cirrhosis of the liver. *J. Hepatol.* 9, 105–113. doi:10.1016/0168-8278(89)90083-4

Fujisaka, S., Usui, I., Bukhari, A., Ikutani, M., Oya, T., Kanatani, Y., et al. (2009). Regulatory mechanisms for adipose tissue M1 and M2 macrophages in diet-induced obese mice. *Diabetes* 58, 2574–2582. doi:10.2337/db08-1475

Fujisaka, S., Usui, I., Ikutani, M., Aminuddin, A., Takikawa, A., Tsuneyama, K., et al. (2013). Adipose tissue hypoxia induces inflammatory M1 polarity of macrophages in an HIF-1α-dependent and HIF-1α-independent manner in obese mice. *Diabetologia* 56, 1403–1412. doi:10.1007/s00125-013-2885-1

Fujisaka, S., Usui, I., Nawaz, A., Takikawa, A., Kado, T., Igarashi, Y., et al. (2016). M2 macrophages in metabolism. *Diabetol. Int.* 7, 342–351. doi:10.1007/s13340-016-0290-y

Gonzalez, O., Fontanes, V., Raychaudhuri, S., Loo, R., Loo, J., Arumugaswami, V., et al. (2009). The heat shock protein inhibitor Quercetin attenuates hepatitis C virus production. *Hepatology* 50, 1756–1764. doi:10.1002/hep.23232

Haid, S., Novodomská, A., Gentzsch, J., Grethe, C., Geuenich, S., Bankwitz, D., et al. (2012). A plant-derived flavonoid inhibits entry of all HCV genotypes into human hepatocytes. *Gastroenterology* 143, 213–222. doi:10.1053/j.gastro.2012.03.036

Hoofnagle, J. H., Mullen, K. D., Jones, D. B., Rustgi, V., Di Bisceglie, A., Peters, M., et al. (1986). Treatment of chronic non-A,non-B hepatitis with recombinant human alpha interferon. A preliminary report. *N. Engl. J. Med.* 315, 1575–1578. doi:10.1056/NEJM198612183152503

Hsu, W.-C., Chang, S.-P., Lin, L.-C., Li, C.-L., Richardson, C. D., Lin, C.-C., et al. (2015). Limonium sinense and gallic acid suppress hepatitis C virus infection by blocking early viral entry. *Antivir. Res.* 118, 139–147. doi:10.1016/j.antiviral.2015.04.003

Ito, M., Kusunoki, H., and Mizuochi, T. (2011). Peripheral B cells as reservoirs for persistent HCV infection. *Front. Microbiol.* 2, 177. doi:10.3389/fmicb.2011.00177

Jacobson, I. M., Cacoub, P., Dal Maso, L., Harrison, S. A., and Younossi, Z. M. (2010). Manifestations of chronic hepatitis C virus infection beyond the liver. *Clin. Gastroenterol. Hepatol.* 8, 1017–1029. doi:10.1016/j.cgh.2010.08.026

Jardim, A. C. G., Shimizu, J. F., Rahal, P., and Harris, M. (2018). Plant-derived antivirals against hepatitis c virus infection. *Virology J.* 15, 34. doi:10.1186/s12985-018-0945-3

Jesus, M., Martins, A. P., Gallardo, E., and Silvestre, S. (2016). Diosgenin: recent highlights on Pharmacology and analytical methodology. *J. Anal. Methods Chem.* 2016, 4156293. doi:10.1155/2016/4156293

Kazankov, K., Jørgensen, S. M. D., Thomsen, K. L., Møller, H. J., Vilstrup, H., George, J., et al. (2019). The role of macrophages in nonalcoholic fatty liver disease and nonalcoholic steatohepatitis. *Nat. Rev. Gastroenterology Hepatology* 16, 145–159. doi:10.1038/s41575-018-0082-x

Lam, P., Cheung, F., Tan, H. Y., Wang, N., Yuen, M. F., and Feng, Y. (2016). Hepatoprotective effects of Chinese medicinal herbs: a focus on anti-inflammatory and anti-oxidative activities. *Int. J. Mol. Sci.* 17, 465. doi:10.3390/ijms17040465

Lan, K. H., Wang, Y. W., Lee, W. P., Lan, K. L., Tseng, S. H., Hung, L. R., et al. (2012). Multiple effects of Honokiol on the life cycle of hepatitis C virus. *Liver Int.* 32, 989–997. doi:10.1111/j.1478-3231.2011.02621.x

Li, J. Y., Cao, H. Y., Liu, P., Cheng, G. H., and Sun, M. Y. (2014). Glycyrrhizic acid in the treatment of liver diseases: literature review. *Biomed. Res. Int.* 2014, 872139. doi:10.1155/2014/872139

Liu, M. M., Zhou, L., He, P. L., Zhang, Y. N., Zhou, J. Y., Shen, Q., et al. (2012). Discovery of flavonoid derivatives as anti-HCV agents via pharmacophore search combining molecular docking strategy. *Eur. J. Med. Chem.* 52, 33–43. doi:10.1016/j.ejmech.2012.03.002

Li, X., Sun, R., and Liu, R. (2019). Natural products in licorice for the therapy of liver diseases: progress and future opportunities. *Pharmacol. Res.* 144, 210–226. doi:10.1016/j.phrs.2019.04.025

Li, Y., Yu, S., Liu, D., Proksch, P., and Lin, W. (2012). Inhibitory effects of polyphenols toward HCV from the mangrove plant *Excoecaria agallocha* L. *Bioorg Med. Chem. Lett.* 22, 1099–1102. doi:10.1016/j.bmcl.2011.11.109

Lovelace, E. S., Wagoner, J., Macdonald, J., Bammler, T., Bruckner, J., Brownell, J., et al. (2015). Silymarin suppresses cellular inflammation by inducing reparative stress signaling. *J. Nat. Prod.* 78, 1990–2000. doi:10.1021/acs.jnatprod.5b00288

Luo, H., Mu, W. C., Karki, R., Chiang, H. H., Mohrin, M., Shin, J. J., et al. (2019). Mitochondrial stress-initiated aberrant activation of the NLRP3 inflammasome regulates the functional deterioration of hematopoietic stem cell aging. *Cell Rep.* 26, 945–954. doi:10.1016/j.celrep.2018.12.101

Matsumoto, Y., Matsuura, T., Aoyagi, H., Matsuda, M., Hmwe, S. S., Date, T., et al. (2013). Antiviral activity of glycyrrhizin against hepatitis C virus *in vitro*. *PLoS One* 8, e68992. doi:10.1371/journal.pone.0068992

Mcgarvey, P., Helling, R. B., Lee, J. Y., Engelke, D. R., and El-Gewely, M. R. (1988). Initiation of rrn transcription in chloroplasts of Euglena gracilis bacillaris. *Curr. Genet.* 14, 493–500. doi:10.1007/BF00521275

Mchutchison, J. G., Gordon, S. C., Schiff, E. R., Shiffman, M. L., Lee, W. M., Rustgi, V. K., et al. (1998). Interferon alfa-2b alone or in combination with ribavirin as initial treatment for chronic hepatitis C. Hepatitis Interventional Therapy Group. *N. Engl. J. Med.* 339, 1485–1492. doi:10.1056/NEJM199811193392101

Mekky, R. Y., El-Ekiaby, N., El Sobky, S. A., Elemam, N. M., Youness, R. A., El-Sayed, M., et al. (2019). Epigallocatechin gallate (EGCG) and miR-548m reduce HCV entry through repression of CD81 receptor in HCV cell models. *Arch. Virol.* 164, 1587–1595. doi:10.1007/s00705-019-04232-x

Moustafa, H., Madkour, M., Hamed, F., Abouelnazar, S., Abo Elwafa, R., and Moaaz, M. (2020). Modulation of memory B cell phenotypes and toll-like receptor-7 in chronic hepatitis C virus infection during direct-acting antiviral interferon-free therapy: correlation with interleukin-7. *Viral Immunol.* 34, 227–240. doi:10.1089/vim.2020.0110

Nahmias, Y., Goldwasser, J., Casali, M., Van Poll, D., Wakita, T., Chung, R. T., et al. (2008). Apolipoprotein B-dependent hepatitis C virus secretion is inhibited by the grapefruit flavonoid naringenin. *Hepatology* 47, 1437–1445. doi:10.1002/hep.22197

Nainan, O. V., Alter, M. J., Kruszon-Moran, D., Gao, F.-X., Xia, G., Mcquillan, G., et al. (2006). Hepatitis C virus genotypes and viral concentrations in participants of a general population survey in the United States. *Gastroenterology* 131, 478–484. doi:10.1053/j.gastro.2006.06.007

Nawaz, A., Aminuddin, A., Kado, T., Takikawa, A., Yamamoto, S., Tsuneyama, K., et al. (2017a). CD206+ M2-like macrophages regulate systemic glucose metabolism by inhibiting proliferation of adipocyte progenitors. *Nat. Commun.* 8, 286. doi:10.1038/s41467-017-00231-1

Nawaz, A., Kado, T., Igarashi, Y., Kunimasa, Y., Usui, I., Fujisaka, S., et al. (2017b). Adipose tissue-resident macrophages and obesity. *RADS J. Pharm. Pharm. Sci.* 5, 3. (2017): Contents of Volume 5(3) July-September 2017.

Nawaz, A., Nazar, H., Usmanghani, K., Sheikh, Z. A., Chishti, M. A., and Ahmad, I. (2016). Ways to manage hepatitis C without cirrhosis: treatment by comparison of coded eastern medicine hepcinal with interferon alpha 2b and ribavirin. *Pak J. Pharm. Sci.* 29, 919–927.

Nawaz, A., Zaidi, S. F., Usmanghani, K., and Ahmad, I. (2015). Concise review on the insight of hepatitis C. *J. Taibah Univ. Med. Sci.* 10, 132–139. doi:10.1016/j.jtumed.2014.08.004

Nsibirwa, S., Anguzu, G., Kamukama, S., Ocama, P., and Nankya-Mutyoba, J. (2020). Herbal medicine use among patients with viral and non-viral Hepatitis in Uganda: prevalence, patterns and related factors. *BMC Complementary Med. Ther.* 20, 169. doi:10.1186/s12906-020-02959-8

Polyak, S. J., Morishima, C., Lohmann, V., Pal, S., Lee, D. Y., Liu, Y., et al. (2010). Identification of hepatoprotective flavonolignans from silymarin. *Proc. Natl. Acad. Sci. U. S. A.* 107, 5995–5999. doi:10.1073/pnas.0914009107

Polyak, S. J., Morishima, C., Shuhart, M. C., Wang, C. C., Liu, Y., and Lee, D. Y. (2007). Inhibition of T-cell inflammatory cytokines, hepatocyte NF-kappaB signaling, and HCV infection by standardized Silymarin. *Gastroenterology* 132, 1925–1936. doi:10.1053/j.gastro.2007.02.038

Ravikumar, Y. S., Ray, U., Nandhitha, M., Perween, A., Raja Naika, H., Khanna, N., et al. (2011). Inhibition of hepatitis C virus replication by herbal extract: Phyllanthus amarus as potent natural source. *Virus Res.* 158, 89–97. doi:10.1016/j.virusres.2011.03.014

Reidy, P. T., Mckenzie, A. I., Mahmassani, Z. S., Petrocelli, J. J., Nelson, D. B., Lindsay, C. C., et al. (2019). Aging impairs mouse skeletal muscle macrophage polarization and muscle-specific abundance during recovery from disuse. *Am. J. Physiology-Endocrinology Metabolism* 317, E85–E98. doi:10.1152/ajpendo.00422.2018

Sakai, M., Troutman, T. D., Seidman, J. S., Ouyang, Z., Spann, N. J., Abe, Y., et al. (2019). Liver-derived signals sequentially reprogram myeloid enhancers to initiate and maintain kupffer cell identity. *Immunity* 51, 655–670. doi:10.1016/j.immuni.2019.09.002

Shibata, C., Ohno, M., Otsuka, M., Kishikawa, T., Goto, K., Muroyama, R., et al. (2014). The flavonoid apigenin inhibits hepatitis C virus replication by decreasing mature microRNA122 levels. *Virology* 462-463, 42–48. doi:10.1016/j.virol.2014.05.024

Singh, G. K., and Hoyert, D. L. (2000). Social epidemiology of chronic liver disease and cirrhosis mortality in the United States, 1935-1997: trends and differentials by ethnicity, socioeconomic status, and alcohol consumption. *Hum. Biol.* 72, 801–820.

Stanaway, J. D., Flaxman, A. D., Naghavi, M., Fitzmaurice, C., Vos, T., Abubakar, I., et al. (2016). The global burden of viral hepatitis from 1990 to 2013: findings from the Global Burden of Disease Study 2013. *Lancet* 388, 1081–1088. doi:10.1016/S0140-6736(16)30579-7

Takebe, Y., Saucedo, C. J., Lund, G., Uenishi, R., Hase, S., Tsuchiura, T., et al. (2013). Antiviral lectins from red and blue-green algae show potent *in vitro* and *in vivo* activity against hepatitis C virus. *PLoS One* 8, e64449. doi:10.1371/journal.pone.0064449

Takikawa, A., Usui, I., Fujisaka, S., Tsuneyama, K., Okabe, K., Nakagawa, T., et al. (2019). Macrophage-specific hypoxia-inducible factor-1α deletion suppresses the development of liver tumors in high-fat diet-fed obese and diabetic mice. *J. Diabetes Investig.* 10, 1411–1418. doi:10.1111/jdi.13047

Tanamly, M. D., Tadros, F., Labeeb, S., Makld, H., Shehata, M., Mikhail, N., et al. (2004). Randomised double-blinded trial evaluating silymarin for chronic hepatitis C in an Egyptian village: study description and 12-month results. *Dig. Liver Dis.* 36, 752–759. doi:10.1016/j.dld.2004.06.015

Tong, M. J., Blatt, L. M., Mchutchison, J. G., Co, R. L., and Conrad, A. (1997). Prediction of response during interferon alfa 2b therapy in chronic hepatitis C patients using viral and biochemical characteristics: a comparison. *Hepatology* 26, 1640–1645. doi:10.1002/hep.510260637

Vanni, E., Bugianesi, E., and Saracco, G. (2016). Treatment of type 2 diabetes mellitus by viral eradication in chronic hepatitis C: myth or reality? *Dig. Liver Dis.* 48, 105–111. doi:10.1016/j.dld.2015.10.016

Wagoner, J., Negash, A., Kane, O. J., Martinez, L. E., Nahmias, Y., Bourne, N., et al. (2010). Multiple effects of silymarin on the hepatitis C virus lifecycle. *Hepatology* 51, 1912–1921. doi:10.1002/hep.23587

Wang, Y. J., Pan, K. L., Hsieh, T. C., Chang, T. Y., Lin, W. H., and Hsu, J. T. (2011). Diosgenin, a plant-derived sapogenin, exhibits antiviral activity *in vitro* against hepatitis C virus. *J. Nat. Prod.* 74, 580–584. doi:10.1021/np100578u

Wang, Y., Li, J., Wang, X., Peña, J. C., Li, K., Zhang, T., et al. (2016). (-)-Epigallocatechin-3-Gallate enhances hepatitis C virus double-stranded RNA intermediates-triggered innate immune responses in hepatocytes. *Sci. Rep.* 6, 21595. doi:10.1038/srep21595

WHO (2022). Hepatitis C (2021). Available online at: https://www.who.int/news-room/fact-sheets/detail/hepatitis-c (Accessed May 7, 2022).

Wu, S. F., Lin, C. K., Chuang, Y. S., Chang, F. R., Tseng, C. K., Wu, Y. C., et al. (2012). Anti-hepatitis C virus activity of 3-hydroxy caruilignan C from Swietenia macrophylla stems. *J. Viral Hepat.* 19, 364–370. doi:10.1111/j.1365-2893.2011.01558.x

Zakaryan, H., Arabyan, E., Oo, A., and Zandi, K. (2017). Flavonoids: promising natural compounds against viral infections. *Archives Virology* 162, 2539–2551. doi:10.1007/s00705-017-3417-y

Zhang, H., Rothwangl, K., Mesecar, A. D., Sabahi, A., Rong, L., and Fong, H. H. (2009). Lamiridosins, hepatitis C virus entry inhibitors from Lamium album. *J. Nat. Prod.* 72, 2158–2162. doi:10.1021/np900549e

Zhang, H., Ryu, D., Wu, Y., Gariani, K., Wang, X., Luan, P., et al. (2016). NAD$^+$ repletion improves mitochondrial and stem cell function and enhances life span in mice. *Science* 352, 1436–1443. doi:10.1126/science.aaf2693

frontiers | Frontiers in Pharmacology

TYPE Systematic Review
PUBLISHED 29 January 2024
DOI 10.3389/fphar.2024.1315584

OPEN ACCESS

EDITED BY
Rongrui Wei,
Jiangxi University of Traditional Chinese Medicine, China

REVIEWED BY
Feng Zhang,
Nanjing University of Chinese Medicine, China
Mengnan Liu,
Southwest Medical University, China

*CORRESPONDENCE
Jinhao Zeng,
zengjinhao@cdutcm.edu.cn
Yu Chen,
735405661@qq.com
Xiao Ma,
tobymaxiao@cdutcm.edu.cn

†These authors have contributed equally to this work and share first authorship

RECEIVED 10 October 2023
ACCEPTED 08 January 2024
PUBLISHED 29 January 2024

CITATION
Feng W, Kao T-c, Jiang J, Zeng X, Chen S, Zeng J, Chen Y and Ma X (2024), The dynamic equilibrium between the protective and toxic effects of matrine in the development of liver injury: a systematic review and meta-analysis. *Front. Pharmacol.* 15:1315584. doi: 10.3389/fphar.2024.1315584

The dynamic equilibrium between the protective and toxic effects of matrine in the development of liver injury: a systematic review and meta-analysis

Weiyi Feng[1,2,3†], Te-chan Kao[1,2,3†], Jiajie Jiang[1,2,3†], Xinyu Zeng[2,4], Shuang Chen[2,4], Jinhao Zeng[1,3,5*], Yu Chen[1,3,5*] and Xiao Ma[2,4*]

[1]TCM Regulating Metabolic Diseases Key Laboratory of Sichuan Province, Hospital of Chengdu University of Traditional Chinese Medicine, Chengdu, China, [2]State Key Laboratory of Southwestern Chinese Medicine Resources, Chengdu University of Traditional Chinese Medicine, Chengdu, China, [3]School of Clinical Medicine, Chengdu University of Traditional Chinese Medicine, Chengdu, China, [4]School of Pharmacy, Chengdu University of Traditional Chinese Medicine, Chengdu, China, [5]Hospital of Chengdu University of Traditional Chinese Medicine, Chengdu, China

Background: Matrine, an alkaloid derived from the dried roots of *Sophora flavescens* Aiton, has been utilized for the treatment of liver diseases, but its potential hepatotoxicity raises concerns. However, the precise condition and mechanism of action of matrine on the liver remain inconclusive. Therefore, the objective of this systematic review and meta-analysis is to comprehensively evaluate both the hepatoprotective and hepatotoxic effects of matrine and provide therapeutic guidance based on the findings.

Methods: The meta-analysis systematically searched relevant preclinical literature up to May 2023 from eight databases, including PubMed, Web of Science, Cochrane Library, Embase, China National Knowledge Infrastructure, WanFang Med Online, China Science and Technology Journal Database, and China Biomedical Literature Service System. The CAMARADES system assessed the quality and bias of the evidence. Statistical analysis was conducted using STATA, which included the use of 3D maps and radar charts to display the effects of matrine dosage and frequency on hepatoprotection and hepatotoxicity.

Results: After a thorough screening, 24 studies involving 657 rodents were selected for inclusion. The results demonstrate that matrine has bidirectional effects on ALT and AST levels, and it also regulates SOD, MDA, serum TG, serum TC, IL-6, TNF-α, and CAT levels. Based on our comprehensive three-dimensional analysis, the optimal bidirectional effective dosage of matrine ranges from 10 to 69.1 mg/kg. However, at a dose of 20–30 mg/kg/d for 0.02–0.86 weeks, it demonstrated high liver protection and low toxicity. The molecular docking analysis revealed the interaction between MT and SERCA as well as SREBP-SCAP complexes. Matrine could alter Ca^{2+} homeostasis in liver injury via multiple pathways, including the SREBP1c/SCAP, Notch/RBP-J/HES1, IκK/NF-κB, and Cul3/Rbx1/Keap1/Nrf2.

Conclusion: Matrine has bidirectional effects on the liver at doses ranging from 10 to 69.1 mg/kg by influencing Ca^{2+} homeostasis in the cytoplasm, endoplasmic reticulum, Golgi apparatus, and mitochondria.

Systematic review registration: https://inplasy.com/, identifier INPLASY202340114

KEYWORDS

matrine, hepatotoxicity, hepatoprotection, liver injury, meta-analysis

1 Introduction

Liver injury (LI) is a prevalent liver disease and a significant global health concern due to its high mortality rates. The European Association for the Study of the Liver (EASL) has reported that liver disease ranks 11th as the leading cause of death worldwide, accounting for 4% of all deaths. In 2023, Devarbhavi et al. estimated over two million fatalities annually due to liver disease (Devarbhavi et al., 2023). As a preliminary stage of liver disease, LI can be caused by various factors such as alcohol, infection, immunity, and drug-induced toxicity (Younossi et al., 2023). The severity of LI can range from mild inflammation to more severe conditions like liver cirrhosis, liver failure and even death. Symptoms of LI consist of abnormalities in liver function test abnormalities, fever, nausea, vomiting, jaundice, and right epigastric pain (Knight, 2005). Hepatocellular damage, fibrosis, and inflammatory infiltration are key pathological features of LI. Anti-viral drugs, liver protective agents, and immunosuppressive drugs are the mainstream drugs used to treat LI. While corticosteroids, pioglitazone, cholestyramine, and other medications are commonly prescribed to treat different types of LI (Devarbhavi et al., 2023), their hepatotoxicity can lead to drug-induced liver injury (DILI) in clinical settings. Therefore, exploring more effective and safer alternatives for LI is necessary.

The dried roots of *Sophora flavescens* Aiton (well-documented in The Plant List www.theplantlist.org), a Traditional Chinese Medicine (TCM) herb, commonly known as KuShen, was initially discovered for its therapeutic properties in the ancient text *Shen Nong Ben Cao Jing*. For thousands of years, the dried roots of *S. flavescens* Aiton has been widely used to treat various digestive disorders, such as dysentery, bloody stools, jaundice, and especially liver diseases (Chinese Pharmacopoeia Commission, 2020). Kushen Decoction and Longdan Kushen Decoction are the representative TCM prescriptions that incorporate the dried roots of *S. flavescens* Aiton for treating liver disease. Contemporary pharmacological studies have revealed that extracts of the dried roots of *S. flavescens* Aiton have hepatoprotective effects due to their anti-inflammatory and antiviral properties (He et al., 2015).

Matrine ((1R,2R,9S,17S)-7,13-diazatetracyclo [7.7.1.02,7.013,17] heptadecan-6-one; $C_{15}H_{24}N_2O$; MW = 248.36) is an alkaloid extracted from the dried roots of *S. flavescens* Aiton and can be dissolved in various solvents such as water, ethanol, benzene, etc .,(Sun et al., 2022). As an active ingredient of the dried roots of *S. flavescens* Aiton, the total content of matrine and oxymatrine should not be less than 1.2% according to the Pharmacopoeia of the People's Republic of China (Chinese Pharmacopoeia Commission, 2020). Numerous studies have shown that MT has anti-inflammatory, anti-viral, anti-tumor, and immune-suppressive abilities (Zhou et al., 2014; Wang et al., 2018; Peng et al., 2020; Chu et al., 2021; Jing et al., 2021). MT has been reported to regulate liver protective function, hepatic regeneration, and alleviate LI through several signaling pathways, such as TGF-β/Smad, NF-κB, Wnt/β-catenin, Notch/Jagged1/recombination signal binding protein for immunoglobulin kappa J (RBP-Jκ, RBP-J)/hairy and enhancer of split-1 (HES1) (Yu H. B. et al., 2011; Yu et al., 2014; Yang et al., 2016; Yin et al., 2018). Due to its extensive pharmacological effects, MT is often used as an injection in clinical practice for hepatitis B, tumors, and immune diseases (Liu and Zhang, 2021). In the clinical pharmacokinetic study of MT, serum MT concentrations ranged from 1 to 6 ug/mL after a large-dose intravenous infusion (6 mg/kg) (Zhang et al., 2009). In rats, the maximum blood concentration of MT was found to reach 2,412 ± 362 ng/mL and 94.6 ± 38.6 ng/mL after intravenous or oral

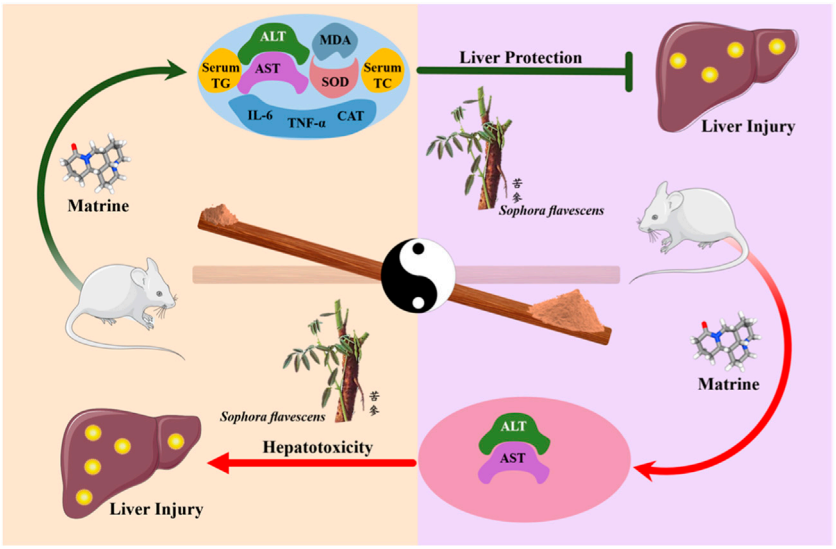

GRAPHICAL ABSTRACT

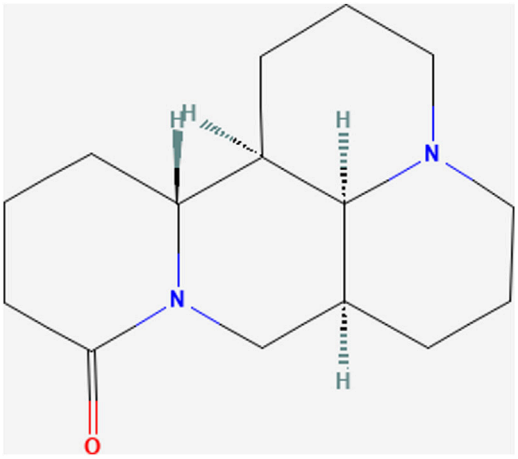

FIGURE 1
Chemical structure of Matrine. (PubChem Identifier: CID 91466, URL: https://pubchem.ncbi.nlm.nih.gov/compound/91466#section=2D-Structure).

administration of MT at a dose of 2 mg/kg (Yang et al., 2010). However, in recent years, several studies have demonstrated that MT can lead to DILI, reproductive toxicity, and neurotoxicity (Wang et al., 2017). MT has been demonstrated to induce hepatotoxicity through inhibiting the Nrf2 pathway and stimulating the reactive oxygen species (ROS)-mediated mitochondrial apoptosis pathway (You et al., 2019). Nevertheless, the mechanisms of MT in liver protection and hepatotoxicity are continually being improved and elucidated (Figure 1).

Calcium ion (Ca^{2+}), a multifunctional intracellular messenger, affects cellular metabolism, energy generation, and intracellular homeostasis under physiological conditions. Extracellular stress stimulation on the cell membrane could enhance Ca^{2+} influx, and increased cytoplasmic Ca^{2+} would be transported into the Endoplasmic reticulum (ER) lumen and stored via cross specific Ca^{2+} ion channels, such as sarcoendoplasmic reticulum calcium transport ATPase (SERCA) (Periasamy and Kalyanasundaram, 2007; Chemaly et al., 2018). Loss of Ca^{2+} homeostasis and irregular Ca^{2+} channels on the cell membrane, ER, and mitochondria might cause ER stress and modify the mitochondrial membrane potential, raising total ROS in hepatocytes (Kaufman and Malhotra, 2014; Zeeshan et al., 2016). Based on the current literature, distinct MT concentration gradients can influence diverse SERCA responses on the ER, regulate mitochondrial activity, and balance intracellular Ca^{2+} levels to alleviate or promote hepatocyte stress (Gao et al., 2019).

Previous studies have demonstrated that MT exhibits both hepatoprotective effects and the potential to cause liver damage, yet the underlying mechanisms remain unclear. Therefore, the objective of this study is to conduct a systematic review and meta-analysis to investigate the impact of MT on LI and elucidate the dynamic processes through which MT leads to liver protection and hepatotoxicity. Additionally, this study aims to explore the role of Ca^{2+} in these processes, offering innovative insights into the mechanisms involved.

2 Methods

2.1 Registration of the meta-analysis

The meta-analysis followed the PRISMA 2020 guidelines and has been submitted to the International Platform of Registered Systematic Review and Meta-analysis Protocols (INPLASY) database (https://inplasy.com/). The registration number for this submission is INPLASY202340114.

2.2 Data sources and search strategy

The retrieved databases included four English databases and four Chinese databases according to the five articles (Ju et al., 2018; Xiong et al., 2019; Liu et al., 2021; Luo et al., 2021; Zheng et al., 2021). The four English databases were: PubMed, Web of science, Cochrane library, Embase. And the four Chinese databases: China National Knowledge Infrastructure, WanFang Med Online, China Science and Technology Journal Database, and China Biomedical Literature Service System. The literature search in this study encompassed all pertinent literature up until May 2023.

The search terms were "Matrine," "liver injury," "hepatoprotection," and "hepatotoxicity". (Figure 2 and Supplementary Table S1).

2.3 Included criteria and excluded criteria

Considering the difference between hepatotoxicity and hepatoprotection of MT, this article has formulated appropriate included and excluded criteria to address these dual effects.

2.3.1 Included criteria

Research of hepatoprotection needs to meet the following requirements: 1) Subjects: the study involved rats or mice as the population. 2) Control(C) group and intervention(I) group: each study included at least 1 LI group as the C group and 1 MT group as the I group. 3) The I groups were comprised of LI models and received MT monotherapy exclusively. The C groups consisted of LI models that either received no treatment or received non-functional intervention. 4) The indicators of the studies should encompass AST, ALT, MDA, SOD, serum TG, serum TC, IL-6, CAT, and TNF-α, either in their entirety or partially. 5) The quality evaluation results were above 5 points.

Research of hepatotoxicity needs to meet the following requirements: 1) Subjects: the study involved rats or mice as the population. 2) C group and I group: each study included at least 1 LI group as the C group and 1 MT group as the I group. 3). The I groups were comprised of normal animals and received MT monotherapy exclusively. The C groups consisted of normal animals that either received no treatment or received non-functional intervention. 4) The indicators of the studies should encompass AST and ALT, either in their entirety or partially. 5) The quality evaluation results were above 5 points.

2.3.2 Excluded criteria

Excluded criteria for the research of hepatoprotection: 1) LI rats or mice were not selected as animal subjects for hepatoprotection

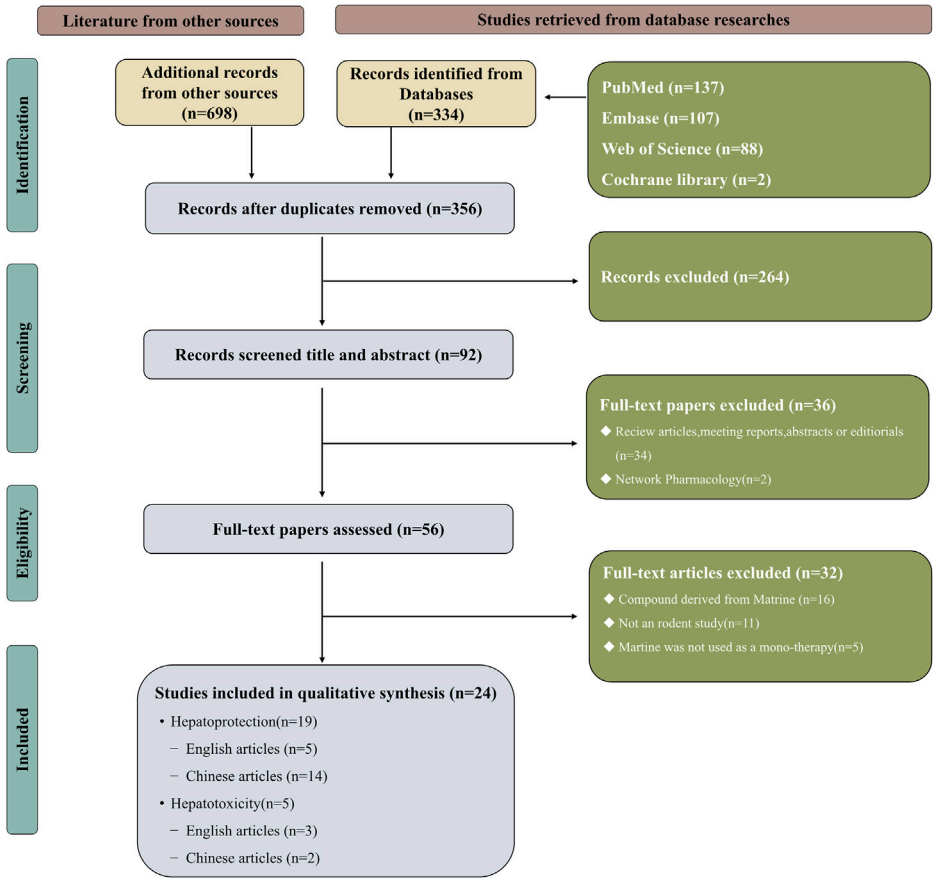

FIGURE 2
Selection of studies for the meta-analysis.

studies. 2) The experiments did not form controls. 3) The I group did not receive MT monotherapy. The C group used functional drugs (including Western medicines, TCMs and integrative medicines) as interventions, and could not provide specific outcome indices. 4) The common indicators of LI were not included in the study. 5) Quality evaluation results below 5 points.

Excluded criteria for the research of hepatotoxicity: 1) Normal rats or mice were not selected as subjects for hepatotoxicity studies. 2) The experiments did not form controls. 3) The I group did not receive MT monotherapy. The C group used functional drugs (including Western medicines, TCMs and integrative medicines) as interventions, and could not provide specific outcome indices. 4) The common indicators of LI were not included in the study. 5) Quality evaluation results below 5 points.

2.4 Data extraction

Two researchers extracted the following data from the included articles: 1) The first author's name and publication year; 2) Basic animal characteristics: including the number, species (mice or rats), strain, sex, and weight; 3) Modeling details: including the method of modeling and criteria for successful modeling; 4) Specific intervention methods: including the drug used, dosage, and frequency of administration; 5) Outcome measures. (Table 1).

Regarding the preset indicators, we recorded only the highest dose group in the gradient dosages. For the experiments that observed data from multiple time points, only the last were recorded. We collected the experimental data by Universal Desktop Ruler and calculated the mean and standard deviation (SD) of the continuous variables. Results of the measurements were displayed in graphics rather than digital text.

2.5 Risk of bias and quality of evidence

The CAMARADES (Collaborative Approach to Meta-Analysis and Review of Animal Data from Experimental Studies) 10-point scoring scale, an internationally recognized criteria published in 2004, is utilized to assess and calculate a methodological quality score (Macleod et al., 2004). Two researchers made an independently assessment of the methodological quality of the surveys. The quality measures were changed in accordance with the study's specificity. When there was a disagreement in the evaluation, the correspondence author came to an agreement or used arbitration. The specific methods were also provided in Figure 3.

TABLE 1 The key characteristics of all 24 Studies.

Author(s)/ Year	Species	Gender (M/F)	Weight of the animal	Sample size (n)MT/ Model	Drug dosage	Treatment courses	Main outcome indicators
Song2009	Kunming mice	NM	18–22 g	12/12	MT: MT,62.5 mg/kg	10 days	ALT, AST
					Mod: No drugs		
Liang2015	ICR mice	Female and male	18–22 g	10/10	MT: MT,40 mg/kg	60 days	ALT, AST
					Mod: Equal volume water		
Gu2019	C57BL/ 6 mice	Male	18–20 g	11/10	MT: MT,69.1 mg/kg	90days	ALT, AST
					Mod: Distilled water (constant volume)		
Liu2020	BALB/c mice	Male	17.7–18.1 g	10/10	MT: MT,100 mg/kg	1 week	ALT, AST
					Mod: Normal saline		
Rao2022	ICR mice	Male	18–22 g	10/10	MT: MT,60 mg/kg	2 weeks	ALT, AST
					Mod: Normal saline		
Li2005	NIH mice	Male	18–22 g	10/10	MT: Con A,20 mg/kg + MT,25 mg/kg	3 days	ALT, TNF-α
					Mod: Con A,20 mg/kg		
Liu2008	Sprague Dawley rats	Male	210–230 g	92/92	MT: HIRI + MT,60 mg/kg	1 day	ALT, AST, IL-6, TNF-α
					Mod: HIRI		
Zhou2009	NIH mice	Male	18–22 g	13/11	MT: Con A,20 mg/kg + MT,25 mg/kg	5 days	ALT, AST
					Mod: Con A,20 mg/kg		
Yang2013	Sprague Dawley rats	Male	180–220 g	24/24	MT: 2-AAF, 15 mg/kg + MT,20 mg/kg	3 weeks	ALT
					Mod: 2-AAF, 15 mg/kg		
Shi2013	C57BL/ 6 mice	Female	NM	8/8	MT: CCl_4,0.6 mL/kg + MT,30 mg/kg	6 weeks	ALT
					Mod: CCl_4,0.6 mL/kg		
Zhang2013	Wistar rats	Male	180–200 g	6/6	MT: High-fructose diet + MT,160 mg/kg	4 weeks	ALT, AST, Serum TG, TNF-α, CAT, MDA, SOD
					Mod: High-fructose diet		
Gao2013	Sprague Dawley rats	Female and male	100–140 g	12/12	MT: Chinese liquor,43% vol + MT, 50 mg/kg	30 days	ALT, AST, Serum TG, Serum TC, CAT, MDA, SOD
					Mod: Chinese liquor,43% vol		
Tang2013	Wistar rats	Female and male	113–118 g	10/10	MT: High fatty diet + MT,36 mg/kg	30 days	Serum TG, Serum TC
					Mod: High fatty diet		
Wu2014	Kunming mice	Male	18–22 g	10/10	MT: ethanol,5 g/kg + MT,80 mg/kg	6 days	ALT, AST, MDA, SOD
					Mod: ethanol,5 g/kg		
Zhu2015	Sprague Dawley rats	Male	200–250 g	15/15	MT: HIRI + MT,30 mg/kg	4 h	ALT, AST, TNF-α
					Mod: HIRI		
Zhao2015	Wistar rats	Male	180–220 g	12/12	MT: CCl_4,1 mL/kg + MT,10 mg/kg	1 week	ALT, AST, TNF-α
					Mod: CCl_4,1 mL/kg		

(Continued on following page)

TABLE 1 (*Continued*) The key characteristics of all 24 Studies.

Author(s)/ Year	Species	Gender (M/F)	Weight of the animal	Sample size (n)MT/ Model	Drug dosage	Treatment courses	Main outcome indicators
Li2016	Sprague Dawley rats	Female and male	100–140 g	12/12	MT: Chinese liquor,43% vol + MT, 100 mg/kg	30 days	ALT, AST, Serum TG, Serum TC, CAT, MDA, SOD
					Mod: Chinese liquor,43% vol		
Guo2017	Sprague Dawley rats	Male	180–220 g	8/8	MT: CCl_4,3 mL/kg + MT,72.8 mg/kg	3 weeks	ALT, AST
					Mod: CCl_4,3 mL/kg		
Gao2018	C57BL/ 6 mice	Male	NM	10/10	MT: High-fat diet + MT,10 mg/kg	7 weeks	ALT, AST, Serum TG, Serum TC, TNF-α
					Mod: High-fat diet		
Bai2018	Sprague Dawley rats	Male	200–250 g	10/10	MT: HIRI + MT,50 mg/kg	4 h	ALT, AST, TNF-α
					Mod: HIRI		
Khan2019	BALB/c mice	Male	24–35 g	5/5	MT: CCL_4,1 mL/kg + MT,50 mg/kg	1 day	ALT, AST, MDA
					Mod: CCL_4,1 mL/kg		
Yuan2020	Sprague Dawley rats	Male	200–250 g	6/6	MT: HIRI + MT,40 mg/kg	1 week	ALT, AST, MDA, SOD
					Mod: HIRI		
Chang2021	C57BL/ 6 mice	Male	18–22 g	8/8	MT: acetaminophen,400 mg/kg + MT,2.8 mg/kg	1 week	ALT, AST, TNF-α, MDA, SOD
					Mod: acetaminophen, 400 mg/kg		
Du2021	Kunming mice	Male	18–22 g	6/6	MT: ethanol,5.4 g/kg + MT,2.8 mg/kg	2 weeks	ALT, AST, CAT, MDA, SOD
					Mod: ethanol,5.4 g/kg		

Abbreviations: Green area: in the matter of hepatotoxicity of MT (n = 5); Yellow area: in the matter of hepatoprotection of MT(n = 19) **NM**, not mentioned; **ICR**, Institute of Cancer Research; **MT**, matrine; **Mod**, model; **2-AAF**, N-2-acetylaminofluorene; **HIRI**, hepatic ischemia-reperfusion injury (clip-closed portal vein and hepatic artery followed by reperfusion); **ALT**, alanine aminotransferase; **AST**, aspartate aminotransferase; **IL-6**, interleukin-6; **TNF-α**, tumor necrosis factor alpha; Serum TG, serum triglyceride; **Serum TC**, serum cholesterol; **CAT**, catalase; **SOD**, superoxide dismutase; **MDA**, malondialdehyde.

2.6 The dose-time-effect relationship and mechanism analysis of MT

To visualize the dose-time-effect relationship for hepatoprotection and hepatotoxicity of MT, this study unified the time units of all experiments into weeks (W), as well as constructed 3D maps and radar charts. In addition, the regulatory mechanism of MT role in the literature is summarized.

2.7 Quantitative synthesis and statistical analyses

Statistical analysis of indicators in this study was conducted using STATA 16.0 software. When the results are statistically significant, the *p*-value should be less than 0.05 ($p < 0.05$). Results were quantified using the standardized mean differences (SMD) and accompanying 95% confidence intervals (95% CI). The I-squared (I^2) test was used to assess the degree of heterogeneity and consistency between research (random-effects model [I^2>50%] or fixed-effects model [$I^2 \leq 50\%$]). Results were deemed to exhibit significant heterogeneity when I^2 exceeded 50%. Investigators conducted subgroup analyses for animal species (rat, mouse), dose administered (low (L)≤25 mg/kg, 25<medium (M)≤50 mg/kg, high (H)>50 mg/kg), and time of administration (<4w, ≥4w) in order to identify the source of heterogeneity. To establish whether the findings were trustworthy enough to draw inferences, sensitivity analysis was done.

2.8 Molecular docking

The compounds and ligands were obtained from the PubChem database (https://pubchem.ncbi.nlm.nih.gov) and RCSB Protein Data Bank database (https://www.rcsb.org/structure). Molecular docking was performed using AutoDockTools 1.5.6 and AutoDock Vina 4.2. Here is a brief summary of the docking process.

1) The structure of MT was downloaded from the PubChem database. It was then converted into a 3D structure using ChemDraw software to minimize the structural energy. The 3D structure was calculated using AutoDockTools 1.5.6 software and

Category	First author	Publication year	A	B	C	D	E	F	G	H	I	J	Total
hepatotoxicity (n=5)	Bing Song	2009	√	√	√	√			√	√		√	7
	Pei Liang	2015	√	√	√	√			√	√		√	7
	Yingmin Gu	2019	√	√	√	√		√	√	√	√	√	9
	Jie Liu	2020	√		√	√			√	√	√	√	7
	Siwei Rao	2021	√	√	√	√			√	√	√	√	8
Hepatoprotection (n=19)	Changqing Li	2005	√		√	√			√	√		√	6
	Hao Liu	2008	√		√	√			√	√		√	6
	Minchao Zhou	2009	√	√	√	√			√	√		√	7
	Zhiyun Yang	2013	√	√	√	√			√	√	√	√	8
	Bin Tang	2013	√	√	√	√			√	√	√	√	8
	Duo Shi	2013	√	√	√	√		√	√	√	√	√	9
	Hefang Zhang	2013	√	√	√	√		√	√	√	√	√	9
	Yan Gao	2013	√	√	√	√			√	√	√	√	8
	Yang Wu	2014	√	√	√	√			√	√	√	√	8
	Jun Zhu	2015	√	√	√	√		√	√	√	√	√	9
	Yan Zhao	2015	√		√	√			√	√	√	√	7
	Xiaohua Li	2016	√	√	√	√			√	√	√	√	8
	Shun Guo	2017	√	√	√	√			√	√	√	√	8
	Xiaobo Gao	2018	√	√	√	√			√	√	√	√	8
	Ning Bai	2018	√	√	√	√		√	√	√	√	√	9
	Adnan Khan	2019	√	√	√	√		√	√	√	√	√	9
	Fang Yuan	2020	√	√	√	√			√	√		√	7
	Lele Chang	2021	√	√	√	√			√	√	√	√	8
	Mengfan Du	2021	√	√	√	√			√	√	√	√	8

A: peer reviewed publication; B: control of temperature; C: random allocation to treatment or control; D:construct suitable animal models according to the purpose of the study; E: blinded assessment of outcome; F: use of anesthetic without significant intrinsic neuroprotective activity; G: animal model (rats or mice); H: sample size calculation; I: compliance with animal welfare policies; and J: statement of potential conflict of interests.

FIGURE 3
Risk of bias and quality assessment scores in each study.

saved as a pdbqt file. 2) The ligands were obtained from the RCSB protein bank. They were imported into PyMOL, dehydrated, hydrogenated, and prepared for ligand separation. The docking grid box was constructed in AutoDockTools 1.5.6 at the active site for each target protein and saved in pdbqt format. 3) AutoDock Vina 1.1.2 was used for molecular docking of the potential targets and active compounds, as well as to evaluate free binding energies. 4) PyMOL 2.6 and Discovery Studio 2019 were utilized for visualizing and analyzing interactions.

3 Results

3.1 Comprehensive literature review and selection

By using keywords, 1,032 articles in all could be found (334 articles from the four English databases and 698 articles from the four Chinese databases). After eliminating 676 duplicate articles, the researchers further examined the rest 356 articles. Depending upon the inclusion and exclusion criteria, the researchers excluded 264 articles after reviewing the titles and abstracts. And 34 articles on MT reviews, conference reports, abstracts or editorials and web pharmacology were subsequently eliminated from consideration. The remaining 32 articles were excluded after reviewing the full text. This meta-analysis eventually comprised 24 publications, 16 of which were in Chinese (Li et al., 2005; Liu et al., 2008; Song et al., 2009; Zhou et al., 2009; Gao et al., 2013; Tang et al., 2013; Wu et al., 2014; Liang et al., 2015; Zhao, 2015; Zhu et al., 2015; Li et al., 2016; Guo et al., 2017; Bai et al., 2018; Yuan and Yang, 2020; Chang et al., 2021; Du et al., 2021) and others were in English (Shi et al., 2013; Yang et al., 2013; Zhang et al., 2013; Gao et al., 2018; Gu et al., 2019; Khan et al., 2019; Liu et al., 2020; Rao et al., 2022). Figure 2 illustrates a flowchart of the study selection process.

3.2 Study quality

A modified 10-item CAMARADES checklist was used to assess the methodological quality of the included publications. Peer-reviewed articles were among the criteria; temperature management; construction of appropriate rodent models according to the study objectives; experimental animals were randomly assigned to treatment or control groups; blinded assessment of outcomes; explicit presentation of the use of anaesthetics without significant intrinsic neuroprotective activity; sample size calculations; compliance with animal welfare policies; and avoidance of potential conflicts of interest. All 24 articles used appropriate rodent models and reasonable groupings, all clearly reported sample sizes for each group and competing interests, and all were published in peer-reviewed publications. However, only 6 articles explicitly reported the use of anaesthetics with no apparent intrinsic neuroprotective activity, 4 did not mention temperature control in the experiments, 5 did not mention animal welfare policies, and no studies assessed outcomes blinded. The included articles' overall quality ratings ranged from 6 to 9. Two of the 24 articles received a score of 6 (8.33%), six received a score of 7 (25.00%), ten received a score of 8 (41.67%), and six received a score of 9 (25.00%). The methodological quality of each selected article is demonstrated in Figure 3.

3.3 Basic information and features of the articles included

The 24 papers had enough information to conduct a meta-analysis. These trials involved a total of 657 rodents, 330 of which were divided into the treatment group and the others were control group (Table 1).

Based on their biological traits, the animals used in the included researches were roughly categorized. The creatures were categorized into seven groups based on their species: 8.52% (56/657) Kunming

mice, 6.09% (40/657) ICR mice, 11.11% (73/657) C57BL/6 mice, 4.57% (30/657) BALB/c mice, 54.49% (358/657) Sprague Dawley Rats, 8.52% (56/657) Wistar rats and 6.70% (44/657) NIH mice. 63.01% (414/657) of rodents were rats, and 36.99% (243/657) of rodents were mice. The percentage of female and male rodents was 9.13% (60/657) and 87.21% (573/657) respectively regarding sex categorization, while 3.65% (24/657) of the rodents' sexes were unknown. Furthermore, according to the quality assessment scores, 25.00% (6/24) had 9 points, 41.67 (10/24) had 8 points, 25.00% (6/24) had 7 points, and 8.33% (2/24) had 6 points. Regarding the intervention time of MT, all experiments were divided into two subgroups: 76.10% (500/657) <4W groups and 23.90% (157/657) ≥4W groups. And the dosage of each experiment was divided into three groups: 24.96% (164/657) L-dosage groups, 23.14% (152/657) M-dosage group and 51.90% (341/657) H-dosage group (Supplementary Figure S1).

Across the studies, the weight of the animals included in the analysis varied from 17.7 g to 250 g, with a total number of examinations ranging from 10 to 184. The daily dosage of MT administered ranged from 2.8 mg/kg to 160 mg/kg, and the frequency of administration varied from a single dose to a maximum of 90 days.

3.4 Effects of MT on LI

The levels of ALT, AST, TNF-α and SOD which were the primary outcomes were assessed after MT therapy as well as the levels of MDA, IL-6, serum TG, serum TC and CAT were also changed by MT (Supplementary Tables S2, S3). Liver tissues from animals with LI exhibited significant inflammatory cell infiltration, hepatocyte swelling, vacuolar degeneration, and hepatocellular necrosis, as evidenced by H&E staining. The pathogenic alterations were significantly improved with MT treatment at dosage of 1.4–100 mg/kg, but the most effective dosage was the medium (25–50 mg/kg/d).

3.4.1 MT can improve the primary outcomes of LI

3.4.1.1 ALT levels

Because there was considerable heterogeneity (I^2 > 50%), we performed a random-effects analysis. The findings revealed that the ALT levels were significantly reduced in the MT groups compared to the LI model groups (n = 532; *95% CI* [−4.34, −2.50]; *SMD* = |−3.42| > 1; I^2 = 90.30%; p < 0.0001) (Figure 4).

3.4.1.2 AST levels

The random-effect analysis was used for further analysis as the significant heterogeneity (I^2 > 50%). The random-effect analysis revealed that the AST levels between the MT and LI model groups were significantly different. The levels of AST were shown to be reduced by MT (n = 448; *95% CI* [-4.74, −2.78]; *SMD* = |−3.76| > 1; I^2 = 87.50%; p < 0.0001) (Figure 4).

3.4.1.3 SOD levels

Significant heterogeneity (I^2 > 50%) was observed, and a random-effects analysis was conducted. The results indicated that the amounts of SOD protein in the MT groups were substantially greater than in the LI model groups (n = 120; *95% CI* [2.66,5.33]; *SMD* = |4.00| > 1; I^2 = 75.60%; p < 0.0001) (Figure 5).

3.4.1.4 MDA levels

The MDA levels in the mammalian models in the included study varied according to random-effects analyses. MDA levels in the MT groups were considerably lower than in the model groups (n = 130; *95% CI* [-3.59, −1.81]; *SMD* = |-2.70| > 1; I^2 = 64.40%; p < 0.0001) (Figure 5).

3.4.2 MT can administer the secondary outcomes of LI

3.4.2.1 Serum TG levels

The random-effects analysis showed that there were differences in serum TG levels between the MT and LI model groups. The MT groups had significantly lower levels of serum TG compared to the LI model group (n = 100; *95% CI* [-2.70, −0.67]; *SMD* = |-1.68| > 1; I^2 = 77.00%; p = 0.001) (Supplementary Figure S2).

3.4.2.2 Serum TC levels

In accordance with the random-effects analysis, the animal models in the included research had different serum TC levels. The MT groups had considerably lower serum TC levels than the model groups (n = 88; *95% CI* [-2.59, −0.78]; *SMD* = |-1.69| > 1; I^2 = 68.60%; p < 0.0001) (Supplementary Figure S2).

3.4.2.3 IL-6 levels

A random-effects analysis found notable IL-6 levels discrepancies between the MT and LI model groups. When compared to the LI model groups, IL-6 levels were substantially lower in the MT groups (n = 254; *95% CI* [-4.87, −2.67]; *SMD* = |-3.77| > 1; I^2 = 66.80%; p < 0.0001) (Supplementary Figure S3).

3.4.2.4 TNF-α levels

Because there was considerable heterogeneity (I^2 > 50%), we performed a random-effects analysis for additional research. Regarding the random-effect analysis, the MT and LI model groups showed significantly different levels of TNF-α. TNF-α levels was observed to be reduced by MT (n = 326; *95% CI* [-5.50, −1.95]; *SMD* = |-3.72| > 1; I^2 = 94.60%; p < 0.0001) (Supplementary Figure S3).

3.4.2.5 CAT levels

The animal models in the included studies showed several differences between the MT and LI model groups in CAT levels, according to random-effect analysis. The MT groups had significantly higher levels of CAT than model groups (n = 72; *95% CI* [2.23,3.62]; *SMD* = |2.93| > 1; I^2 = 0.00%; p < 0.0001) (Supplementary Figure S3).

3.4.3 Subgroup analysis

3.4.3.1 Subgroup analysis of ALT levels

In comparison to the LI model groups, the levels of ALT were found to be significantly reduced in the MT groups. MT was effective in both rats (n = 394; 95% *CI* [-4.96, −2.44]; *SMD* = |−3.70| > 1; I^2 = 92.20%; p < 0.0001) and mice (n = 138; 95% *CI* [-4.42, −1.67]; *SMD* = |−3.05| > 1; I^2 = 85.90%; p < 0.0001) (Figure 4A1). The ALT levels were found to reduced most by MT in the M-dosage subgroups (n = 112; 95% *CI* [-8.90,-2.86]; *SMD* = |−5.88| > 1;

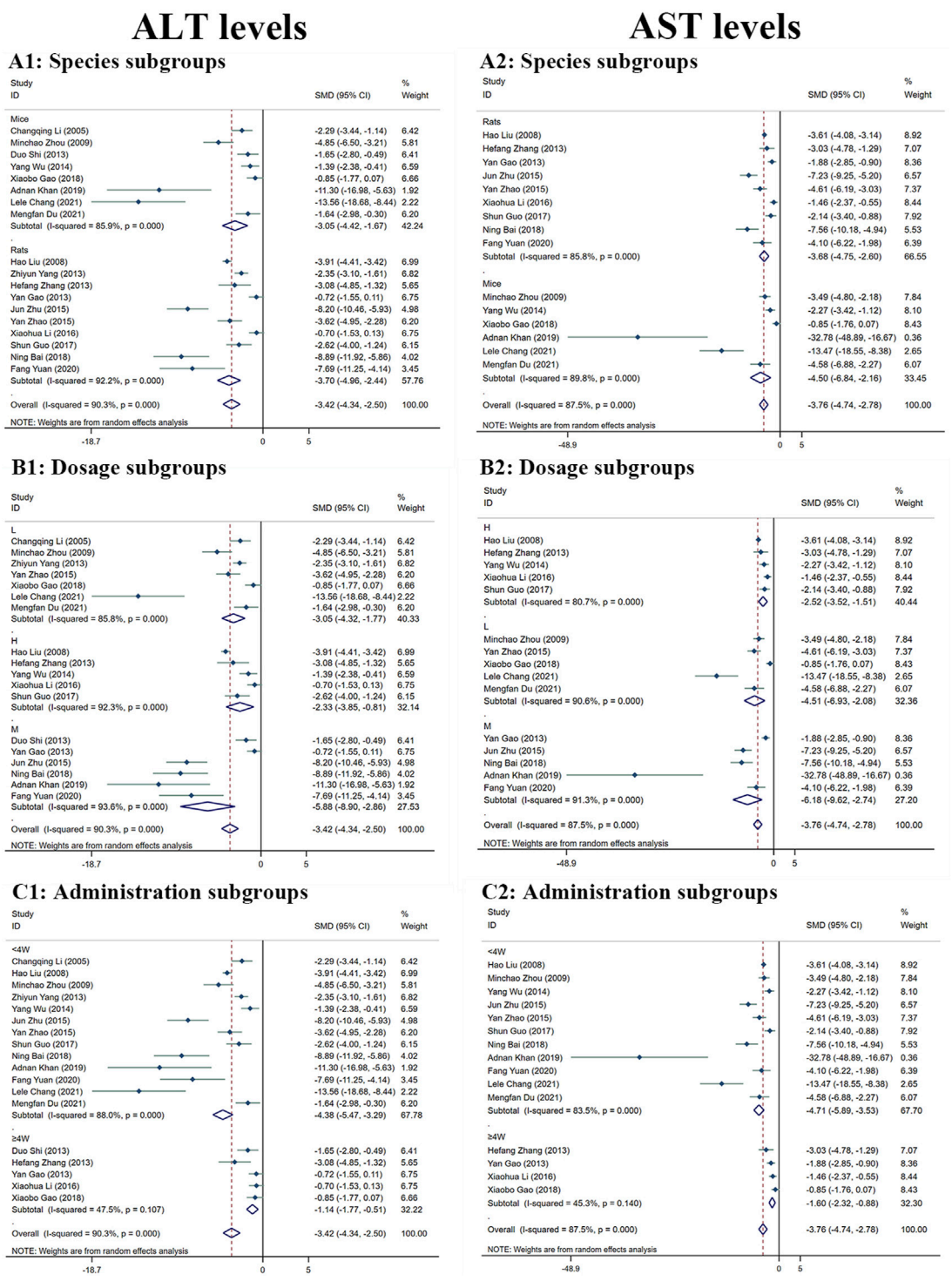

FIGURE 4
Forest plot (effect size and 95% CI) summarising the effects of MT on ALT **(A1–C1)** and AST **(A2–C2)** levels in hepatoprotection. **(A)** Rat and mice subgroups; **(B)** L, M and H dosage subgroups; **(C)** < 4 weeks and ≥4 weeks of administration subgroups.

I^2 = 93.60%; p < 0.0001) than H-dosage (n = 256; 95% *CI* [-3.85,-0.81]; *SMD* = |–2.33| > 1; I^2 = 92.30%; p = 0.003) and L-dosage subgroups (n = 164; 95% *CI* [-4.32,-1.77]; *SMD* = |–3.05| > 1; I^2 = 85.80%; p < 0.0001) (Figure 4B1). Furthermore, it worked in both '≥4W' subgroups (n = 96; 95% *CI* [-1.77, –0.51]; *SMD* = |–1.14| > 1; I^2 = 47.50%; p < 0.0001) and '<4W' subgroups (n = 436; 95% *CI* [-5.47, –3.29]; *SMD* = |–4.38| > 1; I^2 = 88.00%; p < 0.0001), but the lower levels were in the '<4W' subgroups (Figure 4C1).

3.4.3.2 Subgroup analysis of AST levels

Compared with the LI model group, the levels of AST in MT groups were significantly lower. MT reduced substantially the AST

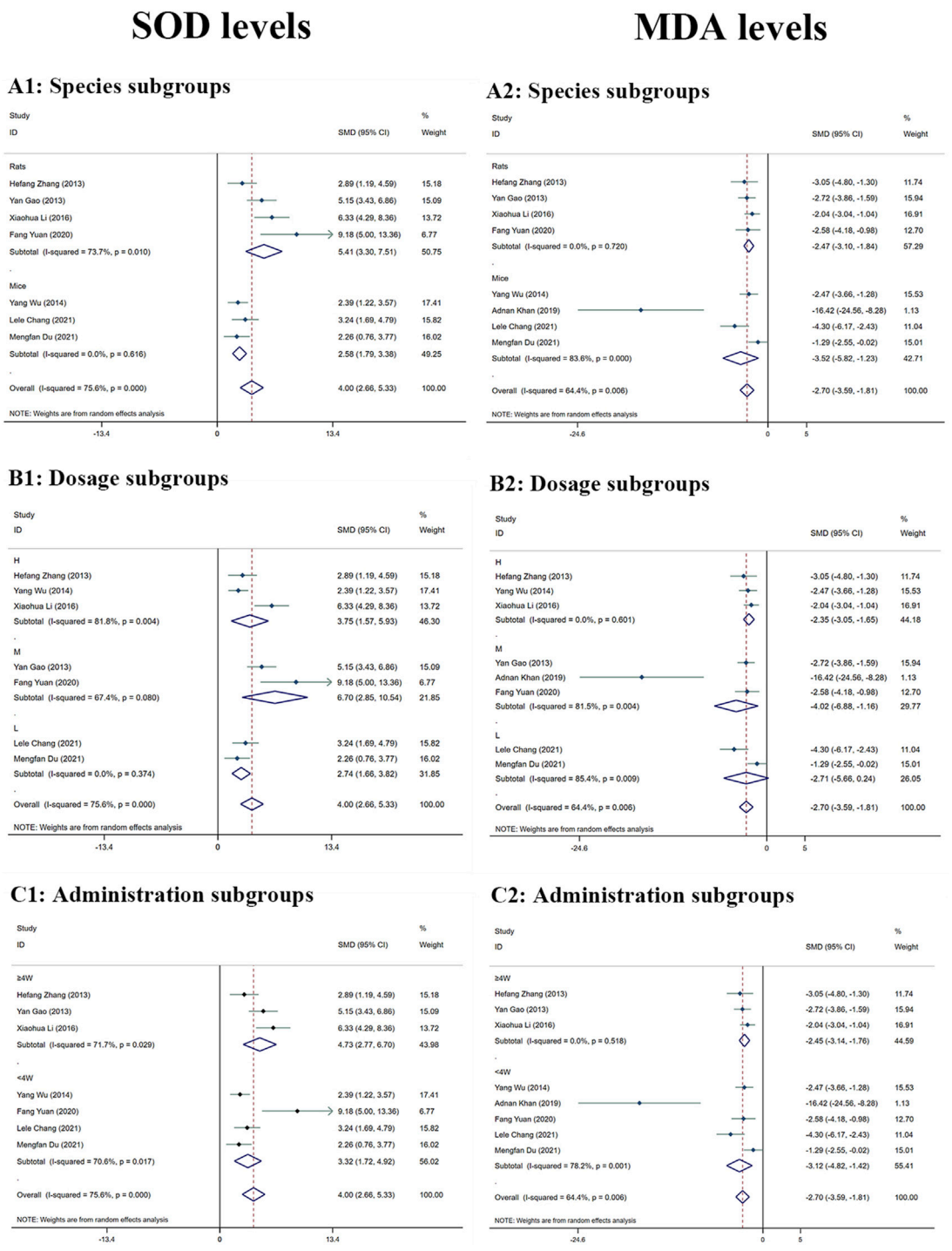

FIGURE 5
Forest plot (effect size and 95% CI) summarising the effects of MT on SOD **(A1–C1)** and MDA **(A2–C2)** levels in hepatoprotection. **(A)** Rat and mice subgroups; **(B)** L, M and H dosage subgroups; **(C)** < 4 weeks and ≥4 weeks of administration subgroups.

levels in both rats' subgroups (n = 346; 95% *CI* [-4.75, −2.60]; *SMD* = |−3.68| > 1; I^2 = 85.80%; $p < 0.0001$) and mice subgroups (n = 102; 95% *CI* [-6.84, −2.16]; *SMD* = |−4.50| > 1; I^2 = 89.80%; $p < 0.0001$) (Figure 4A2). MT had the most significant effect in the M-dosage subgroups (n = 96; 95% *CI* [-9.62,-2.74]; *SMD* = |−6.18| > 1; I^2 = 91.30%; $p < 0.0001$) than the other two subgroups (H-dosage subgroups: n = 256; 95% *CI* [-3.52,-1.51]; *SMD* = |−2.52| > 1; I^2 = 80.70%; $p < 0.0001$) (L-dosage subgroups: n = 96; 95% *CI* [-6.93,-2.08]; *SMD* = |-4.51| > 1; I^2 = 90.60%; $p < 0.0001$) (Figure 4B2). The levels of AST were decreased in the both two time-subgroups, but the lower groups were '<4W' subgroups ('≥4W' subgroups: n = 80; 95% *CI* [-2.32,-0.88]; *SMD* = |-1.60| > 1; I^2 = 45.30%; $p < 0.0001$) ('<4W' subgroups: n = 368; 95% *CI* [-5.89,-3.53]; *SMD* = |-4.71| > 1; I^2 = 83.50%; $p < 0.0001$) (Figure 4C2).

3.4.3.3 SOD levels subgroup analysis

The amount of SOD was significantly greater in the groups treated with MT than in the LI model groups. The levels of SOD were increased by MT in both rats subgroups (n = 72; 95% *CI* [3.30,7.51]; *SMD* = |5.41| > 1; I^2 = 73.70%; $p < 0.0001$) and mice subgroups (n = 48; 95% *CI* [1.79,3.38]; *SMD* = |2.58| > 1; I^2 = 0.00%; $p < 0.0001$) (Figure 5A1). The levels of SOD of M-dosage subgroups (n = 36; 95% *CI* [2.85,10.54]; *SMD* = |6.70| > 1; I^2 = 67.40%; $p = 0.001$) were the highest by MT than H-dosage subgroups (n = 56; 95% *CI* [1.57,5.93]; *SMD* = |3.75| > 1; I^2 = 81.80%; $p = 0.001$) and L-dosage subgroups (n = 28; 95% *CI* [1.66,3.82]; *SMD* = |2.74| > 1; I^2 = 0.00%; $p < 0.0001$) (Figure 5B1). Furthermore, it worked in both '≥4W' subgroups (n = 60; 95% *CI* [2.77,6.70]; *SMD* = |4.73| > 1; I^2 = 71.70%; $p < 0.0001$) and '<4W' subgroups (n = 60; 95% *CI* [1.72,4.92]; *SMD* = |3.32| > 1; I^2 = 70.60%; $p < 0.0001$), but the higher levels were in the '<4W' subgroups (Figure 5C1).

3.4.3.4 Subgroup analysis of MDA levels

The MDA levels in the MT groups were lower than those in the LI model groups. The MDA levels were decreased by MT in both rats subgroups (n = 72; 95% *CI* [-3.10, −1.84]; *SMD* = |-2.47| > 1; I^2 = 0.00%; $p < 0.0001$) and mice subgroups (n = 58; 95% *CI* [-5.82, −1.23]; *SMD* = |-3.52| > 1; I^2 = 83.60%; $p = 0.003$) (Figure 5A2). MT reduced the MDA levels most in the M-dosage subgroups (n = 46; 95% *CI* [-2.55,-0.02]; *SMD* = |-4.02| > 1; I^2 = 81.50%; $p = 0.006$) among the time subgroups (H-dosage subgroups: n = 56; 95% *CI* [-3.05,-1.65]; *SMD* = |−2.35| > 1; I^2 = 0.00%; $p < 0.0001$) (L-dosage subgroups: n = 28; 95% *CI* [-5.66,0.24]; *SMD* = |-4.51| > 1; I^2 = 85.40%; $p = 0.071$) (Figure 5B2). Moreover, it substantially lowered MDA levels in both '≥4W' subgroups (n = 60; 95% *CI* [-3.14, −1.76]; *SMD* = |-2.45| > 1; I^2 = 0.00%; $p < 0.0001$) and '<4W' subgroups (n = 70; 95% *CI* [-4.82, −1.42]; *SMD* = |-3.12| > 1; I^2 = 78.20%; $p < 0.0001$) (Figure 5C2).

3.4.4 Sensitivity analysis and publication bias of outcome indicators

The sensitivity of ALT, AST, SOD, and MDA levels in detecting LI in mouse models did not differ significantly. To identify publication bias, we used the |t|-value and conducted Egger's test. The |t|-values of these four factors did not indicate any publication bias in LI research (Supplementary Figures S4, S5).

3.5 The toxic effects of MT on liver

ALT and AST levels were examined as significant main indicators of toxic effects of MT on liver in five investigations. All the five investigations showed that MT can significantly increase ALT and AST levels. According to the results, MT may increase hepatotoxicity by influencing ALT and AST levels (Supplementary Table S4). H&E staining of normal animal liver tissues revealed significant hepatotoxicity with inflammatory cell infiltration, cell edema, cytoplasmic loosening and vacuolar degeneration of cytoplasm. Significant pathogenic alterations occurred with the intervention of MT at 10–69.1 mg/kg, but the most toxic dosage was the 30–62.5 mg/kg/d.

3.5.1 MT can affect the main indicators of liver function

3.5.1.1 ALT levels

Because of the considerable heterogeneity (I^2 > 50%), the random-effects analysis was utilized for further investigation. The random-effects analysis revealed that the ALT levels between the MT and control groups were significantly different. The level of ALT was shown to be elevated by MT (n = 105; *95% CI* [0.79, 3.02]; *SMD* = |1.91| > 1; I^2 = 81.30%; $p < 0.0001$) (Figure 6A).

3.5.1.2 AST levels

The random-effect analysis revealed that the AST levels between the MT and control groups were significantly different. The level of AST was shown to be elevated by MT (n = 105; 95% *CI* [0.75, 3.68]; *SMD* = |2.21| > 1; I^2 = 87.90%; $p < 0.0001$) (Figure 6B).

3.6 Dose–time–effect/dose–time–toxicity relationship

To achieve effective treatment for a disease, it is crucial to not only use the appropriate medications but also carefully consider the dosage and duration of drug administration. The three key elements in clinical treatment are identifying the most suitable medication, determining the ideal dosage, and establishing the optimal timing. In this study, we utilized three-dimensional mappings and radar charts to analyze the treatment duration and dosage in each research, aiming to identify the optimal length of treatment and dosage for MT that would yield the most effective results. Figures 7, 8 displayed 3D maps and radar charts corresponding to the four key indications.

3.6.1 The dose–time–effect/dose–time–toxicity relationship of ALT and AST levels

3.6.1.1 Effective dose and time length of MT on ALT and AST levels

The ALT and AST levels can be effectively reduced by MT in LI models at a dose of 1.4 mg/kg/d to 100 mg/kg/d, if all other conditions (except the dose of MT) are suitable. However, if the MT dose is less than 1.4 mg/kg/d or greater than 100 mg/kg/d, these effects are not observed. To ascertain the precise MT dosage that is effective, additional research are necessary. Considering the treatment period, 3D maps and radar charts indicate that MT effectively decrease ALT and AST levels at 0.02 W-4 W, but is unsuccessful in reducing these levels over 4.29 W. However, if the treatment period was 0.02W–0.86W at a medium dose (25–50 mg/kg/d), MT reduced ALT and AST levels more effectively than at a low dose (0–25 mg/kg/d) or a high dose (>50 mg/kg/d). Further study needs to be performed to determine the specific effective dose and administration of MT for a treatment duration of more than 4.29 W (Figures 7A,B; Figures 8A,B).

3.6.1.2 Toxic dose and time length of MT on ALT and AST levels

The levels of ALT and AST are increase by MT in normal models at a dosage of 10 mg/kg/d to 69.1 mg/kg/d, if all other conditions (except the dose of MT) are suitable. However, if the

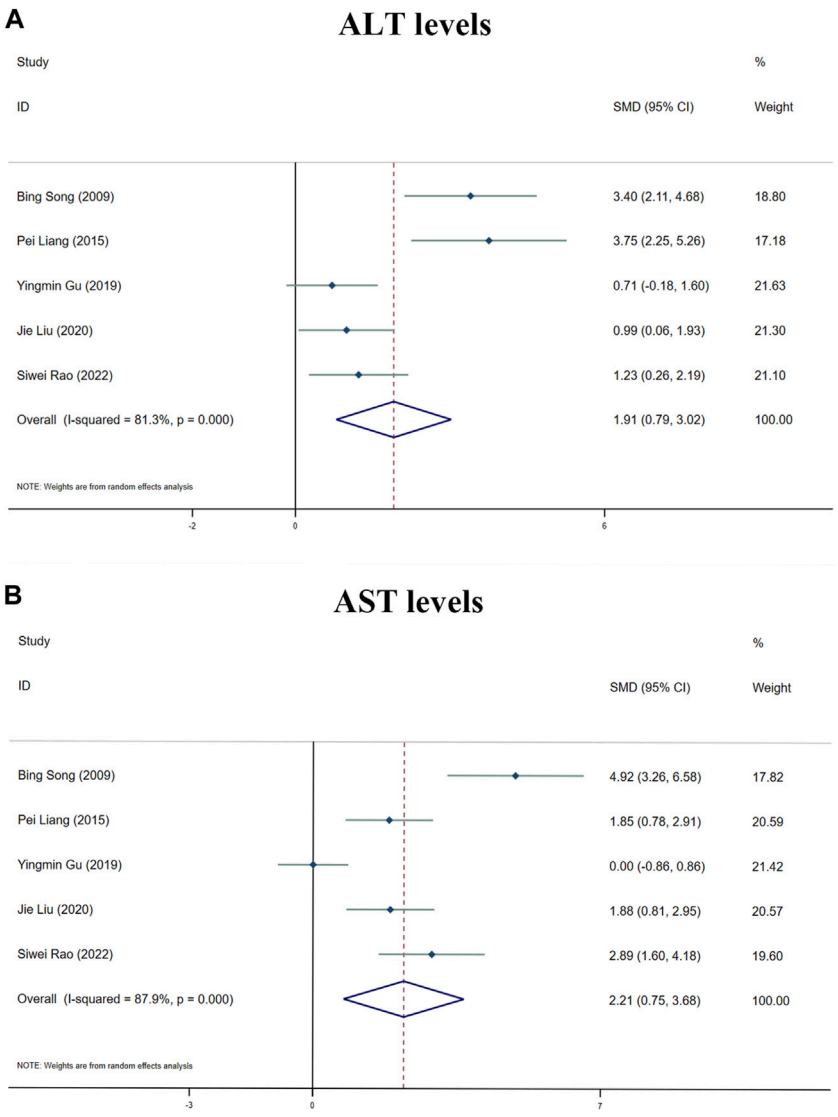

FIGURE 6
Forest plot (effect size and 95% CI) summarising the effects of MT on hepatotoxicity. **(A)** ALT levels; **(B)** AST levels.

MT dose is less than 10 mg/kg/d or greater than 100 mg/kg/d, the toxicity of MT is not observed. Considering the treatment period, 3D maps and radar charts indicate that MT effectively increase ALT and AST levels at 1W-2 W or 8.57W-12.86W, but is unknown at 2W-8.57W. Additional investigation needs to be conducted to study the specific toxic dose and administration of MT *in vivo* (Figures 7A,B; Figures 8A,B).

3.6.2 The impact of the effective dose and time length on SOD and MDA levels

According to the 3D maps and radar charts, the SOD levels in the MT groups were higher than those in the LI model groups at a dose of 1.4 mg/kg/d to 100 mg/kg/d. At 1W-4.29W, MT was found to increase the amounts of SOD in the MT groups. MT, in contrast with MDA, can lower MDA levels at a dosage of 0.7 mg/kg/d to 100 mg/kg/d and a duration of 0.14 W–4.29 W (Figures 7C,D; Figures 8C,D).

3.7 Potential mechanisms of action of MT

The hypothesized bilateral impacts of MT on LI are extensive and complicated. The identified signalling transduction pathways, namely, SERCA, SREBP1c/SCAP, Notch/RBP-J/HES1, IκK/NF-κB, Cul3/Rbx1/Keap1/Nrf2, and Bcl-2/ROS/Bax/caspase-9/caspase-3 have been evaluated in Supplementary Tables S5–S6.

3.8 Molecular docking of key targets

To validate the potential mechanisms of action of MT, we utilized molecular docking to assess the binding affinity between MT and key targets. The molecular docking analysis demonstrated the interaction of MT with SERCA and SREBP-SCAP complexes, and the thermodynamic data was analyzed. The estimated free energy of −7.8 kcal/mol suggests that MT interacts with Phe256,

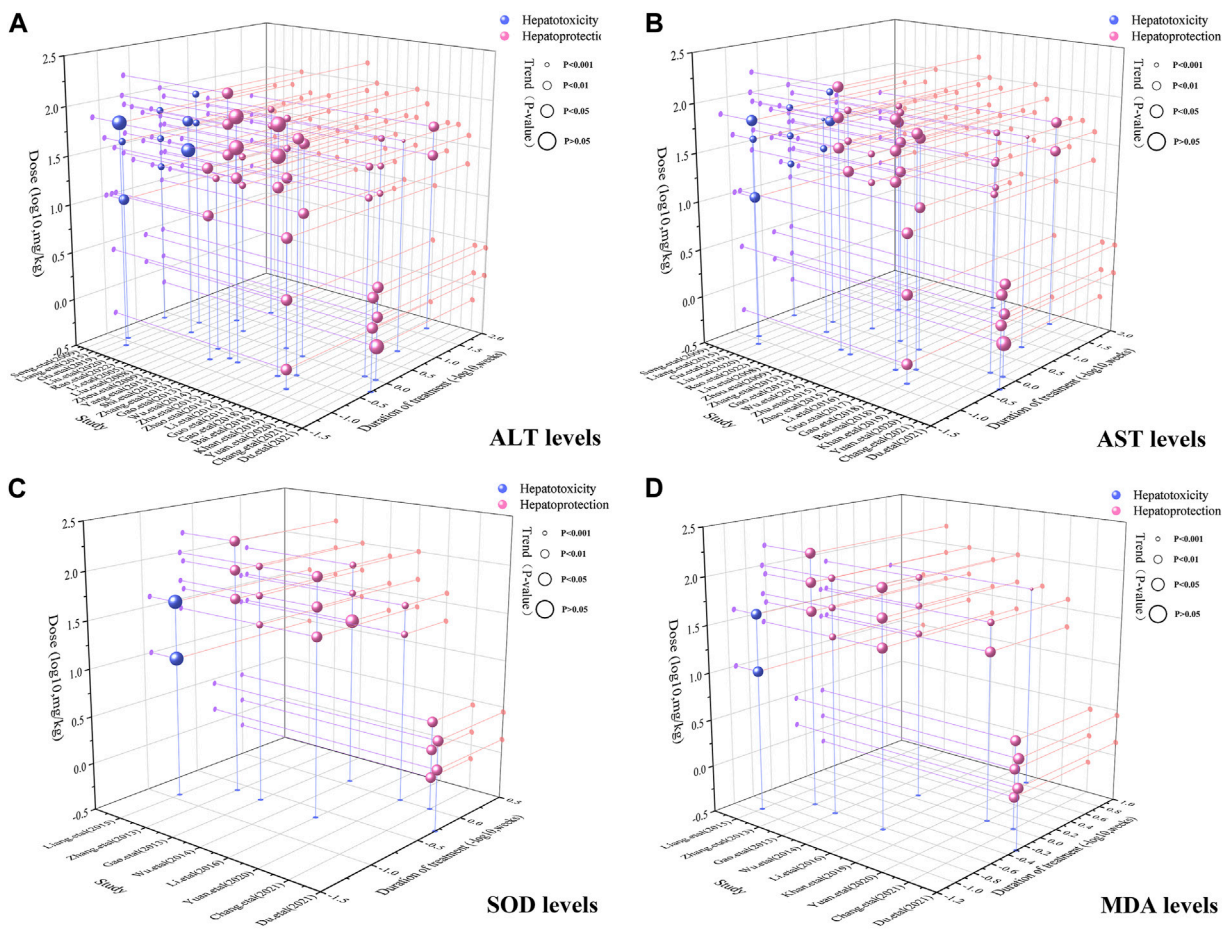

FIGURE 7
3D maps of dose–time–effect relationship. **(A)** ALT levels; **(B)** AST levels; **(C)** SOD levels; **(D)** MDA levels.

Phe834, Ile829, Ile765, Tyr837, Val769, Val263, and Met83 on the SERCA protein. Additionally, with an estimated free energy of −6.8 kcal/mol, MT exhibits significant interactions with Glu605, Leu647, Pro649, Trp690, Ala646, Ala602, Val688, Val603, and Ile645 on the SREBP-SCAP complexes. These interactions between MT and the targets involve beneficial patterns of hydrogen bonds and hydrophobic interactions. The compound–target interactions were visualized using PyMoL 2.6 and Discovery Studio 2019 (Figure 9).

4 Discussion

According to our meta-analysis, consisting of 24 published studies with 657 rodent models, MT provides information on liver protection and hepatotoxicity. We analyzed a range of indicators, such as TNF-α, IL-6, serum TG, serum TC, SOD, MDA, CAT, ALT, and AST, to establish the biological efficacy and diverse dosages of MT for treating and managing LI. Furthermore, by utilizing molecular docking techniques, we confirmed the interaction of MT with SERCA and SREBP-SCAP complexes, while also summarizing the mechanisms of MT as described in relevant literature. These findings aimed to gain a better understanding of the potential protective and harmful signaling pathways linked to the included indicators of MT on the LI (Figure 10).

4.1 The protective molecular mechanism of MT on LI

The comprehensive meta-analyses indicated that MT can protect from hepatotoxicity in animal models, and this protective effect is associated with variations in TNF-α, IL-6, serum TG, serum TC, MDA, ALT, AST, SOD, and CAT. Several signal transduction pathways are responsible for MT-induced alterations in these important indications of LI.

4.1.1 MT could inhibit SREBP1c in the LI models

Sterol regulatory element-binding protein-1c (SREBP1c), a transcription factor which is generated from ER, might have a critical function in the regulation of lipogenesis and be activated by different nutrient states in the liver (Sekiya et al., 2008). SREBPs and SREBP cleavage activating protein (SCAP) interact to form a complex on the endoplasmic reticulum membrane. When cells in mammals lack cholesterol, SREBP-SCAP complexes assemble

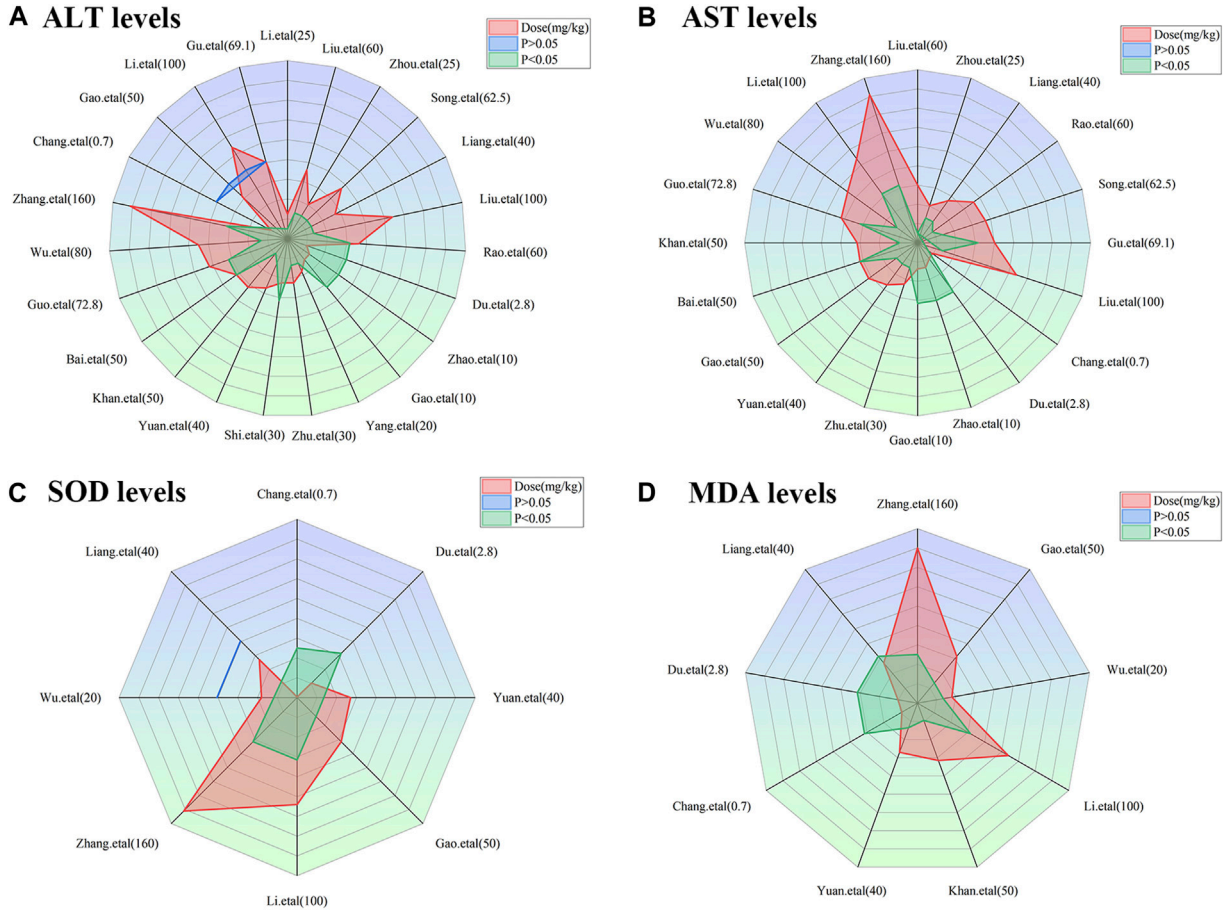

FIGURE 8
Radar charts of dose–time–effect relationship. **(A)** ALT levels; **(B)** AST levels; **(C)** SOD levels; **(D)** MDA levels.

complexes in coat protein II (COPII) vesicles, facilitating transportation from the ER to the Golgi apparatus. To release the bHLH-Zip domains, SREBPs would be proteolyzed at the Golgi by site-1 and site-2 proteases (S1P and S2P) (Horton et al., 2002; Shimano and Sato, 2017; Lee et al., 2020). The translocated bHLH domain of SREBP1c interacts with the sterol regulatory element (SRE) in the nucleus, regulating the transcription of downstream lipid homeostasis genes such as fatty acid synthase (Fas), acetyl-CoA carboxylase (Acc), and stearoyl-CoA desaturase-1 (Scd1). SREBP1c also enhances the synthesis and accumulation of triacylglycerol (TG) in hepatocytes (Eberle et al., 2004). Previous studies have shown that the mechanistic target of rapamycin complex 1 mediates the nucleocytoplasmic transport of SREBP-1 and SREBP-2 (Peterson et al., 2011). A few findings indicate SREBP1c/2 may interact with NF-κB to modulate inflammation and cholesterol stability (Fowler et al., 2022; Guo et al., 2017). NF-κB enhances SCAP protein expression and promotes the activity of the SCAP-SREBP complex, which causes an inflammatory response and the accumulation of cholesterol (Lee et al., 2020; Li et al., 2013). In an animal model of nonalcoholic fatty liver disease (NAFLD) and nonalcoholic steatohepatitis (NASH) induced by a high-fat diet (HFD) or methionine-choline deficit (MCD), SREBP1c, Fas, Acc, ALT, AST, TNF-α, IL-6, and serum TC/TG levels are elevated. However, MT can reduce the levels of SREBP1c, Fas, Acc, ALT, AST, TNF-α, and IL-6 in hepatocytes of HFD and MCD mice by decreasing SREBP1c expression (Rinella et al., 2008; Gao et al., 2018). Modulation of SREBP1c may be positively correlated with the production of liver damage indicators, and MT may have a potential impact on hepatic injury biomarkers (Yang et al., 2022).

4.1.2 MT might regulate Ca^{2+} homeostasis via SERCA to protect hepatocyte

Ca^{2+} is a second messenger that is required for cellular homeostasis through mTORC1, calmodulin, mitochondrial nitric oxide synthase, citric acid cycle (TCA cycle, Kreb cycle) and electron transport chain (ECT) and associated with ROS generation (Wan et al., 1989; O-Uchi et al., 2014; Jin et al., 2016; Tang et al., 2017; Diaz-Garcia et al., 2021; Stork et al., 2022). Extracellular stress stimuli such as CCl4, hepatic ischemia-reperfusion injury (HIRI), alcohol, and so on would increase Ca^{2+} transport from the extracellular area to the cytosol and mitochondria during the development of hepatic damage. The activation of Kupffer cells by hepatic I/R injuries is probably produced by the stimulation of store-operated Ca^{2+} channels (SOC), which increases Ca^{2+} influx into the cells and exacerbates the I/R-induced Kupffer cell injury (Pan et al., 2012). In rat liver, CCl4 might increase the expression and distribution of acid-sensing ion channel 1 (ASIC-1) (Pan et al., 2012). Consistent consumption of alcohol improves Ca^{2+}-mediated

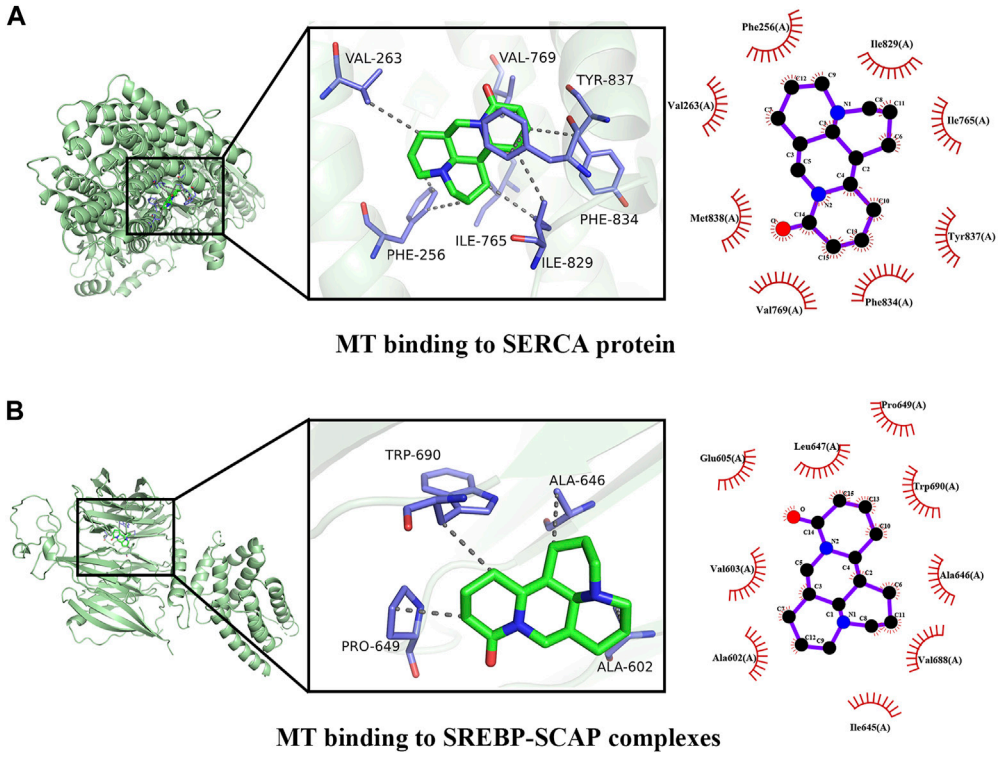

FIGURE 9
Docking patterns of MT and key targets. **(A)** MT binding to SERCA protein; **(B)** MT binding to SREBP-SCAP complexes.

mitochondrial permeability transition pore opening and raises cyclophilin D levels within the liver (King et al., 2010).

A steady Ca^{2+} concentration gradient across the cell membrane is maintained by eukaryotic cells (~100 nM within the cytoplasm and ~1 mM extracellular milieu) (Bagur and Hajnoczky, 2017). The ER and mitochondria play essential roles in the storage, transport, and upkeep of Ca2+ within the cell. Ca^{2+} dysregulation in ER and mitochondria is associated with LI, including chronic viral hepatitis, alcoholic liver disease, and nonalcoholic fatty liver disease (Li et al., 2007; Mantena et al., 2008; King et al., 2010; Xiao et al., 2017). The connection between ER stress and lipid metabolism is linked to intracellular Ca^{2+} homeostasis in the liver. Recent accumulating investigations have connected Ca^{2+} concentration disruption to ER stress, proving to be a significant risk factor during the progression of NAFLD to NASH, leading to increased inositol-requiring enzyme 1α(IRE1α), activating transcription factor 6α (ATF6α), phosphor-plasmic reticulum kinase (p-PERK), the 78 kDa glucose-regulated protein (GRP78), and C/EBP homologous protein (CHOP) expression (Bartlett et al., 2014; Park and Lee, 2014; Rieusset, 2017; Gao et al., 2018). Inactive GRP78, an ER chaperone protein, binds to three transmembrane unfolded protein response (UPR) stress sensors under physiological conditions: IRE1, ATF6α, and PERK. When unfolding proteins assemble within the ER lumen, raising ER stress, GRP78 dissociates from these UPRs to capture the unfolding proteins and activate the UPR stress sensors.

ATF6 is transported from the ER to the Golgi apparatus once it has been separated from GRP78, where it can be cleaved by S1P and S2P. An activated form of ATF6α might migrate to the nucleus and activate downstream target genes related to X-box-binding protein 1 (XBP1) and CHOP. ATF6α signaling pathways may be able to alleviate ER stress. A serine-threonine kinase domain and an endoribonuclease domain have been identified in IRE1. The active IRE1 endonuclease activity could remove the introns of XBP1 mRNA to generate spliced XBP1 (sXBP1) mRNA. The sXBP1 protein functions as a transcription factor, translocating into the nucleus to stimulate the production of ER chaperones and the HSP40 family member P58 ^{IPK} gene. Activated PERK might cause dimerization and autophosphorylation of the kinase, allowing it to phosphorylate eukaryotic initiation factor 2 (eIF2). Phosphorylated eIF2 could block new protein translation while minimizing ER stress, hence assisting cell survival via transcription factor 4 (ATF4) activation. ATF4 could cate to the nucleus and stimulates the production of the survival gene and the apoptotic cell death gene CHOP (Harding et al., 2003; Szegezdi et al., 2006).

Ca^{2+} is transported across the plasma membrane, the endoplasmic reticulum, and the mitochondria through Ca^{2+} channels. Prior studies have demonstrated that the sarco/endoplasmic reticulum Ca^{2+}-ATPase (SERCA) pump, a member of the P-type ATPase family of ion channels, transports intracellular Ca^{2+} from the cytosol to the ER and maintains Ca^{2+} homeostasis between the cytoplasm and ER lumen. Diminished SERCA activity could increase cytosolic Ca^{2+} level, ER stress, and apoptosis in NALFD, whereas increased SERCA activity would reverse the process (Zhang et al., 2014; Lai et al., 2017). Lai et al. revealed that suppressing protein kinase C delta (PKCδ) could increase SERCA activity, thereby reducing ER stress (Lai et al., 2017). Meanwhile, Gao et al. demonstrated that exposing PA-induced

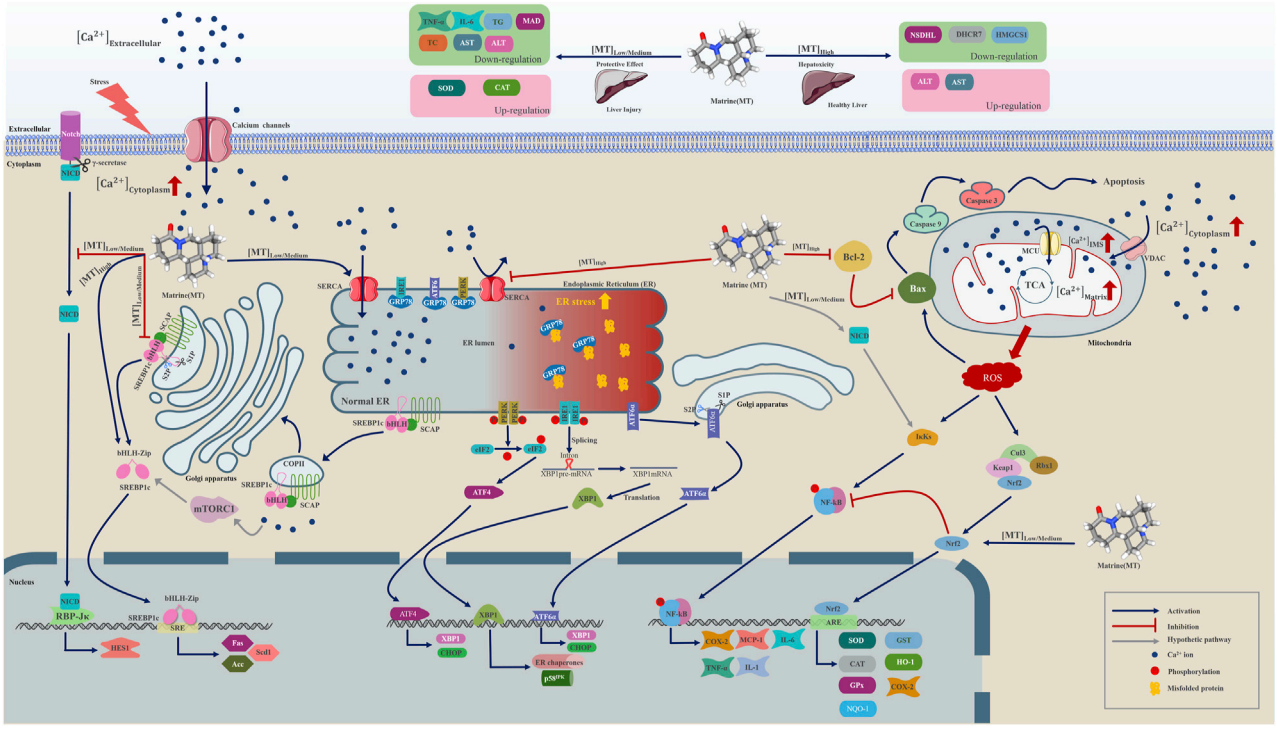

FIGURE 10
A graphical representation illustrates multiple molecular processes of matrine protection and toxicity in liver injury by modifying SERCA, SREBP1c/SCAP, Notch/RBP-J/HES1, IK/NF-B, Cul3/Rbx1/Keap1/Nrf2, and Bcl-2//Bax/caspase 9/caspase 3 signalling pathways. Matrine probably plays a significant role in Ca2+ homeostasis regulation within the endoplasmic reticulum, Golgi apparatus, and mitochondria. Matrine could additionally influence the expression of three essential metabolically related genes, including DHCR7, NSDHL, and HMGCS1. Please check the abbreviation list.

L02 cells to low (200 μM) and medium (400 μM) doses of MT enhanced SERCA activity and facilitated Ca^{2+} influx from the cytosol into the ER lumen (Gao et al., 2018). These findings suggest that changes in SERCA function may contribute to the development of LI and provide a potential therapeutic target for various hepatic disorders.

4.1.3 MT would downregulate Notch/RBP-J/HES1 signaling cascade in the LI

Previous research found that inhibiting Notch signaling using RBP-J deletion or a Notch inhibitor worsened hepatic I/R damage, demonstrated by impaired liver function and increased hepatocyte apoptosis (Yu H. C. et al., 2011; Yue et al., 2018). The intracellular transmembrane domain (NICD) of the Notch receptor is released through the catalytic action of an integral membrane protein γ-secretase complex. NICD might enter the nucleus and bind the DNA-binding protein RBP-J, allowing Notch target genes such as HES1 to be transcribed. Earlier research proposed that MT may diminish HES1 mRNA levels by downregulating RBP-Jκ mRNA expression to safeguard liver function and regeneration (Yang et al., 2013). The current study reveals that MT may promote hepatic progenitor cell development by obstructing the Notch/Jagged1/HES1 signaling pathway *in vivo* (Yang et al., 2016). By reducing SERCA activity and increasing ER stress in T-ALL cells, unmatured Notch signaling transduction pathways would be activated, contributing to apoptosis (De Ford et al., 2016). We hypothesize that MT can suppress the Notch/RBP-J/HES1 signaling cascade by promoting SERCA activity and minimize apoptosis in LI; however, more investigations are required.

4.1.4 MT might indirectly regulate NF-κB activity via modifying SERCA in the LI

The nuclear factor kappa B (NF-κB) is a recognized transcription factor in pro-inflammatory pathways. NF-κB could potentially have an impact on controlling the processes of cell proliferation, differentiation, and cell death (Gerondakis et al., 2006; Khandelwal et al., 2011; Mitchell et al., 2016). TNF-α and IL-1, pro-inflammatory cytokines, may mediate NF-κB signaling transduction pathways and encourage downstream target gene expression. NF-κB activation will trigger the transcription and translation of COX-2, IL-6, MCP-1, TNF-α, and IL-1. The IκK complex, which is composed of α and β subunits, is necessary for NF-κB pathway activation via phosphorylation and ubiquitination. Previous literature has indicated that the activity of IκK and NF-κB is linked to various chronic liver injuries, including steatohepatitis, hepatocellular carcinoma, alcoholic liver disease, NAFLD, viral hepatitis, and biliary liver disease. Present results demonstrated that IκKα would interact with NICD directly to maintain the nuclear factor-kappa B (NF-κB) activity in the T-ALL cells model (Vacca et al., 2006), and we proposed that MT therapeutic effect on Ca^{2+} ion channel SERCA might regulate the process of inflammation and apoptosis in the LI through NICD/NF-κB interaction.

4.1.5 MT could increase Nrf2 translocation to nucleus and protective effect

Under normal state, nuclear factor erythroid 2-related factor 2 (Nrf2), as a protective molecule, could have a crucial function in preventing oxidation in the liver. In a physiological condition, Nrf2 might attach to the kelch-like ECH-associated protein 1 (Keap1), which is an adaptor to the E3 ubiquitin ligase complex Cullin3 (Cul3)/ring box protein 1 (Rbx1), and subsequently be ubiquitinated and suppressed by Cul3 in the cytoplasm. Recently research showed oxidative stress, the main pathologic feature of most liver diseases, could modify Keap1 and inhibit Nrf2 ubiquitination (Kobayashi et al., 2006; Saito et al., 2016). Nrf2 accumulation in the cytoplasm would translocate into the nucleus and bind to antioxidant-responsive elements (ARE) to transcript anti-oxidative and anti-inflammation genes expression involving superoxide dismutase (SOD), glutathione-S transferase (GST), glutathione peroxidase (GPx), catalase (CAT), heme oxygenase-1 (HO-1), quinone oxidoreductase-1 (NQO-1), and cyclooxygenase-2 (COX-2) (Prestera et al., 1995; Raghunath et al., 2018; Bardallo et al., 2022). Additionally, active Nrf2 may inhibit NF-κBp65 phosphorylation and reduce NF-κBp65 translocation to the nucleus in animal models to minimize inflammation and apoptosis. The PERK may collaborate with Nrf2 to improve cell survival after exposure to ER stress (Cullinan et al., 2003; Dai et al., 2018). We identified that MT could enhance the protective impact against hepatic damage via Nrf2 moving to the nucleus and activate downstream transcription of genes including CAT, SOD, and HO-1 in HFD-induced liver injury mouse models (Zhang et al., 2013).

4.2 The hepatoxicity and molecular mechanism of MT on liver

As with the ER, mitochondria can potentially play an essential role in regulating Ca^{2+} homeostasis under physiological conditions. Specifically, Ca^{2+} could be transported to the outer membrane of mitochondria (OMM) through the voltage-dependent anion channels (VDACs) in the hepatocytes, and VDCAs would be regulated by a series of proteins, including inositol 1,4,5-trisphosphate receptors (IP3Rs), ryanodine receptor (RyR), glucose-regulated protein 75 (GRP75), and sigma-1 receptor (S1R), to transfer Ca^{2+} into the intermembranous space (IMS). Elevated Ca^{2+} levels in the IMS could lead the mitochondrial Ca^{2+} uniporter (MCU) on the inner mitochondrial membrane (IMM) to interact with the mitochondrial Ca^{2+} uptake 1/2 (MICU1/2) and promote Ca^{2+} influx to the matrix (Hirata et al., 2002; Csordas et al., 2013; Williams et al., 2015; Shoshan-Barmatz et al., 2018). Furthermore, previous research has suggested that matrix Ca^{2+} can influence the cycle of TCA and the process of oxidative phosphorylation for ATP production. Interestingly, the required ROS might be created simultaneously in aerobic metabolism to maintain microdomain cell signaling (Bertero and Maack, 2018).

Gao et al. observed that excessive amounts of MT (800 μM) elevated SREBP1c, Fas, and Acc expression in PA-induced L02 cells. In comparison to low and medium dosages of MT, overdosage treatment results in the opposite effect. High-MT treatment causes toxicity and ultimately loss of protective capacity in the PA-induced L02 cell line (Gao et al., 2018). Furthermore, at low and medium levels, MT might have a therapeutic function of active SERCA to increase Ca^{2+} ion influx to the ER in response to stress, but excessive MT would have a negative influence on this reaction. MT given in high doses inhibits SERCA activity, limiting Ca^{2+} transport from the cytosol to the ER lumen and increasing ER stress. Nonetheless, increased cytosolic Ca^{2+} may be transported across the mitochondria via VDACs, leading to a surge in Ca^{2+} accumulation within the IMS (Rapizzi et al., 2002; Shoshan-Barmatz et al., 2018). Ca^{2+} accumulation in the IMS stimulates the MCU to transport Ca^{2+} into the matrix. This process accelerates the metabolic rate of the TCA cycle and oxidative phosphorylation, resulting in an increase in mitochondrial ROS and apoptosis (Traaseth et al., 2004; Mallilankaraman et al., 2012; Csordas et al., 2013).

Overdosage of MT induces hepatotoxicity in animal models, and high-level MT may promote hepatocytes to produce higher ROS, increased HO-1, and the pro-apoptotic protein BAX while inhibiting the anti-apoptotic protein Bcl-2 synthesis. According to current research, mitochondrial ROS would activate NF-κB, improve the production of inflammatory cytokines, and prevent Nrf2 degradation, hence increasing HO-1 expression (Wang et al., 2015; Lingappan, 2018; Kasai et al., 2020; Liu et al., 2020; Li et al., 2021). The present literature has demonstrated that raising cytosolic Ca^{2+} concentration could also activate the NF-κB through elevating Ca2+/Calmodulin-Dependent Protein Kinase II (CaMKII) activity to phosphorylate and degrade IκK in the neurons (Snow and Albensi, 2016). Additionally, Rao et al. have discovered that MT-induced hepatotoxicity in the mice model suppresses three genes connected to steroid synthesis and metabolic processes in LI. These genes include 7-dehydrocholesterol reductase (DHCR7), NAD-(P)-dependent steroid dehydrogenase-like (NSDHL), and 3-hydroxy-3-methylglutaryl-coenzyme A synthase 1 (HMGCS1). However, the detailed mechanism is still to be further researched in the future (Rao et al., 2022).

4.3 The dual effects of matrine depend on dosage and molecular docking

The distinctive and dose-dependent effects of MT have been utilized to investigate various mechanisms of liver protection and hepatotoxicity. The suggested dosage, according to our data, is between 30–62. 5 mg/kg/d, which can be harmful to rodent animal models. When given at a dosage of 20 mg/kg/d from 0.02W to 0.86W, MT demonstrated significant liver protection with no hepatotoxicity. Finally, our findings show that a dosage of 20–30 mg/kg/d of 0.02–0.86 W has a considerable liver-protective effect with low hepatotoxicity. A dosage of more than 30–62.5 mg/kg/d of MT therapy, on the other hand, caused liver damage in animal models. Through the activation of SERCA, SREBP-SCAP complexes, and MT, the pharmacological actions of MT can produce both liver protection and damage. These complexes are responsible for linking the IRE1, ATF6, and PERK proteins, all of which play important roles in regulating ER stress. The interaction of MT with SERCA and SREBP-SCAP complexes was demonstrated utilizing molecular docking, and the thermodynamic data was analyzed. With an estimated free energy of −7.8 kcal/mol, the molecule MT interacts with Phe256, Phe834, Ile829, Ile765, Tyr837, Val769, Val263, and Met83 on the SERCA protein.

With an estimated free energy of −6.8 kcal/mol, MT interacts substantially with the Glu605, Leu647, Pro649, Trp690, Ala646, Ala602, Val688, Val603, and Ile645 on the SREBP-SCAP complexes. SERCA and SREBP-SCAP complexes exhibit beneficial patterns of hydrogen bond and hydrophobic interactions.

4.4 Limitations

This meta-analysis adhered to the PRISMA standards (http://prisma-statement.org/), despite several limitations. 1) As only four English and four Chinese databases were utilized for article inclusion, selective bias was inevitable. In addition, we have not been able to compile all the relevant literature. 2) The heterogeneity of various studies could not be unified because of instrument index measurement error, different units of indicators, different experimental methods, *etc.* 3) Even though articles with quality scores of less than 5 points were disregarded, there may be heterogeneity in the results due to differences in the quality of the included articles. 4) The absence of a standardized method for animal intervention, drug dosage, treatment regimens, and model species across studies was another factor that might have caused the high heterogeneity. The reliability of MT's results in treating LI or causing hepatotoxicity was confirmed by the sensitivity analysis, Egger's test, and subgroup analysis. 5) Although the primary pharmacological mechanisms of MT in terms of liver protection and hepatotoxicity have been summarized, not all mechanisms could be summarized due to the complex pathogenic mechanisms involved. 6) The reliability of MT for hepatotoxicity may be lower than for hepatoprotection because only 5 articles on this condition were included. Future research should be conducted to investigate the hepatotoxicity of MT. 7) For ethical reasons, there is a paucity of literature on the toxicological effects of MT in the human body. Therefore, we only included studies using animal models. It is important to conduct relevant clinical trials to confirm the efficacy and reliability of MT in the clinical management of hepatoprotection and hepatotoxicity. 8) We validated the binding of MT to key proteins using molecular docking, but experiments were still needed to prove it.

Although this meta-analysis has several limitations, the findings may provide new strategies for clinical medication and drug development.

5 Conclusion

In summary, our study revealed that within the dose range of 10–69.1 mg/kg and time range of 1–2 weeks, MT could have a bilateral impact on liver damage. However, at a dose of 20–30 mg/kg/d for 0.02–0.86 weeks, it demonstrated high protection and low toxicity on the liver. Molecular docking analysis indicated that MT interacts with SERCA and SREBP-SCAP complexes. These interactions involve beneficial patterns of hydrogen bonds and hydrophobic interactions. By activating SERCA, a Ca^{2+} ion channel on the ER, MT could play a crucial role in regulating Ca^{2+} homeostasis in damaged hepatocytes. This helps maintain the balance among the cytoplasm, ER, Golgi apparatus, and mitochondria. Our findings suggest that MT doses ranging from 1.4 mg/kg/d to 100 mg/kg/d may have a preventive and therapeutic effect on LI by modulating the expression of biomarkers such as TNF-α, IL-6, serum TG, serum TC, SOD, MDA, CAT, ALT, and AST. Additionally, signaling pathways such as SREBP1c/SCAP, Notch/RBP-J/HES1, IκK/NF-κB, and Cul3/Rbx1/Keap1/Nrf2 are likely involved in the protective process. It is interesting to note that many of these signaling pathways directly or indirectly interact with Ca^{2+} homeostasis. However, in normal hepatocytes, a high dosage of MT can suppress SERCA activity, leading to an adverse impact on Ca^{2+} homeostasis. This, in turn, can cause hepatotoxicity and promote apoptosis through the reduction of Bcl-2 and activation of the Ros/Bax/caspase 9/caspase 3 pathway. Elevated MT levels can also modulate the expression of various metabolic indicators, including AST, ALT, DHCR7, NSDHL, and HMGCS1. Further investigation is required to fully understand how MT influences the expression of these genes.

Data availability statement

The original contributions presented in the study are included in the article/Supplementary Material, further inquiries can be directed to the corresponding authors.

Author contributions

WF: Conceptualization, Data curation, Methodology, Visualization, Writing–original draft. T-CK: Conceptualization, Data curation, Formal Analysis, Methodology, Visualization, Writing–original draft. JJ: Conceptualization, Data curation, Formal Analysis, Methodology, Visualization, Writing–original draft. XiZ: Data curation, Visualization, Writing–original draft. SC: Data curation, Visualization, Writing–original draft. JZ: Conceptualization, Writing–review and editing. YC: Conceptualization, Writing–review and editing. XM: Conceptualization, Writing–review and editing.

Funding

The author(s) declare financial support was received for the research, authorship, and/or publication of this article. This work was supported by Sichuan Science and Technology Program (2023NSFSC0687), Xinglin Scholar Research Promotion Project of Chengdu University of TCM (grant nos. QJRC2022028 and QJJJ2022010), Major scientific research problems and key topics of medical technology problems of China Medical Education Association (2022KTZ016) and "The Hundred Talents Program" of the Hospital of the Chengdu University of Traditional Chinese Medicine (grant no. 22- B09).

Acknowledgments

This paper has been greatly improved by the advice of the reviewers and the authors of all references. The authors wish to thank the reviewers and the authors of all references.

Conflict of interest

The authors declare that the research was conducted in the absence of any commercial or financial relationships that could be construed as a potential conflict of interest.

Publisher's note

All claims expressed in this article are solely those of the authors and do not necessarily represent those of their affiliated organizations, or those of the publisher, the editors and the reviewers. Any product that may be evaluated in this article, or claim that may be made by its manufacturer, is not guaranteed or endorsed by the publisher.

Supplementary material

The Supplementary Material for this article can be found online at: https://www.frontiersin.org/articles/10.3389/fphar.2024.1315584/full#supplementary-material

References

Bagur, R., and Hajnoczky, G. (2017). Intracellular Ca(2+) sensing: its role in calcium homeostasis and signaling. *Mol. Cell* 66 (6), 780–788. doi:10.1016/j.molcel.2017.05.028

Bai, N., Wang, D., Ouyang, X., Zhou, L., and Wang, Z. (2018). Inhibitory effect of matrine against hepatic ischemia-reperfusion injury in rats and its mechanis. *Chin. J. General Surg.* 27, 81–86. doi:10.3978/j.issn.1005-6947.2018.01.013

Bardallo, R. G., Panisello-Rosello, A., Sanchez-Nuno, S., Alva, N., Rosello-Catafau, J., and Carbonell, T. (2022). Nrf2 and oxidative stress in liver ischemia/reperfusion injury. *FEBS J.* 289 (18), 5463–5479. doi:10.1111/febs.16336

Bartlett, P. J., Gaspers, L. D., Pierobon, N., and Thomas, A. P. (2014). Calcium-dependent regulation of glucose homeostasis in the liver. *Cell Calcium* 55 (6), 306–316. doi:10.1016/j.ceca.2014.02.007

Bertero, E., and Maack, C. (2018). Calcium signaling and reactive oxygen species in mitochondria. *Circ. Res.* 122 (10), 1460–1478. doi:10.1161/CIRCRESAHA.118.310082

Chang, L., Wang, S., Dou, L., Jia, M., Wang, T., and Xu, B. (2021). Protective mechanism of matrine against liver injury induced by acetaminophen in mice. *China J. Mod. Med.* 31, 58–63. doi:10.3969/j.issn.1005-8982.2021.19.011

Chemaly, E. R., Troncone, L., and Lebeche, D. (2018). SERCA control of cell death and survival. *Cell Calcium* 69, 46–61. doi:10.1016/j.ceca.2017.07.001

Chinese Pharmacopoeia Commission (2020). *The Pharmacopoeia of the people's Republic of China, 2020*. ed. Part I. Beijing, China: China Medical Science Press, 211.

Chu, Y., Jing, Y., Zhao, X., Wang, M., Zhang, M., Ma, R., et al. (2021). Modulation of the HMGB1/TLR4/NF-κB signaling pathway in the CNS by matrine in experimental autoimmune encephalomyelitis. *J. Neuroimmunol.* 352, 577480. doi:10.1016/j.jneuroim.2021.577480

Csordas, G., Golenar, T., Seifert, E. L., Kamer, K. J., Sancak, Y., Perocchi, F., et al. (2013). MICU1 controls both the threshold and cooperative activation of the mitochondrial Ca^{2+} uniporter. *Cell Metab.* 17 (6), 976–987. doi:10.1016/j.cmet.2013.04.020

Cullinan, S. B., Zhang, D., Hannink, M., Arvisais, E., Kaufman, R. J., and Diehl, J. A. (2003). Nrf2 is a direct PERK substrate and effector of PERK-dependent cell survival. *Mol. Cell Biol.* 23 (20), 7198–7209. doi:10.1128/MCB.23.20.7198-7209.2003

Dai, Y., Zhang, H., Zhang, J., and Yan, M. (2018). Isoquercetin attenuates oxidative stress and neuronal apoptosis after ischemia/reperfusion injury via Nrf2-mediated inhibition of the NOX4/ROS/NF-κB pathway. *Chem. Biol. Interact.* 284, 32–40. doi:10.1016/j.cbi.2018.02.017

De Ford, C., Heidersdorf, B., Haun, F., Murillo, R., Friedrich, T., Borner, C., et al. (2016). The clerodane diterpene casearin J induces apoptosis of T-ALL cells through SERCA inhibition, oxidative stress, and interference with Notch1 signaling. *Cell Death Dis.* 7 (1), e2070. doi:10.1038/cddis.2015.413

Devarbhavi, H., Asrani, S. K., Arab, J. P., Nartey, Y. A., Pose, E., and Kamath, P. S. (2023). Global burden of liver disease: 2023 update. *J. Hepatol.* 79 (2), 516–537. doi:10.1016/j.jhep.2023.03.017

Diaz-Garcia, C. M., Meyer, D. J., Nathwani, N., Rahman, M., Martinez-Francois, J. R., and Yellen, G. (2021). The distinct roles of calcium in rapid control of neuronal glycolysis and the tricarboxylic acid cycle. *Elife* 10, e64821. doi:10.7554/eLife.64821

Du, M., Xu, B., Xiang, R., Guo, D., Fan, Y., Shi, X., et al. (2021). The protective effect of Matrine injection on acute alcoholic liver injury in mice. *China J. Mod. Med.* 31, 13–18. doi:10.3969/j.issn.1005-8982.2021.24.003

Eberle, D., Hegarty, B., Bossard, P., Ferre, P., and Foufelle, F. (2004). SREBP transcription factors: master regulators of lipid homeostasis. *Biochimie* 86 (11), 839–848. doi:10.1016/j.biochi.2004.09.018

Fowler, J. W. M., Zhang, R., Tao, B., Boutagy, N. E., and Sessa, W. C. (2022). Inflammatory stress signaling via NF-kB alters accessible cholesterol to upregulate SREBP2 transcriptional activity in endothelial cells. *Elife* 86 (11). doi:10.7554/eLife.79529

Gao, X., Guo, S., Zhang, S., Liu, A., Shi, L., and Zhang, Y. (2018). Matrine attenuates endoplasmic reticulum stress and mitochondrion dysfunction in nonalcoholic fatty liver disease by regulating SERCA pathway. *J. Transl. Med.* 16 (1), 319. doi:10.1186/s12967-018-1685-2

Gao, X., Guo, S., Zhang, S., Liu, A., Shi, L., and Zhang, Y. (2019). Correction to: matrine attenuates endoplasmic reticulum stress and mitochondrion dysfunction in nonalcoholic fatty liver disease by regulating SERCA pathway. *J. Transl. Med.* 17 (1), 277. doi:10.1186/s12967-019-2020-2

Gao, Y., Zheng, P., Yan, L., and Dai, G. (2013). Preliminary mechanism study of matrine on chronic alcohol-induced hepatic injury in rats. *Chin. Pharmacol. Bull.* 29, 1012–1016. doi:10.3969/j.issn.1001-1978.2013.07.028

Gerondakis, S., Grumont, R., Gugasyan, R., Wong, L., Isomura, I., Ho, W., et al. (2006). Unravelling the complexities of the NF-kappaB signalling pathway using mouse knockout and transgenic models. *Oncogene* 25 (51), 6781–6799. doi:10.1038/sj.onc.1209944

Gu, Y., Lu, J., Sun, W., Jin, R., Ohira, T., Zhang, Z., et al. (2019). Oxymatrine and its metabolite matrine contribute to the hepatotoxicity induced by radix Sophorae tonkinensis in mice. *Exp. Ther. Med.* 17 (4), 2519–2528. doi:10.3892/etm.2019.7237

Guo, S., Zhang, S., Wei, H., Shi, L., Hu, N., Dang, X., et al. (2017). Protective effect and mechanism of matrine combined with glycyrrhizic acid in the treatment of chronic liver injury induced by carbon tetrachloride. *China Pharm.* 20, 1153–1158.

Harding, H. P., Zhang, Y., Zeng, H., Novoa, I., Lu, P. D., Calfon, M., et al. (2003). An integrated stress response regulates amino acid metabolism and resistance to oxidative stress. *Mol. Cell* 11 (3), 619–633. doi:10.1016/s1097-2765(03)00105-9

He, X., Fang, J., Huang, L., Wang, J., and Huang, X. (2015). Sophora flavescens Ait.: traditional usage, phytochemistry and pharmacology of an important traditional Chinese medicine. *J. Ethnopharmacol.* 172, 10–29. doi:10.1016/j.jep.2015.06.010

Hirata, K., Pusl, T., O'Neill, A. F., Dranoff, J. A., and Nathanson, M. H. (2002). The type II inositol 1,4,5-trisphosphate receptor can trigger Ca2+ waves in rat hepatocytes. *Gastroenterology* 122 (4), 1088–1100. doi:10.1053/gast.2002.32363

Horton, J. D., Goldstein, J. L., and Brown, M. S. (2002). SREBPs: activators of the complete program of cholesterol and fatty acid synthesis in the liver. *J. Clin. Investigation* 109 (9), 1125–1131. doi:10.1172/JCI15593

Jin, Y., Bai, Y., Ni, H., Qiang, L., Ye, L., Shan, Y., et al. (2016). Activation of autophagy through calcium-dependent AMPK/mTOR and PKCθ pathway causes activation of rat hepatic stellate cells under hypoxic stress. *FEBS Lett.* 590 (5), 672–682. doi:10.1002/1873-3468.12090

Jing, Y., Ma, R., Chu, Y., Dou, M., Wang, M., Li, X., et al. (2021). Matrine treatment induced an A2 astrocyte phenotype and protected the blood-brain barrier in CNS autoimmunity. *J. Chem. Neuroanat.* 117, 102004. doi:10.1016/j.jchemneu.2021.102004

Ju, J., Li, J., Lin, Q., and Xu, H. (2018). Efficacy and safety of berberine for dyslipidaemias: a systematic review and meta-analysis of randomized clinical trials. *Phytomedicine* 50, 25–34. doi:10.1016/j.phymed.2018.09.212

Kasai, S., Shimizu, S., Tatara, Y., Mimura, J., and Itoh, K. (2020). Regulation of Nrf2 by mitochondrial reactive oxygen species in physiology and pathology. *Biomolecules* 10 (2), 320. doi:10.3390/biom10020320

Kaufman, R. J., and Malhotra, J. D. (2014). Calcium trafficking integrates endoplasmic reticulum function with mitochondrial bioenergetics. *Biochim. Biophys. Acta* 1843 (10), 2233–2239. doi:10.1016/j.bbamcr.2014.03.022

Khan, A., Shal, B., Naveed, M., Shah, F. A., Atiq, A., Khan, N. U., et al. (2019). Matrine ameliorates anxiety and depression-like behaviour by targeting hyperammonemia-induced neuroinflammation and oxidative stress in CCl4 model of liver injury. *Neurotoxicology* 72, 38–50. doi:10.1016/j.neuro.2019.02.002

Khandelwal, N., Simpson, J., Taylor, G., Rafique, S., Whitehouse, A., Hiscox, J., et al. (2011). Nucleolar NF-κB/RelA mediates apoptosis by causing cytoplasmic relocalization of nucleophosmin. *Cell Death Differ.* 18 (12), 1889–1903. doi:10.1038/cdd.2011.79

King, A. L., Swain, T. M., Dickinson, D. A., Lesort, M. J., and Bailey, S. M. (2010). Chronic ethanol consumption enhances sensitivity to Ca(2+)-mediated opening of the mitochondrial permeability transition pore and increases cyclophilin D in liver. *Am. J. Physiol. Gastrointest. Liver Physiol.* 299 (4), G954–G966. doi:10.1152/ajpgi.00246.2010

Knight, J. A. (2005). Liver function tests: their role in the diagnosis of hepatobiliary diseases. *J. Infus. Nurs.* 28 (2), 108–117. doi:10.1097/00129804-200503000-00004

Kobayashi, A., Kang, M. I., Watai, Y., Tong, K. I., Shibata, T., Uchida, K., et al. (2006). Oxidative and electrophilic stresses activate Nrf2 through inhibition of ubiquitination activity of Keap1. *Mol. Cell Biol.* 26 (1), 221–229. doi:10.1128/MCB.26.1.221-229.2006

Lai, S., Li, Y., Kuang, Y., Cui, H., Yang, Y., Sun, W., et al. (2017). PKCδ silencing alleviates saturated fatty acid induced ER stress by enhancing SERCA activity. *Biosci. Rep.* 37 (6). doi:10.1042/BSR20170869

Lee, S. H., Lee, J. H., and Im, S. S. (2020). The cellular function of SCAP in metabolic signaling. *Exp. Mol. Med.* 52 (5), 724–729. doi:10.1038/s12276-020-0430-0

Li, L. C., Varghese, Z., Moorhead, J. F., Lee, C. T., Chen, J. B., and Ruan, X. Z. (2013). Cross-talk between TLR4-MyD88-NF-κB and SCAP-SREBP2 pathways mediates macrophage foam cell formation. *Am J. Physiol. Heart Circ. Physiol.* 304 (6), H874–H884. doi:10.1152/ajpheart.00096.2012

Li, C., Liu, L., Mo, C., and Huang, L. (2005). Effects of Matrine on release of interferon and pathological changes in concanavalin A-induced liver injury in mice. *World Chin. J. Dig.* 13, 640–643.

Li, D., Hong, X., Zhao, F., Ci, X., and Zhang, S. (2021). Targeting Nrf2 may reverse the drug resistance in ovarian cancer. *Cancer Cell Int.* 21 (1), 116. doi:10.1186/s12935-021-01822-1

Li, X., Cheng, G., and Zhou, F. (2016). The effects of matrine on blood lipids and antioxidant capacity in rats with chronic alcoholic liver injury. *Chin. J. Geriatrics* 36, 1838–1839. doi:10.3969/j.issn.1005-9202.2016.08.021

Li, Y., Boehning, D. F., Qian, T., Popov, V. L., and Weinman, S. A. (2007). Hepatitis C virus core protein increases mitochondrial ROS production by stimulation of Ca2+ uniporter activity. *FASEB J.* 21 (10), 2474–2485. doi:10.1096/fj.06-7345com

Liang, P., Yuan, T., Gu, L., and Lu, H. (2015). Study of hepatotoxicity and neural behavioral changes of Sophora flavescens and matrine in mice. *Chin. J. Mod. Appl. Pharm.* 32, 1444–1448. doi:10.13748/j.cnki.issn1007-7693.2015.12.008

Lingappan, K. (2018). NF-κB in oxidative stress. *Curr. Opin. Toxicol.* 7, 81–86. doi:10.1016/j.cotox.2017.11.002

Liu, H., Qiu, Y., Mao, L., Zhu, X., and Ding, Y. (2008). Protective effect of matrine against ischemia and reperfusion injury in rat partial liver transplantation. *World Chin. J. Dig.* 16, 1617–1621. doi:10.11569/wcjd.v16.i15.1617

Liu, J., Zhao, Y., Xia, J., and Qiu, M. (2020). Matrine induces toxicity in mouse liver cells through an ROS-dependent mechanism. *Res. Vet. Sci.* 132, 308–311. doi:10.1016/j.rvsc.2020.07.006

Liu, M., Pu, Y., Gu, J., He, Q., Liu, Y., Zeng, Y., et al. (2021). Evaluation of Zhilong Huoxue Tongyu capsule in the treatment of acute cerebral infarction: a systematic review and meta-analysis of randomized controlled trials. *Phytomedicine* 86, 153566. doi:10.1016/j.phymed.2021.153566

Liu, Q., and Zhang, X. S. (2021). Analysis of clinical application literature on matrine injection. *Chin. Jof Clin. Ration. Drug Use* 14, 12A. doi:10.15887/j.cnki.13-1389/r.2021.34.072

Luo, X., Ni, X., Lin, J., Zhang, Y., Wu, L., Huang, D., et al. (2021). The add-on effect of Chinese herbal medicine on COVID-19: a systematic review and meta-analysis. *Phytomedicine* 85, 153282. doi:10.1016/j.phymed.2020.153282

Macleod, M. R., O'Collins, T., Howells, D. W., and Donnan, G. A. (2004). Pooling of animal experimental data reveals influence of study design and publication bias. *Stroke* 35 (5), 1203–1208. doi:10.1161/01.Str.0000125719.25853.20

Mallilankaraman, K., Doonan, P., Cardenas, C., Chandramoorthy, H. C., Muller, M., Miller, R., et al. (2012). MICU1 is an essential gatekeeper for MCU-mediated mitochondrial Ca(2+) uptake that regulates cell survival. *Cell* 151 (3), 630–644. doi:10.1016/j.cell.2012.10.011

Mantena, S. K., King, A. L., Andringa, K. K., Eccleston, H. B., and Bailey, S. M. (2008). Mitochondrial dysfunction and oxidative stress in the pathogenesis of alcohol- and obesity-induced fatty liver diseases. *Free Radic. Biol. Med.* 44 (7), 1259–1272. doi:10.1016/j.freeradbiomed.2007.12.029

Mitchell, S., Vargas, J., and Hoffmann, A. (2016). Signaling via the NFκB system. *Wiley Interdiscip. Rev. Syst. Biol. Med.* 8 (3), 227–241. doi:10.1002/wsbm.1331

O-Uchi, J., Ryu, S. Y., Jhun, B. S., Hurst, S., and Sheu, S. S. (2014). Mitochondrial ion channels/transporters as sensors and regulators of cellular redox signaling. *Antioxid. Redox Signal* 21 (6), 987–1006. doi:10.1089/ars.2013.5681

Pan, L. J., Zhang, Z. C., Zhang, Z. Y., Wang, W. J., Xu, Y., and Zhang, Z. M. (2012). Effects and mechanisms of store-operated calcium channel blockade on hepatic ischemia-reperfusion injury in rats. *World J. Gastroenterol.* 18 (4), 356–367. doi:10.3748/wjg.v18.i4.356

Park, H. W., and Lee, J. H. (2014). Calcium channel blockers as potential therapeutics for obesity-associated autophagy defects and fatty liver pathologies. *Autophagy* 10 (12), 2385–2386. doi:10.4161/15548627.2014.984268

Peng, W., Xu, Y., Han, D., Feng, F., Wang, Z., Gu, C., et al. (2020). Potential mechanism underlying the effect of matrine on COVID-19 patients revealed through network pharmacological approaches and molecular docking analysis. *Arch. Physiol. Biochem.* 129, 253–260. doi:10.1080/13813455.2020.1817944

Periasamy, M., and Kalyanasundaram, A. (2007). SERCA pump isoforms: their role in calcium transport and disease. *Muscle Nerve* 35 (4), 430–442. doi:10.1002/mus.20745

Peterson, T. R., Sengupta, S. S., Harris, T. E., Carmack, A. E., Kang, S. A., Balderas, E., et al. (2011). mTOR complex 1 regulates lipin 1 localization to control the SREBP pathway. *Cell* 146 (3), 408–420. doi:10.1016/j.cell.2011.06.034

Prestera, T., Talalay, P., Alam, J., Ahn, Y. I., Lee, P. J., and Choi, A. M. (1995). Parallel induction of heme oxygenase-1 and chemoprotective phase 2 enzymes by electrophiles and antioxidants: regulation by upstream antioxidant-responsive elements (ARE). *Mol. Med.* 1, 827–837. doi:10.1007/bf03401897

Raghunath, A., Sundarraj, K., Nagarajan, R., Arfuso, F., Bian, J., Kumar, A. P., et al. (2018). Antioxidant response elements: Discovery, classes, regulation and potential applications. *Redox Biol.* 17, 297–314. doi:10.1016/j.redox.2018.05.002

Rao, S. W., Duan, Y. Y., Zhao, D. S., Liu, C. J., Xu, S. H., Liang, D., et al. (2022). Integrative analysis of transcriptomic and metabolomic data for identification of pathways related to matrine-induced hepatotoxicity. *Chem. Res. Toxicol.* 35 (12), 2271–2284. doi:10.1021/acs.chemrestox.2c00264

Rapizzi, E., Pinton, P., Szabadkai, G., Wieckowski, M. R., Vandecasteele, G., Baird, G., et al. (2002). Recombinant expression of the voltage-dependent anion channel enhances the transfer of Ca2+ microdomains to mitochondria. *J. Cell Biol.* 159 (4), 613–624. doi:10.1083/jcb.200205091

Rieusset, J. (2017). Endoplasmic reticulum-mitochondria calcium signaling in hepatic metabolic diseases. *Biochim. Biophys. Acta Mol. Cell Res.* 1864 (6), 865–876. doi:10.1016/j.bbamcr.2017.01.001

Rinella, M. E., Elias, M. S., Smolak, R. R., Fu, T., Borensztajn, J., and Green, R. M. (2008). Mechanisms of hepatic steatosis in mice fed a lipogenic methionine choline-deficient diet. *J. Lipid Res.* 49 (5), 1068–1076. doi:10.1194/jlr.M800042-JLR200

Saito, R., Suzuki, T., Hiramoto, K., Asami, S., Naganuma, E., Suda, H., et al. (2016). Characterizations of three major cysteine sensors of Keap1 in stress response. *Mol. Cell Biol.* 36 (2), 271–284. doi:10.1128/MCB.00868-15

Sekiya, M., Hiraishi, A., Touyama, M., and Sakamoto, K. (2008). Oxidative stress induced lipid accumulation via SREBP1c activation in HepG2 cells. *Biochem. Biophys. Res. Commun.* 375 (4), 602–607. doi:10.1016/j.bbrc.2008.08.068

Shi, D., Zhang, J., Qiu, L., Li, J., Hu, Z., and Zhang, J. (2013). Matrine inhibits infiltration of the inflammatory gr1(hi) monocyte subset in injured mouse liver through inhibition of monocyte chemoattractant protein-1. *Evid. Based Complement. Altern. Med.* 2013, 580673. doi:10.1155/2013/580673

Shimano, H., and Sato, R. (2017). SREBP-regulated lipid metabolism: convergent physiology - divergent pathophysiology. *Nat. Rev. Endocrinol.* 13 (12), 710–730. doi:10.1038/nrendo.2017.91

Shoshan-Barmatz, V., Krelin, Y., and Shteinfer-Kuzmine, A. (2018). VDAC1 functions in Ca(2+) homeostasis and cell life and death in health and disease. *Cell Calcium* 69, 81–100. doi:10.1016/j.ceca.2017.06.007

Snow, W. M., and Albensi, B. C. (2016). Neuronal gene targets of NF-κB and their dysregulation in alzheimer's disease. *Front. Mol. Neurosci.* 9, 118. doi:10.3389/fnmol.2016.00118

Song, B., Han, C., and Zhang, H. (2009). Toxicity of three Sophora flavescens ait alkaloids to mice. *Acta Bot. Boreali-Occidentalia Sin.* 29, 818–823.

Stork, B. A., Dean, A., Ortiz, A. R., Saha, P., Putluri, N., Planas-Silva, M. D., et al. (2022). Calcium/calmodulin-dependent protein kinase kinase 2 regulates hepatic fuel metabolism. *Mol. Metab.* 62, 101513. doi:10.1016/j.molmet.2022.101513

Sun, X. Y., Jia, L. Y., Rong, Z., Zhou, X., Cao, L. Q., Li, A. H., et al. (2022). Research advances on matrine. *Front. Chem.* 10, 867318. doi:10.3389/fchem.2022.867318

Szegezdi, E., Logue, S. E., Gorman, A. M., and Samali, A. (2006). Mediators of endoplasmic reticulum stress-induced apoptosis. *EMBO Rep.* 7 (9), 880–885. doi:10.1038/sj.embor.7400779

Tang, B., Ai, Z., and Yao, S. (2013). Effects of Matrine on the expression of COX-2 and iNOS in rats with non-alcoholic fatty liver disease. *Chin. J. Clin. Electron. Ed.* 7, 2011–2015. doi:10.3877/cma.j.issn.1674-0785.2013.05.038

Tang, B. D., Xia, X., Lv, X. F., Yu, B. X., Yuan, J. N., Mai, X. Y., et al. (2017). Inhibition of Orai1-mediated Ca(2+) entry enhances chemosensitivity of HepG2 hepatocarcinoma cells to 5-fluorouracil. *J. Cell Mol. Med.* 21 (5), 904–915. doi:10.1111/jcmm.13029

Traaseth, N., Elfering, S., Solien, J., Haynes, V., and Giulivi, C. (2004). Role of calcium signaling in the activation of mitochondrial nitric oxide synthase and citric acid cycle. *Biochim. Biophys. Acta* 1658 (1-2), 64–71. doi:10.1016/j.bbabio.2004.04.015

Vacca, A., Felli, M. P., Palermo, R., Di Mario, G., Calce, A., Di Giovine, M., et al. (2006). Notch3 and pre-TCR interaction unveils distinct NF-kappaB pathways in T-cell development and leukemia. *Embo j.* 25 (5), 1000–1008. doi:10.1038/sj.emboj.7600996

Wan, B., LaNoue, K. F., Cheung, J. Y., and Scaduto, R. C. (1989). Regulation of citric acid cycle by calcium. *J. Biol. Chem.* 264 (23), 13430–13439. doi:10.1016/s0021-9258(18)80015-1

Wang, F., Yang, J. L., Yu, K. K., Xu, M., Xu, Y. Z., Chen, L., et al. (2015). Activation of the NF-κB pathway as a mechanism of alcohol enhanced progression and metastasis of human hepatocellular carcinoma. *Mol. Cancer* 14 (1), 10. doi:10.1186/s12943-014-0274-0

Wang, L., Lu, J., Sun, W., Gu, Y., Zhang, C., Jin, R., et al. (2017). Hepatotoxicity induced by radix Sophorae tonkinensis in mice and increased serum cholinesterase as a potential supplemental biomarker for liver injury. *Exp. Toxicol. Pathol.* 69 (4), 193–202. doi:10.1016/j.etp.2017.01.003

Wang, Y., Zhang, S., Liu, J., Fang, B., Yao, J., and Cheng, B. (2018). Matrine inhibits the invasive and migratory properties of human hepatocellular carcinoma by regulating epithelial-mesenchymal transition. *Mol. Med. Rep.* 18 (1), 911–919. doi:10.3892/mmr.2018.9023

Williams, G. S., Boyman, L., and Lederer, W. J. (2015). Mitochondrial calcium and the regulation of metabolism in the heart. *J. Mol. Cell Cardiol.* 78, 35–45. doi:10.1016/j.yjmcc.2014.10.019

Wu, Y., Wang, Y., and Ma, X. (2014). Protective effects of matrine on acute ethanol-induced liver injury in mice. *Asia-Pacific Tradit. Med.* 10, 6–9.

Xiao, F., Zhang, J., Zhang, C., and An, W. (2017). Hepatic stimulator substance inhibits calcium overflow through the mitochondria-associated membrane compartment during nonalcoholic steatohepatitis. *Lab. Invest.* 97 (3), 289–301. doi:10.1038/labinvest.2016.139

Xiong, X., Wang, P., Duan, L., Liu, W., Chu, F., Li, S., et al. (2019). Efficacy and safety of Chinese herbal medicine Xiao Yao San in hypertension: a systematic review and meta-analysis. *Phytomedicine* 61, 152849. doi:10.1016/j.phymed.2019.152849

Yang, Z., Yu, G. L., Zhu, X., Peng, T. H., and Lv, Y. C. (2022). Critical roles of FTO-mediated mRNA m6A demethylation in regulating adipogenesis and lipid metabolism: Implications in lipid metabolic disorders. *Genes Dis.* 9 (1), 51–61. doi:10.1016/j.gendis.2021.01.005

Yang, Z., Gao, S., Yin, T., Kulkarni, K. H., Teng, Y., You, M., et al. (2010). Biopharmaceutical and pharmacokinetic characterization of matrine as determined by a sensitive and robust UPLC-MS/MS method. *J. Pharm. Biomed. Anal.* 51, 1120–1127. doi:10.1016/j.jpba.2009.11.020

Yang, Z., Wang, L., and Wang, X. (2016). Matrine induces the hepatic differentiation of WB-F344 rat hepatic progenitor cells and inhibits Jagged 1/HES1 signaling. *Mol. Med. Rep.* 14 (4), 3841–3847. doi:10.3892/mmr.2016.5668

Yang, Z. Y., Wang, L., Hou, Y. X., and Wang, X. B. (2013). Effects of matrine on oval cell-mediated liver regeneration and expression of RBP-Jκ and HES1. *Mol. Med. Rep.* 7 (5), 1533–1538. doi:10.3892/mmr.2013.1398

Yin, H., Que, R., Liu, C., Ji, W., Sun, B., Lin, X., et al. (2018). Survivin-targeted drug screening platform identifies a matrine derivative WM-127 as a potential therapeutics against hepatocellular carcinoma. *Cancer Lett.* 425, 54–64. doi:10.1016/j.canlet.2018.03.044

You, L., Yang, C., Du, Y., Liu, Y., Chen, G., Sai, N., et al. (2019). Matrine exerts hepatotoxic effects via the ROS-dependent mitochondrial apoptosis pathway and inhibition of nrf2-mediated antioxidant response. *Oxid. Med. Cell Longev.* 2019, 1045345. doi:10.1155/2019/1045345

Younossi, Z. M., Wong, G., Anstee, Q. M., and Henry, L. (2023). The global burden of liver disease. *Clin. Gastroenterol. Hepatol.* 21 (8), 1978–1991. doi:10.1016/j.cgh.2023.04.015

Yu, H. B., Zhang, H. F., Li, D. Y., Zhang, X., Xue, H. Z., and Zhao, S. H. (2011a). Matrine inhibits matrix metalloproteinase-9 expression and invasion of human hepatocellular carcinoma cells. *J. Asian Nat. Prod. Res.* 13 (3), 242–250. doi:10.1080/10286020.2010.551641

Yu, H. C., Qin, H. Y., He, F., Wang, L., Fu, W., Liu, D., et al. (2011b). Canonical notch pathway protects hepatocytes from ischemia/reperfusion injury in mice by repressing reactive oxygen species production through JAK2/STAT3 signaling. *Hepatology* 54 (3), 979–988. doi:10.1002/hep.24469

Yu, J. L., Li, J. H., Chengz, R. G., Ma, Y. M., Wang, X. J., and Liu, J. C. (2014). Effect of matrine on transforming growth factor β1 and hepatocyte growth factor in rat liver fibrosis model. *Asian Pac J. Trop. Med.* 7 (5), 390–393. doi:10.1016/s1995-7645(14)60062-6

Yuan, F., and Yang, Z. (2020). Influence of matrine on liver function and MAPK signaling pathway after hepatic ischemic reperfusion injury in rats. *J. Guangdong Pharm. Univ.* 36, 657–661. doi:10.16809/j.cnki.2096-3653.2020052003

Yue, Z.-S., Ruan, B., Duan, J.-L., Han, H., and Wang, L. (2018). The role of the Notch signaling pathway in liver injury and repair. *J. Bio-X Res.* 1 (2), 95–104. doi:10.1097/jbr.0000000000000014

Zeeshan, H. M., Lee, G. H., Kim, H. R., and Chae, H. J. (2016). Endoplasmic reticulum stress and associated ROS. *Int. J. Mol. Sci.* 17 (3), 327. doi:10.3390/ijms17030327

Zhang, H. F., Shi, L. J., Song, G. Y., Cai, Z. G., Wang, C., and An, R. J. (2013). Protective effects of matrine against progression of high-fructose diet-induced steatohepatitis by enhancing antioxidant and anti-inflammatory defences involving Nrf2 translocation. *Food Chem. Toxicol.* 55, 70–77. doi:10.1016/j.fct.2012.12.043

Zhang, J., Li, Y., Jiang, S., Yu, H., and An, W. (2014). Enhanced endoplasmic reticulum SERCA activity by overexpression of hepatic stimulator substance gene prevents hepatic cells from ER stress-induced apoptosis. *Am. J. Physiol. Cell Physiol.* 306 (3), C279–C290. doi:10.1152/ajpcell.00117.2013

Zhang, X. L., Xu, H. R., Chen, W. L., Chu, N. N., Li, X. N., Liu, G. Y., et al. (2009). Matrine determination and pharmacokinetics in human plasma using LC/MS/MS. *J. Chromatogr. B Anal. Technol. Biomed. Life Sci.* 877 (27), 3253–3256. doi:10.1016/j.jchromb.2009.08.026

Zhao, Y. (2015). Effects of Matrine on inflfl ammatory factor in rats with liver injury of carbon tetrachloride. *Clin. J. Traditional Chin. Med.* 27, 727–728. doi:10.16448/j.cjtcm.2015.0275

Zheng, Y., Ding, Q., Wei, Y., Gou, X., Tian, J., Li, M., et al. (2021). Effect of traditional Chinese medicine on gut microbiota in adults with type 2 diabetes: a systematic review and meta-analysis. *Phytomedicine* 88, 153455. doi:10.1016/j.phymed.2020.153455

Zhou, M., Li, Q., and Su, J. (2009). Effects of matrine on the expression of fas and fasL in liver tissue of mice injured by immune reaction. *China Trop. Med.* 9, 1445–1447.

Zhou, Y., Wu, Y., Deng, L., Chen, L., Zhao, D., Lv, L., et al. (2014). The alkaloid matrine of the root of Sophora flavescens prevents arrhythmogenic effect of ouabain. *Phytomedicine* 21 (7), 931–935. doi:10.1016/j.phymed.2014.02.008

Zhu, J., Zhu, J., Tang, F., Feng, Y., Zhou, Q., Jin, Q., et al. (2015). Influence of matrine on liver functions and TNF-α level following liver ischemic reperfusion injury in rats. *Chin. J. Clin. Res.* 28, 1147–1150. doi:10.13429/j.cnki.cjcr.2015.09.007

10.3389/fphar.2024.1315584

Glossary

Acc	Acetyl-coenzyme A-carboxylase
ALT	Alanine aminotransferase
ARE	Antioxidant-responsive elements
AST	Aspartate aminotransferase
ASIC-1	Acid-sensing ion channel 1
ATF4	Transcription factor 4
ATF6α	Activating transcription factor 6α
Bax	Bcl-2-associated X protein
Bcl-2	B-cell lymphoma-2
C	Control
CAT	Catalase
Ca^{2+}	Calcium ion
CaMKII	Ca2+/Calmodulin-Dependent Protein Kinase II
CHOP	C/EBP homologous protein
Cul3	Cullin3
COPII	Complexes in coat protein II
COX-2	Cyclooxygenase 2
DHCR7	7-dehydrocholesterol reductase
DILI	Drug-induced liver injury
EASL	European Association for the Study of the Liver
ECT	Electron transport chain
ER	Endoplasmic reticulum
eIF2	eukaryotic initiation factor 2
Fas	Fatty acid synthase
GRP75	Glucose-regulated protein 75
GRP78	78 kDa glucose-regulated protein
GST	Glutathione-S transferase
GPx	Glutathione peroxidase
H	High
HES1	Hairy and enhancer of split 1
HFD	High-fat die
HIRI	Hepatic ischemia-reperfusion injury
HMGCS1	3-hydroxy-3-methylglutaryl-coenzyme A synthase 1
HO-1	Heme oxygenase-1
I	Intervention
I^2	I-squared
ICR mice	Institute of Cancer Research mice
IL-1	Interleukin 1
IL-6	Interleukin 6
IRE1α	Inositol-requiring enzyme 1 α
IMS	Intermembranous space
IMM	Inner mitochondrial membrane
IP3Rs	Inositol 1,4,5-trisphosphate receptors
Keap1	kelch-like ECH-associated protein 1
L	Low
M	Medium
MCD	Methionine choline deficient
MCU	Mitochondrial Ca^{2+} uniporter
MDA	Malondialdehyde
MICU1/2	Mitochondrial Ca^{2+} uptake 1/2
MT	Matrine
mTORC1	mechanistic target of rapamycin complex 1
NASH	Nonalcoholic steatohepatitis
NAFLD	Nonalcoholic fatty liver disease
NAFLD	Non-alcoholic fatty liver disease
NICD	Intracellular transmembrane domain
Nrf2	Nuclear factor erythroid 2-related factor 2
NSDHL	NAD-(P)-dependent steroid dehydrogenase-like
NPS	Natural products
NF-κB	Nuclear factor kappa-B
NQO-1	Quinone oxidoreductase-1
OMM	Outer membrane of mitochondria
PKCδ	Protein kinase C delta
p-PERK	phosphor-plasmic reticulum kinase
Rbx1	Ring box protein 1
RyR	Ryanodine receptor
ROS	Reactive oxygen species
RBP-J(κ)	Recombination signal binding protein (kappa) J
Scd1	Stearoyl-coenzyme A desaturase 1
SCAP	SREBP cleavage activating protein
SD	Standard deviation
SERCA	Sarco/endoplasmic reticulum Ca^{2+}-ATPase
SOD	Superoxide dismutase
SOC	Store-operated Ca^{2+} channels
SRE	Sterol regulatory element
SREBP	Sterol regulatory element binding protein
sXBP1	spliced XBP1
S1P	Site-1 proteases
S2P	Site-2 proteases
S1R	Sigma-1 receptor

TC	Total cholesterol
TCM	Traditional Chinese medicine
TG	Triglyceride
TGF-β	Transforming growth factor beta
TNF-α	Tumor necrosis factor alpha
UPR	Unfolded protein response
VDACs	Voltage-dependent anion channels
W	Week(s)
WHO	World Health Organization
XBP1	X-box-binding protein 1
95%CI	95% confidence interval

frontiers | Frontiers in Pharmacology

TYPE Original Research
PUBLISHED 22 February 2024
DOI 10.3389/fphar.2024.1344983

OPEN ACCESS

EDITED BY
Rongrui Wei,
Jiangxi University of Traditional Chinese Medicine, China

REVIEWED BY
Irina Ielciu,
University of Medicine and Pharmacy Iuliu Hatieganu, Romania
Subhalakshmi Ghosh,
Kolkata Biotech Park, India

*CORRESPONDENCE
Xin Feng,
fengxin0303@163.com
Jun-Song Wang,
wang.junsong@gmail.com

†These authors have contributed equally to this work and share first authorship

RECEIVED 27 November 2023
ACCEPTED 14 February 2024
PUBLISHED 22 February 2024

CITATION
Liu W-Y, Xu D, Hu Z-Y, Meng H-H, Zheng Q, Wu F-Y, Feng X and Wang J-S (2024), Total cucurbitacins from *Herpetospermum pedunculosum* pericarp do better than Hu-lu-su-pian (HLSP) in its safety and hepatoprotective efficacy.
Front. Pharmacol. 15:1344983.
doi: 10.3389/fphar.2024.1344983

Total cucurbitacins from *Herpetospermum pedunculosum* pericarp do better than Hu-lu-su-pian (HLSP) in its safety and hepatoprotective efficacy

Wen-Ya Liu[1†], Di Xu[1†], Zi-Yun Hu[1], Hui-Hui Meng[1], Qi Zheng[1], Feng-Ye Wu[1], Xin Feng[2*] and Jun-Song Wang[1*]

[1]Center of Molecular Metabolism, Nanjing University of Science and Technology, Nanjing, China, [2]Beijing Hospital of Tibetan Medicine, China Tibetology Research Center, Beijing, China

The pericarp of *Herpetospermum pedunculosum* (HPP) has traditionally been used for treating jaundice and hepatitis. However, the specific hepatoprotective components and their safety/efficacy profiles remain unclear. This study aimed to characterize the total cucurbitacins (TCs) extracted from HPP and evaluate their hepatoprotective potential. As a reference, Hu-lu-su-pian (HLSP), a known hepatoprotective drug containing cucurbitacins, was used for comparison of chemical composition, effects, and safety. Molecular networking based on UHPLC-MS/MS identified cucurbitacin B, isocucurbitacin B, and cucurbitacin E as the major components in TCs, comprising 70.3%, 26.1%, and 3.6% as determined by RP-HPLC, respectively. TCs treatment significantly reversed CCl_4-induced metabolic changes associated with liver damage in a dose-dependent manner, impacting pathways including energy metabolism, oxidative stress and phenylalanine metabolism, and showed superior efficacy to HLSP. Safety evaluation also showed that TCs were safe, with higher LD_{50} and no observable adverse effect level (NOAEL) values than HLSP. The median lethal dose (LD_{50}) and NOAEL values of TCs were 36.21 and 15 mg/kg body weight (BW), respectively, while the LD_{50} of HLSP was 14 mg/kg BW. In summary, TCs extracted from HPP demonstrated promising potential as a natural hepatoprotective agent, warranting further investigation into synergistic effects of individual cucurbitacin components.

KEYWORDS

***Herpetospermum pedunculosum* pericarp, total cucurbitacins, hepatoprotective activity, NMR, median lethal dosage, no observed adverse effect level**

1 Introduction

Herpetospermum pedunculosum (Ser.) C. B. Clarke (Cucurbitaceae family, Figure 1) is an annual climbing herb widely distributed in southwest China, Nepal and northeast India, growing at 2000–3,500 m altitude (Libin et al., 2003). Its dried mature seeds (HPS) known as "Se-ji-mei-duo" in Tibetan medicine (Yang, 1989), have been used for jaundice, hepatitis and dyspepsia treatment for decades. Early phytochemical studies revealed the presence of lignans (Kaouadji and Pieraccini, 1984; Dai et al., 2017), fatty acids (Zhao et al., 2009) and terpenes (Jiang et al., 2016) in HPS, conferring anti-inflammatory (Fang et al., 2007),

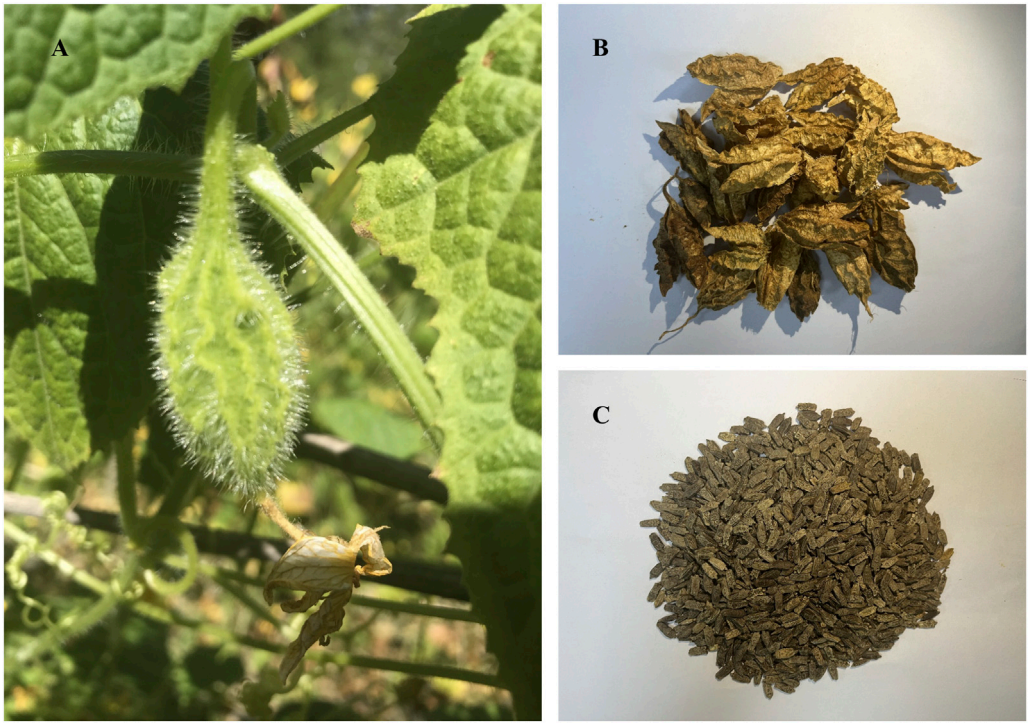

FIGURE 1
(A) Cucurbitaceous *Herpetospermum pedunculosum* (Ser) **(C) (B)**. Clarke and its fruit; **(B)** the dried pericarp of *Herpetospermum pedunculosum* (HPP); **(C)** the mature seed of *Herpetospermum pedunculosum* (HPS).

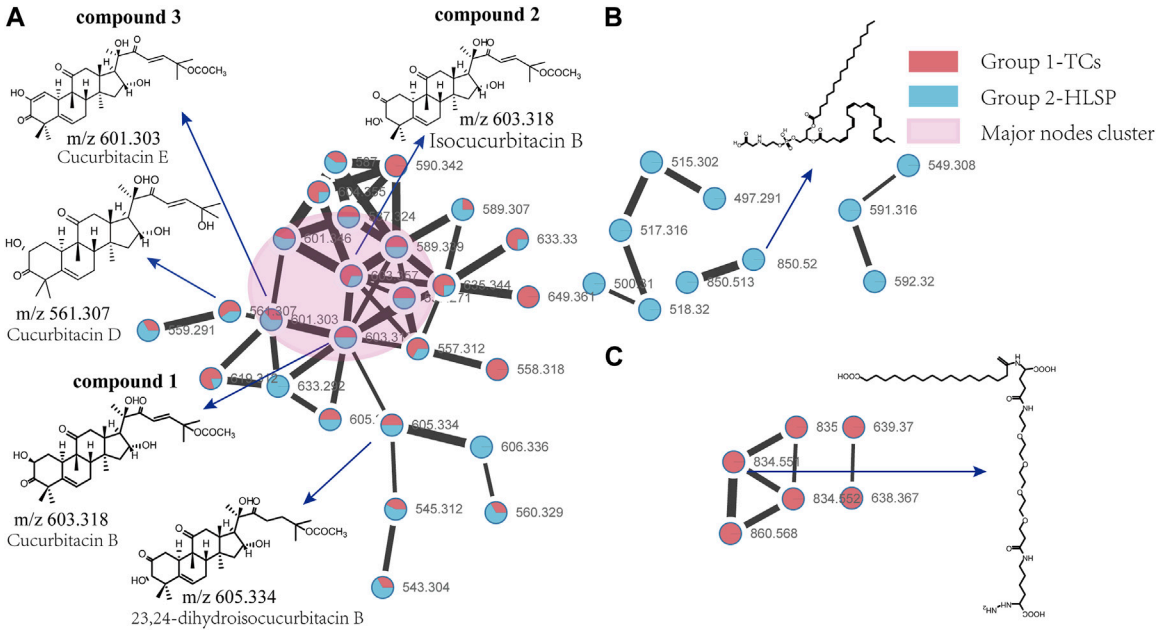

FIGURE 2
Molecular Network of TCs and HLSP obtained using GNPS platform and visualized with cytoscape 3.6.0 software. **(A)** Shared nodes with TCs and HLSP; **(B)** Blue and **(C)** red nodes represent the unique compounds of HLSP and TCs, respectively. The pink part was the major nodes cluster shared with TCs and HLSP.

TABLE 1 Identification of cucurbitacins in TCs and HLSP by UHPLC–QTOF–MS-MS.

No.	Rt (min)	Formula	Addut ions (measured) [M + Na]+	Addut ions (measured) /[M + FA-H]-	MassError (ppm) ESI(+/–)	MS/MS fragments ESI(+)	MS/MS fragments ESI(–)	Identification
1	6.612	$C_{32}H_{46}O_8$	581.3075	603.3178	−1.7/0.6	581.3054, 521.2845	603.3147, 557.3108, 539.3020, 497.2886, 411.2180, 301.1435, 59.0138	Cucurbitacin B
2	6.737	$C_{32}H_{46}O_8$	581.3069	603.3173	−2.8/-0.3	581.3049, 521.2839	603.3173, 557.3102, 539.3011, 497.2811, 411.2167, 385.2013, 59.0133	Isocucurbitacin B
3	6.966	$C_{32}H_{44}O_8$	579.2914	601.302	−2.5/0.3	579.2906, 519.2691	601.2986, 555.2944, 537.2854, 495.2737, 409.2015, 299.1275, 59.0134	Cucurbitacin E
4	6.027	$C_30H_{42}O_7$	537.2816	559.2895	−1.2/-3.2	537.2790, 281.0507	559.2888, 513.2820, 495.2712, 477.2561, 462.2493, 163.0797, 44.9983	Cucurbitacin I
5	5.780	$C_{30}H_{44}O_7$	539.2971	561.3059	−1.5/-1.8	539.2934	561.3013, 515.3010, 497.2902, 479.2852, 455.2763, 385.2206, 301.1819, 165.0929	Isocucurbitacin D
6	5.857	$C_{30}H_{44}O_7$	539.2954	561.3081	−4.6/2.1	539.2938	561.3081, 515.2976, 501.3167, 255.1703, 165.0916, 59.0140	3-epi-isocucurbitacin D
7	6.704	$C_{32}H_{48}O_8$	583.3209	605.3302	−5.6/-4.8	583.3166, 523.2981	605.3283, 559.3268, 541.3158, 499.3041, 481.2957, 341.2121, 301.1812, 165.0922, 59.0142	23,24-dihydrocucurbitacin B
8	6.850	$C_{32}H_{48}O_8$	583.3214	605.3340	−4.7/1.4	583.3206, 523.2996	605.3287, 559.3288, 541.3199, 499.3038, 481.2929, 301.1807, 165.0926, 59.0134	23,24-dihydroisocucurbitacin B
9	7.079	$C_{32}H_{46}O_8$	581.3061	603.3180	−4.2/0.9	581.3030, 521.2815	603.3123, 557.3108, 539.2982, 497.2890, 479.2789, 163.0765, 59.0141	3-epi-isocucurbitacin B
10	5.695	$C_{30}H_{46}O_7$	541.3111	563.3202	−4.6/-2.4	541.3111, 523.2956	563.3121, 517.3149, 499.3057, 385.2394, 165.0911, 137.0948	23,24-dihydrocucurbitacin D
11	5.703	$C_{30}H_{44}O_7$	539.2958	561.3050	−3.9/-3.5	539.2961	561.3033, 515.2968, 497.2845, 479.2748, 439.2458, 165.0935, 59.0129	Cucurbitacin D
12	5.765	$C_{30}H_{46}O_7$	541.3098	563.3209	−6.2/-4.2	541.3101, 523.3070	563.3121, 517.3149, 499.3048, 457.3000, 385.2373, 165.0932, 59.0133	dihydro-epi-iso-cucurbitacin D

anti-tumour (Teodor et al., 2020), anti-HBV (Gong et al., 2016), and hepatoprotective effects (Wang et al., 2014; Yu et al., 2014; Shen et al., 2015; Liu et al., 2017; Linghu et al., 2023). Our group reported the existence of series of lignans in HPS, which exhibited protection against CCl_4-induced hepatic fibrosis (Feng et al., 2018; Li et al., 2019).

Compared to HPS (the seed, the traditional medicinal part), a significantly larger quantity of HPP is currently being discarded as industrial waste during seed processing. However, limited research has explored utilizing the HPP despite it being reported to have equivalent hepatoprotective properties (Yang, 1989) in Tibetan medicine to the seed, wasting this potential resource. Our preliminary experiments revealed that HPP is rich in total cucurbitacins (TCs), which are tetracyclic triterpenoids differing in functional groups and ring saturation (Chen et al., 2005; Wang et al., 2017). Cucurbitacins are characteristic components of Cucurbitaceae plants, attracting attention for diverse activities including anti-inflammatory (Peters et al., 1997; Bernard and Olayinka, 2010; Marzouk et al., 2013; Nagarani et al., 2014; Silvestre et al., 2022), anti-tumor (Jayaprakasam et al., 2003; Molavi et al., 2008; Lee et al., 2010), and hepatoprotection (Bartalis, 2005; Asadi-Samani et al., 2015; Arjaibi et al., 2017) over decades. However, there are few studies on the chemical composition of TCs from HPP and whether they have hepatoprotective effects.

Hu-lu-su-pian tablets (HLSP, approval number: Z43021002) have been utilized in the medicinal market since the 1980s for the treatment of hepatitis and primary hepatocellular carcinoma (Hu et al., 1982; Mei et al., 2021; Kanani and Pandya, 2022). However, the clinical application of HLSP has been limited due to adverse reactions such as diarrhea, dizziness, and nausea following drug administration. HLSP is derived from the fruit stalk of *C. melo* L (Cucurbitaceae family) and has a historical usage in Chinese medicine for treating liver diseases. The fruit

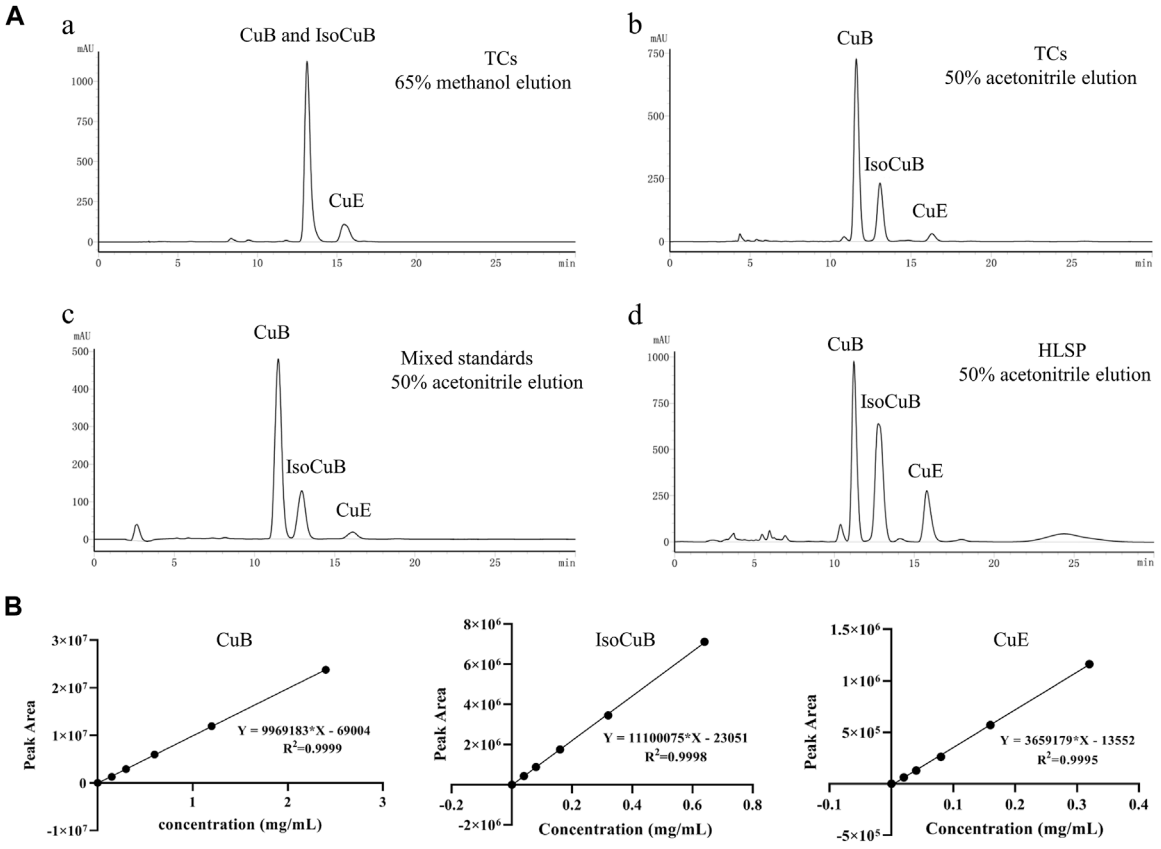

FIGURE 3
(A) HPLC chromatograms of TCs and HLSP, (a) TCs eluted with 65% methanol; (b) TCs eluted with 50% acetonitrile; (c) mixed standards eluted with 50% acetonitrile; (d) HLSP eluted with 50% acetonitrile. **(B)** Standard curves for CuB, IsocuB and CuE.

TABLE 2 Content of CuB, IsocuB and CuE in TCs and HLSP (n = 3, mean ± SD).

No.	Name*	TCs			HLSP		
		tR (min)	Peak area (×10^6)	Content (%)	tR (min)	Peak area (×10^6)	Content (%)
1	CuB	11.5 ± 0.1	15.8 ± 0.2	70.3 ± 0.4	11.5 ± 0.3	21.7 ± 0.9	41.0 ± 1.1
2	IsocuB	13.0 ± 0.1	5.9 ± 0.06	26.1 ± 0.2	12.9 ± 0.2	22.6 ± 0.6	42.8 ± 0.7
3	CuE	16.1 ± 0.2	8.2 ± 0.05	3.6 ± 0.3	16.1 ± 0.3	8.6 ± 0.2	16.2 ± 0.6

TABLE 3 Mortality induced by gavage administration of TCs to mice and survival times corresponding with each treatment.

Does (mg/kg)	Mortality	Survival Times(h)
80	3/3	2.53, 3.67, 4.9
40	3/5	2.85, 3.75, 5.1
30	2/7	14.69,14.69–20.5
20	0/7	>336
15	0/9	>336
10	0/9	>336

stalk of *Cucumis melo* was first documented in the ancient Chinese Pharmacy monograph, Shen Nong Ben Cao Jing (Wu, 2016), compiled around 200 BC. Subsequently, in the influential Materia Medica compiled by Li Shizhen during the 16th century AD, its efficacy in treating jaundice was emphasized (Li, 1975). While *C. melo* itself is an edible plant, the fruit stalk concentrates cucurbitacins as a chemical defense mechanism. Similarly, HPP also biosynthesizes cucurbitacins for defense purposes. However, cucurbitacins exhibit significant chemical variations and proportions among different Cucurbitaceae plants, which can result in diverse biological effects in terms of medicinal value, toxicity, antioxidant properties, anti-inflammatory properties, and

TABLE 4 Symptoms registered after TCs administration. The ratio between mice with the symptom *versus* the total mice treated.

Symptoms	TCs Dose (mg/kg)					
	80	40	30	20	15	10
Apathy	3/3	5/5	7/7	2/9	0/9	0/9
Piloerection	3/3	3/5	5/7	1/9	0/9	0/9
Shortness of breath	1/3	1/5	0/7	0/9	0/9	0/9
Slight convulsion	3/3	0/5	2/7	0/9	0/9	0/9
Semi-closed eye	3/3	4/5	4/7	0/9	0/9	0/9

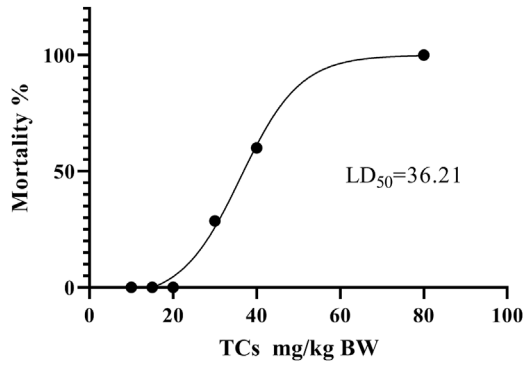

FIGURE 4
Dose-response mortality curve of oral TCs in mice. Percentage mortality *versus* concentration of the TCs. The LD_{50} value is indicated.

antibacterial properties. By comparing the cucurbitacin profiles in HPP and the HLSP product, it becomes possible to evaluate HPP as a potential alternative medicinal source to the established HLSP. Therefore, a comprehensive evaluation of the chemical composition, proportion, safety, and effectiveness of TCs and HLSP is necessary.

This study aims to compare the hepatoprotective efficacy and safety of total cucurbitacins (TCs) extracted from fruit pericarp (HPP) of *H. pedunculosum* to HLSP. While similar active components may confer comparable therapeutic effects, variations in chemical profiles can impact safety and efficacy. We performed UHPLC-MS/molecular networking to qualitatively analyze and compare TCs in HPP and HLSP. Metabolic profiling and mice studies were then used to comprehensively evaluate the hepatoprotective effects and safety of TCs from HPP *versus* HLSP. Comparing HPP to the more toxic HLSP may identify potential candidates from HPP for safer hepatoprotection, advancing development and utilization of this understudied plant resource.

2 Materials and methods

2.1 Reagents and materials

Methanol and acetonitrile of HPLC grade were bought from Tedia Company (Fairfield, United States). 3-(trimethylsilyl) propionic-2, 2, 3, 3-d_4 acid sodium salt (TSP) and Deuterium oxide (D_2O, 99.9%) were purchased from Sigma-Aldrich (St. Louis, MO, United States). Deionized water was ordered from Watsons (Watsons, Hong Kong, China). The three standards, including Cucurbitacin B (CuB), Isocucurbitacin B (IsocuB), and Cucurbitacin E (CuE) were laboratory-made and identified by ^{1}H and ^{13}C NMR. Hu-lu-su-pian (HLSP, the main ingredients are CuB and CuE, 0.1 mg/tablet) was used as a positive drug and was obtained from Hunan Dinuo Pharmaceutical Co., Ltd. (Changsha, China). The Nanjing Jiancheng Bioengineering Institute (Nanjing, China) supplied the assay kits for the enzymes aspartate aminotransferase (AST) and alanine aminotransferase (ALT). HPP were provided by Beijing Tibetology Research Center (Linzhi City, Tibet Autonomous Region, China). Other reagents were all analytically pure.

2.2 Preparation of TCs

5 kg HPP was crushed to 30 mesh with a multifunctional crusher, and then extracted twice with ethanol (1:10, w/v) under reflux for 2 h each time. The two filtrates were collected and concentrated under reduced pressure to obtain 390 g of an ethanol extract. The extracts were extracted using petroleum ether and ethyl acetate after being suspended in water. The extract (48.5 g) of ethyl acetate was successively eluted with petroleum ether-acetone (8:2, 7:3, 6:4, 5:5, 4:6, v/v) on a silica gel column (50 cm × 8 cm i.d.), and the thin fractions were checked by thin layer chromatography (TLC). Fractions 11-14 were collected, concentrated under reduced pressure, and fully dried in a vacuum drying oven to obtain 3.42 g of TCs.

2.3 Qualitative profiling of TCs and HLSP by UHPLC-QTOF-MS/MS

2.3.1 UHPLC-Q-TOF MS analysis

An UHPLC-Q-TOF MS system comprised of an AB SCIEX Triple-TOF 5600$^+$ mass spectrometer (MA, United States) and a SCIEX Exion ultra-high performance liquid chromatography (UHPLC) system was used to conduct the LC-MS analysis (Hu et al., 2023). LC separation was performed using a Phenomenex Kinetex® Biphenyl C18 column (100 × 2.1 mm i.d., 2.6 m; Torrance, CA, United States) with a flow rate of 0.4 mL/min at 40°C. As mobile phases, formic acid in water (solvent A, 0.1%, v/v) and acetonitrile (solvent B) were employed. The procedure for a gradient elution was as follows: 0–1 min, 1% B; 1–10 min, 1–99 %B; 10–13 min, 99% B; 13–14 min, 99%–1% B; 14–17 min, 1% B. the inject volume was 2 μL.

Information-dependent acquisition (IDA) was used to acquire the MS data, which included a TOF MS scan and an intensity-dependent TOF MS/MS scan with high sensitivity mode selected. In the TOF MS-IDA-MS/MS acquisition, the TOF MS spectral mass scanning range was 50–1,000 m/z, the accumulation time was set at 0.10 s/spectrum, and the product ion scanning mass range was 40–1,000 m/z, with the accumulation time being 0.05 s/spectrum. The following settings were made for the IDA mode: maximum candidate ions, 10; mass tolerance, 50 mDa; declustering potential (DP), 80 V (ESI^+)/−80 V (ESI^-); collision energy (CE), 35 V ± 15 V (+)/−35 V ± 15 V (−); intensity threshold, 100 cps; with the dynamic

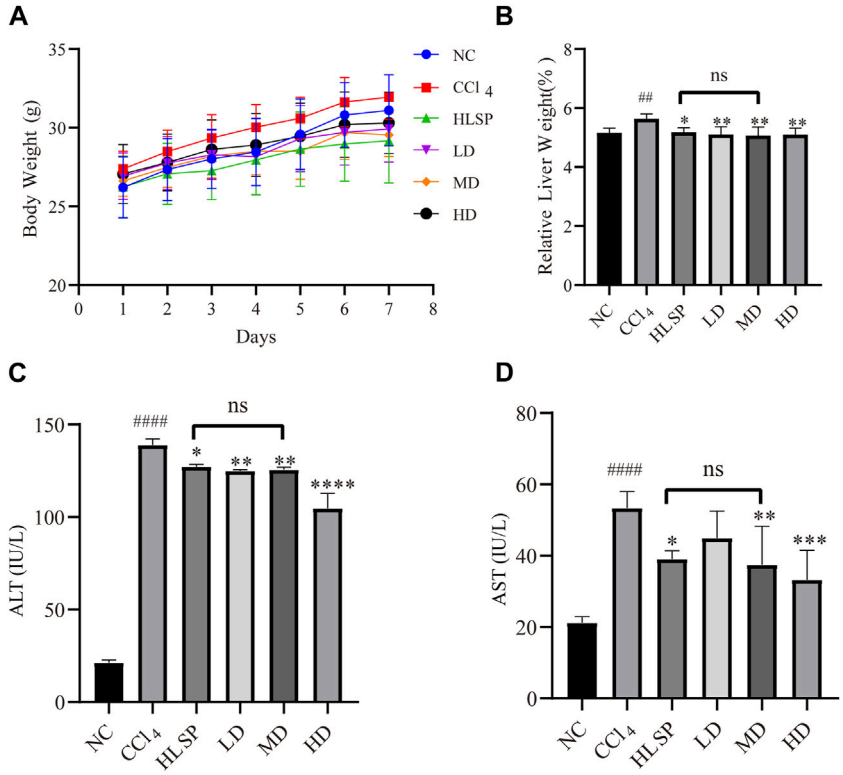

FIGURE 5
Effects of TCs on body weight and relative liver weight, serum AST and ALT activities inCCl_4 -induced mice. **(A)** Body weight changes, **(B)** serum biochemical levels (n = 5) relative to liver weight (n = 10), ALT **(C)** and AST **(D)**. Data are expressed as mean ± SD. Compared with NC, $^{\#}p < 0.05$, $^{\#\#}p < 0.01$, $^{\#\#\#\#}p < 0.0001$; compared with CCl_4 group, $^{*}p < 0.05$, $^{**}p < 0.01$, ** $^{*}p < 0.001$, $^{****}p < 0.0001$, ns: not significant.

background subtraction (DBS) function on. The following detailed ESI settings were made: source temperature was set to 550°C, nebulizing gas (GS1) was set to 55 psi, auxiliary gas (GS2) was set to 55 psi, curtain gas was set to 35 psi, and spray voltage was set to 5,500 V (+)/−4500 V (−). Calibration was carried out using an external calibration reference to ensure mass accuracy before injection.

2.3.2 Molecular networking

Molecular networks were established by the online workflow at Global Natural Products Social Molecular Networking (GNPS) platform (http://gnps.ucsd.edu).The raw MS data (.wiff format) were obtained by SCIEX Analyst TF 1.8.1 Software (version 1.8.1, MA, United States), they were first converted into.mzML files by ProteoWizard-MS Convert (version 3.0, Proteowizard Software Foundation, CA, United States) and then uploaded on the GNPS Web platform (Wang et al., 2016; Quinn et al., 2017; Ramos et al., 2019). The following parameters were used for the development of molecular networks: both the precursor and fragment ion mass tolerance were of 0.02 Da, molecular networking was constructed using 10 minimum matched fragment ions and a minimum cosine score of 0.8, the other parameters were default values. The MS/MS molecular network is accessible at the GNPS Web site with the following link: https://gnps.ucsd.edu/ProteoSAFe/status.jsp?task=78587ed5c58f4cfbac4923ede9b305a8. Data were visualized using Cytoscape 3.6.0 software (https://cytoscape.org/).

Formula Finder and the structural elucidation tool inside SCIEX OS Software (version 2.0, MA, United States) were used to further assess the MS and MS/MS data for characteristics of interest.

2.4 Quantitative analysis of TCs and HLSP by HPLC

2.4.1 Chromatographic conditions

The TCs analysis (Chanda et al., 2020) was carried out using a Shimadu LC-20AT series HPLC system (Shimadu, Tokyo, Japan) with an autosampler and an InertSustain C18 column (250 × 4.6 mm, 5 μm). A mobile phase consisting of 50% acetonitrile and water was used on an isocratic elution procedure at a flow rate of 1 mL/min over 30 min, the column temperature was 30°C, and 230 nm was selected as detection wavelength.

2.4.2 Standard curve creation

The quantitative analysis of the three cucurbitacins was performed by the use of an external standard method (Scherer et al., 2012), and a mixed standard solution containing CuB (2.4 mg), IsocuB (0.64 mg) and CuE (0.32 mg) was prepared in a 1 mL volumetric flask. Use the double dilution method to serially dilute 4 times, so that the concentration of CuB is 0.15, 0.3, 0.6, 1.2, 2.4 mg/mL, and the concentration of IsocuB is 0.04, 0.08, 0.16, 0.32, 0.64 mg/mL, the concentrations of CuE were 0.02, 0.04, 0.08, 0.16,

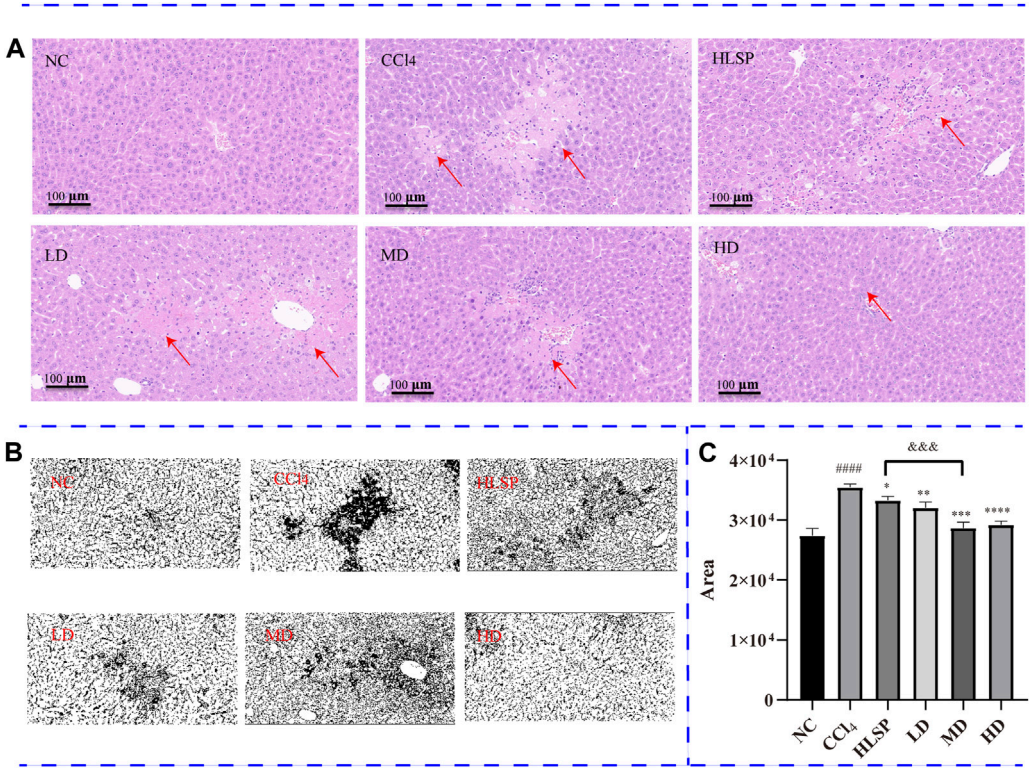

FIGURE 6
(A) H&E-stained liver sections of each group (HE×200), **(B)** RGB channels separation of the original HE staining image of liver tissue sections in each group. The figure shows the green stack under the appropriate threshold. The black part represents the degree of focal necrosis of liver. The darker the color, the greater the degree of necrosis. **(C)** Quantifying H&E-stained liver tissue area using ImageJ (x ± s, $n = 3$). Note: compared with NC group, $^{\#}p < 0.05$, $^{\#\#\#\#}p < 0.0001$; compared with CCl_4 group <0.0001, $^{*}p < 0.05$, $^{**}p < 0.01$, $^{***}p < 0.001$, $^{****}p < 0.0001$; compared with HLSP group, $^{\text{and}\&}p < 0.001$.

0.32 mg/mL. A 10 μL aliquot of each solution was injected and analyzed three times using HPLC, and the standard curves were obtained by plotting peak area *versus* concentration.

2.4.3 Content determination

Accurately weigh 10 mg of TCs and prepare a 1 mg/mL test solution with methanol in a 10 mL volumetric flask. Take 10 tablets of HLSP, grind in a mortar, 5 mL of methanol was added, then ultrasonic extraction was performed twice for 30 min, the two extract solutions were combined and transferred into a 10 mL volumetric flask and diluted with methanol to volume. After filtration through a 0.22 μm microporous membrane, it was used as another test solution. According to the chromatographic conditions of 2.4.1, an injection volume of 10 μL sample solution was performed, the contents of three components were determined based on the corresponding peak area by external standard method.

2.5 Animal experiments

ICR mice (20.0 ± 2 g) were obtained from Qinglongshan Animal Breeding ground in Nanjing. All animals were kept in a specified pathogen-free (SPF) laboratory with unrestricted access to food and water at a temperature of 25°C, with a humidity of 55% ± 5%, and a 12-h light/dark cycle. The animals used in this study have been handled in accordance with the National Institutes of Health (NIH) guidelines, and the experimental protocol has been approved by the Animal Care and Use Committee of Nanjing University of Science and Technology.

2.5.1 Safety assessment of TCs—LD_{50} and NOAEL

We employed a modified "up and down" method (Abal et al., 2017) with four dose levels to assess the safety of TCs and determine the LD_{50} and NOAEL. Female ICR mice weighing 20.0 ± 2 g were fasted overnight prior to administration of a single dose of TCs (20 mL/kg BW, suspended in 2% Tween-80 physiological saline) by gavage the following morning. After that, the animals were kept in metabolic cages with free access to food and water for the following 2 weeks. The first, second, third, and fourth dose levels were tested on groups of three, five, seven, and nine mice, respectively, with a starting dose of 80 mg/kg BW. Doses were decreased if more than 50% of the mice died or increased if less than 50% of the mice died. Detailed observations and recordings of symptoms, including apathy, piloerection, shortness of breath, slight convulsion, semi-closed eyes, and survival time, were recorded after gavage administration for each mouse.

2.5.2 Metabolomics study

After 7 days of acclimation in the laboratory environment, male ICR mice were randomly divided into 6 groups (10 mice in each group): normal control (NC) group, CCl_4 group, HLSP group, the low dose of TCs-treated (LD) group, the medium dose of TCs-treated (MD) group

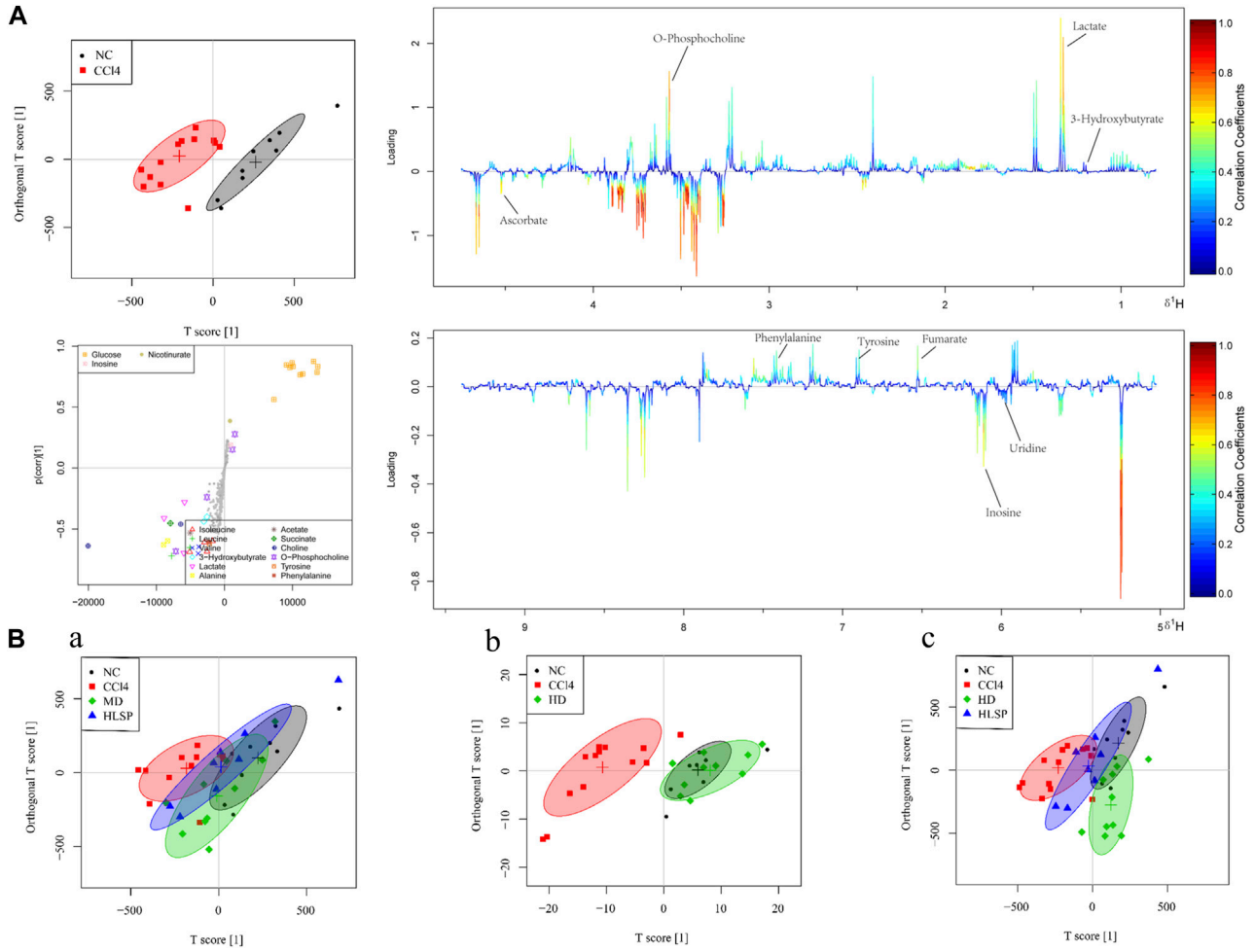

FIGURE 7
(A) OPLS-DA analysis of liver samples from mice in NC and CCl_4 groups. Score plots (upper left), corresponding S plots (bottom left), and color-coded loading plots (right). The change from blue to red represents a significant increase in change. **(B)** OPLS-DA score plot of NC, CCl_4, HLSP, MD and HD.

and the high dose of TCs-treated (HD) group. The LD, MD and HD groups were gavaged with TCs (suspended in 0.5% CMC-Na solution) at 0.1, 0.2, 0.4 mg/kg BW, respectively. Mice in the HLSP group were fed with HLSP tablets (equivalent to a MD of TCs), and the 0.5% CMC-Na solution was administered in the same amount to the NC and CCl_4 groups. In addition, the body weight of each mouse was recorded every morning at 9 a.m. All groups were treated once a day for consecutive 7 days (Yang et al., 2015). After 2 h of administration on the 7th day, except for the NC group, mice in the other groups were intraperitoneally injected with 0.3% CCl_4 olive oil (10 mL/kg BW), while the NC group was given an equal volume of olive oil. Mice in each group were fasted for 24 h, and then were anesthetized with isoflurane controlled by a small animal anesthesia machine (medical supplies andservices INT. LTD. Keighley, UK). The orbital blood was immediately collected for serum biochemical analysis and ^{1}H NMR analysis. Each mouse was then sacrificed, the liver was collected for histopathological examination and ^{1}H NMR analysis, and the relative liver weight was calculated (relative liver weight (%) = liver weight/body weight × 100). Blood samples were centrifuged (3,000 rpm, 10 min, 4°C) to obtain serum samples and stored at −80°C until biochemical analysis.

2.6 Histopathological evaluation and biochemical analysis

For histopathology, liver tissues were quickly removed, and then fixed with 10% formalin to prepare paraffin sections with 5 μm sections for H&E staining, and the remainder were stored at −80°C for other analyses.

For serum biochemical analysis, ALT and AST levels were assessed using a commercial kit in accordance with the manufacturer's recommendations.

2.7 Liver and serum preparation for ^{1}H NMR analysis

Liver tissue sample preparation for ^{1}H NMR analysis (Ruan et al., 2018): Frozen liver tissue samples were crushed in a mortar and pestle in the presence of liquid nitrogen and immediately weighed, then homogenized (5 mL/g) using pre-cooled acetonitrile-water (50:50, v/v). The homogenate was centrifuged for 10 min at 16,000 g at 4°C, and

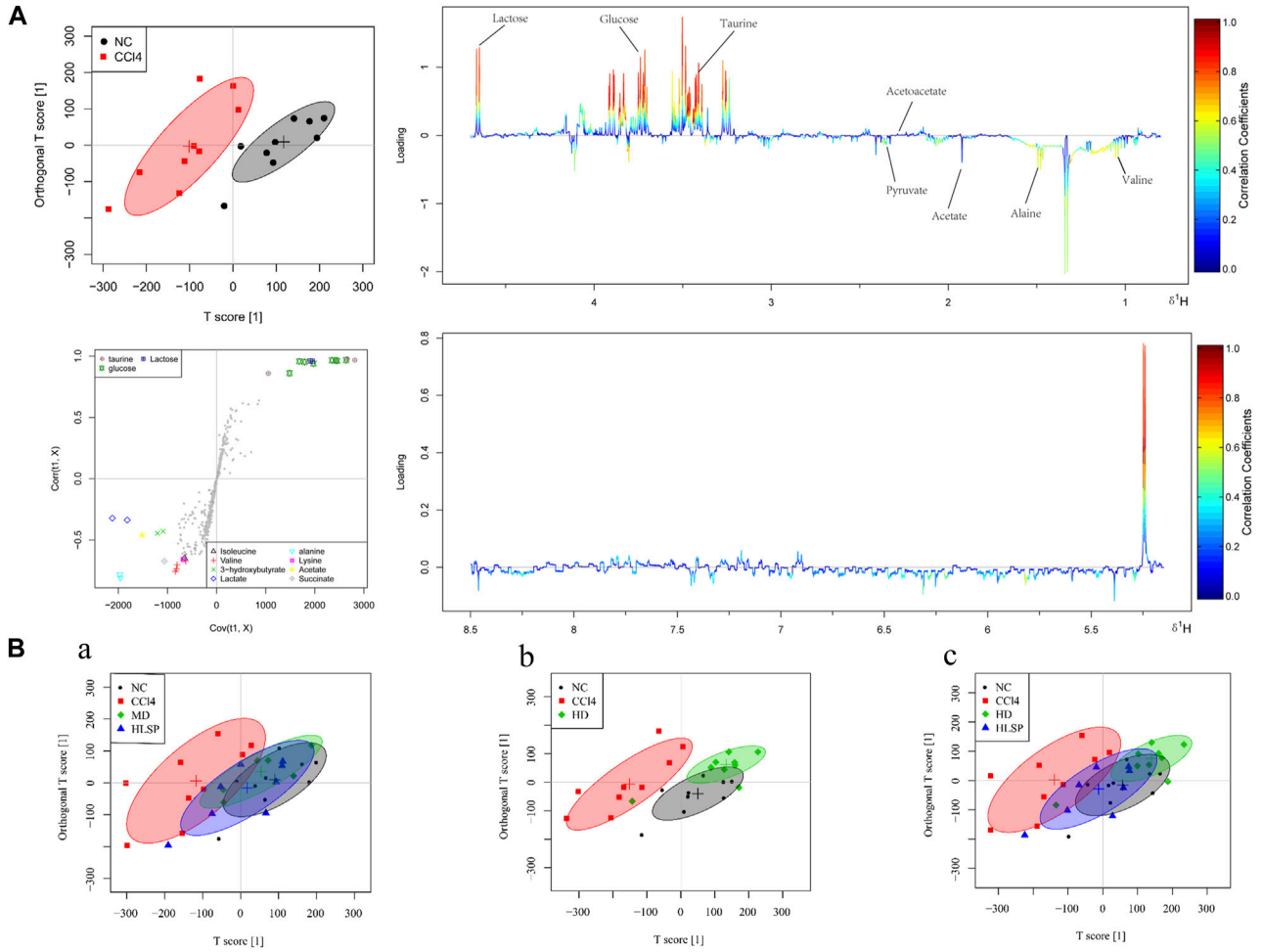

FIGURE 8
(A) OPLS-DA analysis of serum samples from mice in NC and CCl_4 groups. Score plots (upper left), corresponding S plots (bottom left), and color-coded loading plots (right). The change from blue to red represents a significant increase in change. **(B)** OPLS-DA score plot of NC, CCl_4, HLSP, MD and HD.

the supernatant was then transferred to a centrifuge tube. With the removal of acetonitrile under a nitrogen blower, it was then lyophilized and kept at −80°C for future use.

Serum sample preparation for ^{1}H NMR analysis (Fu et al., 2019): Slowly thawing serum samples on ice was followed by the addition of twice as much methanol, the mixture was vortexed and left to stand at −20°C for 20 min. The supernatant was evaporated with a nitrogen blower to remove methanol following centrifugation at 14,000 g for 15 min at 4°C. It was then freeze-dried and kept at −80°C for future use.

The dried liver and serum extracts were added with a new mixture of 600 μL99.8% D_2O phosphate buffer (0.2 M, Na_2HPO_4 and 0.2 M NaH_2PO_4, pH 7.0) containing 0.05% (w/v) sodium 3-(trimethylsilyl) propionate-2,2,3,3-d_4 (TSP). After vortex and 14,000 g centrifugation for 10 min, the supernatant was transferred to the 5 mm NMR tube for the ^{1}H NMR analysis.

2.8 ^{1}H NMR recording

We acquired ^{1}H NMR spectra of liver and serum samples using a Bruker Avance 500 MHz spectrometer (Bruker GmbH, Karlsruhe, Germany). The pulse sequence was edited with a lateral (perpendicular to the main magnetic field direction) relaxation-edited Call-Purcell-Meiboom-Gil (CPMG) sequence (90 (τ-180-τ) n-acquisition) and a spin echo delay of 10 ms (2 nτ) in order to suppress residual macromolecular protein signal in the sample. The number of scans was 32 (32 K data points) and the spectral width was 20 ppm. The spectra were Fourier transformed after multiplying the free induction decay (FID) curve by an exponential weighting function (corresponding to a 0.5 Hz linewidth).

2.9 Data preprocessing and multivariate statistical analysis of ^{1}H NMR data

Using the software Topspin 3.0 from Bruker BioSpin, all NMR spectra were manually pre-processed for baseline, phase, and TSP zero (0.0 ppm). MestReNova (version 6.1.0, Mestrelab Research SL) was used to convert the files to ASCII format, which was then imported into "R" (http://cran.r-project.org/) for multivariate statistical analysis. To minimize the data

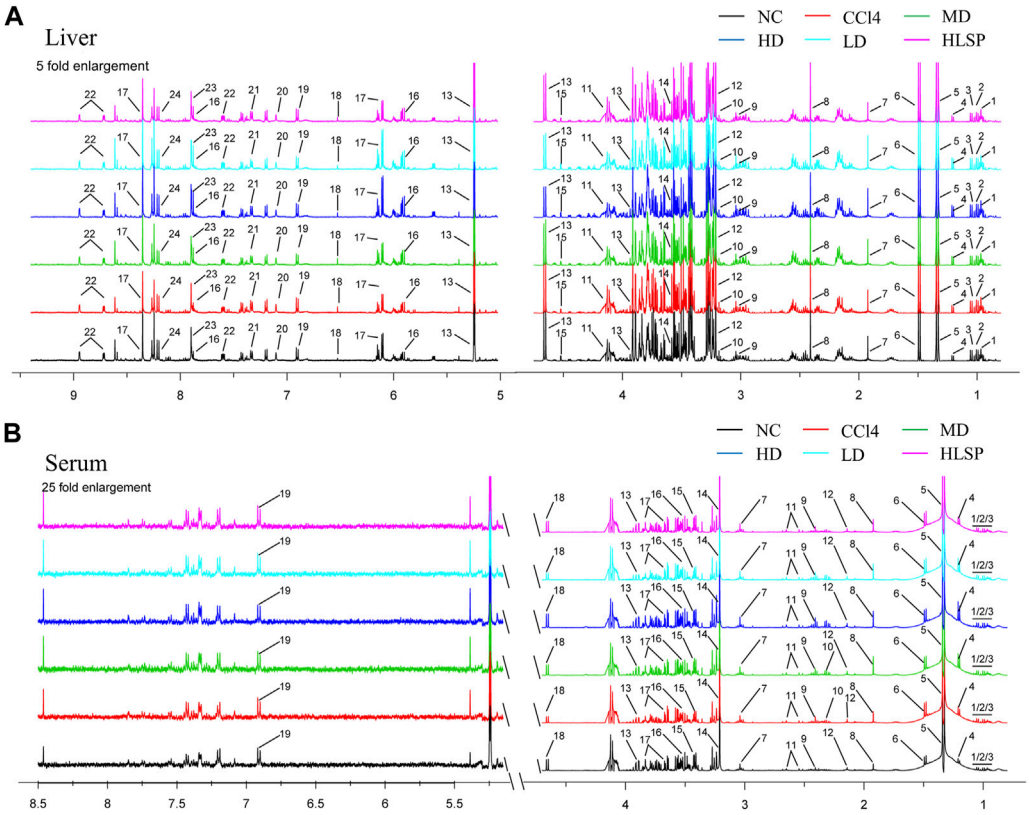

FIGURE 9
Typical 500 MHz ^{1}H NMR spectra of liver and serum extracts. **(A)** Typical 500 MHz hydrogen spectrum of liver extract, 1, Isoleucine; 2, Leucine; 3, Valine; 4, 3-Hydroxybutyrate; 5, Lactate; 6, Alanine; 7, Acetate; 8, Succinate; 9, Creatine; 10, Choline; 11, O-Phosphocholine; 12, Betaine; 13, Glucose; 14, Glycine; 15, Ascorbate; 16, Uridine; 17, Inosine; 18, Fumarate; 19, Tyrosine; 20, Histamine; 21, Phenylalanine; 22, Nicotinurate; 23, Xanthine; 24, Hypoxanthine. **(B)** Typical 500 MHz hydrogen spectrum of serum extract, 1, Isoleucine; 2, Leucine; 3, Valine; 4, 3-hydroxybutyrate; 5, Lactate; 6, alanine; 7, Lysine; 8, Acetate; 9, Succinate; 10, Pyruvate; 11, Citrate; 12, Acetoacetate; 13, creatine; 14, Choline; 15, taurine; 16, Glycine; 17, glucose; 18, Lactose; 19, Tyrosine.

dimension, segmental integration is carried out in the chemical potential range of 0.5 ppm–9 ppm using an adaptive binning approach with an average bin width of 0.015 ppm. Between 4. 47 and 5.50 ppm, the remaining signals of water and its affected regions were eliminated. Finally, the data were subjected to Pareto scaling (Karaman, 2017) and probability quotient normalization (Dieterle et al., 2006) to eliminate systematic differences between sample concentrations.

Orthogonal signal correction-partial least squares discriminant analysis (OSC-PLSDA) was then performed on the processed data, revealing differential metabolic changes in serum and liver tissue. The orthogonal signal correction (OSC) filter is applied to remove uninteresting variations, such as systematic variation, from spectral data before performing PLS-DA. To evaluate the fitting ability and predictive ability of the established OPLS-DA model, repeated two-fold cross-validation (2CV) and permutation test (n = 200) were performed. R^2 (total explained variance) and Q^2 (model predictability) values were used to assess the model's quality. Differences and clusters between groups were displayed using score plots, and metabolites that changed between groups were displayed using colored loading plots.

2.10 Metabolites identification and univariate analysis

Metabolites of liver tissue and serum were identified using the commercial software Chenomx NMR Suite v.8.1 (Chenomx, Edmonton, Canada) and statistical total correlation spectroscopy (STOCSY) techniques, and then by querying public metabolite databases such as the Human Metabolite Database (HMDB, http://www.hmdb.ca) and the Madison-Qingdao Metabolomics Database (MMCD, http://mmcd.nmrfam.wisc.edu).The preliminary identification of metabolites was further confirmed by using 2 dimensional (2D) heteronuclear single quantum correlation (HSQC) and a ^{1}H–^{1}H total correlation (TOCSY) NMR spectroscopy.

For univariate analysis, a parametric test (t-test) and a non-parametric statistical test (Wilcoxon signed rank test) were employed to validate key increased or decreased metabolites across groups using "R". The fold change (FC) values of metabolites adjusted by the Benjamin-Hochberg modification approach and their correlated p values were calculated and exhibited as colored tables. The significance threshold for all tests was set at $p < 0.05$.

2.11 Statistical analysis

All data are expressed as mean ± SD, and statistical analysis was performed using GraphPad Prism 8.0 software (GraphPad Software, CA, United States).

3 Results

3.1 Characterization of the major cucurbitacins in TCs and HLSP by molecular networking

Molecular networking is a powerful complement to screening and identification of undescribed compounds from natural products (Yang et al., 2013). The molecules exhibiting similar fragmentation patterns were clustered together while the molecules with dissimilar MS/MS spectra were displayed as independent nodes (Wang et al., 2016). The visualized molecular networking of TCs and HLSP using Cytoscape 3.6.0 software is presented in Figure 2. Each node represents a compound, inside which the molecular mass of parent ion of the compound is indicated. The nodes of compounds are linked by lines indicating structural similarity, with thicker lines representing greater similarity between the structures. The red and blue node represents TCs and HLSP, respectively. The Pink area represents major cucurbitacin clusters. Clusters that formed by red nodes and blue nodes represent the unique compounds of TCs (Figure 2B) and HLSP (Figure 2C), respectively. Compounds 1 and 2 showed identical $[M + FA\text{-}H]^-$ ions at m/z 603.3 in negative ion mode, suggesting that they were isomers. Furthermore, their MS/MS spectra exhibited the typical daughter ions at m/z 497.3, corresponding to the loss of CH_3COOH (60 Da). In addition, the other fragment ions were nearly alike except for some disparities in relative abundance (Supplementary Figures S1, S2). This revealed that they were two configurational isomers. Thus, Compounds 1 and 2 were therefore tentatively identified as cucurbitacin B and isocucurbitacin B by comparing their retention times and MS/MS spectra with those of authentic standards.

Compound 3 showed a $[M + FA–H]^-$ ion at m/z 601.3, as well as the typical daughter ion at m/z 495.3 which were 2 Da less than compound 1 and 2 (Supplementary Figures S1, S2), indicating that the core structure of compound 3 contained one additional double bond compared to Compound 1 and 2. Therefore, by comparing its retention time and MS/MS spectra with those of an authentic standard, compound 3 was tentatively identified as cucurbitacin E. The retention time, molecular formula, mass errors, MS/MS fragment ions, and detected monoisotopic masses in the four-decimal format provided by QTOF-MS for the major cucurbitacins and the other nine derivatives are summarized in Table 1. Other untargeted compounds (with an MS^2 spectrum) were also annotated by matches to the GNPS spectral libraries (data not shown).

3.2 Contents of CuB, IsocuB and CuE in TCs and HLSP

In order to further investigate the amount of each component in TCs, three primary components were quantified by HPLC technique. CuB and IsocuB could not be completely separated by 65% methanol (Figure 3Aa), whereas the two overlapping isomers could be completely separated by 50% acetonitrile (Figures 3Bb, c, d) with a resolution R > 1.5, therefor, an isocratic elution with 50% acetonitrile was used to determine CuB, IsocuB, and CuE in TCs and HLSP (Figure 3B). The contents of CuB, IsocuB, and CuE were respectively 70.3% ± 0.4%, 26.1% ± 0.2%, and 3.6% ± 0.3% in TCs and 41.0% ± 1.1%, 42.8% ± 0.7% and 16.2% ± 0.6% in HLSP, as shown in Table 2.

3.3 Safety assessment of TCs

LD_{50} and NOAEL values are two metrics commonly used to assess the safety of drugs (Vilariño et al., 2018). Following gavage administration of TCs, all mice died within 5 hours at a dosage of 80 mg/kg. Therefore, the second level dosage was reduced to 40 mg/kg, leading to the death of three out of five mice. At the third level, a dosage of 20 mg/kg resulted in no deaths, prompting a further reduction to 10 mg/kg for the fourth level. None of the nine mice who received this dose died. An additional dose level of 30 mg/kg was introduced between the second and third levels, resulting in the death of two out of seven mice. Lastly, nine mice were given a dosage of 15 mg/kg, with no deaths observed (Table 3). Symptoms of apathy and piloerection were observed within 30 min across all groups, except at 15 and 10 mg/kg. Convulsions increased in frequency over time, occurring every 15 s. Semi-closed eyes were observed an hour before death. At a dosage of 20 mg/kg, 1 mouse showed signs of apathy and another had a minor piloerection. At 15 and 10 mg/kg, none of the mice died and there were no side effects over the following 2 weeks (Table 4). Based on these findings, the oral NOAEL for mice was established at 15 mg/kg, and this modified four-level “up and down” procedure revealed dose-dependent mortality. The results, presented as a percentage of mouse deaths in relation to TCs dosage, are shown in Figure 4. Nonlinear regression fitting software was used to calculate the oral LD_{50} of TCs to be 36.21 mg/kg (GraphPad Prism, version 8.0, GraphPad Software, CA, United States).

3.4 Effects of TCs on body weight, relative liver weight, serum AST and ALT activities

Throughout the treatment period, the body weight of mice in all groups exhibited an upward trend (Figure 5A). This suggests that both TCs and HLSP had minimal effect on the animals’ eating behavior at treatment doses. Hepatomegaly, as evidenced by the mean relative liver weight (also known as liver index), was induced by CCl_4, with the CCl_4 group having a significantly higher liver index than the NC group ($p < 0.01$). Treatment with TCs and HLSP, on the other hand, resulted in a significant decrease in liver index compared to the CCl_4 group ($p < 0.01$), with no significant difference observed between the HLSP and MD groups (Figure 5B). The disturbance of the hepatocyte membrane structure caused by CCl_4 led to a substantial rise in serum AST and ALT levels ($p < 0.0001$) (Figures 5C,D). Dose-dependent treatment with TCs resulted in a significant and substantial drop in ALT and AST levels in the MD and HD groups ($p < 0.01$ and $p < 0.0001$) (Figures

5C,D), with no significant difference observed between the HLSP and MD groups. It can be concluded that TCs can prevent hepatomegaly in CCl_4-induced mice.

3.5 Histopathological observation

The purpose of histopathological observation is to reveal morphological alterations in liver cells, as well as inflammatory cell infiltration and other pathological conditions, which cannot be fully captured by serum biochemistry. Histological sections of liver tissue showed that the NC group had a morphologically normal liver lobular and cellular structure (Figure 6A). In contrast, the CCl_4 group exhibited clear localised necrosis of hepatocytes, loss of hepatocyte structure, and infiltration of inflammatory cells, particularly around the central vein (indicated by the red arrow). Inflammatory cell infiltration was most common in the portal area and manifested as a decrease in nuclear volume, loss of cell structure, or aberrant cell shape. The HLSP group exhibited considerable improvement in hepatocyte shape and inflammatory infiltration. Perivascular inflammatory cell infiltration was lower in the LD group than in the CCl_4 group. Increased dosages of TCs reduced inflammatory cell infiltration and improved cell morphology, resulting in a decrease in liver tissue necrosis area in a dose-dependent manner (Figures 6B,C). The HD group had the greatest hepatoprotective effect, reducing the necrotic area of liver tissue by 77.9% compared to the CCl_4 group ($p < 0.0001$). The hepatoprotective effect showed a significant dose-response relationship, with the MD group performing marginally better than the HLSP group ($p < 0.001$), and the HD group performing the best.

3.6 Metabolite analysis and biomarker identification

The main metabolic differences across groups were investigated using the OPLS-DA model, and the CCl_4 and NC groups were clearly separated in liver and serum samples (Figure 7A; Figure 8A). Following TCs therapy, both the MD and HD groups distinguished themselves from the CCl_4 group (Figures 7Ba and 8Ba), and the HD group nearly overlapped with the NC group (Figures 7Bb and 8Bb). The HD group exhibited greater separation from the CCl_4 group than the HLSP group (Figures 7Bc and 8Bc), suggesting that TCs can dose-dependently reverse CCl_4-induced metabolic abnormalities in mice.

Using the OPLS-DA model, different metabolites were represented by various-sized points of different colors and shapes in the S-plot (Figure 7 bottom left). Among these metabolites, a total of 19 endogenous metabolites were identified (Figure 9) in liver and serum, 11 metabolites were chosen for potential biomarkers to distinguish between the NC and CCl_4 groups. Lactate, fumaric acid, succinic acid, inosine, O-phosphocholine, ascorbate, taurine, tyrosine, phenylalanine, valine, and alanine were chosen based on fold changes and associated *p*-values between groups (see Supplementary Tables S3, S4 for details).

4 Discussion

We qualitatively analyzed the chemical composition of TCs and found that it primarily consists of CuB, IsocuB, CuE and cucurbitacin derivatives by MN. The MN provided comprehensive compound profiling of the constituents in TCs and HLSP. Notably, we discovered for the first time that HLSP, a positive medication used for treating hepatitis and primary liver cancer, also contains IsocuB in addition to the previously reported CuB and CuE. This is attributed to our choice of acetonitrile rather than methanol as the mobile phase. After optimization, we found that isocratic elution with 50% acetonitrile can well separate CuB and its configuration isomer IsocuB, and achieve the resolution required for quantification. The three major components in TCs and HLSP showed an enormous variance in values of IsocuB and CuE. Interestingly, it confirmed our previous hypothesis that different species in the same plant family may lead to huge differences in chemical composition. The content of CuB in TCs was much higher than in HLSP, while the contents of IsocuB and CuE were much lower than in HLSP.

The plant species compared are affected by differences in their growth environments, which impacts gene expression and leads to variations in chemical profiles (Zhou et al., 2016; Nikalje et al., 2023). *H. pedunculosum* grows at high altitudes in cold and drought Tibet, while *C. melo* grows in warmer, humid lowland areas. The cold and drought environment upregulates genes related to cucurbitacin synthesis in *H. pedunculosum*, resulting in higher levels of CuB and its isomer compared to *C. melo*. This finding is consistent with literature showing cucurbitacin accumulation increases under drought stress (Mkhize et al., 2023). Ultimately, growing in different climates impacts the plant biochemistry and results in divergence of therapeutic efficacy and safety between taxa (Panossian, 2023), warranting further evaluation of understudied species like *H. pedunculosum* that may have unexplored benefits.

In safety evaluations, the LD_{50} value of TCs was 36.21 mg/kg BW, 2.6-fold more than the LD_{50} value of HLSP in mice, indicating its higher safety. Bartalis et al. found that the IC_{50} of CuE, CuB are 0.1 μM, 0.8 μM, respectively in HeLa cells (Bartalis and Halaweish, 2011). Therefore, we have a hypothesis that the lower content of CuE (3.6%) may be one of the factors leading to lower cell toxicity than HLSP. To our knowledge, no value of NOAEL as an important indicator of non-clinical experimental research has been published for HLSP. In this study, through continuous observation for 2 weeks of any clinical signs in mice treated with TCs (15 mg/kg BW), no deaths, abnormal behavior or other adverse effects were observed. Previous studies have reported that CuB at an oral dose of 1 mg/kg BW could effectively improve the abnormal liver function in mice induced by concanavalin A (Yang et al., 2020) and mitigated sepsis-induced pulmonary pathological damage in rats (Hua et al., 2017). In this study, TCs at a dose of 0.4 mg/kg BW lower than the above study could significantly reduce serum ALT and AST levels after CCl_4-induced liver injury. In addition, the effective dosage of TCs were 37-fold and 90-fold less than LD_{50} and NOAEL values, respectively, which ensure the safety of TCs use in preclinical study.

Our study further explored the protective mechanism of TCs on CCl_4-induced liver damage in mice through liver tissue and

serum metabolomics. After CCl_4 treatment, lactate involved in pyruvate metabolism and fumarate involved in the TCA cycle were significantly increased compared with the normal group, which disrupted the energy metabolism. Previous studies have been reported that increased levels of lactate and fumarate are markers of live injury (Wolf et al., 2017; Haonon et al., 2021; Ma et al., 2023). Whereas, TCs treatment restored the increased levels of lactate and fumarate to normal levels. This demonstrate that TCs treatment effectively regulates the imbalance of energy metabolism caused by liver injury. In addition, our study identified significant alterations associated with oxidative stress, and amino acid metabolism. Ascorbic acid and taurine have been reported to act as ROS free radical scavengers (Das et al., 2008; Jong et al., 2012; Tian et al., 2021). In this study, ascorbic acid and taurine in the liver and serum were significantly decreased, indicating that oxidative free radicals attacked and impaired the liver's cell membrane. Liver cells store ascorbic acid and taurine to combat oxidative stress, but membrane damage allows their leakage from cells. This results in lower intracellular concentrations. However, after TCs treatment, ascorbic acid in liver tissue and taurine in serum were significantly increased. It demonstrated that TCs can decrease oxidative stress and protect cell membranes from oxidative damage. This result is consistent with a previous study that CuB and CuE minimised cell damage caused by oxidative stress under drought-stressed environments (Mkhize et al., 2023). Since the liver is the primary site of amino acid metabolism (Ammar et al., 2022), CCl_4 injury leads to the disruption of amino acid metabolism. Increased phenylalanine levels have been associated to immunological activation and inflammatory reactions *in vivo* (Moosmann and Behl, 2000). In our study, CCl_4-induced liver damage is commonly accompanied by an increased level of phenylalanine, indicative of activated inflammatory response.

Previous studies have reported that HPS and its major lignan components have hepatoprotective effects (Shen et al., 2015; Shen et al., 2016; Feng et al., 2018). However, the hepatoprotective effects of HPP have been seldomly investigated. This study provides new insights into the hepatoprotective effects of TCs from HPP. Although the results confirmed that TCs showed significant protective effects against carbon tetrachloride-induced liver injury in mice, and exhibited superior efficacy and safety compared to the positive control drug, further work is still needed, including studies in other experimental animals and human validation. Future research directions should investigate the synergistic effects of the three monomeric components in TCs, and their dose-toxicity and dose-efficacy relationships. Overall, by developing a hepatoprotective formulation from the HPP that is rich in bioactive cucurbitacins, this study aims to remedy both the wastage of resources through disposal of this byproduct as well as mitigate ecological damage. Characterizing the pharmacological potential of cucurbitacins in the underutilized pericarp facilitates full utilization of the plant which previously led to resource wastage and environmental pollution upon disposal. Repurposing this byproduct for medicinal applications therefore represents an important example of sustainable phytomedicine development with significant reference value.

5 Conclusion

Our study demonstrated that the chemical composition of TCs primarily consists of CuB, IsocuB, and CuE. Interestingly, we discovered for the first time that HLSP, a positive control medication used for treating hepatitis and primary liver cancer, also contains IsocuB in addition to the previously reported CuB and CuE. This suggests the possibility that HPP could serve as a raw material for HLSP. We established the NOAEL values of TCs for the first time and found that the LD_{50} of TCs was significantly higher than that of HLSP, indicating greater safety. TCs exhibit a greater capacity to alleviate CCl_4-induced liver damage in mice relative to HLSP. In conclusion, our findings demonstrate the protective effect of TCs against CCl_4-induced liver injury in mice and reveal their potential for development into a hepatoprotective drug. The chemical composition and safety evaluation provide a basis for quality control. These results lay a foundation for the production and application of HPP.

Data availability statement

The datasets presented in this study can be found in online repositories. The names of the repository/repositories and accession number(s) can be found in the article/Supplementary Material.

Ethics statement

The animal study was approved by the Animal Care and Use Committee of Nanjing University of Science and Technology. The study was conducted in accordance with the local legislation and institutional requirements.

Author contributions

W-YL: Data curation, Formal Analysis, Investigation, Writing–original draft. DX: Data curation, Investigation, Funding acquisition, Writing–review and editing. Z-YH: Writing–review and editing, Formal Analysis. H-HM: Writing–review and editing, Data curation, Software. QZ: Data curation, Writing–review and editing. F-YW: Writing–review and editing, Resources. XF: Writing–review and editing, Conceptualization, Project administration. J-SW: Conceptualization, Writing–review and editing, Funding acquisition, Supervision.

Funding

The author(s) declare financial support was received for the research, authorship, and/or publication of this article. This research work was supported by the National Natural Science Foundation of China (Nos 81773857 and 82104356).

Acknowledgments

We sincerely thank Open Funding Project of Large Apparatus and equipment (Nanjing University of Science and Technology).

Conflict of interest

The authors declare that the research was conducted in the absence of any commercial or financial relationships that could be construed as a potential conflict of interest.

The authors declare that the research was conducted in the absence of any commercial or financial relationships that could be construed as a potential conflict of interest.

Publisher's note

Supplementary material

The Supplementary Material for this article can be found online at: https://www.frontiersin.org/articles/10.3389/fphar.2024.1344983/full#supplementary-material

References

Abal, P., Louzao, M., Antelo, A., Alvarez, M., Cagide, E., Vilariño, N., et al. (2017). Acute oral toxicity of tetrodotoxin in mice: determination of lethal dose 50 (LD_{50}) and No observed adverse effect level (NOAEL). *Toxins* 9 (3), 75. doi:10.3390/toxins9030075

Ammar, N. M., Hassan, H. A., Abdallah, H. M. I., Afifi, S. M., Elgamal, A. M., Farrag, A. R. H., et al. (2022). Protective effects of naringenin from *Citrus sinensis* (var. Valencia) peels against CCl_4-induced hepatic and renal injuries in rats assessed by metabolomics, histological and biochemical analyses. *Nutrients* 14 (4), 841. doi:10.3390/nu14040841

Arjaibi, H. M., Ahmed, M. S., and Halaweish, F. T. (2017). Mechanistic investigation of hepato-protective potential for cucurbitacins. *Med. Chem. Res.* 26 (7), 1567–1573. doi:10.1007/s00044-017-1872-3

Asadi-Samani, M., Kafash-Farkhad, N., Azimi, N., Fasihi, A., Alinia-Ahandani, E., and Rafieian-Kopaei, M. (2015). Medicinal plants with hepatoprotective activity in Iranian folk medicine. *Asian pac. J. Trop. Biomed.* 5 (2), 146–157. doi:10.1016/S2221-1691(15)30159-3

Bartalis, J. (2005). "Hepatoprotective activity of cucurbitacin," (Brookings (South Dakota): South Dakota State University). [dissertation].

Bartalis, J., and Halaweish, F. T. (2011). *In vitro* and QSAR studies of cucurbitacins on HepG2 and HSC-T6 liver cell lines. *Bioorg. Med. Chem.* 19 (8), 2757–2766. doi:10.1016/j.bmc.2011.01.037

Bernard, S. A., and Olayinka, O. A. (2010). Search for a novel antioxidant, anti-inflammatory/analgesic or anti-proliferative drug: cucurbitacins hold the ace. *J. Med. Plants Res.* 4 (25), 2821–2826. doi:10.5897/JMPR.9001120

Chanda, J., Biswas, S., Kar, A., and Mukherjee, P. K. (2020). Determination of cucurbitacin E in some selected herbs of ayurvedic importance through RP-HPLC. *J. Ayurveda Integr. Med.* 11 (3), 287–293. doi:10.1016/j.jaim.2019.01.002

Chen, J. C., Chiu, M. H., Nie, R. L., Cordell, G. A., and Qiu, S. X. (2005). Cucurbitacins and cucurbitane glycosides: structures and biological activities. *Nat. Prod. Rep.* 22 (3), 386–399. doi:10.1039/B418841C

Dai, Y. X., Wu, W. J., and Tan, R. (2017). Study on the chemical components of the ethyl acetate extract from *Herpetospermum caudigerum*. *N. Am. J. Med. Sci.* 10 (4), 136–138. doi:10.7156/najms.2017.1004136

Das, J., Ghosh, J., Manna, P., and Sil, P. C. (2008). Taurine provides antioxidant defense against NaF-induced cytotoxicity in murine hepatocytes. *Pathophysiology* 15 (3), 181–190. doi:10.1016/j.pathophys.2008.06.002

Dieterle, F., Ross, A., Schlotterbeck, G., and Senn, H. (2006). Probabilistic quotient normalization as robust method to account for dilution of complex biological mixtures. Application in ^{1}H NMR metabonomics. *Anal. Chem.* 78 (13), 4281–4290. doi:10.1021/ac051632c

Fang, Q. M., Zhang, H., Cao, Y., and Wang, C. (2007). Anti-inflammatory and free radical scavenging activities of ethanol extracts of three seeds used as "Bolengguazi". *J. Ethnopharmacol.* 114 (1), 61–65. doi:10.1016/j.jep.2007.07.024

Feng, X., Zhong, G. J., Deng Ba, D. J., Yang, B., Chen, L., and Du, S. (2018). Hepatoprotective effect of *Herpetospermum caudigerum* Wall. on carbon tetrachloride-induced hepatic fibrosis in rats. *J. Cell. Mol. Med.* 22 (7), 3691–3697. doi:10.1111/jcmm.13568

Fu, X., Wang, J., Liao, S., Lv, Y., Xu, D., Yang, M., et al. (2019). ^{1}H NMR-Based metabolomics reveals refined-Huang-Lian-Jie-Du-decoction (BBG) as a potential ischemic stroke treatment drug with efficacy and a favorable therapeutic window. *Front. Pharmacol.* 10, 337. doi:10.3389/fphar.2019.00337

Gong, P. Y., Yuan, Z. X., Gu, J., Tan, R., Li, J. C., Ren, Y., et al. (2016). Anti-HBV activities of three compounds extracted and purified from *Herpetospermum* seeds. *Molecules* 22 (1), 14. doi:10.3390/molecules22010014

Haonon, O., Liu, Z., Dangtakot, R., Intuyod, K., Pinlaor, P., Puapairoj, A., et al. (2021). *Opisthorchis viverrini* infection induces metabolic and fecal microbial disturbances in association with liver and kidney pathologies in hamsters. *J. Proteome Res.* 20 (8), 3940–3951. doi:10.1021/acs.jproteome.1c00246

Hu, G., Liu, W., and Li, L. (2023). Identification and quantification of cucurbitacin in watermelon frost using molecular networking integrated with ultra-high-performance liquid chromatography-tandem mass spectrometry. *J. Sep. Sci.* 46 (16), e2300019. doi:10.1002/jssc.202300019

Hu, R., Peng, Y., Chen, B., Chen, Y., and Hou, X. (1982). Study on tian gua di (*Cucumis melo* L.), an antihepatitis Chinese medicine. Preparation and assay of gua di su and cucurbitacin B and E. *Zhongcaoyao* 13 (10), 445–447.

Hua, S., Liu, X., Lv, S., and Wang, Z. (2017). Protective effects of cucurbitacin B on acute lung injury induced by sepsis in rats. *Med. Sci. Monit.* 23, 1355–1362. doi:10.12659/MSM.900523

Jayaprakasam, B., Seeram, N. P., and Nair, M. G. (2003). Anticancer and antiinflammatory activities of cucurbitacins from *Cucurbita andreana*. *Cancer Lett.* 189 (1), 11–16. doi:10.1016/S0304-3835(02)00497-4

Jiang, H. Z., Tan, R., Jiao, R. H., Deng, X. Z., and Tan, R. X. (2016). Herpecaudin from *Herpetospermum caudigerum*, a xanthine oxidase inhibitor with a novel isoprenoid scaffold. *Planta Med.* 82 (11/12), 1122–1127. doi:10.1055/s-0042-108210

Jong, C. J., Azuma, J., and Schaffer, S. (2012). Mechanism underlying the antioxidant activity of taurine: prevention of mitochondrial oxidant production. *Amino Acids* 42 (6), 2223–2232. doi:10.1007/s00726-011-0962-7

Kanani, S. H., and Pandya, D. J. (2022). Cucurbitacins: nature's wonder molecules. *Curr. Tradit. Med.* 8 (3), 26–34. doi:10.2174/2215083808666220107104220

Kaouadji, M., and Pieraccini, E. (1984). Herpetetradione, nouveau lignoide tetramere isole d'*Herpetospermum caudigerum* wall. *Tetrahedron Lett.* 25 (45), 5135–5136. doi:10.1016/S0040-4039(01)81544-6

Karaman, I. (2017). Preprocessing and pretreatment of metabolomics data for statistical analysis. *Metabolomics Fundam. Clin. Appl.* 965, 145–161. doi:10.1007/978-3-319-47656-8_6

Lee, D. H., Iwanski, G. B., and Thoennissen, N. H. (2010). Cucurbitacin: ancient compound shedding new light on cancer treatment. *Sci. World J.* 10, 413–418. doi:10.1100/tsw.2010.44

Li, M. H., Feng, X., Chen, C., Ruan, L. Y., Xing, Y. X., Chen, L. Y., et al. (2019). Hepatoprotection of *Herpetospermum caudigerum* Wall. against CCl_4-induced liver fibrosis on rats. *J. Ethnopharmacol.* 229, 1–14. doi:10.1016/j.jep.2018.09.033

Li, S. (1975). *Bencao gangmu* (Compendium of Materia Medica). Beijing, China: People's Medical Publishing House Co., LTD.

Libin, Y., Yourui, S., Changfan, Z., Yulin, L., and Honglun, W. (2003). Study on trace elements in seeds of *Herpetospermum penduculosum* (ser) baill. *Guangdong Weiliang Yuansu Kexue* 10 (12), 45–47. doi:10.3969/j.issn.1006-446X.2003.12.010

Linghu, L., Zong, W., Liao, Y., Chen, Q., Meng, F., Wang, G., et al. (2023). Herpetrione, a new type of PPARα ligand as a therapeutic strategy against nonalcoholic steatohepatitis. *Research* 6, 0276. doi:10.34133/research.0276

Liu, W., Fu, X. H., Huang, S. Y., Shi, Y. C., Shi, L. L., and Gu, J. (2017). Protective effect and mechanism of total lignans from Tibetan medicinal *Herpetospermum* seeds on

carbon tetrachloride-induced liver fibrosis in rats. *China J. Chin. Mat. Med.* 24, 567–571. doi:10.19540/j.cnki.cjcmm.20161222.063

Ma, Y. L., Ke, J. F., Wang, J. W., Wang, Y. J., Xu, M. R., and Li, L. X. (2023). Blood lactate levels are associated with an increased risk of metabolic dysfunction-associated fatty liver disease in type 2 diabetes: a real-world study. *Front. Endocrinol.* 14, 1133991. doi:10.3389/fendo.2023.1133991

Marzouk, B., Mahjoub, M. A., Bouraoui, A., Fenina, N., Aouni, M., and Marzouk, Z. (2013). Anti-inflammatory and analgesic activities of a new cucurbitacin isolated from *Citrullus colocynthis* seeds. *Med. Chem. Res.* 22 (8), 3984–3990. doi:10.1007/s00044-012-0406-2

Mei, J., Wu, X., Zheng, S., Chen, X., Huang, Z.-L., and Wu, Y. (2021). Improvement of cucurbitacin B content in *Cucumis melo* pedicel extracts by biotransformation using recombinant β-glucosidase. *Separations* 8 (9), 138. doi:10.3390/separations8090138

Mkhize, P., Shimelis, H., and Mashilo, J. (2023). Cucurbitacins B, E and I concentrations and relationship with drought tolerance in bottle gourd [*Lagenaria siceraria* (molina) standl.]. *Plants* 12 (19), 3492. doi:10.3390/plants12193492

Molavi, O., Ma, Z., Mahmud, A., Alshamsan, A., Samuel, J., Lai, R., et al. (2008). Polymeric micelles for the solubilization and delivery of STAT3 inhibitor cucurbitacins in solid tumors. *Int. J. Pharm.* 347 (1-2), 118–127. doi:10.1016/j.ijpharm.2007.06.032

Moosmann, B., and Behl, C. (2000). Cytoprotective antioxidant function of tyrosine and tryptophan residues in transmembrane proteins. *Eur. J. Biochem.* 267 (18), 5687–5692. doi:10.1046/j.1432-1327.2000.01658.x

Nagarani, G., Abirami, A., and Siddhuraju, P. (2014). Food prospects and nutraceutical attributes of Momordica species: a potential tropical bioresources – a review. *Food Sci. Hum. Wellness.* 3 (3-4), 117–126. doi:10.1016/j.fshw.2014.07.001

Nikalje, G. C., Rajput, V. D., and Ntatsi, G. (2023). Editorial: putting wild vegetables to work for sustainable agriculture and food security. *Front. Plant Sci.* 14, 1268231. doi:10.3389/fpls.2023.1268231

Panossian, A. (2023). Challenges in phytotherapy research. *Front. Pharmacol.* 14, 1199516. doi:10.3389/fphar.2023.1199516

Peters, R., Farias, M., and Ribeiro-do-Valle, R. (1997). Anti-inflammatory and analgesic effects of cucurbitacins from *Wilbrandia ebracteata*. *Planta Med.* 63 (06), 525–528. doi:10.1055/s-2006-957755

Quinn, R. A., Nothias, L. F., Vining, O., Meehan, M., Esquenazi, E., and Dorrestein, P. C. (2017). Molecular networking as a drug discovery, drug metabolism, and precision medicine strategy. *Trends Pharmacol. Sci.* 38 (2), 143–154. doi:10.1016/j.tips.2016.10.011

Ramos, A. E. F., Evanno, L., Poupon, E., Champy, P., and Beniddir, M. A. (2019). Natural products targeting strategies involving molecular networking: different manners, one goal. *Nat. Prod. Rep.* 36 (7), 960–980. doi:10.1039/C9NP00006B

Ruan, L. Y., Fan, J. T., Hong, W., Zhao, H., Li, M. H., Jiang, L., et al. (2018). Isoniazid-induced hepatotoxicity and neurotoxicity in rats investigated by ^{1}H NMR based metabolomics approach. *Toxicol. Lett.* 295, 256–269. doi:10.1016/j.toxlet.2018.05.032

Scherer, R., Rybka, A. C. P., Ballus, C. A., Meinhart, A. D., Teixeira Filho, J., and Godoy, H. T. (2012). Validation of a HPLC method for simultaneous determination of main organic acids in fruits and juices. *Food Chem.* 135 (1), 150–154. doi:10.1016/j.foodchem.2012.03.111

Shen, B., Chen, H., Shen, C., Xu, P., Li, J., Shen, G., et al. (2015). Hepatoprotective effects of lignans extract from *Herpetospermum caudigerum* against CCl_4-induced acute liver injury in mice. *J. Ethnopharmacol.* 164, 46–52. doi:10.1016/j.jep.2015.01.044

Shen, G., Cheng, L., Wang, L. Q., Zhang, L. H., Shen, B. D., Liao, W. B., et al. (2016). Formulation of dried lignans nanosuspension with high redispersibility to enhance stability, dissolution, and oral bioavailability. *Chin. J. Nat. Med.* 14 (10), 757–768. doi:10.1016/S1875-5364(16)30090-5

Silvestre, G. F. G., de Lucena, R. P., and da Silva Alves, H. (2022). Cucurbitacins and the immune system: update in research on anti-inflammatory, antioxidant, and immunomodulatory mechanisms. *Curr. Med. Chem.* 29 (21), 3774–3789. doi:10.2174/0929867329666220107153253

Teodor, E. D., Moroeanu, V., and Radu, G. L. (2020). Lignans from medicinal plants and their anticancer effect. *Mini-Rev. Med. Chem.* 20 (12), 1083–1090. doi:10.2174/1389557520666200212110513

Tian, Y., Zhang, X., Du, M., Li, F., Xiao, M., and Zhang, W. (2021). Synergistic antioxidant effects of araloside A and L-ascorbic acid on H_2O_2-induced HEK293 cells: regulation of cellular antioxidant status. *Oxid. Med. Cell. Longev.* 2021, 9996040–9996120. doi:10.1155/2021/9996040

Vilariño, N., Louzao, M. C., Abal, P., Cagide, E., Carrera, C., Vieytes, M. R., et al. (2018). Human poisoning from marine toxins: unknowns for optimal consumer protection. *Toxins* 10 (8), 324. doi:10.3390/toxins10080324

Wang, M., Carver, J. J., Phelan, V. V., Sanchez, L. M., Garg, N., Peng, Y., et al. (2016). Sharing and community curation of mass spectrometry data with global natural products social molecular networking. *Nat. Biotechnol.* 34 (8), 828–837. doi:10.1038/nbt.3597

Wang, O., Cheng, Q., Liu, J., Wang, Y., Zhao, L., Zhou, F., et al. (2014). Hepatoprotective effect of *Schisandra chinensis* (Turcz.) Baill. lignans and its formula with *Rubus idaeus* on chronic alcohol-induced liver injury in mice. *Food Funct.* 5 (11), 3018–3025. doi:10.1039/C4FO00550C

Wang, X., Tanaka, M., Peixoto, H. S., and Wink, M. (2017). Cucurbitacins: elucidation of their interactions with the cytoskeleton. *PeerJ* 5, e3357. doi:10.7717/peerj.3357

Wolf, A., Mulier, K. E., Muratore, S. L., and Beilman, G. J. (2017). D-β-Hydroxybutyrate and melatonin for treatment of porcine hemorrhagic shock and injury: a melatonin dose-ranging study. *BMC Res. Notes.* 10 (1), 649–657. doi:10.1186/s13104-017-2975-0

Wu, P. (2016). Zhong hua chuan tong yi yao jing dian gu ji: shen Nong ben Cao jing, *48*. Guangxi: Science and Technology Press.

Yang, B. Y., Zhang, X. Y., Guan, S. W., and Hua, Z. C. (2015). Protective effect of procyanidin B2 against CCl_4-induced acute liver injury in mice. *Molecules* 20 (7), 12250–12265. doi:10.3390/molecules200712250

Yang, J. (1989). *Diqing zang yao (diqing medicinal plants)*. Kunming: Yunnan Ethnic Publishing House.

Yang, J. J., Sanchez, L. M., Rath, C. M., Liu, X., Boudreau, P., Bruns, N., et al. (2013). Molecular networking as a dereplication strategy. *J. Nat. Prod.* 76 (9), 1686–1699. doi:10.1021/np400413s

Yang, L., Ao, Q., Zhong, Q., Li, W., and Li, W. (2020). SIRT1/IGFBPrP1/TGF β1 axis involved in cucurbitacin B ameliorating concanavalin A-induced mice liver fibrosis. *Basic Clin. Pharmacol. Toxicol.* 127 (5), 371–379. doi:10.1111/bcpt.13446

Yu, J. Q., Hang, W., Duan, W. J., Wang, X., Wang, D. J., and Qin, X. M. (2014). Two new anti-HBV lignans from *Herpetospermum caudigerum*. *Phytochem. Lett.* 10, 230–234. doi:10.1016/j.phytol.2014.10.001

Zhao, X. E., Liu, Y. J., Wang, H. L., and Suo, Y. R. (2009). HPLC and GC-MS analysis of fatty acids in Tibetan medicine *Herpetospermum* seed oil. *Nat. Prod. Res. Dev.* 21 (1), 76. doi:10.3969/j.issn.1001-6880.2009.01.018

Zhou, Y., Ma, Y., Zeng, J., Duan, L., Xue, X., Wang, H., et al. (2016). Convergence and divergence of bitterness biosynthesis and regulation in Cucurbitaceae. *Nat. Plants* 2 (12), 16183–16188. doi:10.1038/nplants.2016.183

frontiers | Frontiers in Pharmacology

TYPE Systematic Review
PUBLISHED 23 February 2024
DOI 10.3389/fphar.2024.1362391

OPEN ACCESS

EDITED BY
Rongrui Wei,
Jiangxi University of Traditional Chinese Medicine, China

REVIEWED BY
Allah Nawaz,
Joslin Diabetes Center and Harvard Medical School, United States
Ishtiaq Jeelani,
University of California, San Diego, United States

*CORRESPONDENCE
Myung-Ho Kim,
check8x8@woosuk.ac.kr
Chang-Gue Son,
ckson@dju.kr

RECEIVED 28 December 2023
ACCEPTED 12 February 2024
PUBLISHED 23 February 2024

CITATION
Kim M-H, Ahn S, Hur N, Oh S-Y and Son C-G (2024), The additive effect of herbal medicines on lifestyle modification in the treatment of non-alcoholic fatty liver disease: a systematic review and meta-analysis.
Front. Pharmacol. 15:1362391.
doi: 10.3389/fphar.2024.1362391

The additive effect of herbal medicines on lifestyle modification in the treatment of non-alcoholic fatty liver disease: a systematic review and meta-analysis

Myung-Ho Kim[1,2]*, Subin Ahn[2], Nayeon Hur[2], Seung-Yun Oh[3] and Chang-Gue Son[1]*

[1]Liver and Immunology Research Center, Daejeon Korean Medicine Hospital of Daejeon University, Daejeon, Republic of Korea, [2]Department of Internal Korean Medicine, Woosuk University Medical Center, Jeonju, Republic of Korea, [3]Department of Sasang Constitutional Medicine, Woosuk University Medical Center, Jeonju, Republic of Korea

Introduction: Non-alcoholic fatty liver disease (NAFLD) is difficult to manage because of its complex pathophysiological mechanism. There is still no effective treatment other than lifestyle modification (LM) such as dietary modifications, regular physical activity, and gradual weight loss. Herbal medicines from traditional Chinese Medicine and Korean Medicine have been shown to be effective in the treatment of NAFLD based on many randomized controlled trials. This systematic review and meta-analysis aims to evaluate the additive effects of herbal medicines on LM in the treatment of NAFLD.

Methods: Two databases (PubMed and Cochrane library) were searched using keywords related to NAFLD and herbal medicines. Then the randomized controlled trials (RCTs) evaluating the therapeutic effects of herbal medicines combined with LM were selected. The pooled results were analyzed as mean difference (MD) with 95% confidence interval (CI) for continuous data, and risk ratio (RR) with 95% CI for dichotomous data.

Results and Discussion: Eight RCTs with a total of 603 participants were included for this review study. Participants were administered with multi-herbal formulas (Yiqi Sanju Formula, Tiaogan Lipi Recipe, and Lingguizhugan Decoction) or single-herbal extracts (Glycyrrhiza glabra L., Magnoliae offcinalis, Trigonella Foenum-graecum L. semen, Portulaca oleracea L., and Rhus Coriaria L. fructus) along with LM for 12 weeks. The meta-analysis showed a significant improvement in ultrasoundbased liver steatosis measured by odds ratio (OR) in the herbal medicine group than those with LM alone (OR = 7.9, 95% CI 0.7 to 95.2, $p < 0.1$). In addition, herbal medicines decreased the levels of aspartate transferase (MD -7.5, 95% CI -13.4 to –1.7, $p = 0.01$) and total cholesterol (MD -16.0, 95% CI -32.7 to 0.7, $p = 0.06$) more than LM alone. The meta-analysis partially showed

clinical evidence supporting the additive benefits of herbal medicines for NAFLD in combination with LM. Whereas, it is necessary to provide a solid basis through higher-quality studies using a specific herbal medicine.

KEYWORDS

non-alcoholic fatty liver disease, herbal medicine, lifestyle modification, systematic review, meta-analysis

1 Introduction

Non-alcoholic fatty liver disease (NAFLD) is a condition in which excess fat (>5–10% of the liver weight) accumulates in the liver without excessive drinking, resulting in steatohepatitis, liver fibrosis, and cirrhosis (Younossi et al., 2021). With a prevalence of 30%–40% worldwide, NAFLD has become a widespread health concern (Im et al., 2021; Riazi et al., 2022). NAFLD has the potential to progress to cirrhosis, hepatocellular carcinoma (HCC), and death. The escalating prevalence of NAFLD in the general population highlights the increasing role of NAFLD in HCC epidemiology (Fernando et al., 2019). NAFLD sometimes develops into HCC without progressing to liver fibrosis or cirrhosis, therefore early diagnosis and management of liver steatosis are important (Berkan-Kawińska and Piekarska, 2020).

However, there is still no effective treatment other than lifestyle modification (LM) for NAFLD (Younossi et al., 2021). While there has been progress in understanding how NAFLD develops and finding potential treatments, significant challenges persist. There is currently no medication specifically approved for NAFLD (Friedman et al., 2018). The pathophysiological mechanisms of NAFLD are complex and involve systemic metabolic dysfunction and inflammation, making it difficult to manage NAFLD with single-target drugs. Therefore, combination therapies modulating multiple targets have recently been investigated (Makri et al., 2022). In traditional Chinese Medicine and Korean Medicine, herbal medicines are multi-compound and multi-target drugs that appear to have potential for the prevention and treatment of NAFLD (Dai et al., 2021). However, its effectiveness has not yet been clearly demonstrated.

Many randomized controlled trials (RCTs) have been conducted on herbal medicines for the treatment of NAFLD over 2 decades, which suggest that herbal medicines improve NAFLD and are superior to conventional drugs such as silymarin and ursodeoxycholic acid (Lee et al., 2022). As mentioned earlier, LM should not be overlooked when considering any treatment modalities.

Therefore, the purpose of this study was to find out whether herbal medicines have additive effect on LM in the treatment of NAFLD.

2 Methods

2.1 Search strategy

This systematic review and meta-analysis was conducted based on the PRISMA guidelines. Two major databases (PubMed and Cochrane library) were searched using keywords related to NAFLD and herbal medicine through February 2023.

2.2 Selection criteria

The studies that met the following criteria were included: RCTs evaluating the therapeutic effects of herbal medicines which are used in traditional Chinese Medicine and traditional Korean Medicine, combined with LM for NAFLD. The studies that did not use placebo as a control were excluded. There was no limit on the language.

2.3 Risk of bias assessment

The quality of the included RCTs was evaluated using the Cochrane library risk of bias assessment tool. The 7 items used to assess bias in each trial included random sequence generation, allocation concealment, double blindness of participants and trial performers, blindness of outcome assessment, incomplete outcome data, selective reporting, and other biases. Each quality item was divided and categorized into high risk, low risk, and unclear. This work was completed by two independent reviewers, and a third was responsible for resolving controversial issues.

2.4 Data extraction and review process

After screening the title and abstract of all the studies, the full text of the relevant articles was assessed by two reviewers. We conducted a systematic review on the additive effect of herbal medicines on LM in the treatment of NAFLD. We extracted the following data: name of the authors, patient information, sample size, name of herbal medicine, duration of herbal medicine treatment, observation period, and outcome measurements [ultrasound (US) liver steatosis grade, computed tomography (CT) liver/spleen ratio, body mass index (BMI), homeostatic model assessment for insulin resistance (HOMA-IR), alanine transaminase (ALT), aspartate transaminase (AST), gamma-glutamyl transferase (GGT), triglyceride, and total cholesterol] in the study.

A meta-analysis was performed using odds ratio (OR) for the improvement of US liver steatosis grade, and mean difference (MD) for the CT liver/spleen ratio, BMI, HOMA-IR, ALT, AST, GGT, triglyceride, and total cholesterol with 95% confidence interval (CI). Random-effect models were used due to heterogeneity. Dichotomous data are expressed as the OR with 95% CI. MD with the 95% CI were calculated for continuous data. Statistical significance was set at $p < 0.05$. Review Manager 5.4.1 was used for the analysis (http://www.tech.cochrane.org/revman) (accessed on 13 January 2023).

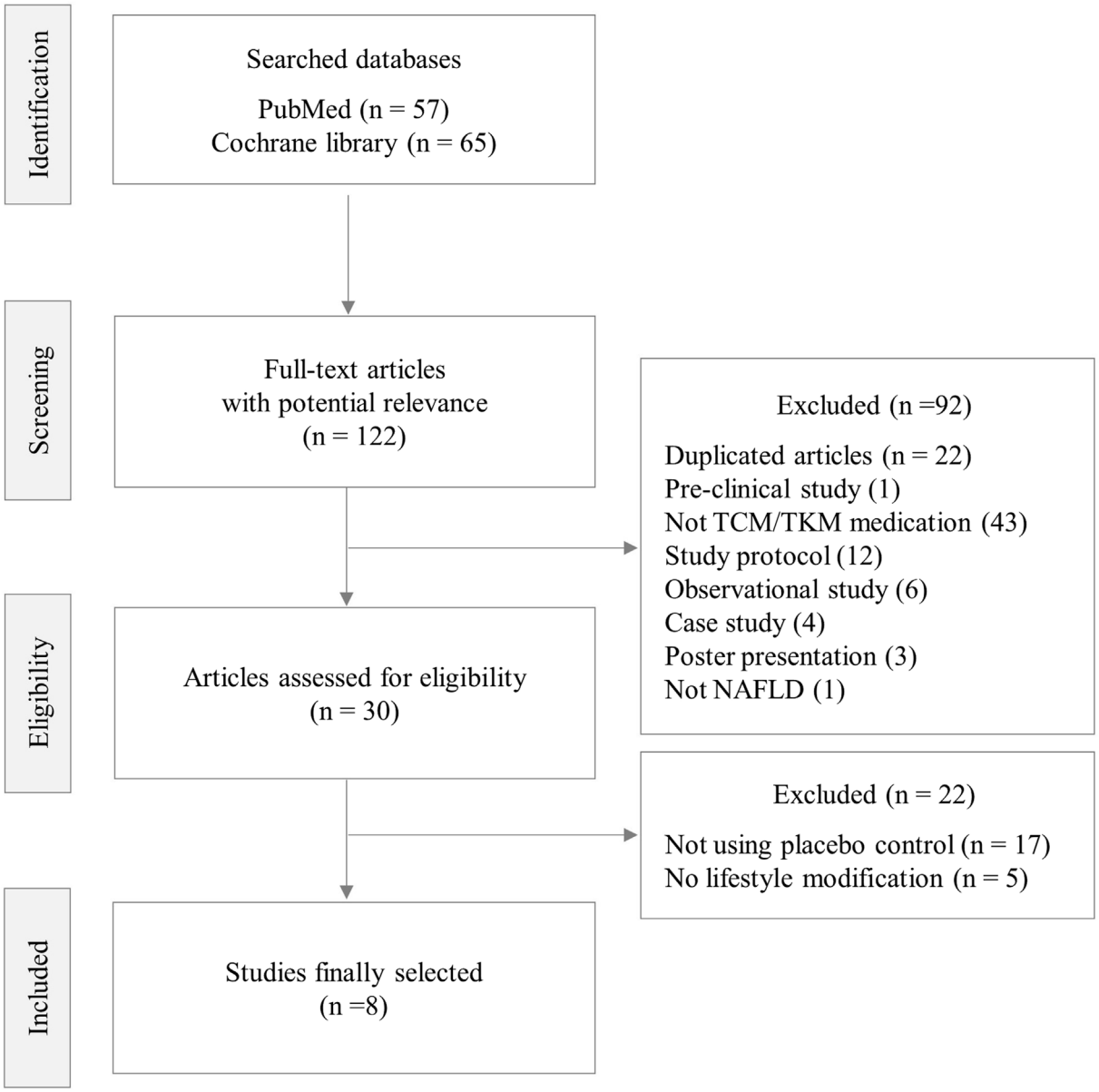

FIGURE 1
Flowchart of the literature search and study selection.

3 Results

3.1 Characteristics of the included studies

From 249 articles initially searched, 8 studies finally met the criteria of this review, which enrolled 603 participants (male 302, female 301, 326 in LM plus herbal medicine versus 277 in LM plus placebo) (Figure 1; Table 1). Risk of bias of each included study was generally assessed as low (Supplementary Figures S1A, S1B).

Regarding LM, all participants in both groups were guided to restrict the high-carbohydrate and high-fat foods, and to increase their physical activity to at least 150 min per week. Herbal medicine group were administered with multi-herbal formulas [Yiqi Sanju Formula: 益气散聚方 (Lou et al., 2008), Tiaogan Lipi Recipe: 调肝理脾方 (Yu et al., 2015), Lingguizhugan Decoction: 苓桂术甘汤 (Dai et al., 2021)] or single-herb extract [*Glycyrrhiza glabra* L.: 甘草 (Rostamizadeh et al., 2022), *Magnoliae officinalis*: 厚朴 (Jeong et al., 2017), *Trigonella Foenum-graecum* L. semen: 胡芦巴 (Babaei et al., 2020), *Portulaca oleracea* L.: 马齿苋 (Darvish Damavandi et al., 2021), and *Rhus Coriaria* L. fructus (Kazemi et al., 2020)], respectively (Supplementary Table S1). After 12-week intervention, the changes of liver steatosis (US and/or CT), liver enzymes (ALT, AST, and GGT) and/or extra-hepatic parameters (BMI, HOMA-IR, TG and TC) were evaluated.

3.2 Change in hepatic steatosis

The US-based measurement of liver steatosis (3 studies, 190 participants) revealed that herbal medicines notably increased the case of improvement in liver steatosis grade: as

TABLE 1 Characteristics of the included 8 studies.

Items		Lifestyle modification + Herbal medicine	Lifestyle modification + Placebo
Participants			
Total number (Male/Female)		326 (166/160)	277 (137/140)
Mean number ± SD		40.8 ± 22.5	37.6 ± 20.8
Mean age of participants[a]		46.3 ± 6.4	46.7 ± 6.3
Study duration, week		12.0 ± 0.0	
Country (n of study)		Iran (4), China (3), South Korea (1)	
Intra-hepatic outcomes (n of study, participants)			
Liver steatosis using US (3, 193)	Grade 1, %	35.8 ± 22.4	38.6 ± 22.3
	Grade 2, %	49.7 ± 19.0	39.0 ± 25.0
	Grade 3, %	15.7 ± 4.7	5.8 ± 3.2
CT liver/spleen ratio (2, 166)[a]		0.79 ± 0.01	0.77 ± 0.05
Hepatic enzymes (U/L)[a]	ALT (8, 603)	56.6 ± 23.4	54.5 ± 21.0
	AST (8, 603)	38.3 ± 14.9	35.6 ± 12.4
	GGT (4, 603)	41.6 ± 19.5	45.3 ± 21.0
Extra-hepatic outcomes (n of study, participants)			
Triglyceride (mg/dL,7, 504)[a]		197.3 ± 44.7	220.2 ± 65.5
Total cholesterol (mg/dL, 7, 504)[a]		200.7 ± 19.6	195.5 ± 22.0
BMI (kg/m^2, 7, 504)[a]		29.0 ± 2.2	28.6 ± 1.8
HOMA-IR (6, 480)[a]		3.9 ± 1.5	3.6 ± 0.4

US, ultrasound; CT, computed tomography; ALT, alanine transaminase; AST, aspartate transaminase; GGT, gamma-glutamyl transferase; BMI, body mass index; HOMA-IR, homeostatic model assessment for insulin resistance.
[a]The mean was estimated using the presented mean value of each study.

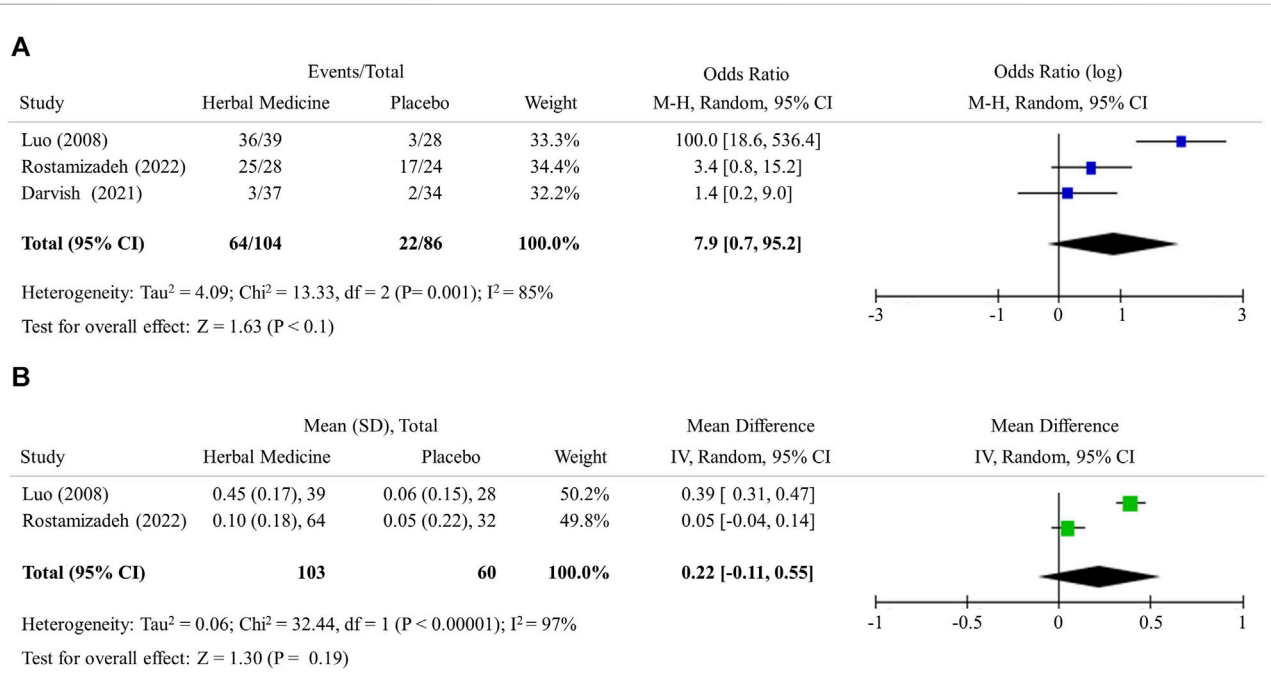

FIGURE 2
Hepatic steatosis. **(A)** Improvement in ultrasound liver steatosis grade **(B)** Computed tomography liver/spleen ratio.

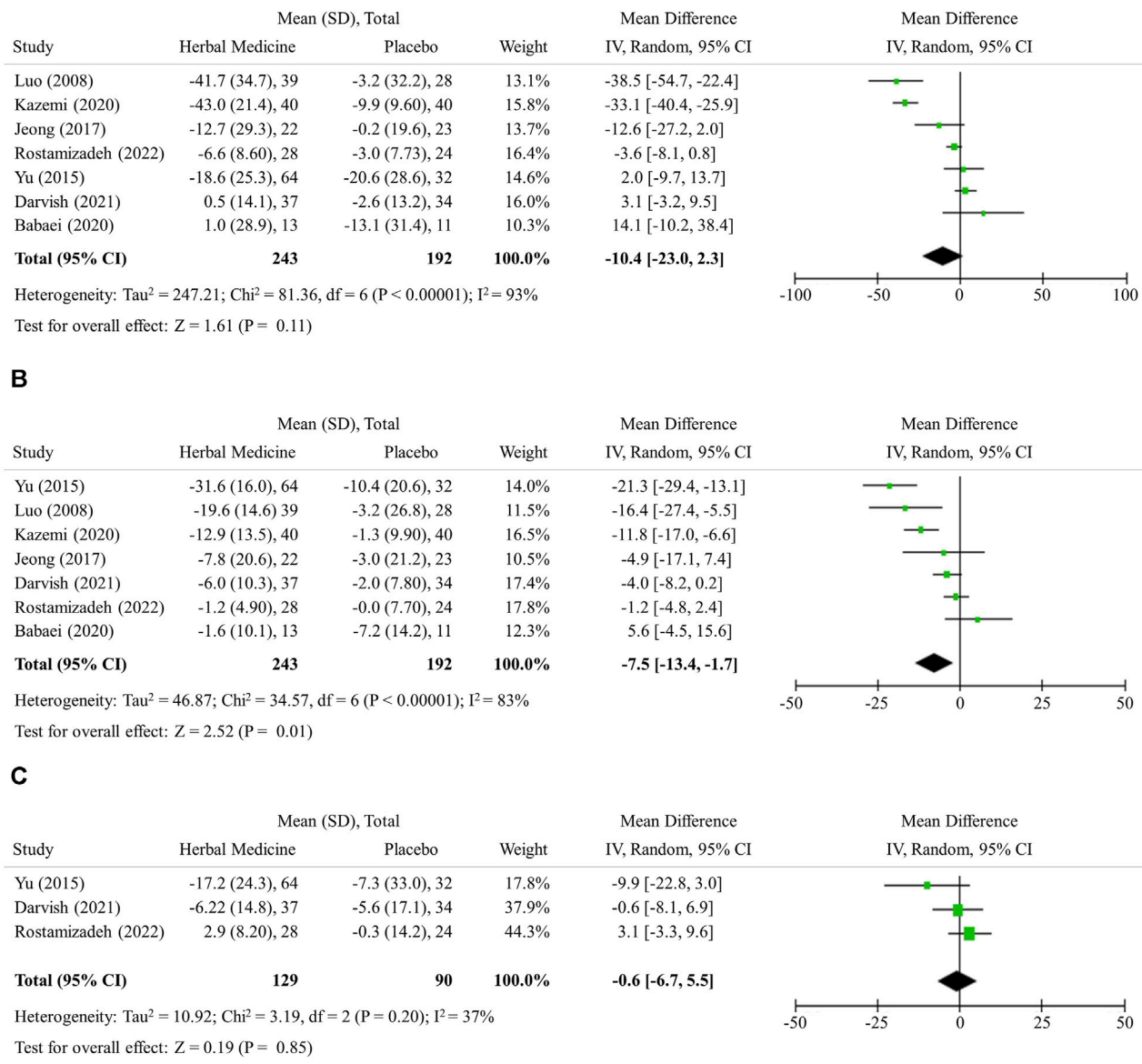

FIGURE 3
Hepatic inflammation. **(A)** Alannine transaminase **(B)** Aspartate transaminase **(C)** Gamma-glutamyl transferase.

OR = 7.9 (95% CI 0.7 to 95.2, $p < 0.1$) (Figure 2A). Meanwhile, CT-based liver/spleen ratio (2 studies, 163 participants) did not show the significant mean difference between 2 groups as 0.2 (95% CI −0.1 to 0.6, $p = 0.19$) (Figure 2B).

3.3 Change in hepatic inflammation

The hepatic enzyme levels were further lowered by herbal medicines compared with LM alone, however no statistical significance was observed in the mean difference; ALT −10.34 (95% CI −23.0 to 2.3, 7 studies, 435 participants), AST −7.5 (95% CI −13.4 to −1.7, 7 studies, 435 participants), and GGT −0.6 (95% CI −6.7 to 5.5, 3 studies, 219 participants), respectively (Figures 3A–C).

3.4 Change in lipid profile

The herbal medicines further lowered serum levels of both TG and TC, but without statistical significance in mean difference, likely −15.7 (95% CI -50.3 to 19.0, 7 studies, 528 participants) and −16.0 (95% CI −32.7 to 0.7, 7 studies, 528 participants), respectively (Figures 4A, B).

3.5 Obesity and insulin resistance

The herbal medicines further lowered serum levels of both BMI and HOMA-IR, but without statistical significance in mean difference; −0.5 (95% CI −1.2 to 0.2, 7 studies, 501 participants) and −0.6 (95% CI −1.5 to 0.3, 6 studies, 477 participants), respectively (Figures 4C, D).

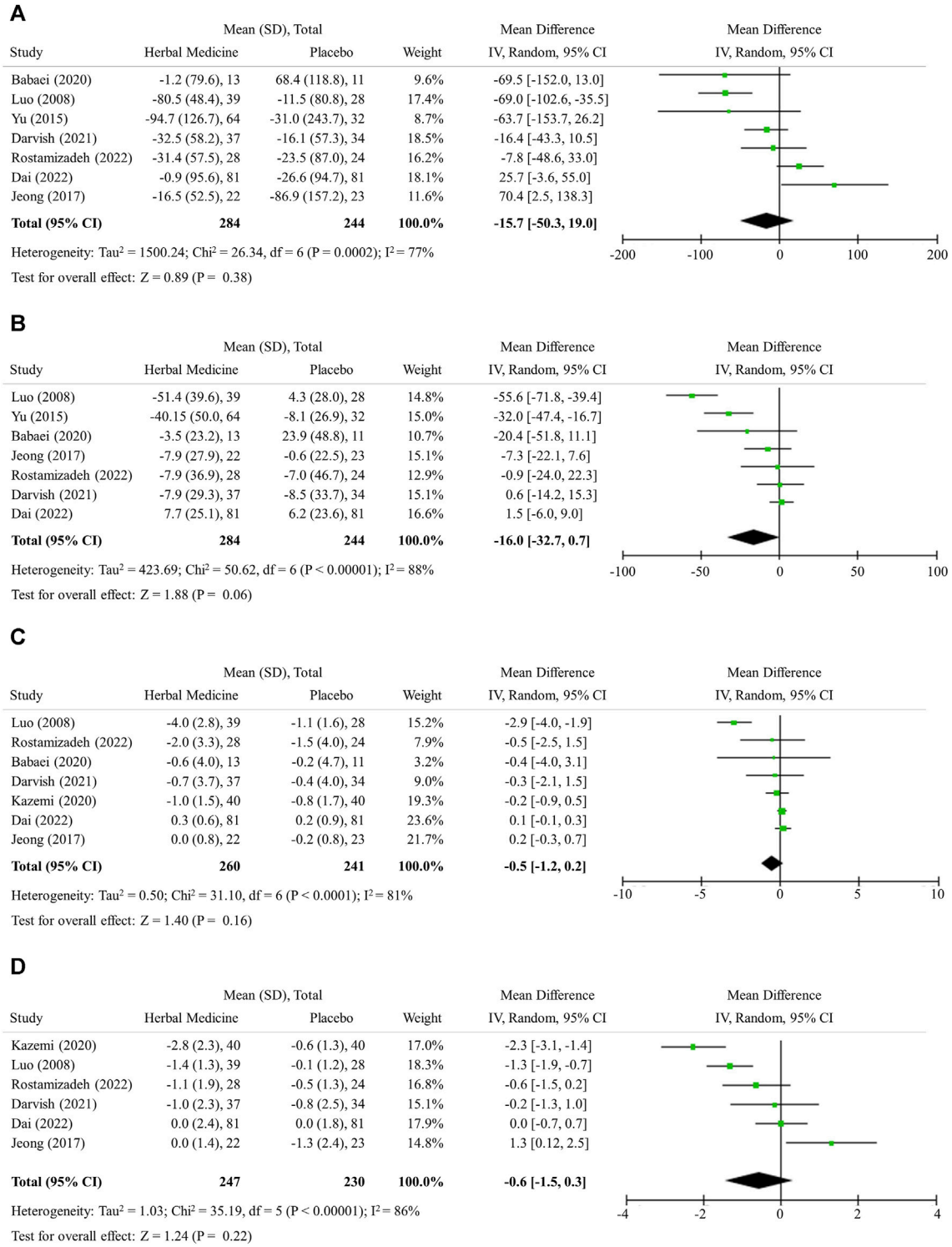

FIGURE 4
Lipid profile, obesity, and insulin resistance. **(A)** Triglyceride **(B)** Total cholesterol **(C)** Body mass index **(D)** HOMA-IR.

4 Discussion

NAFLD is attracting attention from the medical community due to its high prevalence worldwide and as a major components of metabolic syndrome as well as chronic liver diseases (Wong et al., 2023). LM is currently the only way to control this disease, which underscores the demand for the development of effective treatments (Younossi et al., 2021). Based on the partial evidence for the potential of herbal medicines against NAFLD (Dai et al., 2021). We herein performed a meta-analysis to evaluate the additive effect of herbal medicines on LM in the treatment of NAFLD.

Biopsy-derived histological examination is a classical standard to assess the levels of steatosis, inflammation and fibrosis in the liver. Biopsy is however invasive; thus, the multiple tests are almost impossible (Segura-Azuara et al., 2022). Accordingly, US and/or CT examinations are primary tools when evaluating intervention-induced changes in clinics and RCTs, (Schwenzer et al., 2009). As a non-invasive method, US detects fat accumulation in the liver by observing ultrasound attenuation and CT measures the density of the tissue passed by the X-ray beam and identifies fatty liver by comparing the density of liver with that of the spleen. If the ratio of the density of liver to that of spleen is less than 1.0, it is diagnosed with fatty liver. Transient elastography which is an enhanced form of ultrasound detect liver fibrosis in NAFLD or other liver diseases (Sanyal et al., 2023). In this study, 3 RCTs (Lou et al., 2008; Darvish Damavandi et al., 2021; Rostamizadeh et al., 2022) employed US examination and the meta-analysis showed the effect of herbal medicines in improving hepatic steatosis was 7.9 times higher than LM alone (Figure 2A). Two RCTs (Lou et al., 2008; Yu et al., 2015) utilized CT examination and it appeared that herbal medicines had the effect of increasing the liver to spleen ratio to closer to 1.0 in the meta-analysis (Table 1; Figure 2B).

In addition to histological examination, the levels of ALT, AST, and GGT are widely used to check for the damage of hepatic cells and inflammation in the liver. The reference ranges for ALT, AST, and GGT can vary depending on the laboratory and the method used for testing. However, on average, normal ranges are ALT: 0–45 IU/L, AST: 0–35 IU/L, GGT: 0–30 IU/L (Paul, 2020). If fatty liver exists but there is no relevant hepatic cell damage or inflammation, the ALT, AST, and GGT levels should be within normal range. In this study, herbal medicines were shown to have additive effect to LM in decreasing ALT and AST levels by about 10 (Figures 3A, B). This degree of the changes can be regarded as the extent to which herbal medicines normalize the ALT level, since the baseline ALT level of the subjects were around 55 (Table 1). However, it should be noted that the number of studies included in the analysis is small, which limits the interpretation of the results in terms of selection bias and statistical significance.

It has been known that NAFLD is present in up to 75% of overweight people and in more than 90% of people with severe obesity (Rinella et al., 2023). Obesity significantly contributes to NAFLD progression by disrupting lipid metabolism and promoting systemic inflammation. This dysregulation exacerbates hepatic fat accumulation, advancing NAFLD. Additionally, obesity-induced inflammation extends beyond the liver, impacting systemic inflammation and worsening underlying NAFLD processes through increased oxidative stress, mitochondrial dysfunction, and gut dysbiosis (Lim et al., 2021). Therefore, patients with NAFLD are recommended to lose weight through LM. Recently, GLP-1R agonists have been shown that they effectively reduce body weight and may aid in reversing NAFLD (Andreasen et al., 2023). Herbal medicines have been extensively studied that they help reduce body weight and attenuate NAFLD by suppressing appetite and reducing oxidative stress, improving mitochondrial function, and modulating intestinal dysbiosis (Dai et al., 2021).

In this study, the additive effect of herbal medicines in reducing BMI was not found to be significant (Figure 4C). It has been known that weight loss more than 5% (BMI reduction of 1.5 or more, assuming a patient with BMI 30) can improve NAFLD (Younossi et al., 2021). However, LM alone (placebo) did not sufficiently reduce BMI in the studies included in this analysis (Figure 4C). Considering that many patients find it difficult to successfully lose weight through LM, herbal medicines might help weight loss when combined with LM. When HOMA-IR drops below 2, it is regarded that insulin resistance is improved (Isokuortti et al., 2017). In situation where LM alone does not improve HOMA-IR enough, herbal medicine treatment can help to some extent (Figure 4D). In addition, although the levels of TG and TC were in the normal range at baseline, they were reduced by herbal medicines confirming the effect of improving lipid metabolism as previously known (Dai et al., 2021). However, further study on herbal medicines is needed to ensure that herbal medicines can effectively treat metabolic disorders as well as NAFLD.

The herbal medicines and their doses used in the RCTs included in this study are listed in Supplementary Table S1. There was not significant safety issue in the RCTs. Regarding the efficacy of the herbal medicines used in the RCTs included in this study, it has been extensively studied for anti-oxidant, anti-inflammatory, hypoglycemic, and lipid-lowering effects of *Astragali* Radix, *Atractylodis* Rhizoma Alba, *Salviae Miltiorrhizae* Radix, *Bupleuri* Radix, *Artemisiae* Capillaris Herba, *Polygoni Cuspidati* Radix, *Cassiae* Semen, *Crataegi* Fructus, *Poria Sclerotium*, *Cinnamomi Ramulus*, *Glycyrrhiza* Rhizoma in the treatment of NAFLD (Dai et al., 2021). In addition, several studies demonstrated *Coptidis* Rhizoma (Li et al., 2024), *Polygoni orientalis* (Chen et al., 2021), *Magnoliae offcinalis* (Kuo et al., 2020), *and Tegillarca granosa* L. (Jiang et al., 2024) improve glucose and lipid metabolism by modulating PI3K-AKT and AMPK signaling pathway, and *Coicis* Semen (Chiang et al., 2020), *Cyperi* Rhizoma (Wang et al., 2022), *Verbena officinalis* L. (Kubica et al., 2020), *Trigonella Foenum-graecum* L. semen (Yadav and Baquer, 2014), *Portulaca oleracea* L. (Rahimi et al., 2019), and Rhus Coriaria L. fructus (Alsamri et al., 2021) exhibit anti-oxidant, anti-inflammatory effects by enhancing superoxide dismutase and glutathione activity and inhibiting the production of inflammatory mediators such as nitric oxide, tumor necrosis factor-α, interleukin-1β, interleukin-6, and prostaglandin E2. Since the ingredients and their chemical structure of herbal medicines above have been identified (Abu-Reida et al., 2014; Zhou et al., 2015; Pang et al., 2016; Dong et al., 2017; Yang et al., 2017; Wang et al., 2018; Luo et al., 2019; Wang et al., 2019; Kubica et al., 2020; Li et al., 2020; Liu et al., 2020; Zhu et al., 2020; Chen et al., 2021; Hsueh et al., 2021; Xue et al., 2021; Zhang et al., 2021; Chang et al., 2022; Lu et al., 2022; Singh et al., 2022), it is expected that therapeutics will be developed through analog development based on the previous studies.

The limitations of this study are as follows. First, although total 30 RCTs were conducted using herbal medicines for the treatment of NAFLD (Figure 1), there were a few studies using placebo control, so a sufficient number of studies could not be analyzed. Second, the levels of AST, GGT, TG, and TC at baseline were within normal range, which suggest that the patients included in this analysis had mild NAFLD. Third, there were not many studies in which imaging were conducted, even in studies mainly targeting patients with mild NAFLD. In addition, it is imperative to address the role of genetic and epigenetic factors in NAFLD. The examination of genetic (e.g., *PNPLA3*, *TM6SF2*, *MBOAT7*, and *TMC4* variants) and epigenetic (e.g., DNA

methylation) factors becomes crucial in understanding the multifaceted nature of NAFLD progression (Younossi et al., 2018). Several studies have shown that *PNPLA3* genotype and characteristic epigenetic alterations vary depending on nationality and ethnicity (Szanto et al., 2019; Krawczyk et al., 2020). Therefore, it is necessary to consider genetic and epigenetic factors depending on nationality and ethnicity when applying the finding of this study, given that the RCTs included in this study predominantly originate from Asian and Middle Eastern countries (China, South Korea, and Iran).

5 Conclusion

Given some limitations above, this systematic review and meta-analysis at least partially evidenced the add-on efficacy of herbal medicines on LM in the treatment of NAFLD, which produce a reference data for herb-derived drug developments against NAFLD in the future. The further well-designed and larger scaled RCTs are however necessary to provide a solid basis for NAFLD treatment.

Data availability statement

The original contributions presented in the study are included in the article/Supplementary Material, further inquiries can be directed to the corresponding authors.

Author contributions

M-HK: Writing–original draft, Writing–review and editing. SA: Writing–original draft, Writing–review and editing. NH: Writing–original draft, Writing–review and editing. S-YO: Writing–original draft, Writing–review and editing. C-GS: Writing–original draft, Writing–review and editing.

Funding

The author(s) declare financial support was received for the research, authorship, and/or publication of this article. This work was supported by the Woosuk University, a grant of the Korea Health Technology R&D Project through the Korea Health Industry Development Institute (KHIDI), and funded by the Ministry of Health and Welfare, Republic of Korea (Grant No. HF23C0074).

Conflict of interest

The authors declare that the research was conducted in the absence of any commercial or financial relationships that could be construed as a potential conflict of interest.

The author(s) declared that they were an editorial board member of Frontiers, at the time of submission. This had no impact on the peer review process and the final decision.

Publisher's note

Supplementary material

The Supplementary Material for this article can be found online at: https://www.frontiersin.org/articles/10.3389/fphar.2024.1362391/full#supplementary-material

References

Abu-Reida, I. M., Jamous, R. M., and Ali-Shtayeh, M. S. (2014). Phytochemistry, pharmacological properties and industrial applications of Rhus coriaria L.(sumac). *Jordan J. Biol. Sci.* 147 (1573), 233–244. doi:10.12816/0008245

Alsamri, H., Athamneh, K., Pintus, G., Eid, A. H., and Iratni, R. (2021). Pharmacological and antioxidant activities of Rhus coriaria L. (Sumac). *Antioxidants (Basel)* 10 (1), 73. doi:10.3390/antiox10010073

Andreasen, C. R., Andersen, A., and Vilsbøll, T. (2023). The future of incretins in the treatment of obesity and non-alcoholic fatty liver disease. *Diabetologia* 66, 1846–1858. doi:10.1007/s00125-023-05966-9

Babaei, A., Taghavi, S. A., Mohammadi, A., Mahdiyar, M. A., Iranpour, P., Ejtehadi, F., et al. (2020). Comparison of the efficacy of oral fenugreek seeds hydroalcoholic extract versus placebo in nonalcoholic fatty liver disease; a randomized, triple-blind controlled pilot clinical trial. *Indian J. Pharmacol.* 52 (2), 86–93. doi:10.4103/ijp.IJP_17_19

Berkan-Kawińska, A., and Piekarska, A. (2020). Hepatocellular carcinoma in non-alcohol fatty liver disease–changing trends and specific challenges. *Curr. Med. Res. Opin.* 36 (2), 235–243. doi:10.1080/03007995.2019.1683817

Chang, X., Chen, X., Guo, Y., Gong, P., Pei, S., Wang, D., et al. (2022). Advances in chemical composition, extraction techniques, analytical methods, and biological activity of Astragali Radix. *Molecules* 27 (3), 1058. doi:10.3390/molecules27031058

Chen, K., Qu, J., Chen, H., Wang, J., Hua, H., Li, J., et al. (2021). Investigating the medicinal potential, material basis and mechanism of Polygoni Orientalis Fructus based on multi-technology integrated network pharmacology. *Phytomedicine* 91, 153685. doi:10.1016/j.phymed.2021.153685

Chiang, H., Lu, H.-F., Chen, J.-C., Chen, Y.-H., Sun, H.-T., Huang, H.-C., et al. (2020). Adlay seed (*Coix lacryma-jobi* L.) extracts exhibit a prophylactic effect on diet-induced metabolic dysfunction and nonalcoholic fatty liver disease in mice. *Evidence-Based Complementary Altern. Med.* 2020, 9519625. doi:10.1155/2020/9519625

Dai, X., Feng, J., Chen, Y., Huang, S., Shi, X., Liu, X., et al. (2021). Traditional Chinese Medicine in nonalcoholic fatty liver disease: molecular insights and therapeutic perspectives. *Chin. Med.* 16 (1), 68–17. doi:10.1186/s13020-021-00469-4

Darvish Damavandi, R., Shidfar, F., Najafi, M., Janani, L., Masoodi, M., Akbari-Fakhrabadi, M., et al. (2021). Effect of Portulaca Oleracea (purslane) extract on liver enzymes, lipid profile, and glycemic status in nonalcoholic fatty liver disease: a randomized, double-blind clinical trial. *Phytother. Res.* 35 (6), 3145–3156. doi:10.1002/ptr.6972

Dong, X., Fu, J., Yin, X., Yang, C., Zhang, X., Wang, W., et al. (2017). Cassiae semen: a review of its phytochemistry and pharmacology (Review). *Mol. Med. Rep.* 16 (3), 2331–2346. doi:10.3892/mmr.2017.6880

Fernando, D. H., Forbes, J. M., Angus, P. W., and Herath, C. B. (2019). Development and progression of non-alcoholic fatty liver disease: the role of advanced glycation end products. *Int. J. Mol. Sci.* 20 (20), 5037. doi:10.3390/ijms20205037

Friedman, S. L., Neuschwander-Tetri, B. A., Rinella, M., and Sanyal, A. J. (2018). Mechanisms of NAFLD development and therapeutic strategies. *Nat. Med.* 24 (7), 908–922. doi:10.1038/s41591-018-0104-9

Hsueh, T.-P., Lin, W.-L., Dalley, J. W., and Tsai, T.-H. (2021). The pharmacological effects and pharmacokinetics of active compounds of Artemisia capillaris. *Biomedicines* 9 (10), 1412. doi:10.3390/biomedicines9101412

Im, H. J., Ahn, Y. C., Wang, J.-H., Lee, M. M., and Son, C. G. (2021). Systematic review on the prevalence of nonalcoholic fatty liver disease in South Korea. *Clin. Res. Hepatology Gastroenterology* 45 (4), 101526. doi:10.1016/j.clinre.2020.06.022

Isokuortti, E., Zhou, Y., Peltonen, M., Bugianesi, E., Clement, K., Bonnefont-Rousselot, D., et al. (2017). Use of HOMA-IR to diagnose non-alcoholic fatty liver disease: a population-based and inter-laboratory study. *Diabetologia* 60 (10), 1873–1882. doi:10.1007/s00125-017-4340-1

Jeong, J. Y., Sohn, J. H., Baek, Y. H., Cho, Y. K., Kim, Y., and Kim, H. (2017). New botanical drug, HL tablet, reduces hepatic fat as measured by magnetic resonance spectroscopy in patients with nonalcoholic fatty liver disease: a placebo-controlled, randomized, phase II trial. *World J. Gastroenterol.* 23 (32), 5977–5985. doi:10.3748/wjg.v23.i32.5977

Jiang, Q., Chen, L., Wang, R., Chen, Y., Deng, S., Shen, G., et al. (2024). Hypoglycemic mechanism of *Tegillarca granosa* polysaccharides on type 2 diabetic mice by altering gut microbiota and regulating the PI3K-akt signaling pathwaye. *Food Sci. Hum. Wellness* 13 (2), 842–855. doi:10.26599/fshw.2022.9250072

Kazemi, S., Shidfar, F., Ehsani, S., Adibi, P., Janani, L., and Eslami, O. (2020). The effects of sumac (Rhus coriaria L.) powder supplementation in patients with non-alcoholic fatty liver disease: a randomized controlled trial. *Complement. Ther. Clin. Pract.* 41, 101259. doi:10.1016/j.ctcp.2020.101259

Krawczyk, M., Liebe, R., and Lammert, F. (2020). Toward genetic prediction of nonalcoholic fatty liver disease trajectories: PNPLA3 and beyond. *Gastroenterology* 158 (7), 1865–1880. doi:10.1053/j.gastro.2020.01.053

Kubica, P., Szopa, A., Dominiak, J., Luczkiewicz, M., and Ekiert, H. (2020). Verbena officinalis (common vervain)–a review on the investigations of this medicinally important plant species. *Planta medica* 86 (17), 1241–1257. doi:10.1055/a-1232-5758

Kuo, N.-C., Huang, S.-Y., Yang, C.-Y., Shen, H.-H., and Lee, Y.-M. (2020). Involvement of HO-1 and autophagy in the protective effect of magnolol in hepatic steatosis-induced NLRP3 inflammasome activation *in vivo* and *in vitro*. *Antioxidants* 9 (10), 924. doi:10.3390/antiox9100924

Lee, H. A., Chang, Y., Sung, P. S., Yoon, E. L., Lee, H. W., Yoo, J.-J., et al. (2022). Therapeutic mechanisms and beneficial effects of non-antidiabetic drugs in chronic liver diseases. *Clin. Mol. Hepatology* 28 (3), 425–472. doi:10.3350/cmh.2022.0186

Li, F., Liu, B., Li, T., Wu, Q., Xu, Z., Gu, Y., et al. (2020). Review of constituents and biological activities of triterpene saponins from Glycyrrhizae Radix et Rhizoma and its solubilization characteristics. *Molecules* 25 (17), 3904. doi:10.3390/molecules25173904

Li, J., Ma, Z., Yang, Z., Yang, M., Li, C., Li, M., et al. (2024). Integrating transcriptomics and network pharmacology to reveal the mechanisms of total Rhizoma Coptidis alkaloids against nonalcoholic steatohepatitis. *J. Ethnopharmacol.* 322, 117600. doi:10.1016/j.jep.2023.117600

Lim, S., Kim, J.-W., and Targher, G. (2021). Links between metabolic syndrome and metabolic dysfunction-associated fatty liver disease. *Trends Endocrinol. Metabolism* 32 (7), 500–514. doi:10.1016/j.tem.2021.04.008

Liu, J., Zhang, Q., Li, R.-L., Wei, S.-J., Huang, C.-Y., Gao, Y.-X., et al. (2020). The traditional uses, phytochemistry, pharmacology and toxicology of Cinnamomi ramulus: a review. *J. Pharm. Pharmacol.* 72 (3), 319–342. doi:10.1111/jphp.13189

Lou, S. Y., Liu, Y., Ma, Y. Y., Chen, H. Y., Chen, W. H., Ying, J., et al. (2008). Effects of Yiqi Sanju Formula on non-alcoholic fatty liver disease: a randomized controlled trial. *Zhong Xi Yi Jie He Xue Bao* 6 (8), 793–798. doi:10.3736/jcim20080805

Lu, J., Li, W., Gao, T., Wang, S., Fu, C., and Wang, S. (2022). The association study of chemical compositions and their pharmacological effects of Cyperi Rhizoma (Xiangfu), a potential traditional Chinese medicine for treating depression. *J. Ethnopharmacol.* 287, 114962. doi:10.1016/j.jep.2021.114962

Luo, H., Wu, H., Yu, X., Zhang, X., Lu, Y., Fan, J., et al. (2019). A review of the phytochemistry and pharmacological activities of Magnoliae officinalis cortex. *J. Ethnopharmacol.* 236, 412–442. doi:10.1016/j.jep.2019.02.041

Makri, E. S., Makri, E., and Polyzos, S. A. (2022). Combination therapies for nonalcoholic fatty liver disease. *J. Personalized Med.* 12 (7), 1166. doi:10.3390/jpm12071166

Pang, H., Wu, L., Tang, Y., Zhou, G., Qu, C., and Duan, J.-A. (2016). Chemical analysis of the herbal medicine Salviae miltiorrhizae Radix et Rhizoma (Danshen). *Molecules* 21 (1), 51. doi:10.3390/molecules21010051

Paul, J. (2020). Recent advances in non-invasive diagnosis and medical management of non-alcoholic fatty liver disease in adult. *Egypt. Liver J.* 10 (1), 37. doi:10.1186/s43066-020-00043-x

Rahimi, V. B., Ajam, F., Rakhshandeh, H., and Askari, V. R. (2019). A pharmacological review on Portulaca oleracea L.: focusing on anti-inflammatory, anti- oxidant, immuno-modulatory and antitumor activities. *J. Pharmacopuncture* 22 (1), 7–15. doi:10.3831/KPI.2019.22.001

Riazi, K., Azhari, H., Charette, J. H., Underwood, F. E., King, J. A., Afshar, E. E., et al. (2022). The prevalence and incidence of NAFLD worldwide: a systematic review and meta-analysis. *lancet gastroenterology hepatology* 7, 851–861. doi:10.1016/S2468-1253(22)00165-0

Rinella, M. E., Neuschwander-Tetri, B. A., Siddiqui, M. S., Abdelmalek, M. F., Caldwell, S., Barb, D., et al. (2023). AASLD Practice Guidance on the clinical assessment and management of nonalcoholic fatty liver disease. *Hepatology* 77 (5), 1797–1835. doi:10.1097/HEP.0000000000000323

Rostamizadeh, P., Asl, S., Far, Z. G., Ahmadijoo, P., Mahmudiono, T., Bokov, D. O., et al. (2022). Effects of licorice root supplementation on liver enzymes, hepatic steatosis, metabolic and oxidative stress parameters in women with nonalcoholic fatty liver disease: a randomized double-blind clinical trial. *Phytother. Res.* 36 (10), 3949–3956. doi:10.1002/ptr.7543

Sanyal, A. J., Foucquier, J., Younossi, Z. M., Harrison, S. A., Newsome, P. N., Chan, W.-K., et al. (2023). Enhanced diagnosis of advanced fibrosis and cirrhosis in individuals with NAFLD using FibroScan-based Agile scores. *J. hepatology* 78 (2), 247–259. doi:10.1016/j.jhep.2022.10.034

Schwenzer, N. F., Springer, F., Schraml, C., Stefan, N., Machann, J., and Schick, F. (2009). Non-invasive assessment and quantification of liver steatosis by ultrasound, computed tomography and magnetic resonance. *J. hepatology* 51 (3), 433–445. doi:10.1016/j.jhep.2009.05.023

Segura-Azuara, N. Á., Varela-Chinchilla, C. D., and Trinidad-Calderón, P. A. (2022). MAFLD/NAFLD biopsy-free scoring systems for hepatic steatosis, NASH, and fibrosis diagnosis. *Front. Med.* 8, 774079. doi:10.3389/fmed.2021.774079

Singh, N., Yadav, S. S., Kumar, S., and Narashiman, B. (2022). Ethnopharmacological, phytochemical and clinical studies on Fenugreek (Trigonella foenum-graecum L.). *Food Biosci.* 46, 101546. doi:10.1016/j.fbio.2022.101546

Szanto, K. B., Li, J., Cordero, P., and Oben, J. A. (2019). Ethnic differences and heterogeneity in genetic and metabolic makeup contributing to nonalcoholic fatty liver disease. *Diabetes, metabolic syndrome Obes. targets Ther.* 12, 357–367. doi:10.2147/DMSO.S182331

Wang, F., Zhang, S., Zhang, J., and Yuan, F. (2022). Systematic review of ethnomedicine, phytochemistry, and pharmacology of Cyperi Rhizoma. *Front. Pharmacol.* 13, 965902. doi:10.3389/fphar.2022.965902

Wang, J., Wang, L., Lou, G.-H., Zeng, H.-R., Hu, J., Huang, Q.-W., et al. (2019). Coptidis Rhizoma: a comprehensive review of its traditional uses, botany, phytochemistry, pharmacology and toxicology. *Pharm. Biol.* 57 (1), 193–225. doi:10.1080/13880209.2019.1577466

Wang, X., Qin, Y., Li, G.-Q., Chen, S., Ma, J.-Q., Guo, Y.-L., et al. (2018). Study on chemical constituents in Polygoni Cuspidati folium and its preparation by UPLC-ESI-Q-TOF-MS/MS. *J. Chromatogr. Sci.* 56 (5), 425–435. doi:10.1093/chromsci/bmy017

Wong, V. W.-S., Ekstedt, M., Wong, G. L.-H., and Hagström, H. (2023). Changing epidemiology, global trends and implications for outcomes of NAFLD. *J. Hepatology* 79, 842–852. doi:10.1016/j.jhep.2023.04.036

Xue, Q., Wang, Y., Fei, C., Ren, C., Li, W., Li, W., et al. (2021). Profiling and analysis of multiple constituents in Crataegi Fructus before and after processing by ultrahigh-performance liquid chromatography quadrupole time-of-flight mass spectrometry. *Rapid Commun. Mass Spectrom.* 35 (7), e9033. doi:10.1002/rcm.9033

Yadav, U. C., and Baquer, N. Z. (2014). Pharmacological effects of Trigonella foenum-graecum L. in health and disease. *Pharm. Biol.* 52 (2), 243–254. doi:10.3109/13880209.2013.826247

Yang, F., Dong, X., Yin, X., Wang, W., You, L., and Ni, J. (2017). Radix Bupleuri: a review of traditional uses, botany, phytochemistry, pharmacology, and toxicology. *BioMed Res. Int.* 2017, 7597596. doi:10.1155/2017/7597596

Younossi, Z., Anstee, Q. M., Marietti, M., Hardy, T., Henry, L., Eslam, M., et al. (2018). Global burden of NAFLD and NASH: trends, predictions, risk factors and prevention. *Nat. Rev. Gastroenterology Hepatology* 15 (1), 11–20. doi:10.1038/nrgastro.2017.109

Younossi, Z. M., Corey, K. E., and Lim, J. K. (2021). AGA clinical practice update on lifestyle modification using diet and exercise to achieve weight loss in the management of nonalcoholic fatty liver disease: expert review. *Gastroenterology* 160 (3), 912–918. doi:10.1053/j.gastro.2020.11.051

Yu, Q., Zhang, S. S., Zhou, T., Xiong, Y., Zhao, L. Q., and Ding, Y. (2015). Treating non-alcoholic fatty liver disease patients of Gan stagnation Pi deficiency syndrome by tiaogan lidi recipe: a randomized controlled clinical trial. *Zhongguo Zhong Xi Yi Jie He Za Zhi* 35 (4), 401–405.

Zhang, W.-J., Zhao, Z.-Y., Chang, L.-K., Cao, Y., Wang, S., Kang, C.-Z., et al. (2021). Atractylodis Rhizoma: a review of its traditional uses, phytochemistry, pharmacology, toxicology and quality control. *J. Ethnopharmacol.* 266, 113415. doi:10.1016/j.jep.2020.113415

Zhou, Y.-X., Xin, H.-L., Rahman, K., Wang, S.-J., Peng, C., and Zhang, H. (2015). Portulaca oleracea L.: a review of phytochemistry and pharmacological effects. *BioMed Res. Int.* 2015, 925631. doi:10.1155/2015/925631

Zhu, R., Xu, X., Shan, Q., Wang, K., Cao, G., and Wu, X. (2020). Determination of differentiating markers in coicis semen from multi-sources based on structural similarity classification coupled with UPCC-Xevo G2-XS QTOF. *Front. Pharmacol.* 11, 549181. doi:10.3389/fphar.2020.549181

frontiers | Frontiers in Pharmacology

TYPE Original Research
PUBLISHED 12 April 2024
DOI 10.3389/fphar.2024.1363131

OPEN ACCESS

EDITED BY
Rongrui Wei,
Jiangxi University of Traditional Chinese Medicine, China

REVIEWED BY
Allah Nawaz,
Joslin Diabetes Center and Harvard Medical School, United States
Lili Sheng,
Shanghai University of Traditional Chinese Medicine, China
Beatriz Garcia Mendes,
Federal University of Santa Catarina, Brazil

*CORRESPONDENCE
Songtao Li,
lisongtao@zcmu.edu.cn
Xiaobing Dou,
xbdou77@163.com
Zhongyan Du,
duzhongyan@zcmu.edu.cn

†These authors have contributed equally to this work

RECEIVED 29 December 2023
ACCEPTED 03 April 2024
PUBLISHED 12 April 2024

CITATION
Chang K, Guo R, Hu W, Wang X, Cao F, Qiu J, Li J, Han Q, Du Z, Dou X and Li S (2024), Xie Zhuo Tiao Zhi formula ameliorates chronic alcohol-induced liver injury in mice. *Front. Pharmacol.* 15:1363131. doi: 10.3389/fphar.2024.1363131

Xie Zhuo Tiao Zhi formula ameliorates chronic alcohol-induced liver injury in mice

Kaixin Chang[1†], Rui Guo[2†], Wenbo Hu[3†], Xuezhu Wang[2], Feiwei Cao[2], Jiannan Qiu[1], Jiaomei Li[2], Qiang Han[2], Zhongyan Du[4*], Xiaobing Dou[1*] and Songtao Li[2*]

[1]School of Life Science, Zhejiang Chinese Medical University, Hangzhou, China, [2]School of Public Health, Zhejiang Chinese Medical University, Hangzhou, China, [3]The First School of Clinical Medicine, Zhejiang Chinese Medical University, Hangzhou, China, [4]Key Laboratory of Blood-Stasis-Toxin Syndrome of Zhejiang Province, Zhejiang Engineering Research Center for 'Preventive Treatment' Smart Health of Traditional Chinese Medicine, School of Basic Medical Sciences, Zhejiang Chinese Medical University, Hangzhou, China

This study aimed to evaluate the protective role and potential mechanisms of Xie Zhuo Tiao Zhi decoction (XZTZ) on alcohol-associated liver disease (ALD). XZTZ significantly alleviated alcohol-induced liver dysfunction, based on histological examinations and biochemical parameters after 4-week administration. Mechanically, alcohol-stimulated hepatic oxidative stress was ameliorated by XZTZ, accompanied by the improvement of Nrf2/Keap1 expression and alcohol-activated phosphorylation of pro-inflammatory transcription factors, including JNK, P38, P65, and IκBα, were rescued by XZTZ. In conclusion, XZTZ demonstrates potential in alleviating alcohol-induced liver injury, oxidative stress, and inflammation possibly through modulation of Nrf2/Keap1 and MAPKs/NF-κB signaling pathways, suggesting its potential as a therapeutic option for patients with alcoholic liver disease.

KEYWORDS

Xie Zhuo Tiao Zhi decoction, alcohol-associated liver disease, liver injury, oxidative stress, liver inflammation

1 Introduction

The widespread consumption of alcohol has led to a significant health burden in the form of alcohol-associated liver disease (ALD), impacting a large number of individuals globally (Patel and Flamm, 2023). ALD encompasses a range of metabolic disturbances, from reversible hepatic steatosis to various forms of liver damage such as irreversible alcoholic hepatitis, decompensated cirrhosis, and hepatocellular carcinoma (Dukic et al., 2023). Research indicates that alcohol intake contributes to hepatic oxidative stress, exacerbates liver inflammation, and heightens susceptibility to liver injury in male individuals who consume alcohol (Noonberg et al., 1985).

Despite the development of numerous contemporary pharmaceutical interventions for the prevention and treatment of alcohol-induced liver injury, ALD remains a significant public health concern, primarily attributable to its constrained effectiveness and adverse reactions. To date, minimal progress has been made in the therapeutic approaches for ALD, with abstinence from alcohol being the primary recommended strategy. Consequently, there is an urgent requirement for innovative and more efficacious management strategies.

TABLE 1 The herbs of The Xie Zhuo Tiao Zhi decoction.

Chinese name	Latin name	Medicinal part	Production methods	Place of origin	Batch number	Percentage (%)
Zexie	*Alisma orientale* (Sam.) Juzep	Rhizome	Dried	Sichuan Province	20230601	22.3
Baizhu	*Atractylodes macrocephala* Koidz	Rhizome	Dried	Zhejiang Province	20230401	18.5
Fuling	*Poria cocos* (Schw.)Wolf	Thizome	Dried	Anhui Province	20230801	18.5
Zhiqiao	*Citrus* × *aurantium* Engl	Fuit rind	Dried	Jiangxi Province	20220909	7.4
Shanzha	*Crataegus pinnatifida* Bunge	Fruit	Dried	Shandong Province	20230101	18.5
Heye	*Nelumbo nucifera* Gaertn	Leafs	Dried	Zhejiang Province	20230401	14.8

The traditional herbal formula, rooted in the long history of Chinese medicine and characterized by diverse theories and practices, has been utilized in clinical settings for millennia. Traditional Chinese medicines, particularly compound medicines (known as prescriptions or Fu Fangs in Chinese), have garnered significant global interest for their superior efficacy and safety profiles in the prevention and treatment of various diseases (Cheung, 2011). Current research indicates a growing interest in utilizing traditional herbal formulae as novel therapeutic approaches for treating ALD due to their efficacy, minimal adverse effects, and cost-effectiveness (Chen et al., 2010; Mo et al., 2020; Fang et al., 2023). Among these formulae, maintaining the equilibrium of Yin and Yang is considered a fundamental strategy for restoring health. In contemporary medical terminology, the concept of Yin and Yang can be interpreted as the equilibrium between antioxidants and oxidants (Ou et al., 2003; Szeto and Benzie, 2006).

The Xie Zhuo Tiao Zhi decoction (XZTZ), composed of six herbs: *Shanzha, Heye, Zhiqiao, Baizhu, Fuling*, and *Zexie*, is a modified formulation of Zexie Decoction from the "Golden Chamber • Phlegm and Cough Disease". Notably, in the Traditional Chinese Medicine Pharmacy of Zhejiang Provincial Hospital of Traditional Chinese Medicine, the XZTZ has been often used in the therapy of metabolic disorders, such as obesity, hyperlipidemia, non-alcoholic fatty liver disease, and other diseases, with the principle of "simultaneously treating symptoms and root causes", "overall adjustment", and the advantages of six herbal interactions. Nevertheless, while the pharmacological properties of XZTZ are known, there is a lack of scientific evidence regarding its hepato-protective effects on alcohol-induced liver injury. Thus, the objective of our study was to examine the hepato-protective properties of XZTZ and its potential mechanisms of action in the ALD mice model. This investigation has the potential to offer valuable insights for the prevention and treatment of alcohol-induced liver injury.

2 Materials and methods

2.1 Drugs and reagents

XZTZ consists of six traditional Chinese medicines, including Shan zha as *Crataegus pinnatifida Bunge [Rosaceae; Crataegi fructus]*, He ye as *Nelumbo nucifera Gaertn. [Nelumbonaceae; Nelumbinis folium]*, Zhi qiao as *Citrus* × *aurantium Engl [Rutaceae; Aurantii fructus]*, Bai zhu as *Atractylodes macrocephala Koidz. [Compositae; Atractylodis macrocephalae rhizoma]*, Fu ling as *Poria cocos (Schw) Wolf [Polyporaceae; Poria]*, Ze xie as *Alisma orientale (Sam.) Juzep. [Alismataceae; Alismatis rhozoma]*. The original botanical drugs were purchased from Traditional Chinese Medicine Pharmacy of Zhejiang Provincial Hospital of Traditional Chinese Medicine. The details of the specific metabolites and contents of the XZTZ dosage are shown in Table 1. The herbs in the XZTZ were soaked in 10 times the amount of distilled water for 1 h, and then extracted by reflux for 3 times. The extract was concentrated to the relative density of 1.05, dried under 60°C, lyophilized into dry powder, and the lyophilized powder was used for subsequent experiments (1 g of lyophilized powder is equal to 12.05 g original herb). Then, it was diluted with normal saline to achieve two concentrations, including 291.2 mg/kg (low dose, XZTZ-L) and 582.4 mg/kg (high dose, XZTZ-H), based on the body surface area of adults (Standard weight 70 kg). Commencing in the second week of the modeling process, the mice were subjected to daily oral gavage administration of XZTZ at the prescribed dosages for a period of 3 weeks. In a previous study by our group, the analysis of the main metabolites of XZTZ using High Performance Liquid Chromatography revealed the following six metabolites in the extract of XZTZ: mannitol (1.23 min) from Shan zha, citric acid (1.7 min) from Shan zha and He ye, quercetin 3-O-β-D-glucuronopyranoside (16.90 min) from He ye, naringin (19.33 min) from Zhi qiao, hesperidin (20.94 min) from Zhi qiao, and alisol A (32.24 min) from Ze xie (Qiu et al., 2023). The chemical composition of the drug in XZTZ complies with the ConPhyMP statement and has been validated for classification at "http://www.plantsoftheworldonline.org".

Kits for testing the levels of ALT, AST, MDA, SOD, CAT, and GSH-Px were purchased from Nanjing Jiancheng Bioengineering Institute (Nanjing, China). The BCA kit was purchased from the Beyotime Institute of Biotechnology (Jiangsu, China).

2.2 Animal experiments

The traditional Lieber-DeCarli alcohol liquid diet and an isocaloric control diet were purchased from Trophic Animal Feed High-tech Co., Ltd (Nantong, China). Twenty male C57BL/6J mice (8 weeks old, 21.00 ± 1.00 g) were provided by the Animal

TABLE 2 The Growth parameters of mice.

	PF	AF	AF + XZTZ-L	AF + XZTZ-H
Body weight g)	26.21 ± 0.70	23.56 ± 1.13[a]	24.70 ± 0.77[a]	25.35 ± 0.50[b]
Liver weight g)	0.99 ± 0.06	1.10 ± 0.04[a]	1.07 ± 0.11	1.04 ± 0.03[b]
Liver/body weight ratio	0.038 ± 0.002	0.047 ± 0.002[a]	0.043 ± 0.004	0.041 ± 0.002[b]

Data are expressed as mean ± SD.
[a]$p < 0.05$ vs. PF.
[b]$p < 0.05$ vs. AF.

Experiment Center of Zhejiang Chinese Medical University. Animal experiments were reviewed by the Laboratory Animal Management and Ethics Committee (approval number: IACUC-20220321-08). Mice were housed in an environment of 55% ± 5% relative humidity with 23°C ± 2°C and 12 h of light-dark cycle (lights on at 7:30 a.m.). To acclimate the mice, they were continuously free access to regular food and water for 3 days following their acquisition. After 3-day of acclimatization, mice were randomly assigned to four groups for 4 weeks of intervention: a) PF group, fed Lieber-DeCarli liquid diets containing isocaloric maltose dextrin; b) AF group, fed alcohol-containing modified Lieber-DeCarli liquid diets; c) AF with XZTZ-L (AF + XZTZ-L) group; d) AF with XZTZ-H (AF + XZTZ-H) group. After 12 h of fasting, mice were anesthetized with pentobarbital solution (80 mg/kg body weight (Guo et al., 2023)) and euthanized. Blood samples were collected and stored at −80°C until being assayed. Liver tissue was rapidly excised, weighed, and stored at −80°C for further analysis. The Growth parameters of mice among four groups are shown in Table 2.

2.3 Histological examination

The liver was fixed in a 4% buffered paraformaldehyde (Biosharp Biotechnology, Shanghai, China) for 24 h. Then it was embedded with an optimum cutting temperature embedding agent and sliced on a cryostat. The 4 μm thick liver sections were stained with H&E.

2.4 Immunohistochemistry analysis

The myeloperoxidase (MPO) staining (equivalent to monocytes and neutrophils), the 4 μm thick liver sections were de-paraffinized, and re-hydrated in descending grades of alcohol, followed by heat mediated antigen retrieval procedure. According to the manufacturer's instruction, sections were incubated in BloxALL solution (Vector Laboratories, Burlingame, CA, United States) to block endogenous peroxidase activity. Then, sections were incubated with anti-MPO antibody (Servicebio, Wuhan, GB12224) overnight at 4°C in a humidified chamber. The secondary antibody was HRP-labeled goat anti-mouse antibodies (Servicebio, Wuhan, G23301) and the DAB chromogenic agent kit (Servicebio, Wuhan, GB12224) was used for histochemical chromography. The MPO staining was evaluated with a light fluorescence microscope at a 20-fold magnification. Three slides were randomly selected for each tissue, and the MPO-positive cells were quantifed by ImageJ software.

2.5 IQuantitative real-time polymerase chain reaction (qRT-PCR)

Total RNA was extracted from mice livers using TRIzol reagent (Invitrogen, UK), based on the manufacturer's protocol. qRT-PCR was performed with the SYBR Green PCR Master Mix (Applied Biosystems, Foster City, CA, United States). Genes levels were normalized to that of 18S and were calculated by the $2^{-\Delta\Delta CT}$ method. All primers were synthesized by Sangon Biotech Co., Ltd. (Shanghai, China). The sequences of all primers used in this study are listed in Table 3.

2.6 Western blot

Protein concentrations of mice livers were detected using BCA protein assay kits. Samples (approximately 20 μg) were separated by sodium dodecyl sulfate polyacrylamide gel electrophoresis and transferred to polyvinylidene fluoride membranes. The primary antibodies were used as follows: cleaved-Caspase3 (Cell Signaling Techonology, Cat. No. 9664S, rabbit monoclonal, 1:1000), Bcl-2 (Santa Cruz, Cat. No. sc-7382, mouse monoclonal, 1:500), CYP2E1 (Abcam, Cat. No. ab28146, rabbit polyclonal, 1:5000), Nrf2 (Cell Signaling Techonology, Cat. No. 12721S, rabbit monoclonal, 1:1000), Keap1 (Abcam, Cat. No. ab227828, rabbit polyclonal, 1:2000), p-JNK (Cell Signaling Techonology, Cat. No. 9255S, mouse monoclonal, 1:1000), JNK (Cell Signaling Techonology, Cat. No. 9252S, rabbit monoclonal, 1:1000), p-P38 (Cell Signaling Techonology, Cat. No. 4511S, rabbit monoclonal, 1:1000), P38 (Cell Signaling Techonology, Cat. No. 8690S, rabbit monoclonal, 1:1000), p-P65 (Cell Signaling Techonology, Cat. No. 3033S, rabbit monoclonal, 1:1000), P65 (Cell Signaling Techonology, Cat. No. 8242S, rabbit monoclonal, 1:1000), p-IκBα (Cell Signaling Techonology, Cat. No. 2859S, rabbit monoclonal, 1:1000), IκBα (Cell Signaling Techonology, Cat. No. 4814S, mouse monoclonal, 1:1000), LaminB (Cell Signaling Techonology, Cat. No. 17416S, rabbit monoclonal, 1:1000), and β-Actin (Santa Cruz, Cat. No. sc-4778, mouse monoclonal, 1:5000). β-Actin and LaminB were used as the internal control. The secondary antibodies were anti-rabbit (Boster Biological Technology, ba1054, 1:5000) and anti-mouse (Boster Biological Technology, ba1050, 1:5000). Moreover, a nuclear extraction kit (KeyGEN BioTECH, KGP1100) was used for Nrf2 protein. Bands were quantified by the ImageJ software.

2.7 Statistics

All data were expressed as the mean ± SD. Statistical analysis was performed using unpaired Student's t-test with GraphPad Prism

TABLE 3 The sequences of all primers.

Target genes	Forward primer (5′to 3′)	Reverse primer (5′to 3′)
18S	GAATGGGGTTCAACGGGTTA	AGGTCTGTGATGCCCTTAGA
HO-1	AAGCCGAGAATGCTGAGTTCA	GCCGTGTAGATATGGTACAAGGA
GCLC	GGGGTGACGAGGTGGAGTA	GTTGGGGTTTGTCCTCTCCC
GPX-1	AGTCCACCGTGTATGCCTTT	GAGACGCGACATTCTCAATGA
TNFA	CCCAGGGACCTCTCTCTAATCA	GCTACAGGCTTGTCACTCGG
IL-6	GATGCTACCAAACTGGATATAATC	GGTCCTTAGCCACTCCTTCTGTG
IL-1B	TGGGATAGGGCCTCTCTTGC	CCATGGAATCCGTGTCTTCCT
MCP-1	AAAACACGGGACGAGAAACCC	ACGGGAACCTTTATTAACCCCT

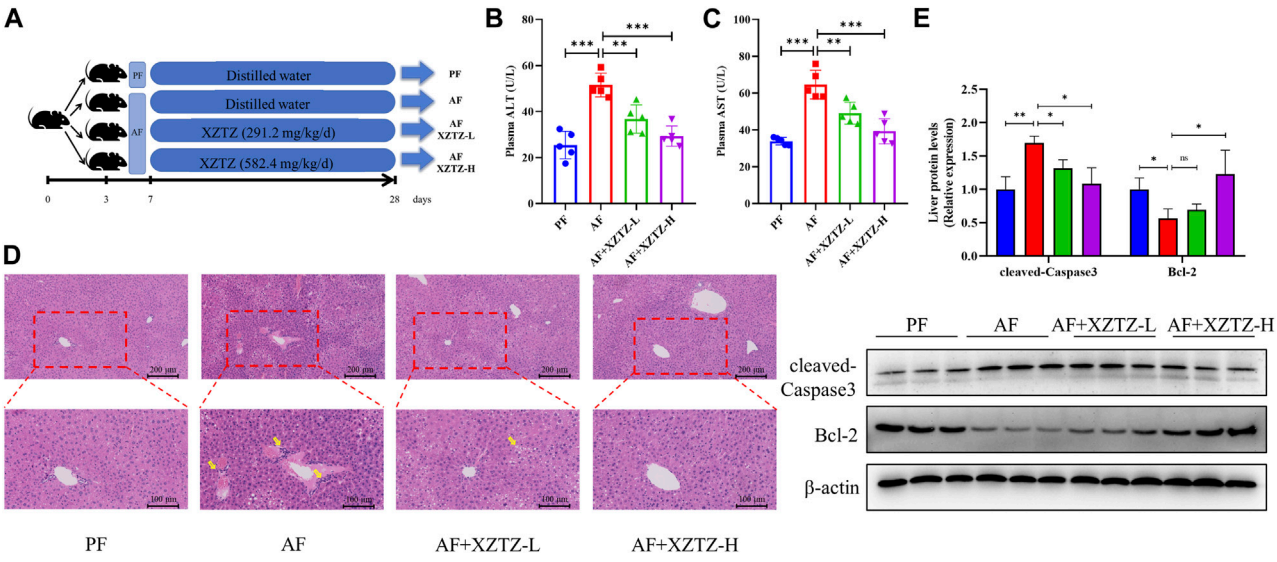

FIGURE 1
The XZTZ rescues alcohol-induced liver injury in C57BL/6J mice. **(A)** The experimental design graphic; **(B, C)** Serum levels of ALT and AST; **(D)** H&E stained sections of the liver (×200 and ×400); **(E)** Western blot verifying the effects of XZTZ on expression of cleaved-Caspase3 and Bcl-2 with alcohol treatment. ns, not significant; *$p < 0.05$, **$p < 0.01$ and ***$p < 0.001$ indicate statistically significant differences.

8.02 software (GraphPad Software, San Diego, CA). The p-value <0.05 was statistically significant.

3 Results

3.1 The XZTZ rescues alcohol-induced liver injury in C57BL/6J mice

In our study, we developed a mouse alcohol-induced liver injury model to evaluate potential recuperative effect of the XZTZ treatment (Figure 1A, Supplementary Figure S1). The increased activities of serum ALT and AST are gold indicators of liver injury. As shown in Figures 1B,C, the activities of serum ALT and AST in the AF group were obviously increased by 2.03-fold and 1.91-fold compared with that in the PF group. The elevations of ALT and AST induced by alcohol were effectively inhibited by the XZTZ, accompanied by a dose-response relationship. We also observed the hepatic pathophysiological changes by H&E staining, and found that XZTZ significantly alleviated alcohol-induced liver injury (Figure 1D). In addition, the elevated hepatic protein level of cleaved-Caspase3 and the decreased hepatic protein level of Bcl-2 induced by alcohol was rescued by the XZTZ (Figure 1E).

3.2 The XZTZ alleviates alcohol-induced hepatic oxidative stress in C57BL/6J mice

Oxidative stress is an essential pathological mechanism of alcohol-induced liver injury. Hence, we measured the levels of oxidative stress products and the activities of antioxidant enzymes in alcohol-fed mice livers. As shown in Figure 2A, the hepatic level of MDA was increased in the AF group compared with that in the PF group, while the intervention of the XZTZ

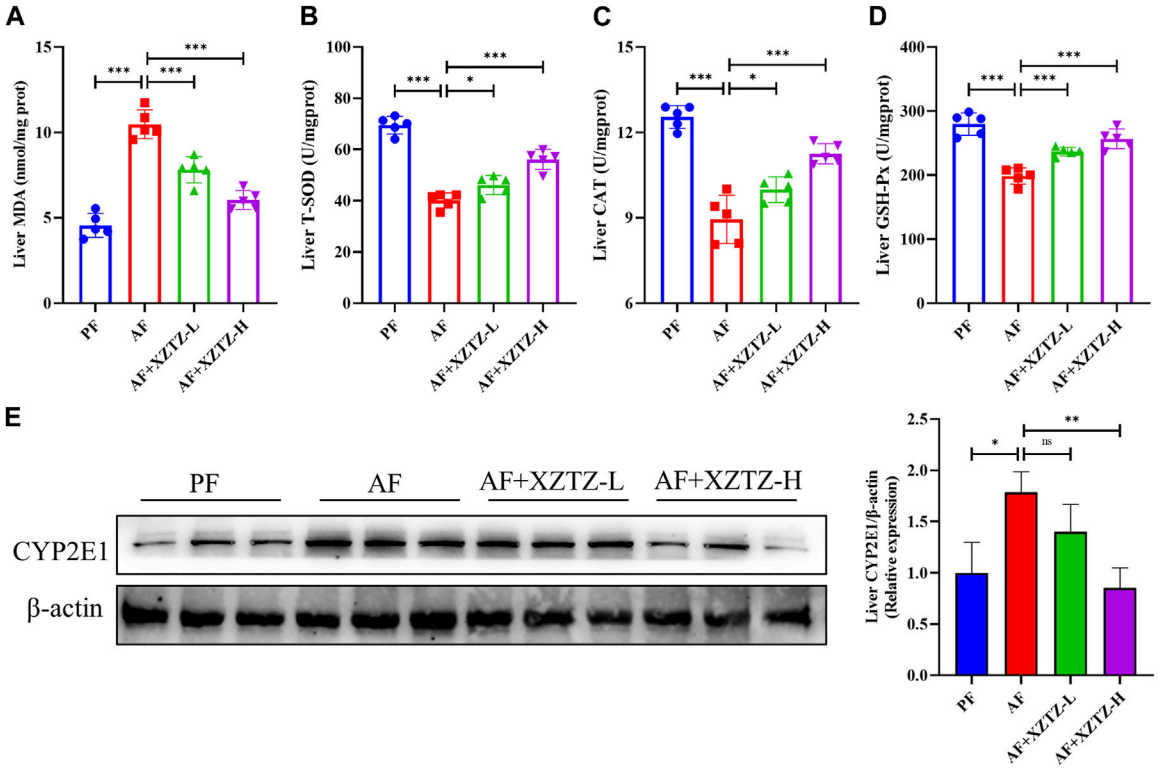

FIGURE 2
The XZTZ alleviates alcohol-induced hepatic oxidative stress in C57BL/6J mice. **(A)** The level of MDA in mice livers; **(B–D)** The activities of SOD, CAT, and GSH-Px in mice livers; **(E)** The protein level of CYP2E1 in the liver of mice. ns, not significant; *$p < 0.05$, **$p < 0.01$ and ***$p < 0.001$ indicate statistically significant differences.

significantly reversed the MDA increase induced by alcohol. Also, the activities of SOD, CAT, and GSH-Px were disrupted by alcohol, while the intervention of the XZTZ clearly rescued the activities of the above antioxidant enzymes (Figures 2B–D). Furthermore, CYP2E1 was analyzed in mice model induced by alcohol. Compared with that in the PF group, the expression of CYP2E1 in the liver tissue of mice was significantly increased in the AF group, while the XZTZ treatment decreased its expression (Figure 2E).

3.3 The XZTZ inhibits hepatic oxidative stress via activating Nrf2-Keap1 pathway

To further discover the molecular mechanism of the XZTZ on inhibiting oxidative stress, the nuclear protein level of Nrf2 and the total protein level of Keap1 were measured by Western blot. As shown in Figure 3A, compared with the PF group, the hepatic protein level of nuclear-Nrf2 was decreased and the hepatic protein level of Keap1 was increased in the AF group, whereas the levels of Nrf2 and Keap1 were obviously reversed by the XZTZ pretreatment. Moreover, we measured the gene expression levels of *HO-1*, *GCLC*, and *GPX-1* by qRT-PCR in mice livers. The result showed that the XZTZ groups had significantly increased *HO-1*, *GCLC*, and *GPX-1* mRNA expressions compared with the AF group (Figure 3B).

3.4 The XZTZ improves alcohol-induced liver inflammation in C57BL/6J mice

The inflammation is also a critical pathological process of alcohol-induced liver injury. The MPO staining in our study was performed to visualize monocytes and neutrophils in the different groups. As shown in Figure 4A, there was a robust increase of MPO-positive cells in the AF group compared to other groups, while MPO-positive cells in XZTZ groups were significantly increased compared to the PF group. Additionally, pro-inflammatory cytokines including *TNFA*, *IL-6*, *IL-1B*, and *MCP-1* in mice livers were significantly increased in the AF group, while the XZTZ supplementation reduced their expressions (Figure 4B).

3.5 The XZTZ eases hepatic inflammatory response via MAPKs/NF-kB pathways

To further explore the molecular mechanism of the XZTZ on alleviating inflammatory response, the expression of proteins involved in MAPKs and NF-κB pathways was measured by Western blot. As shown in Figure 5A, the XZTZ pretreatment significantly reduced alcohol-stimulated both JNK and P38 phosphorylation in a dose-dependent manner. Furthermore, the ratios of p-P65/P65 and p-IκBα/IκBα also decreased clearly after pretreatment with the XZTZ (Figure 5B).

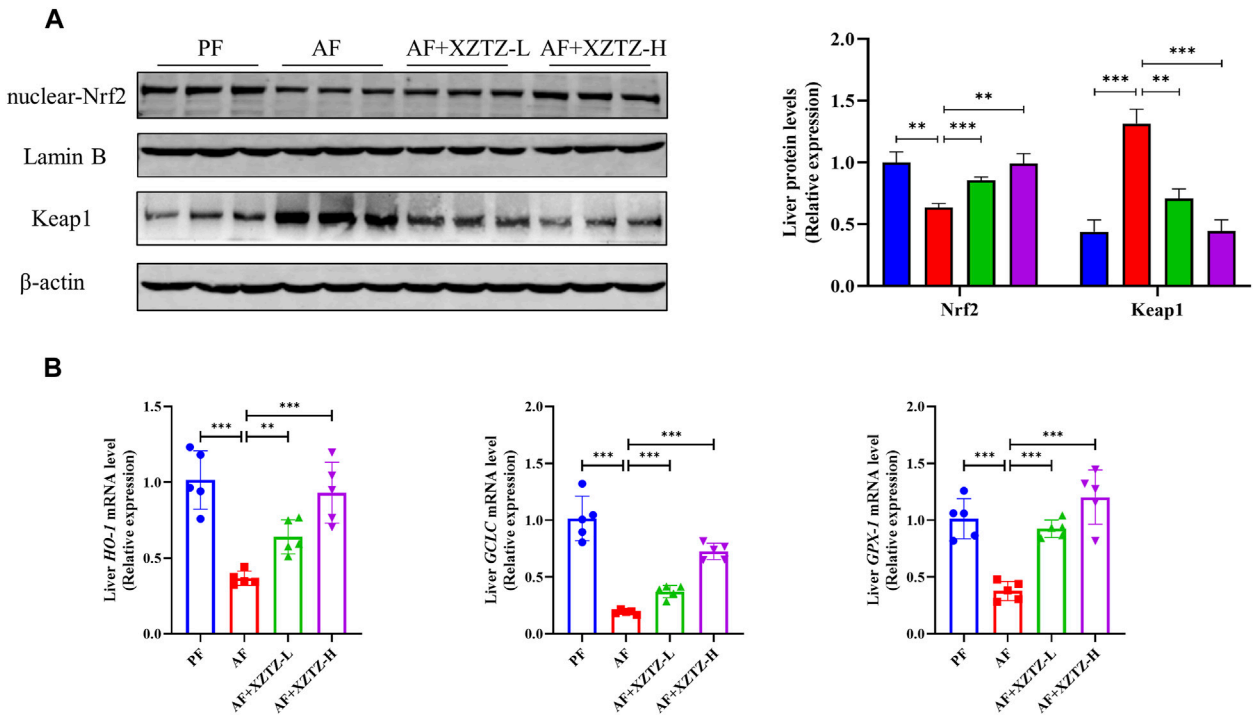

FIGURE 3
The XZTZ inhibits hepatic oxidative stress via activating the Nrf2-Keap1 pathway. **(A)** Western blot verifying the nuclear protein level of Nrf2 and the total protein level of Keap1. LaminB is used as an internal control for nuclear protein and β-actin is used as an internal control for total protein; **(B)** qRT-PCR verifying the expression levels of *HO-1*, *GCLC*, and *GPX-1* mRNAs. ns, not significant; *$p < 0.05$, **$p < 0.01$ and ***$p < 0.001$ indicate statistically significant differences.

4 Discussion

Alcohol consumption is a major global issue for liver damage, with a growing focus on research into preventing and treating alcohol-related liver injury using Chinese herbal medicines (Chen et al., 2010; Feng et al., 2019; Foghis et al., 2023). This study presents the initial evidence that XZTZ, a modified version of the historic prescription 'Golden Chamber • Phlegm and Cough Disease', alleviated alcohol-induced liver injury, oxidative stress in the liver, and liver inflammation in C57BL/6J mice in a dose-dependent manner (Figure 6). Using a well-established mice model of ALD, we demonstrated the positive effect of XZTZ in rescuing alcohol-induced liver injury. This was evidenced by decreased ALT and AST activities, reduced hepatic cleaved-Caspase3 expression, elevated hepatic Bcl-2 expression, and H&E staining results (Figure 1). XZTZ also reduced the liver index and aided in the recovery of body weight *in vivo* (Table2).

The contribution of hepatic oxidative stress and liver inflammation to alcohol-induced liver injury is well recognized in the scientific community (Yang et al., 2022; Ding et al., 2023). Many of the herbs in XZTZ exhibit strong antioxidant and anti-inflammatory properties. For instance, *Shanzha* and *Fuling* have demonstrated potential in preventing ALD (Martinez-Rodriguez et al., 2019; Jiang et al., 2022), while *Heye*, *Zhiqiao*, and *Baizhu* have shown protective effects against liver injury by modulating oxidative stress and inflammation levels *in vivo* (Liu et al., 2019; Wu et al., 2020; Guo et al., 2021). The fingerprint analysis of XZTZ has identified six principal compounds: naringin, neo-hesperidin, Atractylenolide III, 23-o-Acetylalisol B, pachymic acid, and ursolic acid. Extensive literature supports the diverse bioactivities and health benefits associated with these compounds, including antioxidant, anti-inflammatory, and hepatoprotective effects (Qiu et al., 2023). MDA, an aldehyde formed during free radical-induced lipid peroxidation, serves as a marker for assessing lipid peroxidation and oxidative stress in the body (Zheng et al., 2019; Yamada et al., 2020). CAT, an essential oxidoreductase, plays a crucial role in breaking down hydrogen peroxide into oxygen and water, thereby safeguarding cells from oxidative stress (Zhao et al., 2019). Our study establishes the hypothesis that the compound medicine XZTZ may offer hepatoprotective effects against ALD by mitigating hepatic oxidative stress and inflammation. Indeed, in our study, ALD mice exhibited elevated MDA levels and reduced activities of SOD, CAT, and GSH-Px, along with decreased CYP2E1 levels in the liver, all of which were reversed upon treatment with XZTZ (Figure 2).

Nrf2, a crucial stress-activated transcription regulator, has been shown to trigger a defense mechanism against hepatic oxidative stress damage. The activation of Nrf2 is typically inhibited by its negative regulator Keap1, but can detach from Keap1 and move into the nucleus during oxidative stress conditions (Jayasuriya et al., 2021). Activation of the Nrf2-Keap1 signaling pathway is a well-established method for reducing oxidative stress-induced liver damage (Choi et al., 2023). Furthermore, in stressful environments, the Nrf2-Keap1 pathway can bind to antioxidant response elements and activate downstream genes like *HO-1*, *GCLC*, and *GPX-1*. The study depicted in Figure 3 demonstrates that pretreatment with XZTZ led to an increase in nuclear Nrf2 protein levels, a decrease in Keap1 protein levels, and

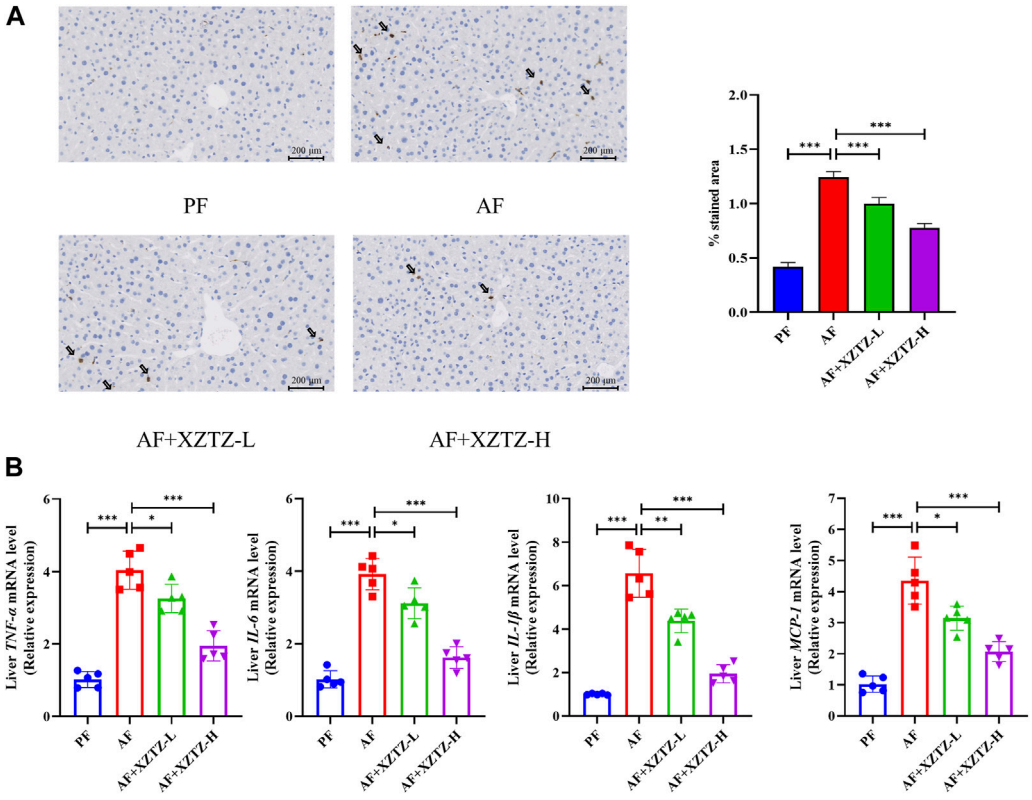

FIGURE 4
The XZTZ improves alcohol-induced liver inflammation in C57BL/6J mice. **(A)** Representative stainings of MPO-positive cells in mice livers. Scale bars: 200μM; **(B)** Gene expression levels of hepatic *TNFA, IL-6, IL-1B*, and *MCP-1*. *$p < 0.05$, **$p < 0.01$ and ***$p < 0.001$ indicate statistically significant differences.

an upregulation of downstream genes *HO-1*, *GCLC*, and *GPX-1* in the livers of mice. This suggests that XZTZ may mitigate alcohol-induced hepatic oxidative stress through the Nrf2/Keap1-dependent antioxidant system.

Alcohol-induced acute liver injury triggers the expression of proinflammatory factors like *IL-1B, IL-6*, and *TNFA*, exacerbating organ damage, particularly hepatocyte injury, leading to liver damage (Effenberger et al., 2023). This inflammatory response is recognized as a fundamental mechanism of alcohol-induced liver injury (Wang et al., 2021). Additionally, NF-κB stimulates the production of various proinflammatory factors that play crucial roles in liver pathology (Nowak and Relja, 2020). Alcohol-induced hepatotoxicity can cause the nuclear translocation of NF-κB (p65), leading to the transcription of inflammatory genes such as *IL-1B*, *IL-6*, and *TNFA* (Ghare et al., 2023). MPO staining revealed a significant reduction in MPO-positive cells in the XZTZ groups compared to the AF group. Moreover, XZTZ pretreatment notably decreased the high levels of pro-inflammatory cytokines induced by alcohol in the liver, including *TNFA, IL-6, IL-1B*, and MCP-1, indicating that XZTZ could ameliorate alcohol-induced liver inflammation (Figure 4).

Mechanistically, XZTZ significantly decreased alcohol-induced JNK and p38 phosphorylation in mouse livers (Figure 5A), associated with the MAPKs pathway (Kim and Choi, 2015). Furthermore, XZTZ reduced the ratios of p-P65/P65 and p-IκBα/IκBα, linked to the NF-κB pathway (Lawrence, 2009), in the livers of ALD mice models. In conclusion, XZTZ appears to alleviate alcohol-induced liver inflammation through the MAPKs- and NF-κB-dependent anti-inflammatory mechanisms.

This study is limited by the use of only the classic Lieber-Decarli model to simulate human alcoholic liver disease, which may not fully represent the complexity of the disease. The modified model used is more suitable for studying the early stages of alcoholic liver disease, but further investigation is required to determine the effectiveness of XZTZ in treating late-stage alcoholic liver disease. Additionally, the study did not conduct reverse verification, and the exact mechanism by which XZTZ improves alcoholic liver disease remains unclear, requiring further research. The XZTZ compound used in the experiment contains active ingredients from multiple traditional Chinese medicines, prompting the need to identify the specific ingredients responsible for improving ALD in future research.

5 Conclusion

Our research presents evidence suggesting that XZTZ significantly influences alcohol-induced liver injury by mitigating hepatic oxidative stress and decreasing liver inflammation. The antioxidant characteristics of XZTZ could be linked to the Nrf2-Keap1 axis, while its anti-inflammatory properties might be regulated by the MAPKs/NF-κB pathways. These results enhance

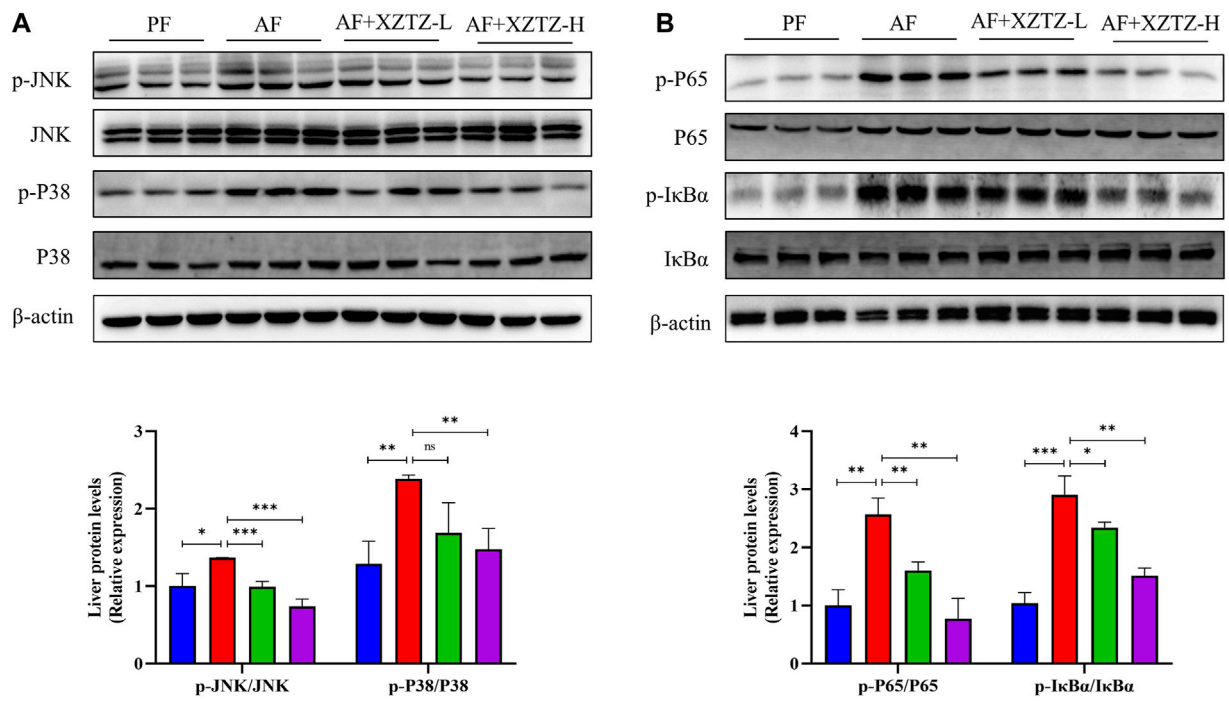

FIGURE 5
The XZTZ eases hepatic inflammatory response via MAPKs/NF-kB pathways. **(A)** The expression of hepatic p-JNK/JNK and p-P38/P38; **(B)** The expression of hepatic p-P65/P65 and p-IκBα/IκBα. ns, not significant; *$p < 0.05$ and **$p < 0.01$ indicate statistically significant differences.

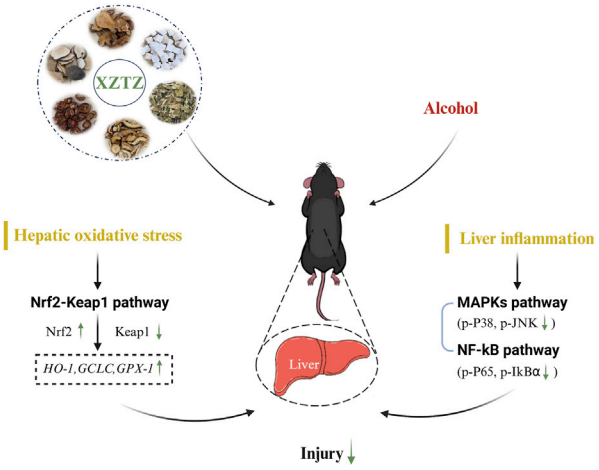

FIGURE 6
Schematic diagram of our study.

our comprehension of the therapeutic potential of XZTZ in managing alcohol-induced liver injury within the context of traditional Chinese medicine formulations.

Data availability statement

The original contributions presented in the study are included in the article/Supplementary Material, further inquiries can be directed to the corresponding authors.

Ethics statement

The animal study was approved by the Laboratory Animal Management and Ethics Committee of the Animal Experiment Center of Zhejiang Chinese Medical University. The study was conducted in accordance with the local legislation and institutional requirements.

Author contributions

KC: Data curation, Formal Analysis, Writing–original draft. RG: Data curation, Methodology, Writing–original draft. WH: Data curation, Methodology, Writing–original draft. XW: Data curation, Investigation, Writing–original draft. FC: Data curation, Investigation, Writing–original draft. JQ: Data curation, Investigation, Writing–original draft. JL: Data curation, Investigation, Writing–original draft. QH: Data curation, Investigation, Writing–original draft. ZD: Conceptualization, Writing–review and editing. XD: Conceptualization, Writing–review and editing. SL: Conceptualization, Writing–review and editing.

Funding

The author(s) declare that financial support was received for the research, authorship, and/or publication of this article. This work was supported by the Natural Science Foundation of China (82004353, 82273625), Zhejiang Natural Science Foundation (LQ20H290005), the Special Support Program for High Level Talents in Zhejiang Province (ZJWR0308092), the Research Project of Zhejiang Chinese Medical University (2023JKZKTS11, 2022RCZXZK20), and Zhejiang Provincial

Science and Technology Innovation Program (New Young Talent Program) for College Students (2022R410A004).

Acknowledgments

The authors appreciate the technical support from the public platform of the Medical Research Center, Academy of Chinese Medical Science, Zhejiang Chinese Medical University.

Conflict of interest

The authors declare that the research was conducted in the absence of any commercial or financial relationships that could be construed as a potential conflict of interest.

Publisher's note

Supplementary material

The Supplementary Material for this article can be found online at: https://www.frontiersin.org/articles/10.3389/fphar.2024.1363131/full#supplementary-material

References

Chen, M. L., Tsai, S. H., Ip, S. P., Ko, K. M., and Che, C. T. (2010). Long-term treatment with a "Yang-invigorating" Chinese herbal formula, Wu-Zi-Yan-Zong-Wan, reduces mortality and liver oxidative damage in chronic alcohol-intoxicated rats. *Rejuvenation Res.* 13 (4), 459–467. doi:10.1089/rej.2009.0985

Cheung, F. (2011). TCM: made in China. *Nature* 480 (7378), S82–S83. doi:10.1038/480S82a

Choi, E. J., Kim, H., Hong, K. B., Suh, H. J., and Ahn, Y. (2023). Hangover-relieving effect of ginseng berry kombucha fermented by *Saccharomyces cerevisiae* and gluconobacter oxydans in ethanol-treated cells and mice model. *Antioxidants (Basel)* 12 (3), 774. doi:10.3390/antiox12030774

Devarbhavi, H., Asrani, S. K., Arab, J. P., Nartey, Y. A., Pose, E., and Kamath, P. S. (2023). Global burden of liver disease: 2023 update. *J. Hepatol.* 79 (2), 516–537. doi:10.1016/j.jhep.2023.03.017

Ding, Q., Pi, A., Hao, L., Xu, T., Zhu, Q., Shu, L., et al. (2023). Genistein protects against acetaldehyde-induced oxidative stress and hepatocyte injury in chronic alcohol-fed mice. *J. Agric. Food Chem.* 71 (4), 1930–1943. doi:10.1021/acs.jafc.2c05747

Dukic, M., Radonjic, T., Jovanovic, I., Zdravkovic, M., Todorovic, Z., Kraisnik, N., et al. (2023). Alcohol, inflammation, and microbiota in alcoholic liver disease. *Int. J. Mol. Sci.* 24 (4), 3735. doi:10.3390/ijms24043735

Effenberger, M., Widjaja, A. A., Grabherr, F., Schaefer, B., Grander, C., Mayr, L., et al. (2023). Interleukin-11 drives human and mouse alcohol-related liver disease. *Gut* 72 (1), 168–179. doi:10.1136/gutjnl-2021-326076

Fang, C., Zhang, J., Han, J., Lei, Y., Cao, Z., Pan, J., et al. (2023). Tiaogan Jiejiu Tongluo Formula attenuated alcohol-induced chronic liver injury by regulating lipid metabolism in rats. *J. Ethnopharmacol.* 317, 116838. doi:10.1016/j.jep.2023.116838

Feng, R., Chen, J. H., Liu, C. H., Xia, F. B., Xiao, Z., Zhang, X., et al. (2019). A combination of Pueraria lobata and Silybum marianum protects against alcoholic liver disease in mice. *Phytomedicine* 58, 152824. doi:10.1016/j.phymed.2019.152824

Foghis, M., Bungau, S. G., Bungau, A. F., Vesa, C. M., Purza, A. L., Tarce, A. G., et al. (2023). Plants-based medicine implication in the evolution of chronic liver diseases. *Biomed. Pharmacother.* 158, 114207. doi:10.1016/j.biopha.2022.114207

Ghare, S. S., Charpentier, B. T., Ghooray, D. T., Zhang, J., Vadhanam, M. V., Reddy, S., et al. (2023). Tributyrin mitigates ethanol-induced lysine acetylation of histone-H3 and p65-nfκb downregulating CCL2 expression and consequent liver inflammation and injury. *Nutrients* 15 (20), 4397. doi:10.3390/nu15204397

Guo, R., Chen, L., Zhu, J., Li, J., Ding, Q., Chang, K., et al. (2023). Monounsaturated fatty acid-enriched olive oil exacerbates chronic alcohol-induced hepatic steatosis and liver injury in C57BL/6J mice. *Food Funct.* 14 (3), 1573–1583. doi:10.1039/d2fo03323b

Guo, S., Li, W., Chen, F., Yang, S., Huang, Y., Tian, Y., et al. (2021). Polysaccharide of Atractylodes macrocephala Koidz regulates LPS-mediated mouse hepatitis through the TLR4-MyD88-NFκB signaling pathway. *Int. Immunopharmacol.* 98, 107692. doi:10.1016/j.intimp.2021.107692

Jayasuriya, R., Dhamodharan, U., Ali, D., Ganesan, K., Xu, B., and Ramkumar, K. M. (2021). Targeting Nrf2/Keap1 signaling pathway by bioactive natural agents: possible therapeutic strategy to combat liver disease. *Phytomedicine* 92, 153755. doi:10.1016/j.phymed.2021.153755

Jiang, Y. H., Wang, L., Chen, W. D., Duan, Y. T., Sun, M. J., Huang, J. J., et al. (2022). Poria cocos polysaccharide prevents alcohol-induced hepatic injury and inflammation by repressing oxidative stress and gut leakiness. *Front. Nutr.* 9, 963598. doi:10.3389/fnut.2022.963598

Kim, E. K., and Choi, E. J. (2015). Compromised MAPK signaling in human diseases: an update. *Arch. Toxicol.* 89 (6), 867–882. doi:10.1007/s00204-015-1472-2

Lawrence, T. (2009). The nuclear factor NF-kappaB pathway in inflammation. *Cold Spring Harb. Perspect. Biol.* 1 (6), a001651. doi:10.1101/cshperspect.a001651

Liu, B., Li, J., Yi, R., Mu, J., Zhou, X., and Zhao, X. (2019). Preventive effect of alkaloids from Lotus plumule on acute liver injury in mice. *Foods* 8 (1), 36. doi:10.3390/foods8010036

Martinez-Rodriguez, J. L., Gutierrez-Hernandez, R., Reyes-Estrada, C. A., Granados-Lopez, A. J., Perez-Veyna, O., Arcos-Ortega, T., et al. (2019). Hepatoprotective, antihyperlipidemic and radical scavenging activity of hawthorn (Crataegus oxyacantha) and rosemary (rosmarinus officinalis) on alcoholic liver disease. *Altern. Ther. Health Med.* 25 (4), 54–63.

Mo, Q., Zhou, G., Xie, B., Ma, B., Zang, X., Chen, Y., et al. (2020). Evaluation of the hepatoprotective effect of Yigan mingmu oral liquid against acute alcohol-induced liver injury in rats. *BMC Complement. Med. Ther.* 20 (1), 32. doi:10.1186/s12906-020-2817-9

Noonberg, A., Goldstein, G., and Page, H. A. (1985). Premature aging in male alcoholics: "accelerated aging" or "increased vulnerability. *Alcohol Clin. Exp. Res.* 9 (4), 334–338. doi:10.1111/j.1530-0277.1985.tb05555.x

Nowak, A. J., and Relja, B. (2020). The impact of acute or chronic alcohol intake on the NF-κB signaling pathway in alcohol-related liver disease. *Int. J. Mol. Sci.* 21 (24), 9407. doi:10.3390/ijms21249407

Ou, B., Huang, D., Hampsch-Woodill, M., and Flanagan, J. A. (2003). When east meets west: the relationship between yin-yang and antioxidation-oxidation. *FASEB J.* 17 (2), 127–129. doi:10.1096/fj.02-0527hyp

Patel, P. V., and Flamm, S. L. (2023). Alcohol-related liver disease including new developments. *Clin. Liver Dis.* 27 (1), 157–172. doi:10.1016/j.cld.2022.08.005

Qiu, J., Chen, L., Zhang, L., Xu, F., Zhang, C., Ren, G., et al. (2023). Xie Zhuo Tiao Zhi formula modulates intestinal microbiota and liver purine metabolism to suppress hepatic steatosis and pyroptosis in NAFLD therapy. *Phytomedicine Int. J. phytotherapy Phytopharm.* 121, 155111. doi:10.1016/j.phymed.2023.155111

Szeto, Y. T., and Benzie, I. F. (2006). Is the yin-yang nature of Chinese herbal medicine equivalent to antioxidation-oxidation? *J. Ethnopharmacol.* 108 (3), 361–366. doi:10.1016/j.jep.2006.05.033

Wang, H., Mehal, W., Nagy, E. L., and Rotman, Y. (2021). Immunological mechanisms and therapeutic targets of fatty liver diseases. *Cell Mol. Immunol.* 18 (1), 73–91. doi:10.1038/s41423-020-00579-3

Wu, J., Huang, G., Li, Y., and Li, X. (2020). Flavonoids from Aurantii fructus immaturus and Aurantii fructus: promising phytomedicines for the treatment of liver diseases. *Chin. Med.* 15, 89. doi:10.1186/s13020-020-00371-5

Yamada, N., Karasawa, H. T., Kimura, S., Watanabe, T., Komada, R., Kamata, A., et al. (2020). Ferroptosis driven by radical oxidation of n-6 polyunsaturated fatty acids mediates acetaminophen-induced acute liver failure. *Cell Death Dis.* 11 (2), 144–216. doi:10.1038/s41419-020-2334-2

Yang, Y. M., Cho, Y. E., and Hwang, S. (2022). Crosstalk between oxidative stress and inflammatory liver injury in the pathogenesis of alcoholic liver disease. *Int. J. Mol. Sci.* 23 (2), 774. doi:10.3390/ijms23020774

Zhao, M. X., Wen, J. L., Wang, L., Wang, X. P., and Chen, T. S. (2019). Intracellular catalase activity instead of glutathione level dominates the resistance of cells to reactive oxygen species. *Cell Stress Chaperones* 24 (3), 609–619. doi:10.1007/s12192-019-00993-1

Zheng, H., J, J., Guo, Q., Jia, Y. S., Huang, W.-J., Huang, W., et al. (2019). The effect of probiotic and synbiotic supplementation on biomarkers of inflammation and oxidative stress in diabetic patients: a systematic review and meta-analysis of randomized controlled trials. *Pharmacol. Res.* 142, 303–313. doi:10.1016/j.phrs.2019.02.016

frontiers | Frontiers in Pharmacology

TYPE Mini Review
PUBLISHED 06 May 2024
DOI 10.3389/fphar.2024.1332027

OPEN ACCESS

EDITED BY
Chunlei Zhang,
China Pharmaceutical University, China

REVIEWED BY
Liang Shan,
Anhui Medical University, China

*CORRESPONDENCE
Lei Zhao,
leizhao@hust.edu.cn
Yiping Dang,
244927160@qq.com

RECEIVED 02 November 2023
ACCEPTED 10 April 2024
PUBLISHED 06 May 2024

CITATION
Liu C, Fisher D, Pronyuk K, Musabaev E, Thu Hien NT, Dang Y and Zhao L (2024), Therapeutic potential of natural products in schistosomiasis-associated liver fibrosis. *Front. Pharmacol.* 15:1332027. doi: 10.3389/fphar.2024.1332027

Therapeutic potential of natural products in schistosomiasis-associated liver fibrosis

Cuiling Liu[1], David Fisher[2], Khrystyna Pronyuk[3], Erkin Musabaev[4], Nguyen Thi Thu Hien[5], Yiping Dang[6]* and Lei Zhao[1]*

[1]Department of Infectious Diseases, Union Hospital, Tongji Medical College, Huazhong University of Science and Technology, Wuhan, China, [2]Department of Medical Biosciences, Faculty of Natural Sciences, University of the Western Cape, Bellville, South Africa, [3]Infectious Diseases Department, O.Bogomolets National Medical University, Kyiv, Ukraine, [4]The Research Institute of Virology, Ministry of Health, Tashkent, Uzbekistan, [5]Hai Phong University of Medicine and Pharmacy, Hai Phong, Vietnam, [6]Department of Vascular Surgery, Union Hospital, Tongji Medical College, Huazhong University of Science and Technology, Wuhan, China

Schistosomiasis is a parasitic disease that endangers human health and social development. The granulomatous reaction of Schistosoma eggs in the liver is the main cause of hepatosplenomegaly and fibrotic lesions. Anti liver fibrosis therapy is crucial for patients with chronic schistosomiasis. Although Praziquantel is the only clinical drug used, it is limited in insecticide treatment and has a long-term large-scale use, which is forcing the search for cost-effective alternatives. Previous research has demonstrated that plant metabolites and extracts have effective therapeutic effects on liver fibrosis associated with schistosomiasis. This paper summarizes the mechanisms of action of metabolites and some plant extracts in alleviating schistosomiasis-associated liver fibrosis. The analysis was conducted using databases such as PubMed, Google Scholar, and China National Knowledge Infrastructure (CNKI) databases. Some plant metabolites and extracts ameliorate liver fibrosis by targeting multiple signaling pathways, including reducing inflammatory infiltration, oxidative stress, inhibiting alternate macrophage activation, suppressing hepatic stellate cell activation, and reducing worm egg load. Natural products improve liver fibrosis associated with schistosomiasis, but further research is needed to elucidate the effectiveness of natural products in treating liver fibrosis caused by schistosomiasis, as there is no reported data from clinical trials in the literature.

KEYWORDS

natural products, plant extracts, schistosomiasis, liver disease, fibrosis

1 Introduction

Schistosomiasis is a parasitic disease, in which trematodes infections poses a serious threat to human health and social development. Schistosomiasis is found in 78 countries in the tropics and subtropics and is predominantly endemic in sub-Saharan Africa (WHO, 2022). Intestinal schistosomiasis and urogenital schistosomiasis are two primary pathologies caused by Schistosoma infections in humans, with the former being primarily caused by *S. japonicum* and *S. mansoni* and the latter by *S. haematobium*. (McManus et al., 2018). Worms parasitize the veins of human hosts to

mate and lay eggs are excreted in feces or urine. These eggs hatch as miracidia and infect intermediate species-specific host snails in fresh water. After 4–6 weeks, the eggs develop into infectious cercariae that can penetrate human skin and cause disease. Acute infections occur mostly in locals, travelers and immigrants and present symptoms of transient urticaria rash, allergic pneumonia, and Katayama syndrome. (Clerinx and Van Gompel, 2011). The progression of these infections can be characterized by chronic abdominal pain, loss of appetite, and liver polyps, and eventually lead to hepatosplenomegaly, portal hypertension, ascites, gastrointestinal varices, and even life-threatening gastrointestinal bleeding (Colley et al., 2014). Currently, the only clinically effective drug for treating schistosomiasis is praziquantel (Kabuyaya et al., 2023). However, due to the incomplete efficacy of praziquantel and the potential for drug resistance, there is an urgent need to find cost-effective alternatives or complementary treatments (Santana et al., 2021). More research is crucial to investigate novel targeting mechanisms of schistosome-induced liver fibrosis in order to discover new drugs or praziquantel analogs that can treat schistosomiasis.

2 Pathogenesis of chronic schistosomiasis

Fibrosis of the liver and portal system is the main pathological manifestation of intestinal schistosomiasis and is the result of an immune response caused by the invasion of schistosome eggs into the liver and blood vessels. The deposition of eggs causes a granulomatous inflammatory response mediated by CD4 T lymphocytes^{+}, which is characterized by a markedly active Th2 immune response, such as increased levels of cytokines and chemokines, and the recruitment of lymphocytes, neutrophils, eosinophils, macrophages, and fibroblasts, followed by extracellular matrix (ECM) and collagen fibril production of liver tissue, with the eggs being trapped in the liver and unable to be excreted, finally resulting in a fibrotic inflammatory infiltrate forming around the eggs (Chiu et al., 2003; Amaral et al., 2017; Ho et al., 2022). The expedited Th2 response during the schistosomiasis infection may be related to alternate activation of macrophages. During the chronic infection phase, alternatively activated macrophages (M2 macrophages) are stimulated by IL-13, IL-33, IL-4, and ROS to regulate the expression of Arg1, IL-10, and TGF-β1, which act directly or indirectly on hepatic stellate cells and contribute to α-SMA and collagen production, leading to liver fibrosis (Peng et al., 2017; Tan et al., 2018; Yu et al., 2021). The soluble egg antigen (SEA) can also activate M2 macrophages via STAT6 and PI3K signaling pathways or directly activate hepatic stellate cells via the P38/JNK MAPK signaling pathway (Liu P. et al., 2013; Tang et al., 2017). In addition, the deposition of eggs significantly reduced the enzymatic activities of $O_2^{\cdot-}$ and H_2O_2 detoxification, by superoxide dismutase (SOD), catalase, and glutathione peroxidase (GSHPx) and increased the levels of hepatic products from lipid peroxidation, which may stimulate the progression of liver fibrosis (Gharib et al., 1999).

3 Natural products against schistosomiasis-associated liver fibrosis

An increasing number of studies have demonstrated that bioactive ingredients of medicinal plants are a promising alternative to current clinical therapy. The current direction of anti-schistosomiasis drug research is focused on the screening of compounds with therapeutic targets and the development of praziquantel analogs. Anti-fibrotic treatment is essential for patients with chronic schistosomiasis as even deworming does not completely stop the progression of liver fibrosis (Bergquist et al., 2017; LoVerde et al., 2021). In schistosomiasis-endemic countries such as China, Brazil, Zimbabwe, and Kenya, the anti-schistosomiasis pharmacological effects of natural products or plant extracts have been extensively studied in an attempt to discover alternative drugs (Molgaard et al., 2001). Currently, the active mechanism of various natural products in the treatment of schistosomiasis-associated liver fibrosis has been reported, which may modulate fibrotic factors such as IL-13, growth stimulation expressed gene 2 (ST2), TGF-β1, TNF-α and anti-fibrotic factors such as IL-10, Tregs, MHC II through intracellular signaling pathways such as NF-κB pathway, PI3K/AKT pathway and TGF-β1/Smad pathway (Liu et al., 2014; Tang et al., 2017; Kamdem et al., 2018; Huang et al., 2020).

3.1 Natural compounds

Based on the diversity that biological exploration of natural products provides for drug discovery, the active substances of natural products and their independent pharmacological effects in mixtures have attracted much attention (Phillipson, 2001; Simoben et al., 2018). Traditional medicinal plants are highly diverse and many metabolites have been shown to have therapeutic effects on liver fibrosis in schistosomiasis (Table 1).

3.1.1 Artemisinin and its derivatives

Artemisinin is a sesquiterpene lactone derived from *Artemisia annua L.*, and artemisinin-based combination therapies (ACTs) are widely used to treat malaria. *Artemisinin* including its derivatives such as *artesunate*, *dihydroartemisinin*, and *artemether* has also been shown to have pharmacological effects such as anti-cancer, anti-viral, anti-inflammatory, and anti-parasitic (Ho et al., 2014). *Artemisinin* and its derivatives have been shown to kill helminths in animal models (rabbits, rats, dogs) with worm reduction rates ranging from 41% to 98%, which is based on its high lethality to larvae and females (You et al., 1992; Xiao et al., 1994; Gold et al., 2017; Correa et al., 2019). In *Schistosoma mansoni* infected mice, the combination of artesunate (400 mg/kg) and praziquantel (500 mg/kg) significantly decreased hepatic P53 expression and increased Bcl-2 expression (Hegazy et al., 2018). Lower doses of artemether (50 mg/kg), artemether reduced the number of eggs in mice's feces, whereas higher doses of 400 mg/kg artemether greatly reduced the number and diameter of liver granulomas (Lescano et al., 2004; El-Beshbishi et al., 2013). A possible mechanism for this reduction is the inhibition of the expression of schistosomal metabolic enzymes such as glycolytic key enzymes as well as

TABLE 1 Natural compounds for schistosomiasis-associated liver fibrosis.

Natural compounds	Main source	Experimental model	Mechanisms	Efficacy	References
Artemisinin and its derivatives	*Artemisia annua L*	Mice by S. mansoni/S. japonicum	Inhibition of apoptosis; Affects female worms metabolism	Reduced worm and egg loads, reduced liver granulomas	Zhai et al. (2000), Abdin et al. (2013), El-Lakkany and Seif El-Din (2013), Madbouly et al. (2015), Hegazy et al. (2018)
Chlorogenic acid	Green coffee beans	Mice by S. japonicum; LX2 induced by TGF-β1/rIL-13	Regulating IL-13/miR-21/Smad7 and TGF-β1/Smad7 Signaling Pathway	Inhibition of HSCs proliferation; Inhibits collagen deposition	Wang et al. (2017), Yang et al. (2017)
Corilagin	*Phyllanthus niruri L*	Mice by S. japonicum	Regulating IL-13/miR-21/Smad Signaling Pathway; M2 macrophages polarization	Reduced expression of fibrosis factor; Reduced hepatic fibrosis and granuloma area	Yang et al. (2016), Li et al. (2017)
Resveratrol	Grape	Mice by S. mansoni/S. japonicum; HSC-T6 induced by TGF-β1	Reduced ROS accumulation and enhanced oxidase activity; SIRT1/NF-κB signaling pathway	Reduced ECM deposition; Suppression of inflammation	Soliman et al. (2017), Chen et al. (2019), Hao et al. (2022), Mostafa et al. (2023)
Curcumin	*Curcuma longa L*	Mice by S. mansoni/S. japonicum	Enhanced oxidase activity; Immunomodulation (NF-κB)	Reduced worm and egg loads, reduced liver granulomas; Inhibition of pro-fibrotic mediators	Jagetia and Aggarwal (2007), Allam, 2009; Chen et al. (2009), Abu Almaaty et al. (2021)
Genistein	*Glycine* max *(L.) Merr*	Mice by S. japonicum; HSCs induced by MφCM (stimulated by SEA)	SIRT1/TGFβ/Smad3 pathway	Suppression of inflammations; Inhibition of HSCs activity; Reduced liver granulomas	Wan et al. (2017), Zhou et al. (2021a)
Paeoniflorin	*Paeonia lactiflora Pall*	Mice by S. japonicum; HSCs induced by TGF-β1(PMCM stimulated by SEA)	TGFβ/Smad Signaling Pathway; Alternative activation of macrophages	Inhibition of HSCs proliferation; Inhibition of pro-fibrotic mediators	Chu et al. (2007), Li et al. (2010), Chu et al. (2011)

Abbreviations: S. mansoni/S. japonicum, Schistosoma mansoni/Schistosoma japonicum; IL-4/6/10/12/13, interleukin 4/6/10/12/13; TGF-β1, transforming growth factor beta 1; M2, alternatively activated macrophage; SEA, soluble egg antigen; MφCM, macrophage-conditioned medium; NF-κB, nuclear transcription factor-κB; SIRT1, sirtuin 1/silent mating type information regulation two homolog-1; HSC, hepatic stellate cell; PMCM, peritoneal macrophage-conditioned medium.

thioredoxin glutathione reductase (TGR), cytochrome c peroxidase (CcP) and SOD (Zhai et al., 2000; Abdin et al., 2013; El-Lakkany and Seif El-Din, 2013). Furthermore artemether has been shown to mediate a shift from a Th2 to a Th1 response in schistosomes, characterized by an increase in IFN-γ levels and a decrease in IL-4 and IL-10 levels (Madbouly et al., 2015). Interestingly, Keiser et al. found that artemether did not rely on synergy with the immune response for its anti-schistosomal effects, even though immunomodulation was beneficial in suppressing egg-induced hepatotoxicity (Keiser et al., 2010). In summary, *artemisinin* and its derivatives may be a potential treatment for schistosomiasis liver fibrosis.

3.1.2 Chlorogenic acid

Chlorogenic acid, 5-O-caffeoylquinic acid (5-CQA), a natural polyphenolic compound, is widely found in various fruits, vegetables, and medicinal plants, such as apples, eggplants, coffee beans, *Lonicera japonica* Thunb. And *Eucommia ulmoides Oliv*. It is most abundant in green coffee beans. It has significant protective effects on cardiovascular, gastrointestinal, liver, nerve, and metabolism due to its antioxidant, antibacterial, and anticancer biological activities (Naveed et al., 2018; Lu et al., 2020). *Chlorogenic acid* has been reported to protect against different types of liver fibrosis through NOX/ROS/MAPK, ERK/Nrf2, TLR4, and NF-κB pathways (Shi et al., 2013; Shi et al., 2016; Yuan et al., 2017; Wei et al., 2018). *Chlorogenic acid* inhibited the elevated expression of TGF-β receptor I, CTGF, and α-SMA after IL-13 treatment of LX2 cells in a dose-dependent manner, ranging from 56 μM to 225 μM. *In vivo* studies in *Schistosoma japonicum*-infected mice have shown that the use of *chlorogenic acid* (5–20 mg/kg for 4 weeks) reduces IL-13 expression and significantly reduces the size of liver granulomas (Wang et al., 2017). Further mechanisms suggest that IL-13 affects miR-21/Smad7 signaling, which in turn affects liver fibrosis. IL-13 is a key factor in the progression of schistosomiasis disease which is consistent with the view of Wynn et al. (2004). Furthermore, 56–225 μM *chlorogenic acid* also directly interferes with miR-21-regulated TGF-β1/Smad7 signaling, which reduces the expression of CTGF, TIMP and MMP-9 and decreases collagen and ECM deposition (Yang et al., 2017).

3.1.3 Corilagin

Corilagin, β-1-O-galloyl-3,6-(R)-hexahydroxydiphenoyl-d-glucose, a natural ellagitannin, mainly derived from plants such as *Phyllanthus niruri L.* and *Geranium sibiricum L.*, has a variety of pharmacological activities including anti-cancer, anti-inflammatory, antioxidant and hepatoprotective (Li et al., 2018; Gupta et al., 2019). Polarization of M2 macrophages induced by IL-4/IL-13 plays an important role in the granuloma response of *Schistosoma* eggs (Herbert et al., 2004). *Corilagin* (20, 40, 80 mg/kg/day for 28 days)

significantly reduced hepatic fibrosis by decreasing the expression of pro-fibrotic factors (e.g., IL-13, IL-13 receptor α1, IL-4 receptor α), as well as by decreasing the expression of PPARγ, KLF4, SOCS1, and p-STAT6, and by inhibiting the polarization of M2 macrophage in *Schistosoma* hepatic tissues in mice (Du et al., 2016). Li et al. showed that *Corilagin* (39–157 μM, 24 h) significantly inhibited downstream fibrotic factors by interfering with the binding of IL-13 to IL-13Rα1 in Ana-1 cells (Li et al., 2017). Yang et al. found that treatment of schistosome mice with 20 mg/kg Corilagin reduced the number of liver eggs and effectively protected against liver fibrosis by inhibiting miR21 regulation of Smad7 and Smad1/2 phosphorylation (Yang et al., 2016). The above studies show that *Corilagin* is an effective drug in the treatment of schistosomiasis-induced liver fibrosis.

3.1.4 Resveratrol

Resveratrol (3,5,4 0-trihydroxy-trans-stilbene) is a non-flavonoid polyphenol found in over 70 plants such as *Veratrum grandiflorum (Maxim. ex Miq.) O. Loes.*, *Polygonum cuspidatum* Siebold & Zucc., grapes and peanuts. *Resveratrol* (RSV) is highly valued for its antioxidant, anti-inflammatory, anti-cancer, anti-diabetic, anti-aging, cardioprotective, and neuroprotective effects (Zhang L. X. et al., 2021). RSV-containing nanocarriers reduced ROS levels, inhibited the growth of activated HSC-T6 cells *in vitro* (20 μM) and significantly reduced hepatic ECM accumulation *in vivo* (5 mg) (Hao et al., 2022). The reduction of GSH and SOD expression in livers infected with schistosomes was significantly reversed in 2 weeks of treatment with 20 mg/kg RSV (Soliman et al., 2017). Chen et al. showed that RSV (400 mg/kg for 3 days) increased mitochondrial membrane potential (Δφm) and peroxisome proliferator-activated receptor-γ coactivator 1α (PGC-1α) expression in mouse liver. Interestingly, the improvement of mitochondrial function was not the only factor that affected liver fibrosis amelioration with RSV(Chen et al., 2019). As a Sirt-1 activator, RSV (20 mg/kg or 100 mg/kg for 4 weeks) reduced anti-inflammatory markers and anti-fibrotic markers in schistosome-infected mice via the SIRT1/NF-κB signaling pathway (Mostafa et al., 2023). In addition, RSV (20 mg/kg for 3 weeks) inhibited the development and progression of liver granulomas by regulating Th17/Treg responses (Han et al., 2019). Therefore, RSV may exert its anti-schistosomal liver fibrosis effects through the above mechanisms.

3.1.5 Curcumin

Curcumin (1,7-bis-(4-hydroxy-3-methoxyphenyl)-hepta-1,6-diene-3,5-dione), is a natural polyphenolic compound, mainly extracted from the rhizome of *Curcuma longa L. Curcumin* is the key active component of turmeric, showing antioxidant, anti-inflammatory, anti-cancer, anti-microbial, and tissue (heart, nerve, liver) protective effects (Sohn et al., 2021; El-Saadony et al., 2022). The protective effects of curcumin against different types of liver injury are mainly mediated by reducing lipid peroxidation, activating the Nrf2 signal and inhibiting NF-κB activity (Khan et al., 2019). *Curcumin* (50–200 mg/kg) was found to upregulate MMP-1 and inhibit TIMP-1, resulting in a reduction in liver granuloma volume by up to 79% and collagen content by 38.6% (Li et al., 2007). Low expression of GSH, GST, SOD, and CAT caused by *S. mansoni* infection increased significantly after 2 weeks of treatment with 40 mg/kg *curcumin* (Abu Almaaty et al., 2021). A total dose of 400 mg/kg *curcumin* treatment was found to suppress serum levels of IL-12 and TNF-α in the infected group, possibly related to immune regulation triggered by inhibition of NF-κB activity (Jagetia and Aggarwal, 2007; Allam, 2009). Additionally, it significantly raised the mRNA expression of PPAR while reducing TGF-β1 (Chen et al., 2009). These studies suggest that *curcumin* may be an effective in the treatment of schistosomiasis-induced liver fibrosis.

3.1.6 Genistein

Genistein (5,7-dihydroxy-3-(4-hydroxyphenyl) chromium-4-one) is the most potent functional component of soy (*Glycine* max *(L.) Merr.*) isoflavone products, with anti-cancer, anti-oxidant, anti-atherosclerotic and anti-inflammatory activities (Mukund et al., 2017; Sharifi-Rad et al., 2021). 25, 50 mg/kg *genistein* significantly inhibited NF-κB signaling in schistosome-infected liver tissues, as evidenced by decreased mRNA levels of MCP1, TNFα, and IL10, and decreased expression of TGF-β1 and α-SMA (Wan et al., 2017). The same concentration of *genistein* reversed the reduction of STRT1 expression and activity in schistosome liver fibrosis tissues. By suppressing SIRT1 activity, 5–10 and 20 μM doses of *genistein* significantly decreased HSC-T6 cell activation (Zhou C. et al., 2021). Previous studies have demonstrated that *genistein* attenuates hepatic fibrosis by inhibiting TGF-β/Smad signaling through downregulation of p-Smad3 (Ganai and Husain, 2017). Interestingly, the knockdown of SIRT1 enhanced TGF-β1-induced Smad3 phosphorylation (Ma et al., 2019). Thus, *genistein* may also ameliorate schistosomiasis liver fibrosis via the SIRT1/TGFβ/Smad3 pathway. The above studies suggest that *genistein* may be an effective drug for the treatment of schistosomiasis liver fibrosis.

3.1.7 Paeoniflorin

Paeoniflorin is the main active ingredient of the *Paeonia lactiflora Pall.*, a monoterpene glycoside compound used in the treatment of cancer, depression, diabetes, liver disease, and autoimmune disorders (Ma et al., 2020; Zhang and Wei, 2020). Mouse peritoneal macrophages that are stimulated to produce TGF-β1 by SEA, causing the promotion of the proliferation of HSC and the synthesis of collagen. Chu et al. demonstrated for the first time that 7.5–120 mg/L of *paeoniflorin* (colchicine, positive control, 1 μM) selectively downregulated the level of Smad3 phosphorylation through TGF-β1 signaling and inhibited the proliferation of HSC(Chu et al., 2007). Another study found that 30 mg/kg *paeoniflorin* significantly reduced schistosome-induced elevated levels of IL-13 and decreased STAT6 phosphorylation levels and collagen I expression by increasing SOCS-1 expression (Li et al., 2010). Further studies showed that 100 μg/mL *paeoniflorin* directly or indirectly inhibited alternative activation of Kupffer cells by reducing JAK2 and STAT6 phosphorylation (Chu et al., 2011). *Paeoniflorin* may be a promising drug for the treatment of fibrosis in schistosomiasis.

3.2 Plant extracts

The roots, stems, leaves, flowers, and fruits of plants are processed using certain technological methods to obtain herbal bioactive ingredients that affect diseases.

3.2.1 Silymarin

Silymarin is a standardized dried extract of the fruit and seeds of *Silybum marianum (L.) Gaertn*. *Silybin, isosilybin, silydianin and silychristin*, are the four major flavonoid lignan isomers in *silymarin*. *Silybin* is the main active ingredient and is known for its anti-inflammatory, antioxidant, anti-fibrotic, and hepatoprotective effects (Abenavoli et al., 2018; Gillessen and Schmidt, 2020). Mata-Santos et al. found that *silymarin* (*silybin* content,47%) reduced the size of liver granulomas and alleviated liver fibrosis by inhibiting the production of pro-inflammatory and fibrotic factors, including IL-13, IL-4, TNF-α and TGF-β1, and HSC proliferation (Mata-Santos et al., 2010; Mata-Santos et al., 2014; El-Sayed et al., 2016). In a study of acute and chronic schistosomiasis liver fibrosis, *silymarin* (750 mg/kg/day, 5 days/week for 6 weeks) significantly reduced hepatic HYP levels, TGF-β1 and MMP-2 expression and restored GSH levels in both stages, reducing hepatic egg load and regulating granuloma size (El-Lakkany et al., 2012).

3.2.2 Green tea extract

Camellia sinensis (L.) Kuntze is a perennial woody plant whose young leaves and flowers are processed into beverages or medicines (Butt et al., 2015). Green tea has been widely demonstrated to have preventive effects against diabetes, cancer, and cardiovascular disease. Its health properties are attributed to the bioactive polyphenols contained in it, particularly catechins (Xing et al., 2019). Epigallocatechin gallate contains 30%–50% of green tea catechins and is known for its potent antioxidant, anti-obesity, anti-inflammatory, anti-cancer, and other pharmacological activities (Yang et al., 2020). Bin Dajem et al. showed that green tea at a concentration of 3% (w/v) reduced hepatocellular necrosis and perivascular collagen fibers by decreasing lipid peroxidation, but failed to significantly improve liver function (Bin Dajem et al., 2011). Another study found Matcha (a Japanese green tea powder made from finely powdered dried tea leaves) to have lower levels of polyphenols and higher levels of caffeine, quercetin, and rutin than traditional green tea (Ramez et al., 2021). Matcha (3 g/kg b. w) contained more theanine and rutin than other green teas, reducing TNF-α, IFN-γ, and IL-13 levels, increasing IL10 levels, which led to the inhibition of the development of liver granulomas, the restoration of SOD, CAT and GSH-Px activity as well as MDA and TAC levels through antioxidant capacity (Kochman et al., 2020). The natural components of green tea may be a promising complementary treatment therapy for schistosomiasis.

3.2.3 Boswellia serrata resin extract

Frankincense is the resin that exudes from the bark of the *Boswellia Roxb.* tree, a member of the olive family, and boswellic acid is the most important triterpenoid of *frankincense*, especially 3-O-acetyl-11-keto-β-boswellic acid (β-AKBA) (Al-Harrasi et al., 2021). Liu et al. combined *frankincense* oil resin extract with cyclodextrin (BSE-CD) to address hydrophilicity issues. They first found that liver egg granulomas formed by the eggs of *S. japonicum* contained high levels of leukotriene B_4. BSE-CD (280 mg/kg for 3 weeks) significantly reduced the size of liver granulomas, possibly caused by the reduced expression of MMP-9, LTB_4, and PGE_2 (Liu M. et al., 2013). Further postulated mechanisms suggested that it could reduce the inflammatory response around eggs by inhibiting NF-κB signaling and reducing the expression of VEGF, TNF-α, and MCP-1 in mice (Liu et al., 2014).

3.2.4 Ampelopsis grossedentata extract

Ampelopsis grossedentata (Hand. -Mazz.) W.T. Wang, also known as vine tea, is a plant of the genus Ampelopsis in the family Vitaceae, mainly distributed in southern China. The pharmacological effects of vine tea are mainly summarized as anti-inflammatory and analgesic, hepatoprotective, hypotensive, hypolipidemic, antitumor, and anti-aging (Xie et al., 2019; Tong et al., 2020; Wang et al., 2023). Flavonoids are the main efficacy components of vine tea, which includes *dihydromyricetin, myricitrin, myricetin, quercetin, rutin,* and *kaempferol* (Xu et al., 2012). *Dihydromyricetin* has the largest content with a mass fraction of 34% and is considered to be foundational for the health benefits of vine tea (Feng et al., 2018; Zhang Q. et al., 2021). The total flavonoids of vine tea have been proven to have anti-liver fibrosis effects (Li et al., 2022). *Ampelopsis grossedentata* extract containing 90% *dihydromyricetin* (150 mg/kg for 8 weeks) significantly ameliorated hepatic fibrosis in *S. japonicum*-infected mice, which was superior to praziquantel alone. (Fang et al., 2010). 30 μM *Dihydromyricetin* significantly inhibited the activation of HSC-T6 cells *in vitro*, mediated through the promotion of AMPK phosphorylation and inhibition of the TGF-β1/Smad signaling pathway (Zhang et al., 2018). *In vivo*, it (100, 200, 400 mg/kg) downregulated TGF-β1/Smad signaling, improved liver function and reduced ECM deposition. Colchicine was used as a positive control at a dose of 0.2 mg/kg (Liang et al., 2019). In addition, another active ingredient, *myricetin* was shown to have a toxic effect on *S. japonicum* worms through induction of apoptosis, with an LC50 of 600 μM at 24 h. Interestingly, it (at 250 mg/kg) reduces the number of worms and eggs as well as the size of liver granulomas by modulating the immune response (lowering the ratio of Th2 and Th17 cells) (Huang et al., 2020).

3.2.5 Ginger extract

Ginger (*Zingiber officinale Roscoe*), a perennial herb of the *ginger* family, is a medicinal plant with the same origin as food, and has the effect of promoting sweating and relieving symptoms, causing a warming sensation of the body, and suppresses vomiting (Zhang M. et al., 2021). *Ginger* crude aqueous extract (500 mg/kg) slowed the development of granulomatous inflammatory infiltrates and reduced hepatic egg load after schistosome infection, which was more pronounced after treatment with *ginger*-derived nanoparticles (Mostafa et al., 2011; Abd El Wahab et al., 2021). This may be related to the powerful antioxidant effect of *ginger* extract and its ability to scavenge free radicals, as evidenced by the restoration of CAT activity and MDA levels. Another study showed that ethanolic extract of *ginger* also inhibited oxidative stress and inflammatory mediators to improve schistosomiasis-associated liver fibrosis (Aly and Mantawy, 2013). Interestingly, Sanderson et al. suggested that the ethyl acetate extract of *ginger* (150 mg/kg) did not kill the egg load and helminth load of schistosome-infected mice, which was attributed to the alternative extraction

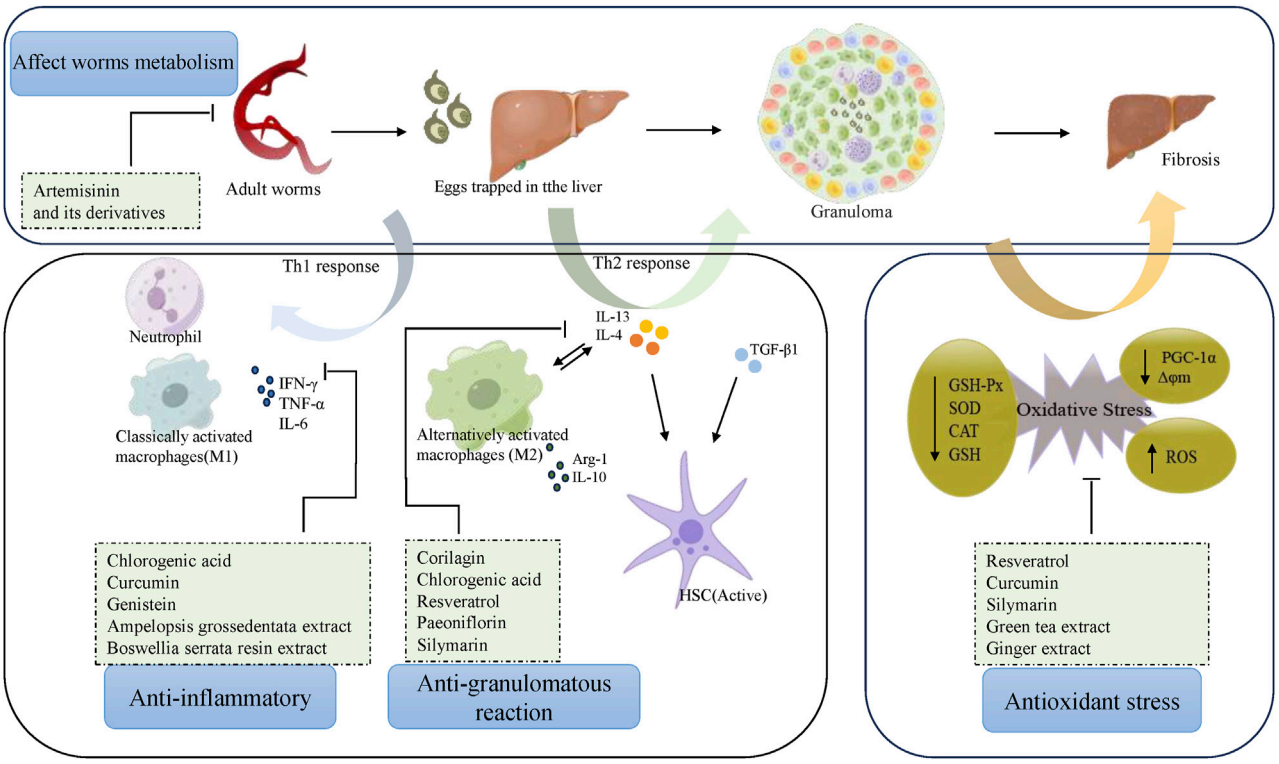

FIGURE 1
Pharmacologic mechanisms of natural products against schistosomiasis-associated liver fibrosis.

solvent and the varying treatment doses of the extracts (Sanderson et al., 2002). Given the lack of data on the role of *ginger* extract as a treatment for schistosomiasis-associated liver fibrosis, further study is required.

3.2.6 Other extracts

Ziziphus spina-christi leaf extract (ZLE) is extracted from *Z. spina-christi (L.) Willd*, alkaloids and flavonoids are the main constituent classes. The pharmacological effects of it include antibacterial, anti-inflammatory, antiparasitic, and anticancer (Abdulrahman et al., 2022). 600 mg/kg Ziziphus spina-christi showed granuloma reduction and anti-hepatic fibrosis in mice infected with *S. haematobium* (Alghamdi et al., 2023). 400 mg/kg ZLE treatment reduces hepatic granuloma area in mice infected with *S. mansoni* and reduces hepatic fibrosis by inhibiting the expression of TGF-β1, VEGF, α-SMA, TIMP-1, and MMP-9, as well as inhibiting oxidative stress and inflammation by upregulating Nrf2 (Almeer et al., 2018). An aqueous extract of *Moringa Oleifera Lam.* Leaves (150 mg/kg for 15 days) significantly reduced NF-κB expression and thereby ameliorated schistosome-induced hepatic fibrosis (Saad El-Din et al., 2023). Ceratonia siliqua pod extract (*Ceratonia siliqua L.*) at doses of 300 mg/kg or 600 mg/kg reduced the area of granulomas and fibrosis by counteracting oxidative stress and decreasing TIMP-2 expression (Al-Olayan et al., 2016). 1.5 g/kg Artichoke leaf extract (*Cynara scolymus L.*) reduces granuloma size by increasing HSC recruitment within the granuloma (Sharaf El-Deen et al., 2017).

4 Conclusion

The main objective of this paper is to summarize the mechanistic studies of selected metabolites and plant extracts for the treatment of schistosomiasis-associated liver fibrosis. Some metabolites or plant extracts that did not address pharmacological mechanisms or were partially uncommon were excluded from the review. In addition, in the literature reviewed reported inconsistent ranges in dosage and varying assessment criteria for fibrosis.

Praziquantel is currently the most commonly used medication for schistosome prophylaxis and treatment. Due to praziquantel's low toxicity to eggs, it is not effective in preventing the progression of liver fibrosis caused by schistosomiasis infection According to pharmacological monographs, current literature, and experimental studies, metabolites or plant extracts have the potential to treat schistosome-induced liver fibrosis. Their therapeutic mechanisms are characterized by 1) reduction of inflammation, 2) reduction of the granulomatous response, 3) reduction of oxidative stress, and 4) reduction of egg loading (Figure 1). There is considerable evidence that therapeutic efficiency is improved by combining metabolites/plant extracts with praziquantel, or with nanocarriers, or by using liposomes. Previous basic and clinical studies have shown good safety and tolerability for metabolic substances like resveratrol and chlorogenic acid, but adverse effects cannot be excluded due to experimental variability, inter-individual variability, and the lack of clinical trial reports. Furthermore, studies on the above metabolites and botanicals for the treatment of hepatic fibrosis due to schistosomiasis have been limited to basic research and no

clinical studies have been reported. In conclusion, the protective role of natural products in the treatment of liver fibrosis in schistosomiasis needs to be confirmed by more standardized cellular studies, and supported by *in vivo* data from animal studies, which if promising should be escalated to randomized controlled clinical trials in humans.

Author contributions

CL: Writing–original draft, Conceptualization. DF: Writing–review and editing. KP: Writing–review and editing. EM: Writing–review and editing, Visualization. NT: Writing–review and editing, Visualization. YD: Writing–review and editing, Supervision. LZ: Funding acquisition, Writing–review and editing.

Funding

The author(s) declare that financial support was received for the research, authorship, and/or publication of this article. The work was supported by grants from the National Natural Science Foundation of China (No. 81974530) and Hubei International Scientific and Technological Cooperation Project (Nos. 2022EHB039, 2023EHA057).

Conflict of interest

The authors declare that the research was conducted in the absence of any commercial or financial relationships that could be construed as a potential conflict of interest.

Publisher's note

All claims expressed in this article are solely those of the authors and do not necessarily represent those of their affiliated organizations, or those of the publisher, the editors and the reviewers. Any product that may be evaluated in this article, or claim that may be made by its manufacturer, is not guaranteed or endorsed by the publisher.

References

Abd El Wahab, W. M., El-Badry, A. A., Mahmoud, S. S., El-Badry, Y. A., El-Badry, M. A., and Hamdy, D. A. (2021). Ginger (Zingiber Officinale)-derived nanoparticles in Schistosoma mansoni infected mice: hepatoprotective and enhancer of etiological treatment. *PLoS Negl. Trop. Dis.* 15 (5), e0009423. doi:10.1371/journal.pntd.0009423

Abdin, A. A., Ashour, D. S., and Shoheib, Z. S. (2013). Artesunate effect on schistosome thioredoxin glutathione reductase and cytochrome c peroxidase as new molecular targets in schistosoma mansoni-infected mice. *Biomed. Environ. Sci.* 26 (12), 953–961. doi:10.3967/bes2013.030

Abdulrahman, M. D., Zakariya, A. M., Hama, H. A., Hamad, S. W., Al-Rawi, S. S., Bradosty, S. W., et al. (2022). Ethnopharmacology, biological evaluation, and chemical composition of ziziphus spina-christi (L.) desf.: a review. *Adv. Pharmacol. Pharm. Sci.* 2022, 4495688. doi:10.1155/2022/4495688

Abenavoli, L., Izzo, A. A., Milic, N., Cicala, C., Santini, A., and Capasso, R. (2018). Milk thistle (Silybum marianum): a concise overview on its chemistry, pharmacological, and nutraceutical uses in liver diseases. *Phytother. Res.* 32 (11), 2202–2213. doi:10.1002/ptr.6171

Abu Almaaty, A. H., Rashed, H. A. E., Soliman, M. F. M., Fayad, E., Althobaiti, F., and El-Shenawy, N. S. (2021). Parasitological and biochemical efficacy of the active ingredients of allium sativum and Curcuma longa in schistosoma mansoni infected mice. *Molecules* 26 (15), 4542. doi:10.3390/molecules26154542

Alghamdi, T., Salem, D. A., and El-Refaei, M. F. (2023). Anti-angiogenic and anti-proliferative activity of ziziphus leaf extract as a novel potential therapeutic agent for reducing hepatic injury in experimental hamster schistosomiasis. *PLoS Negl. Trop. Dis.* 17 (6), e0011426. doi:10.1371/journal.pntd.0011426

Al-Harrasi, A., Khan, A. L., Rehman, N. U., and Csuk, R. (2021). Biosynthetic diversity in triterpene cyclization within the Boswellia genus. *Phytochemistry* 184, 112660. doi:10.1016/j.phytochem.2021.112660

Allam, G. (2009). Immunomodulatory effects of curcumin treatment on murine schistosomiasis mansoni. *Immunobiology* 214 (8), 712–727. doi:10.1016/j.imbio.2008.11.017

Almeer, R. S., El-Khadragy, M. F., Abdelhabib, S., and Abdel Moneim, A. E. (2018). Ziziphus spina-christi leaf extract ameliorates schistosomiasis liver granuloma, fibrosis, and oxidative stress through downregulation of fibrinogenic signaling in mice. *PLoS One* 13 (10), e0204923. doi:10.1371/journal.pone.0204923

Al-Olayan, E. M., El-Khadragy, M. F., Alajmi, R. A., Othman, M. S., Bauomy, A. A., Ibrahim, S. R., et al. (2016). Ceratonia siliqua pod extract ameliorates Schistosoma mansoni-induced liver fibrosis and oxidative stress. *BMC Complement. Altern. Med.* 16 (1), 434. doi:10.1186/s12906-016-1389-1

Aly, H. F., and Mantawy, M. M. (2013). Efficiency of ginger (Zingbar officinale) against Schistosoma mansoni infection during host-parasite association. *Parasitol. Int.* 62 (4), 380–389. doi:10.1016/j.parint.2013.04.002

Amaral, K. B., Silva, T. P., Dias, F. F., Malta, K. K., Rosa, F. M., Costa-Neto, S. F., et al. (2017). Histological assessment of granulomas in natural and experimental Schistosoma mansoni infections using whole slide imaging. *PLoS One* 12 (9), e0184696. doi:10.1371/journal.pone.0184696

Bergquist, R., Utzinger, J., and Keiser, J. (2017). Controlling schistosomiasis with praziquantel: how much longer without a viable alternative? *Infect. Dis. Poverty* 6 (1), 74. doi:10.1186/s40249-017-0286-2

Bin Dajem, S. M., Shati, A. A., Adly, M. A., Ahmed, O. M., Ibrahim, E. H., and Mostafa, O. M. (2011). Green tea (Camellia sinesis) ameliorates female Schistosoma mansoni-induced changes in the liver of Balb/C mice. *Saudi J. Biol. Sci.* 18 (4), 361–368. doi:10.1016/j.sjbs.2011.06.003

Butt, M. S., Ahmad, R. S., Sultan, M. T., Qayyum, M. M., and Naz, A. (2015). Green tea and anticancer perspectives: updates from last decade. *Crit. Rev. Food Sci. Nutr.* 55 (6), 792–805. doi:10.1080/10408398.2012.680205

Chen, H., Zhang, J., and Liu, W. (2009). Jiang Huang su kang xue xi chong bing Gan xian Wei hua ji qi ji zhi de Shi yan yan jiu. *Chin. Traditional Herb. Drugs* 40 (08), 1274–1277. doi:10.3321/j.issn:0253-2670.2009.08.032

Chen, T. T., Peng, S., Wang, Y., Hu, Y., Shen, Y., Xu, Y., et al. (2019). Improvement of mitochondrial activity and fibrosis by resveratrol treatment in mice with schistosoma japonicum infection. *Biomolecules* 9 (11), 658. doi:10.3390/biom9110658

Chiu, B. C., Freeman, C. M., Stolberg, V. R., Komuniecki, E., Lincoln, P. M., Kunkel, S. L., et al. (2003). Cytokine-chemokine networks in experimental mycobacterial and schistosomal pulmonary granuloma formation. *Am. J. Respir. Cell Mol. Biol.* 29 (1), 106–116. doi:10.1165/rcmb.2002-0241OC

Chu, D., Du, M., Hu, X., Wu, Q., and Shen, J. (2011). Paeoniflorin attenuates schistosomiasis japonica-associated liver fibrosis through inhibiting alternative activation of macrophages. *Parasitology* 138 (10), 1259–1271. doi:10.1017/S0031182011001065

Chu, D., Luo, Q., Li, C., Gao, Y., Yu, L., Wei, W., et al. (2007). Paeoniflorin inhibits TGF-beta1-mediated collagen production by Schistosoma japonicum soluble egg antigen *in vitro*. *Parasitology* 134 (11), 1611–1621. doi:10.1017/S0031182007002946

Clerinx, J., and Van Gompel, A. (2011). Schistosomiasis in travellers and migrants. *Travel Med. Infect. Dis.* 9 (1), 6–24. doi:10.1016/j.tmaid.2010.11.002

Colley, D. G., Bustinduy, A. L., Secor, W. E., and King, C. H. (2014). Human schistosomiasis. *Lancet* 383 (9936), 2253–2264. doi:10.1016/S0140-6736(13)61949-2

Correa, S. A. P., de Oliveira, R. N., Mendes, T. M. F., Dos Santos, K. R., Boaventura, S., Jr., Garcia, V. L., et al. (2019). *In vitro* and *in vivo* evaluation of six artemisinin derivatives against Schistosoma mansoni. *Parasitol. Res.* 118 (2), 505–516. doi:10.1007/s00436-018-6188-9

Du, P., Ma, Q., Zhu, Z. D., Li, G., Wang, Y., Li, Q. Q., et al. (2016). Mechanism of Corilagin interference with IL-13/STAT6 signaling pathways in hepatic alternative activation macrophages in schistosomiasis-induced liver fibrosis in mouse model. *Eur. J. Pharmacol.* 793, 119–126. doi:10.1016/j.ejphar.2016.11.018

El-Beshbishi, S. N., Taman, A., El-Malky, M., Azab, M. S., El-Hawary, A. K., and El-Tantawy, D. A. (2013). *In vivo* effect of single oral dose of artemether against early

juvenile stages of Schistosoma mansoni Egyptian strain. *Exp. Parasitol.* 135 (2), 240–245. doi:10.1016/j.exppara.2013.07.006

El-Lakkany, N. M., Hammam, O. A., El-Maadawy, W. H., Badawy, A. A., Ain-Shoka, A. A., and Ebeid, F. A. (2012). Anti-inflammatory/anti-fibrotic effects of the hepatoprotective silymarin and the schistosomicide praziquantel against Schistosoma mansoni-induced liver fibrosis. *Parasit. Vectors* 5, 9. doi:10.1186/1756-3305-5-9

El-Lakkany, N. M., and Seif El-Din, S. H. (2013). Haemin enhances the *in vivo* efficacy of artemether against juvenile and adult Schistosoma mansoni in mice. *Parasitol. Res.* 112 (5), 2005–2015. doi:10.1007/s00436-013-3358-7

El-Saadony, M. T., Yang, T., Korma, S. A., Sitohy, M., Abd El-Mageed, T. A., Selim, S., et al. (2022). Impacts of turmeric and its principal bioactive curcumin on human health: Pharmaceutical, medicinal, and food applications: a comprehensive review. *Front. Nutr.* 9, 1040259. doi:10.3389/fnut.2022.1040259

El-Sayed, N. M., Fathy, G. M., Abdel-Rahman, S. A., and El-Shafei, M. A. (2016). Cytokine patterns in experimental schistosomiasis mansoni infected mice treated with silymarin. *J. Parasit. Dis.* 40 (3), 922–929. doi:10.1007/s12639-014-0606-4

Fang, H., Wang, J., Chen, M., Jia, L., and Li, C. (2010). Therapeutic effects of extract from caulis Ampelopsis grossdentatae on murine SchistosomiasisHepatic fibrosis. *Chin. General Pract.* 13 (18), 2004–2006.

Feng, C., Zhang, N., zhou, D., Jiao, S., Wu, S., Zou, R., et al. (2018). Determination of the content of 4 flavonoids in Ampelopsis grossedentatas leaves by HPLC. *Sci. Technol. Food Industry* 39 (24), 240–245. doi:10.13386/j.issn1002-0306.2018.24.041

Ganai, A. A., and Husain, M. (2017). Genistein attenuates D-GalN induced liver fibrosis/chronic liver damage in rats by blocking the TGF-β/Smad signaling pathways. *Chem. Biol. Interact.* 261, 80–85. doi:10.1016/j.cbi.2016.11.022

Gharib, B., Abdallahi, O. M., Dessein, H., and De Reggi, M. (1999). Development of eosinophil peroxidase activity and concomitant alteration of the antioxidant defenses in the liver of mice infected with Schistosoma mansoni. *J. Hepatol.* 30 (4), 594–602. doi:10.1016/s0168-8278(99)80189-5

Gillessen, A., and Schmidt, H. H. (2020). Silymarin as supportive treatment in liver diseases: a narrative review. *Adv. Ther.* 37 (4), 1279–1301. doi:10.1007/s12325-020-01251-y

Gold, D., Alian, M., Domb, A., Karawani, Y., Jbarien, M., Chollet, J., et al. (2017). Elimination of Schistosoma mansoni in infected mice by slow release of artemisone. *Int. J. Parasitol. Drugs Drug Resist* 7 (2), 241–247. doi:10.1016/j.ijpddr.2017.05.002

Gupta, A., Singh, A. K., Kumar, R., Ganguly, R., Rana, H. K., Pandey, P. K., et al. (2019). Corilagin in cancer: a critical evaluation of anticancer activities and molecular mechanisms. *Molecules* 24 (18), 3399. doi:10.3390/molecules24183399

Han, Q., Zhu, J., Lv, N., Tong, S., and Zhang, W. (2019). Resveratrol inhibited hepatic granulama in mice with schistosomiasis by modulating Th17 and Treg responses. *Chin. Pharmacol. Bull.* 35 (01), 132–138.

Hao, Y., Song, K., Tan, X., Ren, L., Guo, X., Zhou, C., et al. (2022). Reactive oxygen species-responsive polypeptide drug delivery system targeted activated hepatic stellate cells to ameliorate liver fibrosis. *ACS Nano* 16 (12), 20739–20757. doi:10.1021/acsnano.2c07796

Hegazy, L. A. M., Motiam, M. H. A., Abd El-Aal, N. F., Ibrahim, S. M., and Mohamed, H. K. (2018). Evaluation of artesunate and praziquantel combination therapy in murine schistosomiasis mansoni. *Iran. J. Parasitol.* 13 (2), 193–203.

Herbert, D. R., Holscher, C., Mohrs, M., Arendse, B., Schwegmann, A., Radwanska, M., et al. (2004). Alternative macrophage activation is essential for survival during schistosomiasis and downmodulates T helper 1 responses and immunopathology. *Immunity* 20 (5), 623–635. doi:10.1016/s1074-7613(04)00107-4

Ho, C. H., Cheng, C. H., Huang, T. W., Peng, S. Y., Lee, K. M., and Cheng, P. C. (2022). Switched phenotypes of macrophages during the different stages of Schistosoma japonicum infection influenced the subsequent trends of immune responses. *J. Microbiol. Immunol. Infect.* 55 (3), 503–526. doi:10.1016/j.jmii.2021.06.005

Ho, W. E., Peh, H. Y., Chan, T. K., and Wong, W. S. (2014). Artemisinins: pharmacological actions beyond anti-malarial. *Pharmacol. Ther.* 142 (1), 126–139. doi:10.1016/j.pharmthera.2013.12.001

Huang, P., Zhou, M., Cheng, S., Hu, Y., Gao, M., Ma, Y., et al. (2020). Myricetin possesses anthelmintic activity and attenuates hepatic fibrosis via modulating TGFβ1 and akt signaling and shifting Th1/Th2 balance in schistosoma japonicum-infected mice. *Front. Immunol.* 11, 593. doi:10.3389/fimmu.2020.00593

Jagetia, G. C., and Aggarwal, B. B. (2007). Spicing up" of the immune system by curcumin. *J. Clin. Immunol.* 27 (1), 19–35. doi:10.1007/s10875-006-9066-7

Kabuyaya, M., Chimbari, M. J., and Mukaratirwa, S. (2023). Correction: efficacy of praziquantel treatment regimens in pre-school and school aged children infected with schistosomes in sub-Saharan Africa: a systematic review. *Infect. Dis. Poverty* 12 (1), 13. doi:10.1186/s40249-023-01064-5

Kamdem, S. D., Moyou-Somo, R., Brombacher, F., and Nono, J. K. (2018). Host regulators of liver fibrosis during human schistosomiasis. *Front. Immunol.* 9, 2781. doi:10.3389/fimmu.2018.02781

Keiser, J., Vargas, M., and Doenhoff, M. J. (2010). Activity of artemether and mefloquine against juvenile and adult Schistosoma mansoni in athymic and immunocompetent NMRI mice. *Am. J. Trop. Med. Hyg.* 82 (1), 112–114. doi:10.4269/ajtmh.2010.09-0461

Khan, H., Ullah, H., and Nabavi, S. M. (2019). Mechanistic insights of hepatoprotective effects of curcumin: therapeutic updates and future prospects. *Food Chem. Toxicol.* 124, 182–191. doi:10.1016/j.fct.2018.12.002

Kochman, J., Jakubczyk, K., Antoniewicz, J., Mruk, H., and Janda, K. (2020). Health benefits and chemical composition of Matcha green tea: a review. *Molecules* 26 (1), 85. doi:10.3390/molecules26010085

Lescano, S. Z., Chieffi, P. P., Canhassi, R. R., Boulos, M., and Amato Neto, V. (2004). Antischistosomal activity of artemether in experimental Schistosomiasis mansoni. *Rev. Saude Publica* 38 (1), 71–75. doi:10.1590/s0034-89102004000100010

Li, K., Zhang, L., Fan, Z., and Li, W. (2007). The mechanism of curcumin on inhibiting schistosomiasis liver fibrosis in mice. *Chin. J. Endemiology* 26 (06), 643–645.

Li, M., Wang, L., and Li, W. (2022). Improving effect of tengeha flavonoids in mice with liver fibrosis. *J. Guangzhou Univ. Traditional Chin. Med.* 39 (03), 625–630. doi:10.13359/j.cnki.gzxbtcm.2022.03.027

Li, X., Deng, Y., Zheng, Z., Huang, W., Chen, L., Tong, Q., et al. (2018). Corilagin, a promising medicinal herbal agent. *Biomed. Pharmacother.* 99, 43–50. doi:10.1016/j.biopha.2018.01.030

Li, X., Shen, J., Zhong, Z., Peng, J., Wen, H., Li, J., et al. (2010). Paeoniflorin ameliorates schistosomiasis liver fibrosis through regulating IL-13 and its signalling molecules in mice. *Parasitology* 137 (8), 1213–1225. doi:10.1017/S003118201000003X

Li, Y. Q., Chen, Y. F., Dang, Y. P., Wang, Y., Shang, Z. Z., Ma, Q., et al. (2017). Corilagin counteracts IL-13Rα1 signaling pathway in macrophages to mitigate schistosome egg-induced hepatic fibrosis. *Front. Cell Infect. Microbiol.* 7, 443. doi:10.3389/fcimb.2017.00443

Liang, B., Zheng, Z., Gan, C., and Tang, Y. (2019). Effects of dihydromyricetin from Ampelopsis grossedntata on TGF-β1/smad signaling pathwayin hepatic fibrosis mice. *J. Chin. Med. Mater.* 42 (12), 2922–2928. doi:10.13863/j.issn1001-4454.2019.12.034

Liu, M., Chen, P., Buchele, B., Dong, S., Huang, D., Ren, C., et al. (2013a). A boswellic acid-containing extract attenuates hepatic granuloma in C57BL/6 mice infected with Schistosoma japonicum. *Parasitol. Res.* 112 (3), 1105–1111. doi:10.1007/s00436-012-3237-7

Liu, M., Wu, Q., Chen, P., Buchele, B., Bian, M., Dong, S., et al. (2014). A boswellic acid-containing extract ameliorates schistosomiasis liver granuloma and fibrosis through regulating NF-κB signaling in mice. *PLoS One* 9 (6), e100129. doi:10.1371/journal.pone.0100129

Liu, P., Wang, M., Lu, X. D., Zhang, S. J., and Tang, W. X. (2013b). Schistosoma japonicum egg antigen up-regulates fibrogenesis and inhibits proliferation in primary hepatic stellate cells in a concentration-dependent manner. *World J. Gastroenterol.* 19 (8), 1230–1238. doi:10.3748/wjg.v19.i8.1230

LoVerde, P. T., Alwan, S. N., Taylor, A. B., Rhodes, J., Chevalier, F. D., Anderson, T. J., et al. (2021). Rational approach to drug discovery for human schistosomiasis. *Int. J. Parasitol. Drugs Drug Resist* 16, 140–147. doi:10.1016/j.ijpddr.2021.05.002

Lu, H., Tian, Z., Cui, Y., Liu, Z., and Ma, X. (2020). Chlorogenic acid: a comprehensive review of the dietary sources, processing effects, bioavailability, beneficial properties, mechanisms of action, and future directions. *Compr. Rev. Food Sci. Food Saf.* 19 (6), 3130–3158. doi:10.1111/1541-4337.12620

Ma, J. Q., Sun, Y. Z., Ming, Q. L., Tian, Z. K., Yang, H. X., and Liu, C. M. (2019). Ampelopsin attenuates carbon tetrachloride-induced mouse liver fibrosis and hepatic stellate cell activation associated with the SIRT1/TGF-β1/Smad3 and autophagy pathway. *Int. Immunopharmacol.* 77, 105984. doi:10.1016/j.intimp.2019.105984

Ma, X., Zhang, W., Jiang, Y., Wen, J., Wei, S., and Zhao, Y. (2020). Paeoniflorin, a natural product with multiple targets in liver diseases-A mini review. *Front. Pharmacol.* 11, 531. doi:10.3389/fphar.2020.00531

Madbouly, N. A., Shalash, I. R., El Deeb, S. O., and El Amir, A. M. (2015). Effect of artemether on cytokine profile and egg induced pathology in murine schistosomiasis mansoni. *J. Adv. Res.* 6 (6), 851–857. doi:10.1016/j.jare.2014.07.003

Mata-Santos, H. A., Dutra, F. F., Rocha, C. C., Lino, F. G., Xavier, F. R., Chinalia, L. A., et al. (2014). Silymarin reduces profibrogenic cytokines and reverses hepatic fibrosis in chronic murine schistosomiasis. *Antimicrob. Agents Chemother.* 58 (4), 2076–2083. doi:10.1128/AAC.01936-13

Mata-Santos, H. A., Lino, F. G., Rocha, C. C., Paiva, C. N., Castelo Branco, M. T., and Pyrrho Ados, S. (2010). Silymarin treatment reduces granuloma and hepatic fibrosis in experimental schistosomiasis. *Parasitol. Res.* 107 (6), 1429–1434. doi:10.1007/s00436-010-2014-8

McManus, D. P., Dunne, D. W., Sacko, M., Utzinger, J., Vennervald, B. J., and Zhou, X. N. (2018). Schistosomiasis. *Nat. Rev. Dis. Prim.* 4 (1), 13. doi:10.1038/s41572-018-0013-8

Molgaard, P., Nielsen, S. B., Rasmussen, D. E., Drummond, R. B., Makaza, N., and Andreassen, J. (2001). Anthelmintic screening of Zimbabwean plants traditionally used against schistosomiasis. *J. Ethnopharmacol.* 74 (3), 257–264. doi:10.1016/s0378-8741(00)00377-9

Mostafa, D. K., Eissa, M. M., Ghareeb, D. A., Abdulmalek, S., and Hewedy, W. A. (2023). Resveratrol protects against Schistosoma mansoni-induced liver fibrosis by

targeting the Sirt-1/NF-κB axis. *Inflammopharmacology* 32, 763–775. doi:10.1007/s10787-023-01382-y

Mostafa, O. M., Eid, R. A., and Adly, M. A. (2011). Antischistosomal activity of ginger (Zingiber officinale) against Schistosoma mansoni harbored in C57 mice. *Parasitol. Res.* 109 (2), 395–403. doi:10.1007/s00436-011-2267-x

Mukund, V., Mukund, D., Sharma, V., Mannarapu, M., and Alam, A. (2017). Genistein: its role in metabolic diseases and cancer. *Crit. Rev. Oncol. Hematol.* 119, 13–22. doi:10.1016/j.critrevonc.2017.09.004

Naveed, M., Hejazi, V., Abbas, M., Kamboh, A. A., Khan, G. J., Shumzaid, M., et al. (2018). Chlorogenic acid (CGA): a pharmacological review and call for further research. *Biomed. Pharmacother.* 97, 67–74. doi:10.1016/j.biopha.2017.10.064

Peng, H., Zhang, Q., Li, X., Liu, Z., Shen, J., Sun, R., et al. (2017). Erratum: IL-33 contributes to schistosoma japonicum-induced hepatic pathology through induction of M2 macrophages. *Sci. Rep.* 7, 39568. doi:10.1038/srep39568

Phillipson, J. D. (2001). Phytochemistry and medicinal plants. *Phytochemistry* 56 (3), 237–243. doi:10.1016/s0031-9422(00)00456-8

Ramez, A. M., Elmahallawy, E. K., Elshopakey, G. E., Saleh, A. A., Moustafa, S. M., Al-Brakati, A., et al. (2021). Hepatosplenic protective actions of spirulina platensis and Matcha green tea against schistosoma mansoni infection in mice via antioxidative and anti-inflammatory mechanisms. *Front. Vet. Sci.* 8, 650531. doi:10.3389/fvets.2021.650531

Saad El-Din, M. I., Gad El-Hak, H. N., Ghobashy, M. A., and Elrayess, R. A. (2023). Parasitological and histopathological studies to the effect of aqueous extract of Moringa oleifera Lam. leaves combined with praziquantel therapy in modulating the liver and spleen damage induced by Schistosoma mansoni to male mice. *Environ. Sci. Pollut. Res. Int.* 30 (6), 15548–15560. doi:10.1007/s11356-022-23098-2

Sanderson, L., Bartlett, A., and Whitfield, P. J. (2002). *In vitro* and *in vivo* studies on the bioactivity of a ginger (Zingiber officinale) extract towards adult schistosomes and their egg production. *J. Helminthol.* 76 (3), 241–247. doi:10.1079/JOH2002116

Santana, J. B., de Almeida, T., Lopes, D. M., Page, B., Oliveira, S. C., Souza, I., et al. (2021). Phenotypic characterization of CD4(+) T lymphocytes in periportal fibrosis secondary to schistosomiasis. *Front. Immunol.* 12, 605235. doi:10.3389/fimmu.2021.605235

Sharaf El-Deen, S. A., Brakat, R. M., and Mohamed, A. (2017). Artichoke leaf extract protects liver of Schistosoma mansoni infected mice through modulation of hepatic stellate cells recruitment. *Exp. Parasitol.* 178, 51–59. doi:10.1016/j.exppara.2017.05.005

Sharifi-Rad, J., Quispe, C., Imran, M., Rauf, A., Nadeem, M., Gondal, T. A., et al. (2021). Genistein: an integrative overview of its mode of action, pharmacological properties, and health benefits. *Oxid. Med. Cell Longev.* 2021, 3268136. doi:10.1155/2021/3268136

Shi, H., Dong, L., Jiang, J., Zhao, J., Zhao, G., Dang, X., et al. (2013). Chlorogenic acid reduces liver inflammation and fibrosis through inhibition of toll-like receptor 4 signaling pathway. *Toxicology* 303, 107–114. doi:10.1016/j.tox.2012.10.025

Shi, H., Shi, A., Dong, L., Lu, X., Wang, Y., Zhao, J., et al. (2016). Chlorogenic acid protects against liver fibrosis *in vivo* and *in vitro* through inhibition of oxidative stress. *Clin. Nutr.* 35 (6), 1366–1373. doi:10.1016/j.clnu.2016.03.002

Simoben, C. V., Ntie-Kang, F., Akone, S. H., and Sippl, W. (2018). Compounds from african medicinal plants with activities against selected parasitic diseases: schistosomiasis, trypanosomiasis and leishmaniasis. *Nat. Prod. Bioprospect* 8 (3), 151–169. doi:10.1007/s13659-018-0165-y

Sohn, S. I., Priya, A., Balasubramaniam, B., Muthuramalingam, P., Sivasankar, C., Selvaraj, A., et al. (2021). Biomedical applications and bioavailability of curcumin-an updated overview. *Pharmaceutics* 13 (12), 2102. doi:10.3390/pharmaceutics13122102

Soliman, R. H., Ismail, O. A., Badr, M. S., and Nasr, S. M. (2017). Resveratrol ameliorates oxidative stress and organ dysfunction in Schistosoma mansoni infected mice. *Exp. Parasitol.* 174, 52–58. doi:10.1016/j.exppara.2017.02.008

Tan, Z., Liu, Q., Jiang, R., Lv, L., Shoto, S. S., Maillet, I., et al. (2018). Interleukin-33 drives hepatic fibrosis through activation of hepatic stellate cells. *Cell Mol. Immunol.* 15 (4), 388–398. doi:10.1038/cmi.2016.63

Tang, H., Liang, Y. B., Chen, Z. B., Du, L. L., Zeng, L. J., Wu, J. G., et al. (2017). Soluble egg antigen activates M2 macrophages via the STAT6 and PI3K pathways, and schistosoma japonicum alternatively activates macrophage polarization to improve the survival rate of septic mice. *J. Cell Biochem.* 118 (12), 4230–4239. doi:10.1002/jcb.26073

Tong, H., Zhang, X., Tan, L., Jin, R., Huang, S., and Li, X. (2020). Multitarget and promising role of dihydromyricetin in the treatment of metabolic diseases. *Eur. J. Pharmacol.* 870, 172888. doi:10.1016/j.ejphar.2019.172888

Wan, C., Jin, F., Du, Y., Yang, K., Yao, L., Mei, Z., et al. (2017). Genistein improves schistosomiasis liver granuloma and fibrosis via dampening NF-kB signaling in mice. *Parasitol. Res.* 116 (4), 1165–1174. doi:10.1007/s00436-017-5392-3

Wang, Y., Yang, F., Xue, J., Zhou, X., Luo, L., Ma, Q., et al. (2017). Antischistosomiasis liver fibrosis effects of chlorogenic acid through IL-13/miR-21/smad7 signaling interactions *in vivo* and *in vitro*. *Antimicrob. Agents Chemother.* 61 (2), e01347. doi:10.1128/AAC.01347-16

Wang, Z., Jiang, Q., Li, P., Shi, P., Liu, C., Wang, W., et al. (2023). The water extract of Ampelopsis grossedentata alleviates oxidative stress and intestinal inflammation. *Antioxidants (Basel)* 12 (3), 547. doi:10.3390/antiox12030547

Wei, M., Zheng, Z., Shi, L., Jin, Y., and Ji, L. (2018). Natural polyphenol chlorogenic acid protects against acetaminophen-induced hepatotoxicity by activating ERK/Nrf2 antioxidative pathway. *Toxicol. Sci.* 162 (1), 99–112. doi:10.1093/toxsci/kfx230

WHO (2022). *Schistosomiasis and soil-transmitted helminthiases: progress report, 2021*. Weekly epidemiological record, No. 48, 97, 621–632. World Health Organization. Available at: https://www.who.int/publications/i/item/who-wer9748-621-632 (Accessed June 7, 2023).

Wynn, T. A., Thompson, R. W., Cheever, A. W., and Mentink-Kane, M. M. (2004). Immunopathogenesis of schistosomiasis. *Immunol. Rev.* 201, 156–167. doi:10.1111/j.0105-2896.2004.00176.x

Xiao, S. H., You, J. Q., Jiao, P. Y., and Mei, J. Y. (1994). Effect of early treatment of artemether against schistosomiasis in mice. *Zhongguo Ji Sheng Chong Xue Yu Ji Sheng Chong Bing Za Zhi* 12 (1), 7–12.

Xie, K., He, X., Chen, K., Chen, J., Sakao, K., and Hou, D. X. (2019). Antioxidant properties of a traditional vine tea, Ampelopsis grossedentata. *Antioxidants (Basel)* 8 (8), 295. doi:10.3390/antiox8080295

Xing, L., Zhang, H., Qi, R., Tsao, R., and Mine, Y. (2019). Recent advances in the understanding of the health benefits and molecular mechanisms associated with green tea polyphenols. *J. Agric. Food Chem.* 67 (4), 1029–1043. doi:10.1021/acs.jafc.8b06146

Xu, L., Ma, P., Xiao, W., Peng, Y., He, C., and Xiao, P. (2012). Preliminary lnvestigation into the ancient and modern application of vine tea. *Mod. Chin. Med.* 14 (04), 62–66. doi:10.13313/j.issn.1673-4890.2012.04.019

Yang, F., Luo, L., Zhu, Z. D., Zhou, X., Wang, Y., Xue, J., et al. (2017). Chlorogenic acid inhibits liver fibrosis by blocking the miR-21-regulated TGF-β1/smad7 signaling pathway *in vitro* and *in vivo*. *Front. Pharmacol.* 8, 929. doi:10.3389/fphar.2017.00929

Yang, F., Wang, Y., Xue, J., Ma, Q., Zhang, J., Chen, Y. F., et al. (2016). Effect of Corilagin on the miR-21/smad7/ERK signaling pathway in a schistosomiasis-induced hepatic fibrosis mouse model. *Parasitol. Int.* 65 (4), 308–315. doi:10.1016/j.parint.2016.03.001

Yang, Q. Q., Wei, X. L., Fang, Y. P., Gan, R. Y., Wang, M., Ge, Y. Y., et al. (2020). Nanochemoprevention with therapeutic benefits: an updated review focused on epigallocatechin gallate delivery. *Crit. Rev. Food Sci. Nutr.* 60 (8), 1243–1264. doi:10.1080/10408398.2019.1565490

You, J. Q., Mei, J. Y., and Xiao, S. H. (1992). Effect of artemether against Schistosoma japonicum. *Zhongguo Yao Li Xue Bao* 13 (3), 280–284.

Yu, Y., Wang, J., Wang, X., Gu, P., Lei, Z., Tang, R., et al. (2021). Schistosome eggs stimulate reactive oxygen species production to enhance M2 macrophage differentiation and promote hepatic pathology in schistosomiasis. *PLoS Negl. Trop. Dis.* 15 (8), e0009696. doi:10.1371/journal.pntd.0009696

Yuan, Y., Gong, X., Zhang, L., Jiang, R., Yang, J., Wang, B., et al. (2017). Chlorogenic acid ameliorated concanavalin A-induced hepatitis by suppression of Toll-like receptor 4 signaling in mice. *Int. Immunopharmacol.* 44, 97–104. doi:10.1016/j.intimp.2017.01.017

Zhai, Z. L., Zhang, Y., Liu, H. X., Feng, T., and Xiao, S. H. (2000). Effect of artemether on enzymes involved in carbohydrate metabolism of Schistosoma japonicum. *Zhongguo Ji Sheng Chong Xue Yu Ji Sheng Chong Bing Za Zhi* 18 (3), 162–164.

Zhang, L., and Wei, W. (2020). Anti-inflammatory and immunoregulatory effects of paeoniflorin and total glucosides of paeony. *Pharmacol. Ther.* 207, 107452. doi:10.1016/j.pharmthera.2019.107452

Zhang, L. X., Li, C. X., Kakar, M. U., Khan, M. S., Wu, P. F., Amir, R. M., et al. (2021a). Resveratrol (RV): a pharmacological review and call for further research. *Biomed. Pharmacother.* 143, 112164. doi:10.1016/j.biopha.2021.112164

Zhang, M., Zhao, R., Wang, D., Wang, L., Zhang, Q., Wei, S., et al. (2021b). Ginger (Zingiber officinale Rosc.) and its bioactive components are potential resources for health beneficial agents. *Phytother. Res.* 35 (2), 711–742. doi:10.1002/ptr.6858

Zhang, Q., Zhao, Y., Zhang, M., Zhang, Y., Ji, H., and Shen, L. (2021c). Recent advances in research on vine tea, a potential and functional herbal tea with dihydromyricetin and myricetin as major bioactive compounds. *J. Pharm. Anal.* 11 (5), 555–563. doi:10.1016/j.jpha.2020.10.002

Zhang, Y., Zhou, X., Yi, L., Peng, S., Zhang, Q., and Mi, M. (2018). Dihydromyricetin attenuates activation of hepatic stellate cells through TGF-B1/Smad signaling pathway. *J. Army Med. Univ.* 40 (04), 282–289. doi:10.16016/j.1000-5404.201709210

Zhou, C., Li, D., Ding, C., Yuan, Q., Yu, S., Du, D., et al. (2021a). Involvement of SIRT1 in amelioration of schistosomiasis-induced hepatic fibrosis by genistein. *Acta Trop.* 220, 105961. doi:10.1016/j.actatropica.2021.105961

frontiers | Frontiers in Pharmacology

TYPE Original Research
PUBLISHED 30 May 2024
DOI 10.3389/fphar.2024.1378249

OPEN ACCESS

EDITED BY
Rongrui Wei,
Jiangxi University of Traditional Chinese Medicine, China

REVIEWED BY
Gamal Salem,
Zagazig University, Egypt
Tushar Dhanani,
Florida Agricultural and Mechanical University, United States
Alaadin E. El-Haddad,
October 6 University, Egypt
Amal El-Feky,
National Research Centre, Egypt
Amany Abdel-Rahman Mohamed,
Zagazig University, Egypt
Amer Ali,
Cairo University, Egypt

*CORRESPONDENCE
Essa M. Saied,
essa.saied@science.suez.edu.eg

RECEIVED 29 January 2024
ACCEPTED 06 May 2024
PUBLISHED 30 May 2024

CITATION
Elshaer SE, Hamad GM, Sobhy SE, Darwish AMG, Baghdadi HH, H. Abo Nahas H, El-Demerdash FM, Kabeil SSA, Altamimi AS, Al-Olayan E, Alsunbul M, Docmac OK, Jaremko M, Hafez EE and Saied EM (2024), Supplementation of Saussurea costus root alleviates sodium nitrite-induced hepatorenal toxicity by modulating metabolic profile, inflammation, and apoptosis.
Front. Pharmacol. 15:1378249.
doi: 10.3389/fphar.2024.1378249

Supplementation of Saussurea costus root alleviates sodium nitrite-induced hepatorenal toxicity by modulating metabolic profile, inflammation, and apoptosis

Samy E. Elshaer[1], Gamal M. Hamad[2], Sherien E. Sobhy[3], Amira M. Galal Darwish[2,4], Hoda H. Baghdadi[1], Hebatallah H. Abo Nahas[5], Fatma M. El-Demerdash[1], Sanaa S. A. Kabeil[6], Abdulmalik S. Altamimi[7], Ebtesam Al-Olayan[8], Maha Alsunbul[9], Omaima Kamel Docmac[10], Mariusz Jaremko[11], Elsayed E. Hafez[3] and Essa M. Saied[12,13]*

[1]Department of Environmental Studies, Institute of Graduate Studies and Research, Alexandria University, Alexandria, Egypt, [2]Department of Food Technology, Arid Lands Cultivation Research Institute (ALCRI), City of Scientific Research and Technological Applications (SRTA-City), Alexandria, Egypt, [3]Department of Plant Protection and Biomolecular Diagnosis, Arid Lands Cultivation Research Institute (ALCRI), City of Scientific Research and Technological Applications (SRTA-City), Alexandria, Egypt, [4]Food Industry Technology Program, Faculty of Industrial and Energy Technology, Borg Al Arab Technological University (BATU), Alexandria, Egypt, [5]Zoology Department, Faculty of Science, Port Said University, Port Said, Egypt, [6]Department of Protein Research, Genetic Engineering and Biotechnology Research Institute (GEBRI), City of Scientific Research and Technological Applications (SRTA-City), Alexandria, Egypt, [7]Department of Pharmaceutical Chemistry, College of Pharmacy, Prince Sattam Bin Abdulaziz University, Alkharj, Saudi Arabia, [8]Department of Zoology, College of Science, King Saud University, Riyadh, Saudi Arabia, [9]Department of Pharmaceutical Sciences., College of Pharmacy, Princess Nourah bint Abdulrahman University, Riyadh, Saudi Arabia, [10]Anatomy and Embryology Department, Faculty of Medicine, Tanta University, Tanta, Egypt, [11]Smart-Health Initiative and Red Sea Research Center, Division of Biological and Environmental Sciences and Engineering, King Abdullah University of Science and Technology, Thuwal, Saudi Arabia, [12]Chemistry Department (Biochemistry Division), Faculty of Science, Suez Canal University, Ismailia, Egypt, [13]Institute for Chemistry, Humboldt Universität zu Berlin, Berlin, Germany

Sodium nitrite ($NaNO_2$) is a widely used food ingredient, although excessive concentrations can pose potential health risks. In the present study, we evaluated the deterioration effects of $NaNO_2$ additives on hematology, metabolic profile, liver function, and kidney function of male Wistar rats. We further explored the therapeutic potential of supplementation with *S. costus* root ethanolic extract (SCREE) to improve $NaNO_2$-induced hepatorenal toxicity. In this regard, 65 adult male rats were divided into eight groups; Group 1: control, Groups 2, 3, and 4 received SCREE in 200, 400, and 600 mg/kg body weight, respectively, Group 5: $NaNO_2$ (6.5 mg/kg body weight), Groups 6, 7 and 8 received $NaNO_2$ (6.5 mg/kg body weight) in combination with SCREE (200, 400, and 600 mg/kg body weight), respectively. Our results revealed that the $NaNO_2$-treated group shows a significant change in deterioration in body and organ weights, hematological parameters, lipid profile, and hepatorenal dysfunction, as well as immunohistochemical and histopathological alterations. Furthermore, the $NaNO_2$-treated group demonstrated a considerable increase in the expression

of TNF-α cytokine and tumor suppressor gene P53 in the kidney and liver, while a significant reduction was detected in the anti-inflammatory cytokine IL-4 and the apoptosis suppressor gene BCL-2, compared to the control group. Interestingly, SCREE administration demonstrated the ability to significantly alleviate the toxic effects of $NaNO_2$ and improve liver function in a dose-dependent manner, including hematological parameters, lipid profile, and modulation of histopathological architecture. Additionally, SCREE exhibited the ability to modulate the expression levels of inflammatory cytokines and apoptotic genes in the liver and kidney. The phytochemical analysis revealed a wide set of primary metabolites in SCREE, including phenolics, flavonoids, vitamins, alkaloids, saponins and tannins, while the untargeted UPLC/T-TOF−MS/MS analysis identified 183 metabolites in both positive and negative ionization modes. Together, our findings establish the potential of SCREE in mitigating the toxic effects of $NaNO_2$ by modulating metabolic, inflammatory, and apoptosis. Together, this study underscores the promise of SCREE as a potential natural food detoxifying additive to counteract the harmful impacts of sodium nitrite.

KEYWORDS

food additives, sodium nitrite, Saussurea costus, phytochemical profile, hepatorenal protective, metabolic analysis, histopathology analysis, immunohistochemistry analysis

1 Introduction

Food additives are natural or synthetic substances that are incorporated into food products to preserve or enhance their flavor, appearance, and taste (Yılmaz et al., 2009; Bari and Yeasmin, 2018). There are several types of additives, including emulsifiers, stabilizers, preservatives, and coloring agents (Wu et al., 2022). Sodium nitrite is a key component in food additives, commonly used in meat, fish, and certain cheeses for coloring, preservation, and antibacterial agent, and also imparts flavor and color to meat (Osman et al., 2021; Cvetković et al., 2019). Its inhibitory effect on the synthesis of iron-sulfur complexes, particularly notable in frozen meats, effectively suppresses the development of *clostridium botulinum* spores (Milkowski et al., 2010). The vibrant color in meat is the result of the reaction of sodium nitrite with myoglobin that leads to the formation of nitrosyl myoglobin (Sindelar and Milkowski, 2012). Moreover, sodium nitrite effectively delays the onset of oxidative rancidity by binding to heme proteins and metal ions and neutralizing free radicals (Sullivan et al., 2012). However, sodium nitrite can also react with amines and amides in gastric juices, leading to the formation of nitrosamines, potent carcinogens. In addition, this reaction results in the production of free radicals, further complicating the potential health implications of sodium nitrite consumption (Hassan and Ali, 2010; Hassan and Yousef, 2010). Nitrite is also a potent generator of nitric oxide with harmful biological effects (Jensen, 2007). Prolonged consumption of sodium nitrite in food has the potential to induce tissue damage, cardiac toxicity, hepatotoxicity, nephrotoxicity, inflammation, fibrosis, and apoptosis (Hassan et al., 2009; Hassan et al., 2010; El-Sheikh and Khalil, 2011; Salama et al., 2013; Al-Gayyar et al., 2015; Fadda et al., 2018a). Consequently, the rise of considerable environmental and health concerns underscores the importance of intensifying efforts towards the innovation of new and safe food additives and preservatives. These innovations aim to mitigate the deteriorative impact associated with the use of sodium nitrite additives.

Phytochemical substances or secondary metabolites continue to be considered the most promising options. Recent research has placed increasing emphasis on the importance of secondary metabolites in plants, given their numerous biological and medicinal applications. Natural products continue to be a significant source of innovation in drug discovery (Abdallah et al., 2017). Dolomiaea costus (Falc.) Kasana and A.K. Pandey [Asteraceae], a member of the Asteraceae family commonly known as Saussurea costus (Falc.) Lipsch. and Saussurea lappa (Decne.) Sch. Bip is a highly prevalent botanical species employed for several therapeutic purposes. The primary metabolites of Saussurea costus (S. costus) are sesquiterpene lactones, specifically costunolide, dehydrocostus lactone, and cynaropicrin (Abd El-Rahman et al., 2020). The Saussurea genus encompasses many species that are known to contain sesquiterpene lactones, triterpenes, steroids, lignans, and flavonoids. It is worth noting that certain metabolites within this group have intriguing biological activity (Julianti, 2014; Attallah et al., 2023). The essential oil of the roots of S. costus is mainly composed of sesquiterpenoids, which account for approximately 79.80% of its total composition (Hanh et al., 2021). Costunolide, a sesquiterpene lactone that is commonly obtained from the roots of S. costus, exhibits a wide spectrum of biological activity, including antioxidant, anti-inflammatory, neuroprotective, and antidiabetic effects (Moujir et al., 2020). The roots of S. costus were shown to contain acetylated flavone glycosides, palmitic and linoleic acids, as well as chlorogenic acid (El Gizawy et al., 2022). Recent studies have demonstrated that these metabolites exhibit various biological properties, including antifungal (Barrero et al., 2000), antidiabetic, anticancer, and antiprotozoal (Ko et al., 2005), immunostimulant (Kulkarni, 2001), antiulcer (Sutar et al., 2011), antimicrobial (Khalid et al., 2011), anti-inflammatory (Sunkara et al., 2010) and anti-hepatotoxic (Yaeesh et al., 2010) activities. In a recent study conducted by Deabes et al. (2021), it was shown that extracts derived from S. costus have notable efficacy in combating multiantibiotic-resistant human infections. These findings suggest that these extracts could serve as a viable

alternative to antibiotics for the treatment of certain infections. Elshaer et al. (2022) investigated the impact of three distinct extracts derived from roots of S. costus, namely, ethanol, methanol, and water when used as a food additive.

To comprehensively analyze the diverse chemical classes and properties, as well as the wide range of metabolite concentrations in plants, it is necessary to utilize a diverse range of analytical techniques in plant metabolomics. Liquid chromatography tandem mass spectrometry (LC-MS/MS) is a robust analytical technique widely used for the identification and characterization of plant metabolites (Lu et al., 2008). Various LC-MS-based metabolomics platforms have been developed so far for the targeted analysis of primary metabolites (Sawada et al., 2009), photosynthetic intermediates (Arrivault et al., 2009), lipids and fatty acids (Okazaki et al., 2013; Bromke et al., 2015), phytohormones (Seo et al., 2011), secondary metabolites (Tohge and Fernie, 2010), and untargeted metabolome analysis (Shahaf et al., 2016). Analytical approaches are based on untargeted mass spectrometry. The application of advanced liquid chromatography tandem mass spectrometry (LC-MS/MS), distinguished by its exceptional resolution, has enabled thorough exploration of the metabolome in diverse biological samples, including those from herbal medicine. Through the analysis of mass fragmentation (MS/MS) spectra, valuable information on the structural characteristics of metabolites can be inferred from their unique spectral patterns (Beniddir et al., 2021).

Given the wide range of biological activity exhibited by the *S. costus* extract and our ongoing efforts to discover new bioactive molecules with pharmacological potential (Samaha et al., 2020; Khirallah et al., 2022; Salem et al., 2022; Mohamed et al., 2022a; Mohamed et al., 2022b), in this study, we aimed to gain insight into the hepatorenal deterioration effect of sodium nitrite additive in an animal model and to explore the possible protective activity of 70% SCREE to ameliorate these effects. In this regard, we performed several analytical techniques to characterize phytochemical metabolites in SCREE employing several chemical and analytical techniques (HPLC and UPLC/T-TOF–MS/MS-based analysis). Furthermore, we unveiled the possible hepatorenal protective potency of SCREE against NaNO2-induced liver and kidney toxicity by performing multiinformative molecular network analysis including hematological, molecular, metabolic, differential display PCR, histopathological, and immunohistology evaluations.

2 Materials and methods

2.1 Materials

The roots were obtained from an herbal establishment (Mady Herbs) located in Alexandria, Egypt. Subsequently, these roots were subjected to scrutiny, identification, and validation by a plant taxonomy specialist; Assoc. Prof. Maha Elshamy, Department of Botany, Faculty of Science, Mansoura University, Egypt. A voucher specimen (MU_B_Sc10) was kept at the Department of Botany. The roots obtained were recognized and authenticated as Dolomiaea costus (Falc.) Kasana and A.K. Pandey [Asteraceae], a member of the Asteraceae family commonly known as Saussurea costus (Falc.) Lipsch. and Saussurea lappa (Decne.) Sch. Bip. Sodium nitrite was obtained from El-Gomhouria Company for the Trading of Drugs, Chemicals, and Medical Supplies, located in Alexandria, Egypt. Methanol and formic acid (LC-MS grade) were obtained from Fischer Scientific (UK). Acetonitrile (LC-MS grade) was obtained from Sigma-Aldrich (Germany).

2.2 Collection and extraction of S. Costus roots

The ethanol extract was prepared as described by Elshaer et al. (2022), the roots were dried in an oven at 65°C for 3 days and ground to a fairly coarse powder as previously reported by Srivastava et al. (2012). The powder was then carefully kept in sealed containers to prevent exposure to air, ensuring its preservation for subsequent use in the extraction procedure. The powder (400 g) obtained was immersed in 1 L of ethanol (70%) at room temperature and left to soak for 3 days. The solution was subjected to filtration using a Whatman grade-1 filter paper in a funnel under vacuum. Subsequently, the filtrate underwent the rotary evaporation process, in which the liquid was dried and evaporated under conditions of reduced pressure. The crude ethanolic extract of roots of S. costus was obtained and subjected to lyophilization to obtain a dry powder (36 g, 9% wt/wt) (Tag et al., 2016a). Subsequently, the samples were stored at 4°C until use.

2.3 Quantitative assessment of chemical metabolites

The identification and detection of active metabolites in the SCREE was achieved by using chemical assays. Various phytochemicals, including phenolics, flavonoids, alkaloids, saponins, and tannins, were identified using established testing methods.

2.3.1 Phenolics detection

The fat-free specimen was subjected to a boiling process with 50 mL of ether to extract the phenolic metabolite, with the extraction process lasting 15 min. A volume of 5 mL of the extract was transferred using a pipette into a 50 mL flask, followed by the addition of 10 mL of distilled water. In addition, a 2 mL aliquot of ammonium hydroxide solution and 5 mL of concentrated amyl alcohol were introduced. The samples were prepared and then allowed to undergo 30 min of reaction to facilitate color development. The measurement was carried out at a wavelength of 505 nm (Edeoga et al., 2005).

2.3.2 Flavonoids detection

A plant sample weighing 10 g was subjected to multiple extractions using 100 mL of 80% aqueous methanol solution at ambient temperature. The entire solution was subjected to filtration using Whatman filter paper with a diameter of 125 mm. Subsequently, the filtrate was transferred to a crucible and subjected to evaporation until complete dryness was achieved using a water bath. The resulting residue was then repeatedly weighed until a consistent weight was obtained (Boham and Kocipai-Abyazan, 1974; Edeoga et al., 2005).

2.3.3 Alkali detection

Five g of the sample was placed in a beaker with a volume of 250 mL, subsequently; 200 mL of the solution (10% acetic acid in ethanol) was added to the beaker and incubated for 4 h at room temperature. The solution was filtered, followed by concentration in a water bath, resulting in a final volume that was one quarter of the initial volume. The extract was subjected to dropwise addition of concentrated ammonium hydroxide until precipitation reached completion. The entire solution was allowed to undergo sedimentation, and subsequently, the resulting solid was gathered and subjected to a rinsing process utilizing a solution of diluted ammonium hydroxide. Following this, the solids were separated from the solution through filtration. The alkaloid, which had been dried and measured, constitutes the residual (Mir et al., 2016).

2.3.4 Saponin detection

A conical flask was used to contain a total of 20 g of the sample, which was then combined with 100 mL of aqueous ethanol solution with a concentration of 20%. The samples were subjected to a heating process for a duration of 4 h while continuously stirred, using a 55°C water bath. The solution was subjected to filtration and the remaining solid was subsequently subjected to another extraction using an additional 200 mL of 20% ethanol. The mixed extracts were concentrated to a final volume of 40 mL using a water bath maintained at 90°C. The concentrated solution was carefully transferred into a separatory funnel with a volume of 250 mL. Subsequently, 20 mL of diethyl ether was added to the funnel and violently agitated. The aqueous phase was retrieved and the ether phase was discarded. Sixty microliters of n-butanol was added. The n-butanol extracts were mixed and subjected to two washes using 10 mL of a 5% aqueous sodium chloride solution. The solution that remained was subjected to heating using a water bath. Following the evaporation process, the samples were dried in an oven until a consistent weight was achieved. Subsequently, the saponin content was calculated (Obadoni and Ochuko, 2002).

2.3.5 Tannin detection

A quantity of 500 mg of the sample was measured and placed in a plastic bottle with a volume of 50 mL. A volume of 50 mL of distilled water was added and stirred for 1 h. The solution was carefully transferred to a volumetric flask with a capacity of 50 mL and then adjusted to the required volume. Next, 5 mL of the filtered solution was transferred using a pipette into a test tube. Subsequently, it was combined with a volume of 2 mL of a solution containing 0.1 M FeCl3 in 0.1 N HCl and 8 mM potassium ferrocyanide. The absorbance measurement was conducted at a wavelength of 120 nm for 10 min (Robinson and Van Burden, 1981).

2.4 Evaluation of extract proximate composition

2016 AOAC procedures were used, although with minor modifications, to conduct chemical analysis on extract samples, specifically focusing on protein, lipid and ash content (Al-Zayadi et al., 2023). The crude protein content of the materials was determined by the Kjeldahl procedure. Furthermore, the weight of the powdered material was determined using Soxhlet. The determination of the crude fat content of the extract was performed using petroleum ether. The quantity of ash produced is determined by subjecting the substance to combustion at 500°C for 2 h. The quantification of the carbohydrate content was carried out using the methodology proposed by DuBois et al. (1956). This involved the conversion of carbohydrates into furfural derivatives through dehydration, followed by their reaction with phenol to provide a color that could be measured at a wavelength of 490 nm.

2.5 Assessment of phenol metabolites by HPLC analysis

The ethanolic root extract of S. costus was subjected to HPLC analysis using an Agilent 1,260 series to quantify phenolic metabolites (Elshaer et al., 2022). The separation was performed using a Kromasil C18 column of 4.6 mm by 250 mm by 5 mm. The mobile phase consisted of water (A) and 0.05% trifluoroacetic acid in acetonitrile (B), which was flowing at a rate of 1 mL/min. The following linear gradient was sequentially coded into the mobile phase: 12–15 min (85% A), 15–16 min (82% A), 0 min (82% A), 0–5 min (80% A), 5–8 min (60%) and 8–12 min (60%). The wavelength detector was monitored at 280 nm. Specifically, for each of the test solutions, 10 µL of injection volume was used. The column was maintained at a temperature of 35°C (Kolaylı et al., 2010). All standards, including gallic acid, catechin, methyl gallate, chlorogenic acid, caffeic acid, pyro catechol, syringic acid, rutin, coumaric acid, ellagic acid, vanillin, naringenin, ferulic acid, taxifolin and kaempferol, were injected after dissolved in ethanol. The concentration of phenolic metabolites was calculated on the basis of the area under the peak of the standards, and their identities were established by comparing the retention times and UV-vis spectra of the metabolites to those of the standards.

2.6 Untargeted metabolomic analysis by ultraperformance liquid chromatography (UPLC/T-TOF−MS/MS)

Analysis was carried out using an Exion LC Triple TOF 5600+ system manufactured by SCIEX in Framingham, MA, USA. The system was run at a temperature of 40°C and was fitted with an X-select HSS T3 C-18 column provided by Waters Corporation in Milford, CT, USA. The column had dimensions of 2.1 × 150 mm and a particle size of 2.5 µm. Furthermore, a pre-column consisting of Phenomenex In-Line filter discs with dimensions of 0.5 µm × 3.0 mm was used. A SCREE solution (50 mg) was prepared by dissolving it in a solvent working solution consisting of MilliQ water, methanol and acetonitrile in a 50:25:25 ratio. The resulting solution was subjected to sonication for 10 min, followed by centrifugation at a speed of 10,000 rpm for 10 min. The stock solution, consisting of 50 µL, was diluted by adding 1,000 µL of the working solvent. SCREE metabolites were subjected to analysis using UPLC/T-TOF–MS/MS in both negative and positive ionization modes (Eissa et al., 2020). Samples (10 µL), with a concentration of 1 µg/µL were introduced into the system using the designated mobile phases. In the negative mode, solvent A consisted of a 5 mM ammonium format buffer at pH 8, prepared using NaOH, with the addition of 1% methanol. In contrast, in the positive mode, solvent A consisted of a 5 mM

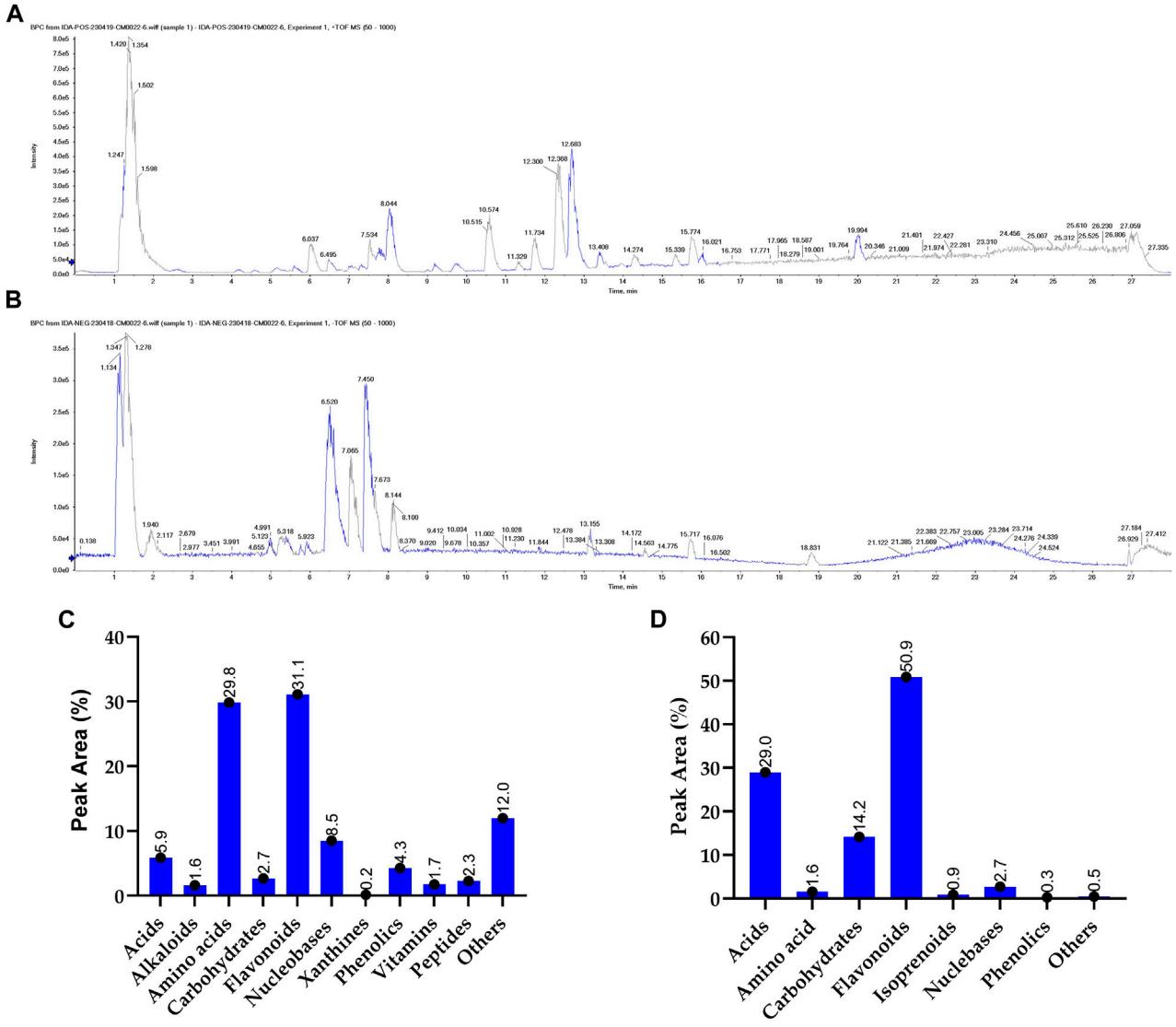

FIGURE 1
Untargeted metabolomic analysis of SCREE by UPLC/T-TOF-MS/MS analysis. The base peak chromatogram of SCREE in the positive **(A)** and negative **(B)** electrospray ionization modes. The classification of the identified primary metabolites in the positive **(C)** and negative **(D)** ionization modes.

ammonium format buffer at pH 3, prepared using formic acid, with the inclusion of 1% methanol. In both modes, solvent B consisted of 100% acetonitrile. The gradient elution procedure was executed in the following manner: The chromatographic method employed in this study involved a series of solvent compositions. The solvent composition was initially established at a ratio of 90% solvent A to 10% solvent B for 0–1 min. Subsequently, a linear gradient was applied, transitioning from 90% solvent A to 10% solvent A and 90% solvent B over 1.1–20.9 min. Following this gradient, the solvent composition was held isocratic in a 10% solvent A to 90% solvent B ratio for 21–25 min. Finally, the solvent composition was kept isocratic at 90% solvent A and 10% solvent B for 25.1–28 min. The recorded flow rate was 0.3 mL/min. A blank sample consisting of the working solvent (10 μL) was injected. Metabolites identified were documented using the Analyst TF 1.7.1 program, Peak view 2.2 software (SCIEX, Framingham, MA, USA), and MS-DIAL 3.70 software for data processing (Tsugawa et al., 2015). Mass spectrometry (MS) analysis was performed using a Triple TOF 5600+ system with a Duo-Spray source working in the electrospray ionization (ESI) mode, manufactured by AB SCIEX in Framingham, MA, USA. The mass range covered during the analysis ranged from 50 to 1,100 m/z. The process of characterization of compounds involved generating a candidate formula while adhering to a mass accuracy restriction of 10 ppm. Additionally, other factors such as retention time (Rt), MS2 data, databases, and reference literature were taken into account (Singh et al., 2017).

2.7 Experimental design

Adult male Wistar Albino rats weighing 160–180 g (9–11 weeks old) were donated by the Animal House of the Institute of Graduate Studies and Research at Alexandria University in Alexandria, Egypt.

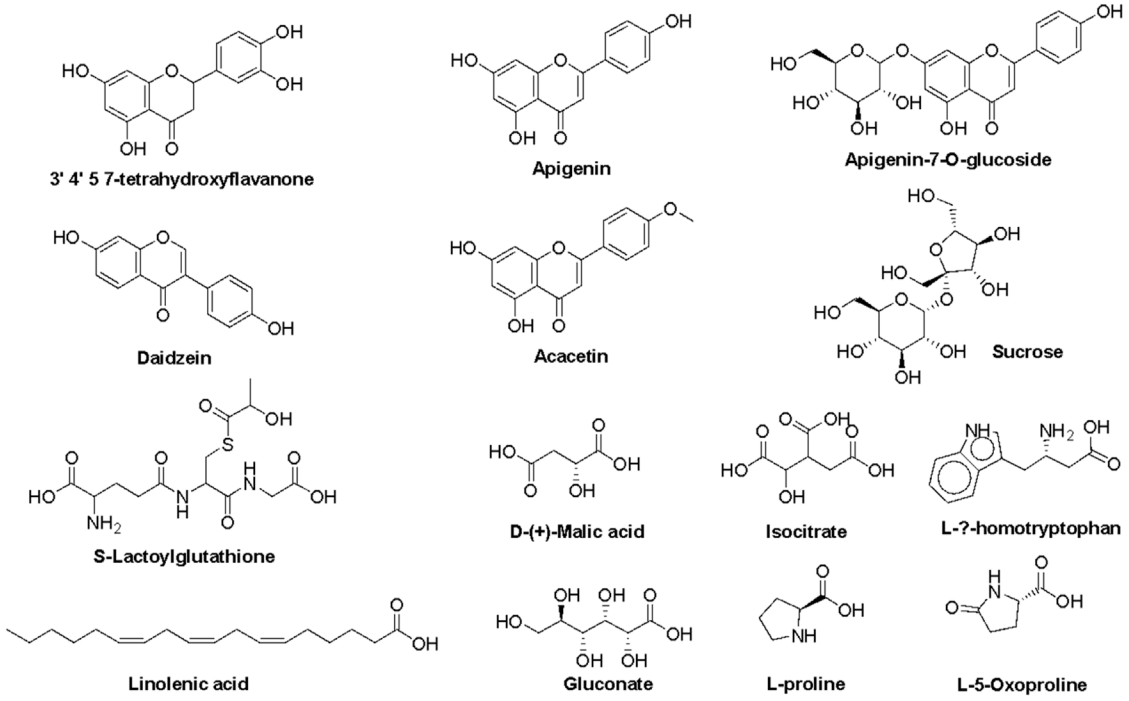

FIGURE 2
Representative metabolites tentatively detected in the roots of the ethanol extract of S. costus using a UPLC/T-TOF–MS/MS spectrometer.

The Local Ethics Committee and the Animal Research Committee authorized the study design and the Laboratory Animal Care Guidelines from the National Institutes of Health (NIH) were followed when handling the animals. (AU14-210126-2-3). The animals were housed in cages with good ventilation and 12-h light/dark cycles every day that ranged in temperature from 20° to 25°C. The rats were supplemented daily with a standard pelleted diet and water *ad libitum*. The animals underwent 2 weeks of monitoring before the study to ensure their successful adaptation. Randomly, eight equal groups of rats were formed, each of seven: Group 1 received distilled water (1 mL/kg body weight), Group 2 received SCREE (200 mg/kg body weight) (Tag et al., 2016a), Group 3 received SCREE (400 mg/kg body weight) (Tag et al., 2016a), Group 4 received SCREE (600 mg/kg body weight) (Tag et al., 2016a), Group 5 was treated with sodium nitrite (NaNO2, 6.5 mg/kg body weight, 1/25 LD50) (Fouad et al., 2017; Abo-EL-Sooud et al., 2019), Groups 6, 7 and 8 received NaNO2 (6.5 mg/kg body weight, 1/25 LD50) in combination with SCREE (200, 400, and 600 mg/kg body weight), respectively. Rats were given NaNO2 and SCREE daily by oral gavage for 28 days. After the experiment, the rats fasted for 12 h before taking blood samples. The rats were hypnotized with isoflurane, sacrificed and then blood, livers, and kidneys were collected for different analyzes.

2.8 Body weight, body weight gain (BWG) and weight of the organs

Rat weights were observed before and after the experimental period, and BWG was also calculated. After scarification, both the liver and kidney weight of the rat were recorded.

2.9 Blood and serum samples

Blood samples were collected through heart piercing and allowed to coagulate for 30 min at 25°C prior to centrifuging for 15 min at 3,000 xg, and the clear serum was carefully separated and stored at −20°C for further analysis. Other blood samples were obtained in EDTA tubes for full blood count (CBC) analysis using an automated analyzer (ABX Micros 60 automated hematologic analyzer, HORIBA ABX Diagnostic Company, France).

2.10 Biochemical investigations of liver function biomarkers

Initially, an examination is conducted to assess the impact of SCREE on liver function in Albino rats treated with sodium nitrite. Rat serum was tested using kits available for purchase from the Cairo Biodiagnostic Company to assess the action of liver aminotransferase action AST; EC 2.6.1.1, CATALOG NO. AS 10 61 and ALT; EC 2.6.1.2, CATALOG NO. AL 10 31, alkaline phosphatase (ALP; EC 3.1.3.1) CATALOG NO. AP 10 20, albumin (CATALOG NO. AB 10 10) and gamma-glutamyl transferase (GGT) (CATALOG NO. GGT 124030) as an additional to the total bilirubin level (CATALOG NO. BR 1111).

2.11 Biochemical investigations of kidney function biomarkers

Second, a comprehensive evaluation is performed to analyze the influence of SCREE on renal function of Albino rats that have

TABLE 1 The main metabolites present in the ethanolic extract of the roots of S. costus (SCREE) were tentatively identified using UPLC/T-TOF–MS/MS in positive and negative ionization modes.

Title	RT (min)	Precursor (m/z)	Area	Error (PPM)	Adduct	Reference (m/z)	Formula	Ontology
D-(+)-Malic acid	0.8788	133.0137	5064285	−0.8	[M-H]-	133.01425	$C_4H_6O_5$	Beta hydroxy acids and derivatives
Gluconate	0.9553	195.05	2141325	3.1	[M-H]-	195.05103	$C_6H_{12}O_7$	Medium-chain hydroxy acids and derivatives
S-Lactoylglutathione	0.9894	380.0954	821,613	0.6	[M + H]+	380.11221	$C_{13}H_{21}N_3O_8S$	Oligopeptides
Choline	1.0284	104.1072	3664216	−0.3	[M]+	104.10645	$C_5H_{14}NO$	Cholines
L-β-homotryptophan-HCl	1.0922	219.0265	2495170	0.4	[M + H]+	219.11281	$C_{12}H_{14}N_2O_2$	Beta amino acids and derivatives
Sucrose	1.1089	341.1085	8329249	0.7	[M-H]-	341.10895	$C_{12}H_{22}O_{11}$	O-glycosyl compounds
L-proline	1.1432	116.0685	6683844	14.6	[M + H]+	116.0706	$C_5H_9NO_2$	Proline and derivatives
Adenosine 3':5'-cyclicmonophosphate	1.5327	330.0566	1103257	6.5	[M + H]+	330.05978	$C_{10}H_{12}N_5O_6P$	3′,5′-cyclic purine nucleotides
L-5-Oxoproline	1.6112	130.0489	882,512	1.8	[M + H]+	130.04987	$C_5H_7NO_3$	Alpha amino acids and derivatives
Apigenin-7-O-glucoside	7.7027	431.101	3585188	−4.3	[M-H]-	431.09836	$C_{21}H_20O_{10}$	Flavonoid-7-O-glycosides
Isocitrate	8.5081	191.035	2382439	−0.2	[M-H]-	191.01973	$C_6H_8O_7$	Tricarboxylic acids and derivatives
3′4′5 7-tetrahydroxyflavanone	10.9264	289.1409	1126044	0.5	[M + H]+	289.07068	$C_{15}H_{12}O_6$	Flavanones
Acacetin	11.0540	285.0754	1473894	1	[M + H]+	285.07574	$C_{16}H_{12}O_5$	4′-O-methylated flavonoids
Apigenin	13.3821	269.0452	38379868	0.8	[M-H]-	269.04553	$C_{15}H_{10}O_5$	Flavones
Daidzein	16.8737	255.1357	3149348	0.3	[M + H]+	255.06519	$C_{15}H_{10}O_4$	Isoflavones
γ-Linolenic acid	19.0706	277.2178	15435236	−0.7	[M-H]-	277.21732	$C_{18}H_{30}O_2$	Lineolic acids and derivatives

received sodium nitrite. The determination of serum levels of urea (CATALOGUE NO. URE 18100), creatinine (CATALOGUE NO. CRE 106100) and uric acid (CATALOGUE NO. UA 119240) was conducted using commercially available kits provided by Egy Chem for Lab Technology Company, located in Cairo, Egypt.

2.12 Biochemical investigation of the lipid profile

At the same time, we examined the impact of SCREE on the lipid profile to investigate its hepatoprotective effect against sodium nitrite-induced damage. A commercial kit from Biodiagnostic Company, Cairo, Egypt, was used to estimate the lipid profile, which included the concentrations of total cholesterol (CATALOG NO. CH 12 20), triglycerides (CATALOG NO. TR 20 30), high-density lipoprotein cholesterol (HDL-C) (CATALOG NO. CH 12 30), low-density lipoprotein cholesterol (LDL-C) (CATALOG NO. CH 12 31), and the very low-density lipoprotein -cholesterol (VLDL-C) concentration was calculated from the following equation.

$$VLDL - C = TG/5$$

2.13 Determination of the serum alpha-fetoprotein tumor marker

In this study, we investigated the hepatoprotective effect of SCREE (Sodium Nitrite-induced liver damage) by examining its impact on the level of AFP (Alpha-Fetoprotein). Elevated levels of alpha-fetoprotein (AFP) can be observed in benign and malignant liver conditions. Alpha-fetoprotein (AFP) is a tumor marker for the detection and diagnosis of liver, testicles, and ovary cancers and was estimated using kits from the Egyptian Company for Biotechnology (SAE) (CATALOG NO. 1317 001). This assay is a solid-phase enzyme immunoassay in the "sandwich" style that is based on an antigen-antibody complex that is created when a sample containing AFP is added to the wells, where it binds to the two antibodies.

2.14 Determination of C-reactive protein

To investigate SCREE's renal protective effect against sodium nitrite-induced damage, we looked at how it affected the level of CRP. The levels of C-reactive protein have been observed to increase

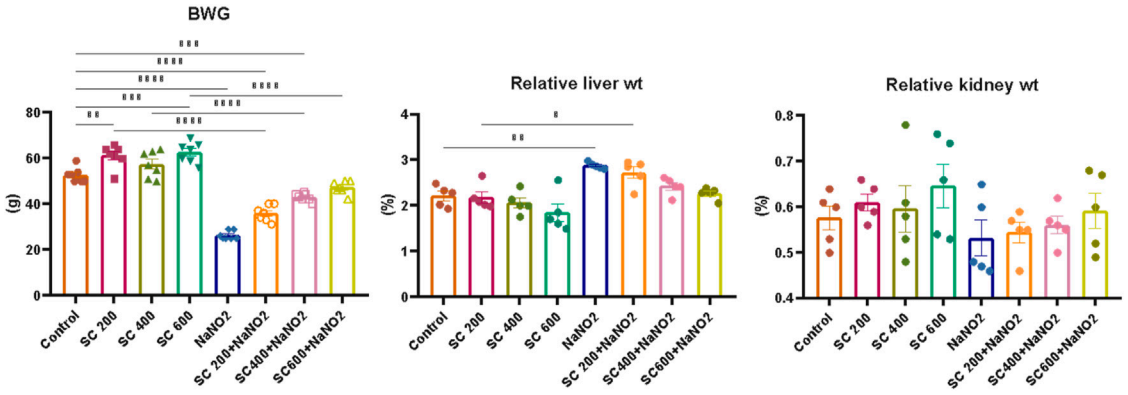

FIGURE 3
Effects of SCREE administration on organ weight, body weight, and body weight gain (BWG) of NaNO2-treated male rats. The results of the statistical tests were reported as mean ± SEM (n = 7). Multiple comparisons were analyzed by one-way ANOVA followed by Tukey's multiple comparison test. Differences between groups were considered significant when $p < 0.05$ (*$p < 0.05$, **$p < 0.01$, ***$p < 0.001$ and ****$p < 0.0001$). Significant data included for each group compared to the control group and for SCREE groups (SCREE 200, SCREE 400, SCREE 600) each compared to its respective treated group (SCREE 200+ NaNO2, SCREE 400+ NaNO2, SCREE 600+ NaNO2).

in correlation with deterioration of renal function. Nephelometry was used to determine an inflammation marker in rat serum based on CRP (CATALOG NO. 52009002) and was estimated using a commercial kit from AGAPPE Diagnostics Switzerland GmbH.

2.15 Molecular analysis using quantitative real-time PCR (Q-RTPCR)

2.15.1 Extraction of RNA and production of cDNA

According to the manufacturer's instructions (Wang et al., 2009), we used Trizol reagent (easy-BLUETM, INTRON Biotechnology, Korea, CATALOG No.17061) to extract total RNA from liver and kidney tissues. Finally, the total RNA was eluted using 20 L of RNase-free water. RNA concentrations and purity were evaluated using a UV spectrophotometer (Nanodrop 8,000, Thermo Scientific, USA). Reverse-transcribed total RNA was used to create cDNA in a 20-L reaction with the following components: A total of 20 L of sterile water, 3 L of total RNA, 2.5 L of dNTP (10 mM), 2.5 L of buffer (10x), 0.3 L of reverse transcriptase, and 5 L of oligo-dT primer were added to the reaction mixture. The completed mixture of the reaction was put into a thermal cycler and subjected to the following cycle: 2 h at 37°C, 20 min of inactivation at 65°C, and then storage at −20°C.

2.15.2 Real-time polymerase chain reaction

The determination of the liver and kidney (IL-4), (P53), (BCL-2), and (TNFα) gene expressions by qRTPCR was performed according to the procedure of (Fan and Robetorye, 2010). Q-RTPCR was performed using an (SYBR® Green PCR Master Mix Kit, CATALOG NO. RT500S) (Fermentas, USA) to examine the expression levels of the genes (IL-4), (P53), (BCL-2), and (TNF-α) genes, both in liver and kidney tissues, the primer sequences of the genes tested are shown in (Table 1). Internal controls were performed using the housekeeping gene, -actin. Several reactions were carried out in a 25 µL mixture, which contained 1 µL of 10 pmol/µ1 of each primer, 1 µL of template cDNA (50 ng), 12.5 µL of 2X SYBR Green PCR Master Mix, and 9.5 µL of nuclease-free water. Before loading the samples into the rotor wells, the samples were spun and a triple of each sample was tested (Supplementary Table S1). During the completion of the 10 min of 95° amplification, there were 40 cycles of denaturation at that temperature for 15 s, followed by 30 s of annealing at 60° and 30 s of extension at 72°. The melting curves were acquired after the cycle process to stop the manufacture of generic goods. Data collection took place during the extension process. A RotorGene 6,000 (QIAGEN, ABI System, USA) was utilized for the reaction. The primers utilized in this study are listed in (Table 1). The gene expression results were analyzed using the 2-ΔΔCTmethod (Livak and Schmittgen, 2001). For three separate amplifications, the data were reported as mean fold changes ±standard error.

2.15.3 Differential display-polymerase chain reaction (DD-PCR)

DD-PCR is an effective method used to investigate the up- and downregulated genes that the treatment affects compared to the control, and DD-PCR was approached on cDNA extracted from the examined animals, blood or tissues, as a template. Furthermore, the conditions for the reaction were carried out according to (Hafez et al., 2013). The total reaction volume is 25 µL containing 2.5 µL 10X Taq buffer, 2.5 µL MgCl2, 2.5 µldNTPs, 1 U Taq DNA polymerase (CAT. No. MB101-0500), 3 µL of 10 pmol of arbitrary primers separately and 2 µL of each cDNA and finally 12 µL of sterile dH2O. The amplification program looked like this; one cycle at 94°C for 5 min (hot start), followed by 40 cycles at 94°C for 1 min, 35°C for 1 min, and 72°C for 1min, and finally extension step at 72°C for 10 min. The down- and up-expressed genes were removed from the 2% agarose gel after the PCR results were imaged using a gel documentation system (Gel Doc, 2000). The sequences of primers used are listed in Table 1, and the examinations were carried out on the quantity and size of the amplified fragments according to (Liang and Pardee, 1992; Hamad et al., 2018).

2.16 Histological and immunohistochemical investigation

For histological analysis using hematoxylin and eosin stain, the kidney and liver were fixed in a 10% buffer neutral formalin solution and handled to create serial paraffin segments, which were then viewed with a light microscope according to (Bancroft et al., 1990). Using DAB staining and the Avidin-Biotin Peroxidase (ABC) immunohistochemical method, the transforming growth factor-beta (TGF-β) protein (TGF-) in liver tissue was determined in deparaffinized sections (5 μm) (Buchwalow and Böcker, 2010).

2.17 Statistical evaluation

All data are shown as mean ± SE. All analyzes were performed using the Social Sciences Statistical Package, the parameters calculated for the Social Sciences (SPSS) program Version 16.0. Multiple comparisons were analyzed using one-way analysis of variance (ANOVA) followed by Tukey's multiple comparison test to assess the data and determine how the groups differed from each other using GraphPad Prism nine software (GraphPad Software, San Diego, CA, USA). The p values were assigned significant if < 0.05 (*, * and ** representing $p < 0.05$, $p < 0.01$, $p < 0.001$ and $p < 0.0001$, respectively).

3 Results and discussion

3.1 Chemical metabolites and proximate analysis of roots of S. Costus

We focus primarily on exploring the phytochemical metabolites of SCREE. Toward this end, we conducted several chemical and analytical assays to gain valuable insight into the root composition and its potential pharmacological applications. As shown in (Supplementary Figure S1), our analysis revealed that SCREE consists of 0.26 g/mL of proteins, 19.26 mg/g of crude lipids, and 3.29 mg/g of carbohydrates, as well as a ash content of 4.72%. While the protein content may be relatively low, the substantial presence of crude lipids and carbohydrates, along with the mineral composition, underscores the potential nutritional and medicinal value of the roots of S. costus. The relatively high presence of crude lipids suggests the presence of fats, which could be important for energy storage and the absorption of fat-soluble vitamins. The carbohydrate content provides information on the energy potential of these roots, and the ash content reflects the mineral composition, which is important for both nutritional and medicinal considerations, as minerals play a crucial role in various physiological functions. Further exploration of metabolite constituents revealed that S. costus roots show notable concentrations of phenolic (58.85 mg/g) and flavonoid metabolites (97.15 mg/g). Phenolic and flavonoids are well recognized for their antioxidant properties (Tungmunnithum et al., 2018), indicating that these roots may possess potential health benefits and therapeutic applications. Additionally, SCREE demonstrated a considerable concentration of alkaloids (0.267 mg/g) and saponins (27.35 mg/g), suggesting the chemical diversity of the roots of S. costus that can facilitate a range of applications, from dietary supplementation to the development of traditional and alternative medicine. Taken together, the presence of macronutrients such as lipids, carbohydrates, and bioactive metabolites, notably phenolics and flavonoids, in SCREE underscores the multifaceted applications of the roots of S. costus in dietary and medicinal contexts. The findings of the phytochemical analysis indicate that the plant exhibits promising characteristics regarding its potential anti-inflammatory, antibacterial, and antioxidant capabilities (Kumar and Pundir, 2022). The primary source of natural antioxidants is derived from plants, predominantly in the form of phenolic chemicals, including flavonoids, phenolic acids, and tocopherols (Asif, 2015). Flavonoids exhibit notable antioxidant properties, anti-inflammatory and anticarcinogenic effects (Saleh-e-In et al., 2016; Vignesh et al., 2021). Tannins are multifaceted metabolites that exhibit a wide range of pharmacological properties, including antioxidant, antibacterial, and anti-inflammatory effects (Saif-Al-Islam, 2020). Saponins have been found to exhibit protective effects against conditions such as hyperglycemia, hypercholesterolemia, and hypertension (Parama et al., 2020), while also possessing antibacterial, anti-inflammatory, and wound healing capabilities (Fromm and DeGolier, 2021). Alkaloids have been documented to possess potent analgesic properties, as well as exerting effects such as reducing fever, lowering blood pressure, combating fungal infections, reducing inflammation, preventing fibrosis, promoting stimulation, inducing anesthesia, and inhibiting the growth of various bacterial strains (Boro et al., 2021; Heinrich et al., 2021). The results of our study indicate that SCREE contains beneficial antioxidants and anti-inflammatory metabolites. Furthermore, it is suggested that SCREE has the ability to reverse oxidative stress and positively impact hematologic parameters. This indicates that the plant has the potential to serve as a valuable source of natural antioxidants and substances that enhance blood function.

3.2 Evaluation of phenolic metabolites in SCREE

Based on the approximate analysis, our results indicated that SCREE has a substantial concentration of phenolic metabolites. Consequently, our investigations were extended to explore the phenolic metabolites of SCREE. In this regard, we conducted phenolic-targeted HPLC analysis for the SCREE. As indicated in (Supplementary Figure S2), our analysis revealed that SCREE exhibits considerable concentrations of gallic acid, emerging as the dominant phenolic metabolite with a concentration of 7881.15 μg/g. The following are closely followed by chlorogenic acid at 3,265.11 μg/g and naringenin at 1,197.63 μg/g. Although other metabolites, such as cinnamic acid, ferulic acid, vanillin, taxifolin, methyl gallate, and ellagic acid, were found in the extract, their concentrations were comparatively lower, ranging from 198.16 μg/g to 71.85 μg/g (Supplementary Figure S2). Caffeic acid and syringic acid were also present in trace amounts (59.77 μg/g and 51.71 μg/g, respectively). On the contrary, kaempferol, coumaric acid, catechin, pyrocatechol, and rutin were not detected in the extract (Supplementary Figure S2). These findings are of significance, as phenolic metabolites are renowned

10.3389/fphar.2024.1378249

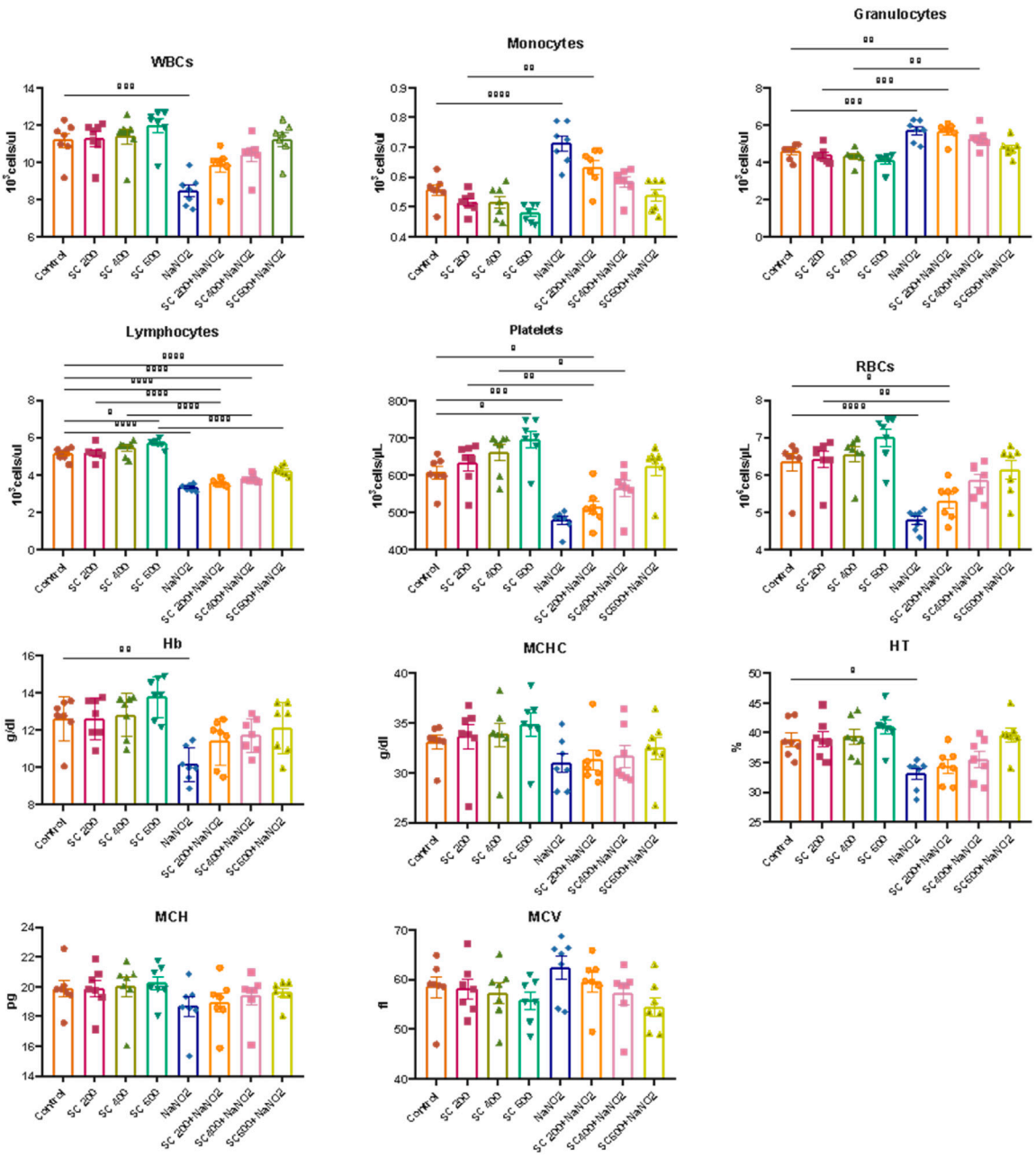

FIGURE 4
Effects of SCREE on the hematological parameters of male rats treated with NaNO2. The results of the statistical analysis were reported as mean ± SE (n = 7). Multiple comparisons were analyzed by one-way ANOVA followed by Tukey's multiple comparison test. Differences between groups were considered significant when $p < 0.05$ (*$p < 0.05$, **$p < 0.01$, ***$p < 0.001$ and * ***$p < 0.0001$). Significant data included for each group compared to the control group and for SCREE groups (SCREE 200, SCREE 400, SCREE 600) each compared to its respective treated group (SCREE 200+ NaNO2, SCREE 400+ NaNO2, SCREE 600+ NaNO2).

for their diverse biological activities, including antioxidant and anti-inflammatory properties. The presence of multiple phenolic metabolites, especially gallic acid and chlorogenic acid, suggests that SCREE may offer potential health benefits. The detected amounts of caffeic acid and syringic acid, although minimal, contribute to the overall phenolic diversity of the extract (Rahman et al., 2022). Collectively, these results shed light on the phenolic composition of SCREE and support the pharmacological and therapeutic potentials of SCREE.

3.3 Untargeted metabolomic analysis by UPLC/T-TOF-MS/MS analysis

Metabolomic analysis is a vital tool to explore the bioactivity of plant extracts, to elucidate their mode of action and to discover key metabolites. By comprehensively profiling and identifying small molecules in these extracts, metabolomics helps uncover the complex chemical compositions and interactions responsible for their biological effects. This approach is essential for

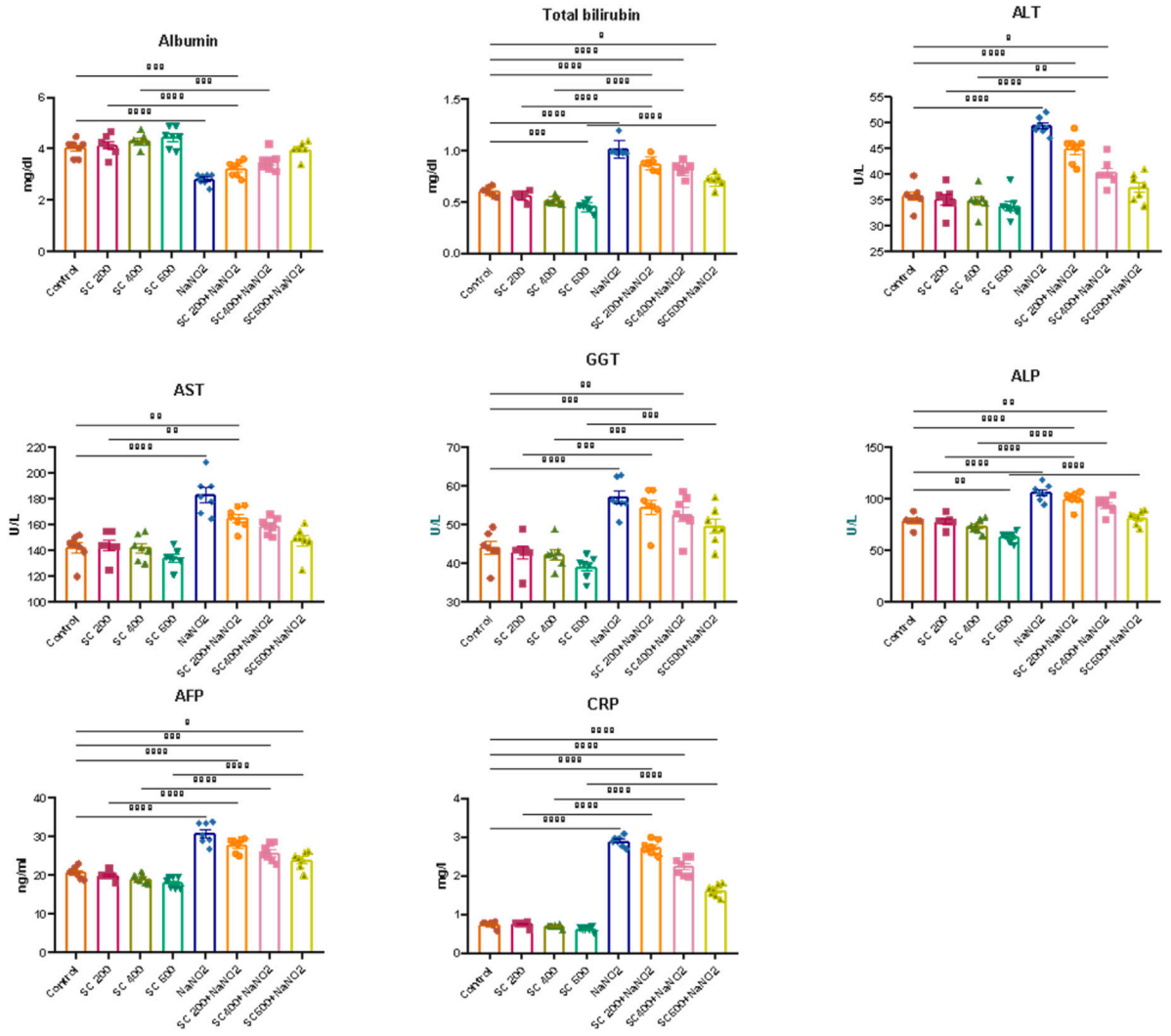

FIGURE 5
Effects of SCREE on liver function biomarkers (ALT, AST, ALP, GGT, total bilirubin, AFP, and CRP) of NaNO2-treated rats. Statistical analysis was reported as mean ± SE (n = 7). Multiple comparisons were analyzed by one-way ANOVA followed by Tukey's multiple comparison test. Differences between groups were considered significant when $p \leq 0.05$ (*$p \leq 0.05$, **$p \leq 0.01$, ***$p \leq 0.001$, and * ***$p < 0.0001$). Significant data included for each group compared to the control group and for SCREE groups (SCREE 200, SCREE 400, SCREE 600) each compared to its respective treated group (SCREE 200+ NaNO2, SCREE 400+ NaNO2, SCREE 600+ NaNO2).

understanding how plant metabolites impact human health, drug discovery, and uncovering potential therapeutic agents or bioactive metabolites from natural sources. To gain more insight into the exact metabolites in the SCREE extract, we performed a detailed untargeted metabolomic analysis utilizing UPLC/T-TOF-MS/MS. Analysis was carried out in both positive and negative modes, leading to the identification of 187 metabolites (Figure 3). In the positive ionization mode, a total of 104 metabolites have been detected, covering a wide spectrum of 11 distinct classes, including acids (5.9%), amino acids (30%), alkaloids (1.6%), nucleobases (8.52956%), xanthines (0.15%), vitamins (1.74%), carbohydrates (2.7%), peptides (2.3%), phenolic metabolites (4.3%), flavonoids (31%) and several other miscellaneous metabolites (12%) (Figure 1; Supplementary Table S4). This diverse array of metabolite classes highlights the comprehensive nature of the analysis, with various metabolites from different classes identified (Figure 1). Our findings underscored that more than 31% of the identified metabolites belong to the flavonoid class. Within this category, two subgroups have been distinguished: one comprising 15 flavonoid metabolites and the other comprising 15 flavonoid–O-glycosides (Supplementary Material). Among flavonoids, four specific flavonoids emerged as the most prevalent metabolites, including daidzein (8.2%), 3, 5, 7-trihydroxy-4′-methoxyflavone (6.7%), acacetin (3.8%), and 3′,4′,5,7-tetrahydroxyflavanone (2.9%). Regarding flavonoid-O-glycosides, apigenin-7-O-glucoside stands out as the most abundant metabolite within the group of 15 metabolites (1.7%). Regarding the detected amino acid metabolites, 15 different amino acid metabolites have been detected, which constitute approximately 30% of the total detected metabolites. L-proline was the most prevalent amino acid metabolite (17.5%), followed by L-ß-homotryptophane (6.5%) and L-5-oxoproline (2.3%). A set of 11 nucleobase-based metabolites was also detected in the extract, which represented about 9% of the total detected metabolites. Adenosine-3′,5′-cyclic monophosphate

10.3389/fphar.2024.1378249

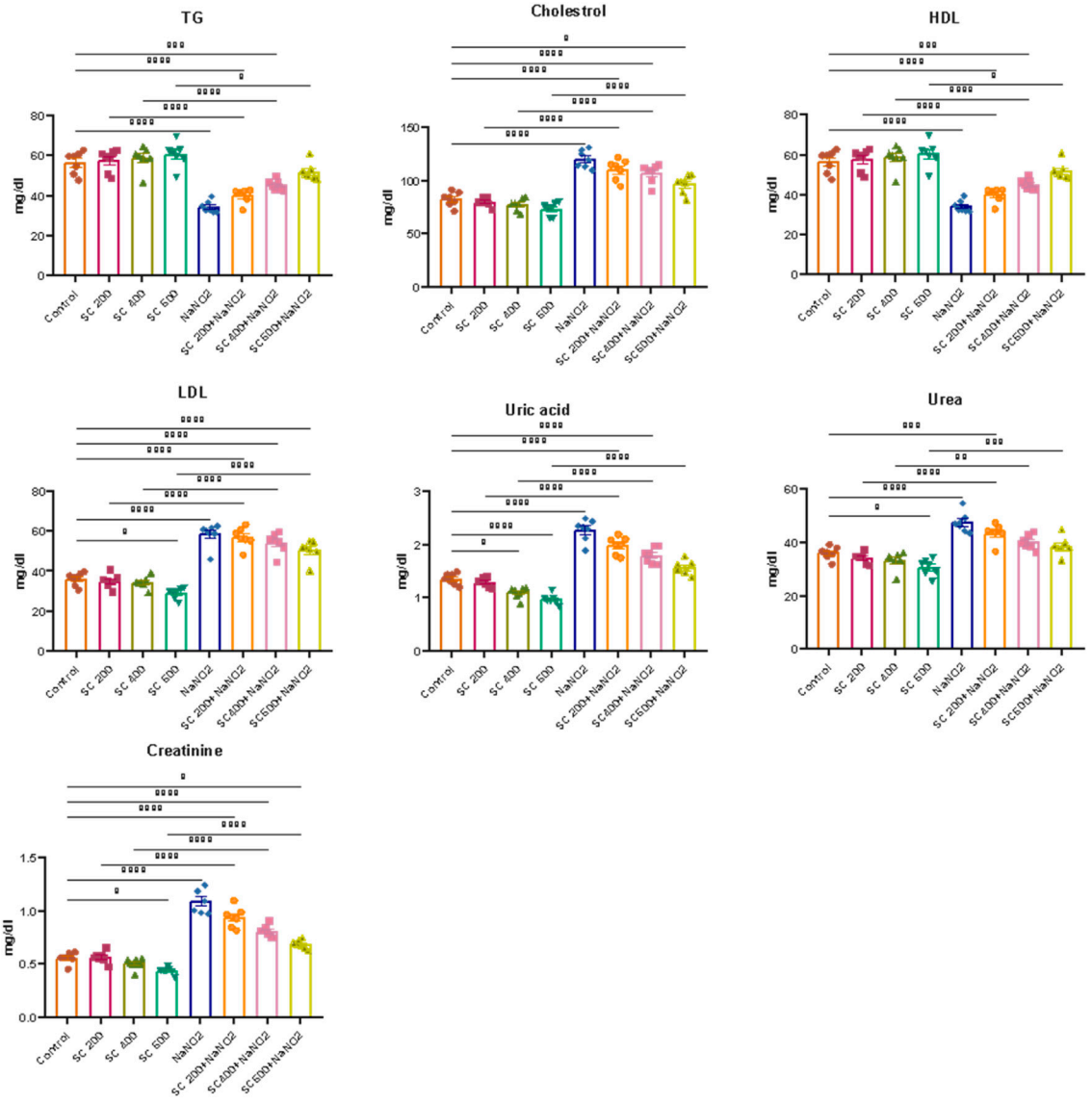

FIGURE 6
Effects of SCREE on kidney function biomarkers and lipid profile of NaNO2-treated rats. Statistical analysis was reported as mean ± SE (n = 7). Multiple comparisons were analyzed by one-way ANOVA followed by Tukey's multiple comparison test. Differences between groups were considered significant when $p \leq 0.05$ (*$p \leq 0.05$, **$p \leq 0.01$, ***$p \leq 0.001$, and * ***$p < 0.0001$). Significant data included for each group compared to the control group and for SCREE groups (SCREE 200, SCREE 400, SCREE 600) each compared to its respective treated group (SCREE 200+ NaNO2, SCREE 400+ NaNO2, SCREE 600+ NaNO2).

represented the most prevalent metabolite (2.9%), followed by 2′-deoxycytidine (1.9%), and xanthosine-5′-monophosphate (1.4%). The detected small peptide metabolites contributed approximately 2.3% of the total detected metabolites and comprised two metabolites, S-lactoylglutathione (2.16%) and leupeptin (0.12%). Phenolic metabolites detected represented approximately 4.3% of the total detected metabolites and were composed of seven metabolites. The metabolite most prominently presented was the coumarin-based metabolite scopoletin (1.61%), followed by 4-aminophenol (1.3%). Acid-based metabolites represented approximately 5.9% of the total detected metabolites, consisting of 17 different metabolites. Chlorogenic acid, a cinnamoyl-based acid, was shown to be the most prevalent metabolite in this class (1.67%), followed by N-acetylneuraminate (1.1%) and urocanic acid (0.69%).

Carbohydrate-based metabolites represented approximately 2.7% of the total detected metabolites and comprised four metabolites. α-Lactose represented the lead metabolite with the highest peak area (1.5%), followed by α-D-glucose-1-phosphate (0.91%). Furthermore, our analysis revealed a set of three xanthine metabolites (total PA%, 0.158) consisting of 3-methylxanthine, 1,3-dimethylurate and uric acid, with 3-methylxanthine being the predominant xanthine metabolite (0.069%). Two alkaloid metabolites were also identified (total PA %, 1.63%), scoulerin being the most prevalent (1.19%). Additionally, miscellaneous metabolites from various classes contributed approximately 12% to the total metabolites, consisting of approximately nine metabolites. In this class of metabolites, choline was the most prevalent (9.6%), followed by Hinokitiol

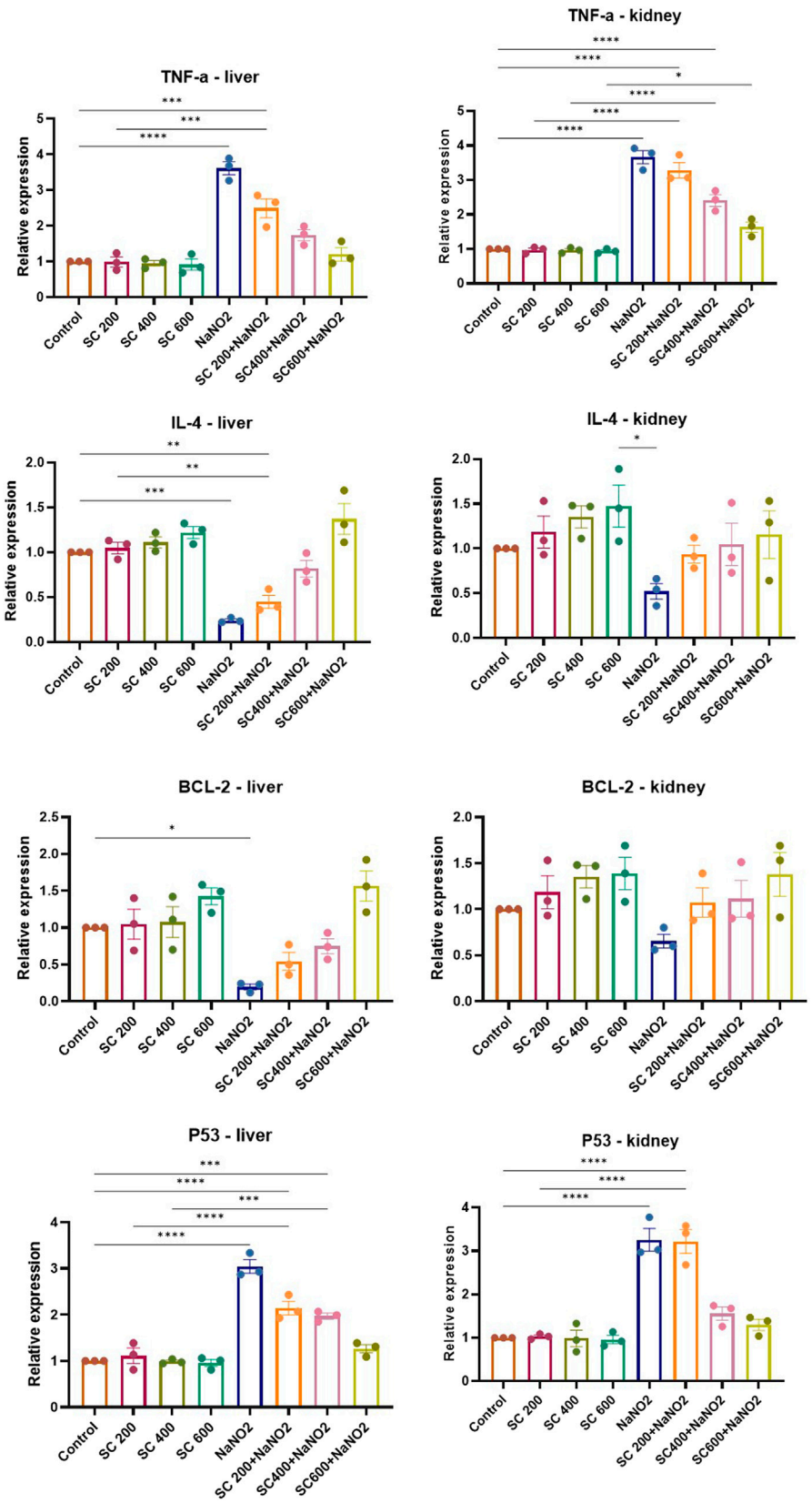

FIGURE 7
Effects of SCREE on the expression of inflammatory (TNF-α, IL-4) and apoptotic genes (P53, Bcl-2) in the liver and kidney of NaNO2-treated rats. Statistical analysis was reported as mean ± SE (n = 7). Multiple comparisons were analyzed by one-way ANOVA followed by Tukey's multiple comparison test. Differences between groups were considered significant when $p \leq 0.05$ (*$p \leq 0.05$, **$p \leq 0.01$, ***$p \leq 0.001$, and ****$p < 0.0001$). Significant data
(*Continued*)

FIGURE 7 (Continued)
included for each group compared to the control group and for SCREE groups (SCREE 200, SCREE 400, SCREE 600) each compared to its respective treated group (SCREE 200+ NaNO2, SCREE 400+ NaNO2, SCREE 600+ NaNO2).

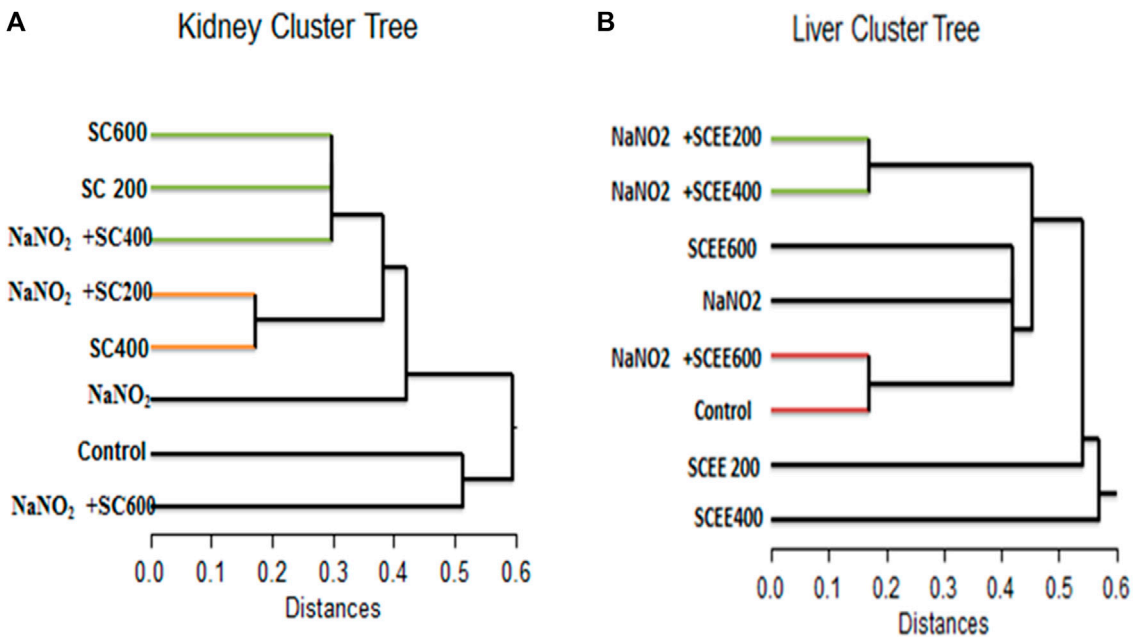

FIGURE 8
A dendrogram was created using the similarity index of the differentially expressed genes of the detected genes (regulated genes from the top) in the collected sera of the white albino rats examined in this study. **(A)** (on the left) for the kidney cluster tree, and **(B)** (on the right) for the liver cluster tree.

(0.73%). Furthermore, a set of three vitamins were also detected that constitute approximately 1.6% of the total detected metabolites, including pyridoxamine (vit B6), calciferol (vit D2), and nicotinamide (vit B3) (Figure 1).

The negative mode of the SCREE UPLC/T-TOF-MS/MS analysis has successfully demonstrated the detection of 84 metabolites, covering a diverse range of eight classes, including acids, amino acids, carbohydrates, alkaloids, isoprenoids, nucleosides, phenols, and others (Figure 1; Supplementary Table S5). Similar to the positive mode analysis, our findings highlighted that more than 50% of the detected metabolites belong to the flavonoid class, with 20 distinct metabolites identified. The detected flavonoid-based metabolites comprised 11 flavonoid metabolites and nine flavonoid O-glycoside metabolites. Among the flavonoid metabolites, apigenin represented the most prevalent metabolite (37.9%), followed by pelargonidin-3-O-glucoside (3.7%) and apigenin-7-O-glucoside (3.5%). Acid-based metabolites represented the second most detected metabolites with 29% of the total detected metabolites. The detected acid-based metabolites comprised 21 different metabolites. γ-Linolenic acid was the most prevalent metabolite in this class with 15.2% of the total detected metabolites, followed by D- (+) -malic (5%) and isocitrate (2.3%). Our analysis also revealed that the SCREE extract contains a set of 11 carbohydrate-based metabolites with 14.2% of the total detected metabolites. Among this class of metabolites, sucrose was the most prominent metabolite (8.2%), followed by gluconate (2.1%). Nucleobase-based detected metabolites represented approximately 2.7% of the total detected metabolites, with eight metabolites identified in this class. Inosine-5′-monophosphate represented the most prominent metabolite in this class (1.3%), followed by 2′-deoxyinosine (0.8%). The amino acid metabolites represented only 1.6% of the total detected metabolites, with eight identified metabolites. DL-5-Hydroxylysine was the main amino acid detected in this group (0.35%). Our analysis also detected a set of three isoprenoid metabolites, which represented about 1% of the total detected metabolites. Gibberellin A4 represented the main isoprenoid metabolite with a peak area of 0.5%. Phenolic-based metabolites represented approximately 0.3% of the total detected metabolites, with three identified metabolites. The most abundant phenolic metabolite was syringaldehyde, accounting for 0.13%. Lastly, a set of eight miscellaneous metabolites was also detected, which represented less than 0.5% of the total detected metabolites. These metabolites represent different classes of metabolites including xanthine, peptides, and coumarin-based metabolites.

The most prominent metabolites detected by untargeted metabolomic analysis are presented in (Table 1). Our LC/MS-MS analysis revealed a set of 16 metabolites that were identified with more than 2% of the total detected metabolites (Figure 2). These metabolites possess diverse biological activities, including anti-inflammatory, antioxidant, and antitumor effects, making them valuable candidates for natural remedies and complementary agents in the treatment of a wide spectrum of health concerns. Therefore, the pronounced biological activity of the SCREE extract attributed to the metabolites is prevalent. Our metabolomic analysis revealed that

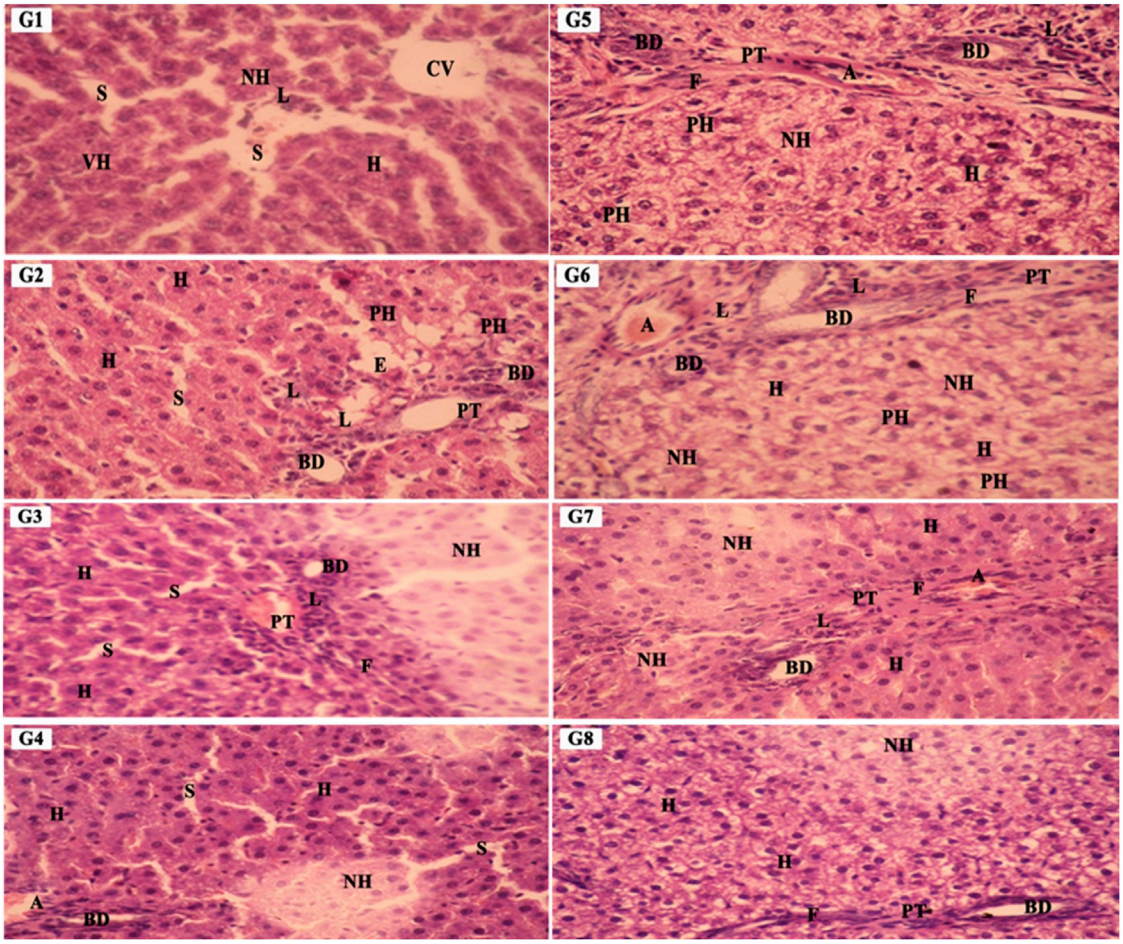

FIGURE 9
The liver sections' photomicrographs in various groups, G1: Control G2: SCREE (200 mg/kg BW), G3: SCREE (400 mg/kg BW), G4: SCREE (600 mg/kg BW), G5: NaNO2 G6: SCREE (200 mg/kg BW) + NaNO2, G7: SCREE (400 mg/kg BW) + NaNO2 and G8: SCREE (600 mg/kg BW) + NaNO2, EH: eosinophilic hepatocytes, CV: central vein, PT: portal tract, H: Hepatocyte, AM: mitotic hepatocytes, BD: bile duct, L: lymphocyte, NH: necrotic hepatocyte, F: fibrotic cells, N: necrotic cells, S: sinusoid, VH: vesiculated nuclei, IF: infiltrating lymphocytes, PH: pyknotic hepatocytes. (H&E stain, ×400magn.)

SCREE possesses a high content of flavonoids, including apigenin, apigenin-7-O-glucoside, daidzein, acacetin, and 3′,4′,5,7-tetrahydroxyflavanone. Apigenin, the most prominent metabolite in the SCREE extract, is renowned for its robust antioxidant and anti-inflammatory characteristics (Romanova et al., 2001; Wang et al., 2014b; Kashyap et al., 2022). It also demonstrates its complications in CNS-related disorders such as multiple sclerosis (Ginwala et al., 2019). Furthermore, apigenin demonstrated antitumor activity both *in vitro* and *in vivo*. It triggers cell apoptosis, induces cell cycle arrest, suppresses cell migration and invasion, and stimulates autophagy (Lotfi and Rassouli, 2024). The SCREE extract also showed a considerable content of daidzein, which functions as a phytoestrogen. It interacts with human estrogen receptors, influencing estrogen sulfation and potentially affecting hormone-related conditions such as breast cancer. Moreover, it exhibits antiviral characteristics and provides lung protection (Poschner et al., 2017). Daidzein demonstrates a potential anti-inflammatory effect by modulating NO levels, pro-inflammatory cytokines (IL-6, TNF-α), inflammatory indicators (COX-2, iNOS), and effectively suppressing NF-κB signaling. Acacetin demonstrates various biological activities, such as its potential as an antidiabetic agent, making it promising for diabetes management by improving insulin sensitivity and blood sugar regulation. It also has potential for cancer prevention, cardiac protection, neuroinflammation control, and antimicrobial effects (Singh et al., 2020). Furthermore, it exhibits potent anti-inflammatory effects by suppressing the expression of pro-inflammatory cytokines, including nitric oxide synthase (iNOS) and COX-2 (Ouyang et al., 2021). Apigenin-7-O-glucoside is known for its various biological activities, including its functions as an antioxidant, effectively countering oxidative stress, and as an anti-inflammatory agent, helping alleviate inflammation-related problems (Armeni et al., 2014; Gallo and GГЎmiz, 2023). Similarly, 3′,4′,5,7-tetrahydroxyflavanone is known for its potential biological activities, which can include antioxidant and anti-inflammatory effects (Lin et al., 2008). Furthermore, SCREE showed a considerable content of amino acid metabolites, including L-proline, L-ß-homo-tryptophan, and L-5-oxoproline. L-proline, the second highly detected metabolite, plays a crucial role in various biological activities, such as collagen synthesis, and contributes to wound healing and neurotransmitter regulation (Li et al., 2019). Another detected amino acid metabolite, L-ß-

TABLE 2 Scores of liver and kidney histological changes in various groups.

Group	parameters	GP1	GP2	GP3	GP4	GP5	GP6	GP7	GP8
Liver									
CV dil	Score	1.01 ± 0.03	0 ± 0.0	0 ± 0.0	0 ± 0.0	0 ± .0	0 ± 0.0	0 ± 0.0	0 ± 0.0
	Change (%)	100	0	0	0	0	0	0	0
PT dil	Score	0 ± 0.0	2.21 ± 0.04	2.04 ± 0.02	0 ± 0.0	3.45 ± 0.06	2.32 ± 0.01	2.23 ± 0.0	2.03 ± 0.01
	Change (%)	0	221	204	0	0	232	223	203
B D dil	Score	0 ± 0.0	2.17 ± 0.03	2.12 ± 0.05	0 ± 0.0	3.48 ± 0.04	3.05 ± 0.03	2.23 ± 0.0	0 ± 0.0
	Change (%)	0	217	212	0	348	305	223	0
Fibrosis	Score	0 ± 0.0	0 ± 0.0	1.02 ± 0.01	1.00 ± 0.01	3.39 ± 0.06	3.23 ± 0.0	2.40 ± 0.09	1.20 ± 0.0
	Change (%)	0	100	102	10.0	33.9	32.3	24.0	12.0
Necrosis	Score	1.16 ± 0.02	0 ± 0.0	1.01 ± 0.01	0 ± 0.0	2.35 ± 0.02	2.23 ± 0.06	0 ± 0.0	0 ± 0.0
	Change (%)	110	0	87.1	0	232.7	220.8	0	0
Regenerative H	Score	0 ± 0.0	2.09 ± 0.02	2.01 ± 0.01	2.02 ± 0.01	0 ± 0.0	0 ± 0.0	0 ± 0.0	2.02 ± 0.01
	Change (%)	0	209	201	202	0	0	0	202
Kidney									
Glomeruliatrophy	Score	0 ± 0.0	2.03 ± 0.01	2.07 ± 0.01	0 ± 0.0	4.29 ± 0.06	2.27 ± 0.06	2.18 ± 0.02	1.18 ± 0.05
	Change (%)	0	203	207	0	429	227	218	118
RT dil	Score	2.06 ± 0.02	3.27 ± 0.02	3.12 ± 0.03	3.03 ± 0.02	4.41 ± 0.1	4.19 ± 0.02	4.05 ± 0.02	3.12 ± 0.03
	Change (%)	100	158.7	151.5	147.1	214.1	203.4	196.6	151.5
Regenerative R.T	Score	0 ± 0.0	0 ± 0.0	2.13 ± 0.05	2.05 ± 0.02	0 ± 0.0	0 ± 0.0	1.24 ± 0.02	2.29 ± 0.06
	Change (%)	0	0	213	205	0	0	124	229

The percentage change was assessed relative to the control group (G1). Data presented as mean ± SE, values.

homotryptophan, serves as a precursor to serotonin, contributing to the modulation of growth and the immunometabolic state (Roager and Licht, 2018). Its structural similarity to tryptophan gives rise to the intriguing possibility of interacting with similar metabolic pathways and receptors, potentially affecting functions linked to immune regulation and neural processes. L-5-oxoproline is also recognized for its anticancer potential, which has been linked to its antioxidant properties, cell cycle regulation, immune system modulation, and chemo-preventive potential (Sasaki et al., 2015). Acid-based metabolites also represented a substantial content of SCREE extract, including γ-Linolenic acid, D-(+)-Malic acid, and Isocitrate. γ-Linolenic acid plays a pivotal role in modulating inflammatory responses. It is essential to produce anti-inflammatory eicosanoids and regulation of gene expression, affecting immune function and cell apoptosis (Kapoor and Huang, 2006). D-(+)-Malic acid exhibits notable biological activities, mainly known for its hepatoprotective effects (Madrigal-Santillán et al., 2014). Additionally, it plays a role in the regulation of acidity in the body and participates in the citric acid cycle, an essential metabolic pathway (Tuncel et al., 2015). Isocitrate demonstrates, as an antioxidant, the ability to combat oxidative stress by participating in the citric acid cycle, which is essential for energy production and the neutralization of harmful free radicals (White and Someya, 2022). The SCREE extract exhibited several carbohydrate-based metabolites, including sucrose and gluconate. Sucrose is known for its multifaceted activity, including its role as a readily available energy source in metabolism and its importance in various biological processes such as glycolysis and cell respiration (Huestis, 2007). Gluconate exhibits robust anti-inflammatory characteristics through its ability to efficiently decrease the production of inflammatory chemokines (Nii et al., 2019). Other metabolites have also been detected in the SCREE extract, including choline and S-lactoylglutathione. Choline is known for its liver protective and cholesterol-lowering effects (Mehedint and Zeisel, 2013). It also serves as a precursor to acetylcholine, affecting brain development, cognition, the gut microbiota, and metabolic health (Gallo and GÜmiz, 2023). Although S-lactoylglutathione exhibits a significant role as a precursor to the important antioxidant glutathione. It contributes to cell protection against oxidative stress, detoxification processes, and overall maintenance of cell health (Armeni et al., 2014).

3.4 Evaluation of the effect of SCREE on organ weight changes and body weight gain

Our initial examinations evaluated the impact of SCREE on body and organ weight, focusing on the liver and kidneys. As depicted in (Figure 3), rats treated with NaNO2 for 28 days showed a significant reduction in body weight, weight gain, and kidney weight, but also an elevation in liver weight compared to the control group. These reductions in body weight can be attributed to reduced food intake (Grant and Butler, 1989) or lack of vitamin C

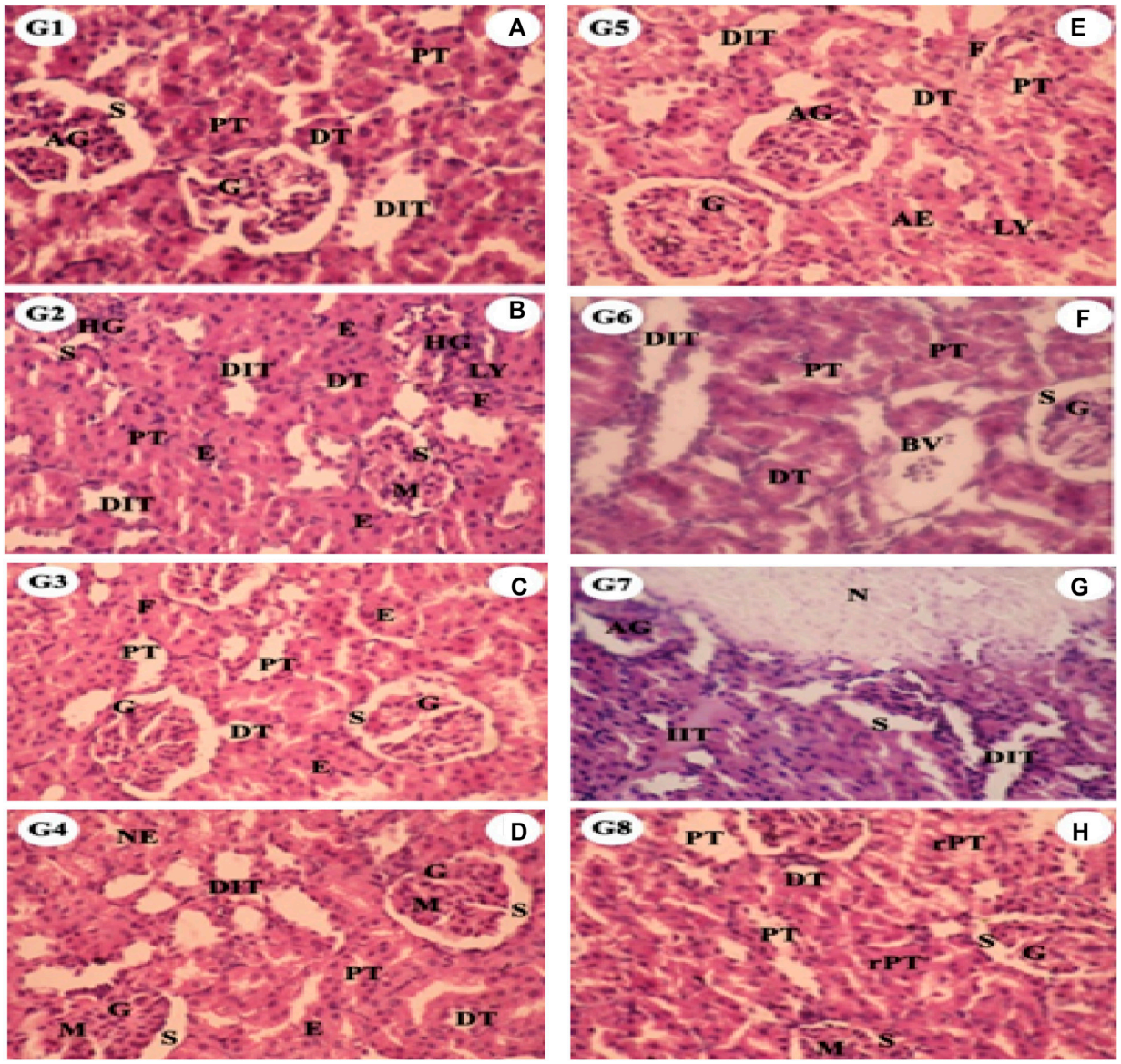

FIGURE 10
The kidney sections' photomicrographs in various groups G1: Control G2: SCREE (200 mg/kg BW), G3: SCREE (400 mg/kg BW), G4: SCREE (high dose), G5: NaNO2 G6: SCREE (200 mg/kg BW) + NaNO2, G7: SCREE (400 mg/kg BW) + NaNO2 and G8: SCREE (600 mg/kg BW)+ NaNO2, G: normal glomeruli, M: mesangial cells, PT: proximal tubule, S: minimal urinary space, IT: interstitial tissue, HG: hyperemic, DT: distal tubule, AG: atrophied glomeruli, (H&E stain, ×400magn.).

(Uchida et al., 1990), or it could be due to an increase in catabolic processes caused by an increase in NaNO2 levels in the body. These findings correspond to those of Poter et al. (Porter et al., 1993), who reported that weight loss was due to a reduction in food intake, a disturbance in hormonal equilibrium, and sodium nitrite therapy has a direct cytotoxic impact. In addition, body weight was found to increase in rats treated with monosodium glutamate, while it decreased in rats that consumed NaNO2 compared to normal rats (Helal et al., 2017). Furthermore, a significant increase in the hepatosomatic index was also caused by the toxic effects of NaNO2 on the nucleic acids, glycogen, lipids and proteins found in the liver, which are responsible for liver growth (Srinivasan and Radhakrishnamurty, 1988; Dikshith et al., 1991). On the other hand, our results revealed that SCREE supplementation with NaNO2 has significant and dose-dependent improvements in body weight, body weight gain, and liver weight, while it exhibits insignificant effects on kidney weight compared to the control group. The improvement observed by SCREE treatment is consistent with the studies by abdul-hussein (2019) and Ahmed (Ahmed, 2017) that showed that rats given ethanolic extract of S. costus exhibit significantly ($p < 0.05$) higher final BW and BWG values compared to the control group. Thyroid hormones play an essential role in growth, development, reproduction, and stress response (Peter, 2011). The decrease in growth rate among the groups exposed to nitrite could be linked to thyroid hormone levels (Ciji et al., 2013). The weight gain observed in our study can be attributed to the presence of tryptophan in SCREE, as this amino acid serves as a crucial factor in the regulation of nutrient metabolism and the promotion of

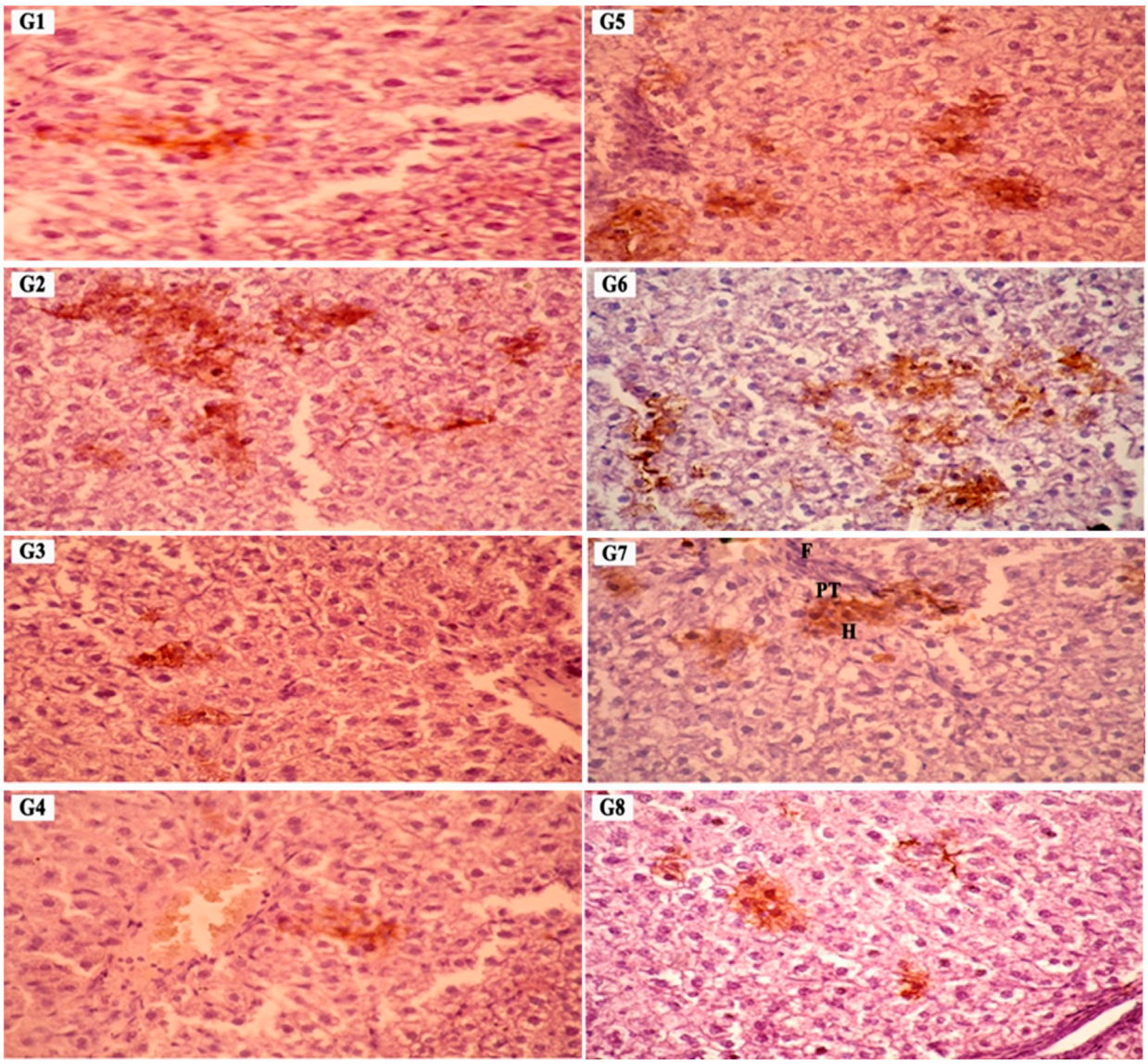

FIGURE 11
Photomicrographs of TGF-β immunoreactivity expression as brownish color in rat liver sections in different groups. G1: Control G2: SCREE (200 mg/kg BW), G3: SCREE (400 mg/kg BW), G4: SCREE (high dose), G5: NaNO2 G6: SCREE (200 mg/kg BW) + NaNO2, G7: SCREE (400 mg/kg BW) + NaNO2 and G8: SCREE (600 mg/kg BW) + NaNO2, PT: portal tract, H: hepatocyte, F: fibrotic cells (DAB 400X stain).

increased body weight. Tryptophan is a vital precursor for neurotransmitters and metabolic regulators that regulate nutrient metabolism (Ruan et al., 2014).

3.5 Assessment of SCREE impact on hematological parameters

Next, we explore the effect of SCREE on the hematological parameters of male rats treated with NaNO2. As shown in (Figure 4), rats subjected to NaNO2 showed a significant reduction in hemoglobin (Hb), RBC, packed cell volume (PCV), mean corpuscular volume (MCV), mean corpuscular hemoglobin (MCH), mean corpuscular hemoglobin concentration (MCHC), white blood cells (WBC), lymphocytes, platelets, and neutrophils, coupled with an increase in granulocytes and monocytes, compared to the control group. These alterations are indicative of altered hematopoiesis and immune function, likely due to adverse effects of NaNO2 on bone marrow, spleen, and liver, as well as oxidative damage and erythrocyte lysis induced by free radical production. On the contrary, the hematological analysis revealed that the administration of SCREE alone exhibits minimal effects on the examined hematological parameters, except for a notable increase in both red blood cell (RBC) and platelet counts at a high dose of 600 mg/kg BW, compared to the control group. Interestingly, the administration of SCREE to NaNO2-treated rats demonstrated, especially at a high dose of 600 mg/kg BW, a tendency toward normalized hematological parameters, approaching levels detected in the control group, which indicates a potential therapeutic effect of SCREE in mitigating NaNO-induced hematological disturbances

TABLE 3 Scores of immunohistochemical observations of TGF- β in the liver in various groups.

Groups	Expression of TGF- β				Notes
	CA		PT		
	Score	Change (%)	Score	Change (%)	
Gp1	0 ± 0.0	0	1.05 ± 0.02	100	-
Gp2	4.25 ± 0.03	425	0 ± 0.0	0	-
Gp 3	0 ± 0.0	0	2.12 ± 0.03	201.9	few fibrotic cells
Gp 4	0 ± 0.0	0	1.03 ± 0.01	98.1	regenerative hepatocytes
Gp 5	4.29 ± 0.06	429	2.43 ± 0.04	231.4	-
Gp 6	4.04 ± 0.01	404	0 ± 0.0	0	-
Gp 7	0 ± 0.0	0	2.11 ± 0.01	201.0	Few fibrotic cells
Gp 8	0 ± 0.0	0	2.02 ± 0.01	192.4	-

The percentage change was assessed relative to the control group (G1),. Data presented as mean ± SE, values.

(Figure 4). The observed changes in hematologic parameters reflect the general health and functioning of rats in response to SCREE administration. The alterations detected in parameters such as RBC count, Hb content, and WBC count indicate disturbances in oxygen transport, immune function, and overall physiological balance. The improvements noted by the SCREE administration suggest a potential protective and regulatory role.

These results are in agreement with previous reports that showed that 4 weeks of NaNO2 administration resulted in significant and dose-dependent reductions in RBC count, WBC count, and hemoglobin (Hb) content (Helal et al., 2008; Hammoud, 2014). These changes were associated with hypochromic microcytic anemia, likely due to the adverse effects of sodium nitrite on the bone marrow, spleen, and liver. The observed decrease in WBC count could also be attributed to insufficient white blood cell production in hematopoietic tissues (El-Sheikh and Khalil, 2011). Furthermore, sodium nitrite administration triggers free radical production, leading to the induction of oxidative damage and promoting the formation of methemoglobin and erythrocyte lysis through oxidation of ferrous ion oxyhemoglobin (Baky et al., 2010). The observed leukopenia was associated with lymphopenia, indicating the suppressive effect of sodium nitrite on the immune system (Gluhcheva et al., 2012). The noticeable decrease in WBCs in NaNO2-treated rats could be associated with the absence of fresh WBC generation from hematopoietic tissues (El-Sheikh and Khalil, 2011). On the other hand, the administration of SCREE extract to sodium nitrite treated rats improved the total leukocytic count. These findings could be attributed to the immunostimulatory activity of the SCREE extract. In this regard, Kadhem (abdul-hussein, 2019) showed that SCREE alleviates the toxic effect of paracetamol by improving hematological indicators (RBC count, WBC count, Hb, PCV, MCV, MCH and MCHC). The improved hematological markers observed could be attributed to L-proline, a significant metabolite within SCREE. L-proline exhibits various biological activities, including its potential role in boosting physiological functions such as improved collagen synthesis, wound healing, and neurotransmitter regulation (Ohtani et al., 2001; Albaugh et al., 2017). The substantial increase in red blood cell and platelet counts, particularly at the higher dose of SCREE (600 mg/kg BW), suggests that L-proline can certainly influence hematological parameters.

3.6 Assessment of the impact of SCREE on liver function

To evaluate the hepatoprotective effect of SCREE against NaNO2-induced liver damage, liver enzymes (ALT, AST, ALP and GGT), total bilirubin, AFP, and CRP activity were evaluated. As shown in (Figure 5), NaNO2-treated rats showed a substantial increase in serum ALT, AST, GGT, ALP, total bilirubin, AFP, and CRP activity, as well as a substantial drop in serum albumin, compared to the control group. Alterations in these markers can be attributed to hepatocellular inflammation and liver necrosis, which can lead to increased membrane permeability and subsequent release into the bloodstream (El-Demerdash et al., 2021a). Hepatocellular damage has also been associated with elevated total bilirubin levels caused by NaNO2 treatment. These results might reflect decreased liver conjugation, increased bilirubin generation by hemolysis, and decreased liver absorption (Le-Vinh et al., 2022). The notable toxic properties of nitroso derivatives, which form in the acidic environment of the stomach and cause severe liver necrosis, could be the cause of elevated liver enzyme activity (Chain et al., 2023). In addition, elevated AST and ALT activities in the NaNO2-treated group could be related to the nitric oxide-induced free radical (ONOO-) (Helal et al., 2020). Both oxygen radicals and NO possess the potential to react further to produce other oxidants and nitro substances, such as peroxynitrite, which can be harmful to the liver and contribute to liver cell death. The shift of the intracellular protein generation pathway may be responsible for the reduction of serum albumin levels, and the alteration of oxidative enzymes has a secondary impact on protein alterations. The observed elevation of AFP and CRP in NaNO2-treated rats was consistent with the findings of Tawfek et al. (Tawfek, 2015) and Elsherbiny et al. (Elsherbiny et al., 2017), who showed that certain food additives increase AFP and CRP levels in

rats. In addition, Elsherbiny et al. (Elsherbiny et al., 2017) reported that NaNO2 administration increased inflammatory markers (CRP, TNF-α, IL-6, IL-1β) while reducing anti-inflammatory markers (IL-10 and IL-4). CRP is also an excellent sign of inflammation and immune dysfunction, as it has been linked to the development of arthritic disease in rats (Kadam and Bodhankar, 2013).

Next, we assessed the effect of SCREE supplementation alone on liver function. As depicted in (Figure 5), our results revealed that the administration of SCREE considerably improved the levels of certain biomarkers that are associated with hepatocellular injury. Interestingly, SCREE administration to the NaNO2-treated group demonstrated significant ($p < 0.05$) decreases ($p < 0.05$) in all parameters examined, except albumin, which increased dose-dependently. These findings suggest that SCREE may have a hepatoprotective effect by mitigating NaNO2-induced liver damage. The potential modulatory effect of SCREE is likely to be attributable to its antioxidant properties inherited by the presence of metabolites such as flavonoids, γ-Linolenic acid, D- (+) -Malic acid and chlorogenic acid, which are known to possess hepatoprotective properties via free radical-induced lipid peroxidation (Selvi et al., 2018). These findings are consistent with previous research that highlights the hepatoprotective potential of SCREE and its ability to modulate inflammatory and immunological responses (Tag et al., 2016b). Further, Elsayed et al. (Elsayed et al., 2015) showed that administration of SCREE root extract to rats treated with CCl4 improved plasma levels of ALT and AST.

3.7 Assessment of SCREE impact on kidney function and lipid profile

We further explored the effect of SCREE on kidney function in NaNO2-treated rats by assessing the levels of certain kidney biomarkers and the lipid profile. Our results revealed that the administration of NaNO2 significantly increases urea, uric acid and creatinine levels, but also cholesterol, LDL-C, and VLDL-C levels. However, TG and HDL-C levels decreased significantly in NaNO2-treated rats, compared to the control group (Figure 6). These findings aligned with several reports that showed that NaNO2 administration increases urea and creatinine levels (Khalil, 2016; Helal et al., 2020). The observed elevation in markers of kidney function (urea, uric acid, and creatinine) suggests renal failure in NaNO2-treated rats (Johnson et al., 2013). On the contrary, high levels of creatinine are related to muscle creatinine catabolism and commonly signal acute kidney injury or chronic kidney disease (El-Demerdash et al., 2020). Most fatty acids in blood, tissues, and cellular membranes are unsaturated fatty acids and are particularly susceptible to ROS. Our results further highlight the nephrotoxic effect of sodium nitrite by triggering lipid peroxidation and oxidative stress that lead to kidney dysfunction (Aita and Mohammed, 2014). Elevated uric acid levels could potentially be attributed to increased uric acid use to counteract increased free radical production induced by NaNO2 treatment. Elevated urea levels observed in NaNO2-treated rats may indicate increased protein breakdown or impaired kidney function. Interestingly, the administration of SCREE to NaNO2-treated rats, particularly at a high dose of 600 mg/kg BW, resulted in decreased levels of uric acid and urea, suggesting that the administration of SCREE could regulate protein metabolism by inhibiting excessive protein breakdown or enhancing kidney function to facilitate efficient urea excretion. The observed changes in the lipid profile suggest an association with lipoprotein and lipid metabolism (El-Demerdash et al., 2021b). Our results revealed that the NaNO2-treated group exhibited elevated levels of cholesterol, TG, and LDL, along with decreased levels of HDL. However, significant improvements in blood lipid profiles were observed after SCREE treatment, characterized by reduced levels of cholesterol, TG and LDL, coupled with increased HDL levels. The elevated levels of lipid profiles observed after NaNO2 administration could potentially be attributed to the release of free fatty acids from adipose tissue into the circulation or the peroxidation of lipids from the cell membrane. These processes may lead to elevated levels of cholesterol production and acetyl CoA (Helal et al., 2000). However, SCREE alone administration demonstrated a beneficial effect on function and lipid profile, suggesting the potential of SCREE as a protective supplement. Consistent with these findings, SCREE administration to NaNO2-treated rats exhibited significant improvements in renal function and lipid profile in a dose-dependent manner (Figure 6). The observed nephroprotective effect of SCREE is consistent with the findings that reported the nephroprotective properties of S. costus extract against paracetamol-induced kidney damage, attributing this effect to the abundant presence of flavonoids and alkaloids (abdul-hussein, 2019). Our detailed metabolomic analysis of SCREE revealed a diverse array of metabolites, including flavonoids such as Apigenin and Luteolin, which possess considerable antioxidant and anti-inflammatory properties, suggesting their potential to mitigate kidney damage (Romanova et al., 2001; Wang et al., 2014a). Furthermore, γ-linolenic acid, a prominent metabolite detected in SCREE, exhibited recognized antioxidant properties and possible nephroprotective effects (Teng et al., 2017). The presence of D-(+)-malic acid, with its known hepatoprotective properties, further highlights the complexity of nephroprotection and the potential value of the SCREE extract (Koriem and Tharwat, 2023). Additionally, our findings indicate that SCREE treatment improved the lipid profile of the NaNO2-treated group. These results are in agreement with the findings of Alnahdi (2017), who demonstrated the beneficial effects of Costus extract in mitigating the adverse impacts of the pesticide deltamethrin on lipid profiles. The ability of SCREE to modify the lipid profile could be attributed to the presence of chlorogenic acid and Luteolin. Chlorogenic acid, a phenolic metabolite, has been extensively investigated for its potential to modulate lipid levels in the bloodstream by promoting fat metabolism leading to a reduction in total cholesterol and triglyceride levels (Murai and Matsuda, 2023). Luteolin, a flavonoid found in various plants, has also been explored for its lipid-modulating properties, potentially reducing total cholesterol and triglycerides while enhancing cholesterol levels that are beneficial for overall cardiovascular health (Muruganathan et al., 2022).

3.8 Evaluation of the anti-inflammatory and antiapoptotic potential of SCREE

To gain insight into the anti-inflammatory and anti-apoptotic impact of SCREE, we evaluated the gene expression of P53, Bcl2, IL-4, and TNF-α in the kidney and liver of control and NaNO2-treated rats. As shown in (Figure 7), our results revealed that administration of SCREE extract alone displays a nonsignificant effect on the expression

of TNF-α and P53 genes in both the liver and the kidney, while increasing the expression of the IL-4 and Bcl2 genes, especially in the kidney. However, rats treated with sodium nitrite showed a considerable increase in the expression of TNF-α cytokine and tumor suppressor P53 gene in the kidney and liver, while a significant reduction was detected in the anti-inflammatory cytokine IL-4 and the apoptosis suppressor gene BCL-2, compared to the control group (Figure 7). These results are consistent with Soliman et al. (Soliman et al., 2022) and Elsherbiny et al. (Elsherbiny et al., 2017) who showed that administration increases the expression of TNF-α and other indicators related to inflammation (CRP, TNF-α, IL-6, IL-1β), but also reduces anti-inflammatory cytokine expression (IL-10 and IL-4). Moreover, Radwan et al. (Radwan et al., 2020) reported that the application of NaNO2 and benzoate mixture triggers alterations in immunohistopathology, biochemical markers, and p53 overexpression. Adu et al. (2020) and El-Nabarawy et al. (2020) showed that nitrite substantially influences the expression of levels of P53 and Bcl-2. Likewise, Soliman et al. (2022) showed that sodium nitrite-treated rats exhibit elevated levels of ROS, triggering numerous stress signaling pathways, including NF-B, which encourages increased expression of TNF-α, IL-1, and IL-6. Interestingly, the administration of SCREE demonstrated the ability to modulate the expression levels of inflammatory cytokines and apoptotic genes in the liver and kidney. In this regard, the administration of SCREE to NaNO2-treated rats exhibited a significant and dose-dependent ability to elevate the expression of the IL-4 and Bcl2 genes, but also downregulate the expression of TNF-α and tumor suppressor gene P53 in both kidney and liver (Figure 7). Our findings aligned with previous findings that revealed that the S. costus extract has the potential to regulate cell apoptosis by controlling the expression of the Bcl-2 and P53 genes (Alotaibi et al., 2021). Moreover, Zhao et al. (2008) found that sesquiterpenes from S. costus exhibit an anti-inflammatory ability to mitigate elevated levels of nitric oxide and TNF- release of TNF-α by LPS-activated macrophages. The observed anti-inflammatory and anti-apoptotic potential of SCREE could be associated with the detected set of metabolites, including apigenin, apigenin-7-O-glucoside, luteolin, daidzein, acacetin and formononetin. The improvement in apoptotic and inflammatory markers could be attributed to the presence of daidzein and apigenin in SCREE, which play a crucial role in the regulation of tumor cell invasion (Singh et al., 2023). Daidzein exerts its anti-inflammatory effects by downregulating TNF-α expression by inhibiting the nuclear factor-kappa B (NF-κB) signaling pathway. Daidzein also enhances IL-4 expression in experimental models by promoting Th2 cell differentiation (Wei et al., 2012). The anti-inflammatory properties of apigenin were observed in LPS-stimulated BV2 microglia, where activation of the GSK-3β/Nrf2 signaling pathway attenuated the expression of IL-6, IL-1β, and TNF-α (Chen et al., 2020). Together, our findings suggest that SCREE exhibits dual effects, comprising anti-inflammatory and anti-apoptotic activities.

4 Evaluation of differential display PCR (DD-PCR)

To gain more insight into the mode of action of SCREE, differential display PCR analysis was performed using the following primers (P5, P4, G23, G24, and NAR) for the kidney and liver. The total number of resolved bands for kidney samples in both control and treated samples was 4, 5, 9, 7, and nine bands for the P5, C24, G23, NAR and P4 primers, respectively. Furthermore, the total bands resolved for the liver for treatment and control samples were 4, 6, 9, 7, and nine bands for the P5, C24, G23, NAR and P4 primers, respectively. The typical number of bands per sample was 6.8 and seven for the kidney and liver, respectively. Of the 69 bands, 34 were for the kidney and 35 for the liver, six monomorphic (17.6%) and 28 (82.4%) polymorphic band recordings were recorded for the kidney, while 13 monomorphic (31.4%) and 24 (68.6%) polymorphic bands were recorded for the liver. Some common bands were seen in both treated samples and controls. There were few treatment-induced bands visible (the genes were turned on). On the contrary, some of the controls noticed bands that disappeared in the treated groups (genes were turned off). Numerous bands were highly lighted, indicating that these genes were overexpressed. Overall, these findings showed that numerous genes were found to be upregulated (overexpressed) and downregulated in various treatments when the chosen primers. Based on the differential display, a liver dendrogram was created that revealed that the eight treatment groups were divided by the tree into two main groups (Figure 8). Cluster one included the SCREE 400 (outer group), while Cluster two had the remaining seven treatments. There were two major subclusters in the second cluster; subcluster one contains SCREE 200, whereas the second subcluster was divided into two groups: the first group was divided into two subgroups, the first for NaNO2 and SCREE 200, the second subgroup for NaNO2 and SCREE 400. The second group was divided into three subgroups, the first subgroup for SCREE 600, the second for NaNO2, and the third subgroup included NaNO2 and SCREE 600 and the control group. In general, the tree topology shows that the NaNO2 + SCREE 600 group is more like the control group (Figure 8). However, the dendrogram constructed based on the differential kidney display indicated that the tree classified the eight treated groups into two main clusters. The first cluster was divided into two groups, the first for control and the second for NaNO2 + SCREE 600, and the remaining six treatments were part of the second cluster. Two subclusters were separated from the second cluster; the first was for the NaNO2 group NaNO2. In the second subgroup, there were two groups: the first group was divided into three subgroups, the first for SCREE 600, the second subgroup for SCREE 600, and the third subgroup for NaNO2 and SCREE 400. The second group was split into two subgroups, the first for NaNO2 and SCREE 200 and the second for SCREE 400. The phylogeny tree has revealed that NaNO2 + SCREE 600 is closer to the control group (Figure 8). Animals given NaNO2 + SCREE 600 were found to have the main genetic profile obtained with the control, which means that SCREE 600 removes any effects on NaNO2, which is observed from the behavior of the mRNA profile. These findings align with the results of Fadda et al. (2018b), who observed that a select few antioxidants were effective in modulating the expression of NF-jB, BcL-2, Bax and flt-1 mRNA. Furthermore, compared to rats exposed to NaNO2-induced toxicity, these antioxidants also exhibited the ability to regulate factors such as oxidative DNA damage, vascular endothelial growth factor (VEGF), and the apoptotic marker caspase 3. The observed enhancement associated with SCREE aligns with the research by Chen et al. (1995), which revealed that the active metabolites within

SCREE, namely, costunolide and dihydrocostus lactone, effectively inhibit the expression of the hepatitis B virus surface antigen gene in human hepatic tissue. In addition, Bains et al. (2019) found that the presence of sesquiterpene lactones gives SCREE its enormous pharmacological potential and molecular efficiency. On the other hand, Fukuda et al. (2001) found that the main sesquiterpene lactone in SCREE, costunolide, has chemoprotective effects on the development of cancer. Further, Kang et al. (2004) found that the biological activity of sesquiterpene lactone extracted from the root of S. costus includes anticarcinogenic and antifungal effects.

4.1 Histopathological analysis of the liver

We further expand our study to explore the effect of SCREE by performing a detailed histopathological analysis of the liver to validate the results and identify any pathological changes. As shown in (Figure 9), histological examination of liver segments stained with hematoxylin and eosin in the control (G1) and SCREE (G2, G3 and G4) rat groups revealed a normal liver architecture compared to the control (Table 2). However, liver sections of NaNO2-treated rats (G5) showed marked dilation of the portal tract and bile duct surrounded by marked fibrotic cells and necrotic cells. According to our biochemical findings, liver sections from rats coadministered with SCREE and NaNO2 (G6, G7, and G8) exhibited a significant modulation of the toxic action of NaNO2, and regenerating hepatocytes were seen especially with the high dose of SCREE compared to the NaNO2 group (Figure 9). In our study, liver sections from rats co-administrated with SCREE and NaNO2 showed a noticeable reduction in the harmful effects of NaNO2. Furthermore, considerable regenerating hepatocytes were observed in the group that received a high dose of SCREE, compared to the NaNO2 group. Several authors reported that in the NaNO2-treated group significant histological changes were observed, indicating hepatotoxicity (Aita and Mohammed, 2014). In this regard, Fouad et al. (Khalil, 2016) showed that NaNO2 toxicity caused degenerative changes, including vacuolar degeneration of hepatocytes, as well as congestion and swelling of the blood sinusoid and portal vein. The potential hepatoprotective and antifibrotic effects of S. costus root may be due to its ability to block the calcium channel that prevents hypoxia and new angiogenesis (Gilani et al., 2007; Ali et al., 2018). Furthermore, it was shown that liver histological structure was significantly improved by the ethanol extract of S. costus (Elshaer et al., 2022). Together, our findings further indicate that SCREE has the ability to decrease the effect of NaNO2 deterioration on liver tissue.

4.2 Kidney histopathological analysis

Next, we evaluated kidney tissues stained with hematoxylin and eosin to examine the effect of SCREE on mitigating the effect of NaNO2 treatment. As shown in Figure 10, the renal cortex of the kidney tissue of control (G1) and SCREE (G2, G3 and G4) showed a normal histological architecture of the glomeruli and renal tubules under light microscopy. Unlike the control group, microscopic examination of renal cortex sections of the NaNO2 group (G5) revealed marked atrophied of many glomeruli (AG) surrounded by marked dilation renal tubules (DIT), marked dilation of proximal and distal tubules with many atrophied epithelial cells (AE), and differentiated fibrotic cell (F) (Figure 10). Compared to the group that received sodium nitrite, co-administration of SCREE with NaNO2 (G6, G7, and G8) altered the toxic action of NaNO2, and regeneration of renal tubules was observed at medium and high doses. Similarly, microscopic examination of the renal tubules revealed a wide variety of necrobiotic alterations, including vacuolization, swelling, and necrosis of the epithelium that encloses the convoluted proximal tubules. These findings are consistent with previous research that demonstrated the nephrotoxic potential of NaNO2 administration by inducing notable kidney effects, particularly tubular degeneration, in conjunction with concurrent hydropic cellular degeneration in the liver. These findings emphasize the significant nephrotoxic potential of sodium nitrite, suggesting a direct detrimental impact on renal tissue integrity and function in rodent models (Özen et al., 2014).

In the current study, co-administration of SCREE altered the toxic effects of NaNO2 and improved the regeneration of renal tubules at medium and high doses, compared to the NaNO2-treated group. These changes are ascribed to NaNO2-inducing hypoxia, leading to the creation of free radicals that cause tissue damage (Aita and Mohammed, 2014). These findings aligned with Ayaz who found that early oral administration of S. costus extract (300 mg/kg BW) for 28 days may protect renal tissue from oxidative stress caused by deltamethrin's harmful effects (Ayaz, 2017). The enhanced architecture of the kidney tissue observed with SCREE administration could be attributed to the presence of metabolites such as apigenin and its derivative, apigenin-7-O-glucoside, which exhibit potent antioxidant properties through multiple mechanisms. They interact directly with radicals and metals, leading to a stop in the chain reaction of oxidative stress. Furthermore, apigenin and its glucoside derivative mitigate lipid peroxidation, thus preserving cell membrane integrity (Kashyap et al., 2022). Collectively, these findings further support the therapeutic potential of SCREE to diminish the deterioration effect of NaNO2 treatment on the histological architecture and kidney function.

4.3 Liver immunohistochemical analysis

Finally, we performed immunohistochemical analysis to assess the distribution of immunostaining expression of the transforming growth factor β protein (TGF- β) in liver tissues. As shown in Figure 11, TGF-ß was shown as a brown color diffuse in the cell membrane and cytoplasm of hepatocytes. The liver sections of the control group (G1) showed weak expression for TGF-β. The control SCREE group (G2, 200 mg/kg BW) showed moderately positive expression (+2) of TGF-β protein in the cytoplasm of the centrilobular area of the hepatocytes (CA), while the SCREE group (G3, 400 mg/kg BW) also showed moderately positive expression (+2) in the cytoplasm of the hepatocytes and the cell membrane in the portal area (PT) surrounded by few fibrotic cells (Table 3). Interestingly, the SCREE group (G4, 600 mg/kg BW) exhibited a mild positive expression (+1) in the cytoplasm of hepatocytes and the cell membrane in the portal area (PT) lack

fibrotic cells and the area of regenerative hepatocytes. On the contrary, the liver segments of the NaNO2-treated group (G5) exhibited a strongly positive reaction (+4) of TGF-β protein in the cytoplasm of hepatocytes in the centrilobular area (CA), moderate positive expression (+2) in the cytoplasm of the hepatocytes cytoplasm and cell membrane in the portal area (PT) and the cell membrane mostly adjacent to the necrotic area of hepatocytes. Furthermore, the liver segments of group (G6) showed strongly positive expression (+4) of TGF-β protein in the cytoplasm of the hepatocytes and the spread of the cell membrane in the centrilobular area (CA), while group (G7) showed moderate positive expression (+2) in the cytoplasm of the hepatocytes and the cell membrane in the portal area (PT) with few fibrotic cells (F). Finally, group (G8) showed moderate positive expression (+2) in the cytoplasm and cell membranes of the few hepatocytes in the fibrotic area of the portal tract (PT) (Table 3). The high expression of TGF-β in liver tissue after NaNO2 treatment could also be attributed to hepatic tissue damage caused by changes in liver function markers. Similarly, AlRasheed et al. found that NaNO2 administration resulted in a highly significant increase in small mothers against expressions of decapentaplegic homlog 2(Smad-2), serine/threonine protein kinase (AKT), and hypoxia-inducible factor 1 alpha (HIF1-) with a simultaneous reduction in BcL-2 expression when compared to control in the hepatic, pulmonary, renal, and cardiac tissues (Al-Rasheed et al., 2017). Furthermore, Sherif et al. reported a significant increase in monocyte chemoattractant protein-1 (MCP-1) and TGF-1 levels in the liver of sodium nitrite treated rats (Imam and Mohammed, 2013). Soliman et al. found that NaNO2 treatment elevated ROS production and activated numerous stress signaling pathways, including TNF-α, and TGF-β (Soliman et al., 2022). The observed improvement in SCREE treated groups is consistent with Jia et al. (2013) who found that sesquiterpene lactones prevent MCP-1/TGF-β pathway and the activation of the nuclear factor kappa B (NF-kB) induced by high glucose in rat mesangial cells. Our results indicate that SCREE has the potential to modulate the expression of TGF-β protein in liver tissue and the ability to mitigate the deterioration effect of NaNO2 treatment.

5 Conclusion

This study sheds light on the critical health implications associated with the use of sodium nitrite as a food additive, particularly on vital organs such as the liver and kidneys. Our presented study explored the potential of SCREE supplementation to mitigate NaNO2-induced toxicity. Administration of SCREE demonstrated a remarkable ability to counteract the toxic effects of NaNO2 in a dose-dependent manner. This improved effect was evident in improvements in hematological parameters, lipid profile, and modulation of histopathological architecture in the liver and kidneys. Furthermore, SCREE exhibited a regulatory effect on TNF-α, P53, IL-4, and BCL-2 markers, suggesting its potential to modulate inflammatory and apoptotic pathways. The comprehensive phytochemical analysis of SCREE identified a diverse array of primary and secondary metabolites, including phenolics, flavonoids, vitamins, alkaloids, saponins, and tannins. This unique phytochemical profile, coupled with the observed therapeutic effects, positions SCREE as a promising natural food detoxifying additive. Taken together, this study highlights the potential of the ethanolic extract of the Saussurea costus root as a valuable natural intervention to mitigate the detrimental effects of sodium nitrite, offering a basis for further exploration and development of SCREE as a safe and effective food detoxification strategy in the realm of human health nutrition.

Data availability statement

The raw data supporting the conclusion of this article will be made available by the authors, without undue reservation.

Ethics statement

The animal study was approved by the Institutional Animal Care's Ethical Committee on Animal Experimentation and Use Committee (ALEXU-IACUC) at Alexandria University, Egypt. The ethical Approval number is (AU14-210126-2-3). The study was conducted in accordance with the local legislation and institutional requirements.

Author contributions

SE: Conceptualization, Data curation, Formal Analysis, Investigation, Methodology, Resources, Validation, Writing–original draft, Writing–review and editing. GH: Conceptualization, Formal Analysis, Investigation, Methodology, Project administration, Resources, Software, Visualization, Writing–original draft. SS: Conceptualization, Data curation, Formal Analysis, Methodology, Project administration, Resources, Software, Validation, Writing–original draft, Writing–review and editing. AD: Data curation, Formal Analysis, Investigation, Methodology, Resources, Software, Supervision, Visualization, Writing–review and editing. HB: Conceptualization, Formal Analysis, Investigation, Methodology, Resources, Software, Visualization, Writing–original draft. HH: Data curation, Formal Analysis, Investigation, Validation, Software, Visualization, Writing–review and editing. FE-D: Data curation, Formal Analysis, Investigation, Validation, Conceptualization, Methodology, Project administration, Resources, Writing–original draft. AA: Data curation, Formal Analysis, Funding acquisition, Investigation, Software, Validation, Visualization, Writing–review and editing. EA-O: Data curation, Formal Analysis, Funding acquisition, Investigation, Software, Validation, Visualization, Writing–review and editing. MA: Investigation, Software, Data curation, Formal Analysis, Funding acquisition, Validation, Visualization, Writing–review and editing. MJ: Investigation, Methodology, Writing–original draft, Software. EH: Conceptualization, Funding acquisition, Investigation, Methodology, Project administration, Resources, Supervision, Writing–original draft, Writing–review and editing, Data curation, Validation. ES: Conceptualization, Funding acquisition, Investigation, Methodology, Project administration, Resources,

Supervision, Visualization, Writing–original draft, Writing–review and editing.

Funding

The author(s) declare that financial support was received for the research, authorship, and/or publication of this article. This research was funded by Alexandria University, City of Scientific Research and Technological Applications (SRTA) and Faculty of Science, Suez Canal University, Egypt. The authors also extend their appreciation to Princess Nourah bint Abdulrahman University for funding this work through the Researchers Supporting Project number (PNURSP2024R736), Princess Nourah bint Abdulrahman University, Riyadh, Saudi Arabia. This study was also supported by Researchers Supporting Project number (RSP2024R111), King Saud University, Riyadh, Saudi Arabia.

Acknowledgments

The authors acknowledge the Princess Nourah bint Abdulrahman University for funding this work through the Researchers Supporting Project number (PNURSP2024R736), Princess Nourah bint Abdulrahman University, Riyadh, Saudi Arabia. This study was also supported by Researchers Supporting Project number (RSP2024R111), King Saud University, Riyadh, Saudi Arabia. The identification and validation of the roots studied were carried out under the guidance of Assistant Professor Maha Elshamy from the Department of Botany, Faculty of Science, Mansoura University, Egypt.

Conflict of interest

The authors declare that the research was conducted in the absence of any commercial or financial relationships that could be construed as a potential conflict of interest.

The author(s) declared that they were an editorial board member of Frontiers, at the time of submission. This had no impact on the peer review process and the final decision.

Publisher's note

Supplementary material

The Supplementary Material for this article can be found online at: https://www.frontiersin.org/articles/10.3389/fphar.2024.1378249/full#supplementary-material

References

Abdallah, E. M., Qureshi, K. A., Ali, A. M., and Elhassan, G. (2017). Evaluation of some biological properties of Saussurea costus crude root extract. *Biosci. Biotech. Res. Comm.* 10 (4), 601–611. doi:10.21786/bbrc/10.4/2

Abd El-Rahman, G. I., Behairy, A., Elseddawy, N. M., Batiha, G. E.-S., Hozzein, W. N., Khodeer, D. M., et al. (2020). Saussurea lappa ethanolic extract attenuates triamcinolone acetonide-induced pulmonary and splenic tissue damage in rats via modulation of oxidative stress, inflammation, and apoptosis. *Inflamm. apoptosis* 9 (5), 396. doi:10.3390/antiox9050396

abdul-hussein, M. (2019). Protective of ethanolic extract of Saussurea lappa against paracetamol-induced hepatic and renal damage in male rabbits. *Asian J. Pharm. Clin. Res.* 12, 68–73. doi:10.22159/ajpcr.2019.v12i18.34218

Abo-El-Sooud, K., Hashem, M. M., Abd ElHakim, Y. M., Kamel, G. M., Eleiwa, M., and Gab-Alllah, A. (2019). Effect of sodium nitrite exposure on the immune responses against of rift valley fever vaccine in mice. *Int. J. Pharm. Pharm. Sci.*, 28–31. doi:10.22159/ijpps.2019v11i7.33443

Adu, A., Sudiana, I., and Martini, S. (2020). The effect of nitrite food preservatives added to se'i meat on the expression of wild-type p53 protein. *Open Chem.* 18, 559–564. doi:10.1515/chem-2020-0094

Ahmed, A. H. A. (2017). The effect of water extracts of Phyllanthus emblica and Costus speciousus on reducing obesity in albino rats. *Alexandria Sci. Exch. J.* 38, 463–472. doi:10.21608/asejaiqjsae.2017.3750

Aita, N., and Mohammed, F. (2014). Effect of marjoram oil on the clinicopathological, cytogenetic and histopathological alterations induced by sodium nitrite toxicity in rats. *Glob. Veterinaria* 12, 606–616. doi:10.5829/idosi.gv.2014.12.05.83186

Albaugh, V. L., Mukherjee, K., and Barbul, A. (2017). Proline precursors and collagen synthesis: biochemical challenges of nutrient supplementation and wound healing. *J. Nutr.* 147 (11), 2011–2017. doi:10.3945/jn.117.256404

Al-Gayyar, M. M., Alyoussef, A., Hamdan, A. M., Abbas, A., Darweish, M. M., and El-Hawwary, A. A. (2015). Cod liver oil ameliorates sodium nitrite-induced insulin resistance and degradation of rat hepatic glycogen through inhibition of cAMP/PKA pathway. *Life Sci.* 120, 13–21. doi:10.1016/j.lfs.2014.11.002

Ali, M., Khan, T., Fatima, K., Ali, Q. u. A., Ovais, M., Khalil, A. T., et al. (2018). Selected hepatoprotective herbal medicines: evidence from ethnomedicinal applications, animal models, and possible mechanism of actions. *Phytotherapy Res.* 32 (2), 199–215. doi:10.1002/ptr.5957

Alnahdi, H. S. (2017). Injury in metabolic gland induced by pyrethroid insecticide could Be reduced by aqueous extract of sassura lappa. *Int. J. Pharm. Res. Allied Sci.* 6 (2), 86–97.

Alotaibi, A. A., Bepari, A., Assiri, R. A., Niazi, S. K., Nayaka, S., Rudrappa, M., et al. (2021). Saussurea lappa exhibits anti-oncogenic effect in hepatocellular carcinoma, HepG2 cancer cell line by bcl-2 mediated apoptotic pathway and mitochondrial cytochrome C release. *Curr. Issues Mol. Biol.* 43, 1114–1132. doi:10.3390/cimb43020079

Al-Rasheed, N. M., Fadda, L. M., Attia, H. A., Ali, H. M., and Al-Rasheed, N. M. (2017). Quercetin inhibits sodium nitrite-induced inflammation and apoptosis in different rats organs by suppressing Bax, HIF1-α, TGF-β, Smad-2, and AKT pathways. *J. Biochem. Mol. Toxicol.* 31 (5), e21883. doi:10.1002/jbt.21883

Al-Zayadi, Z. A., Shanan, H. K., and Al Salihi, K. A. (2023). "Extraction and evaluation of active ingredients of Saussurea costus roots and determination of its antibacterial activity," in *IOP conference series: earth and environmental science* (Bristol, United Kingdom: IOP Publishing).012058

Armeni, T., Cianfruglia, L., Piva, F., Urbanelli, L., Caniglia, M. L., Pugnaloni, A., et al. (2014). S-D-Lactoylglutathione can be an alternative supply of mitochondrial glutathione. *Free Radic. Biol. Med.* 67, 451–459. doi:10.1016/j.freeradbiomed.2013.12.005

Arrivault, S., Guenther, M., Ivakov, A., Feil, R., Vosloh, D., Van Dongen, J. T., et al. (2009). Use of reverse-phase liquid chromatography, linked to tandem mass spectrometry, to profile the Calvin cycle and other metabolic intermediates in Arabidopsis rosettes at different carbon dioxide concentrations. *Plant J.* 59 (5), 826–839. doi:10.1111/j.1365-313X.2009.03902.x

Asif, M. J. C. (2015). Chemistry and antioxidant activity of plants containing some phenolic compounds. *Biomolecules* 1 (1), 35–52. doi:10.31221/osf.io/rygwm

Attallah, N. G. M., Kabbash, A., Negm, W. A., Elekhnawy, E., Binsuwaidan, R., Al-Fakhrany, O. M., et al. (2023). Protective potential of Saussurea costus (falc.) Lipsch. Roots against cyclophosphamide-induced pulmonary injury in rats and its *in vitro* antiviral effect. *Pharmaceuticals* 16 (2), 318. doi:10.3390/ph16020318

Ayaz, N. O. (2017). Modulating impacts of coustus Sassura lappa extract against oxidative stress and genotoxicity induced by deltamethrin toxicity in rat kidneys. *Int. J. Pharm. Res. allied Sci.* 6 (2), 49–60.

Bains, S., Thakur, V., Kaur, J., Singh, K., and Kaur, R. (2019). Elucidating genes involved in sesquiterpenoid and flavonoid biosynthetic pathways in Saussurea lappa by *de novo* leaf transcriptome analysis. *Genomics* 111 (6), 1474–1482. doi:10.1016/j.ygeno.2018.09.022

Baky, N. A. A., Zaidi, Z. F., Fatani, A. J., Sayed-Ahmed, M. M., and Yaqub, H. (2010). Nitric oxide pros and cons: the role of l-arginine, a nitric oxide precursor, and idebenone, a coenzyme-Q analogue in ameliorating cerebral hypoxia in rat. *Brain Res. Bull.* 83 (1), 49–56. doi:10.1016/j.brainresbull.2010.07.004

Bancroft, J. D., Stevens, A., Bancroft, J. D., and Stevens, A. (1990) *Theory and practice of histological techniques*.

Bari, M. L., and Yeasmin, S. (2018). "Foodborne diseases and responsible agents," in *Food safety and preservation* (Amsterdam, Netherlands: Elsevier), 195–229.

Barrero, A. F., Oltra, J. E., Álvarez, M. r., Raslan, D. S., and Akssira, M. (2000). New sources and antifungal activity of sesquiterpene lactones. *Fitoterapia* 71 (1), 60–64. doi:10.1016/s0367-326x(99)00122-7

Beniddir, M. A., Kang, K. B., Genta-Jouve, G., Huber, F., Rogers, S., and Van Der Hooft, J. J. J. N. (2021). Advances in decomposing complex metabolite mixtures using substructure-and network-based computational metabolomics approaches. *Nat. Prod. Rep.* 38 (11), 1967–1993. doi:10.1039/d1np00023c

Boham, B., and Kocipai-Abyazan, R. J. P. (1974). Flavonoids and condensed tannins from leaves of Hawaiian vaccinium vaticulatum and V. calycinium. *Pac Sci.* 48 (4), 458–463.

Boro, H., Das, S., and Middha, S. K. J. A. i. T. M. (2021). The therapeutic potential and the health benefits of Morus indica Linn.: a mini review. *a mini Rev.* 21, 241–252. doi:10.1007/s13596-020-00544-5

Bromke, M. A., Hochmuth, A., Tohge, T., Fernie, A. R., Giavalisco, P., Burgos, A., et al. (2015). Liquid chromatography high-resolution mass spectrometry for fatty acid profiling. *Plant J.* 81 (3), 529–536. doi:10.1111/tpj.12739

Buchwalow, I. B., and Böcker, W. (2010). Immunohistochemistry. *Basics Methods* 1, 1–149. doi:10.4016/16455.01

Chain, E. P., Schrenk, D., Bignami, M., Bodin, L., Chipman, J. K., del Mazo, J., et al. (2023). Risk assessment of N-nitrosamines in food. *EFSA J.* 21 (3), e07884. doi:10.2903/j.efsa.2023.7884

Chen, H.-C., Chou, C.-K., Lee, S.-D., Wang, J.-C., and Yeh, S.-F. (1995). Active compounds from Saussurea lappa Clarks that suppress hepatitis B virus surface antigen gene expression in human hepatoma cells. *Antivir. Res.* 27 (1), 99–109. doi:10.1016/0166-3542(94)00083-k

Chen, P., Huo, X., Liu, W., Li, K., Sun, Z., and Tian, J. (2020). Apigenin exhibits anti-inflammatory effects in LPS-stimulated BV2 microglia through activating GSK3β/Nrf2 signaling pathway. *Immunopharmacol. Immunotoxicol.* 42 (1), 9–16. doi:10.1080/08923973.2019.1688345

Ciji, A., Sahu, N. P., Pal, A. K., and Akhtar, M. S. (2013). Nitrite-induced alterations in sex steroids and thyroid hormones of Labeo rohita juveniles: effects of dietary vitamin E and l-tryptophan. *Fish Physiology Biochem.* 39 (5), 1297–1307. doi:10.1007/s10695-013-9784-8

Cvetković, D., Živković, V., Lukić, V., and Nikolić, S. (2019). Sodium nitrite food poisoning in one family. *Forensic Sci. Med. Pathology* 15 (1), 102–105. doi:10.1007/s12024-018-0036-1

Deabes, M. M., Fatah, A.-E., Sally, I., Salem, S. H. E., and Naguib, K. M. J. E. J. (2021). Antimicrobial activity of bioactive compounds extract from Saussurea costus against food spoilage microorganisms. *Egypt. J. Chem.* 64 (6), 2833–2843. doi:10.21608/EJCHEM.202169572.3528

Dikshith, T. S. S., Raizada, R. B., and Srivastava, M. K. (1991). Long-term dietary study and development of no-observed-effect level (NOEL) of technical HCH to rats. *J. Toxicol. Environ. Health* 34 (4), 495–507. doi:10.1080/15287399109531585

DuBois, M., Gilles, K. A., Hamilton, J. K., Rebers, P. t., and Smith, F. (1956). Colorimetric method for determination of sugars and related substances. *Anal. Chem.* 28 (3), 350–356. doi:10.1021/ac60111a017

Edeoga, H. O., Okwu, D., and Mbaebie, B. (2005). Phytochemical constituents of some Nigerian medicinal plants. *Afr. J. Biotechnol.* 4 (7), 685–688. doi:10.5897/ajb2005.000-3127

Eissa, M. A., Hashim, Y. Z. H., El-Kersh, D. M., Abd-Azziz, S. S., Salleh, H. M., Isa, M. L. M., et al. (2020). Metabolite Profiling of Aquilaria malaccensis leaf extract using Liquid Chromatography-Q-TOF-Mass spectrometry and investigation of its potential antilipoxygenase activity *in-vitro*. *Processes* 8 (2), 202. doi:10.3390/pr8020202

El-Demerdash, F. M., Baghdadi, H. H., Ghanem, N. F., and Mhanna, A. B. A. (2020). Nephroprotective role of bromelain against oxidative injury induced by aluminium in rats. *Environ. Toxicol. Pharmacol.* 80, 103509. doi:10.1016/j.etap.2020.103509

El-Demerdash, F. M., El-Sayed, R. A., and Abdel-Daim, M. M. (2021a). Rosmarinus officinalis essential oil modulates renal toxicity and oxidative stress induced by potassium dichromate in rats. *J. Trace Elem. Med. Biol.* 67, 126791. doi:10.1016/j.jtemb.2021.126791

El-Demerdash, F. M., El-Sayed, R. A., and Abdel-Daim, M. M. (2021b). Hepatoprotective potential of Rosmarinus officinalis essential oil against hexavalent chromium-induced hematotoxicity, biochemical, histological, and immunohistochemical changes in male rats. *Environ. Sci. Pollut. Res.* 28 (14), 17445–17456. doi:10.1007/s11356-020-12126-8

El Gizawy, H. A., El-Haddad, A. E., Saadeldeen, A. M., and Boshra, S. A. J. M. (2022). Tentatively identified (UPLC/T-TOF-MS/MS) compounds in the extract of Saussurea costus roots exhibit *in vivo* hepatoprotection via modulation of HNF-1α, sirtuin-1, C/ebpα, miRNA-34a and miRNA-223. *Sirtuin-1, C/Ebpα, MiRNA-34a MiRNA-223* 27 (9), 2802. doi:10.3390/molecules27092802

El-Nabarawy, N. A., Gouda, A. S., Khattab, M. A., and Rashed, L. A. (2020). Effects of nitrite graded doses on hepatotoxicity and nephrotoxicity, histopathological alterations, and activation of apoptosis in adult rats. *Environ. Sci. Pollut. Res.* 27 (12), 14019–14032. doi:10.1007/s11356-020-07901-6

Elsayed, H., Mohamad, M., Gabr, O., and Badria, F. (2015). Saussurea lappa root extract accelerates the reversion of liver fibrosis induced by carbon tetrachloride in rats. *Benha Med. J.* 32, 116–125. doi:10.4103/1110-208x.180324

Elshaer, S. E., Hamad, G. M., Hafez, E. E., Baghdadi, H. H., El-Demerdash, F. M., and Simal-Gandara, J. (2022). Root extracts of Saussurea costus as prospective detoxifying food additive against sodium nitrite toxicity in male rats. *Food Chem. Toxicol.* 166, 113225. doi:10.1016/j.fct.2022.113225

El-Sheikh, N. M., and Khalil, F. A. (2011). l-Arginine and l-glutamine as immunonutrients and modulating agents for oxidative stress and toxicity induced by sodium nitrite in rats. *Food Chem. Toxicol.* 49 (4), 758–762. doi:10.1016/j.fct.2010.11.039

Elsherbiny, N. M., Maysarah, N. M., El-Sherbiny, M., and Al-Gayyar, M. M. (2017). Renal protective effects of thymoquinone against sodium nitrite-induced chronic toxicity in rats: impact on inflammation and apoptosis. *Life Sci.* 180, 1–8. doi:10.1016/j.lfs.2017.05.005

Fadda, L. M., Attia, H. A., Al-Rasheed, N. M., Ali, H. M., and Al-Rasheed, N. M. (2018a). Roles of some antioxidants in modulation of cardiac myopathy induced by sodium nitrite via down-regulation of mRNA expression of NF-κB, Bax, and flt-1 and suppressing DNA damage. *Saudi Pharm. J.* 26 (2), 217–223. doi:10.1016/j.jsps.2017.12.008

Fadda, L. M., Attia, H. A., Al-Rasheed, N. M., Ali, H. M., and Al-Rasheed, N. M. (2018b). Downregulation of flt-1 and HIF-1α gene expression by some antioxidants in rats under sodium nitrite-induced hypoxic stress. *Dose-Response* 16 (2), 1559325818776204. doi:10.1177/1559325818776204

Fan, H., and Robetorye, R. S. (2010). "Real-time quantitative reverse transcriptase polymerase chain reaction," in *RT-PCR protocols* (Berlin, Germany: Springer), 199–213.

Fouad, S. S., Mohi-Eldin, M. M., Haridy, M. A., and Khalil, A. M. (2017). Ameliorative effects of ascorbic acid (vit. C) against sodium nitrite toxicity in albino rats: hematological, biochemical and histopathological studies. *American-Eurasian J. Toxicol. Sci.* 9 (1), 01–06.

Fromm, O., and DeGolier, T. (2021). The contractile capabilities of various herbal constituents on uterine smooth muscle and their shared constituent presence involved with anti-inflammatory/antioxidant mechanisms. *J. Pharmacogn. Phytochemistry* 10 (4), 28–37.

Fukuda, K., Akao, S., Ohno, Y., Yamashita, K., and Fujiwara, H. (2001). Inhibition by costunolide of phorbol ester-induced transcriptional activation of inducible nitric oxide synthase gene in a human monocyte cell line THP-1. *Cancer Lett.* 164 (1), 7–13. doi:10.1016/s0304-3835(00)00704-7

Gallo, M., and GĬ̆miz, F. (2023). Choline: an essential nutrient for human health. *Nutrients* 15, 2900. doi:10.3390/nu15132900

Gilani, A. H., Shah, A. J., and Yaeesh, S. (2007). Presence of cholinergic and calcium antagonist constituents in Saussurea lappa explains its use in constipation and spasm. *Phytotherapy Res.* 21 (6), 541–544. doi:10.1002/ptr.2098

Ginwala, R., Bhavsar, R., Chigbu, D. G. I., Jain, P., and Khan, Z. K. (2019). Potential role of flavonoids in treating chronic inflammatory diseases with a special focus on the anti-inflammatory activity of apigenin. *Antioxidants* 8, 35. doi:10.3390/antiox8020035

Gluhcheva, Y., Ivanov, I., Petrova, E., Pavlova, E., and Vladov, I. (2012). Sodium nitrite-induced hematological and hemorheological changes in rats. *Ser. Biomechanics* 27, 4–53.

Grant, D., and Butler, W. H. (1989). Chronic toxicity of sodium nitrite in the male F344 rat. *Food Chem. Toxicol.* 27 (9), 565–571. doi:10.1016/0278-6915(89)90015-x

Hafez, E., Hashem, M., Balbaa, M., El-Saadani, M., and Ahmed, S. (2013). Induction of new defensin genes in tomato plants via pathogens-biocontrol agent interaction. *J. Plant Pathol. Microb.* 4 (167), 2. doi:10.4172/2157-7471.1000167

Hamad, G., Hafez, E., Khaled, A., and A. Amara, A. (2018). Amino acids diets as model for investigating cancer induced by acrylamide produced during wrong food cooking. *SOJ Biochem.* 4 (1), 1–14. doi:10.15226/2376-4589/4/1/00126

Hammoud, G. (2014). Protective effect of grape seeds extract against sodium nitrite-induced toxicity and oxidative stress in albino rats. *Al-Azhar J. Pharm. Sci.* 49, 1–34. doi:10.21608/ajps.2014.6956

Hanh, T. T. H., Cham, P. T., My, N. T. T., Cuong, N. T., Dang, N. H., Quang, T. H., et al. (2021). Sesquiterpenoids from Saussurea costus. *Nat. Prod. Res.* 35 (9), 1399–1405. doi:10.1080/14786419.2019.1650357

Hassan, H. A., El-Agmy, S. M., Gaur, R. L., Fernando, A., Raj, M. H., and Ouhtit, A. (2009). *In vivo* evidence of hepato-and reno-protective effect of garlic oil against sodium nitrite-induced oxidative stress. *Int. J. Biol. Sci.* 5 (3), 249–255. doi:10.7150/ijbs.5.249

Hassan, H. A., Hafez, H. S., and Zeghebar, F. E. (2010). Garlic oil as a modulating agent for oxidative stress and neurotoxicity induced by sodium nitrite in male albino rats. *Food Chem. Toxicol.* 48 (7), 1980–1985. doi:10.1016/j.fct.2010.05.001

Hassan, H. A., and Yousef, M. I. (2010). Ameliorating effect of chicory (Cichorium intybus L.)-supplemented diet against nitrosamine precursors-induced liver injury and oxidative stress in male rats. *Food Chem. Toxicol.* 48 (8-9), 2163–2169. doi:10.1016/j.fct.2010.05.023

Hassan, R. O., and Ali, D. S. (2010). Determination of content levels of nitrogen species (Nitrite, Nitrate, and N-Nitrosamines) in processed meat consumed in Erbil City. *Der Pharma Chem.* 2 (6), 31–37.

Heinrich, M., Mah, J., and Amirkia, V. (2021). Alkaloids used as medicines: structural phytochemistry meets biodiversity-an update and forward look. *Molecules* 26 (7), 1836. doi:10.3390/molecules26071836

Helal, E., Zaahkouk, S. A., and Mekkawy, H. A. (2000). Effect of some food colorants (synthetic andNatural products) of young albino rats. *Egypt. J. Hosp. Med.* 1, 103–113. doi:10.21608/ejhm.2000.11021

Helal, E. G. E., Almutairi, A., Abdelaziz, M. A., and Mohamed, A. A. H. (2020). Adverse effects of fast green, sodium nitrate and Glycine on some physiological parameters. *Egypt. J. Hosp. Med.* 80 (3), 964–970. doi:10.21608/ejhm.2020.104304

Helal, E. G. E., El-Sayed, R. A. A., Hedeab, G., and El-Gamal, M. S. (2017). Effects of some food additives on some biochemical parameters in young male albino rats and the ameliorative role of royal jelly. *Egypt. J. Hosp. Med.* 67 (2), 605–613. doi:10.12816/0037812

Helal, E., M, A.-K., H, A. W., S, Z., and Soliman, G. Z. A. (2008). Biochemical studies on the effect of sodium nitrite and/or glutathione treatment on male rats. *Egypt. J. Hosp. Med.* 30 (1), 25–38. doi:10.21608/ejhm.2008.17650

Huestis, M. A. (2007). Human cannabinoid pharmacokinetics. *Chem. Biodivers.* 4 (8), 1770–1804. doi:10.1002/cbdv.200790152

Imam, O. S., and Mohammed, M. H. A.-G. (2013). Antioxidant, anti-inflammatory and hepatoprotective effects of silymarin on hepatic dysfunction induced by sodium nitrite. *Eur. Cytokine Netw.* 24 (3), 114–121. doi:10.1684/ecn.2013.0341

Jensen, F. B. (2007). Nitric oxide formation from nitrite in zebrafish. *J. Exp. Biol.* 210 (19), 3387–3394. doi:10.1242/jeb.008748

Jia, Q.-Q., Wang, J.-C., Long, J., Zhao, Y., Chen, S.-J., Zhai, J.-D., et al. (2013). Sesquiterpene lactones and their derivatives inhibit high glucose-induced NF-κB activation and MCP-1 and TGF-β1 expression in rat mesangial cells. *Molecules* 18, 13061–13077. doi:10.3390/molecules181013061

Johnson, R. J., Nakagawa, T., Jalal, D., SГЎnchez-Lozada, L. G., Kang, D.-H., and Ritz, E. (2013). Uric acid and chronic kidney disease: which is chasing which? *Nephrol. Dial. Transplant.* 28 (9), 2221–2228. doi:10.1093/ndt/gft029

Julianti, T. (2014) *Discovery of natural antiprotozoals from medicinal plants Saussurea costus and Carica papaya*. Basel, Switzerland: University_of_Basel.

Kadam, P., and Bodhankar, S. (2013). Analgesic and anti-inflammatory activity of seed extracts of diplocyclos palmatus (L) C. Jeffrey. *Int. J. Pharma Bio Sci.* 4, P970–P978.

Kang, J. S., Yoon, Y. D., Lee, K. H., Park, S.-K., and Kim, H. M. (2004). Costunolide inhibits interleukin-1beta expression by down-regulation of AP-1 and MAPK activity in LPS-stimulated RAW 264.7 cells. *Biochem. Biophysical Res. Commun.* 313 (1), 171–177. doi:10.1016/j.bbrc.2003.11.109

Kapoor, R., and Huang, Y.-S. (2006). Gamma linolenic acid: an antiinflammatory omega-6 fatty acid. *Curr. Pharm. Biotechnol.* 7 (6), 531–534. doi:10.2174/138920106779116874

Kashyap, P., Shikha, D., Thakur, M., and Aneja, A. (2022). Functionality of apigenin as a potent antioxidant with emphasis on bioavailability, metabolism, action mechanism and *in vitro* and *in vivo* studies: a review. *J. Food Biochem.* 46 (4), e13950. doi:10.1111/jfbc.13950

Khalid, A., Rehman, U., Sethi, A., Khilji, S., Fatima, U., Khan, M. I., et al. (2011). Antimicrobial activity analysis of extracts of Acacia modesta, Artimisia absinthium, Nigella sativa and Saussurea lappa against Gram positive and Gram negative microorganisms. *Afr. J. Biotechnol.* 10 (22), 4574–4580. doi:10.5897/AJB11.109

Khalil, A. (2016). Ameliorative effects of ascorbic acid (vit. C) against sodium nitrite toxicity in albino rats: hematological. *Biochem. Histopathol. Stud.*

Khirallah, S. M., Ramadan, H. M. M., Shawky, A., Qahl, S. H., Baty, R. S., Alqadri, N., et al. (2022). Development of novel 1,3-disubstituted-2-thiohydantoin analogues with potent anti-inflammatory activity; *in vitro* and *in silico* assessments. *Molecules* 27. doi:10.3390/molecules27196271

Ko, S. G., Kim, H.-P., Jin, D.-H., Bae, H.-S., Kim, S. H., Park, C.-H., et al. (2005). Saussurea lappa induces G2-growth arrest and apoptosis in AGS gastric cancer cells. *Cancer Lett.* 220 (1), 11–19. doi:10.1016/j.canlet.2004.06.026

Kolaylı, S., Sahin, H., Ulusoy, E., and Tarhan, Ö. (2010). Phenolic composition and antioxidant capacities of Helichrysum plicatum. *Hacet. J. Biol. Chem.* 38, 269–276.

Koriem, K. M. M., and Tharwat, H. A. K. (2023). Malic acid improves behavioral, biochemical, and molecular disturbances in the hypothalamus of stressed rats. *JIN* 22 (4), 98. doi:10.31083/j.jin2204098

Kulkarni, S. (2001). Immunostimulant activity of inulin isolated from Saussurea lappa roots. *Indian J. Pharm. Sci.* 63 (4), 292.

Kumar, J., and Pundir, M. (2022). Phytochemistry and pharmacology of Saussurea genus (Saussurea lappa, Saussurea costus, Saussurea obvallata, Saussurea involucrata). *Mater. Proc.* 56, 1173–1181. doi:10.1016/j.matpr.2021.11.145

Le-Vinh, B., AkkuЕџ-DaДџdeviren, Z. B., Le, N. M. N., Nazir, I., and Bernkop-SchnГјrch, A. (2022). Alkaline phosphatase: a reliable endogenous partner for drug delivery and Diagnostics. *Adv. Ther.* 5 (2), 2100219. doi:10.1002/adtp.202100219

Li, H., Li, S., Yang, H., Wang, Y., Wang, J., and Zheng, N. J. T. (2019). l-Proline alleviates kidney injury caused by AFB1 and AFM1 through regulating excessive apoptosis of kidney cells. *Toxins (Basel)* 11 (4), 226. doi:10.3390/toxins11040226

Liang, P., and Pardee, A. B. (1992). Differential display of eukaryotic messenger RNA by means of the polymerase chain reaction. *Science* 257 (5072), 967–971. doi:10.1126/science.1354393

Lin, Y., Shi, R., Wang, X., and Shen, H.-M. (2008). Luteolin, a flavonoid with potential for cancer prevention and therapy. *Curr. Cancer Drug Targets* 8 (7), 634–646. doi:10.2174/156800908786241050

Livak, K. J., and Schmittgen, T. D. (2001). Analysis of relative gene expression data using real-time quantitative PCR and the 2(-Delta Delta C(T)) Method. *methods* 25 (4), 402–408. doi:10.1006/meth.2001.1262

Lotfi, M.-S., and Rassouli, F. B. (2024). Natural flavonoid apigenin, an effective agent against nervous system cancers. *Mol. Neurobiol.* doi:10.1007/s12035-024-03917-y

Lu, X., Zhao, X., Bai, C., Zhao, C., Lu, G., and Xu, G. J. J. C. B. (2008). LC–MS-based metabonomics analysis. *J. Chromatogr. B Anal. Technol. Biomed. Life Sci.* 866 (1-2), 64–76. doi:10.1016/j.jchromb.2007.10.022

Madrigal-Santillán, E., Madrigal-Bujaidar, E., Álvarez-González, I., Sumaya-Martínez, M. T., Gutiérrez-Salinas, J., Bautista, M., et al. (2014). Review of natural products with hepatoprotective effects. *World J. gastroenterology* 20 (40), 14787–14804. doi:10.3748/wjg.v20.i40.14787

Mehedint, M. G., and Zeisel, S. H. (2013). Choline's role in maintaining liver function: new evidence for epigenetic mechanisms. *Curr. Opin. Clin. Nutr. metabolic care* 16 (3), 339–345. doi:10.1097/MCO.0b013e3283600d46

Milkowski, A., Garg, H. K., Coughlin, J. R., and Bryan, N. S. (2010). Nutritional epidemiology in the context of nitric oxide biology: a risk–benefit evaluation for dietary nitrite and nitrate. *Nitric oxide* 22 (2), 110–119. doi:10.1016/j.niox.2009.08.004

Mir, M. A., Parihar, K., Tabasum, U., and Kumari, E. J. J. M. P. S. (2016). Estimation of alkaloid, saponin and flavonoid, content in various extracts of Crocus sativa. *J. Med. Plants Stud.* 4 (5), 171–174.

Mohamed, D. I., El-Waseef, D. A. E.-D. A., Nabih, E. S., El-Kharashi, O. A., El-Kareem, H. F. A., Nahas, H. H. A., et al. (2022a). Acetylsalicylic acid suppresses alcoholism-induced cognitive impairment associated with atorvastatin intake by targeting cerebral mirna155 and nlrp3: *in vivo*, and *in silico* study. *Pharmaceutics* 14. doi:10.3390/pharmaceutics14030529

Mohamed, D. I., Ezzat, S. F., Elayat, W. M., El-Kharashi, O. A., El-Kareem, H. F. A., Nahas, H. H. A., et al. (2022b). Hepatoprotective role of carvedilol against ischemic hepatitis associated with acute heart failure via targeting mirna-17 and mitochondrial dynamics-related proteins: an *in vivo* and *in silico* study. *Pharmaceuticals* 15, 832. doi:10.3390/ph15070832

Moujir, L., Callies, O., Sousa, P. M., Sharopov, F., and Seca, A. M. J. A. S. (2020). Applications of sesquiterpene lactones: a review of some potential success cases. *Appl. Sci.* 10 (9), 3001. doi:10.3390/app10093001

Murai, T., and Matsuda, S. (2023). The chemopreventive effects of chlorogenic acids, phenolic compounds in coffee, against inflammation, cancer, and neurological diseases. *Molecules* 28 (5), 2381. doi:10.3390/molecules28052381

Muruganathan, N., Dhanapal, A. R., Baskar, V., Muthuramalingam, P., Selvaraj, D., Aara, H., et al. (2022). Recent updates on source, biosynthesis, and therapeutic potential of natural flavonoid luteolin: a review. *Metabolites* 12 (11), 1145. doi:10.3390/metabo12111145

Nii, T., Yumoto, H., Hirota, K., and Miyake, Y. J. B. O. H. (2019). Anti-inflammatory effects of olanexidine gluconate on oral epithelial cells. *BMC Oral Health.* 19 (1), 239–247. doi:10.1186/s12903-019-0932-0

Obadoni, B., and Ochuko, P. J. G. J. (2002). Phytochemical studies and comparative efficacy of the crude extracts of some haemostatic plants in Edo and Delta States of Nigeria. *Glob. J. Pure Appl. Sci.* 8 (2), 203–208. doi:10.4314/gjpas.v8i2.16033

Ohtani, M., Maruyama, K., Sugita, M., and Kobayashi, K. (2001). Amino acid supplementation affects hematological and biochemical parameters in elite rugby players. *Biosci. Biotechnol. Biochem.* 65 (9), 1970–1976. doi:10.1271/bbb.65.1970

Okazaki, Y., Otsuki, H., Narisawa, T., Kobayashi, M., Sawai, S., Kamide, Y., et al. (2013). A new class of plant lipid is essential for protection against phosphorus depletion. *Nat. Commun.* 4 (1), 1510. doi:10.1038/ncomms2512

Osman, A., Imbabi, T. A., El-Hadary, A., Sabeq, I. I., Edris, S. N., Merwad, A.-R., et al. (2021). Health aspects, growth performance, and meat quality of rabbits receiving diets supplemented with lettuce fertilized with whey protein hydrolysate substituting nitrate. *Biomolecules* 11 (6), 835. doi:10.3390/biom11060835

Ouyang, Y., Rong, Y., Wang, Y., Guo, Y., Shan, L., Yu, X., et al. (2021). A systematic study of the mechanism of acacetin against sepsis based on network pharmacology and experimental validation. *Front. Pharmacol.* 12, 683645. doi:10.3389/fphar.2021.683645

Özen, H., Kamber, U., Karaman, M., Gül, S., Atakişi, E., Özcan, K., et al. (2014). Histopathologic, biochemical and genotoxic investigations on chronic sodium nitrite toxicity in mice. *Exp. Toxicol. pathology* 66 (8), 367–375. doi:10.1016/j.etp.2014.05.003

Parama, D., Boruah, M., Yachna, K., Rana, V., Banik, K., Harsha, C., et al. (2020). Diosgenin, a steroidal saponin, and its analogs: effective therapies against different chronic diseases. *diseases* 260, 118182. doi:10.1016/j.lfs.2020.118182

Peter, M. C. S. (2011). The role of thyroid hormones in stress response of fish. *General Comp. Endocrinol.* 172 (2), 198–210. doi:10.1016/j.ygcen.2011.02.023

Porter, W. P., Green, S. M., Debbink, N. L., and Carlson, I. (1993). Groundwater pesticides: interactive effects of low concentrations of carbamates aldicarb and methomyl and the triazine metribuzin on thyroxine and somatotropin levels in white rats. *J. Toxicol. Environ. Health* 40 (1), 15–34. doi:10.1080/15287399309531773

Poschner, S., Maier-Salamon, A., Zehl, M., Wackerlig, J., Dobusch, D., Pachmann, B., et al. (2017). The impacts of genistein and daidzein on estrogen conjugations in human breast cancer cells: a targeted metabolomics approach. *Front. Pharmacol.* 8, 699. doi:10.3389/fphar.2017.00699

Radwan, E., Hussein, H., Kk, A., and Barakat, I. (2020). The possible effects of sodium nitrite and sodium benzoate as food additives on the liver in male rats. *J. Adv. Biol.* 13, 2347–6893. doi:10.24297/jab.v13i.8717

Rahman, M. M., Rahaman, M. S., Islam, M. R., Rahman, F., Mithi, F. M., Alqahtani, T., et al. (2022). Role of phenolic compounds in human disease: current knowledge and future prospects. *Molecules* 27 (1), 233. doi:10.3390/molecules27010233

Roager, H. M., and Licht, T. R. (2018). Microbial tryptophan catabolites in health and disease. *Nat. Commun.* 9 (1), 3294. doi:10.1038/s41467-018-05470-4

Robinson, T., and Van Burden, W. J. J. A. F. C. (1981). Formation of complexes between protein and tannins acid. *J. Agric. Food Chem.* 1, 77. doi:10.1021/jf60164a003

Romanova, D., Vachalkova, A., Cipak, L., Ovesna, Z., and Rauko, P. J. N. (2001). Study of antioxidant effect of apigenin, luteolin and quercetin by DNA protective method. *Neoplasma* 48 (2), 104–107.

Ruan, Z., Yang, Y., Wen, Y., Zhou, Y., Fu, X., Ding, S., et al. (2014). Metabolomic analysis of amino acid and fat metabolism in rats with l-tryptophan supplementation. *Amino Acids* 46 (12), 2681–2691. doi:10.1007/s00726-014-1823-y

Saif-Al-Islam, M. J. S. M. J. (2020). *Saussurea costus may help Treat. COVID-19* 24 (3), 6–17. doi:10.21608/SMJ.2020.31144.1163

Salama, M. F., Abbas, A., Darweish, M. M., El-Hawwary, A. A., and Al-Gayyar, M. M. (2013). Hepatoprotective effects of cod liver oil against sodium nitrite toxicity in rats. *Pharm. Biol.* 51 (11), 1435–1443. doi:10.3109/13880209.2013.796564

Saleh-e-In, M. M., Sultana, N., Hossain, M. N., Hasan, S., and Islam, M. (2016). Pharmacological effects of the phytochemicals of Anethum sowa L. root extracts. *BMC Complementary Altern. Med.* 16 (1), 464–514. doi:10.1186/s12906-016-1438-9

Salem, M. G., El-Maaty, D. M. A., El-Deen, Y. I. M., Elesawy, B. H., Askary, A. E., Saleh, A., et al. (2022). Novel 1,3-thiazole analogues with potent activity against breast cancer: a design, synthesis, *in vitro*, and *in silico* stu. *Molecules* 27. doi:10.3390/molecules27154898

Samaha, D., Hamdo, H. H., Cong, X., Schumacher, F., Banhart, S., Aglar, Ö., et al. (2020). Liposomal fret assay identifies potent drug-like inhibitors of the ceramide transport protein (CERT). *Chem.–Eur. J.* 26, 16616–16621. doi:10.1002/chem.202003283

Sasaki, S., Futagi, Y., Kobayashi, M., Ogura, J., and Iseki, K. (2015). Functional characterization of 5-oxoproline transport via SLC16A1/MCT1*. *J. Biol. Chem.* 290 (4), 2303–2311. doi:10.1074/jbc.M114.581892

Sawada, Y., Kuwahara, A., Nagano, M., Narisawa, T., Sakata, A., Saito, K., et al. (2009). Omics-based approaches to methionine side chain elongation in Arabidopsis: characterization of the genes encoding methylthioalkylmalate isomerase and methylthioalkylmalate dehydrogenase. *Plant Cell Physiol.* 50 (7), 1181–1190. doi:10.1093/pcp/pcp079

Selvi, E. K., Turumtay, H., Demir, A., and Turumtay, E. A. (2018). Phytochemical profiling and evaluation of the hepatoprotective effect of cuscuta campestris by high-performance liquid chromatography with diode array detection. *Anal. Lett.* 51 (10), 1464–1478. doi:10.1080/00032719.2017.1382502

Seo, M., Jikumaru, Y., and Kamiya, Y. (2011). Profiling of hormones and related metabolites in seed dormancy and germination studies. *Methods Mol. Biol.* 773, 99–111. doi:10.1007/978-1-61779-231-1_7

Shahaf, N., Rogachev, I., Heinig, U., Meir, S., Malitsky, S., Battat, M., et al. (2016). The WEIZMASS spectral library for high-confidence metabolite identification. *Nat. Commun.* 7 (1), 12423. doi:10.1038/ncomms12423

Sindelar, J. J., and Milkowski, A. L. (2012). Human safety controversies surrounding nitrate and nitrite in the diet. *Nitric oxide* 26 (4), 259–266. doi:10.1016/j.niox.2012.03.011

Singh, R., Chahal, K., and Singla, N. J. J. o. P. (2017). Chemical composition and pharmacological activities of Saussurea lappa. *A Rev.* 6 (4), 1298–1308.

Singh, S., Grewal, S., Sharma, N., Behl, T., Gupta, S., Anwer, M. K., et al. (2023). Unveiling the pharmacological and nanotechnological facets of daidzein: present state-of-the-art and future perspectives. *Molecules* 28 (4), 1765. doi:10.3390/molecules28041765

Singh, S., Gupta, P., Meena, A., and Luqman, S. (2020). Acacetin, a flavone with diverse therapeutic potential in cancer, inflammation, infections and other metabolic disorders. *Food Chem. Toxicol.* 145, 111708. doi:10.1016/j.fct.2020.111708

Soliman, M. M., Aldhahrani, A., Elshazly, S. A., Shukry, M., and Abouzed, T. K. (2022). Borate ameliorates sodium nitrite-induced oxidative stress through regulation of oxidant/antioxidant status: involvement of the Nrf2/HO-1 and NF-κB pathways. *Biol. Trace Elem. Res.* 200 (1), 197–205. doi:10.1007/s12011-021-02613-5

Srinivasan, K., and Radhakrishnamurty, R. (1988). Biochemical changes produced by beta- and gamma-hexachlorocyclohexane isomers in albino rats. *J. Environ. Sci. Health, Part B* 23 (4), 367–386. doi:10.1080/03601238809372612

Srivastava, S., Singh, P., Jha, K. K., Mishra, G., Srivastava, S., and Khosa, R. L. (2012). Evaluation of anti-arthritic potential of the methanolic extract of the aerial parts of Costus speciosus. *J. Ayurveda Integr. Med.* 3 (4), 204–208. doi:10.4103/0975-9476.104443

Sullivan, G. A., Jackson-Davis, A. L., Niebuhr, S. E., Xi, Y., Schrader, K. D., Sebranek, J. G., et al. (2012). Inhibition of Listeria monocytogenes using natural antimicrobials in no-nitrate-or-nitrite-added ham. *J. food Prot.* 75 (6), 1071–1076. doi:10.4315/0362-028X.JFP-11-511

Sunkara, Y., Robinson, A., Babu, K., Naidu, V., Vishnuvardhan, M., Ramakrishna, S., et al. (2010). Anti-inflammatory and cytotoxic activity of chloroform extract of roots of Saussurea lappa Clarke. *J. Pharm. Res.* 3 (8), 1775–1778.

Sutar, N., Garai, R., Sharma, U. S., Singh, N., and Roy, S. D. (2011). Antiulcerogenic activity of Saussurea lappa root. *Int. J. Pharm. Life Sci.* 2 (1), 516–520.

Tag, H. M., Khaled, H. E., Ismail, H. A., and El-Shenawy, N. S. (2016a). Evaluation of anti-inflammatory potential of the ethanolic extract of the Saussurea lappa root (costus) on adjuvant-induced monoarthritis in rats. *J. basic Clin. physiology Pharmacol.* 27 (1), 71–78. doi:10.1515/jbcpp-2015-0044

Tag, H. M., Khaled, H. E., Ismail, H. A. A., and El-Shenawy, N. S. (2016b). Evaluation of anti-inflammatory potential of the ethanolic extract of the Saussurea lappa root (costus) on adjuvant-induced monoarthritis in rats. *J. Basic Clin. Physiol. Pharmacol.* 27 (1), 71–78. doi:10.1515/jbcpp-2015-0044

Tawfek, N. A. (2015). H; abdalla, AA; fargali, S adverse effects of some food additives in adult male albino rats. *Curr. Sci. Int.* 4 (4), 525–537.

Teng, H., Lin, Q., Li, K., Yuan, B., Song, H., Peng, H., et al. (2017). Hepatoprotective effects of raspberry (Rubus coreanus Miq.) seed oil and its major constituents. *Food Chem. Toxicol.* 110, 418–424. doi:10.1016/j.fct.2017.09.010

Tohge, T., and Fernie, A. R. J. N. (2010). Combining genetic diversity, informatics and metabolomics to facilitate annotation of plant gene function. *Nat. Protoc.* 5 (6), 1210–1227. doi:10.1038/nprot.2010.82

Tsugawa, H., Cajka, T., Kind, T., Ma, Y., Higgins, B., Ikeda, K., et al. (2015). MS-DIAL: data-independent MS/MS deconvolution for comprehensive metabolome analysis. *Nat. Methods.* 12 (6), 523–526. doi:10.1038/nmeth.3393

Tuncel, A. T., Ruppert, T., Wang, B.-T., Okun, J. G., KГ¶lker, S., Morath, M. A., et al. (2015). Maleic acid--but not structurally related methylmalonic acid--interrupts energy metabolism by impaired calcium homeostasis. *PLOS ONE* 10 (6), e0128770. doi:10.1371/journal.pone.0128770

Tungmunnithum, D., Thongboonyou, A., Pholboon, A., and Yangsabai, A. (2018). Flavonoids and other phenolic compounds from medicinal plants for pharmaceutical and medical aspects: an overview. *Med. (Basel, Switz.)* 5 (3), 93. doi:10.3390/medicines5030093

Uchida, K., Nomura, Y., Takase, H., Tasaki, T., Seo, S., Hayashi, Y., et al. (1990). Effect of vitamin C depletion on serum cholesterol and lipoprotein levels in ODS (od/od) rats unable to synthesize ascorbic acid. *J. Nutr.* 120 (10), 1140–1147. doi:10.1093/jn/120.10.1140

Vignesh, A., Pradeepa Veerakumari, K., Selvakumar, S., Rakkiyappan, R., and Vasanth, K. J. T. (2021). Nutritional assessment, antioxidant, anti-inflammatory and antidiabetic potential of traditionally used wild plant. *Berberis tinctoria Lesch* 5 (2), 71–92. doi:10.30495/tpr.2021.1914719.1186

Wang, J., Liu, Y.-T., Xiao, L., Zhu, L., Wang, Q., and Yan, T. (2014a). Anti-inflammatory effects of apigenin in lipopolysaccharide-induced inflammatory in acute lung injury by suppressing COX-2 and NF-kB pathway. *Inflammation* 37 (6), 2085–2090. doi:10.1007/s10753-014-9942-x

Wang, J., Liu, Y.-T., Xiao, L., Zhu, L., Wang, Q., and Yan, T. J. I. (2014b). Anti-inflammatory effects of apigenin in lipopolysaccharide-induced inflammatory in acute lung injury by suppressing COX-2 and NF-kB pathway. *Inflammation.* 37, 2085–2090. doi:10.1007/s10753-014-9942-x

Wang, Y., Hayatsu, M., and Fujii, T. (2009). Extraction of bacterial RNA from soil: challenges and solutions. *Microbes Environ.* 1202170350. doi:10.1264/jsme2.me11304

Wei, J., Bhatt, S., Chang, L. M., Sampson, H. A., and Masilamani, M. (2012). Isoflavones, genistein and daidzein, regulate mucosal immune response by suppressing dendritic cell function. *PLOS ONE* 7 (10), e47979. doi:10.1371/journal.pone.0047979

White, K., and Someya, S. (2022). The roles of NADPH and isocitrate dehydrogenase in cochlear mitochondrial antioxidant defense and aging. *Hear. Res.* 427, 108659. doi:10.1016/j.heares.2022.108659

Wu, L., Zhang, C., Long, Y., Chen, Q., Zhang, W., and Liu, G. (2022). Food additives: from functions to analytical methods. *Crit. Rev. Food Sci. Nutr.* 62 (30), 8497–8517. doi:10.1080/10408398.2021.1929823

Yaeesh, S., Jamal, Q., Shah, A. J., and Gilani, A. H. (2010). Antihepatotoxic activity of Saussurea lappa extract on D-galactosamine and lipopolysaccharide-induced hepatitis in mice. *Phytotherapy Res.* 24 (S2), S229–S232. doi:10.1002/ptr.3089

Yılmaz, S., Ünal, F., and Yüzbaşıoğlu, D. (2009). The *in vitro* genotoxicity of benzoic acid in human peripheral blood lymphocytes. *Cytotechnology* 60 (1-3), 55. doi:10.1007/s10616-009-9214-z

Zhao, F., Xu, H., He, E.-Q., Jiang, Y.-T., and Liu, K. (2008). Inhibitory effects of sesquiterpenes from Saussurea lappa on the overproduction of nitric oxide and TNF-alpha release in LPS-activated macrophages. *J. Asian Nat. Prod. Res.* 10 (11), 1045–1053. doi:10.1080/10286020802274037

frontiers | Frontiers in Pharmacology

TYPE Review
PUBLISHED 20 June 2024
DOI 10.3389/fphar.2024.1400958

OPEN ACCESS

EDITED BY
Qinge Ma,
Jiangxi University of Traditional Chinese Medicine, China

REVIEWED BY
Aaron Balasingam Koenig,
INOVA Health System, United States
Yanling Zhao,
Fifth Medical Center of the PLA General Hospital, China

*CORRESPONDENCE
Weiwei Zeng,
zwwspring@126.com
Guoping Zhong,
zhonggp@mail.sysu.edu.cn

†These authors have contributed equally to this work

RECEIVED 14 March 2024
ACCEPTED 30 May 2024
PUBLISHED 20 June 2024

CITATION
Wei X, Luo D, Li H, Li Y, Cen S, Huang M, Jiang X, Zhong G and Zeng W (2024), The roles and potential mechanisms of plant polysaccharides in liver diseases: a review.
Front. Pharmacol. 15:1400958.
doi: 10.3389/fphar.2024.1400958

The roles and potential mechanisms of plant polysaccharides in liver diseases: a review

Xianzhi Wei[1,2†], Daimin Luo[1†], Haonan Li[1†], Yagang Li[1,2], Shizhuo Cen[1,2], Min Huang[1,2], Xianxing Jiang[1], Guoping Zhong[1,2*] and Weiwei Zeng[3*]

[1]School of Pharmaceutical Sciences, Sun Yat-sen University, Guangzhou, China, [2]Guangdong Provincial Key Laboratory of New Drug Design and Evaluation, Guangzhou, China, [3]Shenzhen Longgang Second People's Hospital, Shenzhen, China

Plant polysaccharides (PP) demonstrate a diverse array of biological and pharmacological properties. This comprehensive review aims to compile and present the multifaceted roles and underlying mechanisms of plant polysaccharides in various liver diseases. These diseases include non-alcoholic fatty liver disease (NAFLD), alcoholic liver disease (ALD), fibrosis, drug-induced liver injury (DILI), and hepatocellular carcinoma (HCC). This study aims to elucidate the intricate mechanisms and therapeutic potential of plant polysaccharides, shedding light on their significance and potential applications in the management and potential prevention of these liver conditions. An exhaustive literature search was conducted for this study, utilizing prominent databases such as PubMed, Web of Science, and CNKI. The search criteria focused on the formula "(plant polysaccharides liver disease) NOT (review)" was employed to ensure the inclusion of original research articles up to the year 2023. Relevant literature was extracted and analyzed from these databases. Plant polysaccharides exhibit promising pharmacological properties, particularly in the regulation of glucose and lipid metabolism and their anti-inflammatory and immunomodulatory effects. The ongoing progress of studies on the molecular mechanisms associated with polysaccharides will offer novel therapeutic strategies for the treatment of chronic liver diseases (CLDs).

KEYWORDS

plant polysaccharides, anti-inflammation, antifibrotic, non-alcoholic fatty liver disease, alcohol-related liver disease, drug-induced liver injury, hepatocellular carcinoma

Abbreviations: AMPK, adenosine 5′-monophosphate (AMP)-activated protein kinase; ALD, alcohol-related liver disease; CLD, Chronic liver disease; DILI, drug-induced liver injury; LPS, lipopolysaccharide; NAFLD, non-alcoholic fatty liver disease; PPAR-α, peroxisome proliferator-activated receptor-α; PP, Plant Polysaccharides; SREBP-1, sterol-regulatory element binding proteins; ZO-1, zonula occludens-1.

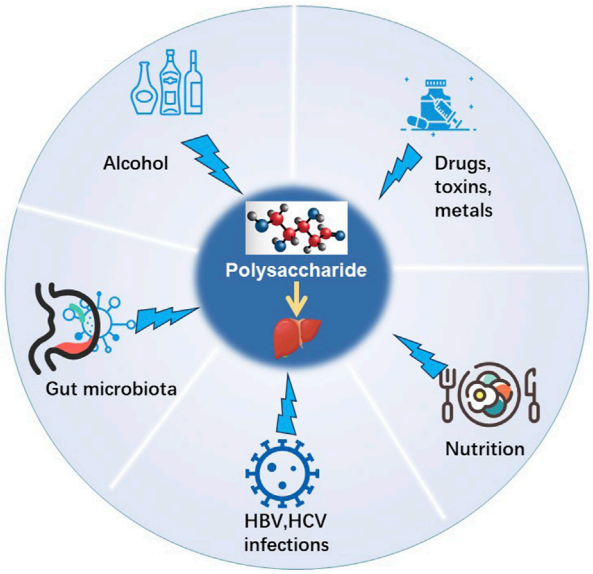

GRAPHICAL ABSTRACT

1 Introduction

Chronic liver disease (CLD) has emerged as a consequential global public health challenge, significantly contributing to morbidity and mortality rates worldwide. In recent decades, the prevalence of liver diseases has been steadily escalating, establishing them as leading causes of death and illness on a global scale. These diseases, encompassing cirrhosis, viral hepatitis, and liver cancer, are responsible for an annual loss of over two million lives, accounting for approximately 4% of all worldwide deaths (equating to 1 out of every 25 deaths). Notably, liver cancer alone contributes to a staggering 600,000 to 900,000 fatalities. Presently, liver disease ranks as the eleventh-leading cause of death, although the actual number of liver-related deaths may be underestimated. A current study indicates that cirrhosis ranks as the tenth-leading cause of death in Africa (thirteenth-leading cause in 2015), the ninth-leading cause in Southeast Asia and Europe, and the fifth-leading cause of death in the Eastern Mediterranean region (Devarbhavi et al., 2023). Notably, the incidence of viral hepatitis has shown a decline in most countries due to progress in disease prevention, diagnosis, and therapeutic interventions. Moreover, the implementation of comprehensive immunization programs targeting the hepatitis B virus has proven effective in reducing the number of new cases in numerous countries (Xiao et al., 2019). With the advancement in living standards, there is an anticipated increase in the prevalence of metabolic liver diseases, namely non-alcoholic fatty liver disease (NAFLD), alcohol-related liver disease (ALD), and drug-induced liver injury (DILI). Consequently, this rise in cases is expected to result in an escalation of end-stage liver diseases, including liver failure, cirrhosis, and liver cancer. As a direct consequence, liver diseases unequivocally emerge as significant contributors to morbidity and mortality rates within the whole world.

Newly discovered elements, such as stem cells and miRNAs targeting specific genes, have emerged as potential novel mechanisms contributing to CLD. These discoveries have significantly influenced liver disease research in the past decade. However, it is important to note that most liver diseases do not have a single cause, but rather multiple concurrent causes. For instance, individuals may experience infection of hepatitis B virus superimposed on metabolic dysfunction–associated steatotic liver disease (MASLD) (Rinella et al., 2023). The molecular mechanisms of liver disease primarily involve synergistic effects and multi-target signaling pathways, rather than relying solely on single targets or signaling pathways. Consequently, the use of a single drug to treat a specific disease inherently presents limitations, as compared to the approach of employing a multi-level, multi-target, and multi-signaling strategy. Future therapeutic interventions aimed at improving liver disease outcomes are anticipated to employ rational structural optimization and design strategies based on the understanding of structure-activity relationships. These interventions will target the modulation of well-established signaling pathways, which hold significant importance in the context of multifactorial liver diseases, to ameliorate CLD. However, the inadequate knowledge regarding the pathogenesis of liver diseases, coupled with delayed diagnoses and rapid disease progression, contribute to the insufficiency of current clinical therapeutic approaches. These limitations directly result in unsatisfactory treatment outcomes.

Natural polysaccharides possess distinctive structural characteristics that encompass factors such as molecular weight, monosaccharide composition, charge properties, and glycosidic bonds. These features not only determine the functional attributes of polysaccharides but also contribute to their extensive utilization in various applications. PP exhibit diverse biological activities and hold tremendous potential in mitigating liver damage caused by conditions such as NAFLD, ALD, DILI, hepatic fibrosis, and HCC.

Plant polysaccharides hold potential as valuable sources of therapeutic agents for liver disease due to their low toxicity and ability to target multiple processes and pathways. However, the

growing number of studies investigating the effective plant-derived compounds have yet to be systematically summarized, particularly with regards to the functions and mechanisms of plant polysaccharides exhibiting hepatoprotective effects. Therefore, this comprehensive review aims to address this gap by specifically focusing on the mechanisms underlying the actions of polysaccharides in liver disease therapy.

2 Methods

The research conducted for this study involved a meticulous search of prominent online academic databases, including PubMed, Web of Science, and CNKI, up until the year 2023. Our search strategy utilized specific terms such as "plant polysaccharides" and "liver disease", as well as various combinations of these terms. Within the timeframe of 2010–2023, more than 140 scholarly articles were identified, focusing on the potential of plant polysaccharides in addressing liver conditions such as NAFLD, ALD, DILI, hepatic fibrosis, and HCC. These articles were systematically categorized based on their primary objectives, and their key findings were summarized for clarity. Additionally, to ensure a comprehensive understanding and provide historical context, a thorough review of influential studies published prior to 2010 was also conducted. This approach ensures a holistic perspective on the topic, encompassing both recent advancements and foundational knowledge.

2.1 Polysaccharides in different liver diseases

2.1.1 Plant polysaccharides against non-alcoholic fatty liver disease

NAFLD represents the hepatic manifestation of a cluster of conditions linked to metabolic dysfunction. The prevalence of NAFLD on a global scale tends to go up (Friedman et al., 2018). Globally, the estimated prevalence of NAFLD stands at approximately 25%, with the highest rates observed in the Middle East and South America, and the lowest in Africa. In North America and Europe, NAFLD is commonly associated with central obesity, accounting for approximately 83% of affected patients. However, it is noteworthy that in Asia, a significant proportion of NAFLD patients, known as "thin NASH" individuals, exhibit normal body mass index (BMI), despite the lower BMI threshold for defining overweight in Asia (BMI > 23) compared to North America and Europe (BMI > 25) (Pereira et al., 2015). NAFLD is characterized by the accumulation of fat (steatosis) in more than 5% of hepatocytes, occurring concurrently with metabolic risk factors, particularly obesity and type 2 diabetes. Notably, NAFLD is distinguished by the absence of excessive alcohol intake (≥30 g per day for men and ≥20 g per day for women), as well as the absence of other chronic liver diseases (Byrne and Targher, 2016). NAFLD encompasses a spectrum that spans from isolated steatosis, in which fat accumulates in the liver without significant progression, to the more severe condition known as non-alcoholic steatohepatitis (NASH). NASH is distinguished by the presence of hepatocellular injury, inflammation, and fibrosis, and is characterized by a progressive clinical course. Left untreated, NASH may lead to the development of cirrhosis, with its associated complications including hepatocellular carcinoma.

PP have shown the potential to alleviate the effects of NAFLD by inhibiting hepatocellular injury, inflammation, and fibrosis. The underlying mechanism is closely associated with the regulation of energy metabolism mediated through signaling pathways such as AMPK and MAPK. Radix *Hedysari* polysaccharide, *Polygonatum sibiricum* polysaccharides, and *Astragalus mongholicus* polysaccharides have been reported to ameliorate disorders in lipid metabolism, regulate hepatic lipid content, and improve liver inflammation and damage by modulating the phosphorylation levels of AMPK (Sun et al., 2014; Huang et al., 2021; Zhou et al., 2021; Zhong et al., 2022). Up to now, APS has been widely used in poultry and animal feed, with the function of improving the utilization of nutrients and promoting animal growth. The application of APS in the human is mainly to prevent and treat cardiovascular diseases. Additionally, the MAPK cascade plays a role in regulating NF-κB gene expression through redox mechanisms. ASP has been shown to mitigate Caspase-3-dependent apoptosis through the involvement of the Caspase-8 and JNK-mediated pathway. Moreover, ASP inhibits the activation of IL-6/STAT3 and NF-κB signaling pathways (Wang et al., 2016). Furthermore, emerging evidence supports the significant involvement of the gut microbiota in the development and progression of NAFLD. This study contributes novel findings by demonstrating the potential of *Astragalus mongholicus* polysaccharides to alleviate hepatic inflammation and reduce lipid accumulation in NAFLD. These beneficial effects are achieved through the modulation of the gut microbiota composition and the SCFA-GPR signaling pathways (Zhong et al., 2022). Moreover, *Poria cocos* polysaccharides have demonstrated the potential to mitigate the disruption of the gut–vascular barrier, the translocation of endotoxins induced by a high-fat diet, and inhibit intestinal pyroptosis. These effects are mediated through the regulation of key factors, including PARP-1 and the administration of pyroptosis inhibitors, such as MCC950 (Ye et al., 2022). Walnut green husk polysaccharide has the potential to enhance the composition and diversity of the gut microbiota, as well as increase the abundance of beneficial bacteria (Wang et al., 2020). Long-term and repetitive inflammation is a contributing factor in the advancement of NAFLD. In the progression of NAFLD, inflammation, fibrosis, autophagy, and apoptosis interact and exacerbate one another. *Gynostemma pentaphyllum* polysaccharides have been shown to inhibit the expression of Toll-like receptor 2 (TLR2) and downregulate the expression of the NOD-like receptor pyrin domain-containing 3 (NLRP3) inflammasome, as well as the pro-inflammatory cytokines TNF-α and IL-1β. These polysaccharides have the potential to improve non-alcoholic steatohepatitis (NASH), possibly through the modulation of gut microbiota and the TLR2/NLRP3 signaling pathway (Yue et al., 2022). *Angelica sinensis* polysaccharide (ASP) has garnered significant attention due to its notable hepatoprotective effects. Previous research has demonstrated that ASP exerts therapeutic effects on NAFLD through the regulation of lipid metabolism via the propionate/ERRα pathway (Luo et al., 2023). Furthermore, ASP has the capacity to enhance the expression of PPARγ and key liver insulin signaling proteins, such as IRS-2, PI3K, Akt, p-Akt, and GLUT2. Moreover, ASP has been shown to increase the levels of the

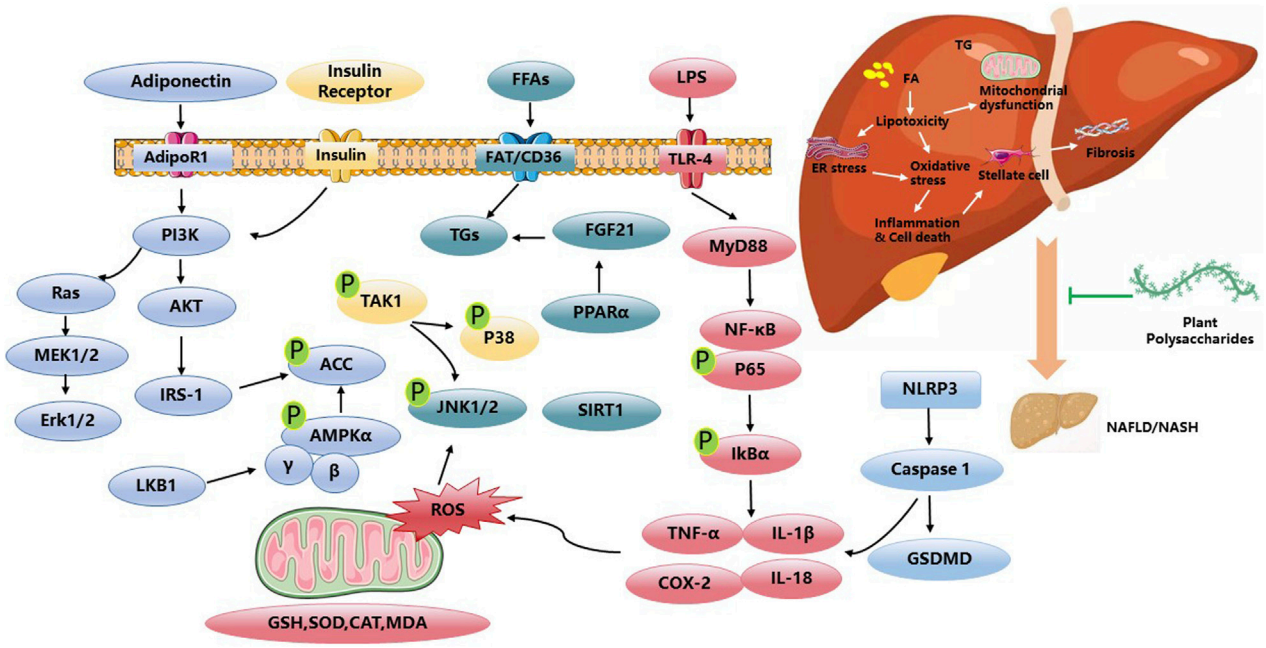

FIGURE 1
Anti-NAFLD activities and related mechanisms of PP.

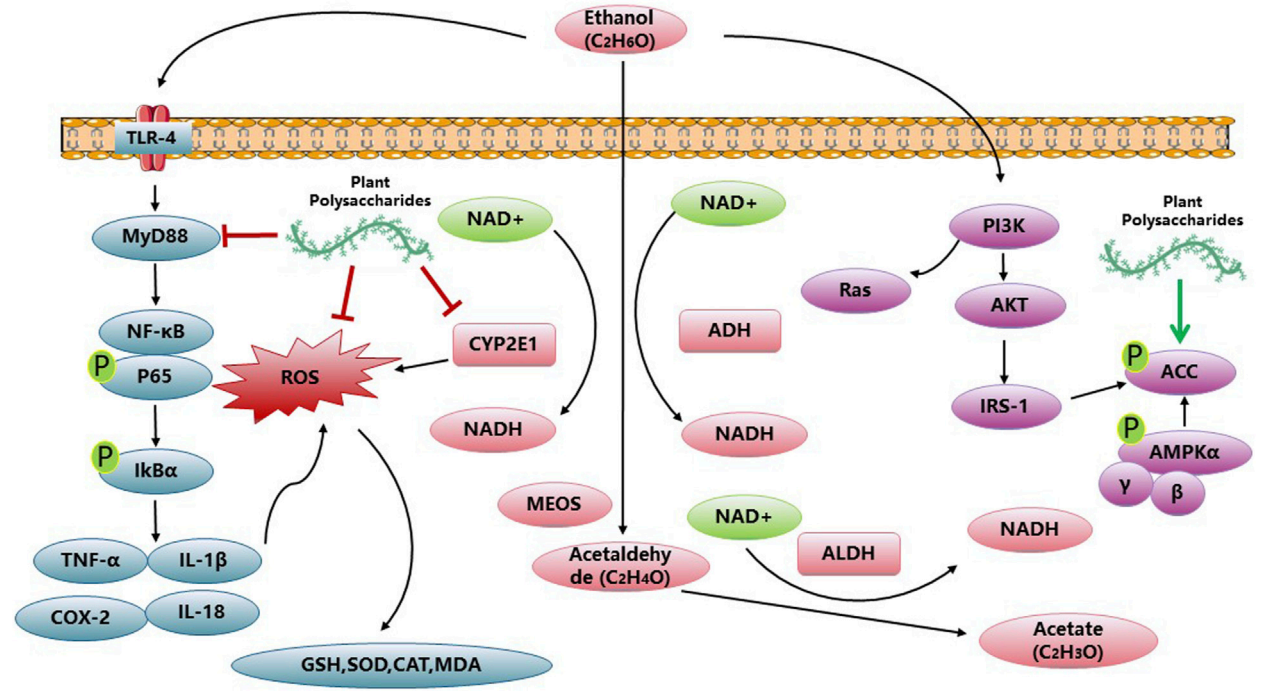

FIGURE 2
Anti-ALD activities and related mechanisms of PP.

anti-apoptotic protein Bcl-2 while concurrently reducing the expression of the pro-apoptotic protein Bax. This multifaceted action of ASP not only provides protection against hepatic damage but also offers promising therapeutic benefits in the context of liver health (Wang et al., 2016). *Gynostemma pentaphyllum* polysaccharides is a pure natural plant with medicinal value, which has broad application prospects in food, health, and drug. At present, the utilization is only for crude

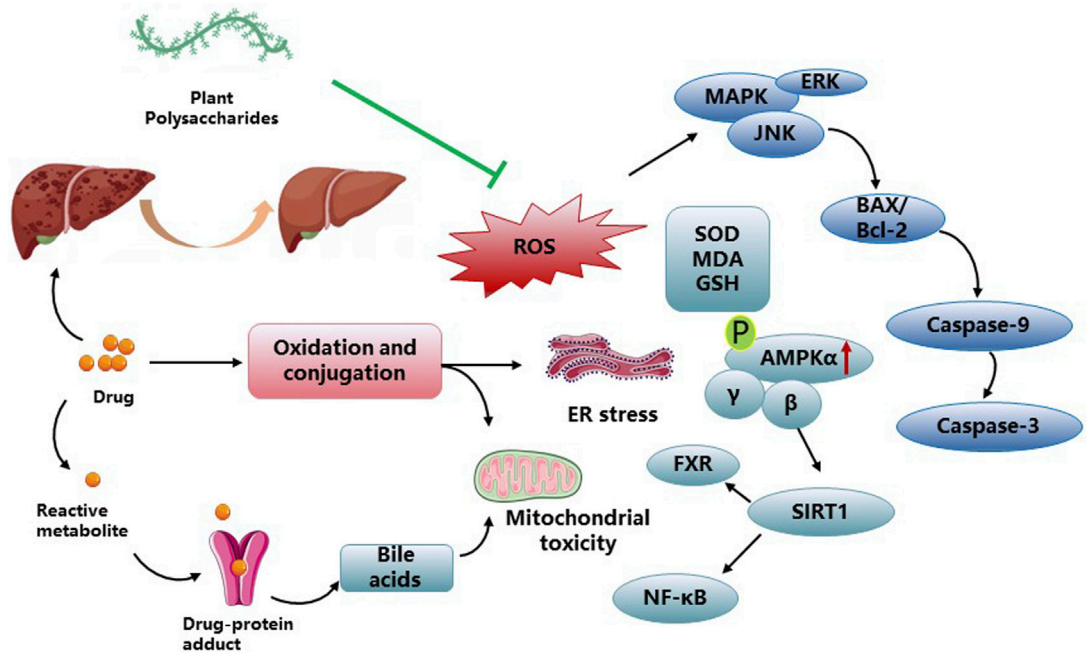

FIGURE 3
PP impact on DILI activities and related mechanisms.

products, and research on it is limited to preclinical studies. Various studies have been done for discovering the anti-NAFLD activity of plant polysaccharides in Figure 1. Table 1 gives an overview of some studies performed in NAFLD.

2.1.2 Plant polysaccharides against ethanol-induced liver disease

ALD encompasses a range of liver conditions resulting from excessive alcohol consumption. These conditions include liver steatosis, steatohepatitis, hepatitis, cirrhosis, and HCC. The progression of ALD is primarily influenced by the duration and quantity of alcohol intake, while genetic, epigenetic, and environmental factors also contribute. Chronic alcohol use is a prominent cause of morbidity and mortality on a global scale, impacting over 200 disease and injury outcomes (Rehm et al., 2017; European Association for the Study of the Liver, 2018). According to the World Health Organization (WHO), there are approximately 2.3 billion current consumers of alcoholic beverages, with around one billion categorized as heavy intermittent drinkers. Among alcohol-attributable conditions, cirrhosis of the liver obtains the highest score, followed by road injuries and other digestive diseases (Saito et al., 2018). Alcohol is widely acknowledged as a carcinogen, being associated with the development and progression of various types of cancer. Furthermore, alcohol consumption has been firmly linked to the advancement of liver-specific diseases, including chronic viral hepatitis and hepatocellular carcinoma (Dolganiuc, 2015; Sahlman et al., 2016; Ganesan et al., 2020).

The liver assumes primary responsibility for ethanol metabolism. When excessive alcohol is consumed, the liver incurs substantial tissue damage as a result of both oxidative stress and the accumulation of acetaldehyde and lipopolysaccharide (LPS) (Meroni et al., 2018; Kong et al., 2019). ALD encompasses various conditions linked to alcohol consumption, such as early-stage asymptomatic ALD characterized by fatty liver or steatosis, steatohepatitis, advanced forms including alcoholic hepatitis and cirrhosis, as well as the development of HCC(Thursz et al., 2019).

Inflammation is a crucial risk factor associated with the progression of ALD, serving as a prerequisite for the development of fibrosis, cirrhosis, and HCC. Activation of Toll-like receptor 4 (TLR4) triggers NF-κB signaling, leading to the production and release of pro-inflammatory cytokines such as tumor necrosis factor (TNF) and interleukin-6 (IL-6). Chronic alcohol consumption increases the levels of TNF and IL-6 in both animal models and human liver biopsy samples. Notably, patients with acute alcoholic hepatitis exhibit significantly elevated circulating levels of TNF and IL-6, which have been implicated in disease severity and the onset of multiorgan failure (Seitz et al., 2018).

PP exhibit notable anti-inflammatory properties, and recent studies have indicated that *Aloe vera* polysaccharides (AVP) can ameliorate ALD. AVP achieves this by upregulating AMPK-α, PPAR-α, and IκB-α, while simultaneously downregulating TLR-4 and MyD88 (Cui et al., 2014). Additionally, *Aloe vera* polysaccharides have been found to reduce hepatic inflammation by inhibiting the toll-like receptor 4 (TLR4)/nuclear factor-kappa B (NF-κB) signaling pathway. Moreover, they improve hepatocyte apoptosis by inhibiting the CYP2E1/ROS/MAPKs signaling pathway (Jiang et al., 2022). *Lycium barbarum* polysaccharide was found to regulate the NLRP3 inflammasome pathway, effectively inhibiting hepatic inflammation in the context of ALD. Moreover, it was observed that *Lycium barbarum* polysaccharide primarily ameliorated ALD through the SCD1-AMPK-CPT pathway, subsequent to ERα (Xiao et al., 2014; Wang et al., 2018). The activation of PPAR-γ signaling by water-insoluble polysaccharide treatment effectively reduces inflammation in

TABLE 1 Summary of known anti-NAFLD activity of PP.

Polysaccharide	Origin plant	Models	Functions	Mechanisms	References
Radix *Hedysari* polysaccharide	Radix *Hedysari*	HFD rat	Ameliorate lipid metabolism disorders	Activate P-AMPK, pparα and downregulate SREBP-1c	Sun et al. (2014)
Ginkgo biloba polysaccharide	*Ginkgo biloba*	HFD rat	Enhance antioxidant defence system	Reduce lipid peroxidation	Yan et al. (2015)
Angelica sinensis polysaccharide	*Angelica sinensis* (Oliv.) Diels	ConA-induced liver damage in mice	Anti-inflammatory and anti-oxidant	Attenuate Caspase-3-dependent apoptosis by Caspase-8 and JNK-mediated pathway	Wang et al. (2016b)
Sophora flavescens polysaccharides	*Sophora flavescens*	ConA-induced hepatitis mice	Anti-inflammatory and anti-oxidant	Inhibit activation of NKT cell, inhibit HBV secretion	Yang et al. (2022)
Enteromorpha prolifera polysaccharide	Enteromorpha prolifera	HFD rat	Upregulate cystathionine-β-synthase	Increase H2S production	Ren et al. (2020)
Artemisia sphaerocephala Krasch polysaccharide	*Artemisia sphaerocephala* Krash seed	HF mice	Maintenance of the intestinal microecosystem	Modulate hepatic SREBP-1c, SCD-1, ACC and FAS expression	Zhang et al. (2019)
Trehalose	The ergot of rye	HFD mice	The induction of autophagy	Inhibit atherosclerosis and attenuate hepatic steatosis	Stachowicz et al., (2019)
Codonopsis lanceolata polysaccharide	Codonopsis lanceolata	HFHS mice	Ameliorate insulin resistance	Impair phosphorylation of PKB/Akt and hyperphosphorylation of IRS-1 at Ser307	Zhang et al. (2019)
Walnut green husk polysaccharide	Walnut green husk	HF mice	Ameliorate oxidative stress, lipid metabolism	Improve the composition of gut microbiota, increase the diversity of gut microbiota and the abundance of beneficial bacteria	Wang et al. (2020)
Noni fruit polysaccharide	Noni fruit	HFD rat	Improve hepatic oxidative stress and inflammation	Modulate short-chain fatty acids (SCFAs), the intestinal barrier, and gut microbiota	Yang et al. (2022)
Polygonatum sibiricum polysaccharides	*Polygonatum sibiricum*	HFD rat	Promote lipid metabolism, decrease body weight, and anti-inflammatory and anti-oxidant	Upregulate insulin receptor expression, increase AMPK phosphorylation, and downregulate SREBP2 and LDLR expression	Huang et al. (2021)
Poria cocos polysaccharides	*Poria cocos*	NAFLD mice	Inhibit pyroptosis	Inhibit the pyroptosis of small intestinal macrophages	Ye et al. (2022)
Astragalus mongholicus polysaccharides	*Astragalus mongholicus*	NAFLD rat	Ameliorate hepatic lipid accumulation and inflammation as well as modulate gut microbiota	Increase p-AMPK and PPAR-α, decrease SREBP-1, TLR4, NF-κB NLRP3, GPR41 and 43. Modulate the gut microbiota and SCFA-GPR signaling pathways	Zhong et al. (2022)
Polygonatum cyrtonema Hua polysaccharides	*Polygonatum cyrtonema* Hua	NAFLD mice	Reduce liver damage, improve lipid metabolism, decrease oxidative stress	Promote the production of short-chain fatty acids, and balances the composition of the intestinal microbiota	Liu et al. (2021)
Pleurotus polysaccharides	Pleurotus	HepG2 cells	Regulate liver-gut axis system	Increase the viabilities and cellular total superoxide dismutase activities	Huang et al. (2021)

colonic epithelial cells and promotes a hypoxic state, which aids in suppressing the excessive growth of fungi and Proteobacteria in the gut. This mechanism holds promise for alleviating ALD (Sun et al., 2020). A polysaccharide known as PFP-1, obtained from the fruiting body of *Pleurotus geesteranus*, has exhibited the ability to mitigate oxidative stress and inflammatory responses. This effect is achieved through the activation of Nrf2-mediated signaling pathways and regulation of the TLR4-mediated NF-κB signaling pathways, presenting a potential therapeutic strategy against ALD (Song et al., 2021). Additionally, research has indicated that the lipid-lowering impact of ASP may stem from its dual inhibition of lipid synthesis and CD36-mediated lipid uptake. The antioxidative properties of ASP can be attributed to its ability to reverse alcohol metabolic pathways, transitioning from cytochrome P450 2E1 (CYP2E1) catalysis to alcohol dehydrogenase (ADH) catalysis. Overall, this study establishes the direct involvement of ASP in lipid metabolism and elucidates its mechanism of action in reducing reactive oxygen species (ROS), thus positioning it as a potential therapeutic agent for the treatment of alcoholic fatty liver disease (AFLD) (He et al., 2022). The polysaccharides derived from *Echinacea purpurea*, known as EPPs, exhibit significant free radical scavenging activity *in vitro*, and have demonstrated the ability to ameliorate alcohol-induced liver injury through the activation of Nrf2/HO-1 pathways *in vivo* (Jiang et al., 2021; Jiang et al., 2022). These findings highlight the remarkable potential of PP in effectively regulating abnormal biochemical

TABLE 2 Given a summary of a few reports on the anti-ALD activity of PP.

Polysaccharide	Origin plant	Models	Functions	Mechanisms	References
Aloe vera polysaccharides	*Aloe vera*	ALD induced-mouse	Anti-oxidation, anti-inflammation and immune enhancement	Upregulate AMPK-α,PPAR-α and IκB-α; downregulation of TLR-4 and MyD88	Cui et al. (2014)
Lycium barbarum polysaccharide	*Lycium barbarum*	ALD induced-mice	Rebalance the dysregulated lipid metabolism	Activate the SCD1-AMPK-CPT pathway; TXNIP-NLRP3 inflammasome pathway	Wang et al. (2018), Xiao et al. (2014)
Crassostrea gigas water-soluble polysaccharide	*Crassostrea gigas*	ALD induced-mice	Antioxidant	Decrease serum AST, ALT, and MDA; increase SOD	Shi et al. (2015)
Dendrobium huoshanense polysaccharide	*Dendrobium huoshanense*	ALD induced-mice	Restore the perturbed metabolism pathways	Alter metabolic levels particularly involved in phosphocholine and l-Proline	Wang et al. (2016)
Mori Fructus polysaccharides	Morus alba L.	ALD induced-rats	Anti-inflammatory antioxidant, and immuno-enhancing activities	Activation of ethanol dehydrogenase, elimination of free radicals, and inhibition of lipid peroxidation	Zhou et al. (2021)
Triticum aestivum sprout-derived polysaccharide	ALD induced-mouse	ALD induced-mice	Inhibit steatosis and improve antioxidant marker levels	Regulated by a phosphatidylinositol 3-kinase (PI3K)/Akt pathway	Nepali et al. (2017)
Schisandra chinensis acidic polysaccharide	Schisandra chinensis acidic	ALD induced-mice	Alleviate oxidative stress	Inhibit the upregulation of CYP2E1	Yuan et al. (2018)

TABLE 3 Summary of articles data about PP impact on DILI activity.

Polysaccharide	Origin plant	Models	Functions	Mechanisms	References
Jujube polysaccharides	*Zizyphus jujube* cv	CCl_4 or APAP induced in mice	Anti-oxidation and detoxification	Enhance SOD and GSH-Px and decrease MDA	Liu et al. (2015)
dandelion root polysaccharide	*dandelion*	APAP induced in mice	Enhance Nrf2, NQO1 and HO-1, decrease Keap1	Activate the Nrf2-Keap1 pathway	Cai et al. (2015)
Seabuckthorn berry polysaccharide	*seabuckthorn*	APAP induced in mice	Increase GSH and GSH-Px, SOD and SOD-2; the ratio of Bcl-2/Bax,Nrf-2; reduced NO and iNOS and p-JNK; Keap-1	The activation of the Nrf-2/HO-1-SOD-2 signaling pathway	Wang et al. (2018)
Periploca polysaccharide	*Periploca*	Cadmium chloride ($CdCl_2$) induced toxicity in male Wistar rats	Antioxidant	Decrease the content of MDA and protein damage, hepatic anti-oxidant	Athmouni et al. (2018)
Schisandra chinensis acidic polysaccharide partially	*Schisandra chinensis*	APAP induced in mice	Antioxidation, anti-inflammation and anti-apoptosis	Reduce ratio of Bax/Bcl-2, prohibit cleaved caspase-3, and elevate p-AMPK, p-Akt, p-GSK 3β, Nrf 2 and HO-1	Che et al. (2019)
Astragalus polysaccharide	*Astragalus*	Cantharidin (CTD)-induced-mice	Inhibit oxidative stress; regulate primary bile acid biosynthesis and glycerophospholipid metabolism	Inhibit ER stress	Huang et al. (2021)
Echinacea purpurea polysaccharide	*Echinacea purpurea*	APAP overdose-induced DILI in mice	Increase autophagy with a reduction in oxidative stress and inflammation	Reduction of autophagy-dependent oxidant, inflammatio-n and apoptosis	Yu et al. (2022)
Salvia miltiorrhiza polysaccharides	*Salvia miltiorrhiza*	Florfenicol induced in chickens	Inflammation and oxidative stress	The phagosome signaling pathway	Wang et al. (2022)

indices associated with ALD. Figure 2 and Table 2 give a summary of a few reports that PP against ALD.

2.1.3 Plant polysaccharides against drug-induced liver injury (DILI)

The liver is highly susceptible to drug toxicity during clinical treatment due to its first-pass effect in gastrointestinal nutrition metabolism. Drug-induced liver injury is estimated to affect around 14–19 cases per 100,000 individuals (Andrade et al., 2019). Although asymptomatic elevated liver enzymes are the most common presentation, drug-induced liver injury constitutes the primary cause of acute liver failure in many Western countries, accounting for over 50% of cases. It can manifest at either excessive or therapeutic doses, potentially as consequence of

direct intrinsic drug hepatotoxicity or idiosyncratic (unpredictable) hepatotoxicity (Hoofnagle and Bjornsson, 2019).

DILI is an infrequent condition that occurs irrespective of drug dose, route, or duration of administration. Moreover, idiosyncratic DILI does not represent a single homogeneous disease, but rather a range of rare disorders presenting diverse clinical, histological, and laboratory characteristics. The pathogenesis of DILI remains incompletely elucidated, with various factors contributing to its development and progression (Fontana, 2014). Intrinsic hepatotoxins, such as acetaminophen, typically exhibit dose-dependent behavior and can be studied using reproducible animal models to understand the underlying pathways leading to hepatocyte injury. Conversely, most cases of DILI observed in clinical practice are considered "idiosyncrasies" because they lack a clear correlation with the dose, route, or duration of administration, which makes them specific to each patient. PP play a significant protective role in mitigating drug-induced liver damage. In addition to the direct toxic effects of drugs, oxidative stress can occur as a result of drug metabolism, leading to the generation of ROS. These ROS can interact with proteins, causing changes in their functional and structural characteristics, and form neoantigens. ROS are responsible for initiating lipid peroxidation, leading to the formation of lipid peroxidation byproducts, such as 4-hydroxynonenal (4-HNE) and malondialdehyde (MDA). Various studies have demonstrated the potential of PP in improving ROS levels associated with DILI. Notable examples include Jujube polysaccharides, Seabuckthorn berry polysaccharide, and *Periploca* polysaccharide (Liu et al., 2015; Athmouni et al., 2018; Wang et al., 2018). *Periploca* polysaccharides have shown significant reductions in MDA content and protein damage in liver tissue, along with improvements in liver function parameters (alanine transaminase, ALT; aspartate aminotransferase, AST; bilirubin). Furthermore, *Periploca* polysaccharides have demonstrated the ability to enhance the activities of hepatic antioxidant enzymes (superoxide dismutase, SOD; catalase, CAT; glutathione peroxidase, GPx; GSH) as a protective response against cadmium chloride ($CdCl_2$)-induced toxicity in male Wistar rats (Athmouni et al., 2018). Schisandra polysaccharide exhibited a significant reduction in ALT, AST, TNF-α, and IL-1β levels, leading to the alleviation of hepatic pathological alterations in the mouse model. Additionally, it demonstrated protective effects on liver injury-associated enzymes and factors, including a notable decrease in MDA levels and GSH depletion, downregulation of Bax/Bcl-2 expression, inhibition of cleaved caspase-3 expression, as well as upregulation of p-AMPK, p-Akt, GSK 3β, Nrf 2, and HO-1 proteins in the liver tissues of the mouse model (Che et al., 2019). The hepatoprotective effect of *Echinacea purpurea* polysaccharide against APAP-induced DILI was observed. This effect was associated with a decrease in autophagy-dependent oxidative stress, inflammation, and apoptosis. Moreover, the observed protective mechanism involved Parkin-dependent autophagy (Yu et al., 2022). ASP pretreatment demonstrated significant attenuation of Caspase-3-dependent apoptosis through the Caspase-8 and JNK-mediated pathway. Furthermore, ASP inhibited the activation of IL-6/STAT3 and NF-κB signaling pathways in ConA-induced liver damage in mice (Wang et al., 2016). Moreover, ASP exhibits potential as a hepatoprotective agent for the management of acetaminophen (APAP)-induced liver injury by increasing glutathione (GSH) levels and inhibiting hepatic apoptosis (Cao et al., 2018). Notably, ASP has also shown efficacy in alleviating chronic liver fibrosis by inhibiting HSC activation via the IL-22/STAT3 pathway (Wang et al., 2020). *Broussonetia papyrifera* polysaccharide demonstrated hepatoprotective properties against APAP-induced liver injury. It effectively attenuated liver apoptosis, enhanced antioxidant capacity, and improved the liver's detoxification ability towards APAP (Xu et al., 2022). Several studies have been conducted to investigate the efficacy of plant polysaccharides on the treatment of drug-induced liver damage in Figure 3 and Table 3.

2.1.4 Plant polysaccharides against hepatic fibrosis

Hepatic fibrosis and cirrhosis pose a substantial global health burden, leading to liver failure or HCC, thereby posing a significant threat to human health on a worldwide scale (Yang et al., 2023). Liver diseases pose a substantial global threat to human health, contributing to approximately 2 million deaths annually. Hepatic cirrhosis alone accounts for approximately 50% of all liver disease-related fatalities (Asrani et al., 2019).

Liver cirrhosis is a progressive complication that arises from liver disease, representing a significant advancement in hepatic fibrosis whereby there is a substantial loss of liver cells accompanied by irreversible scarring. Various factors such as viral infections (HBV and HCV), hepatic lipid accumulation, alcohol consumption, and drug toxicity contribute to chronic damage, impairing the functionality of hepatocytes. This, in turn, triggers inflammation and release of inflammatory factors, which promote excessive accumulation of collagen and extracellular matrix (ECM), resulting in the disruption of liver structure and function. Ultimately, this fibrotic process may progress to clinically significant cirrhosis and subsequent hepatic failure. Cirrhosis can be identified as an advanced stage of fibrosis characterized by the development of regenerative nodules within the liver parenchyma, enclosed by fibrotic septa (Pinzani and Macias-Barragan, 2010).

NAFLD and ALD, as well as DILI, contribute significantly to the development of advanced liver conditions, including hepatic fibrosis and HCC. PP have been reported to exhibit a variety of pharmacological effects such as antioxidation, anti-inflammation, and anti-apoptosis, thereby improving hepatic fibrosis. The polysaccharide derived from *Talinum triangulare* demonstrates remarkable antioxidant activities, effectively reducing the levels of AST, ALT), and MDA in CCl_4-induced liver injuries. Furthermore, it restores the activities of key antioxidant substances, SOD, and reduced GSH, thereby normalizing the liver's defense mechanisms (Liang et al., 2011). *Lycium barbarum* polysaccharides have demonstrated effectiveness in reducing hepatic necrosis, serum ALT levels, and cytochrome P450 2E1 expression. Additionally, they restore the expression levels of antioxidant enzymes, decrease nitric oxide levels, inhibit lipid peroxidation, and alleviate hepatic inflammation. These effects are achieved through the downregulation of NFκB activity induced by CCl_4 (Xiao et al., 2012). *Amomum villosum* polysaccharides exhibited potent *in vitro* free radical scavenging activities and effectively mitigated oxidative stress-induced liver injury in CCl_4-treated mice by suppressing malondialdehyde formation and enhancing the activities of antioxidant enzymes (Zhang et al., 2013). Seabuckthorn berry polysaccharide (SP) administration

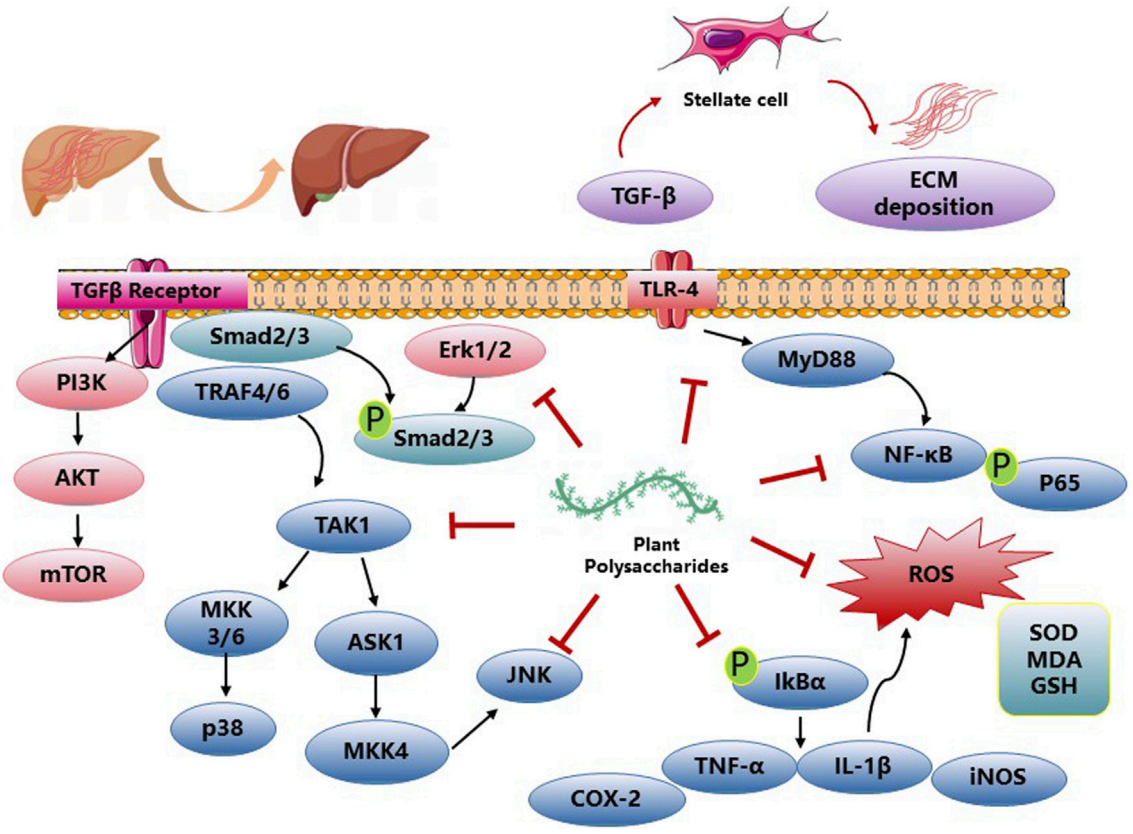

FIGURE 4
PP impact on hepatic fibrosis activities and related mechanisms.

significantly ameliorated liver injury in CCl_4-challenged mice, as evidenced by reduced levels of serum ALT, AST, and total bilirubin (TBIL). Moreover, SP treatment enhanced PALB levels, indicating hepatoprotective effects. These beneficial effects were accompanied by increased activities of antioxidant enzymes SOD and GSH-Px, elevated GSH levels, and reduced MDA content, indicating reduced oxidative stress. SP pre-treatment also attenuated the expression of pro-inflammatory cytokines TNF-α and IL-1β, as well as iNOS and NO production induced by CCl_4. Furthermore, SP pre-treatment suppressed hepatic TLR4 expression and inhibited the phosphorylation of p38 MAPK, p-ERK, p-JNK, and NF-κB signaling pathways in CCl_4-challenged mice (Zhang et al., 2017). *Stipa parviflora* polysaccharides treated rat liver anti-oxidant parameters (SOD, CAT and GPx) were significantly antagonized for the pro-oxidant effect of CCl_4 (Bargougui et al., 2019). *Dictyophora* polysaccharides (DIP) attenuated liver fibrosis induced by arsenic (As) by reducing hepatic pathological alterations and modulating the levels of serum markers including AST, ALT, total protein (TP), albumin (ALB), and Albumin/Globulin (A/G) ratio, as well as diminishing the concentrations of hyaluronic acid (HA), laminin (LN), procollagen type III (PCIII), collagen type Ⅳ (IV-C), TBIL, and direct bilirubin (DBIL). Moreover, DIP exhibited inhibitory effects on the synthesis of TGF-β1, thereby regulating the expression of connective tissue growth factor (CTGF) and subsequently suppressing the proliferation of fibrinogen and fibroblasts. This led to a reduction in fibroblast transformation into myofibroblasts, thus limiting the synthesis of fibroblasts (Wang et al., 2022). Results of the effects of PP on hepatic fibrosis activity are described in Figure 4 and Table 4.

2.1.5 Plant polysaccharides against hepatocellular carcinoma (HCC)

HCC is a prevalent form of primary liver cancer with significant medical implications. It ranks sixth among the most commonly diagnosed tumors worldwide, accounting for 1.100 cases per 100,000 person-years. Moreover, it stands as the third leading cause of cancer-related mortality, resulting in 0.746 million new cases and 0.2012 million deaths. Notably, HCC represents the primary cause of death in individuals with cirrhosis, and its incidence is projected to rise in the coming years (Forner et al., 2018). The incidence of HCC is highest in East Asia and Africa, but there is a growing trend in the United States. In Asia and Africa, 60% of HCC cases are attributed to HBV infection, whereas HCV infection takes predominance in North America, Europe, and Japan. The strongest risk factor for HCC is cirrhosis, with an annual incidence ranging from 1% to 6%. HCC is commonly observed in patients with cirrhosis and is a leading cause of mortality in this population. Alcohol-induced cirrhosis accounts for 15%–30% of HCC cases, varying across geographical regions (Llovet et al., 2021). The polysaccharide derived from *Panax notoginseng* has demonstrated its potential to extend the lifespan of tumor-bearing mice by enhancing the host immune system while

TABLE 4 Summary of articles data about PP impact on hepatic fibrosis activity.

Polysaccharide	Origin plant	Models	Functions	Mechanisms	References
Talinum triangulare polysaccharides	*Talinum triangulare*	CCl_4-induced liver injury in mice	Antioxidant	Decrease AST, ALT and MDA; restored antioxidant; substance SOD and GSH	Liang et al. (2011)
Lycium barbarum polysaccharide	*Lycium barbarum*	CCl_4-induced acute hepatotoxicity in mice	Reduce necroinflammation and oxidative stress	Inhibit cytochrome P450 2E1 and restore antioxidant enzymes; decreased nitric oxide metabolism and lipid peroxidation	Xiao et al. (2012)
Amomum villosum polysaccharides	The seeds of *Amomum villosum*	CCl_4-induced liver injury mice	Antioxidant	Prevent the formation of malondialdehyde and enhanced antioxidant enzymes	Zhang et al. (2013)
Tea polysaccharides	Green tea	CCl_4-induced hepatotoxicity in mice	Antioxidant activity	Against free radicals	Wang et al. (2016)
Angelica and Astragalus polysaccharide	*Angelica and Astragalus*	CCl_4-induced liver injury in mice	Anti-inflammation antioxidant	Ameliorate oxidative stress and to inhibit lipid peroxidation	Pu et al. (2015)
Anoectochilus roxburghii polysaccharides	*Anoectochilus roxburghii*	CCl_4-induced liver injury in mice	Antioxidant	Decrease the oxidative stress marker MDA and the antioxidant enzymes	Zeng et al. (2016)
Seabuckthorn berry polysaccharide	Seabuckthorn	CCl_4-induced liver injury mice	Anti-oxidative and anti-inflammatory	Decrease hepatic TLR4 expression and inhibit the p-p38 p-MAPK, p-ERK, p-JNK and NF-κB	Zhang et al. (2017)
Inulin-type fructan	*Artemisia vulgaris* L.	CCl_4-induced liver injury in mice	Hepatoprotective and antioxidant	Modulate hepatic cytokines and promote a reparative inflammatory response	Correa-Ferreira et al. (2017)
Stipa parviflora polysaccharides	*Stipa parviflora*	CCl_4-induced liver injury in rats	Antioxidant	Anti-oxidant parameters (SOD, CAT and GPx), hepatoprotective activity	Bargougui et al. (2019)
Radix *Cyathulae officinalis* Kuan polysaccharide	Radix *Cyathulae officinalis* Kuan	CCl_4-induced liver injury in mice	Antioxidant	Increase antioxidant enzyme activities; decrease the production of inflammatory	Meng et al. (2019)
Anoectochilus roxburghii polysaccharide	*Anoectochilus roxburghii*	CCl_4-induced liver injury in mice	Mitigate hepatotoxicity	Lipid metabolism, gut bacteria metabolism, and the methylation pathway	Zeng et al. (2020)
Dictyophora polysaccharides	*Dictyophora*	As-induced liver fibrosis in rats	Improve the As-induced liver fibrosis	Inhibit the synthesis of TGF-β1	Wang et al. (2022)
Pectic polysaccharide	*Abelmoschus esculentus* (Linn.) Moench	CCl_4-induced liver injury mice	Ameliorate lipid metabolism, oxidative stress, anti-inflammatory	Regulate intestinal microflora, and promoting SCFA production	Yan et al. (2023)

displaying limited cytotoxicity against hepatocellular carcinoma (Liu et al., 2021). Treatment with *Dictyophora* polysaccharides resulted in a time- and dose-dependent inhibition of HCC-LM3 cell proliferation, accompanied by cell cycle arrest in the G_2/M phase. Moreover, the expression of Bax and caspase-3 exhibited a significant increase following *Dictyophora* polysaccharides administration (Hu et al., 2020). Dandelion polysaccharide (DP) treatment effectively suppressed the protein levels of crucial angiogenesis-related factors involved in HCC, including HIF-1α, VEGF, p-PI3K, and p-AKT. This suggests that DP holds promise as a potential therapeutic agent for HCC (Ren et al., 2020). Astragalus polysaccharide (APS) has been found to mitigate PD-L1-mediated immunosuppression by targeting the miR-133a-3p/MSN axis, thereby facilitating an antitumor response (He et al., 2022). Additionally, ASP has been explored as a targeted drug carrier for HepG2 tumors via ASGPR, enhancing therapy for liver cancer (Zhang et al., 2019). Treatment with *Aconitum coreanum* polysaccharide, a potential therapeutic agent for HCC, led to a significant reduction in p-Akt protein levels, while simultaneously increasing p-p38 MAPK protein levels in H22 cells (Liang et al., 2015). Hypoxia promotes epithelial-mesenchymal transition (EMT) and facilitates migration and invasion of HCC cells. However, Basil polysaccharide (BPS) exhibits inhibitory effects on tumor progression and metastasis, including the reversal of EMT via cytoskeletal remodeling under hypoxic conditions. Furthermore, BPS targets hypoxia-inducible factor 1 alpha (HIF1α) to alleviate tumor hypoxia. We observed downregulation of mesenchymal markers (β-catenin, N-cadherin, and vimentin) along with upregulation of epithelial markers (E-cadherin, VMP1, and ZO-1) after BPS treatment, highlighting its potential for HCC therapy in hypoxic conditions (Feng et al., 2019). The application of *Ginseng polysaccharide* (GSP) mainly includes GSP injection and GSP fermented milk beverage. GSP injection is mainly used as an adjuvant therapy for clinical tumors, reducing the side effects caused by various tumor radiotherapy and chemotherapy, and serving as an immune modulator to improve the immune function. It can also be used to treat acute and chronic hepatitis and various liver injuries, as well as various chronic infections, diabetes, and various immune diseases. Figure 5 and Table 5 give a summary of a few reports on the anti-tumor activity of PP.

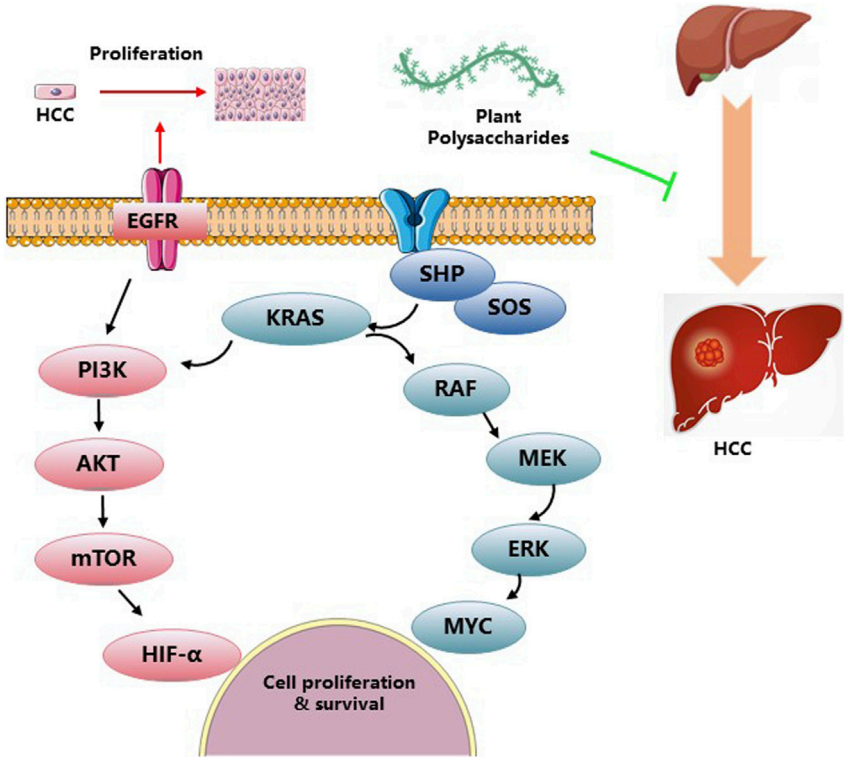

FIGURE 5
Anti-tumor activities and related mechanisms of PP.

3 Conclusion and outlook

Chronic liver disease has a significant impact on global health, resulting in over two million deaths annually and accounting for 4% of all global deaths (Devarbhavi et al., 2023). However, there are limited hepatoprotective drugs available in the market that demonstrate satisfactory efficacy without notable side effects. Natural compounds, characterized by their structural diversity and beneficial biological activities, hold great potential as precursors for clinical drugs. Therefore, the search for natural and low-toxic hepatoprotective compounds is of utmost importance. Plant polysaccharides (PP) from herbs have emerged as active constituents with a wide range of pharmacological effects, including antioxidant, anti-inflammatory, anti-apoptotic, lipid metabolism regulation, and anti-cancer properties. PP have demonstrated promising hepatoprotective effects against various liver conditions such as NAFLD, ALD, DILI, hepatic fibrosis and HCC.

In addition, cholestatic hepatitis is a disorder characterized by aberrant metabolism of bile acids. However, there is limited research on the role of polysaccharides in cholestatic hepatitis. Although polysaccharides with pharmacological effects, including antioxidant, anti-inflammatory, anti-apoptotic, which may have a therapeutic effect like *Yinchenhao decoction* (YCHD). YCHD exhibited the ability to ameliorate cholestasis by stimulating the bile secretion pathway. The YCHD has been proposed for its potential to mitigate cholestasis by activating the bile secretion pathway. This mechanism entails the modulation of various targets, including FXR, by some of the major active components of YCHD. FXR, a vital molecule that interacts with bile acids, exerts inhibitory effects on bile acid synthesis and transport (Keitel et al., 2019). FXR modulates the expression of the bile salt export pump (BSEP), facilitating the translocation of monovalent bile acids from hepatocytes to bile, thereby mitigating the hepatotoxicity associated with bile acids (Luo et al., 2024). In conclusion, this review provides a comprehensive overview of the latest advancements regarding PP and their significance in modulating lipid metabolism, inflammation, fibrosis, and oxidative stress. These effects are predominantly regulated through classical signaling pathways, such as MAPK, AMPK, PPAR, NFκB, and PI3K/AKT, which play crucial roles in the development and progression of diverse liver disorders.

PP have shown great potential for clinical use due to their remarkable properties. However, despite the numerous advantages revealed by several clinical trials, PP utilization in real-world medical settings remains limited. While their safety, effectiveness, and minimal side effects have been verified (Yang et al., 2022; Kuang et al., 2023), unresolved issues persist. For example, the health benefits and medicinal value of *Ganoderma lucidum* polysaccharide (GLP) have been widely recognized in the academic community. Although GLP has not yet been used in clinical medicine, it will have broad application prospects and clinical value as its immunomodulatory, tumor suppressive, and blood glucose regulating effects and mechanisms are gradually elucidated. At present, there are still some controversies regarding the widespread application of GLP: firstly, the composition of GLP is complex, and different types and origins

TABLE 5 Summary of known anti-tumor activity of PP.

Polysaccharide	Origin plant	Models	Functions	Mechanisms	References
Andrographis paniculate polysaccharide	*Andrographis paniculate*	HepG2 cells	Loss of mitochondrial membrane potential and the release of cytochrome c from the mitochondria to the cytosol; caspase-9 and caspase-3 were activated	Mitochondria-mediated signaling pathway	Zou et al. (2015)
Aconitum coreanum polysaccharide	*Aconitum coreanum*	H22 cells in mice	The induction of apoptosis	PTTG1-mediated suppression of the P13K/Akt and activation of p38 MAPK signaling pathway	Liang et al. (2015)
Purified white polysaccharide	Purified white	HepG2 cells	Apoptosis	Induce apoptosis involved a caspase-3-mediated mitochondrial pathway	Shen et al. (2016)
Dandelion Polysaccharide	*Dandelion*	Hepa1-6 cells; H22 cells tumors model	Suppress expression of VEGF and HIF-1α	PI3K/AKT signaling	Ren et al. (2020)
Dictyophora polysaccharide	*Dictyophora*	HCC-LM3 cell line	Modulate Cell cycle and apoptosis-inhibited cell	Proliferation in a time- and dose-dependent manner and block the cell cycle in the G_2/M phase	Hu et al. (2020)
crude Polysaccharide	*Panax notoginseng*	myelosuppression mice induced by CTX	Antitumor activity for the treatment of liver cancer combined with cyclophosphamide	Immunosuppressive	Liu et al. (2021)
Astragalus polysaccharide	*Astragalus*	Hep3B xenograft tumors model	Inhibit exacerbation of ER stress and activation of apoptotic	Promote Dox-induced apoptosis through reducing the O-GlcNAcylation; mediated immunosuppression via miR-133a-3p/MSN axis; decreasing the expression of Notch1	He et al. (2022), Huang et al. (2019), Li et al. (2023)
Mushroom-derived polysaccharide	Mushroom	N-Diethylnitrosamine-Induced Hepatocellular Carcinoma in Wistar Rats	Antioxidant and anti-inflammatory; exerted cytotoxic activities	Inhibit cell proliferation and restore liver architecture, antioxidant enzymes, and cytokines/chemokines balance	Sipping et al. (2022)

of Ganoderma have an impact on the composition of GLP; Secondly, the molecular regulatory mechanisms of GLP in inhibiting tumors and lowering blood sugar are not fully understood and lack in-depth research; Thirdly, research on the efficacy of GLP is still in the experimental stage, with limited clinical research. It is still necessary to study and explore how to determine the clinical value and effective dosage of GLP. The biological activities of PP are strongly impacted by their chemical structure and chain conformations, necessitating further investigation and improved methodologies to establish their efficacy. Two crucial areas for future research can be identified. First and foremost, it is crucial to enhance the bioavailability of plant polysaccharides (PP) and identify their specific molecular targets for the treatment of chronic liver disease (CLD). These factors are essential for advancing research and developing new PP-based drugs in the future. Additionally, with accurate knowledge of the structure and molecular weight of PP, extensive studies have investigated the structure-activity relationship of PP in CLD treatment. However, further investigations are required to attain rational structural optimization and design of PP, thereby influencing critical signaling pathways involved in multifactorial liver diseases to enhance bioavailability and therapeutic efficacy. This research will facilitate a deeper understanding of the precise binding sites and mechanisms through which these polysaccharides operate. This foundational knowledge will pave the way for further research and the potential development of innovative medications. Lastly, it is imperative to conduct clinical trials to evaluate the safety and effectiveness of PP in the management of multifactorial liver disease. Furthermore, the combination of PP with other drugs for comprehensive treatment has emerged as a recent research focus.

There is a general conception that PP, when utilized as health food or dietary supplements are generally considered safe to enhance immune response, exhibit potential antiviral effects, antioxidant properties, modulation of inflammatory pathways and potential anti-cancer properties. For example, Serum glucose was found to be significantly decreased and insulinogenic index increased during OMTT after 3 months administration of *Lycium barbarum* polysaccharide. In addition, a prescription drug, injectable *Astragalus* polysaccharide (PG2) (PhytoHealth Corporation, Taiwan, ROC), is an immunomodulator that has been approved for the alleviation of

TABLE 6 Summary of main findings and side effects of PP in clinicals.

Polysaccharide	Functions	Side effects	References
Lycium barbarum polysaccharide	Improved immune function, antioxidant properties, and potential anti-inflammatory effects	Generally well-tolerated. Some individuals may experience mild gastrointestinal discomfort	Cai et al. (2015), Chen et al. (2020), Gao et al. (2021)
Astragalus polysaccharide	Enhanced immune response, potential antiviral effects, and modulation of inflammatory pathways	Rare cases of allergic reactions or gastrointestinal upset have been reported	Bamodu et al. (2019), Huang et al. (2019), Tsao et al. (2021), Lee et al. (2023)
Ganoderma lucidum polysaccharide (fungal polysaccharides)	Exhibits immunomodulatory effects, potential anti-cancer properties, and antioxidant activity	Rare cases of liver toxicity or allergic reactions have been reported with high doses	Lin et al. (2005), Lin et al. (2006)

cancer-related fatigue. However, they can cause adverse effects when used therapeutically, such as in the examples shown in Table 6. The combined use of PP with other drugs are considered a major problem in clinical practice of PP as they contribute to altering important pharmacokinetic processes, resulting in therapeutic failure or increase toxicity of some prescription drugs. Clinical trials have shown that many over-the-counter dietary supplements can modulate the activity of drug metabolizing enzymes and/or drug transporters and further influence the bioavailability of co-administrated drugs (Abuznait et al., 2011). For example, *Lycium barbarum* polysaccharide could inhibit cytochrome P450 (Xiao et al., 2012), yet herb-drug and food-drug interactions can arise from the modulation of cytochrome P450 isoenzymes. Therefore, the adverse effects of synthetic action of PP with other drugs for comprehensive treatment should be considered in the treatment of patients with chronic liver disease whose liver function may already be compromised. Additionally, a significant challenge in harnessing the full potential of these polysaccharides is their limited solubility, which hampers the development of effective dosage forms. To overcome this limitation, the utilization of nano-formulations has emerged as a promising approach, improving the bioavailability of these compounds. Moving forward, the ongoing advancements in PP research offer great potential for revolutionizing treatment strategies for CLDs.

Author contributions

XW: Investigation, Project administration, Writing–original draft, Writing–review and editing. DL: Data curation, Investigation, Writing–original draft. HL: Formal Analysis, Methodology, Software, Writing–original draft. YL: Validation, Visualization, Writing–original draft. SC: Visualization, Writing–original draft. MH: Supervision, Visualization, Writing–review and editing. XJ: Resources, Supervision, Writing–review and editing. GZ: Project administration, Supervision, Writing–review and editing. WZ: Funding acquisition, Supervision, Validation, Writing–review and editing.

Funding

The author(s) declare financial support was received for the research, authorship, and/or publication of this article. The Project was Supported by the Opening Project of Guangdong Provincial Key Laboratory of New Drug Design and Evaluation, (No. 2020B1212060034).

Conflict of interest

The authors declare that the research was conducted in the absence of any commercial or financial relationships that could be construed as a potential conflict of interest.

Publisher's note

References

Abuznait, A. H., Qosa, H., O'Connell, N. D., Akbarian-Tefaghi, J., Sylvester, P. W., El, S. K., et al. (2011). Induction of expression and functional activity of P-glycoprotein efflux transporter by bioactive plant natural products. *Food. Chem. Toxicol.* 49 (11), 2765–2772. doi:10.1016/j.fct.2011.08.004

Andrade, R. J., Chalasani, N., Bjornsson, E. S., Suzuki, A., Kullak-Ublick, G. A., Watkins, P. B., et al. (2019). Drug-induced liver injury. *Nat. Rev. Dis. Prim.* 5 (1), 58. doi:10.1038/s41572-019-0105-0

Asrani, S. K., Devarbhavi, H., Eaton, J., and Kamath, P. S. (2019). Burden of liver diseases in the world. *J. Hepatol.* 70 (1), 151–171. doi:10.1016/j.jhep.2018.09.014

Athmouni, K., Belhaj, D., El, F. A., and Ayadi, H. (2018). Optimization, antioxidant properties and GC-MS analysis of Periploca angustifolia polysaccharides and chelation therapy on cadmium-induced toxicity in human HepG2 cells line and rat liver. *Int. J. Biol. Macromol.* 108, 853–862. doi:10.1016/j.ijbiomac.2017.10.175

Bamodu, O. A., Kuo, K., Wang, C., Huang, W., Wu, A. T. H., Tsai, J., et al. (2019). Astragalus polysaccharides (PG2) enhances the M1 polarization of macrophages, functional maturation of dendritic cells, and T cell-mediated anticancer immune responses in patients with lung cancer. *Nutrients* 11 (10), 2264. doi:10.3390/nu11102264

Bargougui, K., Athmouni, K., and Chaieb, M. (2019). Optimization, characterization and hepatoprotective effect of polysaccharides isolated from Stipa parviflora Desf. against CCl(4) induced liver injury in rats using surface response methodology (RSM). *Int. J. Biol. Macromol.* 132, 524–533. doi:10.1016/j.ijbiomac.2019.03.216

Byrne, C. D., and Targher, G. (2016). EASL-EASD-EASO Clinical Practice Guidelines for the management of non-alcoholic fatty liver disease: is universal screening appropriate? *Diabetologia* 59 (6), 1141–1144. doi:10.1007/s00125-016-3910-y

Cai, H., Liu, F., Zuo, P., Huang, G., Song, Z., Wang, T., et al. (2015). Practical application of antidiabetic efficacy of Lycium barbarum polysaccharide in patients with type 2 diabetes. *Med. Chem.* 11 (4), 383–390. doi:10.2174/1573406410666141111053858

Cao, P., Sun, J., Sullivan, M. A., Huang, X., Wang, H., Zhang, Y., et al. (2018). Angelica sinensis polysaccharide protects against acetaminophen-induced acute liver injury and cell death by suppressing oxidative stress and hepatic apoptosis *in vivo* and *in vitro*. *Int. J. Biol. Macromol.* 111, 1133–1139. doi:10.1016/j.ijbiomac.2018.01.139

Che, J., Yang, S., Qiao, Z., Li, H., Sun, J., Zhuang, W., et al. (2019). Schisandra chinensis acidic polysaccharide partialy reverses acetaminophen-induced liver injury in mice. *J. Pharmacol. Sci.* 140 (3), 248–254. doi:10.1016/j.jphs.2019.07.008

Chen, L. J., Xu, W., Li, Y. P., Ma, L. T., Zhang, H. F., Huang, X. B., et al. (2020). Lycium barbarum polysaccharide inhibited hypoxia-inducible factor 1 in COPD patients. *Int. J. Chronic Obstr. Pulm. Dis.* 15, 1997–2004. doi:10.2147/COPD.S254172

Correa-Ferreira, M. L., Verdan, M. H., Dos, R. L. F., Galuppo, L. F., Telles, J. E., Alves, S. M., et al. (2017). Inulin-type fructan and infusion of Artemisia vulgaris protect the liver against carbon tetrachloride-induced liver injury. *Phytomedicine* 24, 68–76.

Cui, Y., Ye, Q., Wang, H., Li, Y., Yao, W., and Qian, H. (2014). Hepatoprotective potential of Aloe vera polysaccharides against chronic alcohol-induced hepatotoxicity in mice. *J. Sci. Food. Agric.* 94 (9), 1764–1771. doi:10.1002/jsfa.6489

Devarbhavi, H., Asrani, S. K., Arab, J. P., Nartey, Y. A., Pose, E., and Kamath, P. S. (2023). Global burden of liver disease: 2023 update. *J. Hepatol.* 79 (2), 516–537. doi:10.1016/j.jhep.2023.03.017

Dolganiuc, A. (2015). Alcohol and viral hepatitis: role of lipid rafts. *Alcohol Res.* 37 (2), 299–309.

European Association for the Study of the LiverEuropean Association for the Study of the Liver (2018). EASL clinical practice guidelines: management of alcohol-related liver disease. *J. Hepatol.* 69 (1), 154–181. doi:10.1016/j.jhep.2018.03.018

Feng, B., Zhu, Y., Sun, C., Su, Z., Tang, L., Li, C., et al. (2019). Basil polysaccharide inhibits hypoxia-induced hepatocellular carcinoma metastasis and progression through suppression of HIF-1α-mediated epithelial-mesenchymal transition. *Int. J. Biol. Macromol.* 137, 32–44. doi:10.1016/j.ijbiomac.2019.06.189

Fontana, R. J. (2014). Pathogenesis of idiosyncratic drug-induced liver injury and clinical perspectives. *Gastroenterology* 146 (4), 914–928. doi:10.1053/j.gastro.2013.12.032

Forner, A., Reig, M., and Bruix, J. (2018). Hepatocellular carcinoma. *Lancet* 391 (10127), 1301–1314. doi:10.1016/S0140-6736(18)30010-2

Friedman, S. L., Neuschwander-Tetri, B. A., Rinella, M., and Sanyal, A. J. (2018). Mechanisms of NAFLD development and therapeutic strategies. *Nat. Med.* 24 (7), 908–922. doi:10.1038/s41591-018-0104-9

Ganesan, M., Eikenberry, A., Poluektova, L. Y., Kharbanda, K. K., and Osna, N. A. (2020). Role of alcohol in pathogenesis of hepatitis B virus infection. *World J. Gastroenterol.* 26 (9), 883–903. doi:10.3748/wjg.v26.i9.883

Gao, L. L., Li, Y. X., Ma, J. M., Guo, Y. Q., Li, L., Gao, Q. H., et al. (2021). Effect of Lycium barbarum polysaccharide supplementation in non-alcoholic fatty liver disease patients: study protocol for a randomized controlled trial. *Trials* 22 (1), 566. doi:10.1186/s13063-021-05529-6

He, L., Xu, K., Niu, L., and Lin, L. (2022a). Astragalus polysaccharide (APS) attenuated PD-L1-mediated immunosuppression via the miR-133a-3p/MSN axis in HCC. *Pharm. Biol.* 60 (1), 1710–1720. doi:10.1080/13880209.2022.2112963

He, Z., Guo, T., Cui, Z., Xu, J., Wu, Z., Yang, X., et al. (2022b). New understanding of Angelica sinensis polysaccharide improving fatty liver: the dual inhibition of lipid synthesis and CD36-mediated lipid uptake and the regulation of alcohol metabolism. *Int. J. Biol. Macromol.* 207, 813–825. doi:10.1016/j.ijbiomac.2022.03.148

Hoofnagle, J. H., and Bjornsson, E. S. (2019). Drug-induced liver injury - types and phenotypes. *N. Engl. J. Med.* 381 (3), 264–273. doi:10.1056/NEJMra1816149

Hu, T., Zhang, K., Pan, D., Pan, X., Yang, H., Xiao, J., et al. (2020). Inhibition effect of Dictyophora polysaccharides on human hepatocellular carcinoma cell line HCC-LM3. *Med. Sci. Monit.* 26, e918870. doi:10.12659/MSM.918870

Huang, W., Kuo, K., Bamodu, O. A., Lin, Y., Wang, C., Lee, K., et al. (2019). Astragalus polysaccharide (PG2) ameliorates cancer symptom clusters, as well as improves quality of life in patients with metastatic disease, through modulation of the inflammatory cascade. *Cancers* 11 (8), 1054. doi:10.3390/cancers11081054

Huang, X., Tang, W., Lin, C., Sa, Z., Xu, M., Liu, J., et al. (2021). Protective mechanism of Astragalus Polysaccharides against Cantharidin-induced liver injury determined *in vivo* by liquid chromatography/mass spectrometry metabolomics. *Basic Clin. Pharmacol. Toxicol.* 129 (1), 61–71. doi:10.1111/bcpt.13585

Jiang, W., Zhu, H., Liu, C., Hu, B., Guo, Y., Cheng, Y., et al. (2022). In-depth investigation of the mechanisms of Echinacea purpurea polysaccharide mitigating alcoholic liver injury in mice via gut microbiota informatics and liver metabolomics. *Int. J. Biol. Macromol.* 209 (Pt A), 1327–1338. doi:10.1016/j.ijbiomac.2022.04.131

Jiang, W., Zhu, H., Xu, W., Liu, C., Hu, B., Guo, Y., et al. (2021). Echinacea purpurea polysaccharide prepared by fractional precipitation prevents alcoholic liver injury in mice by protecting the intestinal barrier and regulating liver-related pathways. *Int. J. Biol. Macromol.* 187, 143–156. doi:10.1016/j.ijbiomac.2021.07.095

Jiang, Y. H., Wang, L., Chen, W. D., Duan, Y. T., Sun, M. J., Huang, J. J., et al. (2022). Poria cocos polysaccharide prevents alcohol-induced hepatic injury and inflammation by repressing oxidative stress and gut leakiness. *Front. Nutr.* 9, 963598. doi:10.3389/fnut.2022.963598

Keitel, V., Droge, C., and Haussinger, D. (2019). Targeting FXR in cholestasis. *Handb. Exp. Pharmacol.* 256, 299–324. doi:10.1007/164_2019_231

Kong, L. Z., Chandimali, N., Han, Y. H., Lee, D. H., Kim, J. S., Kim, S. U., et al. (2019). Pathogenesis, early diagnosis, and therapeutic management of alcoholic liver disease. *Int. J. Mol. Sci.* 20 (11), 2712. doi:10.3390/ijms20112712

Kuang, S., Liu, L., Hu, Z., Luo, M., Fu, X., Lin, C., et al. (2023). A review focusing on the benefits of plant-derived polysaccharides for osteoarthritis. *Int. J. Biol. Macromol.* 228, 582–593. doi:10.1016/j.ijbiomac.2022.12.153

Lee, C., Nguyen, A. T., Doan, L. H., Chu, L., Chang, C., Liu, H., et al. (2023). Repurposing Astragalus polysaccharide PG2 for inhibiting ACE2 and SARS-CoV-2 spike syncytial formation and anti-inflammatory effects. *Viruses* 15 (3), 641. doi:10.3390/v15030641

Li, M., Duan, F., Pan, Z., Liu, X., Lu, W., Liang, C., et al. (2023). Astragalus Polysaccharide Promotes Doxorubicin-Induced Apoptosis by Reducing O-GlcNAcylation in Hepatocellular Carcinoma. *Cells-Basel* 12.

Liang, D., Zhou, Q., Gong, W., Wang, Y., Nie, Z., He, H., et al. (2011). Studies on the antioxidant and hepatoprotective activities of polysaccharides from Talinum triangulare. *J. Ethnopharmacol.* 136 (2), 316–321. doi:10.1016/j.jep.2011.04.047

Liang, M., Liu, J., Ji, H., Chen, M., Zhao, Y., Li, S., et al. (2015). A Aconitum coreanum polysaccharide fraction induces apoptosis of hepatocellular carcinoma (HCC) cells via pituitary tumor transforming gene 1 (PTTG1)-mediated suppression of the P13K/Akt and activation of p38 MAPK signaling pathway and displays antitumor activity *in vivo*. *Tumour Biol.* 36 (9), 7085–7091. doi:10.1007/s13277-015-3420-4

Lin, Y., Lee, S., Hou, S., and Chiang, B. (2006). Polysaccharide purified from Ganoderma lucidum induces gene expression changes in human dendritic cells and promotes T helper 1 immune response in BALB/c mice. *Mol. Pharmacol.* 70 (2), 637–644. doi:10.1124/mol.106.022327

Lin, Y. L., Liang, Y. C., Lee, S. S., and Chiang, B. L. (2005). Polysaccharide purified from Ganoderma lucidum induced activation and maturation of human monocyte-derived dendritic cells by the NF-kappaB and p38 mitogen-activated protein kinase pathways. *J. Leukoc. Biol.* 78 (2), 533–543. doi:10.1189/jlb.0804481

Liu, G., Liu, X., Zhang, Y., Zhang, F., Wei, T., Yang, M., et al. (2015). Hepatoprotective effects of polysaccharides extracted from Zizyphus jujube cv. Huanghetanzao. *Huanghetanzao. Int. J. Biol. Macromol.* 76, 169–175. doi:10.1016/j.ijbiomac.2015.01.061

Liu, Y. H., Qin, H. Y., Zhong, Y. Y., Li, S., Wang, H. J., Wang, H., et al. (2021). Neutral polysaccharide from Panax notoginseng enhanced cyclophosphamide antitumor efficacy in hepatoma H22-bearing mice. *BMC Cancer* 21 (1), 37. doi:10.1186/s12885-020-07742-z

Llovet, J. M., Kelley, R. K., Villanueva, A., Singal, A. G., Pikarsky, E., Roayaie, S., et al. (2021). Hepatocellular carcinoma. *Nat. Rev. Dis. Prim.* 7 (1), 6. doi:10.1038/s41572-020-00240-3

Luo, L., Zhang, H., Chen, W., Zheng, Z., He, Z., Wang, H., et al. (2023). Angelica sinensis polysaccharide ameliorates nonalcoholic fatty liver disease via restoring estrogen-related receptor α expression in liver. *Phytother. Res.* 37, 5407–5417. doi:10.1002/ptr.7982

Luo, S., Huang, M., Lu, X., Zhang, M., Xiong, H., Tan, X., et al. (2024). Optimized therapeutic potential of Yinchenhao decoction for cholestatic hepatitis by combined network meta-analysis and network pharmacology. *Phytomedicine* 129, 155573. doi:10.1016/j.phymed.2024.155573

Meng, X., Wang, Z., Liang, S., Tang, Z., Liu, J., Xin, Y., et al. (2019). Hepatoprotective effect of a polysaccharide from Radix Cyathulae officinalis Kuan against CCl(4)-induced acute liver injury in rat. *Int. J. Biol. Macromol.* 132, 1057–1067.

Meroni, M., Longo, M., Rametta, R., and Dongiovanni, P. (2018). Genetic and epigenetic modifiers of alcoholic liver disease. *Int. J. Mol. Sci.* 19 (12), 3857. doi:10.3390/ijms19123857

Pereira, K., Salsamendi, J., and Casillas, J. (2015). The global nonalcoholic fatty liver disease epidemic: what a radiologist needs to know. *J. Clin. Imag. Sci.* 5, 32. doi:10.4103/2156-7514.157860

Nepali, S., Ki, H. H., Lee, J. H., Cha, J. Y., Lee, Y. M., and Kim, D. K. (2017). Triticum aestivum sprout-derived polysaccharide exerts hepatoprotective effects against ethanol-induced liver damage by enhancing the antioxidant system in mice. *Int. J. Mol. Med.* 40, 1243–1252.

Pinzani, M., and Macias-Barragan, J. (2010). Update on the pathophysiology of liver fibrosis. *Expert Rev. Gastroenterol. Hepatol.* 4 (4), 459–472. doi:10.1586/egh.10.47

Pu, X., Fan, W., Yu, S., Li, Y., Ma, X., Liu, L., et al. (2015). Polysaccharides from Angelica and Astragalus exert hepatoprotective effects against carbon-tetrachloride-induced intoxication in mice. *Can. J. Physiol. Pharm.* 93, 39–43.

Rehm, J., Gmel, G. S., Gmel, G., Hasan, O., Imtiaz, S., Popova, S., et al. (2017). The relationship between different dimensions of alcohol use and the burden of disease-an update. *Addiction* 112 (6), 968–1001. doi:10.1111/add.13757

Ren, F., Wu, K., Yang, Y., Yang, Y., Wang, Y., and Li, J. (2020). Dandelion polysaccharide exerts anti-angiogenesis effect on hepatocellular carcinoma by regulating VEGF/HIF-1α expression. *Front. Pharmacol.* 11, 460. doi:10.3389/fphar.2020.00460

Rinella, M. E., Lazarus, J. V., Ratziu, V., Francque, S. M., Sanyal, A. J., Kanwal, F., et al. (2023). A multisociety Delphi consensus statement on new fatty liver disease nomenclature. *Hepatology* 78 (6), 1966–1986. doi:10.1097/HEP.0000000000000520

Sahlman, P., Nissinen, M., Pukkala, E., and Farkkila, M. (2016). Cancer incidence among alcoholic liver disease patients in Finland: a retrospective registry study during years 1996-2013. *Int. J. Cancer.* 138 (11), 2616–2621. doi:10.1002/ijc.29995

Saito, H., Kilpatrick, C., and Pittet, D. (2018). The 2018 world health organization SAVE LIVES: clean your hands campaign targets sepsis in health care. *Intensive Care Med.* 44 (4), 499–501. doi:10.1007/s00134-018-5097-9

Seitz, H. K., Bataller, R., Cortez-Pinto, H., Gao, B., Gual, A., Lackner, C., et al. (2018). Alcoholic liver disease. *Nat. Rev. Dis. Prim.* 4 (1), 16. doi:10.1038/s41572-018-0014-7

Shen, W., Guan, Y., Wang, J., Hu, Y., Tan, Q., Song, X., et al. (2016). A polysaccharide from pumpkin induces apoptosis of HepG2 cells by activation of mitochondrial pathway. *Tumour Biol.* 37, 5239–5245.

Shi, X., Ma, H., Tong, C., Qu, M., Jin, Q., and Li, W. (2015). Hepatoprotective effect of a polysaccharide from Crassostrea gigas on acute and chronic models of liver injury. *Int. J. Biol. Macromol.* 78, 142–148.

Sipping, M., Mediesse, F. K., Kenmogne, L. V., Kanemoto, J., Njamen, D., and Boudjeko, T. (2022). Polysaccharide-rich fractions from ganoderma resinaceum (Ganodermataceae) as chemopreventive agents in N-Diethylnitrosamine-induced hepatocellular carcinoma in wistar rats. *Evid-Based Compl. Alt.* 2022, 8198859.

Song, X., Sun, W., Cui, W., Jia, L., and Zhang, J. (2021). A polysaccharide of PFP-1 from Pleurotus geesteranus attenuates alcoholic liver diseases via Nrf2 and NF-κB signaling pathways. *Food Funct.* 12 (10), 4591–4605. doi:10.1039/d1fo00310k

Sun, S., Wang, K., Sun, L., Cheng, B., Qiao, S., Dai, H., et al. (2020). Therapeutic manipulation of gut microbiota by polysaccharides of Wolfiporia cocos reveals the contribution of the gut fungi-induced PGE (2) to alcoholic hepatic steatosis. *Gut Microbes* 12 (1), 1830693. doi:10.1080/19490976.2020.1830693

Sun, W. M., Wang, Y. P., Duan, Y. Q., Shang, H. X., and Cheng, W. D. (2014). Radix Hedysari polysaccharide suppresses lipid metabolism dysfunction in a rat model of non-alcoholic fatty liver disease via adenosine monophosphate-activated protein kinase pathway activation. *Mol. Med. Rep.* 10 (3), 1237–1244. doi:10.3892/mmr.2014.2327

Thursz, M., Kamath, P. S., Mathurin, P., Szabo, G., and Shah, V. H. (2019). Alcohol-related liver disease: areas of consensus, unmet needs, and opportunities for further study. *J. Hepatol.* 70 (3), 521–530. doi:10.1016/j.jhep.2018.10.041

Tsao, S. M., Wu, T. C., Chen, J., Chang, F., and Tsao, T. (2021). Astragalus polysaccharide injection (PG2) normalizes the neutrophil-to-lymphocyte ratio in patients with advanced lung cancer receiving immunotherapy. *Integr. Cancer Ther.* 20, 1534735421995256. doi:10.1177/1534735421995256

Wang, F., Tipoe, G. L., Yang, C., Nanji, A. A., Hao, X., So, K. F., et al. (2018). Lycium barbarum polysaccharide supplementation improves alcoholic liver injury in female mice by inhibiting stearoyl-CoA desaturase 1. *Mol. Nutr. Food Res.* 62 (13), e1800144. doi:10.1002/mnfr.201800144

Wang, G., Zhang, Y., Zhang, R., Pan, J., Qi, D., Wang, J., et al. (2020). The protective effects of walnut green husk polysaccharide on liver injury, vascular endothelial dysfunction, and disorder of gut microbiota in high fructose-induced mice. *Int. J. Biol. Macromol.* 162, 92–106. doi:10.1016/j.ijbiomac.2020.06.055

Wang, G., Zuo, P., Ding, K., Zeng, Q., Hu, T., Wei, S., et al. (2022). Intervention study of Dictyophora polysaccharides on arsenic-induced liver fibrosis in SD rats. *Biomed. Res. Int.* 2022, 7509620. doi:10.1155/2022/7509620

Wang, K., Song, Z., Wang, H., Li, Q., Cui, Z., and Zhang, Y. (2016a). Angelica sinensis polysaccharide attenuates concanavalin A-induced liver injury in mice. *Int. Immunopharmacol.* 31, 140–148. doi:10.1016/j.intimp.2015.12.021

Wang, K., Tang, Z., Zheng, Z., Cao, P., Shui, W., Li, Q., et al. (2016b). Protective effects of Angelica sinensis polysaccharide against hyperglycemia and liver injury in multiple low-dose streptozotocin-induced type 2 diabetic BALB/c mice. *Food Funct.* 7 (12), 4889–4897. doi:10.1039/c6fo01196a

Wang, K., Wang, J., Song, M., Wang, H., Xia, N., and Zhang, Y. (2020). Angelica sinensis polysaccharide attenuates CCl(4)-induced liver fibrosis via the IL-22/STAT3 pathway. *Int. J. Biol. Macromol.* 162, 273–283. doi:10.1016/j.ijbiomac.2020.06.166

Xiao, J., Liong, E. C., Ching, Y. P., Chang, R. C., So, K. F., Fung, M. L., et al. (2012). Lycium barbarum polysaccharides protect mice liver from carbon tetrachloride-induced oxidative stress and necroinflammation. *J. Ethnopharmacol.* 139 (2), 462–470. doi:10.1016/j.jep.2011.11.033

Xiao, J., Wang, F., Wong, N. K., He, J., Zhang, R., Sun, R., et al. (2019). Global liver disease burdens and research trends: analysis from a Chinese perspective. *J. Hepatol.* 71 (1), 212–221. doi:10.1016/j.jhep.2019.03.004

Xiao, J., Zhu, Y., Liu, Y., Tipoe, G. L., Xing, F., and So, K. F. (2014). Lycium barbarum polysaccharide attenuates alcoholic cellular injury through TXNIP-NLRP3 inflammasome pathway. *Int. J. Biol. Macromol.* 69, 73–78. doi:10.1016/j.ijbiomac.2014.05.034

Xu, B., Hao, K., Chen, X., Wu, E., Nie, D., Zhang, G., et al. (2022). Broussonetia papyrifera polysaccharide alleviated acetaminophen-induced liver injury by regulating the intestinal flora. *Nutrients* 14 (13), 2636. doi:10.3390/nu14132636

Yan, J. K., Wang, C., Chen, T. T., Zhu, J., Chen, X., Li, L., et al. (2023). A pectic polysaccharide from fresh okra (Abelmoschus esculentus L.) beneficially ameliorates CCl(4)-induced acute liver injury in mice by antioxidation, inhibition of inflammation and modulation of gut microbiota. *Food Chem. Toxicol.* 171, 113551.

Yan, Z., Fan, R., Yin, S., Zhao, X., Liu, J., Li, L., et al. (2015). Protective effects of Ginkgo biloba leaf polysaccharide on nonalcoholic fatty liver disease and its mechanisms. *Int. J. Biol. Macromol.* 80, 573–580.

Yang, W., Zhao, P., Li, X., Guo, L., and Gao, W. (2022). The potential roles of natural plant polysaccharides in inflammatory bowel disease: a review. *Carbohydr. Polym.* 277, 118821. doi:10.1016/j.carbpol.2021.118821

Yang, X., Li, Q., Liu, W., Zong, C., Wei, L., Shi, Y., et al. (2023). Mesenchymal stromal cells in hepatic fibrosis/cirrhosis: from pathogenesis to treatment. *Cell. Mol. Immunol.* 20 (6), 583–599. doi:10.1038/s41423-023-00983-5

Ye, H., Ma, S., Qiu, Z., Huang, S., Deng, G., Li, Y., et al. (2022). Poria cocos polysaccharides rescue pyroptosis-driven gut vascular barrier disruption in order to alleviates non-alcoholic steatohepatitis. *J. Ethnopharmacol.* 296, 115457. doi:10.1016/j.jep.2022.115457

Yu, T., He, Y., Chen, H., Lu, X., Ni, H., Ma, Y., et al. (2022). Polysaccharide from Echinacea purpurea plant ameliorates oxidative stress-induced liver injury by promoting Parkin-dependent autophagy. *Phytomedicine* 104, 154311. doi:10.1016/j.phymed.2022.154311

Yuan, R., Tao, X., Liang, S., Pan, Y., He, L., Sun, J., et al. (2018). Protective effect of acidic polysaccharide from Schisandra chinensis on acute ethanol-induced liver injury through reducing CYP2E1-dependent oxidative stress. *Biomed. Pharmacother.* 99, 537–542.

Yue, S. R., Tan, Y. Y., Zhang, L., Zhang, B. J., Jiang, F. Y., Ji, G., et al. (2022). Gynostemma pentaphyllum polysaccharides ameliorate non-alcoholic steatohepatitis in mice associated with gut microbiota and the TLR2/NLRP3 pathway. *Front. Endocrinol.* 13, 885039. doi:10.3389/fendo.2022.885039

Zeng, B., Su, M., Chen, Q., Chang, Q., Wang, W., and Li, H. (2020). Anoectochilus roxburghii polysaccharide prevents carbon tetrachloride-induced liver injury in mice by metabolomic analysis. *J. Chromatogr. B.* 1152, 122202.

Zeng, B., Su, M., Chen, Q., Chang, Q., Wang, W., and Li, H. (2016). Antioxidant and hepatoprotective activities of polysaccharides from Anoectochilus roxburghii. *Carbohyd. Polym.* 153, 391–398.

Zhang, D., Li, S., Xiong, Q., Jiang, C., and Lai, X. (2013). Extraction, characterization, and biological activities of polysaccharides from Amomum villosum. *Carbohydr. Polym.* 95 (1), 114–122. doi:10.1016/j.carbpol.2013.03.015

Zhang, W., Zhang, X., Zou, K., Xie, J., Zhao, S., Liu, J., et al. (2017). Seabuckthorn berry polysaccharide protects against carbon tetrachloride-induced hepatotoxicity in mice via anti-oxidative and anti-inflammatory activities. *Food Funct.* 8 (9), 3130–3138. doi:10.1039/c7fo00399d

Zhang, Y., Cui, Z., Mei, H., Xu, J., Zhou, T., Cheng, F., et al. (2019). Angelica sinensis polysaccharide nanoparticles as a targeted drug delivery system for enhanced therapy of liver cancer. *Carbohydr. Polym.* 219, 143–154. doi:10.1016/j.carbpol.2019.04.041

Zhong, M., Yan, Y., Yuan, H., A, R., Xu, G., Cai, F., et al. (2022). Astragalus mongholicus polysaccharides ameliorate hepatic lipid accumulation and inflammation as well as modulate gut microbiota in NAFLD rats. *Food Funct.* 13 (13), 7287–7301. doi:10.1039/d2fo01009g

Zhou, J., Zhang, N., Zhao, L., Wu, W., Zhang, L., Zhou, F., et al. (2021). Astragalus polysaccharides and saponins alleviate liver injury and regulate gut microbiota in alcohol liver disease mice. *Foods* 10 (11), 2688. doi:10.3390/foods10112688

Zou, Y., Xiong, H., Xiong, H., Lu, T., Zhu, F., Luo, Z., et al. (2015). A polysaccharide from Andrographis paniculata induces mitochondrial-mediated apoptosis in human hepatoma cell line (HepG2). *Tumour. Biol.* 36, 5179–5186.

frontiers | Frontiers in Pharmacology

TYPE Original Research
PUBLISHED 05 July 2024
DOI 10.3389/fphar.2024.1393636

OPEN ACCESS

EDITED BY
Rongrui Wei,
Jiangxi University of Traditional Chinese Medicine, China

REVIEWED BY
I. Made Dwi Mertha Adnyana,
Universitas Hindu Indonesia, Indonesia
Safaet Alam,
Bangladesh Council of Scientific and Industrial Research (BCSIR), Bangladesh
Titilayo Omolara Johnson,
University of Jos, Nigeria
Joyce Ogidigo,
Columbia University, United States

*CORRESPONDENCE
Sophie Aboughe Angone,
sophie.aboughe@iphametra.org,
sophie.aboughe@gmail.com

RECEIVED 29 February 2024
ACCEPTED 04 June 2024
PUBLISHED 05 July 2024

CITATION
Boukandou Mounanga MM, Mezui A, Mewono L, Mogangué JB and Aboughe Angone S (2024), Medicinal plants used in Gabon for prophylaxis and treatment against COVID-19-related symptoms: an ethnobotanical survey.
Front. Pharmacol. 15:1393636.
doi: 10.3389/fphar.2024.1393636

Medicinal plants used in Gabon for prophylaxis and treatment against COVID-19-related symptoms: an ethnobotanical survey

Marlaine Michel Boukandou Mounanga[1], Annais Mezui[2], Ludovic Mewono[3], Jean Bertrand Mogangué[1] and Sophie Aboughe Angone[1]*

[1]Institut de Pharmacopée et de Médecine Traditionnelle (IPHAMETRA), Centre National de la Recherche Scientifique et Technologique (CENAREST), Libreville, Gabon, [2]Centre Hospitalier Universitaire Mère-Enfant, Fondation Jeanne EBORI, Libreville, Gabon, [3]Groupe de Recherche en Immunologie 2, Microbiologie appliquée, Hygiène et Physiologie, Département des Sciences de la Vie et de la Terre-Ecole Normale Supérieure, Libreville, Gabon

Background: Gabon faced COVID-19 with more than 49,000 individuals tested positive and 307 recorded fatalities since the first reported case in 2020. A popular hypothesis is that the low rate of cases and deaths in the country was attributed to the use of medicinal plants in prevention and treatment. This study aimed to document the plants used for remedial and preventive therapies by the Gabonese population during the COVID-19 pandemic and to pinpoint specific potential plant species that merit further investigation.

Methods: An ethnobotanical survey involving 97 participants was conducted in Libreville. Traditional healers and medicinal plant vendors were interviewed orally using a semi-structured questionnaire sheet, while the general population responded to an online questionnaire format. Various quantitative indexes were calculated from the collected data and included the relative frequency of citation (RFC), use value (UV), informant consensus factor (ICF), relative importance (RI), and popular therapeutic use value (POPUT). One-way ANOVA and independent samples *t*-test were used for statistical analyses. *p*-values ≤0.05 were considered significant.

Results: The survey identified 63 plant species belonging to 35 families. Prevalent symptoms treated included fever (18%), cough (16%), fatigue (13%), and cold (12%). The demographic data highlighted that 52.58% of male subjects ($p > 0.94$) aged 31–44 years were enrolled in the survey, of which 48.45% ($p < 0.0001$) and 74.73% ($p < 0.99$) of informants had university-level education. In addition, the results indicated that a total of 66% of the informants used medicinal plants for prophylaxis (34%), for both prevention and treatment (26%), exclusively for treatment (3%), and only for prevention (3%) while suffering from COVID-19, against 34% of the participants who did not use plants for prevention or treatment. *Annickia chlorantha, Citrus* sp., *Alstonia congensis, Zingiber officinale,* and *Carica papaya* emerged as the most commonly cited plants with the highest RFC (0.15–0.26), UV (0.47–0.75), and RI (35.72–45.46) values. Most of these plants were used either individually or in combination with others.

Conclusion: The survey reinforces the use of traditional medicine as a method to alleviate COVID-19 symptoms, thereby advocating for the utilization of medicinal plants in managing coronavirus infections.

KEYWORDS

COVID-19, Gabon, medicinal plants, prevention, treatment, survey

1 Introduction

After the World Health Organization lifted the public health emergency of international concern for COVID-19, statistics indicate that approximately 689 million people tested positive for COVID-19, with approximately 7 million fatalities attributed to the disease (https://www.worldometers.info/coronavirus/). Various therapeutic approaches were explored in the management of COVID-19, including antibiotics (azithromycin), antiparasitic agents (hydroxychloroquine), antiviral medications (remdesivir), monoclonal antibodies (casirivimab), steroids (dexamethasone), and immune modulators (tocilizumab), anticoagulants, as well as oxygen therapy and other supportive measures for patients experiencing respiratory distress (Mehraeen et al., 2022; Murakami et al., 2023; Panahi et al., 2023). Other approaches such as the search for new treatments using traditional remedies were also explored, as well as vaccines (Rahman et al., 2022; Soheili et al., 2023).

Gabon, with a population of approximately 2.3 million, has grappled with COVID-19, with statistics revealing approximately 49,000 individuals testing positive and resulting in 307 recorded fatalities since the first reported case in 2020 (https://www.worldometers.info/coronavirus/country/gabon/). The diagnostic of the disease was carried out by Laboratoire Professeur Daniel Gahouma. The latter was the specialized state-of-the-art technology specifically established to address the challenges posed by the pandemic. In addition, COVID-19 treatment protocols in Gabon have involved antibiotherapy in combination with vitamins, paracetamol, zinc, and vaccine.

However, despite the availability of medications and vaccines, and due to fears regarding potential adverse effects associated with vaccination, the Gabonese population has turned to medicinal plants for the prophylaxis and treatment of symptoms associated with this viral disease, similar to the populations of several other countries including Algeria, Brazil, Colombia, Cameroon, Morocco, and Peru (Belmouhoub et al., 2021; Villena-Tejada et al., 2021; Chebaibi et al., 2022; Cordoba-Tovar et al., 2022; Mvogo Ottou et al., 2022; da Silva et al., 2023). Most Gabonese people often rely on medicinal plants due to their long tradition of plant-based medicine. The Gabonese population strongly believes in the efficacy of medicinal plants, considering them crucial in managing COVID-19, particularly due to symptoms resembling those of malaria and flu. Indeed, several symptoms such as respiratory disorders, colds, coughs, fever, and joint pain commonly associated with flu and malaria are typically treated using plant-based remedies by the population. Ancestral knowledge passed down from generation to generation may contain treasures of effective natural remedies against this virus. Therefore, the present study aimed to document and valorize plants used by the Gabonese population to prevent or cure COVID-19 and to identify specific plant species deserving further investigation as potential treatments against coronavirus infections.

2 Materials and methods

2.1 Data collection

The survey was conducted in Libreville (Figure 1) between February and June 2022 involving participants from the general population, traditional healers, and medicinal plant vendors. A semi-structured questionnaire was developed for conducting direct interviews with randomly selected traditional healers and medicinal plant vendors. Meanwhile, an online questionnaire format was employed to engage the general population. This approach aimed to collect a comprehensive range of information within the population. The questionnaire was converted into a Google Docs form using Google services and was disseminated through various online-based social media platforms such as Facebook, Instagram, Messenger, and WhatsApp. These platforms were chosen as they were perceived to be the most accessible means of reaching the maximum population regarding the governmental measures of partial lockdown and restrictions on movement. A total of 97 participants responded to the survey, comprising both online respondents and those who participated in oral interviews. The questionnaire was designed with two main sections: the first focused on gathering information about the informants (including age, sex, level of education, and ethnic group affiliation), while the second aimed to obtain details regarding medicinal plants, their forms, prescriptions, COVID status, and methods of preparation.

2.2 Data analysis

2.2.1 Quantitative analyses of the ethnobotanical data

Various quantitative indexes were calculated from the collected data and included the relative frequency of citation (RFC), Use Value (UV), Informant Consensus Factor (ICF), Relative Importance (RI) and Popular Therapeutic Use Value (POPUT) (Anwar et al., 2023; Naceiri et al., 2021; Ndhlovu et al., 2023).

2.2.1.1 Relative Frequency of Citation (RFC)

The Relative Frequency of Citation (RFC) demonstrates the local importance of each plant species. The RFC value ranges from 0 (none of the informants indicate a plant species as useful), to 1 (all informants indicate it as useful). RFC has been calculated as follows:

$$\mathbf{RFC = FC/N}$$

Where FC denotes the number of informants mentioning the use of the species in any symptoms and N is the total number of informants participating in the survey.

FIGURE 1
Map of Gabon (source: ANPN, s.d.).

2.2.1.2 The use value (UV)

The UV is an index highlighting the relative importance of plants known locally in traditional medicine. The use value of a plant species varies according to its cultural, geographical, and biological context. The UV determines the most frequently indicated plants in the treatment of an ailment. Use value was calculated using the following formula:

$$\mathbf{UV} = \frac{\sum \boldsymbol{UI}}{\boldsymbol{N}}$$

Where *UI* is number of uses recorded for a given species by each informant, and *N* is the total number of informants participating in the survey.

2.2.1.3 Relative Importance (RI)

RI helps in the prioritization of plants based on their importance and prevalence in local knowledge systems. It is a useful tool for identifying significant plants with cultural, medical, or ritual significance to a society. It was determined as:

$$\mathbf{RI} = \frac{(\boldsymbol{R} \cdot \boldsymbol{Ph} + \boldsymbol{R} \cdot \boldsymbol{BS})}{\mathbf{2}} \times \mathbf{100}$$

Where '*R·Ph*' stands for relative pharmacological properties. '*R·Ph*' is calculated by dividing number of uses (U) by total number of use reports. '*R·BS*' is calculated by dividing number of diseases treated by a plant species by total number of diseases.

2.2.1.4 Informant Consensus Factor (ICF)

This index was calculated for informants' agreement on the reported treatment based on each category of disease. The following formula was used to calculate the informant consensus factor (ICF):

$$\mathbf{ICF} = \frac{(\boldsymbol{Nur} - \boldsymbol{Nt})}{(\boldsymbol{Nur} - \mathbf{1})},$$

where "Nur" is the total use reports for each category and "Nt" is the total number of species used for that category. The ICF scale is 0–1. A number close to 1 implies a high level of agreement or consensus among informants regarding the relevance of a given use category and the plants associated with it. A score closer to 0 shows a lack of consensus, implying that informants may have various or varying ideas regarding the relevance of a certain use category or the plants used for that purpose.

2.1.1.5 Popular therapeutic use value

The popular therapeutic use value (POPUT) shows the significance of a plant species for medicinal and therapeutic uses.

TABLE 1 Sociodemographic data about the participants of the study.

Variable	Demographic category	Number of informants (n = 97)	Frequency (%)	*p*-value
Female		46	47.42	>0.94
Male		51	52.58	
Age	18–30	20	20.62	<0.0001
	31–44	47	48.45	
	45–66	30	30.93	
Education	Primary school	3	3.09	>0.9999
	Secondary	21	21.65	
	University	73	75.26	
Ethnic group	Awandji	1	1.03	>0.9999
	Benga	1	1.03	
	Haussa	1	1.03	
	Kota	1	1.03	
	Kwélé	1	1.03	
	Vili	1	1.03	
	Vungu	1	1.03	
	Adouma	3	3.09	
	Massango	3	3.09	
	Myene	3	3.09	
	Mitsogo	8	8.25	
	Ghisir	11	11.34	
	Ndzebi	12	12.37	
	Punu	18	18.56	
	Fang	32	32.99	

The following formula was used to calculate the popular therapeutic use value:

$$\mathbf{POPUT} = \frac{\boldsymbol{NURIT}}{\boldsymbol{TUR}},$$

where "NURIT" is the number of use reports for each illness or therapeutic effect and "TUR" is the total number of use reports.

2.2.2 Statistical analysis

The recorded data were tabulated on Microsoft Excel spreadsheets. A descriptive and quantitative statistical method was applied (one-way ANOVA and independent samples *t*-test; *p*-values ≤0.05 were considered significant) to analyze and summarize the data.

3 Results

3.1 Sociodemographic features of informants

The social–demographic features of informants are presented in Table 1. The gender distribution revealed that women constituted 47.42% of the respondents, while men were more predominant at 52.58%. The average age of participants was 39.41 years, ranging from 18 to 66 years, with the age group of 31–44 years being the most represented at 48.45% ($p < 0.0001$). A significant majority of informants (74.73%) had attended university, while only 3.3% had completed primary school. The most represented ethnic affiliation was the Fang (30.77%), followed by the Punu (19.78%) and the Nzebi (13.19%). Ethnic groups such as the Awandji, Benga, and Haussa were among the least represented.

3.2 Frequency of COVID-19-related symptoms treated

COVID-19 symptoms are various. In this survey, prevalent symptoms included fever (18%), cough (16%), fatigue (13%), and cold (12%), as shown in Figure 2. Additionally, respiratory conditions (10%), general pain (8%), and breathlessness (7%) were managed by informants to a lesser extent. Sneeze, sore throat, and colic associated with COVID-19 were cited at 2% and 1%.

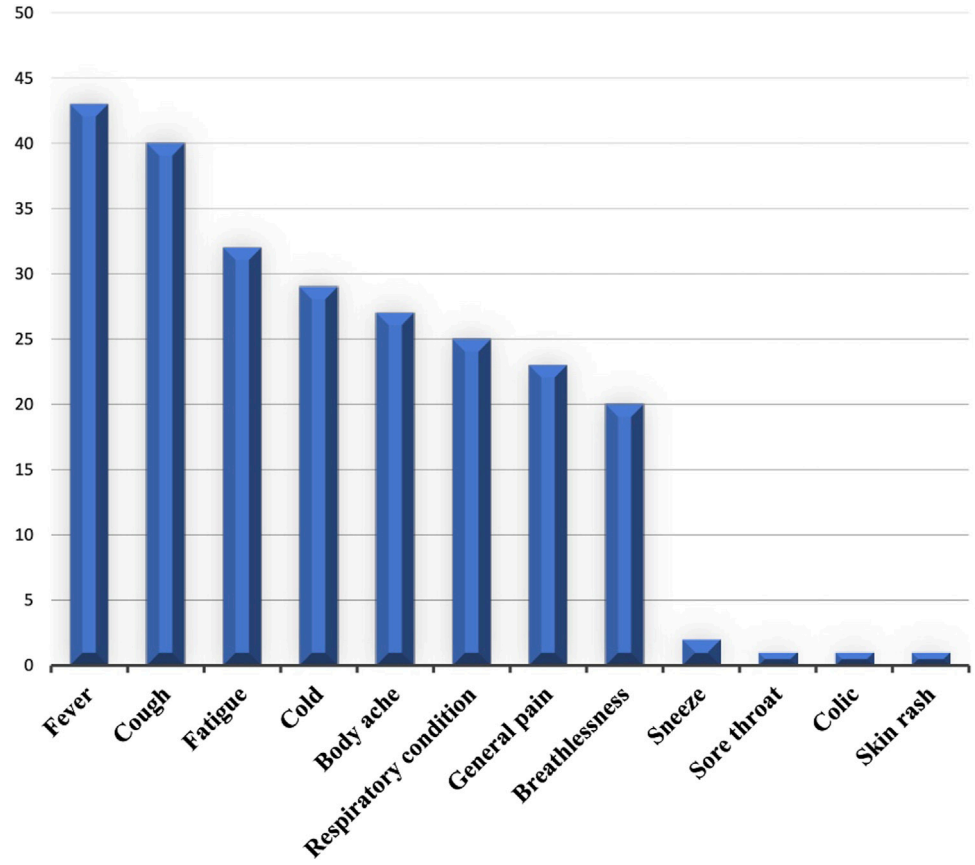

FIGURE 2
Treated symptoms.

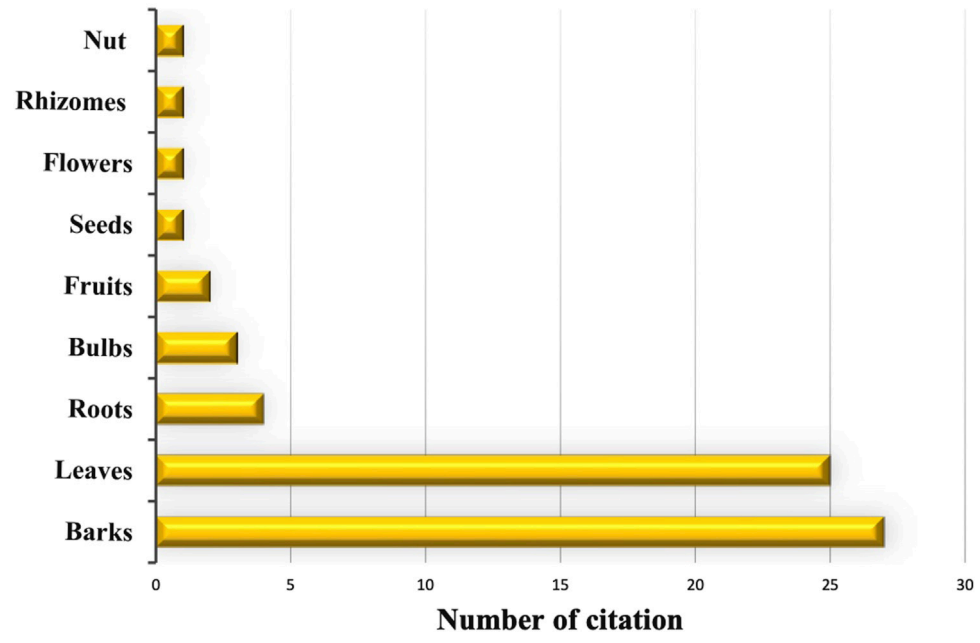

FIGURE 3
Plant parts used.

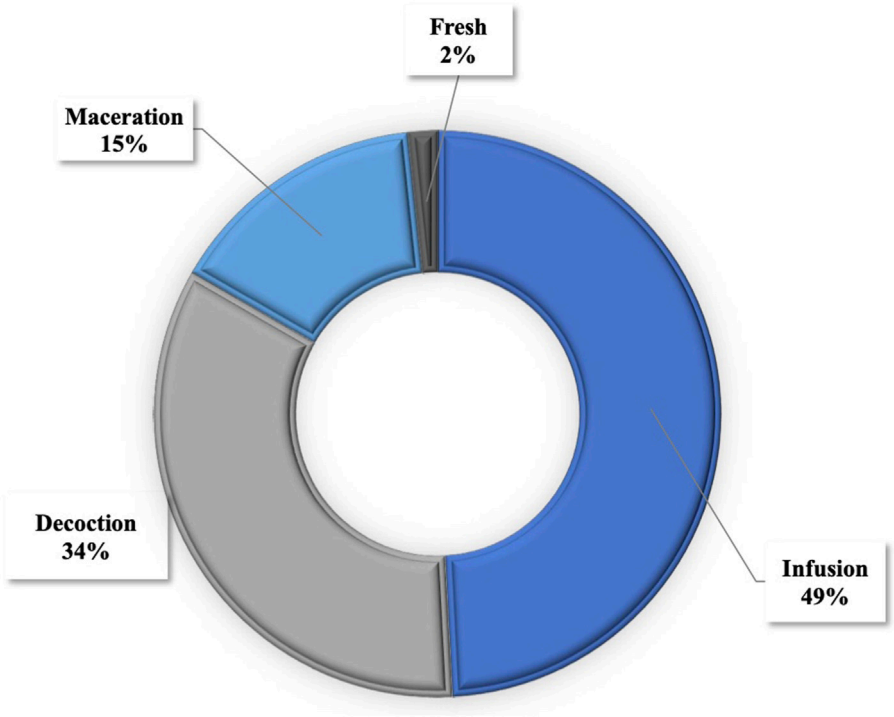

FIGURE 4
Mode of preparation.

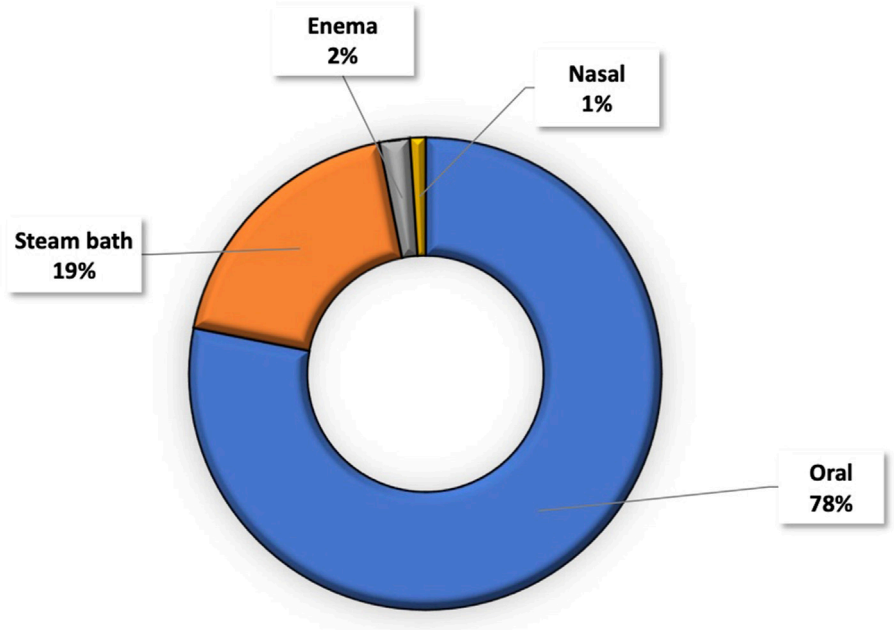

FIGURE 5
Mode of administration.

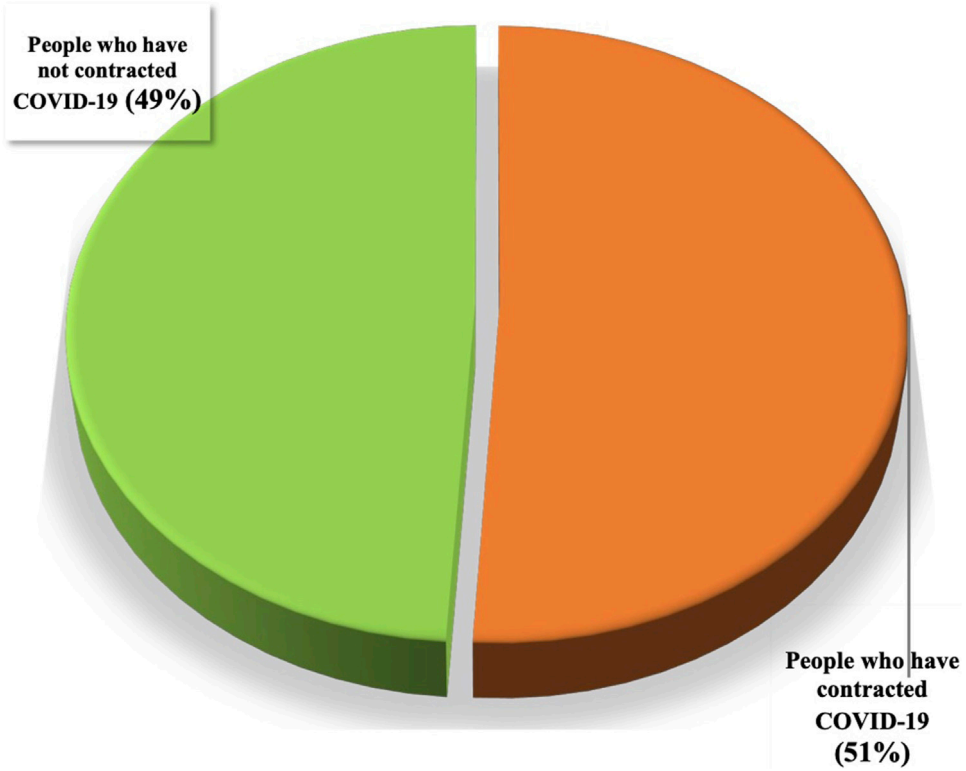

FIGURE 6
Proportion of people who have contracted COVID-19.

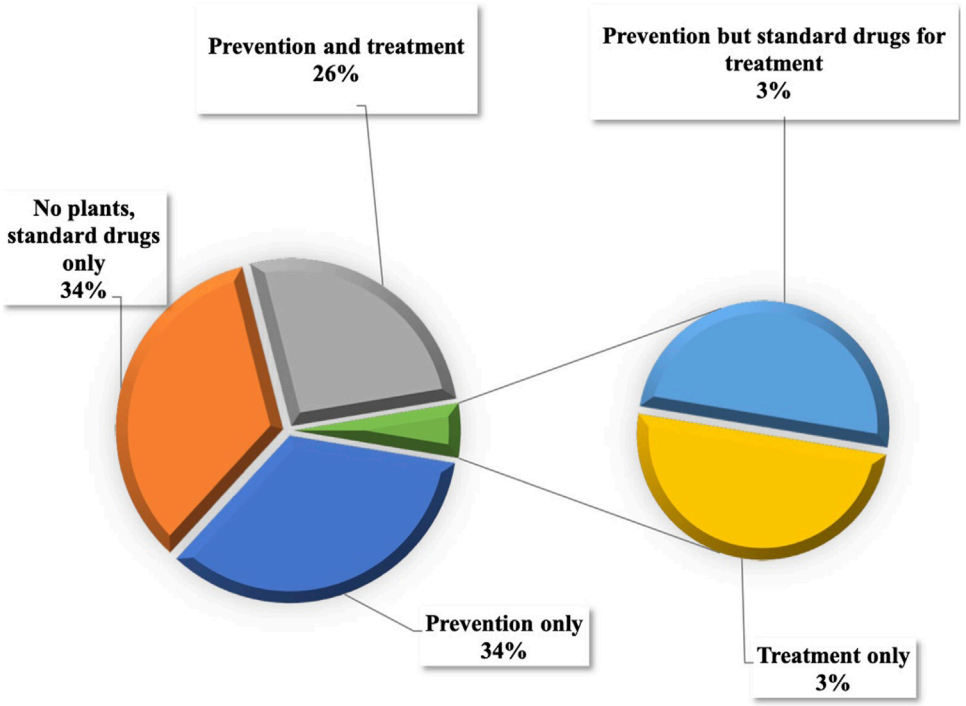

FIGURE 7
Use of medicinal plants in the treatment and/or prevention of COVID-19.

TABLE 2 Ethnobotanical data on plants used to treat and prevent COVID-19.

N°	Family	Scientific name	Vernacular name	Plant parts	Growth form	RFC	UV	RI (%)
1	Acanthaceae	*Acanthus montanus* (Nees) T.Anderson	Mabangue pele	Roots	Perennial	0.02	0.03	12.66
2	Anacardiaceae	*Mangifera indica* L.	Mwiba	Leaves and barks	Tree	0.11	0.32	34.94
3		*Pseudospondias longifolia* Engl.	Musungubali	Barks	Tree	0.01	0.04	16.88
4	Annonaceae	*Annona muricata* Lin.	Corossol	Leaves	Tree	0.02	0.05	21.09
5		*Annickia chlorantha* (Oliv.) Setten and Maas	Nfo'o	Barks	Tree	0.26	0.75	45.46
6		*Xylopia aethiopica* (Dunal) A. Rich	Mugana	Leaves	Tree	0.01	0.02	8.44
7		*Greenwayodendron suaveolens* Engl. and Diels	Muamba noir	Leaves and barks	Tree	0.12	0.3	18.17
8		*Cleistopholis staudtii* Engl. and Diels	Ovoc	Barks	Tree	0.01	0.04	16.88
9	Apocynaceae	*Alstonia congensis* Engl.	Ekouk	Leaves and barks	Tree	0.22	0.71	45.25
10		*Tabernanthe iboga* Baill.	Dibuga	Root barks	Shrub	0.02	0.02	8.44
11		*Picralima nitida* T. Durand and H. Durand	Dugundu	Barks and fresh leaves	Tree	0.06	0.13	21.5
12	Asteraceae	*Ageratum conyzoides* L.	Burongu	Barks	Weed	0.01	0.04	16.88
13		*Artemisia annua* L.		Leaves	Shrub	0.1	0.25	34.58
14		*Gymnanthemum amygdalinum* (Delile) Sch.Bip. syn *Vernonia amygdalina*	Ndole	Leaves	Shrub	0.06	0.23	38.64
15	Bignoniaceae	*Newbouldia laevis* (P.Beauv.) Seem. ex Bureau	Isope	Leaves and barks	Tree	0.08	0.24	34.53
16	Bombacaceae	*Ceiba pentandra* (L.) Gaertn.	Dum	Leaves	Tree	0.01	0.04	16.88
17	Burseraceae	*Aucoumea klaineana* Pierre	Okume	Barks	Tree	0.08	0.3	18.17
18		*Canarium schweinfurthii* Engl.	Aiele	Barks	Tree	0.01	0.02	8.44
19		*Dacryodes edulis* (G.Don.) H. J. Lam.	Safu	Barks and leaves	Tree	0.01	0.05	16.93
20	Caricaceae	*Carica papaya* L.	Mulolu	Leaves	Tree	0.15	0.62	44.78
21	Combretaceae	*Combretum micranthum* G.Don	Kinkeliba	Roots	Shrub	0.08	0.35	35.1
22	Costaceae	*Costus lucanusianus* JA.Braun. and K.Schum.	Mikwissa	Leaves	Perennial herb	0.05	0.21	34.37
23	Euphorbiaceae.	*Alchornea cordifolia* (Schumach) Müll. Arg.	Mumbundjeni	Leaves	Shrub or small tree	0.01	0.03	12.66
24	Fabaceae	*Cylicodiscus gabunensis* Harms	Madume	Leaves	Tree	0.02	0.08	17.08
25		*Copaifera religiosa* J.Léonard	Mutombi	Barks	Tree	0.01	0.01	4.22
26		*Distemonanthus benthamianus* Baill.	Muvengui	Barks	Tree	0.02	0.05	12.76
27		*Osodendron altissimum* (Hook.f.) E.J.M.Koenen	Difyoru balossi	Barks	Tree	0.01	0.01	4.22
28		*Pterocarpus soyauxii* Taub.	Padouk	Barks	Tree	0.03	0.1	17.19
29		*Pentaclethra macrophylla* Benth.	Muvandji	Barks	Tree	0.02	0.04	16.88
30		*Senna occidentalis* (L.) Link	Muwiwisi	Leaves	Shrub	0.02	0.04	16.87
31		*Tetrapleura tetraptera* (Schum. and Thonn.) Taub.	Gyaga	Fruit	Tree	0.03	0.06	25.31
32		*Guibourtia tessmannii* (Harms) J.Léonard.	Kevazingo	Barks	Tree	0.03	0.1	17.19
33	Hypericaceae	*Harungana madagascariensis* Lam. ex Poiret	Musasa	Barks	Tree	0.01	0.02	8.44
34	Irvingiaceae	*Irvingia gabonensis* (Aubry-Lecomte ex O'Rorke) Baill.	Mundjuka	Barks	Tree	0.01	0.04	16.88
35	Lamiaceae	*Mentha suaveolens* Ehrh.		Leaves	Perennial herb	0.03	0.07	17.03
36		*Ocimum gratissimum* L.	Messep	Leaves	Perennial herb	0.07	0.2	42.65

(Continued on following page)

TABLE 2 (*Continued*) Ethnobotanical data on plants used to treat and prevent COVID-19.

N°	Family	Scientific name	Vernacular name	Plant parts	Growth form	RFC	UV	RI (%)
37	Lauraceae	*Persea americana* Mill.	Muvoka	Leaves	Tree	0.01	0.02	8.44
38	Lecythidaceae	*Petersianthus macrocarpus* (P.Beauv.) Liben	Mbindju	Ecorces	Tree	0.01	0.01	4.22
39	Liliaceae	*Allium cepa* L.	Oignon	Bulbs	Perennial herb	0.02	0.03	12.66
40		*Allium sativum* L.	Ail	Bulbs	Perennial herb	0.04	0.1	25.52
41		*Aloe vera* (L.) Burm.f.	Aloe	Leaves	Perennial herb	0.01	0.07	29.53
42	Malvaceae	*Cola nitida* (Vent.) Schott and Endl.	Cola	Nut and barks	Tree	0.05	0.14	25.73
43	Moraceae	*Milicia excelsa* (Welw.) C.C.Berg.	Iroko	Barks	Tree	0.02	0.02	8.44
44	Moringaceae	*Moringa oleifera* Lam.	Moringa	Leaves	Tree	0.04	0.09	21.3
45	Musaceae	*Musa x paradisiaca* L.	Mupala	Leaves	Perennial	0.11	0.26	34.63
46	Myristicaceae	*Pycnanthus angolensis* (Welw.) Warb.	Ilomba	Barks	Tree	0.01	0.01	4.22
47		*Scyphocephalium mannii* (Benth.) Warb.	Sorro	Barks	Tree	0.01	0.07	17.04
48		*Staudtia kamerunensis* Warb.	Niove	Barks	Tree	0.09	0.45	18.95
49	Myrtaceae	*Psidium guajava* L.	Ngwaba	Leaves	Shrub or small tree	0.07	0.2	34.32
50		*Syzygium aromaticum* (L.) Merr. and L.M.Perry.	Clove	Dried flowers	Tree	0.04	0.08	29.58
51	Poaceae	*Cymbopogon citratus* (DC.) Stapf	Esosi	Leaves	Perennial grass	0.1	0.26	34.63
52	Rhamnaceae	*Maesopsis eminii* Engl.	Mosangea	Barks	Tree	0.01	0.01	4.22
53	Rubiaceae	*Mitragyna ciliata* Aubrév. and Pellegr.	Bahia	Barks	Tree	0.09	0.13	17.34
54		*Coffea mannii* (Hook.f.) A.P.Davis	Azeme	Barks	Shrub	0.01	0.02	8.44
55		*Sarcocephalus pobeguinii* Hua ex Pobég. and Pellegr.	Kombe ningo	Barks	Tree	0.01	0.07	17.04
56	Rutaceae	*Citrus* sp.	Diali	Fruits, barks, leaves	Shrubs or small tree	0.23	0.66	36.66
57		*Zanthoxylum heitzii* (Aubrév. and Pellegr.) P. G. Waterman	Ndungu	Leaves and barks	Tree	0.01	0.01	4.22
58	Simabouraceae	*Simaba africana* Baill.	Issindu ighale	Roots	Tree	0.03	0.03	12.66
59	Solanaceae	*Capsicum chinense* Jacq.	Nungu	Seeds	Shrub	0.02	0.04	16.88
60	Tiliaceae	*Ancistrocarpus densispinosus* Oliv.	Eege	Leaves	Shrub or small tree	0.01	0.04	16.88
61	Urticaceae	*Musanga cecropioides* R.Br. ex Tedlie	Parasolier	Barks	Tree	0.03	0.13	17.34
62	Vitaceae	*Cissus quadrangularis* L.	Dyaba	Aerial parts	Perennial herb	0.02	0.08	17.08
63	Zingiberaceae	*Zingiber officinale* Roscoe	Maketa	Rhizomes	Perennial herb	0.17	0.47	35.72

3.3 Frequency of plant parts used

The survey unveiled that nearly all plant parts were used in the treatment of COVID-19. Informants mostly used bark (42%) and leaves (38%) for their remedies, while roots, bulbs, and fruits were used to a lesser extent, accounting for 7%, 6%, and 3%, respectively. Less commonly utilized were parts such as seeds, flowers, rhizomes, and nuts, each representing 1% (Figure 3).

3.4 Frequency of the methods of preparation and administration of ethnomedicinal remedies

In the formulation of plant-based remedies for the prevention and treatment of COVID-19, methods such as infusion, decoction, and maceration were predominantly utilized, comprising 49%, 34%, and 15%, respectively (Figure 4). The administration of these remedies was

TABLE 3 Ten popular recipes used in the prevention and/or treatment of COVID-19-related symptoms.

	Recipe		Plant parts	Preparation	Posology	Administration
1	*Annickia chlorantha* + *Alstonia congensis* + *Syzygium aromaticum*	Nfo'o + Ekouk + Clous de Girofle	Barks and flower	Maceration, infusion, and decoction	2–3 times/day	Drink
2	*Musa x paradisiaca* + *Carica papaya* + *Mangifera indica* + *Cymbopogon citratus* + *Citrus* sp. + *Aloe vera* + *Psidium guajava*	Mupala + Mulolu + Mwiba + Esosi + Diali + Aloe+ Ngwaba	Dead leaves, fresh leaves, and fruit	Decoction	2–3 times/day	Drink
3	*Mangifera indica* + *Psidium guajava* + *Cymbopogon citratus*	Mwiba + Ngwaba + Esosi	Leaves	Decoction	Twice/day	Drink Steam bath
4	*Annickia chlorantha* + *Carica papaya* + *Zingiber officinale* + *Citrus* sp.	Nfo'o + Mulolu + Maketa + Diali	Barks, fruits, rhizome, and leaves	Decoction	2–3 times/day	Drink
5	*Allium sativum* + *Citrus* sp. + *Zingiber officinale*	Ail + Diali + Maketa + Honney	Fruit, bulb and rhizome	Maceration	More than three times/day	Drink
6	*Gymnanthemum amygdalinum* + *Carica papaya* + *Mangifera indica*	Ndolè+ Mulolu + Mwiba	Leaves	Infusion	2–3 times/day	Drink
7	*Moringa oleifera* + *Senna occidentalis*	Moringa + Muwiwisi	Barks and leaves	Infusion	Once/day	Steam bath
8	*Artemisia annua* + *Cymbopogon citratus* + *Annona muricata* + *Tetrapleura tetraptera*	Artemesia + Esosi + corosole + Gyaga	Leaves and fruit	Infusion	Once/day	Enema
9	*Annickia chlorantha* + *Alstonia congensis* + *Ocimum gratissimum*	Ńfo'o + Ekouk + Messep	Barks	Infusion	Once/day	Drink
10	*Senna occidentalis* + *Newbouldia laevis* + *Zingiber officinale* + *Citrus* sp. + *Cymbopogon citratus* + *Allium cepa* + *Allium sativum* + *Syzygium aromaticum* + *Cola nitida*	Kinkéliba + Isope + Maketa + Diali + Esosi + Oignon + Ail + Clous de Girofle + Cola	Leaves, fruit, rhizome, and bulb	Maceration, infusion, and decoction	2–3 times/day	Drink

primarily oral (78%), while 19% were applied through steam baths. Enema and nasal administration accounted for 2% and 1%, respectively (Figure 5).

3.5 Frequency of the disease amongst the informants and use of plants in prevention or treatment

Among the participants, 51% tested positive for COVID-19, as confirmed by PCR analysis, while 49% either did not exhibit any symptoms or did not contract the disease (Figure 6). The survey also uncovered that 34% of the informants did not use plants for either prevention or treatment. Among the remaining participants, 34% utilized plants for prophylaxis, 26% for both prevention and treatment, 3% exclusively for treatment, and 3% used medicinal plants solely for prevention in conjunction with standard drugs while they were sick with COVID-19 (Figure 7).

3.6 Ethnomedicinal plants used

The survey on medicinal plants used for the prevention and treatment of COVID-19 within the general population, traditional healers, and medicinal plant vendors identified 63 plant species belonging to 35 families (Table 2). These plants were utilized either individually or in combination with other species to formulate remedies. The listed species are presented in alphabetical order by family. For each plant, we provide information on the family, scientific name, vernacular name, part used, and growth form.

The family most abundantly represented, with the highest number of species, was Fabaceae (nine species), followed by Annonaceae (five species), Apocynaceae, Asteraceae, Burseraceae, Liliaceae, Myristicaceae, and Rubiaceae (three species each). Other families were represented by only one or two species, such as Lamiaceae, Musaceae, and Zingiberaceae. These plants were primarily characterized as trees, perennials, shrubs, or weeds. Table 3 presents 10 popular recipes cited by the informants for either prevention, treatment, or both. The table indicates the recipe, the plant parts used, the modes of preparation and administration, and the posology, which was mostly 2–3 times per day, especially for the remedies taken orally. The recipes were a mixture of at least two different plants and could be made of more than nine plants.

3.7 Importance of the plants through RFC, UV, and RI

Several indexes allowed the identification of the most valuable plants that were used to treat COVID-19 symptoms in Gabon (Table 2). On a global scale, species exhibiting the highest values across the various indexes calculated are deemed useful and significant for COVID-19 management and should be further assessed through pharmacological analysis for drug development purposes.

The relative frequency of citation (RFC) index varied from 0.01 to 0.26 and indicated that species like *Annickia chlorantha* (0.26), *Citrus* sp. (0.23), *Alstonia congensis* (0.22), *Zingiber officinale* (0.17), and

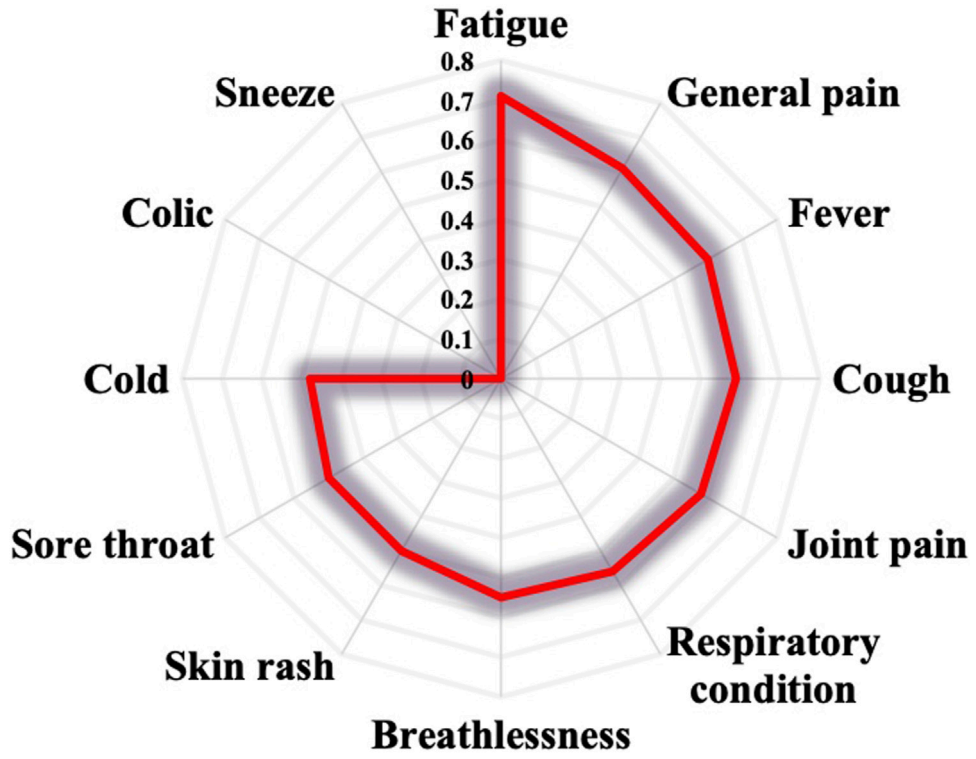

FIGURE 8
Informant consensus factor (ICF).

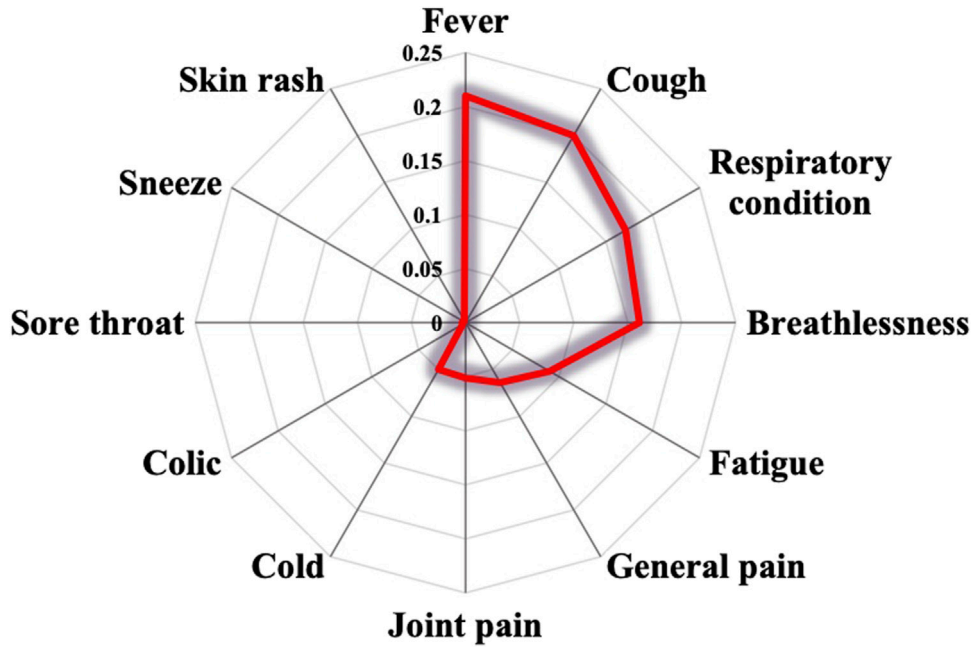

FIGURE 9
Popular therapeutic use value (POPUT).

Carica papaya (0.15) were the most frequently cited by informants. The lowest index calculated (0.01) was for plant species like *Ageratum conyzoides, Dacryodes edulis*, or *Sarcocephalus pobeguini.*

In the present study, the species have use values (UVs) ranging from 0.01 to 0.75. Species such as *Annickia chlorantha* (0.75), *Alstonia congensis* (0.71), *Citrus* sp. (0.66), *Carica papaya* (0.62), *Zingiber*

officinale (0.47), *Staudtia kamerunensis* (0.45), and *Mangifera indica* (0.32) presented the highest values. The lowest value of 0.01 was found for *Zanthoxylum Heitzii* and *Copaifera religiosa.*

The relative importance (RI) index had percentages ranging from 4.22% to 45.46%. The highest values were displayed by *Annickia chlorantha* (45.46%), *Alstonia congensis* (45.25%), *Carica papaya* (44.78%), *Ocimum gratissimum* (42.65%), *Gymnanthemum amygdalinum* (38.64%), *Citrus* sp. (36.66%), *Zingiber officinale* (35.72%), *Combretum micranthum* (35.1%), *Mangifera indica* (34.94%), *Cymbopogon citratus* (34.64%), *Musa x paradisiaca* (34.64%), and *Artemisia annua* (34.58%). The lowest value calculated (4.22%) corresponded to *Zanthoxylum heitzii* and *Copaifera religiosa.*

3.8 ICF and POPUT

The survey results revealed that the cited plants were employed to address various symptoms associated with COVID-19, including cold, cough, breathlessness, fatigue, fever, and general pain. The calculated indexes indicated that ICF values ranged from 0 to 0.71. The highest ICF (0.71) was observed for fatigue, followed by general pain (0.61), fever (0.6), cough (0.59), joint pain (0.58), respiratory condition (0.56), and breathlessness (0.55). The lowest ICF values were obtained for colic and sneezing (Figure 8).

Regarding the POPUT index, the values varied from 0.002 to 0.21. Symptoms such as cough, fever, respiratory condition, and breathlessness obtained the highest values (higher than 0.1), while the lowest values were calculated for skin rashes, colic, and sore throat (Figure 9).

4 Discussion

The present study aimed to highlight the plants used in Gabon to prevent and/or treat symptoms associated with COVID-19. Survey participants included individuals from the general population, traditional healers, and medicinal plant vendors. The findings revealed that most of the participants were male subjects, with the predominant age group being 31–44 years. These results suggest that men displayed a greater interest in the survey compared to women, likely due to the prevalence of male traditional healers and medicinal plant vendors. The age group of 31–44 years was particularly noteworthy as it represents the demographic most inclined to embrace traditional medicine and seek to reclaim traditional knowledge. In addition, a large number of informants had a university education. The high level of education among the majority of respondents indicates that, despite heightened awareness of the ongoing pandemic, the population continues to associate medicinal plants with the prevention and treatment of diseases exhibiting flu-like symptoms. Khadka et al. (2021) supported this finding, reporting that educated people had a preference for modern medicine, but during COVID-19, they used medicinal plants as an alternative medicine option. Gabon is very rich in plant biodiversity, and the knowledge of medicinal plants used to treat infections or conditions such as malaria or influenza is deeply rooted within the population, is transmitted from generation to generation, and is often shared by traditional healers with individuals seeking information. Consequently, when the pandemic emerged, the Gabonese population likened it to a blend of malaria and flu due to the overlapping symptoms with COVID-19, including fever, joint and body ache, fatigue, coughing, and cold symptoms. Subsequently, people began treating these symptoms using plants commonly used to treat influenza and malaria. The study findings indicate that these specific symptoms were the most frequently treated by the population. Surveys conducted in different countries such as Bangladesh and South Africa also described these symptoms as the most commonly treated in their respective countries (Phumthum et al., 2021; Rafiqul Islam et al., 2021; Zondi and Ehaine, 2022). The remedies predominantly involved the use of barks and leaves, prepared through infusion, decoction, or maceration. Notably, steam baths emerged as the second most common mode of administration, a method traditionally employed in Gabon specifically for treating malaria. Other studies also mentioned steam baths or steam inhalation as modes of administration, arguing that this method has been used for decades as a home remedy for cold and pain (Rafiqul Islam et al., 2021; Mvogo Ottou et al., 2022; Zondi and Ehaine, 2022). The study also revealed that the majority of respondents had contracted COVID-19 and that only 3% of them did not take treatment based on medicinal plants. Among the remaining respondents who claimed to have never developed any symptoms, medicinal plants were used for prevention. These results suggest that medicinal plants may have provided protection against coronavirus infection for individuals who used them. Further research, including clinical trials, is necessary to confirm these findings and to determine the safety and efficacy of the plants. In a similar context, results from a study carried out in Peru on the use of medicinal plants for COVID-19 prevention and respiratory symptom treatment showed that most of their respondents did use plants for these purposes (Villena-Tejada et al., 2021).

Ethnobotanical surveys often employ various indexes to unveil or highlight medicinal plants that are most frequently used or deemed most beneficial for the treatment of a specific disease. These indexes help quantify and analyze the importance of different plant species within a particular cultural or ecological context. In the present study, the results indicated that several indexes, including RFC, UV, or RI, collectively highlighted the plants most frequently used for the prevention or treatment of COVID-19. Notably, *Annickia chlorantha, Allium* sp., *Citrus* sp., *Alstonia congensis, Zingiber officinale, Carica papaya, Staudtia kamerunensis, Mangifera indica, Combretum micranthum, Cymbopogon citratus, Newbouldia laevis, Ocimum gratissimum, Gymnanthemum amygdalinum, Musa x paradisiaca,* and *Artemisia annua* emerged as the most commonly cited. Surveys conducted worldwide documented the use of several of these plants in the prevention and/or treatment of the disease, regardless of geographical location, climate diversity, or the variability of flora in the different regions. Hence, plants like *Allium* sp., *Citrus* sp., *Zingiber officinale, Carica papaya, Mentha piperita, Cymbopogon citratus*, and *Ocimum* sp. were used in diverse regions such as Cameroon, Morocco, Iraq, Thailand, Nepal, and Turkey (Akbulut, 2021; Khadka et al., 2021; Phumthum et al., 2021; Abdulrahman et al., 2022; Mvogo Ottou et al., 2022). ICF and POPUT are indispensable tools in ethnopharmacological surveys, offering valuable insights into the consensus, popularity, and cultural significance of medicinal plants within a community (Asiimwe

TABLE 4 Active compounds from medicinal plants with potential anti-SARS-CoV activity.

Plant name	Active compounds	Mechanisms	References
Ageratum conyzoides	Chromene, hydroxamic acid, and apigenin	Inhibit SARS-CoV-2 main protease	Hariono et al. (2021)
Allium cepa	Oleanolic acid, quercitrin, peonidin progesterone, and 3-arabinoside	Inhibit SARS-CoV-2 main protease	Fitriani and Utami (2021)
Allium sativum	Alliin, S-propyl cysteine, S-allylcysteine, squalene, S-ethylcysteine, 1,4-dihydro-2,3-benzoxathiin 3-oxide, 1,2,3-propanetriyl ester, trans-13-octadecenoic acid, and methyl-11-hexadecenoate Fresh bulbs	Inhibit SARS-CoV-2 6LU7 protein Improvement in the general condition with the resolution of most of the symptoms after 2 days	Pandey et al. (2021) Belkessam et al. (2021)
Aloe vera	Feralolide, isoaloeresin, aloeresine, and aloin A	Inhibit SARS-CoV-2 main protease	Mpiana, et al. (2020)
Annona muricata	Roseoside, coreximine Javoricin, 5-(1-hydroxytridecyl)oxolan-2-one, arianacin, annomuricin A, annomuricin B, annomuricin C, muricatocin C, muricatacin, *cis*-annonacin, annonacin-10-one, and *cis*-goniothalamicin	Inhibit the main protease and spike protein Inhibit the spike protein	Adedotun et al. (2023) Prasad et al. (2021)
Artemisia annua	Scopoletin, arteannuin, and artemisinic acid	Inhibit the main protease and spike protein	Baggieri et al. (2023)
Capsicum chinense	Kaempferol, lutein, zeaxanthin, and quercetin	Inhibit main protease, ACE-2, and TMPRSS2 proteins	Rahmattullah et al. (2021)
Carica papaya	Papain, β-cryptoxanthin, lycopene, lutein, β-carotene, dichloro-9,10-diphenylanthracene-9,10-diol, lupeol Deoxyquercetin, riboflavin, kaempferol, catechin, deoxykaempferol, and apigenin	Inhibitory activity against main proteases of SARS-CoV-2, SARS-CoV, and MERS-CoV Inhibit 3-chymotrypsin-like protease, papain-like protease, RNA-dependent RNA-polymerase, endonuclease, and S1 and S2 regions of the spike protein	Nallusamy et al. (2021) Hariyono et al. (2021)
Cissus quadrangularis	Taraxerol and β-amyrin	Inhibitory activity against main proteases of SARS-CoV-2, SARS-CoV, and MERS-CoV	Nallusamy et al. (2021)
Citrus sp.	Naringin, naringenin, hesperetin, hesperidin, nobiletin Obacunone, limonin, nomilin, hesperidin Sakuranetin, isosacuranetin, tetra-o-methylscutallerin, rutoside, eriodictoyl, quercetin, neoeriocitrin, diosmin, and diosmetin	Inhibit ACE2 receptor Virucidal activity on Vero E6-infected cells Inhibit SARS-CoV-2 main protease	Liu et al. (2022) Magurano et al. (2021) Maulydia et al. (2022) Khan et al. (2022)
Cymbopogon citratus	Tannic acid, isoorientin, luteolin, swertiajaponin, chlorogenic acid, cymbopogonol, warfarin, citral diethyl acetal, citral acetate, kaempferol, and cianidanol	Inhibit SARS-CoV-2 main protease	Ahmad et al. (2022)
Gymnanthemum amygdalinum	Veronicoside A, vernodalin and vernolide, vernomygdin and 11, 13-dihydrovernodalin, and neoandrographolide	Inhibit SARS-CoV-2 main protease	Oladele et al. (2021)
Mangifera indica	Ellagic acid, epicatechin, gallic acid, mangiferin, kaempferol Amentoflavone, catechin, mangiferin, and kaempferol	Inhibit SARS-CoV-2 main protease Inhibitory activity against main proteases of SARS-CoV-2, SARS-CoV, and MERS-CoV	Haruna et al. (2021) Nallusamy et al. (2021)
Moringa oleifera	Catechin, ellagic acid, chlorogenic acid, quercetin, Myrecitin, and kaempferol Epicatechin, niazirin, glucotropaeolin, quercetin, apigenin, luteolin, rutin, kaempferol, isorhamnetin, myricetin, astragalin, marumoside A, and moringyne	Inhibit SARS-CoV-2 main protease Inhibit the human TMPRSS2 protein	Haruna et al. (2021) Oyedara et al. (2021)
Musa x paradisiaca	Leucocyanidin, quercetin, sitoindoside-I, 6S-9R-roseoside, hydroxyanigorufone, and 1,2-dihydro-1,2,3-trihydroxy-9-[4 methyphenylphenalene]	Inhibit SARS-CoV-2 main protease	Harini and Gopal (2022)
Ocimum gratissimum	Luteolin, rosmarinic acid, chicoric acid, and myricetin	Inhibit SARS-CoV-2 main protease	Gyebi et al. (2021)
Psidium guajava	Gamma-sitosterol, peri-xanthenoxanthene-4,10-dione,2,8-bis (1-methylethyl) *P. guajava* extract supplementation	Inhibit main protease, papain-like protease, and spike and ACE2 receptor. Neutrophil/lymphocyte ratio reduction, PCR-based conversion time acceleration, and increase in the recovery rate of subjects with mild and asymptomatic COVID-19 infection in a single-blinded, randomized clinical trial	Fadilah et al. (2021) Heppy et al. (2023)
Pycnanthus angolensis	*Pycnanthuquinone C* and *pycnanthuquinone A*	Inhibit SARS-CoV-2 main protease	Chtita et al. (2022)

(Continued on following page)

TABLE 4 (*Continued*) Active compounds from medicinal plants with potential anti-SARS-CoV activity.

Plant name	Active compounds	Mechanisms	References
Syzygium aromaticum	Campesterol, stigmasterol, crategolic acid, oleanolic acid, and bicornin Polysaccharides	Inhibit SARS-CoV-2 main protease Block SARS-CoV-2 replication	Abdelli and Hamed (2023) Jin et al. (2021)
Xylopia aethiopica	Phenolic compounds and essential oils Liriodenine, lysicamine, o-methylmoschatoline, oxoglaucine, and oxophoebine	Antiviral activity against SARS-CoV-1 and SARS-CoV-2 pseudoviruses infecting HeLa ACE-2 cells Inhibit SARS-CoV-2 main protease	Melo et al. (2021) Ogunyemi and Oderinlo (2022)
Zingiber officinale	Gingerenone-A, chlorogenic acid, and hesperidin Cyanin Thujopsene, zingiberol, Gamma-elemene, beta-elemene, and aromadendrene	Block the entry of SARS-CoV-2 through its ACE2 receptors, binding affinities to Mpro and S protein Inhibitory activity against main proteases of SARS-CoV-2, SARS-CoV, and MERS-CoV Inhibit human TMPRSS2 protein	Jahan et al. (2021) Nallusamy et al. (2021) Ogunyemi and Oderinlo (2022)

et al., 2021; Anwar et al., 2023). Their application enhances the understanding of traditional healthcare practices and guides scientific research efforts. In this regard, symptoms such as fever, cough, and fatigue, which displayed high index values, appeared to be well-managed by the population, who are knowledgeable about several plants that can alleviate these symptoms. These plants merit further investigation based on the specific symptoms they are reported to alleviate.

The study findings suggest that plants traditionally used in the treatment of malaria are potential candidates for drug development against coronaviruses. Notably, the species prominently cited in this study have undergone assessment for their antiplasmodial activity, both in animal models and *in vitro*, demonstrating significant potential for managing malaria (Afolabi and Oyewole, 2020; Tajbakhsh et al., 2021; Indradi et al., 2023). These plants include *Annickia chlorantha*, *Zingiber officinale, Alstonia congensis, Newbouldia laevis, Ocimum gratissimum, Gymnanthemum amygdalinum, Artemisia annua*, and *Carica papaya* (Cimanga et al., 2019; Abubakar et al., 2020; Assogba, 2020; Wang et al., 2020; Kshirsagar and Rao, 2021; Tajbakhsh et al., 2021). Furthermore, the same plants demonstrate noteworthy anti-inflammatory and immunomodulatory effects, which are particularly valuable in addressing the cytokine storm induced by COVID-19 (Omoregie and Pal, 2016; Eftekhar et al., 2019; Abubakar et al., 2020; Olaoye et al., 2021; Kshirsagar and Rao, 2021; Mezui et al., 2022; Kamelnia et al., 2023; Nishitha et al., 2023; Ukwubile et al., 2023; Yuandani et al., 2023). In addition, plants such as *Z. officinale, Artemisia annua, Carica papaya*, *Citrus* sp., *Allium sativum,* and *Cymbopogon citratus* were assessed for their antiviral activity against SARS-CoV-2 (Belkessam et al., 2021; Haridas et al., 2021; Oladele et al., 2021; Thuy et al., 2021; Adel et al., 2022) (Table 4). Various studies, using molecular docking, cell-based assays, and clinical trials, were conducted to elucidate the mechanisms underlying the antiviral activity of the cited plants. Collectively, the findings of these studies suggest that all tested plants are potential putative inhibitors of the proliferation of SARS-CoV-2, ACE2 host receptor, and major protease. They impede the attachment, membrane fusion, and internalization of SARS-CoV-2 into host cells, as well as the viral replication and transcription processes. Furthermore, numerous trials currently investigate several promising and potent phyto-based formulations for the treatment of SARS-CoV-2 infections (Alam et al., 2021). These formulations include a range of bioactive metabolites, plant extracts, functional foods, and plant-based preparations. For example, hesperidin, which is present in some of the plants described in our study (Table 4), is involved as primary therapy in a phase II trial (Alam et al., 2021). In addition, a preliminary trial of the effect of *Allium sativum* in patients with SARS-CoV-2 showed an improvement in the general condition with the resolution of most of the symptoms (fever, headache, asthenia, ageusia, anosmia, and diarrhea) (Belkessam et al., 2021).

Analysis of the data highlighted that all the plants described in Table 4 showing promising activity against SARS-CoV-2 are listed in Table 3 as components of the popular recipes used in the prevention and/or treatment of COVID-19. A combination of these plants with antiviral and anti-inflammatory effects in a recipe strengthens the hypothesis that these recipes could effectively prevent or treat the coronavirus infection, thereby sustaining their use by the Gabonese population. So, taken together, the results of the present study showed the potential of medicinal plants as independent therapies, complementary or alternative medicines for the management of symptoms associated with COVID-19.

A concern could be raised regarding the potential overharvesting of certain species such as *Annickia chlorantha, Allium* sp., *Citrus* sp., *Alstonia congensis, Zingiber officinale, Carica papaya, Staudtia kamerunensis, Mangifera indica, Combretum micranthum,* and *Cymbopogon citratus* due to increased demand during the pandemic. However, Gabon is predominantly covered by forest (over 80%), and most of these species are distributed across all regions of the country (Wakefield Adhya, 2024). This suggests that the overharvesting of these species during the pandemic may not have had a significant impact on their abundance. Nevertheless, it is important to develop conservation planning for species with significant bioactivity. Conservation efforts could include measures such as sustainable harvesting practices and community-based management initiatives to ensure the long-term viability of these species and their ecosystems.

4.1 Limitations

The online ethnobotanical survey fell short of the anticipated participant count, primarily attributed to participants' failure to share the survey link and a general lack of interest in responding to online surveys. Furthermore, the use of online surveys is not

common among the Gabonese population, resulting in responders who are likely to possess a certain level of education and understand the significance of the survey. This could lead to potential bias regarding the sociodemographic profile of the responders. Furthermore, a field-based study extended to all the regions of the country might cover responses from all levels and classes of people.

5 Conclusion

COVID-19 has emerged as the most prolonged and deadly coronavirus outbreak witnessed worldwide in the past 50 years. Despite extensive exploration of various treatments, no definitive solution has been identified, and vaccination efforts have encountered limitations in the face of evolving virus variants. Ethnobotanical surveys conducted worldwide have explored the potential of plants to alleviate COVID-19 symptoms, yielding positive results and encouraging the use of medicinal plants for coronavirus infection management. In Gabon, the country's relatively low rate of cases and fatalities has been attributed to the consumption of plants traditionally used to treat malaria and flu, both as a preventive measure and in the treatment of COVID-19. Further investigation into the mechanisms of these plants such as anti-inflammatory, antioxidant, antiviral, and immunomodulatory activities is crucial for the development of plant-based medicines that could effectively act during the early stages of SARS-CoV-2 infection. This research holds promise as a significant alternative in the preparation for the inevitable occurrence of future coronavirus epidemics in the coming years. Understanding and harnessing the potential of these medicinal plants may provide valuable tools for mitigating the impact of such outbreaks.

Data availability statement

The original contributions presented in the study are included in the article/Supplementary Material; further inquiries can be directed to the corresponding author.

Author contributions

MB: conceptualization, data curation, formal analysis, methodology, writing–original draft, and writing–review and editing. AM: conceptualization, data curation, formal analysis, investigation, methodology, and writing–review and editing. JM: formal analysis, investigation, resources, and writing–review and editing. SA: conceptualization, supervision, validation, visualization, and writing–review and editing. LM: conceptualization, methodology, resources, supervision, validation, and writing–review and editing.

Funding

The author(s) declare that financial support was received for the research, authorship, and/or publication of this article. Gabonese government through PAZOPIA project.

Acknowledgments

The authors thank the informants who agreed to participate in this study and share their traditional knowledge.

Conflict of interest

The authors declare that the research was conducted in the absence of any commercial or financial relationships that could be construed as a potential conflict of interest.

Publisher's note

References

Abdelli, W., and Hamed, D. (2023). Molecular docking and pharmacokinetics studies of *Syzygium aromaticum* compounds as potential SARS-CoV-2 main protease inhibitors. *Trop. J. Nat. Prod. Res.* 7 (11), 5155–5163. doi:10.26538/tjnpr/v7i11.18

Abdulrahman, M. D., Mohammed, F. Z., Hamad, S. W., Hama, H. A., and Lema, A. A. (2022). Medicinal plants traditionally used in the management of COVID-19 in Kurdistan region of Iraq. *Aro-The Sci. J. Koya Univ.* 10 (2), 87–98. doi:10.14500/aro.11042

Abubakar, A., Ahmad, N. S., Akanya, H. O., Abdullahi, A., and Asmau, N. A. (2020). Antiplasmodial activity of total alkaloids and flavonoids of stem bark extracts of *Enantia chlorantha* in mice. *Comp. Clin. Pathol.* 29, 873–881. doi:10.1007/s00580-020-03138-4

Adedotun, I. O., Abdul-Hammed, M., Towolawi, B. T., Afolabi, T. I., Mufutau, K. M., and Adegoke, H. M. (2023). Phytochemicals from *Annona muricata* (Sour Sop) as potential inhibitors of SARS-CoV-2 main protease (M^{pro}) and spike receptor protein: a structure-based drug design studies and chemoinformatics analyses. *Phys. Sci. Rev.* doi:10.1515/psr-2022-0338

Adel, A., Elnaggar, M. S., Albohy, A., Elrashedy, A. A., Mostafa, A., Kutkat, O., and et al., (2022). Evaluation of antiviral activity of *Carica papaya* leaves against SARS-CoV-2 assisted by metabolomic profiling. *RSC Adv.* 12 (51), 32844–32852. doi:10.1039/d2ra04600h

Afolabi, O. J., and Oyewole, J. L. (2020). Antiplasmodial efficacy of Vernonia amygdalina in Albino mice infected with Plasmodium berghei. *Int. J. Pediatr. Res.* 6, 115. doi:10.23937/2469-5807/1510115

Ahmad, T., Saif, R., Raza, M. H., Zafar, M. O., Zia, S., Shafiq, M., et al. (2022). Computational prediction of *Cymbopogon citratus* compounds as promising inhibitors of main protease of SARS-CoV-2. *Futur. Biotechnol.* 2 (01), 20–25. doi:10.54393/fbt.v2i01.23

Akbulut, S. (2021). Medicinal plants preferences for the treatment of COVID-19 symptoms in central and Eastern Anatolia. *Kastamonu Univ. J. Forestr. Facult.* 21 (3), 196–207. doi:10.17475/kastorman.1048372

Alam, S., Sarker, M. M. R., Afrin, S., Richi, F. T., Zhao, C., Zhou, J.-R., et al. (2021). Traditional herbal medicines, bioactive metabolites, and plant products against COVID-19: update on clinical trials and mechanism of actions. *Front. Pharmacol.* 12 (671498), 671498. doi:10.3389/fphar.2021.671498

Anwar, T., Qureshi, H., Naeem, H., Shahzadi, S., Sehar, Z., and Hassan, R. (2023). Exploration of the wild edible plants used for basic health care by local people of Bahawalpur and adjacent regions, Pakistan. *Foods.* 12 (19), 3557. doi:10.3390/foods12193557

Asiimwe, S., Namukobe, J., Byamukama, R., and Imanlingat, B. (2021). Ethnobotanical survey of medicinal plant species used by communities around

Mabira and Mpanga Central Forest Reserves, Uganda. *Trop. Med. Health* 49 (52), 52. doi:10.1186/s41182-021-00341-z

Assogba, M. (2020). Usage traditionnel d'*Artemisia annua*: intérêt et limites dans le traitement du paludisme. *Sci. Pharm.* 75.

Baggieri, M., Gioacchini, S., Borgonovo, G., Catinella, G., Marchi, A., Picone, P., et al. (2023). Antiviral, virucidal and antioxidant properties of *Artemisia annua* against SARS-CoV-2. *Biomed. Pharmacother.* 168, 115682. doi:10.1016/j.biopha.2023.115682

Belkessam, N., Messafeur, A., Abderrahmane, R., Abdelkrim, K., and Ghanassi, F. Z. (2021). Etude préliminaire de l'effet de l'ail (*Allium sativum* L.) chez des malades atteints du SARS-CoV-2/preliminary study of the effect of garlic (*Allium sativum* L.) in patients with SARS-CoV-2. *Alger. J. Health Sci.* 3 (2), 9–14.

Belmouhoub, M., Aberkane, B., and Bachir bey, M. (2021). Ethnopharmacological survey on medicinal plants used by Algerian population to prevent SARS-CoV-2 infection. *Ethnobot. Res. Appl.* 22, 1–13. doi:10.32859/era.22.38.1-13

Chebaibi, M., Bousta, D., Bourhia, M., Baammi, S., Salamatullah, A. M., Nafidi, H. A., et al. (2022). Ethnobotanical study of medicinal plants used against COVID-19. *Evidence-Based Complementary Altern. Med.* 2022, 2085297. doi:10.1155/2022/2085297

Chtita, S., Fouedjou, R. T., Belaidi, S., Djoumbissie, L. A., Ouassaf, M., Qais, F. A., et al. (2022). *In silico* investigation of phytoconstituents from Cameroonian medicinal plants towards COVID-19 treatment. *Struct. Chem.* 33, 1799–1813. doi:10.1007/s11224-022-01939-7

Cimanga, R. K., Nsaka, S. L., Tshodi, M. E., Mbamu, B. M., Kikweta, C. M., Makila, F. B., et al. (2019). *In vitro* and *in vivo* antiplasmodial activity of extracts and isolated constituents of *Alstonia Congensis* root bark. *J. Ethnopharmacol.* 242, 111736. doi:10.1016/j.jep.2019.02.019

Cordoba-Tovar, L., Ríos-Geovo, V., Largacha-Viveros, M. F., Salas-Moreno, M., Marrugo-Negrete, J. L., Ramos, P. A., et al. (2022). Cultural belief and medicinal plants in treating COVID 19 patients of Western Colombia. *Acta Ecol. Sin.* 42 (5), 476–484. doi:10.1016/j.chnaes.2021.10.011

da Silva, A. M., Horsth, A. L., Timóteo, E. D., Faria, R. J., Bazoni, P. S., Meira, E. F., et al. (2023). Use of medicinal plants during COVID-19 pandemic in Brazil. *Sci. Rep.* 13, 16558. doi:10.1038/s41598-023-43673-y

Eftekhar, N., Moghimi, A., Mohammadian Roshan, N., Saadat, S., and Boskabady, M. H. (2019). Immunomodulatory and anti-inflammatory effects of hydro-ethanolic extract of *Ocimum basilicum* leaves and its effect on lung pathological changes in an ovalbumin-induced rat model of asthma. *BMC Complement. Altern. Med.* 19 (1), 349. doi:10.1186/s12906-019-2765-4

Fadilah, F., Erlina, L., Paramita, R. I., Istiadi, K. A., and Handayani, R. R. D. (2021). Active constituents and molecular analysis of *Psidium guajava* against multiple protein of SARS-CoV-2. *Res. Sq.* doi:10.21203/rs.3.rs-271919/v1

Fitriani, I., and Utami, W. (2021). Potential phytochemical inhibitor from *Allium cepa* for the medication of COVID-19 using in-silico approach. *Al Kim. J. Ilmu Kim. Terap.* 4 (2), 80–87. doi:10.19109/alkimia.v4i2.7459

Gyebi, G. A., Elfiky, A. A., Ogunyemi, O. M., Ibrahim, I. M., Adegunloye, A. P., Adebayo, J. O., et al. (2021). Structure-based virtual screening suggests inhibitors of 3-Chymotrypsin-Like Protease of SARS-CoV-2 from *Vernonia amygdalina* and *Occinum gratissimum*. *Comput. Biol. Med.* 136, 104671. doi:10.1016/j.compbiomed.2021.104671

Haridas, M., Sasidhar, V., Nath, P., Abhithaj, J., Sabu, A., and Rammanohar, P. (2021). Compounds of *Citrus medica* and *Zingiber officinale* for COVID-19 inhibition: *in silico* evidence for cues from ayurveda. *Futur J. Pharm. Sci.* 7 (1), 13. doi:10.1186/s43094-020-00171-6

Harini, R., and Gopal, V. (2022). *In silico* studies on the phytoconstituents of *Musa paradisiaca* for Sars Cov-2 main protease inhibitory activity. *J. Adv. Pharmacol.* 2 (1), 7.

Hariono, M., Hariyono, P., Dwiastuti, R., Setyani, W., Yusuf, M., Salin, N., et al. (2021). Potential SARS-CoV-2 3CLpro inhibitors from chromene, flavonoid and hydroxamic acid compound based on FRET assay, docking and pharmacophore studies. *Results Chem.* 3 (21), 100195. doi:10.1016/j.rechem.2021.100195

Hariyono, P., Patramurti, C., Candrasari, D., and Hariono, M. (2021). An integrated virtual screening of compounds from *Carica papaya* leaves against multiple protein targets of SARS-Coronavirus-2. *Results Chem.* 3, 100113. doi:10.1016/j.rechem.2021.100113

Haruna, I. U. H. N. D., Sunday, S. J., Tolulope, P. S., Tajudeen, O. J., Adeola, A., and Jamilu, B. D. (2021). In-silico analysis of the inhibition of the SARS-CoV-2 main protease by some active compounds from selected African plants. *J. Taibah Univ. Med. Sci.* 16 (2), 162–176. doi:10.1016/j.jtumed.2020.12.005

Heppy, F., Mulyana, R., Afrainin, S. N., and Tjandrawinata, R. R. (2023). The effect of *Psidium guajava* Leaves' extract for mild and asymptomatic corona virus Disease-19. *Saudi Pharm. J.* 31 (4), 592–596. doi:10.1016/j.jsps.2023.02.012

Indradi, R. B., Muhaimin, M., Barliana, M. I., and Khatib, A. (2023). Potential Plant-Based New Antiplasmodial Agent Used in Papua Island, Indonesia. *Plants.* 12, 1813. doi:10.3390/plants12091813

Jahan, R., Paul, A. K., Bondhon, T. A., Hasan, A., Jannat, K., Mahboob, T., et al. (2021). Zingiber *officinale*: ayurvedic uses of the plant and *in silico* binding studies of selected phytochemicals with Mpro of SARS-CoV-2. *Nat. Prod. Commun.* 16 (10), 1934578X2110317–13. doi:10.1177/1934578X211031766

Jin, C., Feng, B., Pei, R., Ding, Y., Li, M., Chen, X., et al. (2021). Novel pectin from crude polysaccharide of *Syzygium aromaticum* against SARS-CoV-2 activities by targeting 3CLpro. *bioRxiv.* 38. doi:10.1101/2021.10.27.466067

Kamelnia, E., Mohebbati, R., Kamelnia, R., El-Seedi, H. R., and Boskabady, M. H. (2023). Anti-inflammatory, immunomodulatory and anti-oxidant effects of *Ocimum basilicum* L. and its main constituents: a review. *Ira. J. Basic. Med. Sci.* 26 (6), 617–627. doi:10.22038/IJBMS.2023.67466.14783

Khadka, D., Dhamala, M. K., Li, F., Aryal, P. C., Magar, P. R., Bhatta, S., et al. (2021). The use of medicinal plants to prevent COVID-19 in Nepal. *J. Ethnobiol. Ethnomed* 17 (1), 26. doi:10.1186/s13002-021-00449-w

Khan, J., Sakib, S. A., Mahmud, S., Khan, Z., Islam, M. N., Sakib, M. A., et al. (2022). Identification of potential phytochemicals from *Citrus Limon* against main protease of SARS-CoV-2: molecular docking, molecular dynamic simulations and quantum computations. *J. Biomol. Struct. Dyn.* 1 (12), 10741–10752. doi:10.1080/07391102.2021.1947893

Kshirsagar, S. G., and Rao, R. V. (2021). Antiviral and immunomodulation effects of Artemisia. *Med. Kaunas. Lith.* 57 (3), 217. doi:10.3390/medicina57030217

Liu, W., Zheng, W., Cheng, L., Li, M., Huang, J., Bao, S., et al. (2022). Citrus fruits are rich in flavonoids for immunoregulation and potential targeting ACE2. *Nat. Prod. Bioprospect.* 12 (4), 4. doi:10.1007/s13659-022-00325-4

Magurano, F., Sucameli, M., Picone, P., Micucci, M., Baggieri, M., Marchi, A., et al. (2021). Antioxidant activity of citrus limonoids and investigation of their virucidal potential against SARS-CoV-2 in cellular models. *Antioxidants* 10 (11), 1794. doi:10.3390/antiox10111794

Maulydia, N. B., Tallei, T. E., Ginting, B., Idroes, R., Illian, D. N., and Faradilla, M. (2022). Analysis of flavonoid compounds of Orange (Citrus sp.) peel as anti-main protease of SARS-CoV-2: a molecular docking study. *IOP Conf. Ser. Earth. Environ. Sci.* 951 (1), 012078. doi:10.1088/1755-1315/951/1/012078

Mehraeen, E., Najafi, Z., Hayati, B., Javaherian, M., Rahimi, S., Dadras, O., et al. (2022). Current treatments and therapeutic options for COVID-19 patients: a systematic review. *Infect. Disord. Drug Targets* 22 (1), e260721194968. doi:10.2174/1871526521666210726150435

Melo, C., Perdomo, R., Yerima, F., Mahoney, O., Cornejal, N., Alsaidi, S., et al. (2021). Antioxidant, antibacterial, and anti-SARS-CoV activity of commercial products of Xylopia (Xylopia aethiopica). *J. Med. Act. Plants.* 10 (1), 11–23. doi:10.7275/9baf-e988

Mezui, C., Kuissi, M. M., Fanta, S. Y., Amang, P. A., Daptousia, D., Emakoua, J., et al. (2022). Analgesic, anti-inflammatory and non-ulcerogenic properties of *Annickia chlorantha* aqueous stem bark extract. *Discov. Phytom.* 9 (1), 184–192. doi:10.15562/phytomedicine.2022.186

Mpiana, P. T., Tshibangu, D. S., Kilembe, J. T., Gbolo, B. Z., Mwanangombo, D. T., Inkoto, C. L., et al. (2020). Identification of potential inhibitors of SARS-CoV-2 main protease from *Aloe vera* compounds: a molecular docking study. *Chem. Phys. Lett.* 754 (2020), 7. doi:10.1016/j.cplett.2020.137751

Murakami, N., Hayden, R., Hills, T., Al-Samkari, H., Casey, J., Del Sorbo, L., et al. (2023). Therapeutic advances in COVID-19. *Nat. Rev. Nephrol.* 19 (1), 38–52. doi:10.1038/s41581-022-00642-4

Mvogo Ottou, P. B., Fogang, C. W. S., Ndiang, Z., Biyon, J. B. N., Mokake, S. E., Mbezo, F. B., et al. (2022). Assessment of resilience of aromatic plants during the COVID-19 pandemic in Douala, Cameroon. *J. Drug Deliv. Ther.* 12 (5), 8–19. doi:10.22270/jddt.v12i5.5580

Naceiri, M. H., Bouyahya, A., Naceiri Mrabti, N., Jaradat, N., Doudach, L., and Faouzi, M. E. A. (2021). Ethnobotanical survey of medicinal plants used by traditional healers to treat diabetes in the Taza region of Morocco. *Evidence-Based Complement. Altern. Med.* 2021 (5515634), 5515634. doi:10.1155/2021/5515634

Nallusamy, S., Mannu, J., Ravikumar, C., Angamuthu, K., Nathan, B., Nachimuthu, K., et al. (2021). Exploring phytochemicals of traditional medicinal plants exhibiting inhibitory activity against main protease, spike glycoprotein, RNA-dependent RNA polymerase and non-structural proteins of SARS-CoV-2 through virtual screening. *Front. Pharmacol.* 12 (667704), 667704. doi:10.3389/fphar.2021.667704

Ndhlovu, P. T., Asong, J. A., Omotayo, A. O., Otang-Mbeng, W., and Aremu, A. O. (2023). Ethnobotanical survey of medicinal plants used by indigenous knowledge holders to manage healthcare needs in children. *PLoS ONE* 18 (3), e0282113. doi:10.1371/journal.pone.0282113

Nishitha, A., Sindhu, R., and Anjali, S. (2023). Comparative evaluation of anti-inflammatory and antioxidant property of Carica papaya leaf and seed extract—an *in vitro* study. *J. Popul. Ther. Clin. Pharmacol.* 30 (14), 11–18. doi:10.47750/jptcp.2023.30.14.002

Ogunyemi, B. T., and Oderinlo, O. O. (2022). In-silico investigation of oxoaporphine alkaloids of *Xylopia aethiopica* against SARS-COV-2 main protease. *AROC Nat. Prod. Res.* 2 (1), 01–12. doi:10.53858/arocnpr02010112

Oladele, J. O., Oyeleke, O. M., Oladele, O. T., and Oladiji, A. T. (2021). Covid-19 treatment: investigation on the phytochemical constituents of *Vernonia amygdalina* as potential Coronavirus-2 inhibitors. *Comput. Toxicol.* 18 (2021), 100161. doi:10.1016/j.comtox.2021.100161

Olaoye, I. F., Oso, B. J., and Aberuagba, A. (2021). Molecular mechanisms of anti-inflammatory activities of the extracts of *Ocimum gratissimum* and *Thymus vulgaris*. *Avicen. J. Med. Biotech.* 13 (4), 207–216. doi:10.18502/ajmb.v13i4.7206

Omoregie, E. S., and Pal, A. (2016). Antiplasmodial, antioxidant and immunomodulatory activities of ethanol extract of *Vernonia amygdalina* del. leaf in *Swiss mice*. *Avicenna J. Phytomed.* 6 (2), 236–47.

Oyedara, O. O., Agbedahunsi, J. M., Adeyemi, F. M., Juárez-Saldivar, A., Fadare, O. A., Adetunji, C. O., et al. (2021). Computational screening of phytochemicals from three medicinal plants as inhibitors of transmembrane protease serine 2 implicated in SARS-CoV-2 infection. *Phytomed. Plus.* 1 (4), 100135. doi:10.1016/j.phyplu.2021.100135

Panahi, Y., Gorabi, A. M., Talaei, S., Beiraghdar, F., Akbarzadeh, A., Tarhriz, V., et al. (2023). An overview on the treatments and prevention against COVID-19. *Virol. J.* 20 (1), 23. doi:10.1186/s12985-023-01973-9

Pandey, P., Khan, F., Kumar, A., Srivastava, A., and Jha, N. K. (2021). Screening of potent inhibitors against 2019 novel coronavirus (Covid-19) from *Allium sativum* and *Allium cepa*: an in-silico approach. *Biointerface Res. Appl. Chem.* 11 (1), 7981–7993. doi:10.33263/BRIAC111.79817993

Phumthum, M., Nguanchoo, V., and Balslev, H. (2021). Medicinal plants used for treating mild Covid-19 symptoms among Thai Karen and Hmong. *Front. Pharmacol.* 12, 699897. doi:10.3389/fphar.2021.699897

Prasad, S. K., Pradeep, S., Shimavallu, C., Kollur, S. P., Syed, A., Marraiki, N., et al. (2021). Evaluation of *Annona muricata* Acetogenins as potential anti-SARS-CoV-2 agents through computational approaches. *Front. Chem.* 8, 624716. doi:10.3389/fchem.2020.624716

Rafiqul Islam, A. T. M., Ferdousi, J., and Shahinozzaman, M. (2021). Previously published ethno-pharmacological reports reveal the potentiality of plants and plant-derived products used as traditional home remedies by Bangladeshi COVID-19 patients to combat SARS-CoV-2. *Saudi. J. Biol. Sci.* 28 (11), 6653–6673. doi:10.1016/j.sjbs.2021.07.036

Rahman, M. M., Masum, M. H. U., Wajed, S., and Talukder, A. (2022). A comprehensive review on COVID-19 vaccines: development, effectiveness, adverse effects, distribution and challenges. *Virusdisease* 33 (1), 1–22. doi:10.1007/s13337-022-00755-1

Rahmattullah, N., Arumingtyas, E. L., Widyananda, M. H., Ahyar, A. N., and Tabroni, I. (2021). Bioinformatics analysis of bioactive compounds of four capsicum species against SARS-CoV-2 infection. *Int. J. Adv. Biol. Biomed. Res.* 9 (4), 298–319. doi:10.22034/ijabbr.2021.139183.1335

Soheili, M., Khateri, S., Moradpour, F., Mohammadzedeh, P., Zareie, M., Mortazavi, S. M. M., et al. (2023). The efficacy and effectiveness of COVID-19 vaccines around the world: a mini-review and meta-analysis. *Ann. Clin. Microbiol. Antimicrob.* 22 (1), 42. doi:10.1186/s12941-023-00594-y

Tajbakhsh, E., Kwenti, T. E., Kheyri, P., Nezaratizade, S., Lindsay, D. S., and Khamesipour, F. (2021). Antiplasmodial, antimalarial activities and toxicity of African medicinal plants: a systematic review of literature. *Malar. J.* 20, 349. doi:10.1186/s12936-021-03866-0

Thuy, B. T. P., Nhan, V. D., Quang, N. M., Duoc, N. T., and Tat, P. V. (2021). Evaluation of SARS-CoV-2 inhibition of some compounds in *Cymbopogon citratus* oil combining docking and molecular dynamics simulations. *Vietn. J. Chem.* 59 (6), 790–799. doi:10.1002/vjch.202100022

Ukwubile, C. A., Ikpefan, E. O., Dibal, M. Y., Umeano, V. A., Menkiti, D. N., Kaosi, C. C., et al. (2023). Pharmacognostic profiles, evaluation of analgesic, anti-inflammatory and anticonvulsant activities of *Newbouldia laevis* (P. Beauv.) Seem. ex Bureau leaf and root extracts in Wistar rats. *J. Ethnopharmacol.* 314, 116632. doi:10.1016/j.jep.2023.116632

Villena-Tejada, M., Vera-Ferchau, I., Cardona-Rivero, A., Zamalloa-Cornejo, R., Quispe-Florez, M., Frisancho-Triveño, Z., et al. (2021). Use of medicinal plants for COVID-19 prevention and respiratory symptom treatment during the pandemic in Cusco, Peru: a cross-sectional survey. *PLoS ONE* 16 (9), e0257165. doi:10.1371/journal.pone.0257165

Wakefield Adhya, S. (2024). Inspiring the world through action. The nature conservancy. Available at: https://www.nature.org/en-us/what-we-do/our-insights/perspectives/gabon-30-30-leading-conservation/ (Accessed June 26, 2024).

Wang, W. T., Liao, S. F., Wu, Z. L., Chang, C. W., and Wu, J. Y. (2020). Simultaneous study of antioxidant activity, DNA protection and anti-inflammatory effect of Vernonia amygdalina leaves extracts. *PLoS ONE* 15 (7), e0235717. doi:10.1371/journal.pone.0235717

Yuandani, J. I., Haque, M. A., Rohani, A. S., Nugraha, S. E., Salim, E., Septama, A. W., et al. (2023). Immunomodulatory effects and mechanisms of the extracts and secondary compounds of *Zingiber* and *Alpinia* species: a review. *Front. Pharmacol.* 14, 26. doi:10.3389/fphar.2023.1222195

Zondi, L. P., and Ehaine, S. (2022). Perspectives of the rural communities of Impendle, Bulwer, and Kokstad in South Africa using ethnomedicinal plants to cure flu and associated symptoms in the advent of COVID-19. *Int. J. Indig. Herb. Drug.* 7 (3), 62–75. doi:10.46956/ijihd.v7i3.312

frontiers | Frontiers in Pharmacology

TYPE Review
PUBLISHED 30 August 2024
DOI 10.3389/fphar.2024.1451084

OPEN ACCESS

EDITED BY
Zhipei Sang,
Hainan University, China

REVIEWED BY
Angela Ostuni,
University of Basilicata, Italy
Ishtiaq Jeelani,
University of California, San Diego, United States

*CORRESPONDENCE
Xiaoyu Hu,
xiaoyuhu202206@163.com

†These authors have contributed equally to this work

RECEIVED 18 June 2024
ACCEPTED 22 August 2024
PUBLISHED 30 August 2024

CITATION
Li S, Hao L, Yu F, Li N, Deng J, Zhang J, Xiong S and Hu X (2024) Capsaicin: a spicy way in liver disease.
Front. Pharmacol. 15:1451084.
doi: 10.3389/fphar.2024.1451084

Capsaicin: a spicy way in liver disease

Shenghao Li[1,2†], Liyuan Hao[1,2†], Fei Yu[1,2], Na Li[1,2], Jiali Deng[1,2], Junli Zhang[3], Shuai Xiong[1,2] and Xiaoyu Hu[2*]

[1]School of Clinical Medicine, Chengdu University of Traditional Chinese Medicine, Chengdu, China, [2]Department of Infectious Diseases, Hospital of Chengdu University of Traditional Chinese Medicine, Chengdu, China, [3]Jiangsu Province Hospital of Chinese Medicine, Nanjing, China

The incidence of liver disease continues to rise, encompassing a spectrum from simple steatosis or non-alcoholic fatty liver disease (NAFLD) to non-alcoholic steatohepatitis (NASH), cirrhosis and liver cancer. Dietary habits in individuals with liver disease may significantly impact the treatment and prevention of these conditions. This article examines the role of chili peppers, a common dietary component, in this context, focusing on capsaicin, the active ingredient in chili peppers. Capsaicin is an agonist of the transient receptor potential vanilloid subfamily 1 (TRPV1) and has been shown to exert protective effects on liver diseases, including liver injury, NAFLD, liver fibrosis and liver cancer. These protective effects are attributed to capsaicin's anti-oxidant, anti-inflammatory, anti-steatosis and anti-fibrosis effects. This article reviewed the different molecular mechanisms of the protective effect of capsaicin on liver diseases.

KEYWORDS

capsaicin, liver injury, NAFLD, liver fibrosis, liver cancer

1 Introduction

The liver plays a vital role in energy metabolism, bile acid secretion, drug metabolism, detoxification, among other functions (Luo et al., 2022). Liver disease causes 2 million deaths each year, accounting for 4 percent of all deaths, and about two-thirds of liver-related deaths occur in men (Devarbhavi et al., 2023). The incidence of liver disease continues to increase (Yu Y. et al., 2014), encompassing conditions ranging from simple steatosis and non-alcoholic fatty liver disease (NAFLD) to non-alcoholic steatohepatitis (NASH), cirrhosis and liver cancer (Li et al., 2019). Therefore, it is crucial to find effective means to prevent the occurrence of liver diseases.

In recent years, capsaicin has attracted attention for its potential in the prevention and treatment of many diseases (Radhakrishna et al., 2024). Capsaicin (trans-8-methyl-N-vanillyl-6-nonenamide), a naturally occurring alkaloid, is the active component in Capsicum plants and serves as an agonist of transient receptor potential vanilloid subfamily 1 (TRPV1). This spicy substance in red chili peppers features a long hydrophobic carbon end with a polar amide group and a benzene ring (Li et al., 2020). Capsaicin exhibits numerous beneficial properties, including protection against liver damage (Fukuta et al., 2020), anti-diabetic (Wang et al., 2012), anti-obesity (Li et al., 2020), anti-liver fibrosis (Sheng et al., 2020), anti-liver cancer (Ates et al., 2022), relieve pain (Caprodossi et al., 2011) and anti-oxidant (Chen et al., 2015) and so on. This article reviewed the protective effects of capsaicin on liver diseases through various mechanisms of action. A better understanding of the specific role of capsaicin in liver pathogenesis may provide new directions for the treatment and prevention of liver diseases.

2 Capsaicin

Capsaicin (trans-8-methyl-N-vanillyl-6-nonenamide) is the main compound responsible for the spicy flavor of Capsicum plants (Santos et al., 2023). It is insoluble in water and contains a vanillyl group (the head), an amide group (the neck), and a fatty acid chain (the tail) (Musolino et al., 2024). Capsaicin functions through both TRPV1-dependent and TRPV1-independent pathways, with evidence suggesting that its biological effects may be mediated by either mechanism (Sánchez et al., 2022; Zhang et al., 2020). Capsaicin is a high affinity agonist for the TRPV1 (Li et al., 2021). The affinity between capsaicin and TRPV1 channels is highly selective and potent. TRPV1 is a non-selective cation channel that responses to pH, temperature, and endogenous lipids (Alawi and Keeble, 2010). It is activated directly or indirectly by various neuroinflammatory mediators and endogenous inflammatory mediators, such as calcitonin gene-related peptide (CGRP) or substance P (SP). TRPV1 is also involved in various physiological and pathological processes in the body, including cough, pain, inflammation, hearing, taste, gastrointestinal movement, blood pressure regulation, apoptosis, fat metabolism, pruritus and tumor pathologic processes (Li and Wang, 2021). Activation of TRPV1 led to the opening of Ca^{2+} channels, an influx of Ca^{2+}, and increased Ca^{2+} concentration in the cytoplasm, thus promoting the release of neuropeptides, vasoactive intestinal peptides and excitatory amino acids by neurons and their fibers. This depletes and inhibits their formation, and blocking the pain conduction pathway from peripheral nerve to central nerve (Sharma et al., 2013). After activating TRPV1, capsaicin induces pain afferent neurons to release SP. Continuous activation leads to SP exhaustion, eventually preventing the perception and transmission of pain, thus exerting a pain-relieving effect (Caprodossi et al., 2011). While capsaicin exerts many of its effects through TRPV1 activation, some studies have reported capsaicin-induced effects that occur independently of TRPV1. In addition to activating TRPV1, capsaicin also regulates the production of reactive oxygen species (ROS) (Wu et al., 2022), the flux of other ions across cell membranes (Reilly et al., 2012), and the fluidity of cell membranes, impacting various cellular functions (Prakash and Srinivasan, 2010). Consequently, it has also been extensively studied as a powerful anti-oxidant and anti-inflammatory agent (Braga Ferreira et al., 2020). Capsaicin alleviates inflammatory responses and the Warburg effect in a TRPV1-independent manner by targeting PKM2, LDHA and COX-2 (Zhang Q. et al., 2022). Moreover, capsaicin induces AMPK and p53 activation and triggers cell death in a TRPV1-independent manner (Bao et al., 2019). Overall, capsaicin's ability to act through both TRPV1-dependent and independent pathways highlights its therapeutic potential. This dual action allows capsaicin to modulate a wide range of biological processes, making it a valuable compound for further research and clinical applications.

3 Liver injury and capsaicin

3.1 Liver injury

Liver injury is a major threat to human health worldwide, with causes including viral hepatitis, autoimmune liver disease, liver ischemia, and drug toxicity (Stravitz and Lee, 2019). The recent increase in the use of newly developed drugs and herbal or dietary supplements has increased the risk of liver damage. Drug-induced liver injury (DILI) is a rare but significant condition that can appear after exposure to various drugs, herbs, and dietary supplements. The severity of DILI varies, and severe liver damage can progress to acute liver failure, potentially resulting in death within days of onset or liver transplantation (Hassan and Fontana, 2019). Excessive alcohol consumption is another major cause of liver damage and liver failure globally (Koneru et al., 2018). The rapid progression of alcoholic liver disease (ALD) lead to liver fibrosis and cirrhosis. Alcohol metabolism produces toxic metabolites that cause tissue and organ damage through an inflammatory cascade involving numerous cytokines, chemokines, and ROS (Dukić et al., 2023). Currently, effective strategies for treating liver injury are lacking. Therefore, there is an urgent need to develop new therapeutic agents to inhibit liver damage and reduce the risk of severe liver failure in affected patients.

3.2 Roles of capsaicin in the treatment of liver injury

3.2.1 Drug-induced liver injury

Capsaicin has demonstrated a protective effect on liver injury (Table 1). Studies have shown that carbon tetrachloride (CCl4) can significantly increase the levels of aspartate aminotransferase (AST) and alanine aminotransferase (ALT) in the rat model. However, the combined of liposomes encapsulating astaxanthin (Asx)-R (Asx-R-Lipo) and liposomes encapsulating capsaicin (Cap) (Cap-Lipo) significantly reduced CCL4-induced elevation of AST and ALT (Fukuta et al., 2020). Additionally, both the Asx-R-Lipo and Cap-Lipo treatment groups showed a reduction in ALT levels, with Cap-Lipo exhibiting a more pronounced decrease. Capsaicin has also shown a protective effect against N-acetyl-para-aminophenol (APAP)-induced acute liver injury (ALI). This beneficial effect might be attributed to capsaicin's ability to inhibit the high mobility group box 1 (HMGB1)/toll-like receptor 4 (TLR4)/nuclear factor κB (NF-κB) signaling pathway, reduce the release of pro-inflammatory cytokines, diminish hepatic oxidative stress induced by APAP and alleviate hepatocyte apoptosis (Zhan et al., 2020). Cyclophosphamide disrupts the anti-oxidant system by producing ROS and led to liver injury. Capsaicin's hepatoprotective effect in this context is due to its ability to reduce ROS production, inhibit inflammation and suppress the expression of apoptosis protein Caspase-3 (Alam et al., 2023). Moreover, studies have also demonstrated that capsaicin, when used in combination with other therapeutic approaches, enhances its protective effects against liver diseases. Capsaicin and cannabinoids improved liver pathology and liver function following thioacetamide-induced acute injury in mice (Avraham et al., 2008).

3.2.2 Sepsis-induced acute liver injury

Capsaicin is known for its anti-oxidant and anti-inflammatory effects. It has demonstrated beneficial effects on apoptosis and mitochondrial function in acute liver injury (ALI) associated with sepsis. High doses of capsaicin have been shown to reduce serum levels of ALT and AST, reverse and/or improved the expression of apoptosis-related proteins, and regulate mitochondrial and

TABLE 1 Effects of capsaicin on liver injury.

Model	Capsaicin dosage	Main functions	Reference
CCl4-induced liver injury model rat	0.5 μmol Asx/kg and 1 μmol capsaicin/kg	↓ALT, AST	Fukuta et al. (2020)
Alcohol-induced acute liver injury in mice	10 and 20 mg/kg	↓ALT, AST	Koneru et al. (2018)
Acetaminophen-induced acute liver injury in mice	1 mg/kg	↓IL-6, IL-1β, TNF-α, MDA; ↑SOD, GSH	Zhan et al. (2020)
Cyclophosphamide-induced liver injury in rat	10 mg and 20 mg/kg	↓serum liver markers (AST, ALT, ALP, BLI), IL-1β, TNFα, caspase-3	Alam et al. (2023)
Thioacetamide-induced acute injury in mice	1.25 μg/kg	↓AST, ALT, ammonia, and bilirubin	Avraham et al. (2008)
Septic acute liver injury in mice	5 or 20 mg/kg	↓ALT, AST, MDA, ROS, NF-kB, TLR4, IL-1β, TNF-α, caspase 3 ↑sirtuin1, Nrf2, SOD, HO-1	Ghorbanpour et al. (2023)
Alcohol-induced liver injury in mice	0.014%	↑body, liver, and brain weights	Pyun et al. (2014)

metabolic regulators, as well as inflammation-related molecules. These findings suggest that capsaicin protects the liver during ALI in sepsis, likely due to its ability to downregulate oxidation and inflammatory processes and potentially alleviate mitochondrial dysfunction and apoptosis (Ghorbanpour et al., 2023).

3.2.3 Alcoholic liver injury

Studies have shown that a diet rich in capsaicin can be used as an adjunct treatment for liver damage or disease caused by alcohol consumption (Koneru et al., 2018; Pyun et al., 2014). In an earlier study, it has shown that a diet containing capsaicin reduces acute ethanol-induced lipid accumulation in the liver of rats (Sambaiah and Satyanarayana, 1989). Capsaicin inhibits Cytochrome P450 2E1 (CYP2E1) and reduces ROS production. This inhibition lead to a decrease in free radical formation and oxidative stress, restoration of the MMP/TIMP balance, reducing liver injury (Koneru et al., 2018). Furthermore, studies have also demonstrated that capsaicin could be used in combination with dietary modifications enhances its protective effects against liver diseases. Dietary curcumin and capsaicin has been shown to prevent loss of alcohol-induced body, liver, and brain weights and inhibit alcohol-induced oxidative stress in BALB/c mice (Pyun et al., 2014).

4 Non-alcoholic fatty liver disease and capsaicin

4.1 Non-alcoholic fatty liver disease

NAFLD affects 25% of the world's population and is the most prevalent liver disease. It presents a diverse phenotype, ranging from simple steatosis to NASH, fibrosis, cirrhosis, and hepatocellular carcinoma (HCC) (Diehl and Day, 2017). NAFLD is a complex systemic disease characterized by liver lipid accumulation, lipotoxicity, insulin resistance, intestinal dysbiosis, and inflammation (Tilg et al., 2021). The primary driver of NAFLD is excess nutrition, leading to the expansion of the fat pool and the accumulation of ectopic fat (Kragh Petersen et al., 2020). In this case, macrophage infiltration in the visceral adipose tissue produces a pro-inflammatory state that promotes insulin resistance. In insulin resistance, inappropriate lipolysis results in the continuous delivery of fatty acids to the liver, which, along with increased *de novo* lipogenesis, disrupts liver metabolism (Powell et al., 2021). Imbalances in lipid metabolism lead to the formation of lipotoxic lipids, promoting oxidative stress, inflammasome activation and apoptosis, and subsequently stimulate inflammation, tissue regeneration and fibrosis (Friedman et al., 2018; Sanyal, 2019). The multiple parallel hits theory explained the progression of NAFLD (Tilg and Moschen, 2010). Multiple hits induced adipokine secretion, oxidative stress at the endoplasmic reticulum and cellular levels, and subsequently induced hepatic steatosis (Takaki et al., 2013). This phenomenon made the liver vulnerable to multiple effects, including inflammation, mitochondrial dysfunction, lipocytokine imbalances, apoptosis dysregulation, oxidative stress, intestinal dysbiosis, HSCs activation, and production of pro-fibrotic factors, ultimately leading to NASH and cirrhosis (Takai and Jin, 2018). Studies have shown that capsaicin may have a role in improving NAFLD. Capsaicin has been found to reduce liver lipid accumulation, mitigate oxidative stress, and decrease inflammation. These effects suggest that capsaicin could be a potential therapeutic agent for managing NAFLD and its progression to more severe liver diseases.

4.2 Roles of capsaicin in the treatment of non-alcoholic fatty liver disease

4.2.1 Anti-steatosis

Capsaicin exhibits anti-steatosis effect (Table 2). It reduces lipid accumulation and also decreased glucose and fatty acid uptake in HepG2 (Hochkogler et al., 2018). Studies have shown that capsaicin and hesperidin prevent hepatic steatosis and other metabolic syndrome-related changes in rats fed a western diet (Mosqueda-Solís et al., 2018a). Additionally, topical capsaicin cream combined with moderate exercise has been shown to prevent hepatic steatosis, dyslipidemia and elevated blood pressure in hypoestrogenic obese rats (de Lourdes Medina-Contreras et al., 2020). Dietary capsaicin reduces liver steatosis and insulin resistance in obese mice fed a high-fat diet (HFD) (Kang et al., 2010). Capsaicin has been shown to improve lipid metabolism in the liver (Kang et al.,

TABLE 2 Effects of capsaicin on non-alcoholic fatty liver disease.

Model	Capsaicin dosage	Main functions	Reference
3T3-L1 and HepG2 cells	3T3-L1:6.91%; HepG2:100 μM	↓mitochondrial oxygen consumption and reduced glucose and fatty acid uptake	Hochkogler et al. (2018)
Western diet in rats	4 mg/kg	↓hepatic lipid accumulation	Mosqueda-Solís et al. (2018a)
High fat diet in mice	0.015%	↑PPAR-α	Kang et al. (2010)
High fat diet in KKAy mice	0.015%	↓fasting glucose/insulin and triglyceride, inflammatory adipocytokine genes	Kang et al. (2011)
High-fat diet in mice	0.075%	↑CPT-1 and CD36 ↓ACC and FAS	Shin et al. (2020)
High-fat diet in mice	capsaicin 0.4 mg/kg, menthol 20 mg/kg, and cinnamaldehyde 2 mg/kg	↓weight gain, lipid accumulation and insulin resistance ↑brown adipose tissue activation	Kaur et al. (2022)
High-fat diet in mice	2 mg/kg	↓weight gain and food intake, triglyceride, cholesterol, glucose, and insulin levels	Wang et al. (2020)
High-fat diet in mice	2 mg/kg	↑BAT associated genes	Baboota et al. (2014a)
3T3-L1 cells and mice	3T3-L1 cells:0.1–100 μM; mice:2 mg/kg		Baboota et al. (2014b)
HepG2 cells	200 and 300 μM	↑AMPK and PGC-1α	Bort et al. (2019a)
SD rats	30 mg/kg	↓lipid accumulation	Wu et al. (2017)
HepG2 cells	200 μM	↑ROS and AMPK	Bort et al. (2019b)
Caco-2 cells	0.1–100 μM	↑FATP2, FATP4, IFABP, CD36, PPARα and PPARγ	Rohm et al. (2015)
Western diet in rats	4 mg/kg	↑UCP1 and CIDEA	Mosqueda-Solís et al. (2018b)
High-fat diet in rats	10 mg/kg	↓vimentin, peroxiredoxins, and NQO1	Joo et al. (2010)
High-fat diet in rats	bean powder (15%) plus capsaicin (0.015%)	↓hepatic cholesterol and triglycerides	Pande and Srinivasan (2012)
High-fat diet in rats	HCCMS, 3,382 mg/kg/d (containing 30 mg capsaicin); M-CCMS, 1,128 mg/kg/d (10 mg capsaicin); L-CCMS, 367 mg/kg/d (3 mg capsaicin)	↑PPARα, PPARγ, UCP2, and adiponectin ↓ leptin	Tan et al. (2014)
High-fat diet in rats	0.15 g capsaicin/kg and/or 1.5 g curcumin/kg	↓hepatic fat accumulation and leptin	Seyithanoğlu et al. (2016)
High-fat diet in mice	0.015%	↑PPAR-α	Hu et al. (2017)
High-fat diet in mice	0.010%	↑Muc2 and Reg3g	Shen et al. (2017)
High-fat diet in mice	16 mg/kg	↑adiponectin ↓leptin, free fatty acid and insulin concentrations	Shanmugham and Subban (2022)
Overweight women	125 mg green tea, 25 mg capsaicin and 50 mg ginger extracts	↓serum insulin concentrations; ↑quantitative insulin sensitivity check index and GSH	Taghizadeh et al. (2017)

2011). It stimulates the expression of carnitine palmitoyl transferase (CPT)-1 and CD36, enzymes involved in β-oxidation and hepatic fatty acid inflow. Conversely, capsaicin decreases the expression of key enzymes involved in fatty acid synthesis, such as acetyl Co-A carboxylase (ACC) and fatty acid synthase (FAS) (Shin et al., 2020). These changes suggest that capsaicin not only helps in reducing fat accumulation but also improves overall lipid metabolism in the liver, making it a potential therapeutic agent for managing hepatic steatosis and related metabolic disorders.

4.2.2 Anti-obesity

The anti-obesity effect of capsaicin has been confirmed through various models, ranging from cells to animals and humans (Li et al., 2020). Capsaicin promotes weight loss by increasing energy expenditure and increasing satiety (Elmas and Gezer, 2022), inhibiting the production of white adipose tissue (WAT) and activating the activity of brown adipose tissue (BAT) (Kaur et al., 2022). It also improves the gut microbiota (Wang et al., 2020; Baboota et al., 2014a) and other pathways mediated.

In 3T3-L1 cells, capsaicin inhibits adipocyte differentiation by activating TRPV1, which induces the browning of white adipocyte, increases heat production, and decreases intracellular lipid content (Baboota et al., 2014b). Activation of TRPV1 enhances peroxisome proliferator-activated receptor gamma (PPAR-γ) expression and deacetylation, promoting the browning of white adipose tissue (Krishnan et al., 2019). Capsaicin reduces lipid accumulation and glucose and fatty acid uptake in 3T3-L1 cells (Hochkogler et al., 2018). Capsaicin activates AMP-activated protein kinase (AMPK) and inhibits the protein kinase B (AKT)/mammalian target of rapamycin (mTOR) pathway, a major regulator of liver adipogenesis. In addition, capsaicin blocks autophagy and increases peroxisome proliferator-activated receptor gamma coactivator-1A (PGC-1a) protein, suggesting that capsaicin acts as an anti-lipogenic compound in HepG2 cells (Bort et al., 2019a). Studies have indicated that triglyceride content and lipid droplets in hepatocytes are significantly reduced by capsaicin, highlighting its potential to inhibit lipid production in HepG2 cells (Wu et al., 2017). Additionally, capsaicin decreases basal neutral lipid content and increases TRPV1 levels by activating AMPK and PPAR-γ pathways in HepG2 cells (Bort et al., 2019b).

In rats, capsaicin reduces body weight, inhibits fat accumulation and induces heat production (Ludy et al., 2012). Oral administration of capsaicin for 5 weeks in HFD-fed rats results in increased UCP1 expression in WAT, along with changes in protein expression related to thermogenesis, lipid metabolism, redox-regulation, signal transduction and energy metabolism (Joo et al., 2010). Capsaicin-loaded nanoemulsion effectively reduces the body weight gain, serum lipid level and adipose tissue mass in obese male SD (Sprague Dawley) rats induced by HFD (Lu et al., 2016). In addition, capsaicin reduces weight gain and lowered triglyceride levels in HFD-fed rats without affecting feed intake (Pande and Srinivasan, 2012). Capsaicin-chitosan microspheres (CCMSs) can regulate body weight, body mass index, organ index, body fat, fat-to-weight ratio, and blood lipid levels (Tan et al., 2014). Studies have also demonstrated that capsaicin could be used in combination with other treatments or dietary modifications to enhance its protective effects against liver diseases. In rats fed a western diet, capsaicin alone or in combination with hesperidin reduces adipocyte size and induces the browning of WAT and reduces weight gain by upregulating UCP1 and PRDM16 (Mosqueda-Solís et al., 2018b). Additionally, capsaicin inhibits the histological features of NAFLD by decreasing hepatic fat accumulation and increasing leptin levels associated with inflammation (Seyithanoğlu et al., 2016). Moreover, dietary curcumin and capsaicin treatment reduced weight gain and liver lipid levels induced by HFD consumption (Seyithanoğlu et al., 2016). These findings suggest that capsaicin has significant potential in managing obesity and NAFLD through various mechanisms, including promoting the browning of WAT, enhancing thermogenesis, and improving lipid metabolism.

The application of capsaicin has been shown to reduce liver fat in mice fed a HFD. Capsaicin stimulates the expression of CPT-1 and CD36, while decreases the expression of key enzymes involved in fatty acid synthesis, such as acetyl Co-A carboxylase (ACC) and fatty acid synthase (FAS). Additionally, capsaicin treatment increases adiponectin levels in liver tissues. These results suggest that capsaicin inhibits liver fat accumulation in mice by upregulating β-oxidation and *de novo* lipogenesis in HFD-induced NAFLD mice (Shin et al., 2020). Studies have shown that antibiotics treatment significantly reduces intestinal inflammation and leakage caused by HFD. Diet capsaicin increases the expression of PPAR-α in adipose tissue. Animals treated with both capsaicin and antibiotics showed the least weight gain and had the smallest fat pad index. Their livers exhibited the lowest levels of fat accumulation, and this combination therapy also resulted in the highest insulin responsiveness (Hu et al., 2017). Regardless of whether the TRPV1 channel was activated, capsaicin reduced food intake and demonstrated anti-obesity effects, which were mediated by changes in gut microbiota and concentrations of short-chain fatty acids (SCFAs) (Wang et al., 2020). One study has shown that the anti-obesity effects of capsaicin in HFD-fed mice are associated with an increase in the population of gut bacteria *Akkermansia muciniphila* (Shen et al., 2017). Capsanthin-enriched pellets and capsaicin pellets effectively reduced body weight in mice. Treatment with capsanthin-enriched pellets resulted in a 37.0% reduction in inguinal adipose tissue and a 43.64% reduction in epididymal adipose tissue (Shanmugham and Subban, 2022). Capsaicin exhibited an antagonistic effect on HFD-induced obesity in mice without reducing energy intake (Baskaran et al., 2017).

There is a positive correlation between dietary capsaicin consumption and markers of body obesity and fatty liver (Martínez-Aceviz et al., 2023). A study involving fifteen subjects has shown that diet capsaicin increases feelings of fullness when food intake is not restricted, and after dinner, capsaicin prevents the effects of negative energy balance on appetite (Janssens et al., 2014). Adding capsaicin to the diet has been shown to increase energy expenditure, helping to maintain negative energy balance by counteracting the adverse effects of reduced energy expenditure components (Janssens et al., 2013). Taking dietary supplements containing green Tea, capsaicin and ginger extracts for 8 weeks in overweight women has shown beneficial effects on body weight, body mass index, insulin metabolism markers, and plasma glutathione levels (Taghizadeh et al., 2017). Moreover, studies have shown that a combination of capsaicin, green tea, and CH-19 sweet pepper can reduce body weight in humans by reducing energy intake, suppressing hunger, and increasing satiety (Reinbach et al., 2009). These findings suggest that capsaicin could be used in combination with other treatments or dietary modifications play a valuable role in weight management and metabolic health, contributing to improved insulin metabolism and oxidative stress markers, while also enhancing satiety and energy expenditure.

4.2.3 Improve insulin resistance

HFD or overfeeding can reduce muscle glucose uptake and increase liver gluconeogenesis, leading to insulin resistance. Insulin resistance in the liver and skeletal muscle leads to hyperglycemia, hyperinsulinemia, contributing to dyslipidemia and fatty liver (Czech, 2017). Capsaicin has been shown to have protective effects against NAFLD and metabolic disorders by addressing insulin resistance and hepatic steatosis (Kang et al., 2010). It also has preventive effects on insulin resistance in rats fed a western diet (Mosqueda-Solís et al., 2018a). Capsaicin inhibits sugar absorption in the gut (Zhang et al., 2017), reduces liver gluconeogenesis, increases glycogen synthesis, improves intestinal microbiota and bile acids and enhances insulin resistance (Hui et al., 2019). Nonivamide, a capsaicin analog, promotes insulin signaling, stimulates glucose transporter 2 (GLUT2) transport to the membrane, and improves NAFLD

(Wikan et al., 2020). Pelargonic acid vanillylamide (PAVA) alleviates NAFLD by exhibiting anti-inflammatory effects and improving insulin resistance mediated by the Janus kinase 2 (JAK2)/signal transducer and activator of transcription 3 (STAT3) pathway (Wikan et al., 2023). Oral capsaicin attenuates the proliferation and activation of autoreactive T cells in the pancreatic lymph node, protecting mice from the development of type 1 diabetes (Nevius et al., 2012). In type 2 diabetes, dietary capsaicin activation of TRPV1 improved abnormal glucose homeostasis and increases plasma and ileum glucagon-like peptide 1 (GLP-1) levels (Wang et al., 2012). Capsaicin improves glucose tolerance and insulin sensitivity in mice by regulating the gut microbial-bile acid-farnesoid X receptor (FXR) axis (Hui et al., 2019). Studies have suggested that dietary capsaicin reduces fasting blood sugar, insulin, leptin levels and significantly reduces impaired glucose tolerance in obese mice (Kang et al., 2010). It also reduces metabolic disorders in obese/diabetic KKAy mice by increasing the expression of adiponectin and its receptors (Kang et al., 2011). Capsaicin enhances insulin secretion at various stage during hyperglycemic clamp, increases β-cell proliferation and decreases β-cell apoptosis by enhancing insulin/IGF-1 signaling, thereby increasing β-cell mass (Kwon et al., 2013). In addition, regular supplementation of capsaicin improves postprandial hyperglycemia, hyperinsulinemia and fasting lipid metabolism disorders in women with gestational diabetes mellitus (GDM) (Yuan et al., 2016).

In a word, in NAFLD, key molecules and pathways play critical roles in regulating lipid metabolism and disease progression. CPT-1 and CD36 are essential for promoting β-oxidation and hepatic fatty acid uptake, while ACC and FAS are central to fatty acid synthesis. Their expression is tightly controlled, impacting lipid metabolism directly. The activation of AMPK and inhibition of the AKT/mTOR pathway are crucial in suppressing hepatic adipogenesis. Increased PGC-1α levels and autophagy blockade further support hepatic lipid homeostasis. UCP1 and PRDM16 contribute to NAFLD inhibition by inducing the browning of WAT and reducing adipocyte size. The gut microbial-bile acid-FXR axis plays a significant role in enhancing glucose tolerance and insulin sensitivity, while the insulin/IGF-1 signaling pathway increases β-cell mass, further modulating glucose and lipid metabolism.

Capsaicin improves hepatic lipid metabolism by upregulating CPT-1 and CD36 and downregulating ACC and FAS, thus promoting β-oxidation and reducing fatty acid synthesis. This effect is mediated through AMPK activation and AKT/mTOR inhibition, key regulators of liver adipogenesis. Capsaicin also blocks autophagy, elevates PGC-1α levels, reduces adipocyte size, and induces WAT browning by upregulating UCP1 and PRDM16. Additionally, capsaicin improves glucose tolerance and insulin sensitivity via modulation of the gut microbial-bile acid-FXR axis, and enhances β-cell function by increasing proliferation and reducing apoptosis through insulin/IGF-1 signaling, thereby augmenting β-cell mass.

5 Liver fibrosis and capsaicin

5.1 Liver fibrosis

Liver fibrosis and end-stage cirrhosis are common consequences of all major chronic liver diseases, with HSCs activation being the primary mechanism underlying the deposition of fibrotic tissue (Elpek, 2014). Fibrosis serves as a wound-healing defense mechanism triggered by inflammation or injury. However, the immune system's destruction of organ structures and inherent inflammation in the liver lead to immune deficiency and immune paralysis. Liver fibrosis is characterized by extracellular matrix deposition and persistent loss of the tissues that perform liver function (Wang et al., 2023). If left untreated, liver fibrosis can progress to cirrhosis, HCC and eventually liver failure (Cheng et al., 2021). The pathophysiology of liver fibrosis is multifactorial, with the activation of HSCs driving its development. When activated, HSCs are associated with fibrotic matrix deposition and fibrous collagen production (Neshat et al., 2021). Unfortunately, there is currently no effective treatment for liver fibrosis other than liver transplantation (Wang et al., 2023; Cheng et al., 2021).

5.2 Roles of capsaicin in the treatment of liver fibrosis

Liver fibrosis caused by the activation of HSCs is associated with the incidence of liver diseases (Zhang WS. et al., 2022). Previous studies have supported capsaicin's inhibitory effect on HSCs, demonstrating its important role in mitigating liver fibrosis (Table 3). Capsaicin inhibits M1 macrophage polarization by targeting Notch signaling, resulting in decreased secretion of the inflammatory factor TNF-α, which weakens myofibroblast regeneration and fibrosis formation of HSCs (Sheng et al., 2020). Capsaicin inhibits dimethylnitrosamine (DMN)-induced hepatotoxicity, NF-κB activation, and collagen accumulation. Specifically, capsaicin reduces the increase of α-SMA, collagen type I, MMP-2 and TNF-α. In hematopoietic stem cells, capsaicin inhibits TGF-β1-induced increased expression of α-SMA and collagen type I by activating PPAR-γ. These results suggest that capsaicin improves liver fibrosis by inhibiting the TGF-β1/Smad pathway through PPAR-γ activation (Choi et al., 2017). The inhibitory effect of dietary capsaicin on liver fibrosis *in vivo* has been confirmed using two well-established mouse models of liver fibrosis: bile duct ligation (BDL) and CCl4. This is demonstrated by reduced fibrosis related damage, reduced collagen deposition and α-smooth muscle actin $(\alpha SMA)^+$ cells, and reduced expression of profibrogenic markers in isolated HSCs (Bitencourt et al., 2015). Capsaicin also inhibits cell proliferation, reduces cell activation, and reduces hydrogen peroxide production, lowers levels of tissue inhibitor of metalloproteinases-1 (TIMP-1) and transforming growth faction-1 (TGF-1). Consequently, capsaicin effectively reduces the degree of liver fibrosis, inhibits the proliferation of HSCs, and promotes cell apoptosis (Yu FX. et al., 2014).

6 Liver cancer and capsaicin

6.1 Liver cancer

Liver cancer is one of the most common malignancies and the third leading cause of cancer-related death worldwide (Sung et al.,

TABLE 3 Effects of capsaicin on liver fibrosis.

Model	Capsaicin dosage	Main functions	Reference
CCl4-induced liver fibrosis in mice	0, 2.5 and 5 mg/kg	↓TNF-α	Sheng et al. (2020)
DMN-induced liver fibrosis in rats	0.5 and 1.0 mg/kg	↓α-SMA, collagen type I, MMP-2, and TNF-α, TGF-β1 ↑Smad7	Choi et al. (2017)
CCl4-induced fibrosis in mice	0.01%	↓Col1a1, αSMA and Loxl2	Bitencourt et al. (2015)
CCl4-induced fibrosis in rats	0, 2.5, 5.0 and 7.5 mg/kg	↓TIMP-1, TGF-1, Bcl-2 ↑Bax, cyto c, caspase-3	Yu et al. (2014b)

TABLE 4 Effects of capsaicin on liver cancer.

Model	Capsaicin dosage	Main functions	Reference
HepG2 cells	0,25,50,75,100 and 200 μM	↓Bcl-2; Bax/Bcl-2 ratio	Chen et al. (2018)
Trpv1 null ($Trpv1^{-/-}$) mice, wide type C57BL/6 ($Trpv1^{+/+}$) mice, and NOD/SCID female mice	2 mg/kg	↓AFP and Ki67	Xie et al. (2019)
Western-type diet in mice	0.5 mg/kg	↓ALT and AST	Sarmiento-Machado et al. (2021)
HepG2 cells	0,50,100,200 and 250 μM	↑ROS	Lee et al. (2004)
HepG2 cells	50–250 μM	↑ROS	Baek et al. (2008)
HepG2 cells	0–800 μM	↑TOS, 8-OHdG, CASP3, CYC, Bax, and NOX4 levels; ↓Bcl-2, GSH, and SIRT1	Hacioglu (2022)
HepG2 cells	10, 50, 100 and 200 μM	↑ROS	Huang et al. (2009)
HepG2 cells	5, 10, 25, 50, 100 and 200 μM	VROS	Joung et al. (2007)
HepG2 cells	150 and 250 μM	↑intracellular Ca^{2+}	Kim et al. (2005)
Hep3B and HepG2 cells	0,50,100,150,200 and 250 μM	↑DR5	Moon et al. (2012)
SK-Hep-1 cells	0,50,100,150 and 200 μM	↓Bcl-2; ↑Bax	Jung et al. (2001)
HepG2 cells	50, 100 and 200 μM	↑LC3-II and beclin-1	Chen et al. (2016)
Sprague-Dawley rats	1 mg/kg and 2 mg/kg	↓SIRT1 and SOX2	Xie et al. (2022)
LM3, Hep3B, Huh7 cells and BALB/C nude mice	LM cells: capsaicin (0.100,130,160,190,220 μM) and sorafenib (0,2,3,4,5,6,7 μM); Hep3B cells: capsaicin (0,8,16,32,64,128 μM) and sorafenib (0,0.25,0.5,1,2,3,4 μM); Huh7 cells: capsaicin (0,25,50,75,100,125) μM and sorafenib (0,0.5,0.75,1,1.25,1.5,1.75 μM); mice:5 mg/kg capsaicin and 50 mg/kg sorafenib	↓EGFR	Dai et al. (2018)
PLC/PRF/5, Huh7, and HepG2 cells	capsaicin (0, 50, 100, 150, 200, and 250 μM) and sorafenib (0, 0.3, 1, 3, 10, and 30 μM)	↑Bax; ↓Bcl-2	Zhang et al. (2018)
HepG2, Huh-7 cells and nu/nu mice	HepG2 cells: capsaicin (0,20,40,75,150,200 μM) and sorafenib (0,1,1.5,2,2.5,3 μM); Huh7 cells: capsaicin (0,10,20,40,80,100 μM) and sorafenib (0,0.2,0.4,0.75,1.5,3 μM)	↑caspase-9 and PARP	Bort et al. (2017)

2021). The common types of liver cancer include HCC, cholangiocarcinoma (CC), and hepatocellular cholangiocarcinoma (HCC/CC) (Zhang and Zhou, 2019). Liver cancer exhibits high incidence and mortality rates, and traditional treatments, such as transarterial chemoembolization (TACE) or sorafenib, have significant limitations, including cancer recurrence, drug ineffectiveness, and adverse reactions (Kim et al., 2022). Natural products have shown promising anti-liver cancer properties, anti-oxidation, induction of apoptosis, inhibition of cancer cell proliferation and inhibition of angiogenesis (Diab et al., 2022; Guo et al., 2019; Waziri et al., 2018). The pathogenesis of HCC is complex, involving processes such as abnormal cell and tissue regeneration, angiogenesis, genomic instability, cell proliferation and alterations in signal pathway. Studies have found that capsaicin plays a role in various stages of liver cancer progression (Table 4).

6.2 Roles of capsaicin in the treatment of liver cancer

6.2.1 Specific effects of capsaicin on TRPV1

Capsaicin is a natural bioactive compound that activates TRPV1 (Abdillah and Yun, 2024). TRPV1 is a Ca^{2+} permeable cation channel and serves as the primary heat and capsaicin sensor in humans (Kwon et al., 2021). Capsaicin, in combination with a static magnetic field (SMF), synergistically inhibits the growth of HepG2 through the mitochondria-dependent apoptosis pathway. SMF significantly enhanced the inhibitory effect of capsaicin on cancer cells. The mechanism was that SMF enhances the inhibitory effect of capsaicin on cancer cells by inducing conformational changes in the TRPV1 ion channel (Chen et al., 2018). *In vivo* studies have shown that treating tumor-bearing mice with capsaicin significantly reduces tumor volume and improves overall survival rate. In addition, TRPV1 expression is increased in capsaicin-treated mice, while alpha-fetoprotein (AFP) and Ki67 expression are decreased (Xie et al., 2019). Preventive capsaicin dietary (specifically 0.02%) mitigates carcinogenic liver damage and the development of pretumor lesions. Capsaicin reduces diethylnitrosamine (DEN)-induced oxidative damage by improving the glutathione (GSH) axis, and reducing hepatocyte necrosis and inflammation (Sarmiento-Machado et al., 2021).

6.2.2 Oxidative stress

Oxidative stress is a condition where the oxidative and anti-oxidant effects in the body is disrupted. It has become a key factor in the initiation and progression of many diseases, including liver cancer (Tang et al., 2022; Li Z. et al., 2023). ROS are the most prevalent reactive chemical involved in oxidative stress during disease progression. Oxidative stress plays a unique role in the development of HCC, with excessive ROS generation being common in liver diseases of various etiologies (Liu et al., 2023). NADPH oxidase-mediated ROS production plays an important role in the mechanism of capsaicin-induced apoptosis (Lee et al., 2004). Capsaicin increases ROS production in HepG2 cells (Baek et al., 2008). The increase in total oxidant status (TOS) level and the decrease in GSH level indicate that capsaicin induces oxidative stress. The levels of 8-hydroxydeoxyguanosine (8-OHdG) levels are significantly increased in capsaicin-treated HepG2 and HL-7702 cells (Hacioglu, 2022). Capsaicin may covalently bind to NAD(P)H:quinone oxidoreductase (NQO1), thereby inhibiting its activity and leading to ROS production. Furthermore, p-Akt is activated, which increases the nuclear translocation of Nrf2, enhances the binding of ARE, and upregulates the expression of heme oxygenase-1 (HO-1) (Joung et al., 2007).

6.2.3 Cell proliferation, apoptosis and survival

Malignant cells are characterized by abnormal signaling pathways involved in proliferation, apoptosis and angiogenesis (Davis et al., 2010). Capsaicin inhibits cell proliferation and induced apoptosis of HepG2 cells through the downregulation of Bcl-2 and the activation of pro-apoptotic molecules caspase-3 and p53 (Baek et al., 2008). Capsaicin induces apoptosis by promoting the expression of Bax, and decreasing Bcl-2 and increasing caspase-3 activation in HepG2 cells (Huang et al., 2009). Capsaicin has been shown to inhibit the proliferation of HepG2 cell. As an epigenetic marker, the expression of miR-126 is upregulated and the expression of piR-Hep-1 is downregulated after treatment. Additionally, capsaicin treatment leads to a decrease in the expression of Ki-67, phosphoinositide 3-kinase (PI3K), and mTOR, while increasing the expression of non-phosphorylated AKT. This indicates that capsaicin exerts both genetic and epigenetic effects on cell proliferation. Furthermore, capsaicin affects carcinogenesis by modulating the expression of miR-126 and piR-Hep-1 in different ways (Ates et al., 2022). Pepper fruit extracts have been found to alter the anti-oxidant capacity ofHepG2 cell lines, enhancing catalase activity and reducing the activity of NADPH-producing enzymes (Rodríguez-Ruiz et al., 2023). Activation of the Phospholipase C and the release of intracellular Ca^{2+} from inositol 1,4,5-trisphosphate (IP3) sensitive stores (Kim et al., 2005). Capsaicin enhances the apoptotic effect of tumor necrosis factor-related apoptosis-inducing ligand (TRAIL) on various cancer cells by inducing the expression of TRAIL receptor DR5 on the cell surface throughSp1 promoter activation. These findings suggest that capsaicin upregulates DR5 via calcium inflow-dependent Sp1 activation, thereby sensitizing HCC cells to TRAIL-mediated apoptosis (Moon et al., 2012). The inhibitory effect of capsaicin on SK-Hep-1 cells is primarily due to apoptosis induced by DNA fragmentation and nuclear aggregation. In addition, capsaicin effectively induces the apoptosis of SK-Hep-1 cells through a caspase-3-dependent mechanism (Jung et al., 2001). Capsaicin induces autophagy and apoptosis in HCC cells. The ROS-STAT3 pathway is involved in capsaicin-induced autophagy of HCC cells, and inhibition of autophagy enhances capsaicin's effects in HCC cells (Chen et al., 2016). Sirtuin 1 (SIRT1) is overexpressed in liver cancer and acts as a tumor promoter through deacetylation by sex-determining region Y-box 2 (SOX2). Capsaicin treatment downregulates SIRT1, resulting in reduced deacetylation and degradation of SOX2. These results indicate that capsaicin inhibits liver cancer progression through the SIRT1/SOX2 signaling pathway (Xie et al., 2022).

6.2.4 Interaction of capsaicin with sorafenib or 5-FU

Sorafenib is an oral kinase inhibitor known for its ability to inhibit tumor cell proliferation and angiogenesis and while inducing apoptosis in cancer cells, thereby improving survival rates for patients with advanced HCC (Kong et al., 2021). Capsaicin or sorafenib alone could inhibit cell proliferation and induce apoptosis (Dai et al., 2018; Zhang et al., 2018). Notably, capsaicin and sorafenib have shown synergistic effects in inhibiting the growth, invasion and metastasis of liver cancer cells, as well as enhancing cell apoptosis (Dai et al., 2018) (Zhang et al., 2018). And intratumoral injection of capsaicin did not cause significant severe toxicity (Zhang et al., 2018). Sorafenib combined with capsaicin demonstrated an enhanced anti-cancer effect. Sorafenib induced AKT activation, which led to drug resistance, whereas capsaicin's inhibition of AKT might sensitize cells to sorafenib therapy (Bort et al., 2017). Additionally, 5-Fluorouracil (5-FU) is a widely used chemotherapy agent for various cancers (Shi et al., 2023). Capsaicin has been found to enhance the activity of anti-cancer drugs when used in combination. Capsaicin significantly enhanced the drug sensitivity of QBC939 to 5-FU. In addition, the combination of capsaicin and 5-FU demonstrated a synergistic effect in

cholangiocarcinoma (CCA) xenografts, with the combined therapy yielding greater inhibition than 5-FU alone. Further research found that capsaicin inhibited 5-FU-induced autophagy in CCA cells by activating the PI3K/AKT/mTOR pathway (Hong et al., 2015).

7 Conclusion and perspective

This study found that capsaicin has numerous beneficial effects, including protection against liver damage, anti-diabetes, anti-obesity, anti-liver fibrosis, anti-liver cancer, pain relief and anti-oxidant. The studies mentioned indicate limited clinical studies on fatty liver. Most basic studies and a few clinical studies have shown that capsaicin improves liver inflammation and fat infiltration through mechanisms mediated by TRPV1 or independent pathways, preventing the progression of fatty liver, and providing liver protection effect. Capsaicin also improves systemic metabolic issues, including blood lipid, blood sugar, and insulin resistance. Geographically, fatty liver disease is prevalence across China, with higher rates in northern regions compared to the southern and southwestern regions (Yip et al., 2023). Moderate spicy eating may benefit fatty liver, be safe, and potentially reduce mortality. In another study on HCC incidence, patients from two hospitals in western China (Chongqing) and eastern China (Shanghai) were examined, revealing a higher incidence of HCC in eastern China. Epidemiological studies have shown that unhealthy diet, living environment and multiple carcinogenic factors may explain the regional differences in HCC incidence (Liao et al., 2017).

The capsaicin content varies among chili pepper varieties, with some being very hot and others less so or even non-spicy. An intake of 2.56 mg of capsaicin induces satiety, equivalent to 1–2 g of chili pepper. An intake of 5 mg improves blood sugar metabolism, equivalent to 2–4 g of chili pepper (Janssens et al., 2014). Clinical studies have shown that in pregnant women with gestational diabetes, taking 5 mg of capsaicin per day for 4 weeks, without changes in food calories or composition, improved blood sugar control and insulin resistance, and reduced the birth rate of larger-than-gestational-age infants (Yuan et al., 2016). Cancer-related fatigue is common symptom among Cancer patients, and exercise is a treatment (Li J. et al., 2023). Studies have found that capsaicin reduces serum lactate, ammonia, BUN (blood urea nitrogen) and creatine kinase (CK) levels, reduces physical fatigue and improves exercise performance in mice (Hsu et al., 2016). Studies have found that the 8% capsaicin patch appears to be effective in the short and medium term for treating peripheral neuropathic pain, as it not only reduces pain intensity but also decreases the pain area. Most patients tolerate its application well (Goncalves et al., 2020). Moreover, in Europe, capsaicin patches (179 mg) have been approved for the local treatment of peripheral neuropathic pain, either as a monotherapy or in combination with other medications (Maihöfner et al., 2021).

Moreover, whole chili peppers or other capsaicin-containing foods have an effect on liver health. Research indicates that dietary preferences in China vary geographically, influenced by local climate and consumption levels. Spicy regions are mainly in the southwest, centered around Sichuan province, which also has lower diabetes prevalence, possibly due to capsaicin, the main spicy ingredient in chili peppers (Zhao et al., 2020). A 2021 study showed that compared to those who do not eat spicy food, individuals who consume spicy food have reduced risks of esophageal, stomach, and colorectal cancers. The benefits are greater among non-drinkers and non-smokers (Chan et al., 2021). Furthermore, compared to individuals who consume spicy foods less than once a week, even a modest intake of spicy foods-just 1–2 days per week-has been associated with observable health benefits. Notably, consuming spicy foods 6 to 7 times per week is linked to a 14% reduction in all-cause mortality and a 22% reduction in ischemic heart disease-related mortality (Lv et al., 2015). A foreign cohort study with 22,000 participants followed for 8.2 years showed that regular chili pepper consumption reduced all-cause mortality by 23% and cardiovascular event mortality by 34% (Bonaccio et al., 2019). Another cohort study with over 50,000 people found that weekly chili pepper consumption reduced high blood pressure incidence by 28% among non-drinkers (Wang et al., 2021). A meta-study has found that eating chili peppers reduces the risk of death, potentially due to capsaicin promoting fat metabolism, increasing energy expenditure, and controlling blood sugar, thereby reducing obesity and metabolic syndrome risks, and cardiovascular disease mortality (Kaur et al., 2021). Regular chili pepper consumption (at least once a week) was shown to reduce all-cause mortality by 12% and cardiovascular event mortality by 18% (Ofori-Asenso et al., 2021). Moreover, Defatted pepper seed ethanolic extract (DPSE) reduces HFD-induced weight gain and liver cholesterol content (Sung et al., 2016). The study found that the consumption of black pepper or chili is significantly associated with a reduced risk of overall mortality (Hashemian et al., 2019). Additionally, the study also found that green Capsicum annuum exhibits hepatoprotective effects (Das et al., 2018).

While capsaicin has demonstrated significant anti-cancer potential in various preclinical models, its translation into clinical application presents several key challenges, particularly in terms of dosage determination and safety. Firstly, establishing a dosage that is both effective and safe poses a substantial challenge. The effective doses observed in animal models may not be directly applicable to humans due to differences in metabolism and toxicity responses across species. Therefore, extensive dose-escalation studies are necessary to identify an appropriate therapeutic range. Secondly, the safety profile of capsaicin cannot be overlooked. High doses of capsaicin may cause adverse effects such as gastrointestinal cramps, stomach pain, nausea, diarrhea, vomiting, increased circulating blood volume, heart rate, tachycardia and stomach cancer risk (López-Carrillo et al., 2003; Merritt et al., 2022). Some studies suggest capsaicin may also be a carcinogen, promoting cancer metastasis (Cheng et al., 2023a; Deng et al., 2023; Cheng et al., 2023b). Despite its anti-cancer activity, capsaicin's clinical use as an anti-cancer drug remains problematic due to poor bioavailability and water solubility (Giri et al., 2016). Furthermore, the delivery method of capsaicin is another significant challenge. While local delivery may help mitigate systemic toxicity, ensuring sufficient concentration at the tumor site without causing widespread adverse effects remains a critical area for further research, especially in the treatment of systemic cancers (Giri et al., 2016; Lu et al., 2020). Therefore, patients with liver disease are advised to consume spicy food in moderation to satisfy appetite without aggravating their condition.

Research on chronic liver diseases has increasingly focused on fatty liver disease, particularly NAFLD, due to its close association

with metabolic syndrome. Studies have shown that capsaicin consumption may have beneficial effects, such as improving cardiovascular outcomes and reducing all-cause mortality, which is particularly relevant in the context of fatty liver disease. Given these findings, the long-term effects of capsaicin on chronic liver diseases, especially metabolic-related fatty liver, could be a promising area for future research. However, more studies are needed to fully understand its impact compared to other liver conditions, such as hepatic injury or HCC. Future research could focus on determining the optimal dosage and safety profile of capsaicin for clinical use, particularly in the treatment of liver diseases and cancers, while also exploring the mechanisms through which capsaicin exerts its protective effects on liver health and its potential impact on systemic metabolic issues. Additionally, investigating regional dietary habits in China, especially the varying impacts of capsaicin consumption on health outcomes, could provide valuable insights. Exploring novel delivery methods for capsaicin to improve its bioavailability and minimize adverse effects represents another crucial area for future investigation.

Author contributions

SL: Data curation, Formal Analysis, Writing–original draft. LH: Formal Analysis, Writing–original draft. FY: Writing–original draft. NL: Writing–original draft. JD: Writing–original draft. JZ: Writing–original draft. SX: Writing–original draft. XH: Conceptualization, Data curation, Funding acquisition, Writing–original draft.

Funding

The author(s) declare that financial support was received for the research, authorship, and/or publication of this article. The present study was financially supported by Science and Technology Program of Hebei (223777156D); Clinical Medical School Graduate Research Innovation Practice Project (2023KCY06) and National Natural Science Foundation of China (Nos 81973840 and 81273748).

Conflict of interest

The authors declare that the research was conducted in the absence of any commercial or financial relationships that could be construed as a potential conflict of interest.

Publisher's note

References

Abdillah, A. M., and Yun, J. W. (2024). Capsaicin induces ATP-dependent thermogenesis via the activation of TRPV1/β3-AR/α1-AR in 3T3-L1 adipocytes and mouse model. *Arch. Biochem. Biophys.* 755 (109975), 109975. doi:10.1016/j.abb.2024.109975

Alam, M. F., Ajeibi, A. O., Safhi, M. H., Alabdly, A. J. A., Alshahrani, S., Rashid, H., et al. (2023). Therapeutic potential of capsaicin against cyclophosphamide-induced liver damage. *J. Clin. Med.* 12 (3), 911. doi:10.3390/jcm12030911

Alawi, K., and Keeble, J. (2010). The paradoxical role of the transient receptor potential vanilloid 1 receptor in inflammation. *Pharmacol. Ther.* 125 (2), 181–195. doi:10.1016/j.pharmthera.2009.10.005

Ates, B., Öner, Ç., Akbulut, Z., and Çolak, E. (2022). Capsaicin alters the expression of genetic and epigenetic molecules in hepatocellular carcinoma cell. *Int. J. Mol. Cell. Med.* 11 (3), 236–243. doi:10.22088/IJMCM.BUMS.11.3.236

Avraham, Y., Zolotarev, O., Grigoriadis, N. C., Poutahidis, T., Magen, I., Vorobiav, L., et al. (2008). Cannabinoids and capsaicin improve liver function following thioacetamide-induced acute injury in mice. *Am. J. Gastroenterol.* 103 (12), 3047–3056. doi:10.1111/j.1572-0241.2008.02155.x

Baboota, R. K., Murtaza, N., Jagtap, S., Singh, D. P., Karmase, A., Kaur, J., et al. (2014a). Capsaicin-induced transcriptional changes in hypothalamus and alterations in gut microbial count in high fat diet fed mice. *J. Nutr. Biochem.* 25 (9), 893–902. doi:10.1016/j.jnutbio.2014.04.004

Baboota, R. K., Singh, D. P., Sarma, S. M., Kaur, J., Sandhir, R., Boparai, R. K., et al. (2014b). Capsaicin induces "brite" phenotype in differentiating 3t3-L1 preadipocytes. *PLoS One* 9 (7), e103093. doi:10.1371/journal.pone.0103093

Baek, Y. M., Hwang, H. J., Kim, S. W., Hwang, H. S., Lee, S. H., Kim, J. A., et al. (2008). A comparative proteomic Analysis for capsaicin-induced apoptosis between human hepatocarcinoma (Hepg2) and human neuroblastoma (sk-N-sh) cells. *Proteomics* 8 (22), 4748–4767. doi:10.1002/pmic.200800094

Bao, Z., Dai, X., Wang, P., Tao, Y., and Chai, D. (2019). Capsaicin induces cytotoxicity in human osteosarcoma Mg63 cells through trpv1-dependent and -independent pathways. *Cell. cycleGeorget. Tex* 18 (12), 1379–1392. doi:10.1080/15384101.2019.1618119

Baskaran, P., Krishnan, V., Fettel, K., Gao, P., Zhu, Z., Ren, J., et al. (2017). Trpv1 activation counters diet-induced obesity through sirtuin-1 activation and prdm-16 deacetylation in Brown adipose tissue. *Int. J. Obes.* 41 (5), 739–749. doi:10.1038/ijo.2017.16

Bitencourt, S., Stradiot, L., Verhulst, S., Thoen, L., Mannaerts, I., and van Grunsven, L. A. (2015). Inhibitory effect of dietary capsaicin on liver fibrosis in mice. *Mol. Nutr. Food Res.* 59 (6), 1107–1116. doi:10.1002/mnfr.201400649

Bonaccio, M., Di Castelnuovo, A., Costanzo, S., Ruggiero, E., De Curtis, A., Persichillo, M., et al. (2019). Chili pepper consumption and mortality in Italian adults. *J. Am. Coll. Cardiol.* 74 (25), 3139–3149. doi:10.1016/j.jacc.2019.09.068

Bort, A., Sánchez, B. G., Mateos-Gómez, P. A., Díaz-Laviada, I., and Rodríguez-Henche, N. (2019a). Capsaicin targets lipogenesis in Hepg2 cells through ampk activation, akt inhibition and ppars regulation. *Int. J. Mol. Sci.* 20 (7), 1660. doi:10.3390/ijms20071660

Bort, A., Sánchez, B. G., Spínola, E., Mateos-Gómez, P. A., Rodríguez-Henche, N., and Díaz-Laviada, I. (2019b). The red pepper's spicy ingredient capsaicin activates ampk in Hepg2 cells through camkkβ. *PLoS One* 14 (1), e0211420. doi:10.1371/journal.pone.0211420

Bort, A., Spínola, E., Rodríguez-Henche, N., and Díaz-Laviada, I. (2017). Capsaicin exerts synergistic antitumor effect with sorafenib in hepatocellular carcinoma cells through ampk activation. *Oncotarget* 8 (50), 87684–87698. doi:10.18632/oncotarget.21196

Braga Ferreira, L. G., Faria, J. V., Dos Santos, J. P. S., and Faria, R. X. (2020). Capsaicin: trpv1-independent mechanisms and novel therapeutic possibilities. *Eur. J. Pharmacol.* 887 (173356), 173356. doi:10.1016/j.ejphar.2020.173356

Caprodossi, S., Amantini, C., Nabissi, M., Morelli, M. B., Farfariello, V., Santoni, M., et al. (2011). Capsaicin promotes a more aggressive gene expression phenotype and invasiveness in null-trpv1 urothelial cancer cells. *Carcinogenesis* 32 (5), 686–694. doi:10.1093/carcin/bgr025

Chan, W. C., Millwood, I. Y., Kartsonaki, C., Du, H., Guo, Y., Chen, Y., et al. (2021). Spicy food consumption and risk of gastrointestinal-tract cancers: findings from the China kadoorie biobank. *Int. J. Epidemiol.* 50 (1), 199–211. doi:10.1093/ije/dyaa275

Chen, K. S., Chen, P. N., Hsieh, Y. S., Lin, C. Y., Lee, Y. H., and Chu, S. C. (2015). Capsaicin protects endothelial cells and macrophage against oxidized low-density lipoprotein-induced injury by direct antioxidant action. *Chem. Biol. Interact.* 228, 35–45. doi:10.1016/j.cbi.2015.01.007

Chen, W. T., Lin, G. B., Lin, S. H., Lu, C. H., Hsieh, C. H., Ma, B. L., et al. (2018). Static magnetic field enhances the anticancer efficacy of capsaicin on Hepg2 cells via capsaicin receptor Trpv1. *PLoS One* 13 (1), e0191078. doi:10.1371/journal.pone.0191078

Chen, X., Tan, M., Xie, Z., Feng, B., Zhao, Z., Yang, K., et al. (2016). Inhibiting ros-stat3-dependent autophagy enhanced capsaicin-induced apoptosis in human hepatocellular carcinoma cells. *Free Radic. Res.* 50 (7), 744–755. doi:10.3109/10715762.2016.1173689

Cheng, D., Chai, J., Wang, H., Fu, L., Peng, S., and Ni, X. (2021). Hepatic macrophages: key players in the development and progression of liver fibrosis. *Liver Int.* 41 (10), 2279–2294. doi:10.1111/liv.14940

Cheng, P., Wu, J., Zong, G., Wang, F., Deng, R., Tao, R., et al. (2023a). Capsaicin shapes gut microbiota and pre-metastatic niche to facilitate cancer metastasis to liver. *Pharmacol. Res.* 188 (106643), 106643. doi:10.1016/j.phrs.2022.106643

Cheng, P., Wu, J., Zong, G., Wang, F., Deng, R., Tao, R., et al. (2023b). Capsaicin shapes gut microbiota and pre-metastatic niche to facilitate cancer metastasis to liver. *Pharmacol. Res.* 188, 106643. doi:10.1016/j.phrs.2022.106643

Choi, J. H., Jin, S. W., Choi, C. Y., Kim, H. G., Lee, G. H., Kim, Y. A., et al. (2017). Capsaicin inhibits dimethylnitrosamine-induced hepatic fibrosis by inhibiting the TGF-β1/smad pathway via peroxisome proliferator-activated receptor gamma activation. *J. Agric. Food Chem.* 65 (2), 317–326. doi:10.1021/acs.jafc.6b04805

Czech, M. P. (2017). Insulin action and resistance in obesity and type 2 diabetes. *Nat. Med.* 23 (7), 804–814. doi:10.1038/nm.4350

Dai, N., Ye, R., He, Q., Guo, P., Chen, H., and Zhang, Q. (2018). Capsaicin and sorafenib combination treatment exerts synergistic anti-hepatocellular carcinoma activity by suppressing egfr and pi3k/akt/mtor signaling. *Oncol. Rep.* 40 (6), 3235–3248. doi:10.3892/or.2018.6754

Das, M., Basu, S., Banerjee, B., Sen, A., Jana, K., and Datta, G. (2018). Hepatoprotective effects of green Capsicum annum against ethanol induced oxidative stress, inflammation and apoptosis in rats. *J. Ethnopharmacol.* 227, 69–81. doi:10.1016/j.jep.2018.08.019

Davis, C. D., Emenaker, N. J., and Milner, J. A. (2010). Cellular proliferation, apoptosis and angiogenesis: molecular targets for nutritional preemption of cancer. *Semin. Oncol.* 37 (3), 243–257. doi:10.1053/j.seminoncol.2010.05.001

de Lourdes Medina-Contreras, J. M., Mailloux-Salinas, P., Colado-Velazquez, J. I., Gómez-Viquez, N., Velázquez-Espejel, R., Del Carmen Susunaga-Notario, A., et al. (2020). Topical capsaicin cream with moderate exercise protects against hepatic steatosis, dyslipidemia and increased blood pressure in hypoestrogenic obese rats. *J. Sci. Food Agric.* 100 (7), 3212–3219. doi:10.1002/jsfa.10357

Deng, R., Yu, S., Ruan, X., Liu, H., Zong, G., Cheng, P., et al. (2023). Capsaicin orchestrates metastasis in gastric cancer via modulating expression of Trpv1 channels and driving gut microbiota disorder. *Cell. Commun. Signal* 21 (1), 364–01265. doi:10.1186/s12964-023-01265-3

Devarbhavi, H., Asrani, S. K., Arab, J. P., Nartey, Y. A., Pose, E., and Kamath, P. S. (2023). Global burden of liver disease: 2023 update. *J. Hepatol.* 79 (2), 516–537. doi:10.1016/j.jhep.2023.03.017

Diab, K. A., El-Shenawy, R., Helmy, N. M., and El-Toumy, S. A. (2022). Polyphenol content, antioxidant, cytotoxic, and genotoxic activities of Bombax ceiba flowers in liver cancer cells Huh7. *Asian Pac J. Cancer Prev.* 23 (4), 1345–1350. doi:10.31557/APJCP.2022.23.4.1345

Diehl, A. M., and Day, C. (2017). Cause, pathogenesis, and treatment of nonalcoholic steatohepatitis. *N. Engl. J. Med.* 377 (21), 2063–2072. doi:10.1056/NEJMra1503519

Dukić, M., Radonjić, T., Jovanović, I., Zdravković, M., Todorović, Z., Kraišnik, N., et al. (2023). Alcohol, inflammation, and microbiota in alcoholic liver disease. *Int. J. Mol. Sci.* 24 (4), 3735. doi:10.3390/ijms24043735

Elmas, C., and Gezer, C. (2022). Capsaicin and its effects on body weight. *J. Am. Nutr. Assoc.* 41 (8), 831–839. doi:10.1080/07315724.2021.1962771

Elpek, G. (2014). Cellular and molecular mechanisms in the pathogenesis of liver fibrosis: an update. *World J. Gastroenterol.* 20 (23), 7260–7276. doi:10.3748/wjg.v20.i23.7260

Friedman, S. L., Neuschwander-Tetri, B. A., Rinella, M., and Sanyal, A. J. (2018). Mechanisms of nafld development and therapeutic strategies. *Nat. Med.* 24 (7), 908–922. doi:10.1038/s41591-018-0104-9

Fukuta, T., Hirai, S., Yoshida, T., Maoka, T., and Kogure, K. (2020). Protective effect of antioxidative liposomes Co-encapsulating astaxanthin and capsaicin on ccl(4)-induced liver injury. *Biol. Pharm. Bull.* 43 (8), 1272–1274. doi:10.1248/bpb.b20-00116

Ghorbanpour, A., Salari, S., Baluchnejadmojarad, T., and Roghani, M. (2023). Capsaicin protects against septic acute liver injury by attenuation of apoptosis and mitochondrial dysfunction. *Heliyon* 9 (3), e14205. doi:10.1016/j.heliyon.2023.e14205

Giri, T. K., Alexander, A., Ajazuddin, B. T. K., and Maity, S. (2016). Infringement of the barriers of cancer via dietary phytoconstituents capsaicin through novel drug delivery system. *Curr. drug Deliv.* 13 (1), 27–39. doi:10.2174/1567201812666150603151250

Goncalves, D., Rebelo, V., Barbosa, P., and Gomes, A. (2020). 8% capsaicin patch in treatment of peripheral neuropathic pain. *Pain physician* 23 (5), E541–e8.

Guo, Z., Zhou, Y., Yang, J., and Shao, X. (2019). Expression of concern: dendrobium candidum extract inhibits proliferation and induces apoptosis of liver cancer cells by inactivating wnt/B-catenin signaling pathway. *Biomed. Pharmacother.* 110, 371–379. doi:10.1016/j.biopha.2018.11.149

Hacioglu, C. (2022). Capsaicin inhibits cell proliferation by enhancing oxidative stress and apoptosis through sirt1/nox4 signaling pathways in Hepg2 and hl-7702 cells. *J. Biochem. Mol. Toxicol.* 36 (3), e22974. doi:10.1002/jbt.22974

Hashemian, M., Poustchi, H., Murphy, G., Etemadi, A., Kamangar, F., Pourshams, A., et al. (2019). Turmeric, pepper, cinnamon, and saffron consumption and mortality. *J. Am. Heart Assoc.* 8 (18), e012240. doi:10.1161/jaha.119.012240

Hassan, A., and Fontana, R. J. (2019). The diagnosis and management of idiosyncratic drug-induced liver injury. *Liver Int.* 39 (1), 31–41. doi:10.1111/liv.13931

Hochkogler, C. M., Lieder, B., Schachner, D., Heiss, E., Schröter, A., Hans, J., et al. (2018). Capsaicin and nonivamide similarly modulate outcome measures of mitochondrial energy metabolism in Hepg2 and 3t3-L1 cells. *Food Funct.* 9 (2), 1123–1132. doi:10.1039/c7fo01626c

Hong, Z. F., Zhao, W. X., Yin, Z. Y., Xie, C. R., Xu, Y. P., Chi, X. Q., et al. (2015). Capsaicin enhances the drug sensitivity of cholangiocarcinoma through the inhibition of chemotherapeutic-induced autophagy. *PLoS One* 10 (5), e0121538. doi:10.1371/journal.pone.0121538

Hsu, Y. J., Huang, W. C., Chiu, C. C., Liu, Y. L., Chiu, W. C., Chiu, C. H., et al. (2016). Capsaicin supplementation reduces physical fatigue and improves exercise performance in mice. *Nutrients* 8 (10), 648. doi:10.3390/nu8100648

Hu, J., Luo, H., Jiang, Y., and Chen, P. (2017). Dietary capsaicin and antibiotics act synergistically to reduce non-alcoholic fatty liver disease induced by high fat diet in mice. *Oncotarget* 8 (24), 38161–38175. doi:10.18632/oncotarget.16975

Huang, S. P., Chen, J. C., Wu, C. C., Chen, C. T., Tang, N. Y., Ho, Y. T., et al. (2009). Capsaicin-induced apoptosis in human hepatoma Hepg2 cells. *Anticancer Res.* 29 (1), 165–174.

Hui, S., Liu, Y., Chen, M., Wang, X., Lang, H., Zhou, M., et al. (2019). Capsaicin improves glucose tolerance and insulin sensitivity through modulation of the gut microbiota-bile acid-fxr Axis in type 2 diabetic Db/Db mice. *Mol. Nutr. Food Res.* 63 (23), e1900608. doi:10.1002/mnfr.201900608

Janssens, P. L., Hursel, R., Martens, E. A., and Westerterp-Plantenga, M. S. (2013). Acute effects of capsaicin on energy expenditure and fat oxidation in negative energy balance. *PLoS One* 8 (7), e67786. doi:10.1371/journal.pone.0067786

Janssens, P. L., Hursel, R., and Westerterp-Plantenga, M. S. (2014). Capsaicin increases sensation of fullness in energy balance, and decreases desire to eat after dinner in negative energy balance. *Appetite* 77, 44–49. doi:10.1016/j.appet.2014.02.018

Joo, J. I., Kim, D. H., Choi, J. W., and Yun, J. W. (2010). Proteomic Analysis for antiobesity potential of capsaicin on white adipose tissue in rats fed with a high fat diet. *J. Proteome Res.* 9 (6), 2977–2987. doi:10.1021/pr901175w

Joung, E. J., Li, M. H., Lee, H. G., Somparn, N., Jung, Y. S., Na, H. K., et al. (2007). Capsaicin induces heme oxygenase-1 expression in Hepg2 cells via activation of pi3k-nrf2 signaling: nad(P)H:quinone oxidoreductase as a potential target. *Antioxid. Redox Signal* 9 (12), 2087–2098. doi:10.1089/ars.2007.1827

Jung, M. Y., Kang, H. J., and Moon, A. (2001). Capsaicin-induced apoptosis in sk-hep-1 hepatocarcinoma cells involves bcl-2 downregulation and caspase-3 activation. *Cancer Lett.* 165 (2), 139–145. doi:10.1016/s0304-3835(01)00426-8

Kang, J. H., Goto, T., Han, I. S., Kawada, T., Kim, Y. M., and Yu, R. (2010). Dietary capsaicin reduces obesity-induced insulin resistance and hepatic steatosis in obese mice fed a high-fat diet. *Obesity* 18 (4), 780–787. doi:10.1038/oby.2009.301

Kang, J. H., Tsuyoshi, G., Le Ngoc, H., Kim, H. M., Tu, T. H., Noh, H. J., et al. (2011). Dietary capsaicin attenuates metabolic dysregulation in genetically obese diabetic mice. *J. Med. Food* 14 (3), 310–315. doi:10.1089/jmf.2010.1367

Kaur, J., Kumar, V., Shafi, S., Khare, P., Mahajan, N., Bhadada, S. K., et al. (2022). Combination of trp channel dietary agonists induces energy expending and glucose utilizing phenotype in hfd-fed mice. *Int. J. Obes.* 46 (1), 153–161. doi:10.1038/s41366-021-00967-3

Kaur, M., Verma, B. R., Zhou, L., Lak, H. M., Kaur, S., Sammour, Y. M., et al. (2021). Association of pepper intake with all-cause and specific cause mortality - a systematic review and meta-analysis. *Am. J. Prev. Cardiol.* 9 (100301), 100301. doi:10.1016/j.ajpc.2021.100301

Kim, D. B., Lee, D. K., Cheon, C., Ribeiro, R., and Kim, B. (2022). Natural products for liver cancer treatment: from traditional medicine to modern drug discovery. *Nutrients* 14 (20), 4252. doi:10.3390/nu14204252

Kim, J. A., Kang, Y. S., and Lee, Y. S. (2005). A Phospholipase C-dependent intracellular Ca2+ release pathway mediates the capsaicin-induced apoptosis in Hepg2 human hepatoma cells. *Arch. Pharm. Res.* 28 (1), 73–80. doi:10.1007/BF02975139

Koneru, M., Sahu, B. D., Mir, S. M., Ravuri, H. G., Kuncha, M., Mahesh Kumar, J., et al. (2018). Capsaicin, the pungent principle of peppers, ameliorates alcohol-induced acute liver injury in mice via modulation of matrix metalloproteinases. *Can. J. Physiol. Pharmacol.* 96 (4), 419–427. doi:10.1139/cjpp-2017-0473

Kong, F. H., Ye, Q. F., Miao, X. Y., Liu, X., Huang, S. Q., Xiong, L., et al. (2021). Current status of sorafenib nanoparticle delivery systems in the treatment of hepatocellular carcinoma. *Theranostics* 11 (11), 5464–5490. doi:10.7150/thno.54822

Kragh Petersen, S., Bilkei-Gorzo, O., Govaere, O., and Härtlova, A. (2020). Macrophages and scavenger receptors in obesity-associated non-alcoholic liver fatty disease (nafld). *Scand. J. Immunol.* 92 (5), e12971. doi:10.1111/sji.12971

Krishnan, V., Baskaran, P., and Thyagarajan, B. (2019). Troglitazone activates Trpv1 and causes deacetylation of pparγ in 3t3-L1 cells. *Biochim. Biophys. Acta Mol. Basis Dis.* 1 (2), 445–453. doi:10.1016/j.bbadis.2018.11.004

Kwon, D. H., Zhang, F., Suo, Y., Bouvette, J., Borgnia, M. J., and Lee, S. Y. (2021). Heat-dependent opening of Trpv1 in the presence of capsaicin. *Nat. Struct. Mol. Biol.* 28 (7), 554–563. doi:10.1038/s41594-021-00616-3

Kwon, D. Y., Kim, Y. S., Ryu, S. Y., Cha, M. R., Yon, G. H., Yang, H. J., et al. (2013). Capsiate improves glucose metabolism by improving insulin sensitivity better than capsaicin in diabetic rats. *J. Nutr. Biochem.* 24 (6), 1078–1085. doi:10.1016/j.jnutbio.2012.08.006

Lee, Y. S., Kang, Y. S., Lee, J. S., Nicolova, S., and Kim, J. A. (2004). Involvement of nadph oxidase-mediated generation of reactive oxygen species in the apototic cell death by capsaicin in Hepg2 human hepatoma cells. *Free Radic. Res.* 38 (4), 405–412. doi:10.1080/10715760410001665262

Li, F., and Wang, F. (2021). Trpv1 in pain and itch. *Adv. Exp. Med. Biol.* 4254–4812. doi:10.1007/978-981-16-4254-8_12

Li, J., Cheng, Q., Zhu, X., Lin, S., Xiang, H., and Lu, W. (2023b). The relationship of exercise and cancer-related fatigue in patients with advanced liver cancer: a cross-sectional study. *Sci. Rep.* 13 (1), 17341–44655. doi:10.1038/s41598-023-44655-w

Li, J., Wang, T., Xia, J., Yao, W., and Huang, F. (2019). Enzymatic and nonenzymatic protein acetylations control glycolysis process in liver diseases. *Faseb J.* 33 (11), 11640–11654. doi:10.1096/fj.201901175R

Li, L., Chen, C., Chiang, C., Xiao, T., Chen, Y., Zhao, Y., et al. (2021). The impact of Trpv1 on cancer pathogenesis and therapy: a systematic review. *Int. J. Biol. Sci.* 17 (8), 2034–2049. doi:10.7150/ijbs.59918

Li, R., Lan, Y., Chen, C., Cao, Y., Huang, Q., Ho, C. T., et al. (2020). Anti-obesity effects of capsaicin and the underlying mechanisms: a review. *Food Funct.* 11 (9), 7356–7370. doi:10.1039/d0fo01467b

Li, Z., Zhou, H., Zhai, X., Gao, L., Yang, M., An, B., et al. (2023a). Melk promotes hcc carcinogenesis through modulating cuproptosis-related gene dlat-mediated mitochondrial function. *Cell. Death Dis.* 14 (11), 733–06264. doi:10.1038/s41419-023-06264-3

Liao, R., Fu, Y. P., Wang, T., Deng, Z. G., Li, D. W., Fan, J., et al. (2017). Metavir and fib-4 scores are associated with patient prognosis after curative hepatectomy in hepatitis B virus-related hepatocellular carcinoma: a retrospective cohort study at two centers in China. *Oncotarget* 8 (1), 1774–1787. doi:10.18632/oncotarget.12152

Liu, Y., Hao, C., Li, L., Zhang, H., Zha, W., Ma, L., et al. (2023). The role of oxidative stress in the development and therapeutic intervention of hepatocellular carcinoma. *Curr. Cancer Drug Targets* 23 (10), 792–804. doi:10.2174/1568009623666230418121130

López-Carrillo, L., López-Cervantes, M., Robles-Díaz, G., Ramírez-Espitia, A., Mohar-Betancourt, A., Meneses-García, A., et al. (2003). Capsaicin consumption, Helicobacter pylori positivity and gastric cancer in Mexico. *Int. J. Cancer* 106 (2), 277–282. doi:10.1002/ijc.11195

Lu, M., Cao, Y., Ho, C. T., and Huang, Q. (2016). Development of organogel-derived capsaicin nanoemulsion with improved bioaccessibility and reduced gastric mucosa irritation. *J. Agric. Food Chem.* 64 (23), 4735–4741. doi:10.1021/acs.jafc.6b01095

Lu, M., Chen, C., Lan, Y., Xiao, J., Li, R., Huang, J., et al. (2020). Capsaicin-the major bioactive ingredient of chili peppers: bio-efficacy and delivery systems. *Food and Funct.* 11 (4), 2848–2860. doi:10.1039/d0fo00351d

Ludy, M. J., Moore, G. E., and Mattes, R. D. (2012). The effects of capsaicin and capsiate on energy balance: critical review and meta-analyses of studies in humans. *Chem. Senses* 37 (2), 103–121. doi:10.1093/chemse/bjr100

Luo, Y., Lu, H., Peng, D., Ruan, X., Eugene Chen, Y., and Guo, Y. (2022). Liver-humanized mice: a translational strategy to study metabolic disorders. *J. Cell. Physiol.* 237 (1), 489–506. doi:10.1002/jcp.30610

Lv, J., Qi, L., Yu, C., Yang, L., Guo, Y., Chen, Y., et al. (2015). Consumption of spicy foods and total and cause specific mortality: population based cohort study. *BMJ Clin. Res. ed* 351, h3942. doi:10.1136/bmj.h3942

Maihöfner, C., Diel, I., Tesch, H., Quandel, T., and Baron, R. (2021). Chemotherapy-induced peripheral neuropathy (cipn): current therapies and topical treatment option with high-concentration capsaicin. *Support. care cancer* 29 (8), 4223–4238. doi:10.1007/s00520-021-06042-x

Martínez-Aceviz, Y., Sobrevilla-Navarro, A. A., and Ramos-Lopez, O. (2023). Dietary intake of capsaicin and its association with markers of body adiposity and fatty liver in a Mexican adult population of tijuana. *Healthc. Basel, Switz.* 11 (22), 3001. doi:10.3390/healthcare11223001

Merritt, J. C., Richbart, S. D., Moles, E. G., Cox, A. J., Brown, K. C., Miles, S. L., et al. (2022). Anti-cancer activity of sustained release capsaicin formulations. *Pharmacol. Ther.* 238 (108177), 108177. doi:10.1016/j.pharmthera.2022.108177

Moon, D. O., Kang, C. H., Kang, S. H., Choi, Y. H., Hyun, J. W., Chang, W. Y., et al. (2012). Capsaicin sensitizes trail-induced apoptosis through sp1-mediated Dr5 up-regulation: involvement of Ca(2+) influx. *Toxicol. Appl. Pharmacol.* 259 (1), 87–95. doi:10.1016/j.taap.2011.12.010

Mosqueda-Solís, A., Sánchez, J., Portillo, M. P., Palou, A., and Picó, C. (2018b). Combination of capsaicin and hesperidin reduces the effectiveness of each compound to decrease the adipocyte size and to induce browning features in adipose tissue of western diet fed rats. *J. Agric. Food Chem.* 66 (37), 9679–9689. doi:10.1021/acs.jafc.8b02611

Mosqueda-Solís, A., Sánchez, J., Reynés, B., Palou, M., Portillo, M. P., Palou, A., et al. (2018a). Hesperidin and capsaicin, but not the combination, prevent hepatic steatosis and other metabolic syndrome-related alterations in western diet-fed rats. *Sci. Rep.* 8 (1), 15100–32875. doi:10.1038/s41598-018-32875-4

Musolino, M., D'Agostino, M., Zicarelli, M., Andreucci, M., Coppolino, G., and Bolignano, D. (2024). Spice up your kidney: a review on the effects of capsaicin in renal physiology and disease. *Int. J. Mol. Sci.* 25 (2), 791. doi:10.3390/ijms25020791

Neshat, S. Y., Quiroz, V. M., Wang, Y., Tamayo, S., and Doloff, J. C. (2021). Liver disease: induction, progression, immunological mechanisms, and therapeutic interventions. *Int. J. Mol. Sci.* 22 (13), 6777. doi:10.3390/ijms22136777

Nevius, E., Srivastava, P. K., and Basu, S. (2012). Oral ingestion of capsaicin, the pungent component of chili pepper, enhances a discreet population of macrophages and confers protection from autoimmune diabetes. *Mucosal Immunol.* 5 (1), 76–86. doi:10.1038/mi.2011.50

Ofori-Asenso, R., Mohsenpour, M. A., Nouri, M., Faghih, S., Liew, D., and Mazidi, M. (2021). Association of spicy chilli food consumption with cardiovascular and all-cause mortality: a meta-analysis of prospective cohort studies. *Angiology* 72 (7), 625–632. doi:10.1177/0003319721995666

Pande, S., and Srinivasan, K. (2012). Potentiation of hypolipidemic and weight-reducing influence of dietary tender cluster bean (cyamopsis tetragonoloba) when combined with capsaicin in high-fat-fed rats. *J. Agric. Food Chem.* 60 (33), 8155–8162. doi:10.1021/jf301211c

Powell, E. E., Wong, V. W., and Rinella, M. (2021). Non-alcoholic fatty liver disease. *Lancet* 397 (10290), 2212–2224. doi:10.1016/S0140-6736(20)32511-3

Prakash, U. N., and Srinivasan, K. (2010). Beneficial influence of dietary spices on the ultrastructure and fluidity of the intestinal brush border in rats. *Br. J. Nutr.* 104 (1), 31–39. doi:10.1017/s0007114510000334

Pyun, C. W., Kim, J. H., Han, K. H., Hong, G. E., and Lee, C. H. (2014). *In vivo* protective effects of dietary curcumin and capsaicin against alcohol-induced oxidative stress. *Biofactors* 40 (5), 494–500. doi:10.1002/biof.1172

Radhakrishna, G. K., Ammunje, D. N., Kunjiappan, S., Ravi, K., Vellingiri, S., Ramesh, S. H., et al. (2024). A comprehensive review of capsaicin and its role in cancer prevention and treatment. *Drug Res.* 74 (5), 195–207. doi:10.1055/a-2309-5581

Reilly, R. M., McDonald, H. A., Puttfarcken, P. S., Joshi, S. K., Lewis, L., Pai, M., et al. (2012). Pharmacology of modality-specific transient receptor potential vanilloid-1 antagonists that do not alter body temperature. *J. Pharmacol. Exp. Ther.* 342 (2), 416–428. doi:10.1124/jpet.111.190314

Reinbach, H. C., Smeets, A., Martinussen, T., Møller, P., and Westerterp-Plantenga, M. S. (2009). Effects of capsaicin, green tea and ch-19 sweet pepper on appetite and energy intake in humans in negative and positive energy balance. *Clin. Nutr.* 28 (3), 260–265. doi:10.1016/j.clnu.2009.01.010

Rodríguez-Ruiz, M., Ramos, M. C., Campos, M. J., Díaz-Sánchez, I., Cautain, B., Mackenzie, T. A., et al. (2023). Pepper fruit extracts show anti-proliferative activity against tumor cells altering their nadph-generating dehydrogenase and catalase profiles. *Antioxidants* 12 (7), 1461. doi:10.3390/antiox12071461

Rohm, B., Riedel, A., Ley, J. P., Widder, S., Krammer, G. E., and Somoza, V. (2015). Capsaicin, nonivamide and trans-pellitorine decrease free fatty acid uptake without Trpv1 activation and increase acetyl-coenzyme a synthetase activity in caco-2 cells. *Food Funct.* 6 (1), 173–185. doi:10.1039/c4fo00435c

Sambaiah, K., and Satyanarayana, M. N. (1989). Effect of capsaicin on triglyceride accumulation and secretion in ethanol fed rats. *Indian J. Med. Res.* 90, 154–158.

Sánchez, B. G., Bort, A., Mora-Rodríguez, J. M., and Díaz-Laviada, I. (2022). The natural chemotherapeutic capsaicin activates ampk through Lkb1 kinase and Trpv1 receptors in prostate cancer cells. *Pharmaceutics* 14 (2), 329. doi:10.3390/pharmaceutics14020329

Santos, V. A. M., Bressiani, P. A., Zanotto, A. W., Almeida, I. V., Berti, A. P., Lunkes, A. M., et al. (2023). Cytotoxicity of capsaicin and its analogs *in vitro*. *Braz J. Biol.* 31 (83), 1519–6984. doi:10.1590/1519-6984.268941

Sanyal, A. J. (2019). Past, present and future perspectives in nonalcoholic fatty liver disease. *Nat. Rev. Gastroenterol. Hepatol.* 16 (6), 377–386. doi:10.1038/s41575-019-0144-8

Sarmiento-Machado, L. M., Romualdo, G. R., Zapaterini, J. R., Tablas, M. B., Fernandes, A. A. H., Moreno, F. S., et al. (2021). Protective effects of dietary capsaicin on the initiation step of a two-stage hepatocarcinogenesis rat model. *Nutr. Cancer* 73 (5), 817–828. doi:10.1080/01635581.2020.1764067

Seyithanoğlu, M., Öner-İyidoğan, Y., Doğru-Abbasoğlu, S., Tanrıkulu-Küçük, S., Koçak, H., Beyhan-Özdaş, Ş., et al. (2016). The effect of dietary curcumin and

capsaicin on hepatic fetuin-a expression and fat accumulation in rats fed on a high-fat diet. *Arch. Physiol. Biochem.* 122 (2), 94–102. doi:10.3109/13813455.2015.1120753

Shanmugham, V., and Subban, R. (2022). Comparison of the anti-obesity effect of enriched capsanthin and capsaicin from Capsicum annuum L. Fruit in obesity-induced C57bl/6j mouse model. *Food Technol. Biotechnol.* 60 (2), 202–212. doi:10.17113/ftb.60.02.22.7376

Sharma, S. K., Vij, A. S., and Sharma, M. (2013). Mechanisms and clinical uses of capsaicin. *Eur. J. Pharmacol.* 720 (1-3), 55–62. doi:10.1016/j.ejphar.2013.10.053

Shen, W., Shen, M., Zhao, X., Zhu, H., Yang, Y., Lu, S., et al. (2017). Anti-obesity effect of capsaicin in mice fed with high-fat diet is associated with an increase in population of the gut bacterium Akkermansia muciniphila. *Front. Microbiol.* 8 (272), 272. doi:10.3389/fmicb.2017.00272

Sheng, J., Zhang, B., Chen, Y., and Yu, F. (2020). Capsaicin attenuates liver fibrosis by targeting Notch signaling to inhibit TNF-α secretion from M1 macrophages. *Immunopharmacol. Immunotoxicol.* 42 (6), 556–563. doi:10.1080/08923973.2020.1811308

Shi, Y., Ma, J., Chen, K. E., and Chen, B. (2023). Konjac glucomannan enhances 5-fu-induced cytotoxicity of hepatocellular carcinoma cells via tlr4/perk/chop signaling to induce endoplasmic reticulum stress. *Oncol. Res.* 30 (4), 201–210. doi:10.32604/or.2022.027584

Shin, M. K., Yang, S. M., and Han, I. S. (2020). Capsaicin suppresses liver fat accumulation in high-fat diet-induced nafld mice. *Anim. Cells Syst.* 24 (4), 214–219. doi:10.1080/19768354.2020.1810771

Stravitz, R. T., and Lee, W. M. (2019). Acute liver failure. *Lancet* 394 (10201), 869–881. doi:10.1016/S0140-6736(19)31894-X

Sung, H., Ferlay, J., Siegel, R. L., Laversanne, M., Soerjomataram, I., Jemal, A., et al. (2021). Global cancer statistics 2020: globocan estimates of incidence and mortality worldwide for 36 cancers in 185 countries. *CA a cancer J. Clin.* 71 (3), 209–249. doi:10.3322/caac.21660

Sung, J., Yang, J., Kim, Y., Kim, M., Jeong, H. S., and Lee, J. (2016). Effect of defatted pepper (Capsicum annuum L.) seed extracts on high-fat diet-induced obesity in C57bl/6j mice. *Food Sci. Biotechnol.* 25 (5), 1457–1461. doi:10.1007/s10068-016-0226-0

Taghizadeh, M., Farzin, N., Taheri, S., Mahlouji, M., Akbari, H., Karamali, F., et al. (2017). The effect of dietary supplements containing green tea, capsaicin and ginger extracts on weight loss and metabolic profiles in overweight women: a randomized double-blind placebo-controlled clinical trial. *Ann. Nutr. Metab.* 70 (4), 277–285. doi:10.1159/000471889

Takai, S., and Jin, D. (2018). Chymase inhibitor as a novel therapeutic agent for non-alcoholic steatohepatitis. *Front. Pharmacol.* 9 (144), 144. doi:10.3389/fphar.2018.00144

Takaki, A., Kawai, D., and Yamamoto, K. (2013). Multiple hits, including oxidative stress, as pathogenesis and treatment target in non-alcoholic steatohepatitis (nash). *Int. J. Mol. Sci.* 14 (10), 20704–20728. doi:10.3390/ijms141020704

Tan, S., Gao, B., Tao, Y., Guo, J., and Su, Z. Q. (2014). Antiobese effects of capsaicin-chitosan microsphere (ccms) in obese rats induced by high fat diet. *J. Agric. Food Chem.* 62 (8), 1866–1874. doi:10.1021/jf4040628

Tang, D., Zhang, Q., Duan, H., Ye, X., Liu, J., Peng, W., et al. (2022). Polydatin: a critical promising natural agent for liver protection via antioxidative stress. *Oxid. Med. Cell. Longev.* 10, 9218738. doi:10.1155/2022/9218738

Tilg, H., Adolph, T. E., Dudek, M., and Knolle, P. (2021). Non-alcoholic fatty liver disease: the interplay between metabolism, microbes and immunity. *Nat. Metab.* 3 (12), 1596–1607. doi:10.1038/s42255-021-00501-9

Tilg, H., and Moschen, A. R. (2010). Evolution of inflammation in nonalcoholic fatty liver disease: the multiple parallel hits hypothesis. *Hepatology* 52 (5), 1836–1846. doi:10.1002/hep.24001

Wang, H., Chen, L., Shen, D., Cao, Y., Zhang, X., Xie, K., et al. (2021). Association between frequency of spicy food consumption and hypertension: a cross-sectional study in zhejiang province, China. *Nutr. Metab.* 18 (1), 70–00588. doi:10.1186/s12986-021-00588-7

Wang, P., Yan, Z., Zhong, J., Chen, J., Ni, Y., Li, L., et al. (2012). Transient receptor potential vanilloid 1 activation enhances gut glucagon-like peptide-1 secretion and improves glucose homeostasis. *Diabetes* 61 (8), 2155–2165. doi:10.2337/db11-1503

Wang, Y., Tang, C., Tang, Y., Yin, H., and Liu, X. (2020). Capsaicin has an anti-obesity effect through alterations in gut microbiota populations and short-chain fatty acid concentrations. *Food Nutr. Res.* 64 (19). doi:10.29219/fnr.v64.3525

Wang, Z., Du, K., Jin, N., Tang, B., and Zhang, W. (2023). Macrophage in liver fibrosis: identities and mechanisms. *Int. Immunopharmacol.* 120 (110357), 110357. doi:10.1016/j.intimp.2023.110357

Waziri, P. M., Abdullah, R., Rosli, R., Omar, A. R., Abdul, A. B., Kassim, N. K., et al. (2018). Clausenidin induces caspase 8-dependent apoptosis and suppresses production of vegf in liver cancer cells. *Asian Pac J. Cancer Prev.* 19 (4), 917–922. doi:10.22034/APJCP.2018.19.4.917

Wikan, N., Tocharus, J., Oka, C., Sivasinprasasn, S., Chaichompoo, W., Suksamrarn, A., et al. (2023). The capsaicinoid nonivamide suppresses the inflammatory response and attenuates the progression of steatosis in a nafld-rat model. *J. Biochem. Mol. Toxicol.* 37 (3), 21. doi:10.1002/jbt.23279

Wikan, N., Tocharus, J., Sivasinprasasn, S., Kongkaew, A., Chaichompoo, W., Suksamrarn, A., et al. (2020). Capsaicinoid nonivamide improves nonalcoholic fatty liver disease in rats fed a high-fat diet. *J. Pharmacol. Sci.* 143 (3), 188–198. doi:10.1016/j.jphs.2020.03.008

Wu, Q., Bai, P., Guo, H., Guo, M. S. S., Xia, Y., Xia, Y., et al. (2022). Capsaicin, a phytochemical from chili pepper, alleviates the ultraviolet irradiation-induced decline of collagen in dermal fibroblast via blocking the generation of reactive oxygen species. *Front. Pharmacol.* 13, 872912. doi:10.3389/fphar.2022.872912

Wu, S., Pan, H., Tan, S., Ding, C., Huang, G., Liu, G., et al. (2017). *In vitro* inhibition of lipid accumulation induced by oleic acid and *in vivo* pharmacokinetics of chitosan microspheres (ctms) and chitosan-capsaicin microspheres (ccms). *Food Nutr. Res.* 61 (1), 1331658. doi:10.1080/16546628.2017.1331658

Xie, C., Liu, G., Li, M., Fang, Y., Qian, K., Tang, Y., et al. (2019). Targeting Trpv1 on cellular plasticity regulated by ovol 2 and zeb 1 in hepatocellular carcinoma. *Biomed. Pharmacother.* 118 (109270), 109270. doi:10.1016/j.biopha.2019.109270

Xie, Z. Q., Li, H. X., Hou, X. J., Huang, M. Y., Zhu, Z. M., Wei, L. X., et al. (2022). Capsaicin suppresses hepatocarcinogenesis by inhibiting the stemness of hepatic progenitor cells via sirt1/sox2 signaling pathway. *Cancer Med.* 11 (22), 4283–4296. doi:10.1002/cam4.4777

Yip, T. C., Fan, J. G., and Wong, V. W. (2023). China's fatty liver crisis: a looming public health emergency. *Gastroenterology* 165 (4), 825–827. doi:10.1053/j.gastro.2023.06.008

Yu, F. X., Teng, Y. Y., Zhu, Q. D., Zhang, Q. Y., and Tang, Y. H. (2014b). Inhibitory effects of capsaicin on hepatic stellate cells and liver fibrosis. *Biochem. Cell. Biol.* 92 (5), 406–412. doi:10.1139/bcb-2014-0036

Yu, Y., Wang, X., and Nyberg, S. L. (2014a). Application of induced pluripotent stem cells in liver diseases. *Cell. Med.* 7 (1), 1–13. doi:10.3727/215517914X680056

Yuan, L. J., Qin, Y., Wang, L., Zeng, Y., Chang, H., Wang, J., et al. (2016). Capsaicin-containing chili improved postprandial hyperglycemia, hyperinsulinemia, and fasting lipid disorders in women with gestational diabetes mellitus and lowered the incidence of large-for-gestational-age newborns. *Clin. Nutr.* 35 (2), 388–393. doi:10.1016/j.clnu.2015.02.011

Zhan, X., Zhang, J., Chen, H., Liu, L., Zhou, Y., Zheng, T., et al. (2020). Capsaicin alleviates acetaminophen-induced acute liver injury in mice. *Clin. Immunol.* 220 (108578), 108578. doi:10.1016/j.clim.2020.108578

Zhang, Q., Luo, P., Xia, F., Tang, H., Chen, J., Zhang, J., et al. (2022a). Capsaicin ameliorates inflammation in a trpv1-independent mechanism by inhibiting pkm2-ldha-mediated Warburg effect in sepsis. *Cell. Chem. Biol.* 29 (8), 1248–1259.e6. doi:10.1016/j.chembiol.2022.06.011

Zhang, S., Ma, X., Zhang, L., Sun, H., and Liu, X. (2017). Capsaicin reduces blood glucose by increasing insulin levels and glycogen content better than capsiate in streptozotocin-induced diabetic rats. *J. Agric. Food Chem.* 65 (11), 2323–2330. doi:10.1021/acs.jafc.7b00132

Zhang, S., Wang, D., Huang, J., Hu, Y., and Xu, Y. (2020). Application of capsaicin as a potential new therapeutic drug in human cancers. *J. Clin. Pharm. Ther.* 45 (1), 16–28. doi:10.1111/jcpt.13039

Zhang, S., and Zhou, D. (2019). Role of the transcriptional coactivators yap/taz in liver cancer. *Curr. Opin. Cell. Biol.* 61, 64–71. doi:10.1016/j.ceb.2019.07.006

Zhang, S. S., Ni, Y. H., Zhao, C. R., Qiao, Z., Yu, H. X., Wang, L. Y., et al. (2018). Capsaicin enhances the antitumor activity of sorafenib in hepatocellular carcinoma cells and mouse xenograft tumors through increased erk signaling. *Acta Pharmacol. Sin.* 39 (3), 438–448. doi:10.1038/aps.2017.156

Zhang, W. S., Zhang, R., Ge, Y., Wang, D., Hu, Y., Qin, X., et al. (2022b). S100a16 deficiency prevents hepatic stellate cells activation and liver fibrosis via inhibiting Cxcr4 expression. *Metabolism* 135 (155271), 155271. doi:10.1016/j.metabol.2022.155271

Zhao, Z., Li, M., Li, C., Wang, T., Xu, Y., Zhan, Z., et al. (2020). Dietary preferences and diabetic risk in China: a large-scale nationwide internet data-based study. *J. Diabetes* 12 (4), 270–278. doi:10.1111/1753-0407.12967

frontiers | Frontiers in Pharmacology

TYPE Original Research
PUBLISHED 02 October 2024
DOI 10.3389/fphar.2024.1433076

OPEN ACCESS

EDITED BY
Rongrui Wei,
Jiangxi University of Traditional Chinese Medicine, China

REVIEWED BY
Feng Zhang,
Nanjing University of Chinese Medicine, China
Xie-an Yu,
Shenzhen Institute For Drug Control, China

*CORRESPONDENCE
Linlin Lu,
lulinlin2007@hotmail.com
Yongning Xin,
xinyongning@163.com

RECEIVED 15 May 2024
ACCEPTED 16 September 2024
PUBLISHED 02 October 2024

CITATION
Chu X, Liu S, Qu B, Xin Y and Lu L (2024) Salidroside may target PPARα to exert preventive and therapeutic activities on NASH. *Front. Pharmacol.* 15:1433076. doi: 10.3389/fphar.2024.1433076

Salidroside may target PPARα to exert preventive and therapeutic activities on NASH

Xueru Chu[1,2], Shousheng Liu[3], Baozhen Qu[4], Yongning Xin[1,2]* and Linlin Lu[4]*

[1]Department of Infectious Disease, Qingdao Municipal Hospital, School of Medicine and Pharmacy, Ocean University of China, Qingdao, China, [2]Department of Infectious Disease, Qingdao Municipal Hospital, Qingdao, China, [3]Clinical Research Center, Qingdao Municipal Hospital, University of Health and Rehabilitation Sciences, Qingdao, China, [4]Qingdao Cancer Prevention and Treatment Research Institute, Qingdao Central Hospital, University of Health and Rehabilitation Sciences, Qingdao, China

Background: Salidroside (SDS), a phenylpropanoid glycoside, is an antioxidant component isolated from the traditional Chinese medicine *Rhodiola rosea* and has multifunctional bioactivities, particularly possessing potent hepatoprotective function. Non-alcoholic steatohepatitis (NASH) is one of the most prevalent chronic liver diseases worldwide, but it still lacks efficient drugs. This study aimed to assess the preventive and therapeutic effects of SDS on NASH and its underlying mechanisms in a mouse model subjected to a methionine- and choline-deficient (MCD) diet.

Methods: C57BL/6J mice were fed an MCD diet to induce NASH. During or after the formation of the MCD-induced NASH model, SDS (24 mg/kg/day) was supplied as a form of diet for 4 weeks. The histopathological changes were evaluated by H&E staining. Oil Red O staining and Sirius Red staining were used to quantitatively determine the lipid accumulation and collagen fibers in the liver. Serum lipid and liver enzyme levels were measured. The morphology of autophagic vesicles and autophagosomes was observed by transmission electron microscopy (TEM), and qRT-PCR and Western blotting were used to detect autophagy-related factor levels. Immunohistochemistry and TUNEL staining were used to evaluate the apoptosis of liver tissues. Flow cytometry was used to detect the composition of immune cells. ELISA was used to evaluate the expression of serum inflammatory factors. Transcript–proteome sequencing, molecular docking, qRT-PCR, and Western blotting were performed to explore the mechanism and target of SDS in NASH.

Results: The oral administration of SDS demonstrated comprehensive efficacy in NASH. SDS showed both promising preventive and therapeutic effects on NASH *in vivo*. SDS could upregulate autophagy, downregulate apoptosis, rebalance immunity, and alleviate inflammation to exert anti-NASH properties. Finally, the results of transcript–proteome sequencing, molecular docking evaluation, and experimental validation showed that SDS might exert its multiple effects through targeting PPARα.

Conclusion: Our findings revealed that SDS could regulate liver autophagy and apoptosis, regulating both innate immunity and adaptive immunity and alleviating inflammation in NASH prevention and therapy via the PPAR pathway, suggesting that SDS could be a potential anti-NASH drug in the future.

KEYWORDS

salidroside, non-alcoholic steatohepatitis, prevention, therapy, immunity, inflammation, PPARα

1 Introduction

Non-alcoholic fatty liver disease (NAFLD) is the most common chronic liver disease with the prevalence increasing yearly, affecting the health of both adults and children (Younossi et al., 2018). NAFLD is a clinicopathologic syndrome characterized by excessive fat deposition in hepatocytes caused by alcohol and other specific liver damaging factors and an acquired metabolic stress liver injury closely related to insulin resistance and genetic susceptibility. NAFLD consists of a series of hepatic abnormalities extending from a non-alcoholic fatty liver (NAFL) to non-alcoholic steatohepatitis (NASH) with possible developments of liver fibrosis, cirrhosis, and liver cancer (Qu et al., 2022). NASH is considered a hallmark of the progression and deterioration of NAFLD and is characterized by hepatic steatosis, liver cell damage, innate immune cell-mediated inflammation, and varying degrees of fibrosis. The "two-hit" mechanism is the most widely accepted theory to explain the development of NAFLD to NASH. The first hit is mainly caused by the excessive accumulation of lipids in the liver, which is closely associated with mitochondrial disorders caused by lipotoxicity, making the liver sensitive to the second hit. The second hit is related to a combination of inflammatory response, oxidative stress, liver damage, and fibrosis (Gu et al., 2023). Without intervention, the continuous mechanisms of tissue damage and regeneration typical of NASH chronic inflammation can progress to liver fibrosis, cirrhosis, or even hepatocellular carcinoma (Motta et al., 2023). The prevalence of NAFLD among the general population is approximately 20%–25%, whereas the prevalence of NASH is expected to increase by up to 56% by 2030 in China, Europe, Japan, the United Kingdom, and the United States (Motta et al., 2023; Llovet et al., 2023). Recent studies indicated that 20% of the patients with NAFLD histologically show NASH in biopsy specimens (Han S. K. et al., 2023). Due to the increasing prevalence of NASH, it is considered the second most common cause of liver transplantation in the United States after chronic hepatitis C (Aldossari, 2023). The annual incidence of hepatocellular carcinoma (HCC) in patients with NASH-related cirrhosis is about 2%, and about 35%–50% of HCC in NASH occurs in patients with cirrhosis and before routine cancer screening (Llovet et al., 2023; Liu and Chien, 2023). Overall, NASH is associated with an increased risk of HCC and mortality and is expected to become the leading cause of HCC worldwide by 2030 (Quek et al., 2023). However, there are currently no approved preventive treatments or treatments for NASH beyond lifestyle changes (Harrison et al., 2023). NASH is strongly associated with metabolic disorders and obesity. At present, dietary intervention is considered one of the main strategies to prevent NASH, and the development of safe and effective NASH drugs has long-term social and economic significance.

It is well-known that traditional herbal medicines have been used for centuries to cure people with many diseases, and they are essential sources for originating hepatoprotective drugs. Several therapeutic candidate drugs, such as silymarin and berberine, have been selected and verified from these traditional herbs, and they have been in the fourth phase of clinical research for the treatment of NAFLD (Yan et al., 2020). *Rhodiola rosea* (*hong jing tian* in Chinese) is a prestigious plant used in Chinese traditional medicine application for its hepatoprotective and neuroprotective function. Salidroside (SDS), a phenylpropanoid glycoside, is an antioxidant component isolated from *R. rosea* (Fan et al., 2020). Numerous studies have shown that SDS possesses anti-hypoxia, anti-fatigue, anti-viral, anti-cancer, anti-inflammatory, immune-balancing, and lipid-lowering effects, glucose and lipid metabolism improvement, and many other properties both *in vitro* and *in vivo* (Gao et al., 2023; Hu et al., 2021; Rong et al., 2020). In terms of hepatoprotective function, SDS has a protective effect on various types of liver injury, such as alleviating chemical liver injury through the Sirt1-mediated Akt/Nrf2 pathway (Xu et al., 2023), improving inflammation in alcohol-induced liver injury through TLR4/TAK1 (Sun et al., 2016), regulating GSK-3β/Nrf2 to protect against liver ischemia–reperfusion injury (Cai et al., 2017), facilitating the MIF pathway and downstream hippophagia and lipid metabolism to remission NAFLD (Liu et al., 2022), activating the AMP to suppress NASH in mice (Hu et al., 2021), preventing immune-mediated hepatitis in mice (Hu et al., 2014), alleviating liver fibrosis through the NF-κB and TGF-β1/Smad3 pathway (Feng et al., 2018), and inhibiting the activation of the Notch1 signaling pathway to inhibit liver malignant tumor (Lu et al., 2019). However, few studies have investigated the efficacy of the dietary intake of SDS on the prevention and therapy of NASH, and the immune-boosting effects of SDS on NASH are poorly understood. As mentioned above, the "two-hit" mechanism leads to liver lipid accumulation, lipid toxicity, inflammatory response, cell apoptosis, and fibrosis, which are the main reasons for the progression of NASH. In addition, the innate and adaptive immune responses involved in NASH are other important factors promoting liver inflammation and cell injury (Tilg and Moschen, 2010). Hence, exploring an ideal drug that can regulate multiple pathogenetic pathways of NASH will contribute to achieving an effective therapy response to NASH.

Peroxisome proliferator-activated receptors (PPARs) are ligand-activated transcription factors belonging to the nuclear hormone receptor superfamily, which are proven effective therapeutic targets for NASH treatment. There are three identified isoforms of PPARs (α, β/δ, and γ), all of which are involved in lipid metabolism and glucose homeostasis in NAFLD/NASH (Montagner et al., 2016). In addition, PPARs exist in different types of immune cells and may modulate both hepatic and systemic inflammatory responses (Staels et al., 2023).

Thus, PPARs can simultaneously regulate different interrelated mechanisms of NASH pathogenesis due to their regulating whole-body lipid and glucose metabolism and inflammation functions.

In this study, we first investigated and evaluated the potential preventive and protective effects of the dietary administration of SDS in a mouse model of NASH induced by a methionine- and choline-deficient (MCD) diet and then explored the molecular mechanism and target of SDS by transcriptome–proteome sequencing, molecular docking, Western blotting, and qRT-PCR. The results revealed that SDS might target PPARα to regulate autophagy and apoptosis, enhancing immunity and alleviating inflammation, to exert preventive and therapeutic activities on NASH.

2 Materials and methods

2.1 Animals and treatment

All animal experimental procedures were approved by the Institutional Animal Care and Use Committee of the Ocean University of China (approval number: OUC-SMP-2024-04-01). Specific pathogen-free male C57BL/6J mice (7 weeks of age) were purchased from Beijing Weitong Lihua Experimental Animal Technology Co., Ltd. (China), housed in a 23°C–25°C environment with a light–dark cycle of 12 h, and given shredded wood flour bedding for social activity.

The mice were randomly divided into four groups: (1) mice of control groups (n = 15) were fed with a controlled diet (complete semisynthetic column diet containing 18% crude proteins and 5% cellulose, following the Chinese Association for Laboratory Animal Sciences); (2) mice of the MCD group (n = 15) were fed an MCD diet (a diet composed of high sucrose (40%) and fat (10%) but without methionine and choline), which is a classical used nutritional model of NASH; (3) a mouse group (n = 15) was fed an MCD diet supplemented with SDS at a dose of 24 mg/kg of body weight continuously for 28 days to study the preventive effect of SDS during NASH formation (MCD-SP); and (4) a NASH mouse model (MCD-induced) group (n = 15) was fed the controlled diet and SDS at a dose of 24 mg/kg of body weight for 28 days to study the therapeutic effect of SDS on NASH (MCD-ST). SDS was dissolved in distilled water (24 mg/mL). An aliquot portion of the SDS solution (correlated with each mouse's body weight) was administered via gavage. Fresh mineral water in drinking bottles was replaced daily. Throughout the study period, all mice had free access to diet and water. Body weights were measured and recorded every week. At the end of the study, 4 weeks for the control, MCD, and MCD-SP groups or 8 weeks for the MCD-ST group, the mice were fasted overnight and euthanized using pentobarbital. Blood and livers were sampled. Serum samples were centrifuged at 4°C (3,000 rpm, 15 min). The serum and liver (after measuring and photographing) were frozen in liquid nitrogen and stored at −80°C until analysis.

2.2 Serum and hepatic biochemical indicators

The serum lipid profiles, including triglyceride (TG), total cholesterol (TC), and liver functional measures of the levels of serum aspartate aminotransferase (AST) and alanine aminotransferase (ALT), were quantified using commercial kits (Nanjing Jiancheng Institute of Bioengineering, China), following the manufacturer's instructions. The serum concentrations of pro-inflammatory cytokines, such as tumor necrosis factor α (TNF-α), interleukin-2 (IL-2), interleukin-10 (IL-10), and interleukin-17 (IL-17), were determined using sandwich enzyme-linked immunosorbent assay (ELISA) kits (Shanghai Enzyme-linked Biotechnology, China), according to the manufacturer's instructions. Individual liver tissue samples (10 mg each) were homogenized in 90 μL of anhydrous ethanol in a Potter–Elvehjem tissue homogenizer and centrifuged at 2,500 × g for 10 min to obtain the liver tissue extract. The concentrations of TG and TC in the liver were quantified using commercial kits (Nanjing Jiancheng Institute of Bioengineering, China), following the manufacturer's instructions.

2.3 Histological analysis

Here, 5-μm paraffin-embedded liver sections were stained with hematoxylin and eosin (H&E) staining and Sirius red after fixing in 4% paraformaldehyde at 4°C overnight, which was then embedded in paraffin and dehydrated. Then, 5-μm frozen liver sections were stained with Oil Red O solution in 60% isopropanol after embedding in the optimum cutting temperature compound (Tissue-Tek, Laborimpex). Images were obtained using an optical microscope (Olympus, BX51, Tokyo, Japan). Then, the sum of NAFLD activity scores (NASs) was used to determine the severity of NASH. The NAS system mainly included a semi-quantitative analysis of three pathological features of the liver: lobular inflammation (0–3), hepatic steatosis (0–3), and ballooning (0–2). The sum of the three scores was the NAS. NAS of ≥5 was diagnosed as NASH; NAS between 3 and 4 was NASH suspected; and NAS <3 was not diagnosed as NASH (Han Y. et al., 2023).

For immunohistochemistry (IHC) analysis, the paraffin-embedded liver sections were dewaxed and sequentially incubated with an anti-B-cell lymphoma-2 (BCL-2) primary antibody (1:200; abs131701, Absin, China), anti-BCL-2-Associated X Protein (BAX) primary antibody (1:50; A5131, Selleck, China), and anti-nuclear factor kappa-light-chain-enhancer of activated B cell (NF-κB) primary antibody (1:500; 8242T, CST, China) at 4°C overnight. On the following day, the slides were incubated with a biotinylated secondary antibody (Proteintech, Wuhan, China) at room temperature for 1 h. Positive staining was detected using a 3,3′diaminobenzidine chromogenic reagent, and then, all sections were counterstained with hematoxylin. Immunohistochemistry images were acquired using an optical microscope (Olympus, BX51, Tokyo, Japan).

2.4 Transmission electron microscopy

The autophagosomes of liver tissues were observed by transmission electron microscopy (TEM). Parts of the liver were fixed with 1.25% glutaraldehyde for 1 day and then post-fixed in 1% osmium tetroxide for 1 h. Dehydration was done in a

TABLE 1 Forward and reverse primer sequences for qRT-PCR.

Primer	Forward sequence	Reverse sequence
GAPDH	GTGAAGGTCGGTGTGAACGG	GTGATGGCATGGACTGTGGTC
TNF-α	GCCACCACGCTCTCTCTG	GGTGTGGGTGAGGAGCA
IL-2	AAAAGCTTTCAATTGGAAGATGCTG	TTGAGGGCTTGTGTGAGATGA
IL-17	TTTAACTCCCTTGGCGCAAAA	CTTTCCCTCCGCATTGACAC
IL10	GCCTTATCGGAAATGATCCA	AGGGGAGAAATCGATGACAG
p62	AGTGATGAGGAGCTGACAATGGCT	GCCAGCCAAAGTGTCCATGTTTCA
LC3	TAGGCACCCACATAGGGTATTA	CTACAACACCAGACCTGCTTAG
PPARα	AGAGCCCCATCTGTCCTCTC	ACTGGTAGTCTGCAAAACCAAA

concentration gradient of ethanol, followed by propylene oxide. When incubated in 70% ethanol, the pellet was stained embolic with 1% uranyl acetate. Finally, the pellet was embedded in EPON resin. Ultrathin sections were post-stained with uranyl acetate and Reynold's lead citrate routinely. Electron micrographs were taken using a transmission electron microscope at 80 kV (JEM-1400Flash, Tokyo, Japan).

2.5 Quantitative real-time PCR

The total RNA was extracted from the mouse liver tissues using the MolPure® TRIeasy™ Plus Total RNA Kit (Yeasen, Shanghai, China). The cDNA was reverse-transcribed using a FastKing RT SuperMix kit (TIANGEN, Beijing, China), following the manufacturer's protocol. Furthermore, quantitative real-time PCR (qRT-PCR) was performed using the Bio-Rad Laboratories CFX Connect™ Real-Time PCR Detection System using Fast SYBR Green Master Mix (Yeasen, Shanghai, China). The results were quantified by the $2^{-\Delta\Delta CT}$ method relative to the housekeeping gene actin. The primer pairs are listed in Table 1.

2.6 Western blotting

Liver tissues were ground using a grinding machine (KZ-II, Servicebio, Wuhan, CN) and then lysed in a radioimmunoprecipitation assay buffer containing a protease inhibitor (Beyotime, Shanghai, China) to extract the protein. After sodium dodecyl sulfate polyacrylamide gel electrophoresis, the proteins were transferred to 0.45-μm-pore polyvinylidene fluoride membranes (Millipore, MA, United States). After blocking with 5% non-fatty dry milk, the membranes were incubated with primary antibodies against sequestosome-1 (p62) (1:1,000, 5114T, CST, United States), microtubule-associated protein-1 light-chain 3 (LC3) A/B (1:1,000, 12741T, CST, United States), PPARα (1:1,000, 66826-1-Ig, Proteintech, China), and β-actin (1:5,000, 81115-1-RR, Proteintech, China) (Wang et al., 2022). Following the incubation of HRP-labeled goat anti-rabbit IgG (1:5,000, Proteintech, China) or goat anti-mouse IgG (1:5,000, Proteintech, China), the bands were analyzed using the gel documentation system (Bio-Rad, CA, United States).

2.7 TdT-mediated dUTP nick-end labeling staining

Apoptosis of liver tissues was detected using a TdT-mediated dUTP nick-end labeling (TUNEL) staining kit (Roche, Basel, Switzerland). In brief, the mouse liver tissues were cut into sections. Next, these sections were deparaffinized. After that, the sections were permeabilized with 0.2% Triton X-100 for 10 min at room temperature and then stained with 50 μM TUNEL reagent for 1 h at 37°C in the dark. Then, 4′-6-diamino-2-phenylindole (Sigma-Aldrich, St. Louis, MO, United States) was used to stain the cell nuclei for 20 min in the dark. Finally, the positive cells were visualized and counted under a fluorescence microscope (Leica, Wetzlar, Germany).

2.8 Flow cytometry

Intrahepatic immune cells and spleen immune cells were separated from the perfused liver and spleen by enzyme digestion and density gradient centrifugation. Subsequently, anti-CD4 (67786-1-Ig, Proteintech, China) and anti-IL-17 (66148-1-Ig, Proteintech, China) of T helper 17 (Th17) cells were double-labeled; anti-CD3 (17617-1-AP, Proteintech, China) and anti-CD4 of T helper cells were detected by double-labeling; anti-CD3 and anti-CD8 (sc-53063, Santa, United States) of killer T cells were detected by double-labeling; anti-CD4, anti-CD25 (E-AB-F1194C, Elabscience, China), and anti-Foxp3 (12653S, CST, United States) were detected by regulatory T cells (Tregs); anti-CD16 (E-AB-F1236C, Elabscience, China) and anti-CD56 (14255-1-AP, Proteintech, China) of natural killer (NK) cells were double-labeled; anti-CD11b (66519-1-Ig, Proteintech, China) of macrophages was single-labeled; and anti-CD19 (66298-1-Ig, Thermo Fisher, United States) and anti-CD268 (14-9,117-82, Proteintech, China) of B cells were double-labeled. The cells were added to the cell suspension in PBS for 1 h at room temperature. After washing with PBS three times, a secondary fluorescein isothiocyanate (FITC)-conjugated anti-mouse antibody (E-AB-1088, Elabscience, China) or FITC-conjugated anti-rabbit antibody (E-AB-1111, Elabscience, China) was added for further incubation at 4°C for 1 h in dark. The cells were analyzed by flow cytometry using a BD FACSCalibur instrument. Data were analyzed using FlowJo software (v10.2; FlowJo, LLC, Ashland, OR, United States).

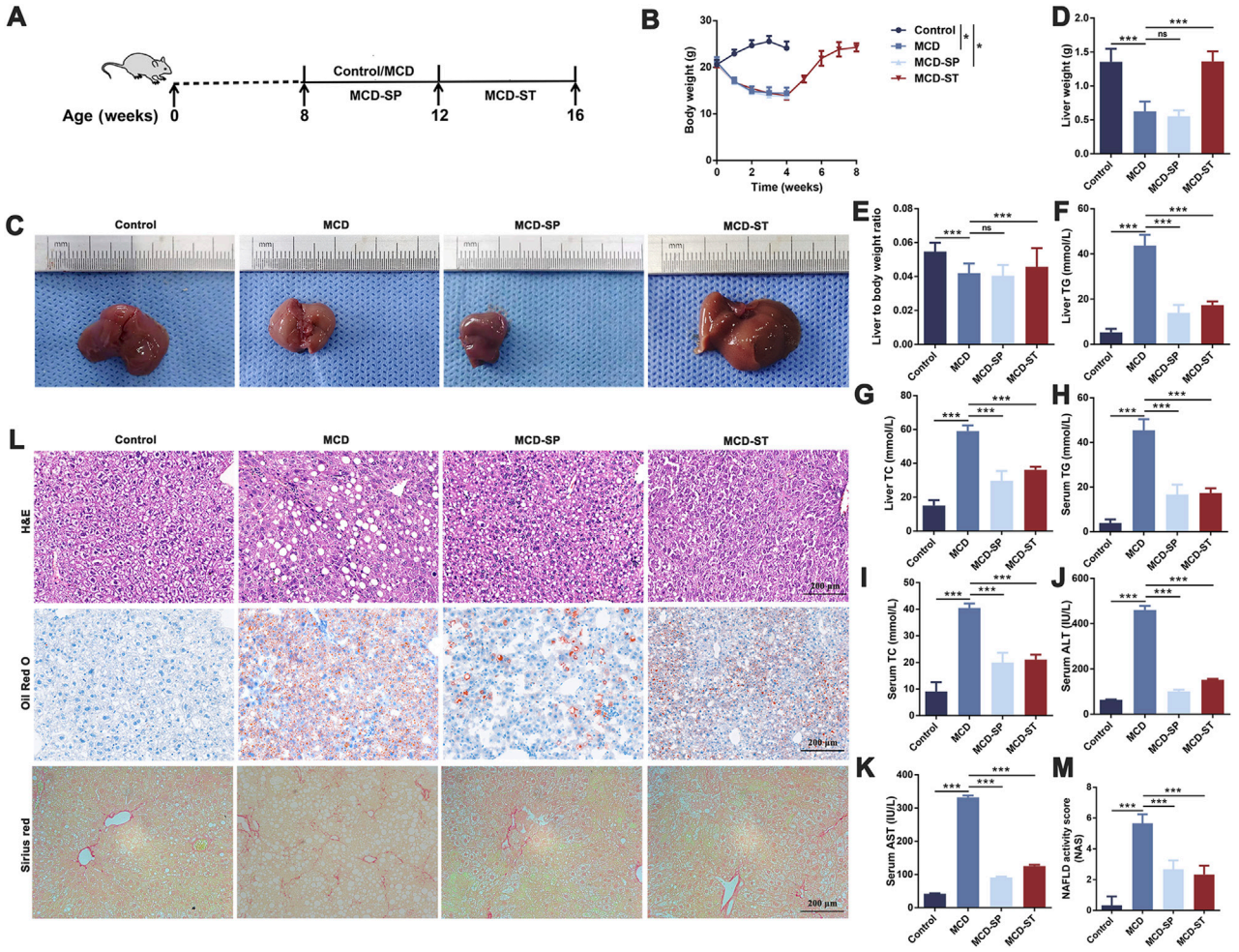

FIGURE 1
SDS significantly inhibited the formation of NASH and had a significant therapeutic effect on the mouse NASH model. **(A)** Schematic diagram of the control, MCD, MCD-SP, and MCD-ST mouse models. **(B)** Changes in the body weight of mice. **(C)** Image of the mouse liver. **(D)** Mouse liver weight. **(E)** Mouse liver-to-body weight ratio. **(F)** Mouse liver TG. **(G)** Mouse liver TC. **(H)** Mouse serum TG. **(I)** Mouse serum TC. **(J)** Mouse serum TG. **(K)** Mouse serum AST. **(L)** H&E, Oil Red O, and Sirius Red staining of liver sections from the indicated groups of mice. Scale bar = 200 μm. **(M)** NAFLD activity score (NAS). NAS is the sum of the steatosis, inflammation, and ballooning score. Data were representative of one or three independent experiments with n = 6 per group. Data were analyzed by Student's *t*-test and expressed as the mean ± SEM. $*p < 0.05$ and $***p < 0.001$; ns, no significance. Control group, MCD group, MCD-SP group, and MCD-ST group. Control, normal diet-fed mice; MCD, MCD-fed mice; MCD-SP, MCD with 24 mg/kg/d of SDS; MCD-ST, NASH model mice were fed with the control diet with 24 mg/kg/d of SDS.

2.9 Transcriptomic analysis

Three liver samples in each group, including the MCD, MCD-SP, and MCD-ST groups, were subjected to total RNA extraction using the RNAiso Plus reagent (9109, TaKaRa, Japan). The RNA sample was checked for a RIN to inspect the RNA integrity using the Bioanalyzer 2100 system (Agilent Technologies, Santa Clara, CA, United States). The qualified total RNA was further purified using an RNAClean XP Kit (A63987, Beckman Coulter, Inc., Kraemer Boulevard Brea, CA, United States) and RNase-Free DNase Set (79254, QIAGEN GmBH, Germany). Sequencing libraries were prepared using the VAHTS mRNA-seq v2 Library Prep Kit (Illumina, United States). The concentration and size of libraries were detected using a Qubit® 2.0 Fluorometer (Life Technologies, United States) and the Agilent Bioanalyzer 2100 system, respectively. After cluster generation and first-way sequencing primer hybridization, the cDNA libraries were sequenced on the Illumina NovaSeq 6000 platform (Illumina, United States), and paired-end reads were generated. Raw read data in fastq format were filtered using Seqtk software to remove the adaptor sequence and low-quality sequence reads. Clean reads were mapped to the genome using HISAT2 (v2.0.4). StringTie (v1.3.0) was used to calculate the fragments of each gene after mapping. The quantification of the gene expression level was estimated as fragments per kilobase of exon model per million mapped reads.

2.10 Proteomic analysis

Next, 300 μL of 8 M urea was added to the liver tissues, and the protease inhibitor was added at 10% of the lysate for proteomic

sequencing. After centrifuging at 14,100 × g for 20 min, the supernatant was collected for protein extraction. The protein concentration was determined using the Bradford method, and the remaining sample was frozen at −80°C.

Next, the protein was digested and desalinated. A 100-μg aliquot of extracted proteins from each sample was then subjected to reduction. The sample was diluted four times by adding 25 mM ammonium bicarbonate buffer after adding 200 mM dithiothreitol solution and incubating at 37°C for 1 h. Then, trypsin was added to the sample (trypsin:protein = 1:50) and incubated at 37°C overnight, and 50 μL 0.1% formic acid (FA) was added to terminate digestion in the next day. Then, 100 μL 100% acetonitrile (ACN) was used to wash the C18 column, and the column was centrifuged at 1,200 rpm for 3 min. The column was washed once with 100 μL of 0.1% FA and centrifuged at 1,200 rpm for 3 min and then transferred to the new EP tubes and centrifuged at 1,200 rpm for 3 min. The column was washed twice with 100 μL of 0.1% FA and centrifuged at 1,200 rpm for 3 min. Then, the column was washed once with 100 μL of pH 10 water and transferred to the new EP tubes and eluted with 70% ACN. The eluents of each sample were combined, lyophilized, and stored at −80°C until loading.

For spectral library generation, samples were fractionated using a high-pH reversed-phase fractionator, as previously described and measured in the data-dependent acquisition (DDA) mode. In brief, the mass spectrometer was operated on a quadrupole Orbitrap mass spectrometer (Q Exactive HF-X, Thermo Fisher Scientific, Bremen, Germany) coupled to an EASY nLC 1200 ultra-high pressure system (Thermo Fisher Scientific) via a nano-electrospray ion source. Then, 500 ng of peptides were loaded on a 25-cm column (150-μm inner diameter, packed using ReproSil-Pur C18-AQ 1.9-μm silica beads). The peptides were separated using a gradient of 8%–12% B in 7 min, then 12%–30% B in 48 min, and stepped up to 40% in 10 min, followed by a 15-min wash at 95% B at 600 mL per minute where solvent A was 0.1% FA in water and solvent B was 80% ACN and 0.1% FA in water. The total duration of the run was 80 min. The column temperature was maintained at 60°C using an in-house-developed oven. In brief, the mass spectrometer was operated in the "top-40" data-dependent mode, collecting MS spectra using the Orbitrap mass analyzer (120,000 resolution, 350–1,500 m/z range) with an automatic gain control (AGC) target of 3E6 and a maximum ion injection time of 80 ms. The most intense ions from the full scan were isolated with an isolation width of 1.6 m/z. Following higher-energy collisional dissociation with a normalized collision energy of 27, the MS/MS spectra were collected in the Orbitrap (15,000 resolution) with an AGC target of 5E4 and a maximum ion injection time of 45 ms. Precursor dynamic exclusion was enabled with a duration of 16 s. For data-independent acquisition (DIA), the acquisition method consisted of one MS1 scan (350–1,500 m/z, resolution 60,000, maximum injection time 50 ms, and AGC target 3E6) and 42 segments at varying isolation windows from 14 m/z to 312 m/z (resolution 30,000, maximum injection time 54 ms, and AGC target 1E6). The stepped normalized collision energy was 25, 27.5, and 30. The default charge state for MS2 was set to 3.

The MS data on the fractionated pools (DDA MS data, six fractions) and the single-shot samples (DIA MS data) were used to generate a DDA library and direct-DIA library, respectively, which were computationally merged into a hybrid library in Spectronaut software (Biognosys, version 15.7.220308.50606). The hybrid spectral library was used to search the MS data on the single-shot samples in Spectronaut software for the final protein identification and quantitation. Carbamidomethylation was used as the fixed modification and acetylation of the protein N-terminus, while the oxidation of methionine was used as variable modifications. Default settings were used for other parameters. In brief, a trypsin/P proteolytic cleavage rule was used, permitting a maximum of two miscleavages and a peptide length of 7–52 amino acids. Protein intensities were normalized using the "Local Normalization" algorithm in Spectronaut based on a local regression model. Spectral library generation stipulated a minimum of three fragments per peptide, and maximally, the six best fragments were included. A protein and precursor false discovery rate of 1% was used, and protein quantities were reported in samples only if the protein passed the filter ("Q-value sparse" mode data filtering).

Gene Ontology (GO) analysis was conducted using the InterProScan-5 program against the non-redundant protein database, and the Kyoto Encyclopedia of Genes and Genomes (KEGG) was used to analyze the protein family and pathway.

2.11 Network pharmacology prediction analysis

The SMILES structure of SDS was obtained using the ChemSpider database (http://www.chemspider.com/) and was introduced into the SwissTargetPrediction online target screening platform (http://www.swisstargetprediction.ch/) to obtain the predicted target information on SDS.

The DisGeNET database (http://www.disgenet.org/) was used to obtain targets related to NASH by using "Non-alcoholic steatohepatitis" as a keyword. The obtained relevant targets were imported into the UniProt (https://www.uniprot.org/) database to correct the target information.

The SDS responding targets and the NASH responding targets were intersected in Draw Venn Diagram (http://bioinformatics.psb.ugent.be/webtools/Venn/), and the intersection targets were obtained, which were the SDS targets of treating NASH. The obtained intersection targets were imported into the STRING database protein–protein interaction (PPI) network, where nodes represent target proteins and edges represent interactions between nodes. PPI network information obtained was saved as a TSV file and imported into the network topology attribute analysis software application Cytoscape to build an SDS-NASH target network. Then, the Network Analyzer function in this software program analyzed the network topology to obtain the degree value of each node, which reflected the importance of SDS-NASH targets in the network based on the degree value.

Molecular docking between SDS and the top five target proteins of SDS in the treatment of NASH was verified using AutoDockTools software. The 2D structure of SDS was downloaded from the ChemSpider database and imported into Chem3D software in mol format, and the mechanical structure was optimized to export in mol2 format. The crystal structure of the target protein was selected by the RCSB PDB (http://www.rcsb.org/) database, and

10.3389/fphar.2024.1433076

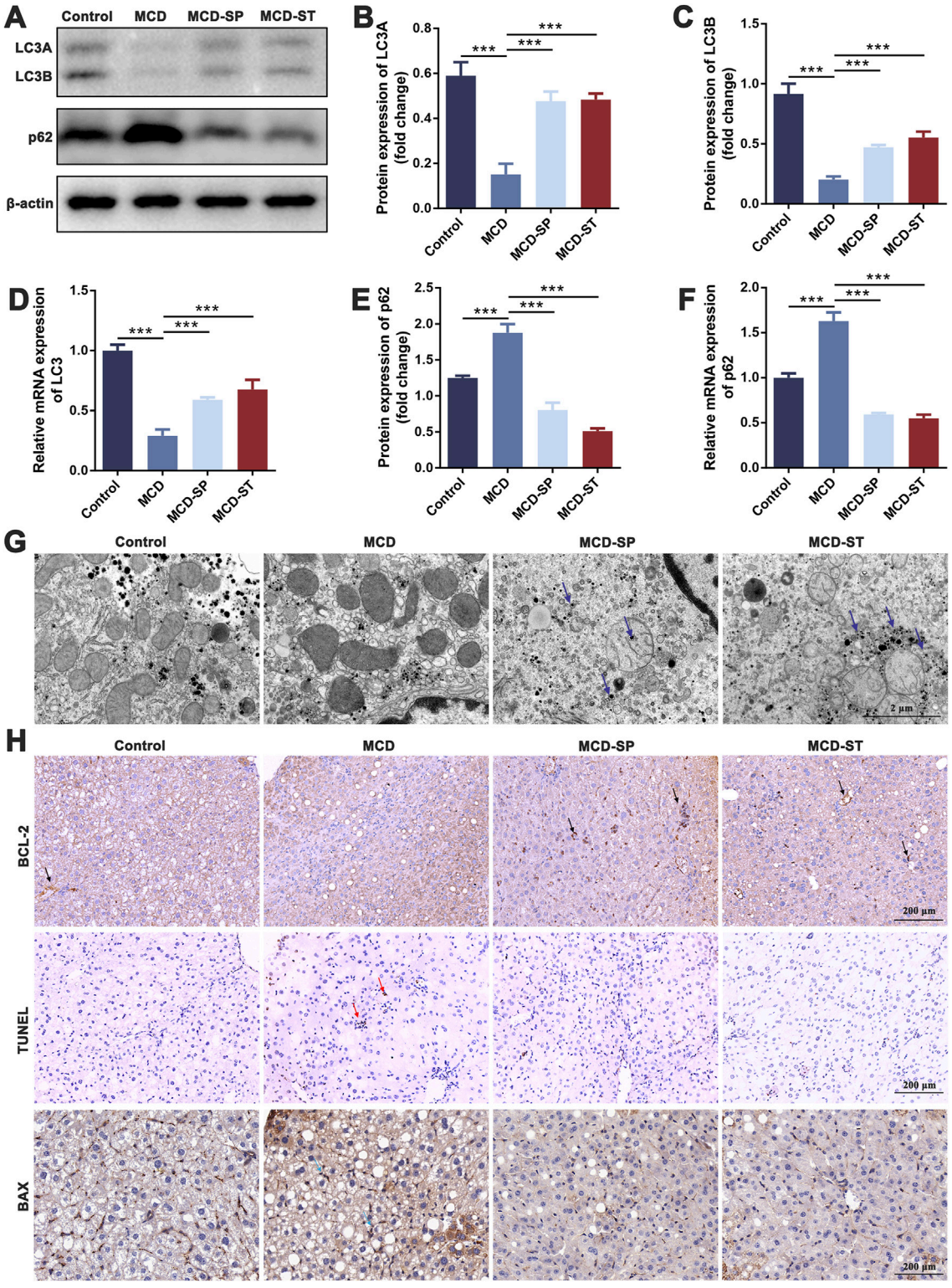

FIGURE 2
SDS significantly upregulates liver autophagy and downregulates liver apoptosis in NASH mice. **(A)** Western blotting of LC3A/B and p62 in the liver of the mice. **(B, C, E)** The relative levels of LC3A, LC3B, and p62 in the liver of the mice were analyzed by Western blotting. **(D, F)** qRT-PCR analyses of the relative expressions of LC3 and p62 in the liver of the mice. **(G)** Mouse liver autophagosome observed by TEM. The blue arrow indicates the autophagosome. Scale bar = 2 μm. **(H)** IHC staining of BCL-2 and BAX and TUNEL staining of liver sections from the indicated groups of mice. The black arrow indicates inhibition of apoptosis in the mouse liver. The red arrow indicates apoptosis of the mouse liver. The blue arrow indicates the promotion of apoptosis in the mouse liver. Scale bar = 200 μm. Data were representative of one or three independent experiments with n = 6 per group. Data were analyzed by Student's *t*-test and expressed as the mean ± SEM. ***$p < 0.001$. Control group, MCD group, MCD-SP and MCD-ST group. Control, normal diet-fed mice; MCD, MCD-fed mice; MCD-SP, MCD with 24 mg/kg/d of SDS; MCD-ST, NASH model mice were fed the control diet with 24 mg/kg/d of SDS.

10.3389/fphar.2024.1433076

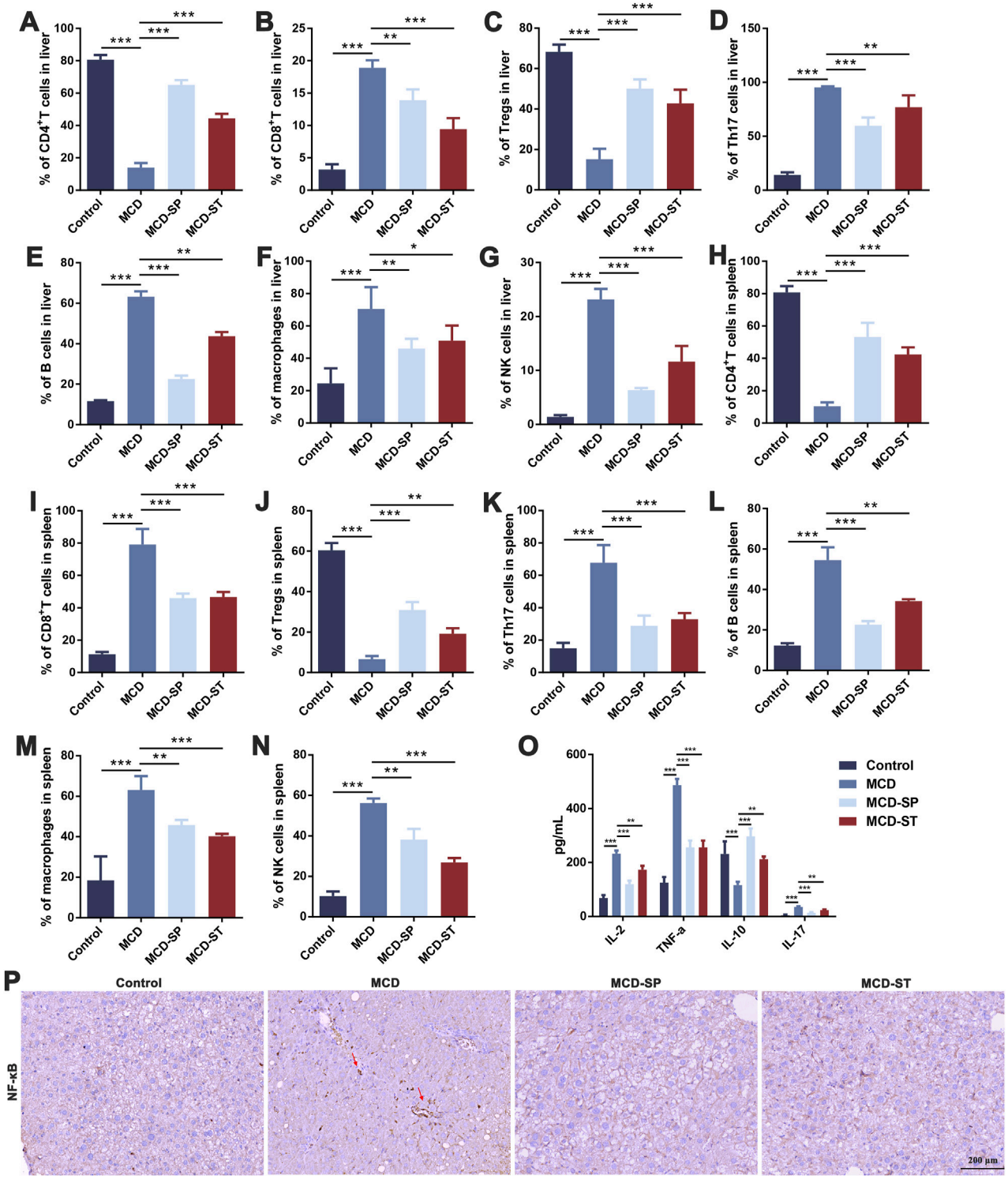

FIGURE 3
SDS significantly balances intrahepatic immunity and improves inflammatory response in NASH mice. **(A–G)** Frequency of $CD4^+$ T cells, $CD8^+$ T cells, Tregs, Th17 cells, B cells, macrophages, and NK cells in the mouse liver. **(H–N)** The frequency of $CD4^+$ T cells, $CD8^+$ T cells, Tregs, Th17 cells, B cells, macrophages, and NK cells in the mouse spleen. **(O)** ELISA of IL-2, TNF-α, IL-10, and IL-17 in mouse serum inflammatory cytokines. **(P)** IHC staining of NF-κB of liver sections from the indicated groups of mice. The red arrow indicates inflammation of the mouse liver. Scale bar = 200 μm. Data were representative of one or three independent experiments with n = 6 per group. Data were analyzed by Student's *t*-test and expressed as the mean ± SEM. $^*p < 0.05$, $^{**}p < 0.01$, and $^{***}p < 0.001$. Control group, MCD group, MCD-SP and MCD-ST group. Control, normal diet-fed mice; MCD, MCD-fed mice; MCD-SP, MCD with 24 mg/kg/d of SDS; MCD-ST, NASH model mice were fed the control diet with 24 mg/kg/d of SDS.

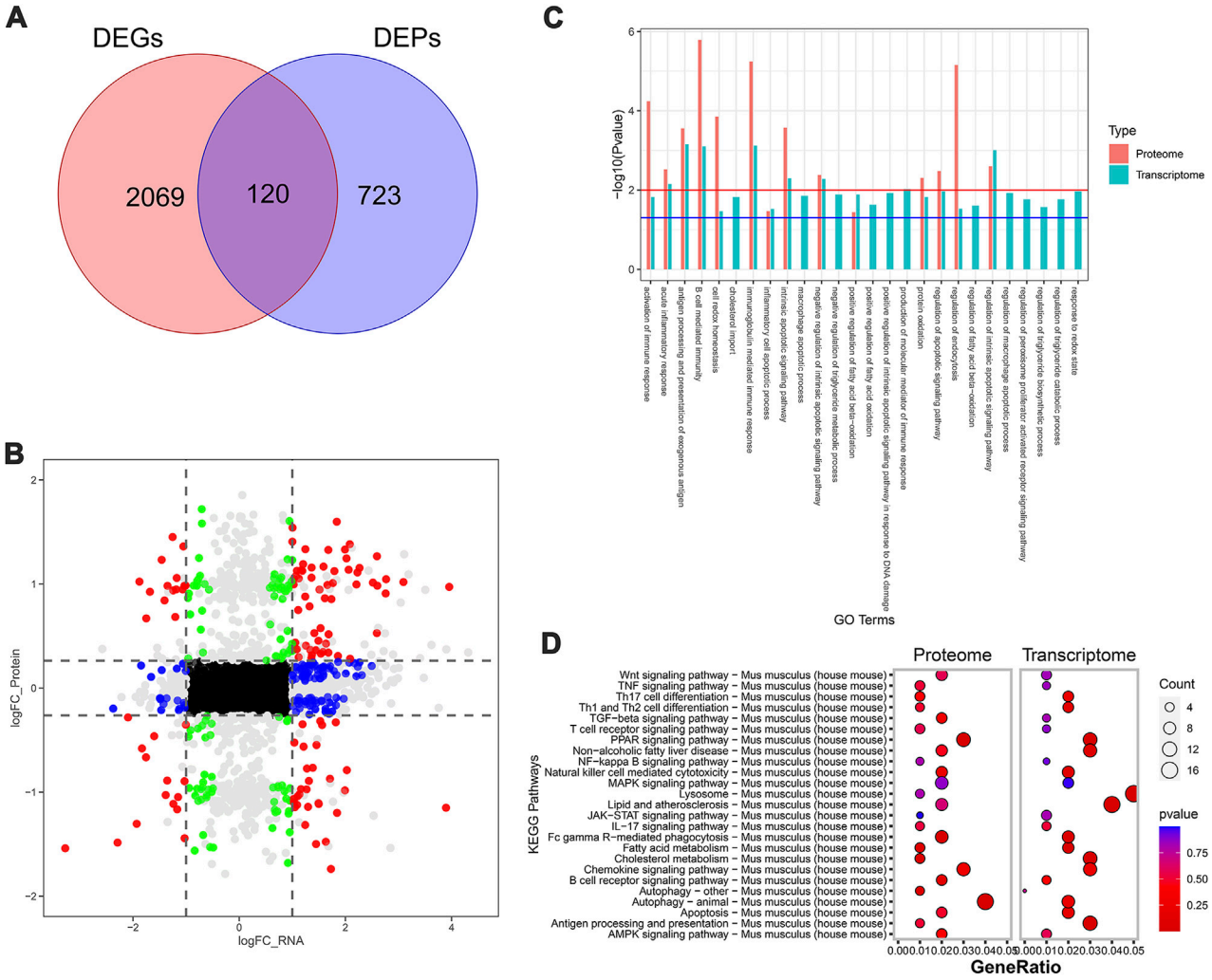

FIGURE 4
Transcriptomic and proteomic analysis in the MCD group and MCD-SP group. **(A)** Venn diagram of DEGs and DEPs in the MCD group and MCD-SP group. **(B)** Transcription protein nine-quadrant diagram of DEPs in the MCD group and MCD-SP group. **(C)** GO enrichment pathway column chart of the MCD group and MCD-SP group. Blue columns represent the genes in the transcriptome, and red columns represent the proteins in the proteome. **(D)** KEGG enrichment top 25 pathways bubble map of the MCD group and MCD-SP group. The size of each circle represents the number of significant DEGs and DEPs enriched in the corresponding pathways. The chromatogram from blue to red represents the *p*-value. Data were representative of one or three independent experiments with n = 3 per group. The topological method adopts relativism-betweenness centrality. Data were analyzed by Student's *t*-test and expressed as the mean ± SEM. The DEGs and DEPs. DEGs, differentially expressed genes; DEPs, differentially expressed proteins.

its docking active center and free binding energy were calculated using AutoDockTools software. Finally, the docking results were visualized using PyMOL software.

2.12 Statistical analysis

Data were presented as the mean ± standard error mean. The comparison between groups was performed by one-way ANOVA and *post hoc* Student's *t*-test, and the multiple comparisons were analyzed by Tukey's honestly significant difference test using SPSS software (version 20.0, IBM, Armonk, NY, United States). The statistically significant difference between various groups was considered when a *p*-value of <0.05 was obtained.

3 Results

3.1 SDS inhibited the MCD-induced NASH formation and exerted promising NASH therapeutic activity *in vivo*

The MCD diet is a classic and useful method to induce NAFLD/NASH in rodents, which was commonly used for the pathogenesis, prevention, and therapy investigation (Parlati et al., 2021). In this study, the positive function of SDS in the progression of NASH was explored using this mouse model. In detail, 7-week-old male C57BL/6J mice were fed with an MCD diet for 4 weeks to develop NASH (Figure 1A). As shown in Figure 1B, notable weight loss was observed in the MCD diet group mice compared to the control group, which was from the beginning of the diet until euthanasia.

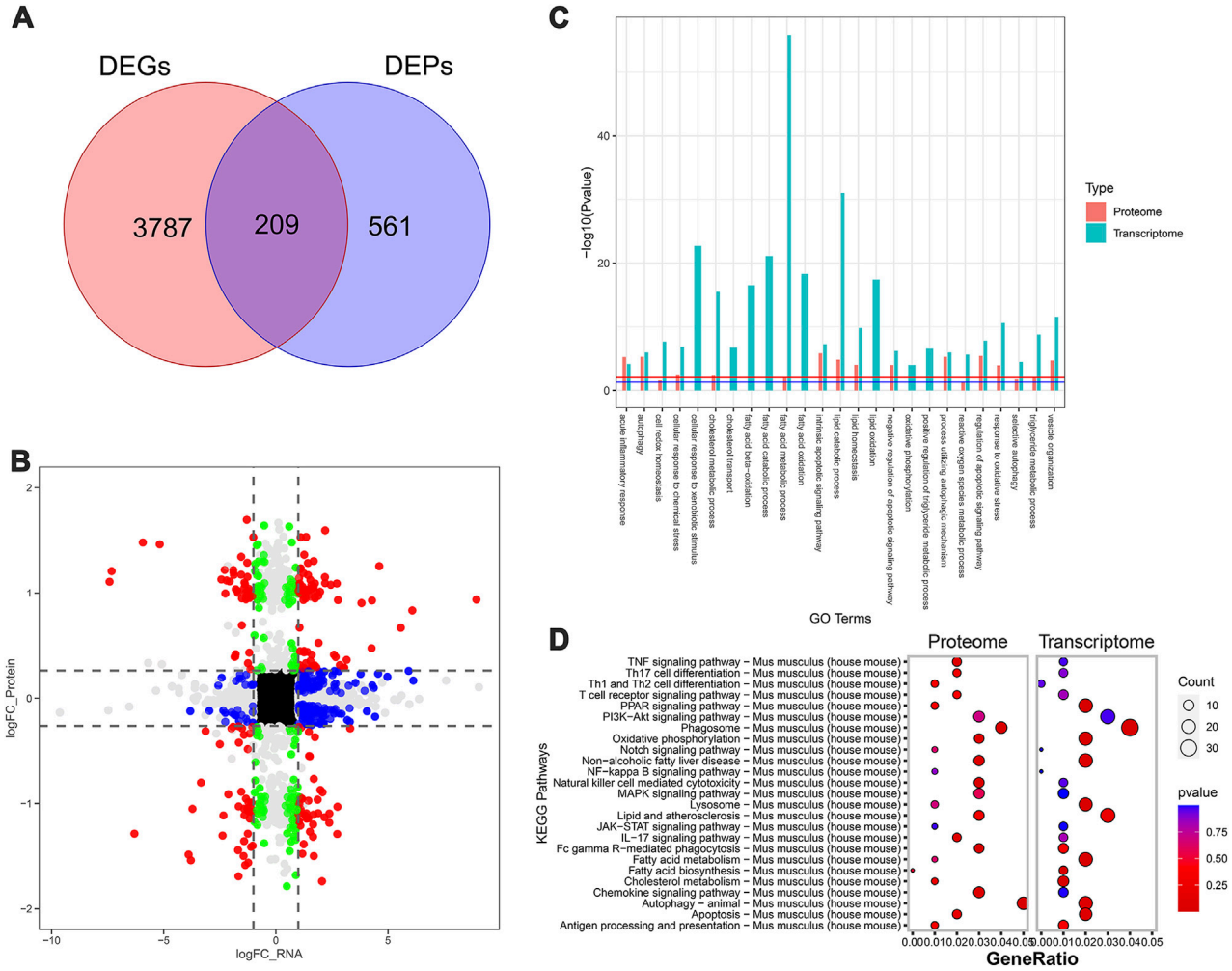

FIGURE 5
Transcriptomic and proteomic analysis in the MCD and MCD-ST groups. **(A)** Venn diagram of DEGs and DEPs in the MCD group and MCD-ST group. **(B)** Transcription protein nine-quadrant diagram of DEPs in the MCD group and MCD-ST group. **(C)** GO enrichment pathway column chart of the MCD group and MCD-ST group. Blue columns represent the genes in the transcriptome, and red columns represent the proteins in the proteome. **(D)** KEGG enrichment top 25 pathways, bubble map of the MCD group and MCD-ST group. The size of each circle represents the number of significant DEGs and DEPs enriched in the corresponding pathways. The chromatogram from blue to red represents the *p*-value. Data were representative of one or three independent experiments with n = 3 per group. The topological method adopts relativism-betweenness centrality. Data were analyzed by Student's *t*-test and expressed as the mean ± SEM. The DEGs and DEPs. DEGs, differentially expressed genes; DEPs, differentially expressed proteins.

Macroscopic observation showed a significant size decrease and yellow color change in the livers of the MCD diet group (Figure 1C). The liver weights of the MCD group mice were significantly decreased compared with the control group (Figure 1D). Furthermore, the liver-to-body weight ratio also confirmed this conclusion (Figure 1E). Blood biochemistry examination revealed a significant upregulation both in the serum and liver tissue levels of TC and TG, as well as the levels of serum ALT and AST in the MCD group compared to these biochemical markers in the control group (Figures 1F–K). The liver histological changes in the MCD group, including hepatic steatosis, ballooning, inflammation, and fibrosis, are the typical pathological findings of human NASH (Tincopa and Loomba, 2023). Specifically, H&E and oil red O staining presented a noticeable increase in the accumulation of lipid droplets, hepatocyte ballooning, and inflammatory cell infiltration in MCD group liver sections, while Sirius red staining revealed significantly increased hepatic fibrosis (Figure 1L). Additionally, the NAS of the MCD group was >5 (Figure 1M). These results demonstrated that the MCD-induced NASH model presented the major features of human NASH, which could be used to study the pathogenesis and therapeutic of NASH.

To explore the potential clinical prevention value of SDS on hepatic steatosis and liver injury, oral administration of SDS (24 mg/kg/day) was supplied accompanied by an MCD diet for 4 weeks (Figure 1A). Compared with the MCD group, SDS treatment had no effect on body weight, liver size, liver weight, and liver to body weight ratio in MCD-SP group mice (Figures 1B–E), but H&E and Oil Red O staining presented that SDS intake remarkably prevented MCD-induced hepatic lipid droplets, hepatocyte ballooning, and inflammatory cell infiltration, and the NAS was significantly reduced in the MCD-SP group (Figures 1L, M). Moreover, SDS treatment sharply decreased serum TG, TC,

ALT, and AST levels, as well as hepatic TG and TC contents in the MCD-SP group, which contrasted with the MCD group (Figures 1F–K). Furthermore, SDS treatment crucially prevented MCD-induced liver fibrosis, as shown by the result of Sirius Red staining (Figure 1L). These results indicated that SDS significantly inhibited NASH formation.

To validate the therapeutic effect of SDS on NASH *in vivo*, we used the mice in the MCD-ST group to study the therapeutic effect of SDS on hepatic steatosis and liver injury. In detail, MCD diet-induced NASH mice were fed a controlled diet with the oral administration of SDS (24 mg/kg/d) continuously for 4 weeks (Figure 1A). As shown in Figures 1B, C, the weight of mice in the MCD-ST group increased significantly once receiving SDS treatment, which almost recovered to the same level as that in the control group in 28 days of SDS administration. Compared with the MCD group, there was no significant difference in liver weight between the MCD-ST group and the control group mice (Figure 1D). The results were consistent with the liver weight-to-body weight ratio (Figure 1E). Compared with the MCD group, the contents of TG and TC in the liver and TG, TC, ALT, and AST in serum were also significantly decreased in the MCD-ST group (Figures 1F–K). Furthermore, H&E and Oil Red O staining presented a notable decrease in the accumulation of lipid droplets, hepatocyte ballooning, and inflammatory cell infiltration in MCD-ST mouse liver sections, while Sirius Red staining revealed significantly decreased hepatic fibrosis (Figure 1L). In addition, it was worth noting that the NAS of the MCD-ST group was <3, indicating that the mice in this group were not diagnosed with NASH. Taken together, these results suggested that SDS exerted a significant therapeutic function in NASH mice.

3.2 SDS treatment upregulated liver autophagy and downregulated liver apoptosis

Programmed cell death, such as autophagy and apoptosis, plays a key role in the development of NASH (Shojaie et al., 2020). Therefore, we first evaluated the effect of SDS on autophagy response. We detected the expression of autophagy marker LC3 in mouse liver tissues by qRT-PCR and Western blotting in these four groups of mice. The results showed that LC3 expression was significantly decreased in the MCD group compared with the control group, while MCD-SP and MCD-ST remarkably reversed this situation (Figures 2A–D). In addition, the p62 expression level was negatively correlated with autophagy activity and can also be used to monitor autophagy flux. The qRT-PCR and Western blotting results showed that the expression of p62 was downregulated in the MCD-SP and MCD-ST groups compared with the MCD group (Figures 2A, E, F). Next, the formation of autophagosomes in liver cells was observed by TEM. As shown in Figure 2G, the results showed that the MCD group formed fewer autophagosomes, while the number of autophagosomes in the liver cells of mice in the MCS-SP and MCS-ST groups was significantly increased, indicating that SDS could significantly upregulate liver autophagy induced by the MCD diet.

Apoptosis is an important biological process that plays a crucial role in cell fate and homeostasis. Hepatocyte apoptosis is a well-defined form of cell death in NASH and is believed to be a major cause of liver inflammation (Zhao et al., 2020). Therefore, we investigated whether SDS could reduce the level of liver apoptosis in MCD mice using BCL-2 and BAX as the marker of apoptosis. Upon daily intake of SDS, the levels of BCL-2 of liver tissues from MCD-SP and MCD-ST groups significantly recovered to a normal level (Figure 2H). Meanwhile, IHC results of the pro-apoptotic marker BAX also confirmed that compared with the MCD group, SDS could suppress the level of BAX in the MCD-SP and MCD-ST groups (Figure 2H). In addition, we used TUNEL staining to detect the DNA breaks formed when DNA fragmentation occurred in the last phase of liver apoptosis. The TUNEL experiment showed that, compared with the control group, the positive area representing apoptotic cells in the liver tissue of mice in the MCD group was significantly larger, while the positive areas in both the MCD-SP and MCD-ST groups were not significantly changed (Figure 2H). Overall, our results showed the ability of SDS to upregulate liver autophagy and downregulate apoptosis of the liver in the NASH mice.

3.3 SDS treatment regulated innate and adaptive immune responses to alleviate inflammation

The hepatic immune cells were reshaped during NASH, which involved the inflammatory processes that triggered liver injury, fibrosis, and evolution toward cirrhosis and hepatocellular carcinoma. Both innate immune and adaptive immunity contribute to NASH-associated inflammation (Zhou et al., 2022). To determine how SDS regulated immune responses to influence the progression of MCD-induced NASH, the liver and spleen were collected to detect immune-related indexes after the mice were euthanized. The frequencies of adapted immune $CD4^+$ T cells, $CD8^+$ T cells, Tregs, Th17 cells, and B cells, as well as innate immune macrophages and NK cells in mouse livers, were first measured by flow cytometry. Compared with the control group, the frequencies of $CD8^+$ T cells, Th17 cells, B cells, macrophages, and NK cells in the MCD group were significantly upregulated, while the frequency of $CD4^+$ T cells and Tregs was significantly downregulated. The above condition could be reversed in the MCD-SP and MCD-ST groups treated with SDS (Figures 3A–G).

To evaluate whether SDS treatment mediated systemic immune responses, spleen lymphocytes were analyzed by flow cytometry. The MCD group significantly increased the frequency of $CD8^+$ T cells, Th17 cells, B cells, macrophages, and NK cells, while it decreased the frequency of $CD4^+$ T cells and Tregs. SDS treatment showed a marked reversal effect to MCD-induced changes of spleen lymphocytes (Figures 3H–N). This was consistent with the results of liver immune-related indexes, indicating that SDS treatment had a significant regulatory effect on the immune responses in NASH mice.

Immune cells in the inflammatory responses secrete various cytokines, and at the same time, cytokines also act on the immune cells. Then, the adapted immune cells will produce more cytokines, thus forming a positive feedback regulation (Duan et al., 2022). Therefore, after evaluating the immune cells mentioned above, we subsequently examined the expression levels of inflammatory factors

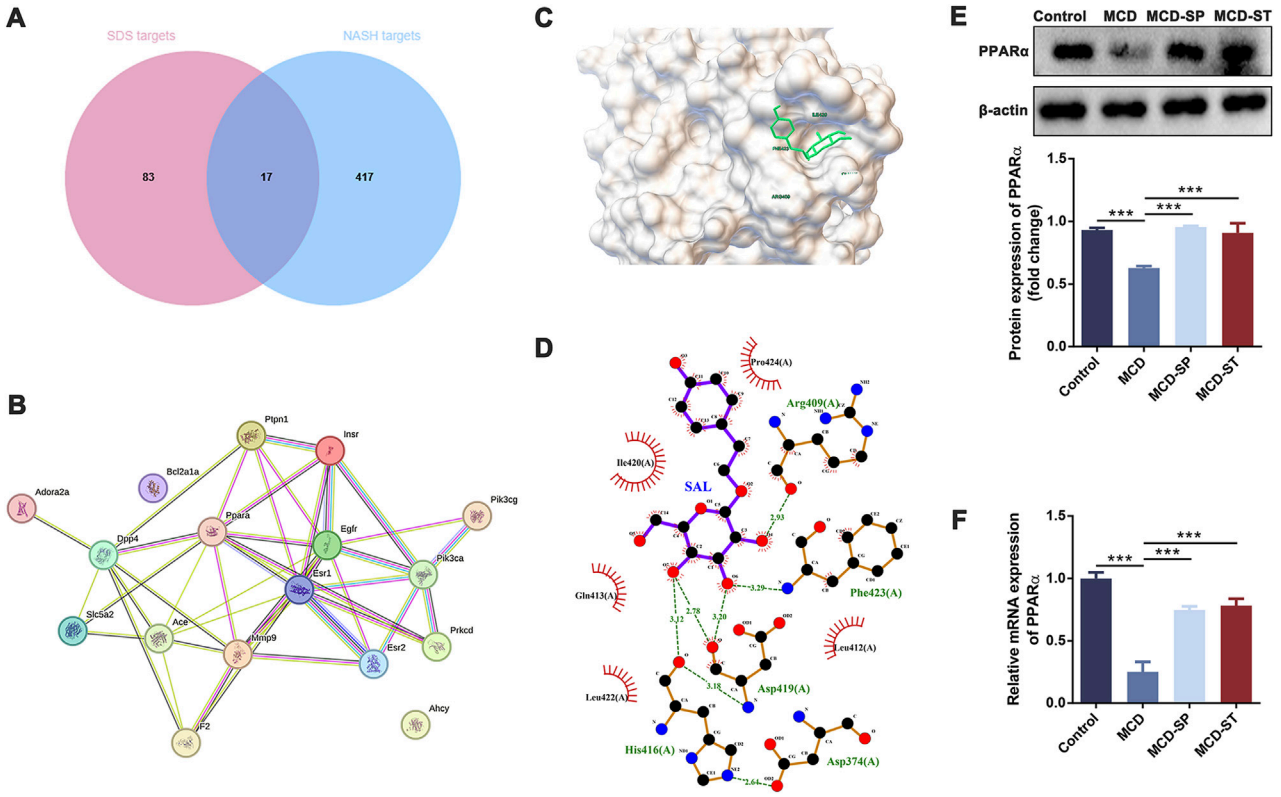

FIGURE 6
SDS may play a role in the prevention and therapy of NASH through PPARα. **(A)** Venn diagram of SDS targets and NASH targets. **(B)** PPI of intersection targets. **(C, D)** Molecular docking of SDS and PPARα. **(E)** Western blotting of PPARα in the liver of the mice. The relative levels of PPARα in the liver of the mice were analyzed. **(F)** qRT-PCR analyses of the relative expressions of PPARα in the liver of the mice. Data were analyzed by Student's *t*-test and expressed as the mean ± SEM. ***$p < 0.001$. Control group, MCD group, and MCD-SP and MCD-ST group. Control, normal diet-fed mice; MCD, MCD-fed mice; MCD-SP, MCD with 24 mg/kg/d of SDS; MCD-ST, NASH model mice were fed with the control diet with 24 mg/kg/d of SDS.

including IL-2, TNF-α, IL-10, and IL-17 in the mouse serum of each group. An ELISA experiment showed that compared with the control group, the levels of IL-2, TNF-α, and IL-17 in the serum of MCD group mice were significantly upregulated, while the level of IL-10 was significantly downregulated. In contrast, the expression levels of IL-2, TNF-α, and IL-17 in MCD-SP and MCD-ST groups were significantly decreased, and the contents of IL-10 were significantly increased (Figure 3O). The IHC results revealed that the NF-κB protein level was significantly increased in the MCD group compared to the control group but decreased in the MCD-SP and MCD-ST groups (Figure 3P). These results suggested that SDS treatment might play a role in rebalancing immunity and inflammatory response.

3.4 RNA-seq transcriptomic and label-free quantitative proteomic analysis of mice

To further systematically elucidate the molecular mechanism by which SDS inhibited the progression of NASH, we performed RNA-seq-based transcriptomics and MS-based marker-free proteomic sequencing on the livers of three mice in each of the MCD, MCD-SP, and MCD-ST groups (NCBI BioProjects: PRJNA1100189). The results of the comparison between the MCD and MCD-SP groups showed a total of 2,189 differentially expressed genes (DEGs) in the transcriptome dataset and 843 differentially expressed proteins (DEPs) in the proteome, of which 120 proteins were shared by the transcriptome and proteome data (Figures 4A, B). Apart from lipid metabolism-related processes or signaling pathways, both Go functional annotation and KEGG pathway analysis indicated that these 120 proteins were also significantly enriched in autophagy, apoptosis, immunity, and inflammation-related processes or signaling pathways (Figures 4C, D). In addition, the Wnt, TGF-β, MAPK, and PPAR signaling pathways were also significantly enriched in the KEGG pathway analysis (Figure 4D).

Next, the MCD and MCD-ST group results showed that 3,996 DEGs and 770 DEPs of the proteome were found in the transcriptome dataset, respectively, of which 209 proteins were shared by the transcriptome and proteome data (Figures 5A, B). Similarly, based on the annotation of the GO database, this overlap between DEGs and DEPs was significantly enriched in the processes related to lipid metabolism, autophagy, apoptosis, and inflammation (Figure 5C). A total of 321 pathways in the SDS treatment of NASH were identified through the KEGG enrichment analysis. Among these pathways, lipid metabolism, autophagy, inflammation, and immune-related signaling pathways were significantly enriched. In addition, the PI3K-AKT, MAPK, and PPAR signaling pathways

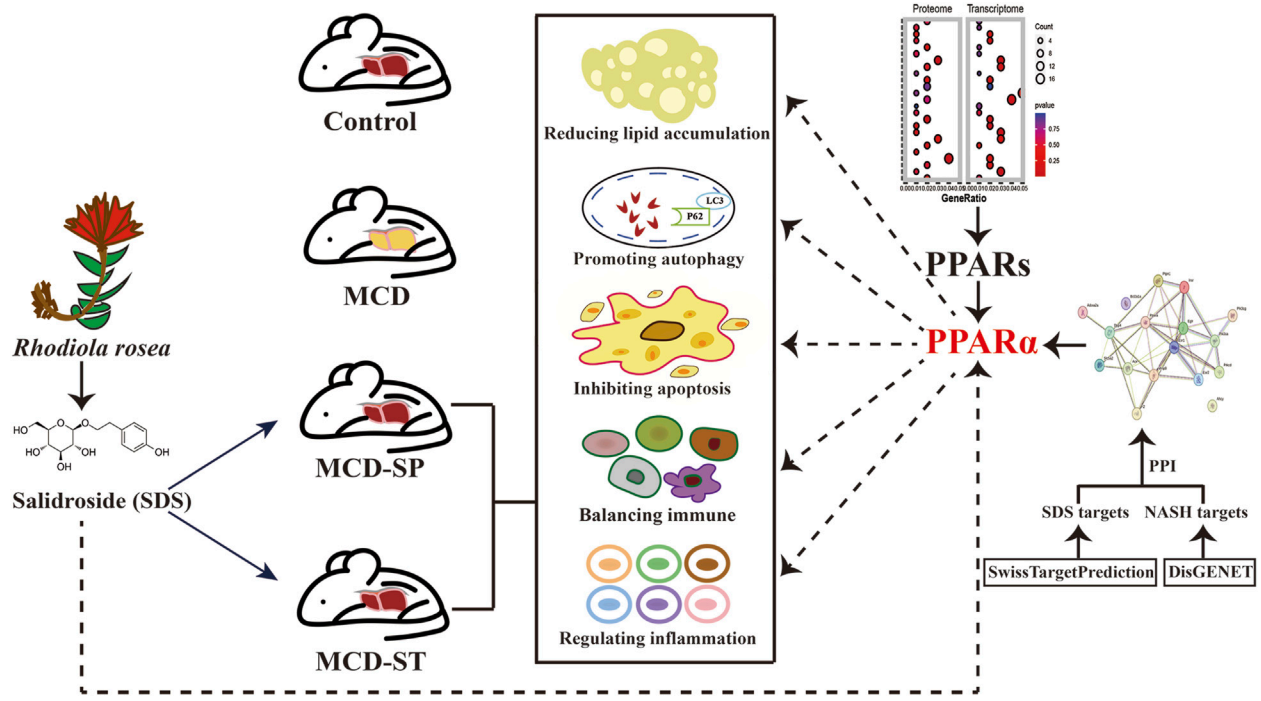

FIGURE 7
Schematic diagram of the mechanism of SDS improving MCD-induced NASH in mice through PPARα.

were significantly enriched (Figure 5D). Notably, the MAPK and PPAR signaling pathways, which participated in the regulatory processes in the MCD-ST group, were also detected to play a significant role in the MCD-SP group. These two signaling pathways have been reported to regulate lipid accumulation, autophagy, apoptosis, immunity, and inflammation in the process of NASH in previous studies. Therefore, based on the above transcriptomic and proteomic analysis results, we speculated that SDS might play a role by regulating MAPK and/or PPAR signaling pathways in NASH mice.

3.5 The multiple anti-NASH effects of SDS may target PPARα

Then, network pharmacology and molecular docking analysis were performed to further confirm the possible role of SDS in preventive and therapeutic activities on NASH. As the results of network pharmacology analysis, 100 SDS-related target genes and 434 NASH-related target genes were obtained. Next, 17 targets of SDS for treating NASH were obtained by plotting Venn diagrams as potential targets (Figure 6A). The 17 targets were imported into the STRING database to obtain protein interaction data, which were imported into Cytoscape software to construct the PPI network (Figure 6B). Topological analysis of the PPI network based on the cyto-NAC function in Cytoscape software identified the top five target genes ranked in the degree of connectivity, namely, EGFR, PPARα, ESR1, ACE, and INSR, which were recognized as key targets for the SDS treatment of NASH. Notably, PPARα is an important component in the PPAR signaling pathway, which has also been shown to play a significant role in the treatment of NASH with SDS in transcriptome and proteomic analysis. In order to evaluate the reliability of the interaction between SDS and PPARα, molecular docking was performed. The minimum binding energy and binding position of SDS and PPARα molecular docking results are shown in Figures 6C, D, which confirmed that SDS and PPARα have binding potential. The minimum binding energy and binding position of SDS and the other four proteins, including EGFR ESR1, ACE, and INSR, are shown in Supplementary Figure S1. Finally, the PPARα expression was verified through the qRT-PCR and Western blot experiments, which showed that PPARα expression was sharply decreased in the MCD group compared with the control group, while MCD-SP and MCD-ST significantly reversed this situation (Figures 6E, F). These findings indicated that SDS might target PPARα to exert preventive and therapeutic activities on NASH.

4 Discussion

Due to the increasing incidence and severe consequences of NASH, patients with NASH have become a major population considered for liver transplantation. The limitation to therapy options aggravates this economic burden, so there is an urgent need to develop effective treatments (Lonardo et al., 2022; Mantovani et al., 2020). SDS is the main biological component extracted from *R. rosea* and has a wide range of biological activities, such as lipid-lowering, immune-balancing, anti-oxidation, anti-aging, anti-inflammation, and anti-cancer effects, both *in vivo* and *in vitro* (Zhang et al., 2021). SDS can improve the NAFLD/NASH status by improving abnormal lipid metabolism, inhibiting

oxidative stress, regulating apoptosis and autophagy, alleviating inflammatory reactions, reducing fibrosis, and regulating intestinal flora (Qu et al., 2022).

In this study, we first comprehensively assessed and confirmed the preventive and therapeutic effects of the oral intake of SDS on NASH (Figure 7). Specifically, although the body weight, liver weight, and liver-to-body weight ratio did not recover in the MCD-SP group, serum and liver biochemical indexes (TG, TC, ALT, and AST) were improved. Comparatively, the MCD-ST group not only reversed the above biochemical indexes but also improved the body weight, liver weight, and liver-to-body weight ratio. Liver pathological sections (H&E, Oil Red O staining and Sirius Red staining) of MCD-SP and MCD-ST mice also thoroughly illustrated that SDS could significantly inhibit the formation of NASH and improve the liver injury of NASH mice. Previous studies revealed that the progression of NASH is closely associated with the processes of autophagy and apoptosis. Autophagy is involved in lipid metabolism and liver injury in NASH, while dysregulated autophagy has also been found to contribute to the development of NASH to liver fibrosis, cirrhosis, and liver cancer (Wu et al., 2018). Apoptosis is an important mechanism contributing to the progression of NASH (Zhao et al., 2024), and the ensuing responses in NASH progression such as cell repair, inflammation, regeneration, and fibrosis may all be triggered by the apoptosis of adjacent cells. In our research, mRNA and protein levels of autophagy markers LC3 and p62 were detected in four groups of mice, and autophagosome formation was observed by TEM, which confirmed that SDS could upregulate liver autophagy. The IHC results of BCL-2, BAX, and TUNEL staining confirmed that SDS could also significantly reduce apoptosis of the mouse liver.

Studies have shown that immune cells and inflammatory factors play important roles in the occurrence and progression of NASH (Peiseler et al., 2022), and SDS was reported to have a good immunomodulatory effect (Yang et al., 2023). The immune system includes adaptive immunity (including $CD4^+$ T cells, $CD8^+$ T cells, Tregs, Th17 cells, and B cells) and innate immunity (including macrophages and NK cells). In adaptive immunity, $CD4^+$ T cells and Tregs are the key regulators of pro-inflammatory and anti-inflammatory immune processes (Woestemeier et al., 2023; Savage et al., 2024). $CD8^+$ T cells are involved in the progression of NASH and liver fibrosis, and the reduction in $CD8^+$ T cells can prevent the progression of NASH and reduce fibrosis. Furthermore, $CD8^+$ T cells can also induce the activation of the NF-κB signaling pathway in hepatocytes and regulate the inflammatory process (Li et al., 2022). Th17 cells secrete IL-17, which can aggravate hepatic steatosis and inflammation and induce the transition from simple steatosis to hepatic steatosis (Zi et al., 2022). In addition, it is reported that there is a large number of B cells in the liver of NASH patients, and these patients have high lobular inflammation and fibrosis, which indicates that B cells may change the course of the disease (Barrow et al., 2021). In innate immunity, macrophages have M1 polarization in NASH and interact with hepatocytes to promote the secretion of inflammatory factors and upregulate the fat synthesis factors, oxidative stress, and endoplasmic reticulum stress, which leads to further deterioration of NASH (Kazankov et al., 2019). Moreover, NK cells play a key role in NAFLD and NASH and can well-coordinate immune responses and regulate inflammation, making it a highly relevant cell type studied under inflammatory conditions (Wang et al., 2021). In this study, for the first time, we evaluated the conditions of adaptive immunity and innate immunity of the mouse liver and spleen to explore how SDS regulated the immune system during the formation of NASH or in NASH patients. Our results revealed that compared with the control group, the frequencies of $CD8^+$ T cells, Th17 cells, B cells, macrophages, and NK cells in the MCD group were significantly increased, while the frequencies of $CD4^+$ T cells and Tregs were significantly reduced. However, in the MCD-SP and MCD-ST groups treated with SDS, the above situation could be reversed, indicating that SDS treatment had a significant regulatory effect on the immune responses in NASH mice.

Under normal circumstances, cytokines such as ILs and TNF-α play roles in regulating and coordinating immune responses in the immune system. Pro-inflammatory cytokines contribute to the occurrence and spread of autoimmune inflammation, while anti-inflammatory factors contribute to the regression of inflammation and the recovery from autoimmune diseases during the acute stage. When the disease occurs, the equilibrium state is broken, which changes the levels of various inflammatory factors (Peiseler et al., 2022). The ELISA results showed that SDS could inhibit the expressions of IL-2, TNF-α, and IL-17 and increase the expression of IL-10. Moreover, the activation of NF-κB can induce liver inflammation, aggravate fatty toxicity, and lead to the activation of hepatic stellate cells, thus further promoting liver fibrosis (Deng et al., 2022). The results of the IHC experiment showed that compared with the control group, the content of the NF-κB protein in the liver tissue of mice in the MCD group significantly increased, while the content of the NF-κB protein in the liver tissue of mice in the MCD-SP group and MCD-ST group decreased. Thus, these results suggested that SDS might play a significant role in regulating inflammatory responses.

Consequently, in order to determine the molecular mechanism of the anti-NASH effect of SDS mentioned above, we conducted a comparative analysis of the transcriptome and proteome of mouse livers in the MCD and MCD-SP groups and MCD and MCD-ST groups, respectively. The GO and KEGG enrichment analyses showed that the pathways that play a major role in the anti-NASH activity of SDS were mainly concentrated in autophagy, apoptosis, immunity, and inflammation. In addition, the MAPK and PPAR signaling pathways were also significantly enriched. The MAPK signaling pathway has been reported to improve lipid accumulation (Liu et al., 2019), autophagy (Vargas-Pozada et al., 2022), and inflammation (Afrin et al., 2017) in NASH mice. Moreover, it is worth noting that PPAR is involved in the regulation of lipid metabolism (Gross et al., 2017), autophagy (Liang et al., 2023), apoptosis (Ren et al., 2017), immunity, and inflammation (Ni et al., 2022) in the process of NASH, and it is a potentially effective target for the treatment of NASH. Based on this, we speculated that SDS might exert its effects by regulating the MAPK and/or PPAR signaling pathways in NASH mice.

To further elucidate the target of SDS, SDS targets and NASH targets were intersected by Venn diagrams, and PPI analysis was performed. PPI is a systematic analysis of the interaction between a large number of proteins in biological systems, which is of great significance for understanding the working principle of proteins in biological systems, the reaction mechanism of biological signals and energy and material metabolism under special physiological states such as diseases, and the functional links between proteins. As a result, 17 targets of SDS for treating NASH were obtained by plotting

Venn diagrams. Subsequently, the top five target genes were identified based on PPI network analysis. As expected, PPARα in the top five genes, which belongs to the PPAR signaling pathway, was shown to play a significant role in the treatment of NASH with SDS treatment. In order to verify the accuracy of the predicted target, the docking analysis between SDS and PPARα was verified through AutoDockTools software. The minimum binding energy and binding position of SDS and PPARα molecular docking results suggested that SDS can play a role in upregulating PPARα in the prevention and therapy of NASH. As reported, the PPAR family is a member of a nuclear receptor superfamily, including PPARα, PPARβ/δ, and PPARγ. PPARα is mainly expressed in the liver, heart, skeletal muscle, brown adipose tissue, intestine, and kidney and promotes energy consumption. PPARα mediates its function by influencing fatty acid transport, esterification, and oxidation. PPARβ/δ is not only widely expressed and participates in fatty acid oxidation but also plays a role in regulating blood glucose levels. In contrast, PPARγ mainly stores energy by promoting lipogenesis and lipid synthesis and shows the highest expression level in white adipose tissue (Christofides et al., 2021). In clinical applications, lanifibranor, an oral PPAR agonist, can activate three PPARs in a balanced way, thus causing beneficial anti-inflammatory, anti-fibrosis, and other vascular and metabolic changes (Francque et al., 2021). At present, it is being analyzed in a global multi-center phase III clinical trial. Lastly, the mRNA and protein levels of PPARα were tested in four groups of mice by experiments, which supported that SDS may regulate liver autophagy, apoptosis, and liver immune environment through the protein of PPARα. To the best of our knowledge, this is the first study to report that the daily oral intake of SDS possesses preventive and therapeutic effects in the NASH formation process or NASH, providing new ideas that SDS could be an ideal candidate drug for the prevention and treatment of NASH.

There were some limitations to this study. The MCD diet used in the current study is considered the most established rodent model of NASH, which mimics classical histopathological features of liver steatosis, apoptosis, oxidative stress, inflammation, and fibrosis, similar to human NASH (Fang et al., 2022; Gallage et al., 2022). However, the model doses do not fully reflect all human NASH characteristics. Mice fed the MCD diet lost weight rather than obesity and lacked insulin resistance, which is commonly observed in patients with NASH (Alshawsh et al., 2022). Thus, in future high-fat and high-fructose models, SDS may play different roles in steatosis, oxidative stress, inflammation, and insulin resistance in obesity-induced 16-week NASH models.

5 Conclusion

The results revealed that SDS may exert preventive and therapeutic activities on NASH by regulating autophagy and apoptosis, enhancing immunity, and alleviating inflammation through targeting the protein of PPARα.

Data availability statement

The data presented in the study are deposited in the NCBI BioProject repository, accession number PRJNA1100189.

Ethics statement

The animal study was approved by the Institutional Animal Care and Use Committee of Ocean University of China. The study was conducted in accordance with the local legislation and institutional requirements.

Author contributions

XC: conceptualization and writing–original draft. SL: conceptualization and writing–original draft. BQ: methodology and writing–original draft. YX: visualization and writing–review and editing. LL: project administration, supervision, and writing–review and editing.

Funding

The author(s) declare that financial support was received for the research, authorship, and/or publication of this article. This study was supported by the National Natural Science Foundation of China (grant number: 31800660).

Conflict of interest

The authors declare that the research was conducted in the absence of any commercial or financial relationships that could be construed as a potential conflict of interest.

Publisher's note

Supplementary material

The Supplementary Material for this article can be found online at: https://www.frontiersin.org/articles/10.3389/fphar.2024.1433076/full#supplementary-material

References

Afrin, M. R., Arumugam, S., Rahman, M. A., Karuppagounder, V., Harima, M., Suzuki, H., et al. (2017). Curcumin reduces the risk of chronic kidney damage in mice with nonalcoholic steatohepatitis by modulating endoplasmic reticulum stress and MAPK signaling. *Int. Immunopharmacol.* 49, 161–167. doi:10.1016/j.intimp.2017.05.035

Aldossari, K. K. (2023). The epidemiology and characteristics of patients with diabetes with or without NASH: a systematic review. *Afr. Health Sci.* 23 (2), 509–518. doi:10.4314/ahs.v23i2.59

Alshawsh, M. A., Alsalahi, A., Alshehade, S. A., Saghir, S. A. M., Ahmeda, A. F., Al Zarzour, R. H., et al. (2022). A comparison of the gene expression profiles of non-alcoholic fatty liver disease between animal models of a high-fat diet and methionine-choline-deficient diet. *Molecules* 27 (3), 858. doi:10.3390/molecules27030858

Barrow, F., Khan, S., Fredrickson, G., Wang, H., Dietsche, K., Parthiban, P., et al. (2021). Microbiota-driven activation of intrahepatic B cells aggravates NASH through innate and adaptive signaling. *Hepatology* 74 (2), 704–722. doi:10.1002/hep.31755

Cai, L., Li, Y., Zhang, Q., Sun, H., Yan, X., Hua, T., et al. (2017). Salidroside protects rat liver against ischemia/reperfusion injury by regulating the GSK-3β/Nrf2-dependent antioxidant response and mitochondrial permeability transition. *Eur. J. Pharmacol.* 806, 32–42. doi:10.1016/j.ejphar.2017.04.011

Christofides, A., Konstantinidou, E., Jani, C., and Boussiotis, V. A. (2021). The role of peroxisome proliferator-activated receptors (PPAR) in immune responses. *Metabolism* 114, 154338. doi:10.1016/j.metabol.2020.154338

Deng, Y. F., Xu, Q. Q., Chen, T. Q., Ming, J. X., Wang, Y. F., Mao, L. N., et al. (2022). Kinsenoside alleviates inflammation and fibrosis in experimental NASH mice by suppressing the NF-κB/NLRP3 signaling pathway. *Phytomedicine* 104, 154241. doi:10.1016/j.phymed.2022.154241

Duan, Y., Pan, X., Luo, J., Xiao, X., Li, J., Bestman, P. L., et al. (2022). Association of inflammatory cytokines with non-alcoholic fatty liver disease. *Front. Immunol.* 13, 880298. doi:10.3389/fimmu.2022.880298

Fan, F., Yang, L., Li, R., Zou, X., Li, N., Meng, X., et al. (2020). Salidroside as a potential neuroprotective agent for ischemic stroke: a review of sources, pharmacokinetics, mechanism and safety. *Biomed. Pharmacother.* 129, 110458. doi:10.1016/j.biopha.2020.110458

Fang, T., Wang, H., Pan, X., Little, P. J., Xu, S., and Weng, J. (2022). Mouse models of nonalcoholic fatty liver disease (NAFLD): pathomechanisms and pharmacotherapies. *Int. J. Biol. Sci.* 18 (15), 5681–5697. doi:10.7150/ijbs.65044

Feng, J., Chen, K., Xia, Y., Wu, L., Li, J., Li, S., et al. (2018). Salidroside ameliorates autophagy and activation of hepatic stellate cells in mice via NF-κB and TGF-β1/Smad3 pathways. *Drug Des. devel. Ther.* 12, 1837–1853. doi:10.2147/DDDT.S162950

Francque, S. M., Bedossa, P., Ratziu, V., Anstee, Q. M., Bugianesi, E., Sanyal, A. J., et al. (2021). A randomized, controlled trial of the pan-PPAR agonist lanifibranor in NASH. *N. Engl. J. Med.* 385 (17), 1547–1558. doi:10.1056/NEJMoa2036205

Gallage, S., Avila, J. E. B., Ramadori, P., Focaccia, E., Rahbari, M., Ali, A., et al. (2022). A researcher's guide to preclinical mouse NASH models. *Nat. Metab.* 4 (12), 1632–1649. doi:10.1038/s42255-022-00700-y

Gao, Z., Zhan, H., Zong, W., Sun, M., Linghu, L., Wang, G., et al. (2023). Salidroside alleviates acetaminophen-induced hepatotoxicity via Sirt1-mediated activation of Akt/Nrf2 pathway and suppression of NF-κB/NLRP3 inflammasome axis. *Life Sci.* 327, 121793. doi:10.1016/j.lfs.2023.121793

Gross, B., Pawlak, M., Lefebvre, P., and Staels, B. (2017). PPARs in obesity-induced T2DM, dyslipidaemia and NAFLD. *Nat. Rev. Endocrinol.* 13 (1), 36–49. doi:10.1038/nrendo.2016.135

Gu, S., Hu, S., Wang, S., Qi, C., Shi, C., and Fan, G. (2023). Bidirectional association between NAFLD and gallstone disease: a systematic review and meta-analysis of observational studies. *Expert Rev. Gastroenterol. Hepatol.* 17 (3), 283–293. doi:10.1080/17474124.2023.2175671

Han, S. K., Baik, S. K., and Kim, M. Y. (2023a). Non-alcoholic fatty liver disease: definition and subtypes. *Clin. Mol. Hepatol.* 29 (Suppl. l), S5–S16. doi:10.3350/cmh.2022.0424

Han, Y., Luo, L., Li, H., Zhang, L., Yan, Y., Fang, M., et al. (2023b). Nomilin and its analogue obacunone alleviate NASH and hepatic fibrosis in mice via enhancing antioxidant and anti-inflammation capacity. *Biofactors* 49 (6), 1189–1204. doi:10.1002/biof.1987

Harrison, S. A., Allen, A. M., Dubourg, J., Noureddin, M., and Alkhouri, N. (2023). Challenges and opportunities in NASH drug development. *Nat. Med.* 29 (3), 562–573. doi:10.1038/s41591-023-02242-6

Hu, B., Zou, Y., Liu, S., Wang, J., Zhu, J., Li, J., et al. (2014). Salidroside attenuates concanavalin A-induced hepatitis via modulating cytokines secretion and lymphocyte migration in mice. *Mediat. Inflamm.* 2014, 314081. doi:10.1155/2014/314081

Hu, M., Zhang, D., Xu, H., Zhang, Y., Shi, H., Huang, X., et al. (2021). Salidroside activates the AMP-activated protein kinase pathway to suppress nonalcoholic steatohepatitis in mice. *Hepatology* 74 (6), 3056–3073. doi:10.1002/hep.32066

Kazankov, K., Jørgensen, S. M. D., Thomsen, K. L., Møller, H. J., Vilstrup, H., George, J., et al. (2019). The role of macrophages in nonalcoholic fatty liver disease and nonalcoholic steatohepatitis. *Nat. Rev. Gastroenterol. Hepatol.* 16 (3), 145–159. doi:10.1038/s41575-018-0082-x

Li, C., Du, X., Shen, Z., Wei, Y., Wang, Y., Han, X., et al. (2022). The critical and diverse roles of CD4-CD8- double negative T cells in nonalcoholic fatty liver disease. *Cell. Mol. Gastroenterol. Hepatol.* 13 (6), 1805–1827. doi:10.1016/j.jcmgh.2022.02.019

Liang, J., Xu, C., Xu, J., Yang, C., Kong, W., Xiao, Z., et al. (2023). PPARα senses bisphenol S to trigger ep300-mediated autophagy blockage and hepatic steatosis. *Environ. Sci. Technol.* 57 (51), 21581–21592. doi:10.1021/acs.est.3c05010

Liu, C. F., and Chien, L. W. (2023). Predictive role of neutrophil-percentage-to-albumin ratio (NPAR) in nonalcoholic fatty liver disease and advanced liver fibrosis in nondiabetic US adults: evidence from NHANES 2017-2018. *Nutrients* 15 (8), 1892. doi:10.3390/nu15081892

Liu, J., Li, D., Dun, Y., Li, H., Ripley-Gonzalez, J. W., Zhang, J., et al. (2022). Rhodiola activates macrophage migration inhibitory factor to alleviate non-alcoholic fatty liver disease. *Life Sci.* 308, 120949. doi:10.1016/j.lfs.2022.120949

Liu, Y., Xu, W., Zhai, T., You, J., and Chen, Y. (2019). Silibinin ameliorates hepatic lipid accumulation and oxidative stress in mice with non-alcoholic steatohepatitis by regulating CFLAR-JNK pathway. *Acta. Pharm. Sin. B* 9 (4), 745–757. doi:10.1016/j.apsb.2019.02.006

Llovet, J. M., Willoughby, C. E., Singal, A. G., Greten, T. F., Heikenwälder, M., El-Serag, H. B., et al. (2023). Nonalcoholic steatohepatitis-related hepatocellular carcinoma: pathogenesis and treatment. *Nat. Rev. Gastroenterol. Hepatol.* 20 (8), 487–503. doi:10.1038/s41575-023-00754-7

Lonardo, A., Mantovani, A., Petta, S., Carraro, A., Byrne, C. D., and Targher, G. (2022). Metabolic mechanisms for and treatment of NAFLD or NASH occurring after liver transplantation. *Nat. Rev. Endocrinol.* 18 (10), 638–650. doi:10.1038/s41574-022-00711-5

Lu, L., Liu, S., Dong, Q., and Xin, Y. (2019). Salidroside suppresses the metastasis of hepatocellular carcinoma cells by inhibiting the activation of the Notch1 signaling pathway. *Mol. Med. Rep.* 19 (6), 4964–4972. doi:10.3892/mmr.2019.10115

Mantovani, A., Scorletti, E., Mosca, A., Alisi, A., Byrne, C. D., and Targher, G. (2020). Complications, morbidity and mortality of nonalcoholic fatty liver disease. *Metabolism* 111S, 154170. doi:10.1016/j.metabol.2020.154170

Montagner, A., Polizzi, A., Fouché, E., Ducheix, S., Lippi, Y., Lasserre, F., et al. (2016). Liver PPARα is crucial for whole-body fatty acid homeostasis and is protective against NAFLD. *Gut* 65 (7), 1202–1214. doi:10.1136/gutjnl-2015-310798

Motta, B. M., Masarone, M., Torre, P., and Persico, M. (2023). From non-alcoholic steatohepatitis (NASH) to hepatocellular carcinoma (HCC): epidemiology, incidence, predictions, risk factors, and prevention. *Cancers (Basel)* 15 (22), 5458. doi:10.3390/cancers15225458

Ni, X. X., Ji, P. X., Chen, Y. X., Li, X. Y., Sheng, L., Lian, M., et al. (2022). Regulation of the macrophage-hepatic stellate cell interaction by targeting macrophage peroxisome proliferator-activated receptor gamma to prevent non-alcoholic steatohepatitis progression in mice. *Liver Int.* 42 (12), 2696–2712. doi:10.1111/liv.15441

Parlati, L., Régnier, M., Guillou, H., and Postic, C. (2021). New targets for NAFLD. *JHEP Rep.* 3 (6), 100346. doi:10.1016/j.jhepr.2021.100346

Peiseler, M., Schwabe, R., Hampe, J., Kubes, P., Heikenwälder, M., and Tacke, F. (2022). Immune mechanisms linking metabolic injury to inflammation and fibrosis in fatty liver disease - novel insights into cellular communication circuits. *J. Hepatol.* 77 (4), 1136–1160. doi:10.1016/j.jhep.2022.06.012

Qu, B., Liu, X., Liang, Y., Zheng, K., Zhang, C., and Lu, L. (2022). Salidroside in the treatment of NAFLD/NASH. *Chem. Biodivers.* 19 (12), e202200401. doi:10.1002/cbdv.202200401

Quek, J., Chan, K. E., Wong, Z. Y., Tan, C., Tan, B., Lim, W. H., et al. (2023). Global prevalence of non-alcoholic fatty liver disease and non-alcoholic steatohepatitis in the overweight and obese population: a systematic review and meta-analysis. *Lancet Gastroenterol. Hepatol.* 8 (1), 20–30. doi:10.1016/S2468-1253(22)00317-X

Ren, T., Zhu, J., Zhu, L., and Cheng, M. (2017). The combination of blueberry juice and probiotics ameliorate non-alcoholic steatohepatitis (NASH) by affecting SREBP-1c/PNPLA-3 pathway via PPAR-α. *Nutrients* 9 (3), 198. doi:10.3390/nu9030198

Rong, L., Li, Z., Leng, X., Li, H., Ma, Y., Chen, Y., et al. (2020). Salidroside induces apoptosis and protective autophagy in human gastric cancer AGS cells through the PI3K/Akt/mTOR pathway. *Biomed. Pharmacother.* 122, 109726. doi:10.1016/j.biopha.2019.109726

Savage, T. M., Fortson, K. T., de Los Santos-Alexis, K., Oliveras-Alsina, A., Rouanne, M., Rae, S. S., et al. (2024). Amphiregulin from regulatory T cells promotes liver fibrosis and insulin resistance in non-alcoholic steatohepatitis. *Immunity* 57 (2), 303–318.e6. doi:10.1016/j.immuni.2024.01.009

Shojaie, L., Iorga, A., and Dara, L. (2020). Cell death in liver diseases: a review. *Int. J. Mol. Sci.* 21 (24), 9682. doi:10.3390/ijms21249682

Staels, B., Butruille, L., and Francque, S. (2023). Treating NASH by targeting peroxisome proliferator-activated receptors. *J. Hepatol.* 79 (5), 1302–1316. doi:10.1016/j.jhep.2023.07.004

Sun, P., Song, S. Z., Jiang, S., Li, X., Yao, Y. L., Wu, Y. L., et al. (2016). Salidroside regulates inflammatory response in raw 264.7 macrophages via TLR4/TAK1 and ameliorates inflammation in alcohol binge drinking-induced liver injury. *Molecules* 21 (11), 1490. doi:10.3390/molecules21111490

Tilg, H., and Moschen, A. R. (2010). Evolution of inflammation in nonalcoholic fatty liver disease: the multiple parallel hits hypothesis. *Hepatology* 52 (5), 1836–1846. doi:10.1002/hep.24001

Tincopa, M. A., and Loomba, R. (2023). Non-invasive diagnosis and monitoring of non-alcoholic fatty liver disease and non-alcoholic steatohepatitis. *Lancet. Gastroenterol. Hepatol.* 8 (7), 660–670. doi:10.1016/S2468-1253(23)00066-3

Vargas-Pozada, E. E., Ramos-Tovar, E., Rodriguez-Callejas, J. D., Cardoso-Lezama, I., Galindo-Gómez, S., Talamás-Lara, D., et al. (2022). Caffeine inhibits NLRP3 inflammasome activation by downregulating TLR4/MAPK/NF-κB signaling pathway in an experimental NASH model. *Int. J. Mol. Sci.* 23 (17), 9954. doi:10.3390/ijms23179954

Wang, F., Zhang, X., Liu, W., Zhou, Y., Wei, W., Liu, D., et al. (2021). Activated natural killer cell promotes nonalcoholic steatohepatitis through mediating JAK/STAT pathway. *Cell. Mol. Gastroenterol. Hepatol.* 13 (1), 257–274. doi:10.1016/j.jcmgh.2021.08.019

Wang, P., Zhang, X., Zheng, X., Gao, J., Shang, M., Xu, J., et al. (2022). Folic acid protects against hyperuricemia in C57bl/6J mice via ameliorating gut-kidney Axis dysfunction. *J. Agric. Food Chem.* 70 (50), 15787–15803. doi:10.1021/acs.jafc.2c06297

Woestemeier, A., Scognamiglio, P., Zhao, Y., Wagner, J., Muscate, F., Casar, C., et al. (2023). Multicytokine-producing $CD4^+$ T cells characterize the livers of patients with NASH. *JCI Insight* 8 (1), e153831. doi:10.1172/jci.insight.153831

Wu, W. K. K., Zhang, L., and Chan, M. T. V. (2018). Autophagy, NAFLD and NAFLD-related HCC. *Adv. Exp. Med. Biol.* 1061, 127–138. doi:10.1007/978-981-10-8684-7_10

Xu, J., Zhao, L., Zhang, X., Ying, K., Zhou, R., Cai, W., et al. (2023). Salidroside ameliorates acetaminophen-induced acute liver injury through the inhibition of endoplasmic reticulum stress-mediated ferroptosis by activating the AMPK/SIRT1 pathway. *Ecotoxicol. Environ. Saf.* 262, 115331. doi:10.1016/j.ecoenv.2023.115331

Yan, T., Yan, N., Wang, P., Xia, Y., Hao, H., Wang, G., et al. (2020). Herbal drug discovery for the treatment of nonalcoholic fatty liver disease. *Acta Pharm. Sin. B* 10 (1), 3–18. doi:10.1016/j.apsb.2019.11.017

Yang, S., Wang, L., Zeng, Y., Wang, Y., Pei, T., Xie, Z., et al. (2023). Salidroside alleviates cognitive impairment by inhibiting ferroptosis via activation of the Nrf2/GPX4 axis in SAMP8 mice. *Phytomedicine* 114, 154762. doi:10.1016/j.phymed.2023.154762

Younossi, Z., Anstee, Q. M., Marietti, M., Hardy, T., Henry, L., Eslam, M., et al. (2018). Global burden of NAFLD and NASH: trends, predictions, risk factors and prevention. *Nat. Rev. Gastroenterol. Hepatol.* 15 (1), 11–20. doi:10.1038/nrgastro.2017.109

Zhang, X., Xie, L., Long, J., Xie, Q., Zheng, Y., Liu, K., et al. (2021). Salidroside: a review of its recent advances in synthetic pathways and pharmacological properties. *Chem. Biol. Interact.* 339, 109268. doi:10.1016/j.cbi.2020.109268

Zhao, P., Sun, X., Chaggan, C., Liao, Z., Wong, K., He, F., et al. (2020). An AMPK-caspase-6 axis controls liver damage in nonalcoholic steatohepatitis. *Science* 367 (6478), 652–660. doi:10.1126/science.aay0542

Zhao, S., Guo, Y., and Yin, X. (2024). Autophagy, ferroptosis, apoptosis and pyroptosis in metabolic dysfunction-associated steatotic liver disease. *Front. Biosci. Landmark Ed.* 29 (1), 30. doi:10.31083/j.fbl2901030

Zhou, Y., Zhang, H., Yao, Y., Zhang, X., Guan, Y., and Zheng, F. (2022). $CD4^+$ T cell activation and inflammation in NASH-related fibrosis. *Front. Immunol.* 13, 967410. doi:10.3389/fimmu.2022.967410

Zi, C., Wang, D., Gao, Y., and He, L. (2022). The role of Th17 cells in endocrine organs: involvement of the gut, adipose tissue, liver and bone. *Front. Immunol.* 13, 1104943. doi:10.3389/fimmu.2022.1104943

frontiers | Frontiers in Pharmacology

TYPE Review
PUBLISHED 13 November 2024
DOI 10.3389/fphar.2024.1499602

OPEN ACCESS

EDITED BY
Qinge Ma,
Jiangxi University of Traditional Chinese Medicine, China

REVIEWED BY
Li Hui,
Guangzhou University of Chinese Medicine, China
Wen-fu Tang,
Sichuan University, China

*CORRESPONDENCE
Jingqing Hu,
gcp306@126.com

†These authors have contributed equally to this work and share first authorship

RECEIVED 21 September 2024
ACCEPTED 30 October 2024
PUBLISHED 13 November 2024

CITATION
Liu Y, Fan Y, Liu J, Liu X, Li X and Hu J (2024) Application and mechanism of Chinese herb medicine in the treatment of non-alcoholic fatty liver disease.
Front. Pharmacol. 15:1499602.
doi: 10.3389/fphar.2024.1499602

Application and mechanism of Chinese herb medicine in the treatment of non-alcoholic fatty liver disease

Yuqiao Liu[1†], Yue Fan[1†], Jibin Liu[1†], Xiyang Liu[1], Xiuyan Li[1] and Jingqing Hu[1,2*]

[1]College of Basic Medical Sciences, Chengdu University of Traditional Chinese Medicine, Chengdu, China, [2]Xin-Huangpu Joint Innovation Institute of Chinese Medicine, Guangzhou, China

Non-alcoholic fatty liver disease (NAFLD) is a chronic liver condition closely associated with metabolic syndrome, with its incidence rate continuously rising globally. Recent studies have shown that the development of NAFLD is associated with insulin resistance, lipid metabolism disorder, oxidative stress and endoplasmic reticulum stress. Therapeutic strategies for NAFLD include lifestyle modifications, pharmacological treatments, and emerging biological therapies; however, there is currently no specific drug to treat NAFLD. However Chinese herb medicine (CHM) has shown potential in the treatment of NAFLD due to its unique therapeutic concepts and methods for centuries in China. This review aims to summarize the pathogenesis of NAFLD and some CHMs that have been shown to have therapeutic effects on NAFLD, thus enriching the scientific connotation of TCM theories and facilitating the exploration of TCM in the treatment of NAFLD.

KEYWORDS

non-alcoholic fatty liver disease (NAFLD), Chinese herb medicine (CHM), insulin resistance, lipid metabolism disorder, mitochondrial dysfunction, oxidative stress, endoplasmic reticulum stress

1 Introduction

Non-alcoholic fatty liver disease (NAFLD) is a growing public health issue worldwide, encompassing a spectrum of liver conditions ranging from simple fatty liver to nonalcoholic steatohepatitis (NASH), which may progress to cirrhosis and hepatocellular carcinoma (Diehl and Day, 2017). In certain parts of the world, the prevalence of NAFLD is thought to reach up to 26.5% (Younossi et al., 2023). Moreover, NAFLD prevalence in China is 32.5% (Teng et al., 2023). NAFLD is closely associated with components of the metabolic syndrome, such as obesity, type 2 diabetes and hyperlipidemia, and its prevalence is rising in tandem with the increasing prevalence of these metabolic disorders (Younossi et al., 2016).

NAFLD presents itself as a syndrome characterized by the accumulation of fat along with hepatocellular steatosis, ballooning degeneration, lobar inflammation, and predominantly fibrosis (Chalasani et al., 2018). The pathogenesis of NAFLD is complex, involving lipid metabolism disorders (Anwar et al., 2023), insulin resistance (Muzurović et al., 2021), inflammatory responses (Tilg and Moschen, 2010), mitochondrial dysfunction (Mansouri et al., 2018), oxidative stress (Karkucinska-Wieckowska et al., 2022), and endoplasmic reticulum stress (Ajoolabady et al., 2023). Currently, the treatment of

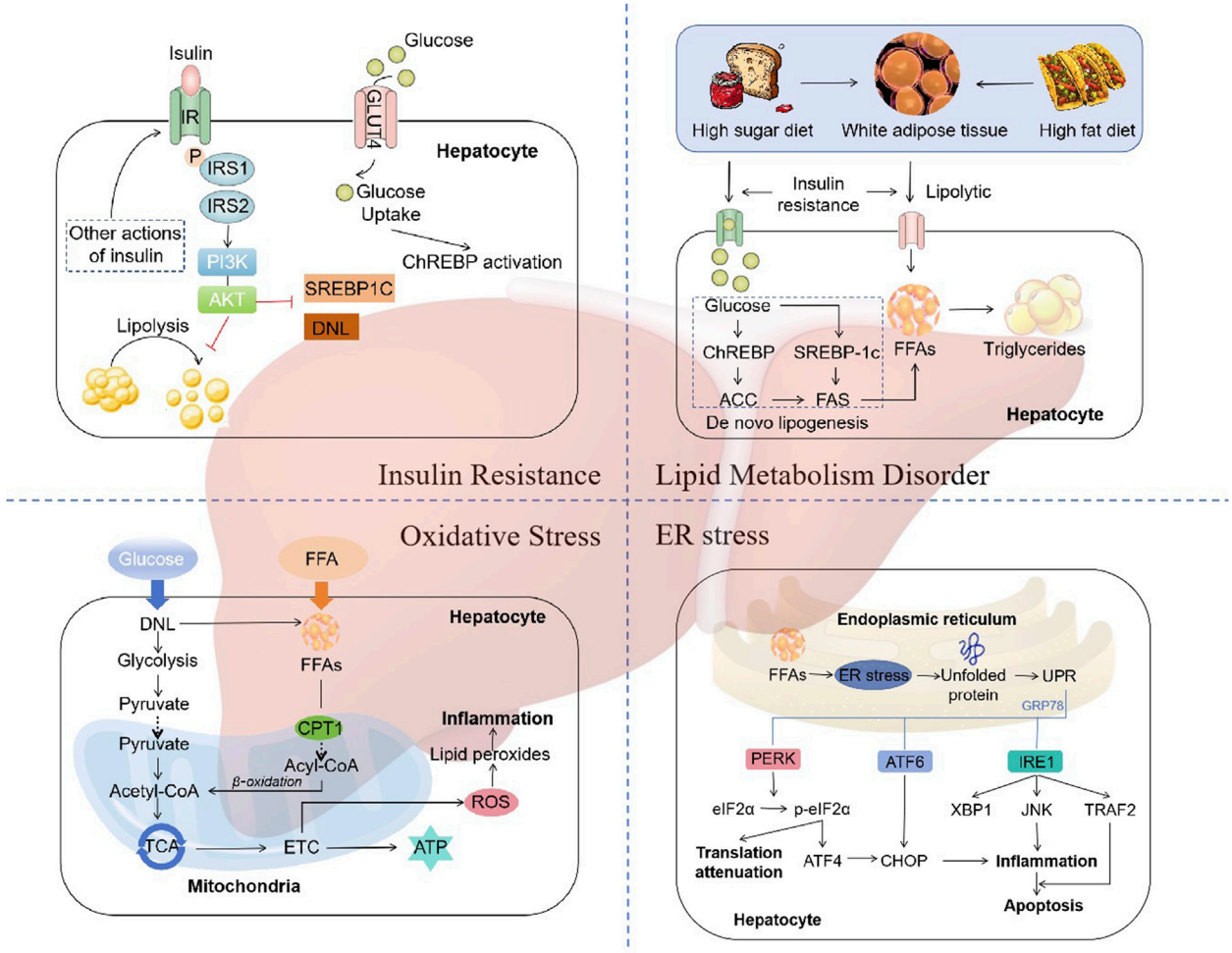

FIGURE 1
The mechanisms of NAFLD. "Multiple hit" theory includes various factors such as insulin resistance, lipid metabolism disorder, mitochondrial dysfunction, oxidative stress, and endoplasmic reticulum (ER) stress. Abbreviations: IRS, insulin receptor substrate; PI3K, phosphatidylinositol 3-kinase; AKT, protein kinase B; SREBP1C, sterol regulatory element binding protein 1c; DNL, *de novo* lipogenesis; ChREBP, carbohydrate regulatory element-binding protein; ACC, acetyl-CoA carboxylase; FAS, fatty acid synthase; TCA, tricarboxylic acid cycle; ETC, electron transport chain; CPT1, carnitine palmitoyltransferase 1; ROS, reactive oxygen species; UPR, unfolded protein response; PERK, RNA-like ER kinase; eIF2α, phosphorylation of eukaryotic initiation factor-2α; ATF4, activation of transcription factor 4; ATF6, activation of transcription factor 6; CHOP, CCAAT-enhancer-binding protein homologous protein; IRE1, inositol-requiring enzyme 1; XBP1, X-box binding protein-1; JNK, c-Jun N-terminal kinase; TRAF2, TNF receptor-related factor 2.

NAFLD primarily relies on lifestyle modifications, including dietary adjustments and increased physical activity (El-Agroudy et al., 2019; Golabi et al., 2016). Contemporary medical approaches to treat NAFLD include the improvement of insulin resistance and the use of lipid-lowering drugs, antioxidants, and hepatocyte-protective agents, all promoting liver lipid metabolism and accelerating intrahepatic fat transport (Nassir, 2022). Although some drugs have entered clinical trials, to date, no specific drug has been approved for the treatment of NAFLD (Friedman et al., 2018). Therefore, it is urgent to develop specific drugs for the treatment of NAFLD, which will generate significant social and economic benefits.

Chinese herb medicine (CHM), as an integral part of traditional Chinese medicine (TCM), has unique theories and practical experiences in treating chronic diseases (Shi et al., 2020). The CHM approach to treating NAFLD is usually based on the principle of syndrome differentiation and treatment, aiming to harmonize the body's yin-yang balance. CHM has been used extensively and safely for millennia to treat liver disorders. In recent years, numerous studies have indicated that certain components of CHM have effects such as modulating insulin resistance (Dai et al., 2022), regulating lipid metabolism (Yang J. M. et al., 2019), anti-inflammation (Lan T. et al., 2021) and antioxidant (Fan et al., 2023), offering new perspectives for the treatment of NAFLD.

With "NAFLD" and "Chinese herb medicine" as key words, we searched CNKI, WanFang, VIP, SinoMed, and PubMed database for relevant literature in the last 10 years. By systematically reviewing relevant literature, this review aims to provide a comprehensive analysis of existing research on the treatment of NAFLD with CHM, explore its mechanisms of action, assess its clinical efficacy, and propose future research directions.

2 Multiple hit theory of NAFLD

The traditional "two hit" hypothesis has gradually transitioned to "multiple hit" theory (Fang et al., 2018). In the "two hit" hypothesis, the first hit is represented by insulin resistance associated with obesity, type 2 diabetes, hyperlipidemia, and other conditions, leading to excessive lipid deposition within hepatocytes. The second hit refers to the occurrence of lipid peroxidation and oxidative stress in hepatocytes with excessive lipid deposition, leading to mitochondrial dysfunction, production of inflammatory mediators, and activation of hepatic stellate cells, thereby resulting in NASH and fibrosis (James and Day, 1998). However, as it is inadequate to explain the several molecular and metabolic changes that take place in NAFLD, the "two-hit" hypothesis is now obsolete. "Multiple hit" theory includes various factors such as insulin resistance, lipid metabolism disorder, mitochondrial dysfunction, oxidative stress, and endoplasmic reticulum (ER) stress, etc (Buzzetti et al., 2016) (Figure 1).

2.1 Insulin resistance

Insulin resistance (IR) is one of the "multiple hits" predisposing to the development of NAFLD and progression to NASH (Peverill et al., 2014). Dietary factors are crucial for the development of NAFLD. Typical western diet, which has high consumption of fat, has been associated with IR (Fan and Cao, 2013). During the intake of calories, the insulin reduces the production of glucose in the liver by inhibiting glycogenolysis and limiting the postprandial rise in glucose. However, this feedback mechanism is impaired in individuals with IR, resulting in the continued elevation of hepatic glucose production despite the postprandial glucose increases (Fujii et al., 2020). The status of IR leads adipose tissue unresponsive to the antilipolytic effect of insulin, resulting in triglyceride (TG) hydrolysis and the ultimate formation of free fatty acids (FFAs) and glycerol (Schweiger et al., 2006). Increased lipolysis in adipocytes leads to an increase in circulating FFAs, which further exacerbates steatosis and IR in muscle tissue (Zhang et al., 2014).

The molecular mechanism of IR refers to the impairment of the appropriate downstream effects of insulin signaling in target tissues, such as the liver, muscle, and adipose tissue. Insulin exerts its effects on all cells by binding to its specific receptor, thereby initiating a cascade of intracellular signaling (Khan et al., 2019). Upon insulin binding, the insulin receptor phosphorylates itself and several members of the insulin receptor substrate (IRS) family. The typical IRS signalling pathways include those that are dependent on IRS1 or IRS2, which utilise the activities of phosphatidylinositol 3-kinase (PI3K), phosphoinositide-dependent kinase (PDK) and protein kinase B (AKT), as well as the RAS-extracellular-signal regulated kinase (ERK) pathway (Eckstein et al., 2017). Activation of IRS2 has been demonstrated to function as a regulator of sterol regulatory element binding protein 1c (SREBP-1c), thereby influencing *de novo* lipogenesis (DNL) (Schreuder et al., 2008). In states of IR, there is a reduction in the expression of IRS-2, which results in an increase in the expression of SREBP-1c and a corresponding elevation in the rate of DNL (Stefan et al., 2008). Additionally, the β-oxidation of FFAs is suppressed in states of insulin resistance, thereby further promoting the accumulation of hepatic lipids (Postic and Girard, 2008). Thus, disorders of lipid metabolism due to dysregulation of insulin signalling are key factors in the development and progression of NAFLD.

2.2 Lipid metabolism disorder

The liver plays a distinctive role in lipid metabolism, acting as a site for lipid uptake, synthesis, oxidation, and distribution of lipids to peripheral tissues (Nguyen et al., 2008). Hepatic fat accumulation results from an imbalance between lipid acquisition and lipid disposal. When energy intake is higher than consumption, excess energy is stored in the form of lipids. In patients with NAFLD, fat accumulates primarily in the form of TG within the liver (Jacome-Sosa and Parks, 2014). The formation of TG is the result of the esterification of glycerol and FFAs. Hepatic steatosis is initiated by an increase in the synthesis of TG in hepatocytes. This synthesis is dependent on the supply of a substrate originating from white adipose tissue (WAT), DNL, and the consumption of a high fat and/or high sugar diet (Donnelly et al., 2005; Heeren and Scheja, 2021; Machado and Cortez-Pinto, 2014).

Dysregulation of DNL is a central feature of liver lipid accumulation in NAFLD patients (Ipsen et al., 2018). The transcriptional regulation of DNL is mainly orchestrated by two key transcription factors: sterol regulatory element-binding protein 1c (SREBP1c) and carbohydrate regulatory element-binding protein (ChREBP) (Eberlé et al., 2004; Sanders and Griffin, 2016). SREBP1c expression is enhanced in NAFLD patients, with higher levels of hepatic triglyceride and upregulating genes coding for acetyl-CoA carboxylase (ACC) and fatty acid synthase (FAS) (Higuchi et al., 2008; Kohjima et al., 2007). In addition, SREBP1c indirectly contributes to the development of hepatic insulin resistance, since enhanced lipogenesis and subsequent accumulation of harmful lipid species, such as diacylglycerides, may interfere with insulin signaling (Kumashiro et al., 2011; Ter Horst et al., 2017). ChREBP is a key transcription factor for enzymes in the fructolysis, glycolysis, gluconeogenesis, and DNL pathways (Iizuka et al., 2004; Iizuka and Horikawa, 2008; Kim et al., 2016). Increased glucose concentration activates ChREBP to regulate the expression of ACC1 and FAS, thereby promoting DNL in hepatocytes (Denechaud et al., 2008; Dentin et al., 2006). Thus, A high fat and/or high sugar diet directly affects the DNL pathways, leading to the accumulation of lipid and the development of NAFLD.

2.3 Oxidative stress

A number of factors contribute to the occurrence of "multiple hits", with oxidative stress being considered the primary cause of liver injury and disease progression in NAFLD (Friedman et al., 2018). An increase in FFAs in the liver, which may result from a number of different causes, can lead to the damage of β-oxidation and mitochondrial dysfunction, resulting in inflammation, which leads to oxidative stress (Chen et al., 2020). Reactive oxygen species (ROS) are important mediators of the inflammatory response (Begriche et al., 2006). ROS, which includes superoxide anion radicals (O2·-) and hydrogen peroxide (H2O2), are continuously

produced intracellularly as byproducts of energetic metabolism in different types of liver cells (Masarone et al., 2018). Normal levels of reactive ROS act as signalling molecules that regulate a number of essential cellular processes, including metabolism, survival, immune defence, proliferation and differentiation through the modulation of transcription factors and epigenetic pathways (Forrester et al., 2018). A reduction in ROS generation leads to a decline in redox status and, consequently, impairs the ability of cells to perform physiological redox signaling (Zhang et al., 2019). In the case of oxidative stress, however, excessive ROS induce oxidative modifications to macromolecules, including DNA, lipids, and proteins, leading to the accumulation of damaged macromolecules and subsequent liver injury (Serviddio et al., 2013). In most cells, mitochondria are considered the most quantitatively relevant ROS generators (Mansouri et al., 2018). The liver contains between 500 and 4,000 mitochondria per hepatocyte, which collectively occupy approximately 18% of the cell volume (Degli Esposti et al., 2012). In addition to the mechanisms for the pathophysiology of NAFLD described above, multiple mitochondria-associated factors contribute to the development and progression of NAFLD. Such factors include reduced β-oxidation, impaired, ETC and ATP depletion, over-production of ROS, oxidative stress-mediated cell damage, and ultra-structural mitochondrial changes (Begriche et al., 2006; Begriche et al., 2013; Pessayre et al., 2002). These changes in mitochondrial function and structure exacerbate hepatic lipid accumulation and trigger inflammatory and fibrogenic processes, thereby contributing to the development and progression of NAFLD.

2.4 Endoplasmic reticulum stress

The main metabolic pathway affected by endoplasmic reticulum (ER) stress is lipogenesis (Flamment et al., 2010). ER stress is implicated in both the development of hepatic steatosis and the progression of NASH. Disruption of ER homeostasis has been observed in liver and adipose tissue of humans with NAFLD (Gentile et al., 2011; Puri et al., 2008). ER stress represents a protective response that restores protein homeostasis through the activation of the unfolded protein response (UPR) (Li W. et al., 2020). The UPR has been linked to lipid biosynthesis, insulin action, inflammation, and apoptosis (Glimcher and Lee, 2009; Hotamisligil, 2010; Kim et al., 2008).

UPR is mediated by three typical ER-resident stress sensors, protein kinase RNA-like ER kinase (PERK), inositol-requiring enzyme 1 (IRE1), and activating transcription factor 6 (ATF6) (Gong J. et al., 2017). These three proximal UPR sensors all regulate lipid storage in the liver (Donnelly et al., 2005). ER stress has been demonstrated to induce apoptosis through the activation of these three sensor dimers and autophosphorylation (Shao et al., 2022). The IRE1-XBP1 and PERK-peIF2α pathways upregulate the adipogenic gene program (Kaufman, 1999). Conversely, the interaction between ATF6, sterol regulatory element-binding protein 2 (SREBP2) and histone deacetylase 1 (HDAC1) can limit adipogenesis (Zeng et al., 2004). In addition, ATF6 upregulates the expression of X-box binding protein-1 (XBP1), which is one of the main regulators of UPR and interacts with the PI3K insulin signaling pathway, with increased nuclear translocation induced by insulin (Park et al., 2010). XBP1 is a crucial transcription factor that regulates the expression of genes encoding the adaptive UPR. The interaction between PI3K and XBP-1 is subject to modulation by both the cellular response to ER stress and the interaction itself (Winnay et al., 2010). Another consequence of UPR is the activation of SREBP-1c pathways, which results in the maintenance of liver fat accumulation and a further exacerbation of ER stress and UPR (Ferré and Foufelle, 2010). Thus, all three proximal UPR sensors, PERK, IRE1α, and ATF6α, can regulate lipid stores in the liver.

3 CHM used in treatment for NAFLD

NAFLD is a complex metabolic disorder that often co-occurs with other metabolic conditions such as dyslipidemia, hypertension, and diabetes mellitus (Zhao et al., 2018). In TCM, while there is no direct equivalent term for NAFLD, the concept of “dampness” and “phlegm” is often used to describe conditions that resemble the symptoms and pathophysiological mechanisms associated with NAFLD. NAFLD can be recognized as hepatic syndromes like distention and fullness, phlegm syndrome like turbidity, hypochondriac pain, lump at the left hypochondrium and damp obstruction disease based on its symptoms and pathogenesis (Zhang and Li, 2017).

In long-term clinical practice, CHM has unique advantages in the treatment of NAFLD. Characterized by a multi-herbal composition and multi-target pharmacological effects, CHM is compatible with the complex pathogenesis of NAFLD. As a result, the majority of NAFLD patients have availed themselves of TCM therapies.

Considering the varying progression of NAFLD, it is imperative to select appropriate CHM for treatment at different stages. Initially, therapeutic interventions for NAFLD focus on soothing the liver, regulating the flow of qi, and bolstering the functions of the spleen and stomach. Xiao Yao San is often used to achieve the effect of soothing the liver and strengthening the spleen in clinical practice. As the condition progresses into the middle and later stages, the primary treatment strategies shift towards strengthening the spleen and nourishing the kidneys, invigorating blood circulation to disperse blood stasis, and additionally incorporating measures to clear heat and resolve dampness. Gexiazhuyu Tang with Erchen Tang are used to activate blood circulation to remove blood stasis, and resolve phlegm to disperse nodules. Sijunzi Tang with Jinguishenqi Pillsis are used to tonify the spleen and kidneys (Zhang and Li, 2017). Meanwhile, the selection of clinical prescriptions should be based on the primary symptom, with consideration given to the other symptoms. It is recommended that a slight variation be made in the selected prescriptions, and that a “differentiation treatment” be employed. Based on clinical experience, the common diagnostic treatment of NAFLD is shown in Table 1.

CHM emphasize on the importance of individualized therapy based on syndrome differentiation, and a variety of CHM formulas are used to alleviate specific symptoms associated with the condition. The selection of formulas is dependent upon the four properties of TCM (cold, hot, warm, cool), the five flavours (sour, bitter, sweet, spicy, salty), and the efficiency. We have assembled a

TABLE 1 The common diagnostic treatment of NAFLD.

TCM Syndrome	Main Symptom	Secondary Symptom	Representive Formula	Prescriptions	TCM therapies
Congestion of dampness turbidity	Distension and fullness in the right hypochondriac region	Obesity, general heaviness and fatigue throughout the body, chest and epigastric stuffiness, dizziness, and nausea	Weiling Tang	*Atractylodes lancea (Thunb.) DC* [Asteraceae; *Rhizoma atractylodis*], *Citrus reticulata Blanco* [Rutaceae; *Tangerine peel*], *Magnolia obovata Thunb.* [Magnoliaceae; *Magnolia officinalis*], *Glycyrrhiza glabra L.* [Fabaceae; *Licorice*], *Alisma plantago-aquatica L.* [Alismataceae; *Rhizoma alismatis*], *Crotalaria albida B.Heyne ex Roth* [Fabaceae; *Polyporus*], *Geranium delavayi Franch.* [Geraniaceae; *Red poria*], *Atractylodes macrocephala Koidz.* [Asteraceae; *Rhizoma atractylodis macrocephalae*], *Neolitsea cassia (L.) Kosterm.* [Lauraceae; *Cinnamon*]	Dispelling dampness and clarifying turbidity
Stagnation of liver-depression with spleen-deficiency	Distending or migratory pain in the right hypochondriac area, triggered by irritability or anger	Abdominal bloating, loose stools, abdominal pain with an urge to defecate, fatigue, chest distress, frequent sighing	Xiaoyao powder	*Levisticum officinale W.D.J.Koch* [Apiaceae;*Radix angelicae sinensis*], *Paeonia lactiflora Pall.* [Paeoniaceae; *Radix paeoniae alba*], *Bupleurum chinense DC.* [Apiaceae;*Radix bupleuri*], *Smilax glabra Roxb.* [Smilacaceae; *Fuling*], *Atractylodes macrocephala Koidz.* [Asteraceae; *Rhizoma atractylodis macrocephalae*], *Glycyrrhiza glabra L.* [Fabaceae; *Prepared liquorice root*], *Zingiber officinale Roscoe* [Zingiberaceae; *Ginger*], *Mentha canadensis L.* [Lamiaceae; *Mint*]	Soothing the liver and strengthening the spleen
Accumulation knot of damp and hot	Distending pain in the right hypochondriac region	Nausea, vomiting, jaundice, chest and epigastric fullness, general heaviness, and loss of appetite	Sanren Tang with Yinchen Wuling powder	*Prunus armeniaca L.* [Rosaceae; *Almonds*], *Talc* [*Mg3(Si4O10)(OH)2*], *Tetrapanax papyrifer (Hook.) K.Koch* [Araliaceae; *Medulla tetrapanacis*], *Myristica fragrans Houtt.* [Myristicaceae; *Roud cardamon seed*], *Zanthoxylum armatum DC.* [Rutaceae; *Bamboo leaves*], *Magnolia obovata Thunb.* [Magnoliaceae; *Magnolia officinalis*], *Coix lacryma-jobi L.* [Poaceae; *Coix Seed*], *Pinellia ternata (Thunb.) Makino* [Araceae; *Rhizoma pinelliae*], *Artemisia capillaris Thunb.* [Asteraceae; *Herba artemisiae scopariae*], *Smilax glabra Roxb.* [Smilacaceae; *Fuling*], *Alisma plantago-aquatica L.* [Alismataceae; *Rhizoma alismatis*], *Crotalaria albida B.Heyne ex Roth* [Fabaceae; *Polyporus*], *Neolitsea cassia (L.) Kosterm.* [Lauraceae; *Ramulus cinnamomi*], *Atractylodes macrocephala Koidz.* [Asteraceae; *Rhizoma atractylodis macrocephalae*]	Clearing heat and transforming dampness
Syndrome of intermin-gled	Lump or stabbing pain in the right hypochondriac region	Loss of appetite, chest and epigastric oppression, and dull complexion	Gexiazhuyu Tang with Erchen Tang	*Juglans regia L.* [Juglandaceae; *Semen persicae*], *Paeonia × suffruticosa Andrews*	Activating blood circulation to remove blood stasis, and

(Continued on following page)

TABLE 1 (*Continued*) The common diagnostic treatment of NAFLD.

TCM Syndrome	Main Symptom	Secondary Symptom	Representive Formula	Prescriptions	TCM therapies
phlegm with blood stasis				*[Paeoniaceae; Cortex moutan], Paeonia lactiflora Pall.* [Paeoniaceae*; Radix paeoniae rubra], Corydalis turtschaninovii Besser* [Papaveraceae; *Yanhusuo], Glycyrrhiza glabra L.*[Fabaceae*; Prepared liquorice root], Conioselinum anthriscoides 'Chuanxiong'* [Apiaceae*; Szechuan lovage rhizome], Levisticum officinale W.D.J.Koch* [Apiaceae;*Radix angelicae sinensis], Trogopterori Faeces, Carthamus tinctorius L.* [Asteraceae; *Carthamus tinctorius], Citrus × aurantium L.* [Rutaceae; *Fructus aurantii], Lindera aggregata (Sims) Kosterm.* [Lauraceae; *Radix linderae], Cyperus rotundus L.* [Cyperaceae; *Rhizoma Cyperi], Citrus reticulata Blanco* [Rutaceae; *Tangerine peel], Pinellia ternata (Thunb.) Makino* [Araceae; *Rhizoma pinelliae], Smilax glabra Roxb.* [Smilacaceae; *Fuling], Prunus mume (Siebold) Siebold & Zucc.* [Rosaceae; *Fructus mume], Zingiber officinale Roscoe* [Zingiberaceae; *Ginger]*	resolving phlegm to disperse nodules
Deficiency of spleen and kidney	Right hypochondriac dull pain	Fatigue, sore and weak waist and knees, frequent nocturnal urination, and loose stools	Sijunzi Tang with Jinguishenqi Pills	*Panax ginseng C.A.Mey.* [Araliaceae; *Ginseng], Smilax glabra Roxb.*[Smilacaceae; *Fuling], Atractylodes macrocephala Koidz.* [Asteraceae; *Rhizoma atractylodis macrocephalae], Glycyrrhiza glabra L.* [Fabaceae; *Prepared liquorice root], Rehmannia glutinosa (Gaertn.) DC.* [Orobanchaceae; *Radix Rehmanniae preparata], Cornus officinalis Siebold & Zucc.* [Cornaceae; *Fructus corni], Dioscorea oppositifolia L.* [Dioscoreaceae; *Wild yam], Alisma plantago-aquatica L.* [Alismataceae; *Rhizoma alismatis], Paeonia × suffruticosa Andrews* [Paeoniaceae; *Cortex moutan]*	Tonifying the spleen and kidneys

diverse set of CHM formulas that are specifically designed to treat NAFLD and clarified the therapeutic mechanisms by which these CHM formulas ameliorate the disease (Table 2). For example, formulas such as Lingguizhugan decoction, Shenling Baizhu San, Chaihu Shugan powder are commonly used in clinical for the treatment of NAFLD.

In China, some TCM compounds have been approved as commercial Chinese polyherbal preparation (CCPP), while more TCM compounds are already in clinical trials (Table 3). Such as Dang Fei Li Gan Ning Capsules are primarily indicated for the treatment of patients with non-alcoholic simple fatty liver disease characterized by internal retention of damp-heat (Xiaoling et al., 2022). Hua Zhi Rou Gan Granules are primarily used for the treatment of patients with NAFLD characterized by damp-heat obstructing the middle burner syndrome (Cao et al., 2024; Liu W. et al., 2022). Each type of CCPP is selected based on the specific symptoms and underlying causes identified by a TCM practitioner, ensuring a personalized approach to treatment.

Currently, many clinical workers combined disease differentiation with syndrome differentiation and used proper prescriptions to effectively improve liver function and clinical symptoms in patients with NAFLD, achieving a satisfactory clinical effect.

TABLE 2 CHM prescriptions that are specifically designed to treat NAFLD.

Commercial Chinese polyherbal preparation	Prescriptions	TCM therapies	Indications	Mechanism	Reference
Dang Fei Li Gan Ning Capsules	*Silybum marianum (L.) Gaertn.* [Asteraceae; *Silymarin*], *Rumex acetosa L.* [*Polygonacea;Swertia pseudochinensis*]	Clearing damp-heat and benefiting the liver to alleviate jaundice	NAFLD with internal damp-heat retention syndrome	Reducing oxidative stress levels in the liver mediated by nuclear factor E2-related factor 2(Nrf2), promoting liver protein synthesis and bile metabolism, and regulating the expression of transforming growth factor-β1 (TGF-β1) and plasminogen activator inhibitor-1(PAI-1) during disease progression, thereby inhibiting the activation of hepatic stellate cells, collagen proliferation, and promoting the degradation of extracellular matrix, thus preventing liver fibrosis and exerting a hepatoprotective effect	Xiaoling et al. (2022)
Hua Zhi Rou Gan Granules	*Artemisia capillaris Thunb.*[Asteraceae;*Herba artemisiae scopariae*], *Senna tora (L.) Roxb.*[Fabaceae; *Semen cassiae*], *Rheum palmatum L.* [Polygonaceae; *Rhubarb*], *Alisma plantago-aquatica L.*[Alismataceae; *Rhizoma alismatis*], *Crotalaria albida B.Heyne ex Roth* [Fabaceae;*Polyporus*], *Crataegus pinnatifida Bunge* [Rosaceae;*Crataegus pinnatifida*], *Atractylodes lancea (Thunb.) DC* [Asteraceae;*Rhizoma atractylodis*], *Atractylodes macrocephala Koidz.*[Asteraceae;*Rhizoma atractylodis macrocephalae*], *Citrus reticulata Blanco* [Rutaceae;*Tangerine peel*], *Trichosanthes kirilowii Maxim.* [Cucurbitaceae;*Fructus trichosanthis*], *Ligustrum lucidum W.T.Aiton*[Oleaceae; *Fructus ligustri lucidi*], *Eclipta prostrata (L.) L.*[Asteraceae; *Herba ecliptae*], *Lycium barbarum L.*[Solanaceae; *Fructus lycii*], *Cirsium arvense* var. *arvense* [Asteraceae;*Herba cirsii*], *Bupleurum chinense DC.*[Apiaceae;*Radix bupleuri*], *Glycyrrhiza glabra L.*[Fabaceae;*Licorice*]	Clearing heat and resolving dampness, purifying turbidity and detoxifying, and removing blood stasis and softening the liver	NALFD with damp-heat obstructing the middle burner syndrome	Reducing insulin resistance, improving intestinal barrier function, inhibiting endotoxemia, and regulating gut microbiota dysbiosis.Inhibition of macrophage apoptosis and improvement of endoplasmic reticulum stress via the Bcl-2/Bax/ Caspase3 signaling pathway	Cao et al. (2024), Liu Y. et al. (2022)
Ke Zhi Capsules	Crustacean shellp [Carapace], Reynoutria multiflora (Thunb.) Moldenke [Polygonaceae; Radix polygoni multiflori], Artemisia capillaris Thunb. [Asteraceae; Herba artemisiae scopariae], Salvia miltiorrhiza Bunge [Lamiaceae; Salvia miltiorrhiza], *Achyranthes*	Digesting dampness and turbidity, activating blood circulation and dispersing lumps, and nourishing the liver and kidneys	NAFLD with internal retention of damp turbidity, qi stagnation and blood stasis, or combined with liver and kidney deficiency and depressive heat syndrome	Upregulating the expression of peroxisome proliferator activated receptor γ (PPARγ), insulin receptor mRNA, and protein in liver tissue, and significantly reducing tumor necrosis factor-α (TNF-α), interleukin-6 (IL-6), to exert effects of reducing insulin resistance, regulating fat	Zhao et al. (2014)

(Continued on following page)

TABLE 2 (*Continued*) CHM prescriptions that are specifically designed to treat NAFLD.

Commercial Chinese polyherbal preparation	Prescriptions	TCM therapies	Indications	Mechanism	Reference
	aspera L. [Amaranthaceae; Radix achyranthis bidentatae]			metabolism, improving liver function, and inhibiting liver inflammation in NAFLD.	
Xue Zhi Kang Capsules	*Monascus purpureus Went* [Monascaceae;*Red yeast rice*]	Clarifying turbidity and reducing lipids, activating blood circulation and resolving stasis, strengthening the spleen and aiding digestion	Hyperlipidemia caused by phlegm obstruction and blood stasis	Regulating blood lipids, having anti-inflammatory effect, and exerting protective effect on liver tissue through anti-inflammation mechanism	Zhang Z. et al. (2018)
Xiao Yao Wan (Granules)	*Bupleurum chinense DC.*[Apiaceae;*Radix bupleuri*], *Paeonia lactiflora Pall.*[Paeoniaceae;*Radix paeoniae alba*], *Levisticum officinale W.D.J.Koch* [Apiaceae;*Radix angelicae sinensis*], *Atractylodes macrocephala Koidz.*[Asteraceae;*Rhizoma atractylodis macrocephalae*], *Smilax glabra Roxb.*[Smilacaceae;*Fuling*], *Mentha canadensis L.*[Lamiaceae;*Mint*], *Glycyrrhiza glabra L.*[Fabaceae;*Licorice*], *Zingiber officinale Roscoe* [Zingiberaceae;*Ginger*]	Soothing the liver and strengthening the spleen, nourishing blood and regulating menstruation	Liver stagnation and spleen deficiency syndrome	Down-regulating PTGS2, up-regulating PPARG, reducing AA content, increasing cAMP, improving insulin resistance, affecting glucose and lipid metabolism, inhibiting oxidative stress and inflammatory response	Ruan et al. (2024)
Hugan Tablets	*Bupleurum chinense DC.*[Apiaceae;*Radix bupleuri*], *Schisandra chinensis (Turcz.) Baill.*[Schisandraceae; *Schisandra chinensis*], *Artemisia capillaris Thunb.*[Asteraceae;*Herba artemisiae scopariae*], *Strobilanthes cusia (Nees) Kuntze* [Acanthaceae;*Radix isatidis*], *Porcine Gall Bladder Powder*, *Vigna radiata (L.) R.Wilczek* [Fabaceae;*Green bean*]	Soothing the liver and regulating qi, strengthening the spleen and aiding digestion	Heart and spleen qi deficiency, with phlegm obstruction and blood stasis syndrome	Regulating the levels of MDA, SOD, and GSH-Px in the liver tissue of the model rats, and reversing the metabolic disorders of lipids, sugars, and amino acids	Gong M. et al. (2017)
Gynostemma Pentaphyllum Total Glycosides Tablets	*Gynostemma pentaphyllum (Thunb.) Makino* [Cucurbitaceae;*Gynostemma pentaphyllum*]	Nourishing the heart and strengthening the spleen, tonifying qi and harmonizing blood, expelling phlegm and resolving stasis	Heart and spleen qi deficiency, with phlegm obstruction and blood stasis syndrome	Improving liver function, lipid metabolism, insulin resistance, and levels of inflammatory factors in NAFLD model by regulating LPS/TLR4 signaling pathway	Shen et al. (2020)
Yin Zhi Huang Granules	*Artemisia capillaris Thunb.*[Asteraceae;*Herba artemisiae scopariae*], *Gardenia jasminoides J.Ellis* [Rubiaceae;*Gardenia*], *Scutellaria baicalensis Georgi* [Lamiaceae;*Scutellaria baicalensis georgi*], *Lonicera japonica Thunb.*[Caprifoliaceae; *Lonicera japonica*]	Clearing heat and detoxifying, resolving dampness and reducing jaundice	Damp-heat internal retention syndrome causing elevated ALT levels in both acute and chronic hepatitis	Downregulating protein expression of ACC1 and FASN, and reduce fatty acid absorption by downregulating protein expression of CD36, thereby affecting fatty liver metabolism	Tan et al. (2023)
Silibinin Capsules	*Silybum marianum (L.) Gaertn.* [Asteraceae;*Silymarin*]	Clearing heat and resolving dampness, soothing the liver and	Restoration of liver function abnormalities in patients with acute and	Reducing *de novo* lipogenesis and increasing FA oxidation and p-AMPKα expression	Cui et al. (2017)

(Continued on following page)

TABLE 2 (*Continued*) CHM prescriptions that are specifically designed to treat NAFLD.

Commercial Chinese polyherbal preparation	Prescriptions	TCM therapies	Indications	Mechanism	Reference
		promoting gallbladder function	chronic hepatitis and fatty liver		
Fu Fang Yi Gan Ling	*Silybum marianum (L.) Gaertn.* [Asteraceae; *Silymarin*], *Schisandra chinensis (Turcz.) Baill.*[Schisandraceae; *Schisandra chinensis*]	Nourishing the liver and the kidneys, detoxifying and dispelling dampness	Liver and kidney yin deficiency, with unresolved damp-toxicity syndrome in chronic hepatitis patients with elevated aminotransferase levels	Regulating the immune response and inflammatory reaction in the liver, modulating the liver's sugar and lipid metabolism, and reducing apoptosis and cell damage in hepatocytes	Guo et al. (2023)

4 Effects and mechanisms of commonly used botanical drugs on NAFLD

In fact, in traditional medicine, botanical drugs play a crucial role in the prevention and mitigation of different human diseases. Due to the complicated metabolites found in botanical drugs, studying the active metabolites became the mainstream of TCM research. According to the literature and clinical experience, the Chinese medicinal herbs commonly used for treatment of NAFLD in clinical practice can be divided into the following types (Table 4). Here, we summarize the pharmacological effects of active metabolites from high-frequency single herbs.

4.1 Shan Zha (*Crataegus pinnatifida* Bunge)

Crataegus pinnatifida Bunge and its subspecies *C. pinnatifida* var. *pubescens* Nakai and *C. pinnatifida* var. *Pinnatifida* [syn.: *Crataegus cuneata* Siebold & Zucc.; Rosaceae] yield Shan Zha (crataegi fructus), is recognized for its ability to enhance digestion and alleviate bloating in TCM. Research has shown that *C. pinnatifida* Bunge possesses potent antioxidant and free radical scavenging activities, which can be attributed to its content of various bioactive metabolites, including chlorogenic acid, epicatechin, hyperoside, vitexin, quercetin, rutin, and procyanidins (Barros et al., 2011; Tadić et al., 2008; Zhang et al., 2001). These metabolites are reported to have many pharmacological effects, which are involved in the treatment of various diseases, including hypertension, cardiovascular, anti-oxidative, atherosclerosis, and hyperlipidemiawhich (Bahorun et al., 2003; Kirakosyan et al., 2003; Yoo et al., 2016). Among them, vitexin and quercetin are reported to intervene NAFLD.

The study showed that 5-week vitexin administration (40 mg/kg, i. g.) could obviously reduce hepatic fat deposition, alleviate lipid metabolism, and inhibit liver inflammation in NAFLD mice. In addition, vitexin significantly reduced hepatic macrophage infiltration, obviously downregulated the mRNA and protein expressions of hepatic SREBP-1c, FAS, ACC, and could significantly inhibit the expressions of TLR4/NF-κB signaling in NAFLD mice (Li C. et al., 2020).

Another metabolite, quercetin is also reported to protect the liver. The finding suggested that antiinflammatory responses, antioxidant, and improve ment of lipid metabolism via farnesoid X receptor 1 (FXR1)/Takeda G protein-coupled receptor 5 (TGR5) signaling pathways played key role in the hepatoprotective effects of quercetin (oral gavaged with the quercetin (100 mg/kg) once a day for 8 weeks) in T2DM-induced NAFLD db/db mice (Yang H. et al., 2019). In additional, quercetin revertes the balance of the gut microbiota and counteracted endotoxemia-induced activation of the TLR-4 pathway, subsequently inhibiting the inflammasome response and the activation of the reticulum stress pathway, which resulted in the prevention of deregulation in the expression of lipid metabolism genes (Porras et al., 2017).

In conclusion, *C. pinnatifida* Bunge can exert therapeutic effects on NAFLD through its anti-inflammatory properties, regulation of lipid metabolism, and modulation of the gut microbiota.

4.2 Ze Xie (*Alisma plantago-aquatica* L.)

The rhizome of *Alisma plantago-aquatica* L. and its subspecies *A. plantago-aquatica subsp. orientale* (Sam.) Sam. [syn.: *Alisma orientale (Sam.)* Juz.; Alismataceae] yield Ze Xie (alismatis rhizoma), which has been used to treat various ailments, such as dysuria, edema, nephropathy, hyperlipidemia, and diabetes. A wide range of metabolites, mainly triterpenoids, sesquiterpenoids, and diterpenoids, have been isolated from *A. plantago-aquatica* L.; among which the protostane-type triterpenoids, termed alisol A and B have been proved to be effective on NAFLD (Gao et al., 2024; Li and Qu, 2012; Zhang et al., 2017).

Alisol A (100 mg/kg/day, intraperitoneal injection once daily for 4 weeks) effectively attenuated HFD-induced obesity, suppressed hepatic steatosis and improved lipid and glucose metabolism, and improved damaged β-oxidation in DIO mice. The pharmacologic action may be mediated through AMPK/ACC/SREBP-1c pathway activation (Ho et al., 2019). In another study, the MCD-induced mice were simultaneously treated with a daily dose of Alisol A (15, 30, and 60 mg·kg^{-1}, ig) for 4 weeks. The results showed that Alisol A can also ameliorate steatohepatitis by inhibiting oxidative stress and stimulating autophagy through the AMPK/mTOR pathway (Wu et al., 2018).

A study indicated that treated with 100 mg/kg Alisol B once daily for 8 weeks showed significant therapeutic effects on DIO + CCl4 and CDA diet-induced murine NASH models. In this study,

TABLE 3 Commonly used commercial Chinese polyherbal preparation (CCPP) for the treatment of NAFLD.

Formula	Prescriptions	Experimental model	Mechanism	References
Lingguizhugan decoction	*Smilax glabra Roxb.* [Smilacaceae; *Fuling*], *Neolitsea cassia (L.) Kosterm.* [Lauraceae; *Ramulus cinnamomi*], *Atractylodes macrocephala Koidz.* [Asteraceae; *Rhizoma atractylodis macrocephalae*], *Glycyrrhiza glabra L.*[Fabaceae;*Licorice*]	C57BL/6J mice with HFD model, Mice bone-marrow-derived macrophages (BMDMs)	Ameliorate HFD-induced hepatic-lipid deposition through inhibiting STING-TBK1-NF-κB pathway in liver macrophages	Cao et al. (2022a)
		Wistar rats with HFD model	Alleviate hepatic steatosis and reduced m6A levels, reduce the m6A methylation levels of suppressor of cytokine signaling 2 (SOCS2), along with the expression of SOCS2 at mRNA and protein levels	Dang et al. (2020)
Zexie–Baizhu Decoction	*Alisma plantago-aquatica L.* [Alismataceae; *Rhizoma alismatis*], *Atractylodes macrocephala Koidz.* [Asteraceae; *Rhizoma atractylodis macrocephalae*]	C57/BL6 mice with gubra-amylin NASH (GAN) diet-induced NAFLD mouse model	Protect the liver and balance lipid disorders in the NAFLD model via influencing AMPK and Sirt1	Cao et al. (2022b)
Jiangzhi granule	*Gynostemma pentaphyllum (Thunb.) Makino* [Cucurbitaceae; *Gynostemma pentaphyllum*], *Reynoutria japonica Houtt.* [Polygonaceae; *Rhizoma polygoni cuspidati*], *Salvia miltiorrhiza Bunge* [Lamiaceae; *Salvia miltiorrhiza*], *Artemisia capillaris Thunb.* [Asteraceae; *Herba artemisiae scopariae*], *Glycyrrhiza glabra L.* [Fabaceae; *Licorice*]	C57BL/6J mice with HFD with vitamin D deficiency	Modulate BA profile and activate VDR in HF-VDD-induced NASH mice	Cao et al. (2022c)
Shenling Baizhu San	*Panax ginseng C.A.Mey.* [Araliaceae; *Ginseng*], *Smilax glabra Roxb.* [Smilacaceae; *Fuling*], *Atractylodes macrocephala Koidz.* [Asteraceae; *Rhizoma atractylodis macrocephalae*], *Paeonia lactiflora Pall.* [Paeoniaceae; *Radix paeoniae alba*], *Lablab purpureus subsp. purpureus* [Fabaceae; *White hyacinth bean*], *Nelumbo nucifera Gaertn.* [Nelumbonaceae; *Lotus seeds*], *Coix lacryma-jobi L.* [Poaceae; *Coix seed*], *Wurfbainia villosa (Lour.) Škorničk. & A.D.Poulsen* [Zingiberaceae; *Fructus amomi*], *Platycodon grandiflorus (Jacq.) A.DC.* [Campanulaceae; *Platycodon grandiflorus*], *Glycyrrhiza glabra L.* [Fabaceae; *Prepared liquorice root*]	C57BL/6J mice with western diet + CCl4 injection (WDC)	Ameliorate NAFLD via specific gut microbiota, gut-derived 5-HT, and related metabolites to decrease fat accumulation in the liver and inflammatory responses	Chen et al. (2024)
		Wistar rats with HFD model	Alleviate NAFLD and abnormal lipid metabolism, SIRT1 activation in the liver	Deng et al. (2019)
			Ameliorates NAFLD involves inducing the activation of autophagy, forming a complex regulatory network of key compounds (quercetin, ellagic acid, kaempferol, formononetin, stigmasterol, isorhamnetin and luteolin), key targets (CAT, AKT, eNOS, NQO1, HO-1 and HIF-1α) and related energy metabolites (NADP and succinate), thereby alleviating oxidative stress, ER stress, and mitochondrial dysfunction	Pan et al. (2024)
			Inhibit NLRP3 inflammasome activation and interleukin-1β release by suppressing LPS-induced TLR4 expression in rats with HFD-induced NAFLD	Pan et al. (2021)
Ganshuang granules	*Bupleurum chinense DC.* [Apiaceae; *Radix bupleuri*] *Dioscorea oppositifolia L.* [Dioscoreaceae; *Wild yam*], *Levisticum officinale W.D.J.Koch* [Apiaceae; *Radix angelicae sinensis*], *Smilax glabra Roxb.* [Smilacaceae; *Fuling*], *Atractylodes macrocephala Koidz.* [Asteraceae; *Rhizoma atractylodis macrocephalae*] *Codonopsis pilosula (Franch.) Nannf.* [Campanulaceae; *Codonopsis pilosula*], *Carapax Trionycis* [*Turtle shell*] *Taraxacum mongolicum Hand.-Mazz.* [Asteraceae; *Dandelion*], *Reynoutria japonica Houtt.* [Polygonaceae; *Rhizoma polygoni cuspidati*], *Prunella vulgaris L.*	C57BL/6J mice with HFD model	Improve liver injury and lipid metabolism disorder by activating the PI3K/AKT signaling pathway, to achieve therapeutic efficacy on NAFLD	Guoguo et al. (2024)

(Continued on following page)

TABLE 3 (*Continued*) Commonly used commercial Chinese polyherbal preparation (CCPP) for the treatment of NAFLD.

Formula	Prescriptions	Experimental model	Mechanism	References
	*[*Lamiaceae; *Prunella vulgaris], Salvia miltiorrhiza Bunge [*Lamiaceae; *Salvia miltiorrhiza], Juglans regia L. [*Juglandaceae; *Semen persicae]*			
Si Miao Formula	*Atractylodes lancea (Thunb.) DC [*Asteraceae; *Rhizoma atractylodis], Phellodendron amurense Rupr. [*Rutaceae; *Phellodendron amurense], Coix lacryma-jobi L. [*Poaceae; *Coix seed], Achyranthes aspera L. [*Amaranthaceae; *Radix achyranthis bidentatae]*	C57BL/6 mice with high fat/high sucrose (HFHS) diet	Attenuate HFHS diet-induced NAFLD and regulates hepatic lipid metabolism pathways, Modulation of the gut microbiota composition and in particular an increased relative abundance of Akkermansia muciniphila	Han et al. (2021)
Yiqi-Bushen-Tiaozhi Recipe	*Astragalus mongholicus Bunge [*Fabaceae; *Radix astragali], Epimedium brevicornu Maxim. [*Berberidaceae; *Herba epimedii], Smilax glabra Roxb. [*Smilacaceae; *Fuling], Atractylodes macrocephala Koidz. [*Asteraceae; *Rhizoma atractylodis macrocephalae], Reynoutria multiflora (Thunb.) Moldenke [*Polygonaceae; *Radix polygoni multiflori], Crataegus pinnatifida Bunge [*Rosaceae; *Crataegus pinnatifida], Elsholtzia splendens Nakai ex F.Maek. [*Lamiaceae; *Seaweed], Curcuma aromatica Salisb. [*Zingiberaceae; *Turmeric], Juglans regia L. [*Juglandaceae; *Semen persicae]*	C57BL/6J mice with HFD model	Alleviate NASH by regulating the expression of mmu-let-7a-5p, mmu-let-7b-5p, mmu-let-7g-3p and mmu-miR106b-3p miRNAs that potentially modulate inflammation/immunity and oxidative stress	Hong et al. (2020)
Mailuoning Oral Liquid (MLN)	*Lonicera japonica Thunb. [*Caprifoliaceae; *Lonicera japonica], Achyranthes aspera L. [*Amaranthaceae; *Radix achyranthis bidentatae] Scrophularia ningpoensis Hemsl. [*Scrophulariaceae; *Radix scrophulariae] Dendrobium nobile Lindl. [*Orchidaceae; *Dendrobium]*	C57BL/6 mice with MCD diet model, HepaRG cell	Improved NASH in MCD-fed mice, and the PGC-1α-PPARα signaling pathway was involved in this process	Jia et al. (2022)
Yinchen Linggui Zhugan Decoction	*Artemisia capillaris Thunb. [*Asteraceae; *Herba artemisiae scopariae], Gardenia jasminoides J.Ellis [*Rubiaceae; *Gardenia], Rheum palmatum L. [*Polygonaceae; *Rhubarb], Smilax glabra Roxb. [*Smilacaceae; *Fuling], Neolitsea cassia (L.) Kosterm. [*Lauraceae; *Ramulus cinnamomi], Atractylodes macrocephala Koidz. [*Asteraceae; *Rhizoma atractylodis macrocephalae], Glycyrrhiza glabra L. [*Fabaceae; *Licorice]*	SD rats with HFD model	Reverse the expression levels of TNF-α, IL-6, IL-1β, and NF-κB in liver tissues of NAFLD rats and decrease the expression of inflammatory chemokines CCL2 and CXCL10	Jiang et al. (2022)
Chaihu Shugan powder	*Bupleurum chinense DC. [*Apiaceae; *Radix bupleuri], Citrus reticulata Blanco [*Rutaceae; *Tangerine peel], Conioselinum anthriscoides "Chuanxiong" [*Apiaceae; *Szechuan lovage rhizome], Cyperus rotundus L. [*Cyperaceae; *Rhizoma Cyperi], Citrus × aurantium L. [*Rutaceae; *Fructus aurantii immaturus], Paeonia lactiflora Pall. [*Paeoniaceae; *Radix paeoniae alba], Glycyrrhiza glabra L. [*Fabaceae; *Licorice]*	SD rats with HFD model	Ameliorate NAFLD with IR by decreasing hypertriglyceridemia, hyperglycemia and hyperinsulinemia; up-regulating the mRNA expression of adiponectin and down-regulating the leptin mRNA expression in liver	Jiang et al. (2018)
		C57BL/6L mice with HFD model	Decrease liver inflammation and inhibiting hepatic fatty acid synthesis, inhibiting the TNFα/TNFR1 signaling pathway	Lei et al. (2022)
Qushi Huayu decoction	*Artemisia capillaris Thunb. [*Asteraceae; *Herba artemisiae scopariae], Reynoutria japonica Houtt. [*Polygonaceae; *Rhizoma polygoni cuspidati], Hypericum japonicum Thunb. [*Hypericaceae; *Herba hyperici japonici], Curcuma longa L. [*Zingiberaceae; *Turmeric], Gardenia jasminoides J.Ellis [*Rubiaceae; *Gardenia]*	Wistar rats with HFD model	Improve the structure of the dysfunctional gut microbiota and regulate DG, TG, PA, LPC, LPE and PAF	Ni et al. (2023)
Qushi Huayu granules		C57BL/6 mice with HFD model	Improve hepatic steatosis and corrected the BCAA disorder in NAFLD mice, and the related mechanisms regulated the	Zhang et al. (2021)

(Continued on following page)

TABLE 3 (*Continued*) Commonly used commercial Chinese polyherbal preparation (CCPP) for the treatment of NAFLD.

Formula	Prescriptions	Experimental model	Mechanism	References
			AMPK/SIRT1/UCP-1 pathway and promoted WAT browning	
Qushi Huayu decoction	*Curcuma longa L.* [Zingiberaceae; *Turmeric*], *Artemisia capillaris Thunb.* [Asteraceae; *Herba artemisiae scopariae*], *Gardenia jasminoides J.Ellis* [Rubiaceae; *Gardenia*], *Hypericum japonicum Thunb.* [Hypericaceae; *Herba hyperici japonici*], *Reynoutria japonica Houtt.* [Polygonaceae; *Rhizoma polygoni cuspidati*]	Wistar rats with MCD diet model	Exerts a hepatoprotective effect against steatosis and fibrosis presumably via depressed MAPK pathways phosphorylation, reinforcement of PPAR-γ and p-p65 translocating into nucleus and enhanced HSCs reprogramming	Lan Q. et al. (2021)
		C57BL/6 mice with HFD model	Inhibit LPS gut-leakage in NASH, which is associated with downregulation of intestinal MAPK pathway	Leng et al. (2020)
			Decreases hepatic DNL by inhibiting XBP1s independent of SREBP1 and ChREBP. Chlorogenic acid, geniposide and polydatin are the potential responsible compounds	Tian et al. (2023)
Huazhi-Rougan formula	*Artemisia capillaris Thunb.* [Asteraceae; *Herba artemisiae scopariae*], *Senna tora (L.) Roxb.* [Fabaceae; *Semen cassiae*], *Rheum palmatum L.* [Polygonaceae; *Rhubarb*], *Alisma plantago-aquatica L.* [Alismataceae; *Rhizoma alismatis*], *Crotalaria albida B.Heyne ex Roth* [Fabaceae; *Polyporus*], *Crataegus pinnatifida Bunge* [Rosaceae; *Crataegus pinnatifida*], *Atractylodes lancea (Thunb.) DC* [Asteraceae; *Rhizoma atractylodis*], *Atractylodes macrocephala Koidz.* [Asteraceae; *Rhizoma atractylodis macrocephalae*], *Citrus reticulata Blanco* [Rutaceae; *Tangerine peel*], *Trichosanthes kirilowii Maxim.* [Cucurbitaceae; *Fructus trichosanthis*], *Ligustrum lucidum W.T.Aiton* [Oleaceae; *Fructus ligustri lucidi*], *Eclipta prostrata (L.) L.* [Asteraceae; *Herba ecliptae*], *Lycium barbarum L.* [Solanaceae; *Fructus lycii*], *Cirsium arvense* var. *arvense* [Asteraceae; *Herba cirsii*], *Bupleurum chinense DC.* [Apiaceae; *Radix bupleuri*], *Glycyrrhiza glabra L.* [Fabaceae; *Licorice*]	C57BL/6J mice with MCD diet model, HepaRG cell	Enhance fecal BA excretion via inhibiting BA transporters, modulates BA profiles, gut dysbiosis as well as the intestinal environment	Li et al. (2022)
Jian Pi Qing Gan Yin decoction	*Atractylodes macrocephala Koidz.* [Asteraceae;*Rhizoma atractylodis macrocephalae*], *Atractylodes lancea (Thunb.) DC* [Asteraceae; *Rhizoma atractylodis*], *Artemisia capillaris Thunb.* [Asteraceae; *Herba artemisiae scopariae*], *Rheum palmatum L.* [Polygonaceae; *Rhubarb*], *Smilax glabra Roxb.* [Smilacaceae; *Fuling*], *Sedum sarmentosum Bunge* [Crassulaceae; *Sedum sarmentosum*]	C57BL/6J mice with HFD model	Ameliorate HFD-induced NAFLD in mice by targeting the first and second phases of hepatic steatosis by stimulating the AMPK/PPARα pathway and inhibiting the LXRα/Srebp1/Nf-κb pathway	Liu W. et al. (2022)
Ginseng-plus-Bai-Hu-Tang	*Panax ginseng C.A.Mey.* [Araliaceae; *Ginseng*], *Plaster of paris[CaSO4·2H2O]*, *Anemarrhena asphodeloides Bunge* [Asparagaceae; *Rhizoma anemarrhenae*], *Oryza sativa L.* [Poaceae; *non-glutinous rice*], *Glycyrrhiza glabra L.* [Fabaceae; *Licorice*]	C57BL/6J mice with HFD model	Modulate lipid and carbohydrate metabolism and be able to restore homeostasis	Lu et al. (2020)
Tianhuang formula	*Panax notoginseng (Burkill) F.H.Chen* [Araliaceae; *Panax notoginseng*], *Coptis chinensis Franch.* [Ranunculaceae; *Rhizoma coptidis*]	C57BL/6J mice with HFD model	Improve NAFLD via the "Lactobacillus-5-MIAA-Nrf2" pathway	Luo et al. (2022)

(Continued on following page)

TABLE 3 (*Continued*) Commonly used commercial Chinese polyherbal preparation (CCPP) for the treatment of NAFLD.

Formula	Prescriptions	Experimental model	Mechanism	References
Shouwu Jiangzhi Granule	*Reynoutria multiflora (Thunb.) Moldenke* [Polygonaceae; *Radix polygoni multiflori*], *Crataegus pinnatifida Bunge* [Rosaceae; *Crataegus pinnatifida*], *Curcuma aromatica Salisb.* [Zingiberaceae; *Turmeric*], *Alisma plantago-aquatica L.* [Alismataceae; *Rhizoma alismatis*], *Rheum palmatum L.* [Polygonaceae; *Rhubarb*], *Sinapis alba L.* [Brassicaceae; *White mustard seed*], *Sedum sarmentosum Bunge* [Crassulaceae; *Sedum sarmentosum*]	C57BL/6J mice with HFD model	Regulated TAGs synthesis to alleviate hepatic lipid accumulation	Qian et al. (2024)
Hedansanqi Tiaozhi Tang	*Panax notoginseng (Burkill) F.H.Chen* [Araliaceae; *Panax notoginseng*], *Salvia miltiorrhiza Bunge* [Lamiaceae; *Salvia miltiorrhiza*], *Crataegus pinnatifida Bunge* [Rosaceae; *Crataegus pinnatifida*], *Nelumbo nucifera Gaertn.* [Nelumbonaceae; *Lotus leaf*]	SD rats with HFD model	Has protective effect against NAFLD *in vitro* and *in vivo* by activating the Nrf2/HO-1 antioxidant pathway	Qiu et al. (2020)
Shenge Formula	*Salvia miltiorrhiza Bunge* [Lamiaceae; *Salvia miltiorrhiza*], *Pueraria montana* var. *thomsonii (Benth.) M.R.Almeida* [Fabaceae; *Pueraria lobata*], *Ligustrum lucidum W.T.Aiton* [Oleaceae; *Fructus ligustri lucidi*], *Atractylodes macrocephala Koidz.* [Asteraceae; *Rhizoma atractylodis macrocephalae*], *Curcuma aromatica Salisb.* [Zingiberaceae; *Rhizoma wenyujin concisa*], *Sedum sarmentosum Bunge* [Crassulaceae; *Sedum sarmentosum*]	C57BL/6 mice with HFD model, AML12 hepatocytes	Activated the PPARα signaling by inhibiting ACOX1, which then promoted mitochondrial fatty acid β-oxidation by upregulating CPT1A, therefore inhibiting hepatocyte lipid accumulation and relieving hepatic steatosis	Shang et al. (2024)
San-Huang-Tang	*Rheum palmatum L.* [Polygonaceae; *Rhubarb*], *Coptis chinensis Franch.* [Ranunculaceae; *Rhizoma coptidis*], *Astragalus mongholicus Bunge* [Fabaceae; *Radix astragali*]	C57BL/6J mice with HFD model, free fatty acids-induced lipotoxicity in HepG2 cells	Contribute to NAFLD by affecting insulin resistance via activating INSR/IRS1/AKT/FoxO1 pathway	Shi et al. (2022)
Zhenqing recipe	*Ligustrum lucidum W.T.Aiton* [Oleaceae; *Fructus ligustri lucidi*], *Eclipta prostrata (L.) L.* [Asteraceae; *Herba ecliptae*], *Dioscorea oppositifolia L.* [Dioscoreaceae; *Wild yam*]	Wistar rats with HFD + STZ model	Ameliorates hepatic gluconeogenesis and lipid storage in diabetic rats induced by HFD and STZ by activating the SIK1/CRTC2 signaling pathway	Song et al. (2020)
Ganjianglingzhu Decoction	*Glycyrrhiza glabra L.* [Fabaceae; *Licorice*], *Zingiber officinale Roscoe* [Zingiberaceae; *Dried ginger*], *Smilax glabra Roxb.* [Smilacaceae; *Fuling*], *Atractylodes macrocephala Koidz.* [Asteraceae; *Rhizoma atractylodis macrocephalae*]	C57BL/6 mice with MCD model	Protect against the development of lean NAFLD by regulating glucose and lipid metabolism, inhibiting the levels of sn-3-O-(geranylgeranyl)glycerol 1-phosphate and lysoPC(P-18:0/0:0) in glycerophospholipid metabolism	Tang et al. (2024)
Danshao Shugan Granule	*Salvia miltiorrhiza Bunge*[Lamiaceae; *Salvia miltiorrhiza*], *Paeonia lactiflora Pall.*[Paeoniaceae;*Radix paeoniae rubra*], *Bupleurum chinense DC.*[Apiaceae;*Radix bupleuri*], *Curcuma aromatica Salisb.* [Zingiberaceae;*Turmeric*], *Cyperus rotundus L.*[Cyperaceae;*Rhizoma Cyperi*], *Levisticum officinale W.D.J.Koch* [Apiaceae;*Radix angelicae sinensis*], *Reynoutria japonica Houtt.*[Polygonaceae;*Rhizoma polygoni cuspidati*], *Astragalus mongholicus Bunge* [Fabaceae;*Radix astragali*], *Artemisia capillaris Thunb.*[Asteraceae;*Tarragon*], *Strobilanthes cusia (Nees) Kuntze* [Acanthaceae;*Radix isatidis*], *Thlaspi arvense L.*[Brassicaceae;*Herba patriniae*], *Artemisia argyi H.Lév. & Vaniot*	260 patients with NAFLD, SD rats with HFD model	Increased activity of superoxide dismutase, a decrease of malondialdehyde as well as reduced NF-κB activity	Wang et al. (2022)

(Continued on following page)

TABLE 3 (*Continued*) Commonly used commercial Chinese polyherbal preparation (CCPP) for the treatment of NAFLD.

Formula	Prescriptions	Experimental model	Mechanism	References
	*[*Asteraceae*;Folium artemisiae argyi], Crataegus pinnatifida* Bunge *[*Rosaceae*; Crataegus pinnatifida], Raphanus raphanistrum subsp. sativus (L.) Domin [*Brassicaceae*;Radish seed], Reynoutria multiflora (Thunb.) Moldenke [*Polygonaceae*;Radix polygoni multiflori], Schisandra chinensis (Turcz.) Baill.[*Schisandraceae*;Schisandra chinensis]*			
Quzhi Formula	*Reynoutria japonica Houtt.[*Polygonaceae*;Rhizoma polygoni cuspidati], Senna tora (L.) Roxb.[*Fabaceae*;Semen cassiae], Crataegus pinnatifida* Bunge *[*Rosaceae*; Crataegus pinnatifida]*	C57BL/6 mice feeding a choline-deficient, l-amino acid-defined, high-fat diet	Protected against NASH by inhibiting lipid accumulation, ER stress, and inflammatory responses	Wu et al. (2022)
Diwuyanggan prescription	*Artemisia capillaris Thunb.[*Asteraceae*; Tarragon], Curcuma longa L.[*Zingiberaceae*;Turmeric], Schisandra chinensis (Turcz.) Baill.[*Schisandraceae*; Schisandra chinensis], Rehmannia glutinosa (Gaertn.) DC.[*Orobanchaceae*; Rehmannia glutinosa], Glycyrrhiza glabra L.[*Fabaceae*;Licorice]*	Kunming mice with HFD model	Reduced the HFD-induced disorders of liver function, which were related to steroid hormone biosynthesis, glycerophospholipid metabolism, sphingolipid signaling pathway, fatty acid beta-oxidation, biosynthesis of unsaturated fatty acids, and amino acid metabolism	Xu et al. (2023)
Yinchenhao Tang	*Artemisia capillaris Thunb.[*Asteraceae*; Tarragon], Gardenia jasminoides J.Ellis [*Rubiaceae*;Gardenia], Rheum palmatum L. [*Polygonaceae*;Rhubarb]*	Kunming mice with HFD model	Reduce body weight and improve the lipid metabolism of HFD induced NAFLD. Ameliorate NAFLD by boosting the expression of NR1H4 and APOA1 in both RNA and protein levels	Xu and Cui (2023)
Huangqin decoction	*Astragalus mongholicus Bunge[*Fabaceae*; Radix astragali], Paeonia lactiflora Pall.[*Paeoniaceae*;Radix paeoniae alba], Glycyrrhiza glabra L.[*Fabaceae*;Prepared liquorice root], Ziziphus jujuba Mill.[*Rhamnaceae*;Chinese date]*	SD rats with HFD model	Ameliorate hepatic inflammation in NAFLD rats by blocking the TLR4/NF-κB/NLRP3 pathway, with multi-components and multi-targets action pattern	Yan et al. (2023)
Huangqin-Huanglian Decoction	*Astragalus mongholicus Bunge[*Fabaceae*; Radix astragali], Coptis chinensis Franch.[*Ranunculaceae*;Rhizoma coptidis], Rehmannia glutinosa (Gaertn.) DC.[*Orobanchaceae*;Radix rehmanniae], Gentiana scabra Bunge[*Gentianaceae*; Gentian]*	C57BL/6 mice with HFD model	Alleviate NAFLD in a multi-target way by lowering fatty acids, and decreasing insulin resistance, inflammation, and apoptosis in the liver	Yang et al. (2024)
Hugan Qingzhi medication	*Alisma plantago-aquatica L.[*Alismataceae*;Rhizoma alismatis], Crataegus pinnatifida* Bunge *[*Rosaceae*; Crataegus pinnatifida], Typha angustifolia L.[*Typhaceae*;Pollen typhae], Nelumbo nucifera Gaertn.[*Nelumbonaceae*;Lotus leaf], Panax notoginseng (Burkill) F.H.Chen [*Araliaceae*;Panax notoginseng]*	Model of hepatic steatosis in the L02 and HepG2 cells	Activate AMPK and PPARα pathways	Yin et al. (2014)
Xiaozhi formula	*Nelumbo nucifera Gaertn.[*Nelumbonaceae*;Lotus leaf], Trichosanthes kirilowii Maxim. [*Cucurbitaceae*;Fructus trichosanthis], Gynostemma pentaphyllum (Thunb.) Makino [*Cucurbitaceae*;Gynostemma pentaphyllum], Benincasa hispida (Thunb.) Cogn.[*Cucurbitaceae*;Chinese waxgourd peel], Salvia miltiorrhiza Bunge[*Lamiaceae*;Salvia miltiorrhiza], Persicaria perfoliata (L.) H.Gross [*Polygonaceae*;Polygonum perfoliatum]*	C57BL/6J mice with HFD model	Attenuate NAFLD by moderating lipid metabolism by activating AMPK and PPAR signaling pathways	You et al. (2024)

(Continued on following page)

TABLE 3 (*Continued*) Commonly used commercial Chinese polyherbal preparation (CCPP) for the treatment of NAFLD.

Formula	Prescriptions	Experimental model	Mechanism	References
Kangtaizhi granule	*Pueraria montana* var. *thomsonii (Benth.) M.R.Almeida*[Fabaceae; *Pueraria lobata*], *Paeonia lactiflora Pall.*[Paeoniaceae;*Radix paeoniae alba*], *Hemerocallis citrina Baroni* [Asphodelaceae;*Daylily*], *Morus alba L.*[Moraceae;*Mulberry leaf*], *Polygonatum odoratum (Mill.) Druce* [Asparagaceae;*Polygonatum odoratum*], *Fructus Mori*[Moraceae;*Mulberry*], *Pseudocydonia sinensis (Dum.Cours.) C.K.Schneid.*[Rosaceae;*Carica papaya*]	SD rats with HFD model, HepG2 cells incubated with 1 mM of FFA	Regulate the AMPK/mTOR signaling pathway	Zhang et al. (2020)
Chai Hu Li Zhong Tang	*Bupleurum chinense DC.*[Apiaceae;*Radix bupleuri*], *Astragalus mongholicus Bunge* [Fabaceae;*Radix astragali*], *Pinellia ternata (Thunb.) Makino* [Araceae; *Rhizoma pinelliae*], *Codonopsis pilosula (Franch.) Nannf.* [Campanulaceae; *Codonopsis pilosula*], *Atractylodes lancea (Thunb.) DC*[Asteraceae;*Rhizoma atractylodis*], *Smilax glabra Roxb.*[Smilacaceae;*Fuling*], *Curcuma longa L.*[Zingiberaceae;*Turmeric*], *Glycyrrhiza glabra L.*[Fabaceae;*Prepared liquorice root*], *Zingiber officinale Roscoe* [Zingiberaceae;*Ginger*], *Ziziphus jujuba Mill.*[Rhamnaceae;*Chinese date*]	SD rats with HFD model, HepG2 cells with 1% long chain fat emulsion	Protects against NAFLD by activating AMPKα, inhibiting ACC activity, down-regulating SREBP2 and HMGR, and up-regulating PPAR-γ	Zhang M. et al. (2018)
Lian-Mei Yin	*Ziziphus jujuba Mill.*[Rhamnaceae; *Chinese date*], *Coptis chinensis Franch.*[Ranunculaceae;*Rhizoma coptidis*], *Ophiopogon japonicus (Thunb.) Ker Gawl.*[Asparagaceae;*Radix ophiopogonis*], *Scrophularia ningpoensis Hemsl.* [Scrophulariaceae;*Radix scrophulariae*], *Zingiber officinale Roscoe* [Zingiberaceae;*Ginger*], *Rehmannia glutinosa (Gaertn.) DC.*[Orobanchaceae; *Rehmannia glutinosa*], *Asini Corii Collap*	C57BL/6 mice with HFD model	Alleviates NAFLD by suppressing Yap1/FOXM1 pathway-mediated lipogenesis, oxidative stress, and inflammation	Zhang et al. (2024)
Chaihu Shugan powder	*Bupleurum chinense DC.*[Apiaceae;*Radix bupleuri*], *Conioselinum anthriscoides 'Chuanxiong'*[Apiaceae;*Szechuan lovage rhizome*], *Citrus × aurantium L.*[Rutaceae;*Fructus aurantii*], *Citrus reticulata Blanco*[Rutaceae;*Tangerine peel*], *Paeonia lactiflora Pall.*[Paeoniaceae;*Radix paeoniae alba*], *Cyperus rotundus L.*[Cyperaceae; *Rhizoma Cyperi*], *Glycyrrhiza glabra L.*[Fabaceae;*Prepared liquorice root*]	Wistar rats with HFD model	Reduce hepatic lipid accumulation of NAFLD rat model induced by HFD, and its mechanism may be through the action of 15 miRNAs such as miR-34a-5p, miR-146a-5p, miR-20b-5p and miR-142-3p. Reduce the gene and protein expression levels of ACACA, FASN and other fatty acid biosynthesis related enzymes, thus reducing fatty acid biosynthesis	Zheng et al. (2024)

Alisol B was found to alleviate hepatocyte lipid accumulation and lipotoxicity in NASH mice via regulating RARα-PPARγ-CD36 cascade. Alisol B was also found to relieve cellular ROS level and decrease inflammatory cytokines expression in mouse primary hepatocytes, along with a robust blockade of JNK/NF-κB pathway (Zhao et al., 2022). In another study, NASH was induced in mice fed a MCD diet for 4 weeks. The mice were simultaneously treated with AB23A (15, 30, and 60 $mg \cdot kg^{-1} \cdot d^{-1}$, ig) for 4 weeks. The study suggested that Alisol B 23A protects against MCD-induced NASH in mice via activating the FXR signaling pathway, thus decreasing the accumulation of lipids in the liver, hepatic lobular inflammation and pericellular fibrosis (Meng et al., 2017).

In summary, *A. plantago-aquatica* L. may treat NAFLD by regulating pathways related to inflammation and lipid metabolism.

4.3 Dan Shen (*Salvia miltiorrhiza* Bunge)

Salvia miltiorrhiza Bunge and its subspecies *S. miltiorrhiza* var. *miltiorrhiza* and *S. miltiorrhiza* var. *charbonnelii* (H.Lév.) C.Y.Wu [syn.: *Salvia przewalskii* Maxim.; Lamiaceae] yield Dan Shen (Radix et rhizoma salviae miltiorrhizae), is a traditional and folk medicine in Asian countries, especially in China and Japan (MEIm et al., 2019). *Salvia miltiorrhiza* Bunge is rich in bioactive metabolites such as tanshinones and salvianolic acids, which are believed to exert hepatoprotective, anti-inflammatory, and antioxidant effects (Shi et al., 2019; Wang Y. C. et al., 2015).

It has been demonstrated that tanshinones can modulate multiple targets, including PPARα, CYP1A2, and MMP2, thereby exerting regulatory effects on lipid metabolism,

TABLE 4 Classification of Chinese medicinal herbs commonly used for NAFLD treatment.

Type	Botanical drugs
Blood-activating and stasis-removing drug	*Salvia miltiorrhiza Bunge*[Lamiaceae;*Salvia miltiorrhiza*], *Paeonia × suffruticosa Andrews* [Paeoniaceae;*Cortex moutan*], *Crataegus pinnatifida Bunge* [Rosaceae;*Crataegus pinnatifida*], *Levisticum officinale W.D.J.Koch* [Apiaceae;*Radix angelicae sinensis*], *Curcuma aromatica Salisb.* [Zingiberaceae;*Turmeric*], *Typha angustifolia L.*[Typhaceae; *Pollen typhae*], *Juglans regia L.*[Juglandaceae;*Semen persicae*], *Rheum palmatum L.* [Polygonaceae;*Rhubarb*], *Paeonia lactiflora Pall.*[Paeoniaceae;*Radix paeoniae rubra*], *Reynoutria japonica Houtt.*[Polygonaceae;*Rhizoma polygoni cuspidati*], *Rehmannia glutinosa (Gaertn.) DC.*[Orobanchaceae;*Radix Rehmanniae preparata*]
Heat-clearing and dampness-drying drug	*Scutellaria baicalensis Georgi*[Lamiaceae;*Scutellaria baicalensis georgi*], *Gardenia jasminoides J.Ellis*[Rubiaceae;*Gardenia*], *Coptis chinensis Franch.*[Ranunculaceae;*Rhizoma coptidis*], *Artemisia capillaris Thunb.*[Asteraceae;*Herba artemisiae scopariae*], *Phellodendron amurense Rupr.*[Rutaceae;*Phellodendron amurense*], *Reynoutria japonica Houtt.*[Polygonaceae;*Rhizoma polygoni cuspidati*]
Spleen-tonifying and qi-supplementing drug	*Atractylodes macrocephala Koidz.*[Asteraceae;*Rhizoma atractylodis macrocephalae*], *Astragalus mongholicus Bunge*[Fabaceae;*Radix astragali*], *Citrus reticulata Blanco* [Rutaceae;*Tangerine peel*], *Codonopsis pilosula (Franch.) Nannf.* [Campanulaceae; *Codonopsis pilosula*]
Aromatic dampness-dispelling drug	*Nelumbo nucifera Gaertn.*[Nelumbonaceae;*Lotus leaf*], *Atractylodes lancea (Thunb.) DC* [Asteraceae;*Rhizoma atractylodis*], *Wurfbainia villosa (Lour.) Škorničk. & A.D.Poulsen* [Zingiberaceae;*Fructus amomi*], *Magnolia obovata Thunb.*[Magnoliaceae;*Magnolia officinalis*]
Spleen-strengthening and dampness-dispelling drug	*Coix lacryma-jobi L.* [Poaceae;*Coix seed*], *Smilax glabra Roxb.*[Smilacaceae;*Fuling*], *Atractylodes macrocephala Koidz.*[Asteraceae;*Rhizoma atractylodis macrocephalae*]
Diuresis-inducing drug	*Alisma plantago-aquatica L.*[Alismataceae;*Rhizoma alismatis*], *Smilax glabra Roxb.*[Smilacaceae;*Fuling*]
Spleen-invigorating for removing food retention drug	*Crataegus pinnatifida Bunge* [Rosaceae;*Crataegus pinnatifida*]
Liver-soothing for qi-regulating drug	*Bupleurum chinense DC.*[Apiaceae;*Radix bupleuri*], *Curcuma aromatica Salisb.* [Zingiberaceae;*Turmeric*], *Lycium barbarum L.*[Solanaceae;*Fructus lycii*], *Mentha canadensis L.*[Lamiaceae;*Mint*]
Liver blood-nourishing drug	Lycium barbarum L. [Solanaceae; Fructus lycii], Levisticum officinale W.D.J.Koch [Apiaceae; Radix angelicae sinensis], Paeonia lactiflora Pall. [Paeoniaceae; Radix paeoniae alba], Reynoutria multiflora (Thunb.) Moldenke [Polygonaceae; Radix polygoni multiflori], Ligustrum lucidum W.T.Aiton [Oleaceae; Fructus ligustri lucidi]
Yin-nourishing and liquid-engendering drug	*Ophiopogon japonicus (Thunb.) Ker Gawl.*[Asparagaceae;*Radix ophiopogonis*], *Rehmannia glutinosa (Gaertn.) DC.*[Orobanchaceae;*Radix Rehmanniae preparata*], *Trichosanthes kirilowii Maxim.* [Cucurbitaceae;*Fructus trichosanthis*]
Heat-clearing for liver-calming drug	*Tagetes erecta L.* [Asteraceae;*african marigold*], *Senna tora (L.) Roxb.*[Fabaceae;*Semen cassiae*], *Scutellaria baicalensis Georgi*[Lamiaceae;*Scutellaria baicalensis georgi*], *Morus alba L.*[Moraceae;*Mulberry leaf*]

providing antioxidant benefits, and inhibiting fibrogenesis (Hong et al., 2017). Following intraperitoneal injection of tanshinone IIA (10 mg/kg/day) for 2 month, liver steatosis was significantly inhibited in mice on a high-fat diet. This study suggested that tanshinones IIA attenuates oxidative stress by decreasing ROS malondialdehyde (MDA) production and enhancing the activity of total superoxide dismutase (T-SOD) and glutathione peroxidase (GSH-PX), which may contribute to the inhibition of apoptosis and amelioration of liver steatosis (Yang et al., 2017). In addition, HFD-induced rats received 10 mg/kg tanshinone IIA by daily intraperitoneal injection for 3 months, the lipid deposition in the livers of hyperlipidemic rats and modulated the expression of miR-33a and SREBP-2/Pcsk9 signaling pathway proteins was attenuated (Jia et al., 2016).

Administration of Salvianolic acid A (20 and 40 mg/kg BW, respectively) via intraperitoneal injection ameliorates liver steatosis and hepatic damage in high-fat and high-carbohydrate diet-fed mice (Li S. et al., 2020). Additionally, Salvianolic acid A protects the liver from NAFLD caused by a high-fat diet by reducing both hepatic lipid accumulation and inflammation. This anti-inflammatory action may be attributed in part to the modulation of the TXNIP/NLRP3 inflammatory pathways (Ding et al., 2016). Salvianolic acid B is capable of modulating the SIRT1-dependent deacetylation of HMGB1, thereby offering protection against hepatic steatosis and inflammation induced by either a high-fat diet or palmitic acid (Zeng et al., 2015).

Thus, *S. miltiorrhiza* Bunge seemed to play its anti-oxidation role in the treatment of NAFLD.

4.4 Chai Hu (*Bupleurum chinense* DC.)

Bupleurum chinense DC. [syn.: *Bupleurum scorzonerifolium* Willd. ; Apiaceae] yield Chai Hu (Bupleuri radix), is a herbal

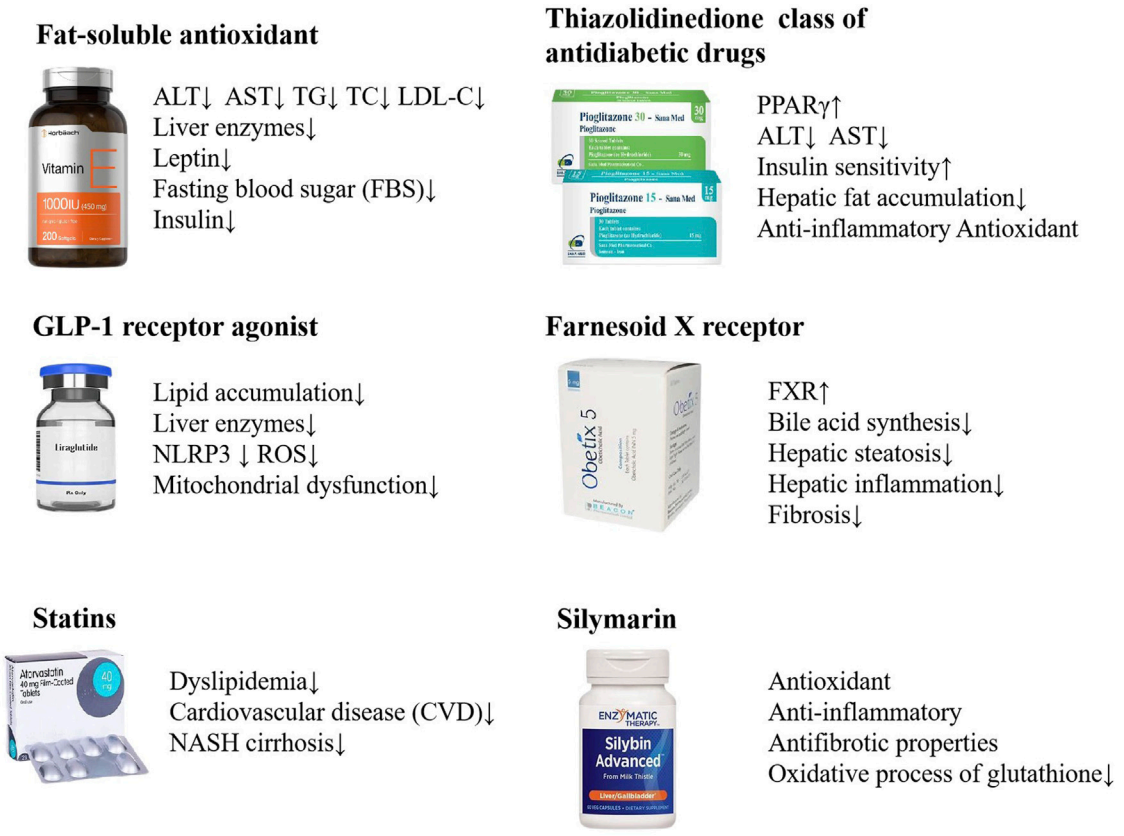

FIGURE 2
NAFLD treatments with biomedicine. Vitamin E, Liraglutide, Statins, Pioglitazone, Obeticholic acid, Silymarin, etc. are used in the treatment of NAFLD.

medicine for harmonizing and soothing liver qi stagnation (Law et al., 2014). Saikosaponins, especially Saikosaponina and Saikosaponind, as the major bioactive metabolites in *B. chinense* DC., represent anti-inflammatory, anti-oxidant, and hepatoprotective effects to treat NAFLD (Li et al., 2018).

Studies suggest that Saikosaponin a may influence key regulatory pathways involved in lipid metabolism, such as the PI3K/Akt/NF-κB/NLRP3 pathway, which is central to the homeostasis of lipid profiles within the liver (He et al., 2016). Additionally, Saikosaponin d improved lipid homeostasis by coordinately regulating PPARα activation-mediated both inhibition of SREBP1c-dependent FA biosynthesis and induction of FA degradation (Gu et al., 2022). Moreover, Saikosaponin d can induce improvement of fatty liver by decreasing ER-stress-related protein expression (Chang et al., 2021).

Overall, for the effects of *B. chinense* DC. on NAFLD, primary mechanisms are anti-inflammation and oxidative stress.

4.5 Jue Ming Zi [*Senna tora* (L.) Roxb.]

Senna tora (L.) Roxb. [syn.: *Senna obtusifolia* (L.). H.S.Irwin & Barneby; Fabaceae] yield Jue Ming Zi (Cassiae semen) has long been used for relieving constipation, improving liver function as well as preventing myopia. Anthraquinones, naphthopyranones, naphthalenes, flavones, polysaccharides and other metabolites, have been isolated and identified from Senna tora (L.) Roxb. (Chen et al., 2023).

It was found that *S. tora* (L.) Roxb. ethanol extract effectively inhibited *de novo* lipogenesis and ameliorated hepatic steatosis by promoting AMPK-mediated autophagy (Ding et al., 2023). Another study found that treatment with *S. tora* (L.) Roxb. extract lessened the effects of HFD-induced NAFLD rats, possibly by increasing the activity of antioxidant enzyme, inhibiting the MDA in liver and upregulated the expression of LDL-R to regulate the lipid metabolism process (Meng et al., 2019).

Naphthalenes can reduce lipid accumulation, liver injury and inflammation, gut microbiota disorders, intestinal barrier injury, and metabolic endotoxemia in HFD induced liver injury (Luo et al., 2021).

Oral administration of rhein (150 mg/kg in water) for 40 days significantly increased energy expenditure, reduced body weight, particularly body fat content, improved insulin resistance, and lowered circulating cholesterol levels in DIO mice. Rhein treatment also reduced liver triglyceride levels, reversed hepatic steatosis, and normalized ALT levels in these mice (Sheng et al., 2011). Rhein can reduce the expression of fat mass and obesity-associated protein and simultaneously alleviating oxidative stress and dysregulation in lipid metabolism within HFD rats. This

beneficial impact might be linked to the downregulation of key inflammatory markers, such as TLR4, MYD88, and Cyr61 (Lin and Yu, 2021; Qin et al., 2013).

In conclusion,the mechanisms of *S. tora* (L.) Roxb. treating on NAFLD may relate to alleviate oxidative stress, reduce lipid accumulation, anti-inflammation, and regulate gut microbiota disorders.

5 Conclusion and perspectives

The rising global prevalence of NAFLD has become a significant public health issue, necessitating the development of effective and comprehensive treatment strategies. Lifestyle modification with healthy eating and regular exercise represent the primary therapeutic approach for NAFLD (Neuschwander-Tetri, 2017). At present, there are no pharmacological treatments that have been approved by the relevant regulatory authorities for the specific treatment of NAFLD. It is, however, the case that certain pharmaceuticals are efficacious in the treatment of NAFLD, such as insulin sensitizer, lipid-lowering drugs, antioxidants, and weight-loss drugs. These drugs aim to improve metabolic imbalance and liver injury occurred in NAFLD (Dai et al., 2021; van Stee et al., 2018). Vitamin E has been found to correlate with a considerable decrease in liver steatosis, ballooning degeneration of hepatocytes, and pericellular fibrosis (Ekhlasi et al., 2016; Polyzos et al., 2017; Sanyal et al., 2010; Sanyal et al., 2004). The GLP-1 receptor agonist Liraglutide has demonstrated its effectiveness in diminishing the accumulation of fat in the liver and in lowering the levels of liver enzymes among patients diagnosed with nonalcoholic steatohepatitis (NASH) (Newsome et al., 2021; Seino et al., 2010; Yu et al., 2019). Statins can be used in the treatment of dyslipidemia in patients with NAFLD and NASH (Ciardullo and Perseghin, 2021; Pessayre et al., 2002). As a PPARγ agonist, pioglitazone is thought to improve insulin sensitivity in the liver, reduce hepatic fat accumulation, and potentially mitigate liver inflammation and injury through anti-inflammatory and antioxidant actions (Chalasani et al., 2018; Cusi et al., 2016). Obeticholic acid (OCA), a potent ligand for the Farnesoid X receptor (FXR), has been investigated as a therapeutic agent for NASH. Studies have demonstrated that OCA can lead to improvements in the clinical parameters of NASH, including the reduction of fibrosis and the amelioration of liver damage markers. Obeticholic acid (OCA), a potent ligand for the Farnesoid X receptor (FXR), has been investigated as a therapeutic agent for NASH. Studies have demonstrated that OCA can lead to improvements in the clinical parameters of NASH, including the reduction of fibrosis and the amelioration of liver damage markers (Neuschwander-Tetri et al., 2015; Stofan and Guo, 2020). In Europe, Silymarin has been historically uesed as a complementary therapy for the management of hepatic disorders. Silymarin is a key ingredient in the management of liver diseases including chronic hepatitis, cirrhosis, steatosis, alcoholic liver disorders and toxic liver injury, due to its antioxidant, anti-inflammatory and antifibrotic properties (Abenavoli et al., 2010; Schrieber et al., 2011; Wang M et al., 2015) (Figure 2).

CHM, with its principle of "holism" and "individualized treatment," has demonstrated potential as a multifaceted treatment for the complex pathophysiology of NAFLD. However, CHM has the characteristics of "multicomponents, multitargets, and multipathways," which also makes it difficult to study. In this review, we summarize the mechanisms of frequently used CCPPs, traditional Chinese formula and single herbs in the treatment of NAFLD. CHM has shown promising therapeutic effects in the treatment of NAFLD by regulating lipid metabolism, reducing inflammation, improving liver function and enhancing antioxidant defenses, with fewer adverse reactions. Thus, the use of CHM in the prevention and treatment of NAFLD has a broad development prospect.

Despite the promising therapeutic effects, there are inherent challenges in CHM treatment for NAFLD. Firstly, most patients with NAFLD do not have obvious symptoms and signs, making the diagnosis of the condition based only on the four diagnostic methods of TCM without objective evidence. Secondly, the CHM in registered clinical trials are limited, because long term effects of CHM are difficult to evaluate. In contrast to numerous synthetic pharmaceuticals, the gradual and nuanced actions of CHM may not manifest immediate outcomes. Consequently, it is essential to conduct comprehensive and prolonged observation periods to fully assess the efficacy and safety profiles. This presents a significant challenge in the design of clinical trials, as they must be sufficiently long-term to accurately assess the true benefits and potential adverse effects of CHM, while also being feasible in terms of resources and patient compliance. Lastly, a comprehensive understanding of the mechanism of CHM on NAFLD are not fully elucidated. The complex interplay of multiple bioactive compounds in CHM presents a great challenge in accurately discerning its precise mode of action. While this complexity is a defining feature of CHM's holistic approach to treatment, it also necessitates advanced research methodologies to elucidate the complex interactions between CHM components and the biological systems with which they interact. Thus, the application of advanced scientific techniques, including metabolomics, transcriptomics, network pharmacology and microbiome analyses, is essential tol to fully elucidate the therapeutic activities of CHM and to substantiate its mechanisms of action in the context of NAFLD treatment. These approaches can facilitate a more systematic understanding of the underlying mechanisms of TCM, paving the way for future investigations.

Author contributions

YL: Writing–original draft, Resources, Methodology, Investigation, Formal Analysis, Conceptualization. YF: Writing–original draft, Visualization, Software, Formal Analysis, Data curation. JL: Writing–review and editing, Project administration, Conceptualization. XL: Writing–original draft, Visualization, Validation, Resources. XL: Writing–original draft, Methodology, Conceptualization. JH: Writing–review and editing, Supervision, Methodology, Funding acquisition.

Funding

The author(s) declare that financial support was received for the research, authorship, and/or publication of this article. This study was funded by the National Natural Science Foundation of China (No. 82074316) and Sichuan Science and Technology Program (No. 2024NSFSC1829).

Acknowledgments

The authors express their gratitude to Quanshen Feng and Dong Wang of the School of Basic Medical Sicience at Chengdu University of TCM for their writing guidance. This study also thanks the editors and reviewers for helping us to improve this manuscript.

Conflict of interest

The authors declare that the research was conducted in the absence of any commercial or financial relationships that could be construed as a potential conflict of interest.

Publisher's note

References

Abenavoli, L., Capasso, R., Milic, N., and Capasso, F. (2010). Milk thistle in liver diseases: past, present, future. *Phytother. Res.* 24 (10), 1423–1432. doi:10.1002/ptr.3207

Ajoolabady, A., Kaplowitz, N., Lebeaupin, C., Kroemer, G., Kaufman, R. J., Malhi, H., et al. (2023). Endoplasmic reticulum stress in liver diseases. *Hepatology* 77 (2), 619–639. doi:10.1002/hep.32562

Anwar, S. D., Foster, C., and Ashraf, A. (2023). Lipid disorders and metabolic-associated fatty liver disease. *Endocrinol. Metab. Clin. North Am.* 52 (3), 445–457. doi:10.1016/j.ecl.2023.01.003

Bahorun, T., Aumjaud, E., Ramphul, H., Rycha, M., Luximon-Ramma, A., Trotin, F., et al. (2003). Phenolic constituents and antioxidant capacities of Crataegus monogyna (Hawthorn) callus extracts. *Nahrung* 47 (3), 191–198. doi:10.1002/food.200390045

Barros, L., Carvalho, A. M., and Ferreira, I. C. (2011). Comparing the composition and bioactivity of Crataegus Monogyna flowers and fruits used in folk medicine. *Phytochem. Anal.* 22 (2), 181–188. doi:10.1002/pca.1267

Begriche, K., Igoudjil, A., Pessayre, D., and Fromenty, B. (2006). Mitochondrial dysfunction in NASH: causes, consequences and possible means to prevent it. *Mitochondrion* 6 (1), 1–28. doi:10.1016/j.mito.2005.10.004

Begriche, K., Massart, J., Robin, M. A., Bonnet, F., and Fromenty, B. (2013). Mitochondrial adaptations and dysfunctions in nonalcoholic fatty liver disease. *Hepatology* 58 (4), 1497–1507. doi:10.1002/hep.26226

Buzzetti, E., Pinzani, M., and Tsochatzis, E. A. (2016). The multiple-hit pathogenesis of non-alcoholic fatty liver disease (NAFLD). *Metabolism* 65 (8), 1038–1048. doi:10.1016/j.metabol.2015.12.012

Cao, L., Xu, E., Zheng, R., Zhangchen, Z., Zhong, R., Huang, F., et al. (2022a). Traditional Chinese medicine Lingguizhugan decoction ameliorate HFD-induced hepatic-lipid deposition in mice by inhibiting STING-mediated inflammation in macrophages. *Chin. Med.* 17 (1), 7. doi:10.1186/s13020-021-00559-3

Cao, Y., Chen, M. L., Yu, S. Y., Zhang, L., and Ji, G. (2024). Study on the mechanism of Huazhi Rougan Granules in alleviating non-alcoholic steatohepatitis by inhibiting endoplasmic reticulum stress. *China J. Traditional Chin. Med. Pharm.* 39 (05), 2195–2203.

Cao, Y., Shi, J., Song, L., Xu, J., Lu, H., Sun, J., et al. (2022b). Multi-omics integration analysis identifies lipid disorder of a non-alcoholic fatty liver disease (NAFLD) mouse model improved by zexie-baizhu decoction. *Front. Pharmacol.* 13, 858795. doi:10.3389/fphar.2022.858795

Cao, Y., Shu, X., Li, M., Yu, S., Li, C., Ji, G., et al. (2022c). Jiangzhi granule attenuates non-alcoholic steatohepatitis through modulating bile acid in mice fed high-fat vitamin D deficiency diet. *Biomed. Pharmacother.* 149, 112825. doi:10.1016/j.biopha.2022.112825

Chalasani, N., Younossi, Z., Lavine, J. E., Charlton, M., Cusi, K., Rinella, M., et al. (2018). The diagnosis and management of nonalcoholic fatty liver disease: practice guidance from the American Association for the Study of Liver Diseases. *Hepatology* 67 (1), 328–357. doi:10.1002/hep.29367

Chang, G. R., Lin, W. L., Lin, T. C., Liao, H. J., and Lu, Y. W. (2021). The ameliorative effects of Saikosaponin in thioacetamide-induced liver injury and non-alcoholic fatty liver disease in mice. *Int. J. Mol. Sci.* 22 (21), 11383. doi:10.3390/ijms222111383

Chen, D., Wang, Y., Yang, J., Ou, W., Lin, G., Zeng, Z., et al. (2024). Shenling Baizhu San ameliorates non-alcoholic fatty liver disease in mice by modulating gut microbiota and metabolites. *Front. Pharmacol.* 15, 1343755. doi:10.3389/fphar.2024.1343755

Chen, Y., Chen, X., Yang, X., Gao, P., Yue, C., Wang, L., et al. (2023). Cassiae Semen: a comprehensive review of botany, traditional use, phytochemistry, pharmacology, toxicity, and quality control. *J. Ethnopharmacol.* 306, 116199. doi:10.1016/j.jep.2023.116199

Chen, Z., Tian, R., She, Z., Cai, J., and Li, H. (2020). Role of oxidative stress in the pathogenesis of nonalcoholic fatty liver disease. *Free Radic. Biol. Med.* 152, 116–141. doi:10.1016/j.freeradbiomed.2020.02.025

Ciardullo, S., and Perseghin, G. (2021). Statin use is associated with lower prevalence of advanced liver fibrosis in patients with type 2 diabetes. *Metabolism* 121, 154752. doi:10.1016/j.metabol.2021.154752

Cui, C. X., Deng, J. N., Yan, L., Liu, Y. Y., Fan, J. Y., Mu, H. N., et al. (2017). Silibinin Capsules improves high fat diet-induced nonalcoholic fatty liver disease in hamsters through modifying hepatic *de novo* lipogenesis and fatty acid oxidation. *J. Ethnopharmacol.* 208, 24–35. doi:10.1016/j.jep.2017.06.030

Cusi, K., Orsak, B., Bril, F., Lomonaco, R., Hecht, J., Ortiz-Lopez, C., et al. (2016). Long-term pioglitazone treatment for patients with nonalcoholic steatohepatitis and prediabetes or type 2 diabetes mellitus: a randomized trial. *Ann. Intern Med.* 165 (5), 305–315. doi:10.7326/m15-1774

Dai, L., Xu, J., Liu, B., Dang, Y., Wang, R., Zhuang, L., et al. (2022). Lingguizhugan Decoction, a Chinese herbal formula, improves insulin resistance in overweight/obese subjects with non-alcoholic fatty liver disease: a translational approach. *Front. Med.* 16 (5), 745–759. doi:10.1007/s11684-021-0880-3

Dai, X., Feng, J., Chen, Y., Huang, S., Shi, X., Liu, X., et al. (2021). Traditional Chinese Medicine in nonalcoholic fatty liver disease: molecular insights and therapeutic perspectives. *Chin. Med.* 16 (1), 68. doi:10.1186/s13020-021-00469-4

Dang, Y., Xu, J., Yang, Y., Li, C., Zhang, Q., Zhou, W., et al. (2020). Ling-gui-zhu-gan decoction alleviates hepatic steatosis through SOCS2 modification by N6-methyladenosine. *Biomed. Pharmacother.* 127, 109976. doi:10.1016/j.biopha.2020.109976

Degli Esposti, D., Hamelin, J., Bosselut, N., Saffroy, R., Sebagh, M., Pommier, A., et al. (2012). Mitochondrial roles and cytoprotection in chronic liver injury. *Biochem. Res. Int.* 2012, 387626. doi:10.1155/2012/387626

Denechaud, P. D., Dentin, R., Girard, J., and Postic, C. (2008). Role of ChREBP in hepatic steatosis and insulin resistance. *FEBS Lett.* 582 (1), 68–73. doi:10.1016/j.febslet.2007.07.084

Deng, Y., Pan, M., Nie, H., Zheng, C., Tang, K., Zhang, Y., et al. (2019). Lipidomic analysis of the protective effects of shenling Baizhu san on non-alcoholic fatty liver disease in rats. *Molecules* 24 (21), 3943. doi:10.3390/molecules24213943

Dentin, R., Benhamed, F., Hainault, I., Fauveau, V., Foufelle, F., Dyck, J. R., et al. (2006). Liver-specific inhibition of ChREBP improves hepatic steatosis and insulin resistance in ob/ob mice. *Diabetes* 55 (8), 2159–2170. doi:10.2337/db06-0200

Diehl, A. M., and Day, C. (2017). Cause, pathogenesis, and treatment of nonalcoholic steatohepatitis. *N. Engl. J. Med.* 377 (21), 2063–2072. doi:10.1056/NEJMra1503519

Ding, C., Zhao, Y., Shi, X., Zhang, N., Zu, G., Li, Z., et al. (2016). New insights into salvianolic acid A action: regulation of the TXNIP/NLRP3 and TXNIP/ChREBP pathways ameliorates HFD-induced NAFLD in rats. *Sci. Rep.* 6, 28734. doi:10.1038/srep28734

Ding, M., Zhou, F., Li, Y., Liu, C., Gu, Y., Wu, J., et al. (2023). Cassiae Semen improves non-alcoholic fatty liver disease through autophagy-related pathway. *Chin. Herb. Med.* 15 (3), 421–429. doi:10.1016/j.chmed.2022.09.006

Donnelly, K. L., Smith, C. I., Schwarzenberg, S. J., Jessurun, J., Boldt, M. D., and Parks, E. J. (2005). Sources of fatty acids stored in liver and secreted via lipoproteins in patients with nonalcoholic fatty liver disease. *J. Clin. Invest* 115 (5), 1343–1351. doi:10.1172/jci23621

Eberlé, D., Hegarty, B., Bossard, P., Ferré, P., and Foufelle, F. (2004). SREBP transcription factors: master regulators of lipid homeostasis. *Biochimie* 86 (11), 839–848. doi:10.1016/j.biochi.2004.09.018

Eckstein, S. S., Weigert, C., and Lehmann, R. (2017). Divergent roles of IRS (insulin receptor substrate) 1 and 2 in liver and skeletal muscle. *Curr. Med. Chem.* 24 (17), 1827–1852. doi:10.2174/0929867324666170426142826

Ekhlasi, G., Kolahdouz Mohammadi, R., Agah, S., Zarrati, M., Hosseini, A. F., Arabshahi, S. S., et al. (2016). Do symbiotic and Vitamin E supplementation have favorite effects in nonalcoholic fatty liver disease? A randomized, double-blind, placebo-controlled trial. *J. Res. Med. Sci.* 21, 106. doi:10.4103/1735-1995.193178

El-Agroudy, N. N., Kurzbach, A., Rodionov, R. N., O'Sullivan, J., Roden, M., Birkenfeld, A. L., et al. (2019). Are lifestyle therapies effective for NAFLD treatment? *Trends Endocrinol. Metab.* 30 (10), 701–709. doi:10.1016/j.tem.2019.07.013

Fan, C., Wang, G., Chen, M., Li, Y., Tang, X., and Dai, Y. (2023). Therapeutic potential of alkaloid extract from Codonopsis Radix in alleviating hepatic lipid accumulation: insights into mitochondrial energy metabolism and endoplasmic reticulum stress regulation in NAFLD mice. *Chin. J. Nat. Med.* 21 (6), 411–422. doi:10.1016/s1875-5364(23)60403-0

Fan, J. G., and Cao, H. X. (2013). Role of diet and nutritional management in non-alcoholic fatty liver disease. *J. Gastroenterol. Hepatol.* 28 (Suppl. 4), 81–87. doi:10.1111/jgh.12244

Fang, Y. L., Chen, H., Wang, C. L., and Liang, L. (2018). Pathogenesis of non-alcoholic fatty liver disease in children and adolescence: from "two hit theory" to "multiple hit model". *World J. Gastroenterol.* 24 (27), 2974–2983. doi:10.3748/wjg.v24.i27.2974

Ferré, P., and Foufelle, F. (2010). Hepatic steatosis: a role for *de novo* lipogenesis and the transcription factor SREBP-1c. *Diabetes Obes. Metab.* 12, 83–92. doi:10.1111/j.1463-1326.2010.01275.x

Flamment, M., Kammoun, H. L., Hainault, I., Ferré, P., and Foufelle, F. (2010). Endoplasmic reticulum stress: a new actor in the development of hepatic steatosis. *Curr. Opin. Lipidol.* 21 (3), 239–246. doi:10.1097/MOL.0b013e3283395e5c

Forrester, S. J., Kikuchi, D. S., Hernandes, M. S., Xu, Q., and Griendling, K. K. (2018). Reactive oxygen species in metabolic and inflammatory signaling. *Circ. Res.* 122 (6), 877–902. doi:10.1161/circresaha.117.311401

Friedman, S. L., Neuschwander-Tetri, B. A., Rinella, M., and Sanyal, A. J. (2018). Mechanisms of NAFLD development and therapeutic strategies. *Nat. Med.* 24 (7), 908–922. doi:10.1038/s41591-018-0104-9

Fujii, H., Kawada, N., and Japan Study Group Of Nafld, J.-N. (2020). The role of insulin resistance and diabetes in nonalcoholic fatty liver disease. *Int. J. Mol. Sci.* 21 (11), 3863. doi:10.3390/ijms21113863

Gao, G., Zhao, J., Ding, J., Liu, S., Shen, Y., Liu, C., et al. (2024). Alisol B regulates AMPK/mTOR/SREBPs via directly targeting VDAC1 to alleviate hyperlipidemia. *Phytomedicine* 128, 155313. doi:10.1016/j.phymed.2023.155313

Gentile, C. L., Frye, M., and Pagliassotti, M. J. (2011). Endoplasmic reticulum stress and the unfolded protein response in nonalcoholic fatty liver disease. *Antioxid. Redox Signal* 15 (2), 505–521. doi:10.1089/ars.2010.3790

Glimcher, L. H., and Lee, A. H. (2009). From sugar to fat: how the transcription factor XBP1 regulates hepatic lipogenesis. *Ann. N. Y. Acad. Sci.* 1173, E2–E9. doi:10.1111/j.1749-6632.2009.04956.x

Golabi, P., Locklear, C. T., Austin, P., Afdhal, S., Byrns, M., Gerber, L., et al. (2016). Effectiveness of exercise in hepatic fat mobilization in non-alcoholic fatty liver disease: systematic review. *World J. Gastroenterol.* 22 (27), 6318–6327. doi:10.3748/wjg.v22.i27.6318

Gong, J., Wang, X. Z., Wang, T., Chen, J. J., Xie, X. Y., Hu, H., et al. (2017). Molecular signal networks and regulating mechanisms of the unfolded protein response. *J. Zhejiang Univ. Sci. B* 18 (1), 1–14. doi:10.1631/jzus.B1600043

Gong, M., Wu, S., Yue, H., Liang, S., and Zou, Z. (2017). Study on the hepatoprotective effects of hugan tablets based on serum and liver metabonomics. *China Pharm.* 28 (34), 4776–4780. doi:10.6039/j.issn.1001-0408.2017.34.06

Gu, Y., Duan, S., Ding, M., Zheng, Q., Fan, G., Li, X., et al. (2022). Saikosaponin D attenuates metabolic associated fatty liver disease by coordinately tuning PPARα and INSIG/SREBP1c pathway. *Phytomedicine* 103, 154219. doi:10.1016/j.phymed.2022.154219

Guo, S., Chen, L., Chen, M., Li, Z., and Fan, Q. (2023). Study on the protective effect and mechanism of compound yiganling on nonalcoholic fatty liver based on network pharmacology and zebrafish model. *Chin. Pharm. J.* 58 (7), 584–591. doi:10.11669/cpj.2023.07.005

Guoguo, Z., Bingjie, S., Tianyan, Z., Shaoxiu, J. I., Jingwei, L. I., Yanni, D., et al. (2024). Efficacy of Ganshuang granules on non-alcoholic fatty liver and underlying mechanism: a network pharmacology and experimental verification. *J. Tradit. Chin. Med.* 44 (1), 122–130. doi:10.19852/j.cnki.jtcm.20231215.001

Han, R., Qiu, H., Zhong, J., Zheng, N., Li, B., Hong, Y., et al. (2021). Si Miao Formula attenuates non-alcoholic fatty liver disease by modulating hepatic lipid metabolism and gut microbiota. *Phytomedicine Stuttg.* 85, 153544. doi:10.1016/j.phymed.2021.153544

He, D., Wang, H., Xu, L., Wang, X., Peng, K., Wang, L., et al. (2016). Saikosaponin-a attenuates oxidized LDL uptake and prompts cholesterol efflux in THP-1 cells. *J. Cardiovasc Pharmacol.* 67 (6), 510–518. doi:10.1097/fjc.0000000000000373

Heeren, J., and Scheja, L. (2021). Metabolic-associated fatty liver disease and lipoprotein metabolism. *Mol. Metab.* 50, 101238. doi:10.1016/j.molmet.2021.101238

Higuchi, N., Kato, M., Shundo, Y., Tajiri, H., Tanaka, M., Yamashita, N., et al. (2008). Liver X receptor in cooperation with SREBP-1c is a major lipid synthesis regulator in nonalcoholic fatty liver disease. *Hepatol. Res.* 38 (11), 1122–1129. doi:10.1111/j.1872-034X.2008.00382.x

Ho, C., Gao, Y., Zheng, D., Liu, Y., Shan, S., Fang, B., et al. (2019). Alisol A attenuates high-fat-diet-induced obesity and metabolic disorders via the AMPK/ACC/SREBP-1c pathway. *J. Cell Mol. Med.* 23 (8), 5108–5118. doi:10.1111/jcmm.14380

Hong, M., Li, S., Wang, N., Tan, H. Y., Cheung, F., and Feng, Y. (2017). A biomedical investigation of the hepatoprotective effect of radix salviae miltiorrhizae and network pharmacology-based prediction of the active compounds and molecular targets. *Int. J. Mol. Sci.* 18 (3), 620. doi:10.3390/ijms18030620

Hong, W., Li, S., Cai, Y., Zhang, T., Yang, Q., He, B., et al. (2020). The target MicroRNAs and potential underlying mechanisms of yiqi-bushen-tiaozhi recipe against-non-alcoholic steatohepatitis. *Front. Pharmacol.* 11, 529553. doi:10.3389/fphar.2020.529553

Hotamisligil, G. S. (2010). Endoplasmic reticulum stress and the inflammatory basis of metabolic disease. *Cell* 140 (6), 900–917. doi:10.1016/j.cell.2010.02.034

Iizuka, K., Bruick, R. K., Liang, G., Horton, J. D., and Uyeda, K. (2004). Deficiency of carbohydrate response element-binding protein (ChREBP) reduces lipogenesis as well as glycolysis. *Proc. Natl. Acad. Sci. U. S. A.* 101 (19), 7281–7286. doi:10.1073/pnas.0401516101

Iizuka, K., and Horikawa, Y. (2008). ChREBP: a glucose-activated transcription factor involved in the development of metabolic syndrome. *Endocr. J.* 55 (4), 617–624. doi:10.1507/endocrj.k07e-110

Ipsen, D. H., Lykkesfeldt, J., and Tveden-Nyborg, P. (2018). Molecular mechanisms of hepatic lipid accumulation in non-alcoholic fatty liver disease. *Cell Mol. Life Sci.* 75 (18), 3313–3327. doi:10.1007/s00018-018-2860-6

Jacome-Sosa, M. M., and Parks, E. J. (2014). Fatty acid sources and their fluxes as they contribute to plasma triglyceride concentrations and fatty liver in humans. *Curr. Opin. Lipidol.* 25 (3), 213–220. doi:10.1097/mol.0000000000000080

James, O. F., and Day, C. P. (1998). Non-alcoholic steatohepatitis (NASH): a disease of emerging identity and importance. *J. Hepatol.* 29 (3), 495–501. doi:10.1016/s0168-8278(98)80073-1

Jia, L., Song, N., Yang, G., Ma, Y., Li, X., Lu, R., et al. (2016). Effects of Tanshinone IIA on the modulation of miR-33a and the SREBP-2/Pcsk9 signaling pathway in hyperlipidemic rats. *Mol. Med. Rep.* 13 (6), 4627–4635. doi:10.3892/mmr.2016.5133

Jia, W., Wang, K., Zhang, S., Lu, W., Du, A., Li, J., et al. (2022). Integrating network pharmacology and *in vivo* experimental validation to reveal the alleviation of mailuoning oral liquid on non-alcoholic fatty liver disease. *J. Artic. Phytomedicine* 104, 154326. doi:10.1016/j.phymed.2022.154326

Jiang, H., Mao, T., Liu, Y., Tan, X., Sun, Z., Cheng, Y., et al. (2022). Protective effects and mechanisms of yinchen linggui zhugan decoction in HFD-induced nonalcoholic fatty liver disease rats based on network pharmacology and experimental verification. *Front. Pharmacol.* 13, 908128. doi:10.3389/fphar.2022.908128

Jiang, W. N., Li, D., Jiang, T., Guo, J., Chen, Y. F., Wang, J., et al. (2018). Protective effects of Chaihu shugan san on nonalcoholic fatty liver disease in rats with insulin resistance. *Chin. J. Integr. Med.* 24 (2), 125–132. doi:10.1007/s11655-016-2252-4

Karkucinska-Wieckowska, A., Simoes, I. C. M., Kalinowski, P., Lebiedzinska-Arciszewska, M., Zieniewicz, K., Milkiewicz, P., et al. (2022). Mitochondria, oxidative stress and nonalcoholic fatty liver disease: a complex relationship. *Eur. J. Clin. Invest* 52 (3), e13622. doi:10.1111/eci.13622

Kaufman, R. J. (1999). Stress signaling from the lumen of the endoplasmic reticulum: coordination of gene transcriptional and translational controls. *Genes Dev.* 13 (10), 1211–1233. doi:10.1101/gad.13.10.1211

Khan, R. S., Bril, F., Cusi, K., and Newsome, P. N. (2019). Modulation of insulin resistance in nonalcoholic fatty liver disease. *Hepatology* 70 (2), 711–724. doi:10.1002/hep.30429

Kim, I., Xu, W., and Reed, J. C. (2008). Cell death and endoplasmic reticulum stress: disease relevance and therapeutic opportunities. *Nat. Rev. Drug Discov.* 7 (12), 1013–1030. doi:10.1038/nrd2755

Kim, M. S., Krawczyk, S. A., Doridot, L., Fowler, A. J., Wang, J. X., Trauger, S. A., et al. (2016). ChREBP regulates fructose-induced glucose production independently of insulin signaling. *J. Clin. Invest* 126 (11), 4372–4386. doi:10.1172/jci81993

Kirakosyan, A., Seymour, E., Kaufman, P. B., Warber, S., Bolling, S., and Chang, S. C. (2003). Antioxidant capacity of polyphenolic extracts from leaves of Crataegus laevigata and Crataegus monogyna (Hawthorn) subjected to drought and cold stress. *J. Agric. Food Chem.* 51 (14), 3973–3976. doi:10.1021/jf030096r

Kohjima, M., Enjoji, M., Higuchi, N., Kato, M., Kotoh, K., Yoshimoto, T., et al. (2007). Re-evaluation of fatty acid metabolism-related gene expression in nonalcoholic fatty liver disease. *Int. J. Mol. Med.* 20 (3), 351–358. doi:10.3892/ijmm.20.3.351

Kumashiro, N., Erion, D. M., Zhang, D., Kahn, M., Beddow, S. A., Chu, X., et al. (2011). Cellular mechanism of insulin resistance in nonalcoholic fatty liver disease. *Proc. Natl. Acad. Sci. U. S. A.* 108 (39), 16381–16385. doi:10.1073/pnas.1113359108

Lan, T., Yu, Y., Zhang, J., Li, H., Weng, Q., Jiang, S., et al. (2021). Cordycepin ameliorates nonalcoholic steatohepatitis by activation of the AMP-activated protein kinase signaling pathway. *Hepatology* 74 (2), 686–703. doi:10.1002/hep.31749

Lan Q., Q., Ren, Z., Chen, Y., Cui, G., Choi, I. C., Ung, C., et al. (2021). Hepatoprotective effect of Qushihuayu formula on non-alcoholic steatohepatitis induced by MCD diet in rat. *Chin. Med.* 16 (1), 27. doi:10.1186/s13020-021-00434-1

Law, B. Y., Mo, J. F., and Wong, V. K. (2014). Autophagic effects of Chaihu (dried roots of Bupleurum chinense DC or Bupleurum scorzoneraefolium WILD). *Chin. Med.* 9, 21. doi:10.1186/1749-8546-9-21

Lei, S., Zhao, S., Huang, X., Feng, Y., Li, Z., Chen, L., et al. (2022). Chaihu Shugan powder alleviates liver inflammation and hepatic steatosis in NAFLD mice: a network pharmacology study and *in vivo* experimental validation. *Front. Pharmacol.* 13, 967623. doi:10.3389/fphar.2022.967623

Leng, J., Huang, F., Hai, Y., Tian, H., Liu, W., Fang, Y., et al. (2020). Amelioration of non-alcoholic steatohepatitis by Qushi Huayu decoction is associated with inhibition of the intestinal mitogen-activated protein kinase pathway. *Phytomedicine* 66, 153135. doi:10.1016/j.phymed.2019.153135

Li, C., Chen, Y., Yuan, X., He, L., Li, X., Huang, S., et al. (2020). Vitexin ameliorates chronic stress plub high fat diet-induced nonalcoholic fatty liver disease by inhibiting inflammation. *Eur. J. Pharmacol.* 882, 173264. doi:10.1016/j.ejphar.2020.173264

Li, C., Yu, S., Li, X., Cao, Y., Li, M., Ji, G., et al. (2022). Medicinal formula huazhi-rougan attenuates non-alcoholic steatohepatitis through enhancing fecal bile acid excretion in mice. *Front. Pharmacol.* 13, 833414. doi:10.3389/fphar.2022.833414

Li, Q., and Qu, H. (2012). Study on the hypoglycemic activities and metabolism of alcohol extract of Alismatis Rhizoma. *Fitoterapia* 83 (6), 1046–1053. doi:10.1016/j.fitote.2012.05.009

Li, S., Qian, Q., Ying, N., Lai, J., Feng, L., Zheng, S., et al. (2020). Activation of the AMPK-SIRT1 pathway contributes to protective effects of Salvianolic acid A against lipotoxicity in hepatocytes and NAFLD in mice. *Front. Pharmacol.* 11, 560905. doi:10.3389/fphar.2020.560905

Li, W., Cao, T., Luo, C., Cai, J., Zhou, X., Xiao, X., et al. (2020). Crosstalk between ER stress, NLRP3 inflammasome, and inflammation. *Appl. Microbiol. Biotechnol.* 104 (14), 6129–6140. doi:10.1007/s00253-020-10614-y

Li, X., Li, X., Huang, N., Liu, R., and Sun, R. (2018). A comprehensive review and perspectives on pharmacology and toxicology of saikosaponins. *Phytomedicine* 50, 73–87. doi:10.1016/j.phymed.2018.09.174

Lin, X. P., and Yu, L. H. (2021). Therapeutic effect analysis of rhubaric acid on non-alcoholic fatty liver disease in mice. *Chin. J. Clin. Med.* 28 (01), 106–110. doi:10.12025/j.issn.1008-6358.2021.20200155

Liu, W., Shang, J., Deng, Y., Han, X., Chen, Y., Wang, S., et al. (2022). Network pharmacology analysis on mechanism of Jian Pi Qing Gan Yin decoction ameliorating high fat diet-induced non-alcoholic fatty liver disease and validated *in vivo*. *J. Ethnopharmacol.* 295, 115382. doi:10.1016/j.jep.2022.115382

Liu, Y., Tan, Y., Huang, J., Wu, C., Fan, X., Stalin, A., et al. (2022). Revealing the mechanism of huazhi rougan granule in the treatment of nonalcoholic fatty liver through intestinal flora based on 16S rRNA, metagenomic sequencing and network pharmacology. *Front. Pharmacol.* 13, 875700. doi:10.3389/fphar.2022.875700

Lu, H. F., Lai, Y. H., Huang, H. C., Lee, I. J., Lin, L. C., Liu, H. K., et al. (2020). Ginseng-plus-Bai-Hu-Tang ameliorates diet-induced obesity, hepatic steatosis, and insulin resistance in mice. *J. Ginseng Res.* 44 (2), 238–246. doi:10.1016/j.jgr.2018.10.005

Luo, D., Yang, L., Pang, H., Zhao, Y., Li, K., Rong, X., et al. (2022). Tianhuang formula reduces the oxidative stress response of NAFLD by regulating the gut microbiome in mice. *Front. Microbiol.* 13, 984019. doi:10.3389/fmicb.2022.984019

Luo, H., Wu, H., Wang, L., Xiao, S., Lu, Y., Liu, C., et al. (2021). Hepatoprotective effects of Cassiae Semen on mice with non-alcoholic fatty liver disease based on gut microbiota. *Commun. Biol.* 4 (1), 1357. doi:10.1038/s42003-021-02883-8

Machado, M. V., and Cortez-Pinto, H. (2014). Non-alcoholic fatty liver disease: what the clinician needs to know. *World J. Gastroenterol.* 20 (36), 12956–12980. doi:10.3748/wjg.v20.i36.12956

Mansouri, A., Gattolliat, C. H., and Asselah, T. (2018). Mitochondrial dysfunction and signaling in chronic liver diseases. *Gastroenterology* 155 (3), 629–647. doi:10.1053/j.gastro.2018.06.083

Masarone, M., Rosato, V., Dallio, M., Gravina, A. G., Aglitti, A., Loguercio, C., et al. (2018). Role of oxidative stress in pathophysiology of nonalcoholic fatty liver disease. *Oxid. Med. Cell Longev.* 2018, 9547613. doi:10.1155/2018/9547613

Meng, Q., Duan, X. P., Wang, C. Y., Liu, Z. H., Sun, P. Y., Huo, X. K., et al. (2017). Alisol B 23-acetate protects against non-alcoholic steatohepatitis in mice via farnesoid X receptor activation. *Acta Pharmacol. Sin.* 38 (1), 69–79. doi:10.1038/aps.2016.119

Meng, Y., Liu, Y., Fang, N., and Guo, Y. (2019). Hepatoprotective effects of Cassia semen ethanol extract on non-alcoholic fatty liver disease in experimental rat. *Pharm. Biol.* 57 (1), 98–104. doi:10.1080/13880209.2019.1568509

Muzurović, E., Mikhailidis, D. P., and Mantzoros, C. (2021). Non-alcoholic fatty liver disease, insulin resistance, metabolic syndrome and their association with vascular risk. *Metabolism* 119, 154770. doi:10.1016/j.metabol.2021.154770

Nassir, F. (2022). NAFLD: mechanisms, treatments, and biomarkers. *Biomolecules* 12 (6), 824. doi:10.3390/biom12060824

Neuschwander-Tetri, B. A. (2017). Non-alcoholic fatty liver disease. *BMC Med.* 15 (1), 45. doi:10.1186/s12916-017-0806-8

Neuschwander-Tetri, B. A., Loomba, R., Sanyal, A. J., Lavine, J. E., Van Natta, M. L., Abdelmalek, M. F., et al. (2015). Farnesoid X nuclear receptor ligand obeticholic acid for non-cirrhotic, non-alcoholic steatohepatitis (FLINT): a multicentre, randomised, placebo-controlled trial. *Lancet* 385 (9972), 956–965. doi:10.1016/s0140-6736(14)61933-4

Newsome, P. N., Buchholtz, K., Cusi, K., Linder, M., Okanoue, T., Ratziu, V., et al. (2021). A placebo-controlled trial of subcutaneous semaglutide in nonalcoholic steatohepatitis. *N. Engl. J. Med.* 384 (12), 1113–1124. doi:10.1056/NEJMoa2028395

Nguyen, P., Leray, V., Diez, M., Serisier, S., Le Bloc'h, J., Siliart, B., et al. (2008). Liver lipid metabolism. *J. Anim. Physiol. Anim. Nutr. Berl.* 92 (3), 272–283. doi:10.1111/j.1439-0396.2007.00752.x

Ni, Y., Wang, X., Wu, Q., Yao, Y., Xu, Y., Li, Y., et al. (2023). Qushi Huayu decoction ameliorates non-alcoholic fatty liver disease in rats by modulating gut microbiota and serum lipids. *Front. Endocrinol. (Lausanne)* 14, 1272214. doi:10.3389/fendo.2023.1272214

Pan, M., Deng, Y., Qiu, Y., Pi, D., Zheng, C., Liang, Z., et al. (2024). Shenling Baizhu powder alleviates non-alcoholic fatty liver disease by modulating autophagy and energy metabolism in high-fat diet-induced rats. *Phytomedicine* 130, 155712. doi:10.1016/j.phymed.2024.155712

Pan, M. X., Zheng, C. Y., Deng, Y. J., Tang, K. R., Nie, H., Xie, J. Q., et al. (2021). Hepatic protective effects of Shenling Baizhu powder, a herbal compound, against inflammatory damage via TLR4/NLRP3 signalling pathway in rats with nonalcoholic fatty liver disease. *J. Integr. Med.* 19 (5), 428–438. doi:10.1016/j.joim.2021.07.004

Park, S. W., Zhou, Y., Lee, J., Lu, A., Sun, C., Chung, J., et al. (2010). The regulatory subunits of PI3K, p85alpha and p85beta, interact with XBP-1 and increase its nuclear translocation. *Nat. Med.* 16 (4), 429–437. doi:10.1038/nm.2099

Pessayre, D., Mansouri, A., and Fromenty, B. (2002). Nonalcoholic steatosis and steatohepatitis. V. Mitochondrial dysfunction in steatohepatitis. *Am. J. Physiol. Gastrointest. Liver Physiol.* 282 (2), G193–G199. doi:10.1152/ajpgi.00426.2001

Peverill, W., Powell, L. W., and Skoien, R. (2014). Evolving concepts in the pathogenesis of NASH: beyond steatosis and inflammation. *Int. J. Mol. Sci.* 15 (5), 8591–8638. doi:10.3390/ijms15058591

Polyzos, S. A., Kountouras, J., Mantzoros, C. S., Polymerou, V., and Katsinelos, P. (2017). Effects of combined low-dose spironolactone plus vitamin E vs vitamin E monotherapy on insulin resistance, non-invasive indices of steatosis and fibrosis, and adipokine levels in non-alcoholic fatty liver disease: a randomized controlled trial. *Diabetes Obes. Metab.* 19 (12), 1805–1809. doi:10.1111/dom.12989

Porras, D., Nistal, E., Martínez-Flórez, S., Pisonero-Vaquero, S., Olcoz, J. L., Jover, R., et al. (2017). Protective effect of quercetin on high-fat diet-induced non-alcoholic fatty liver disease in mice is mediated by modulating intestinal microbiota imbalance and related gut-liver axis activation. *Free Radic. Biol. Med.* 102, 188–202. doi:10.1016/j.freeradbiomed.2016.11.037

Postic, C., and Girard, J. (2008). Contribution of *de novo* fatty acid synthesis to hepatic steatosis and insulin resistance: lessons from genetically engineered mice. *J. Clin. Invest* 118 (3), 829–838. doi:10.1172/jci34275

Puri, P., Mirshahi, F., Cheung, O., Natarajan, R., Maher, J. W., Kellum, J. M., et al. (2008). Activation and dysregulation of the unfolded protein response in nonalcoholic fatty liver disease. *Gastroenterology* 134 (2), 568–576. doi:10.1053/j.gastro.2007.10.039

Qian, F., Ouyang, B., Cai, Z., Zhu, D., Yu, S., Zhao, J., et al. (2024). Compound Shouwu Jiangzhi Granule regulates triacylglyceride synthesis to alleviate hepatic lipid accumulation. *Phytomedicine* 129, 155691. doi:10.1016/j.phymed.2024.155691

Qin, B. C., Zhang, T., Yuan, J. F., Lu, X. L., Xu, J. L., Shi, J. P., et al. (2013). Effect of rhubaric acid on prevention and treatment of nonalcoholic fatty liver disease induced by high fat diet in rats. *Chin. Arch. Tradit. Chin. Med.* 31 (03), 545–547+709. doi:10.13193/j.archtcm.2013.03.99.cenbch.054

Qiu, M., Xiao, F., Wang, T., Piao, S., Zhao, W., Shao, S., et al. (2020). Protective effect of Hedansanqi Tiaozhi Tang against non-alcoholic fatty liver disease *in vitro* and *in vivo* through activating Nrf2/HO-1 antioxidant signaling pathway. *Phytomedicine* 67, 153140. doi:10.1016/j.phymed.2019.153140

Ruan, X., Zhang, X., Liu, L., and Zhang, J. (2024). Mechanism of Xiaoyao San in treating non-alcoholic fatty liver disease with liver depression and spleen deficiency: based on bioinformatics, metabolomics and *in vivo* experiments. *J. Biomol. Struct. Dyn.* 42 (10), 5128–5146. doi:10.1080/07391102.2023.2231544

Sanders, F. W., and Griffin, J. L. (2016). *De novo* lipogenesis in the liver in health and disease: more than just a shunting yard for glucose. *Biol. Rev. Camb Philos. Soc.* 91 (2), 452–468. doi:10.1111/brv.12178

Sanyal, A. J., Chalasani, N., Kowdley, K. V., McCullough, A., Diehl, A. M., Bass, N. M., et al. (2010). Pioglitazone, vitamin E, or placebo for nonalcoholic steatohepatitis. *N. Engl. J. Med.* 362 (18), 1675–1685. doi:10.1056/NEJMoa0907929

Sanyal, A. J., Mofrad, P. S., Contos, M. J., Sargeant, C., Luketic, V. A., Sterling, R. K., et al. (2004). A pilot study of vitamin E versus vitamin E and pioglitazone for the treatment of nonalcoholic steatohepatitis. *Clin. Gastroenterol. Hepatol.* 2 (12), 1107–1115. doi:10.1016/s1542-3565(04)00457-4

Schreuder, T. C., Verwer, B. J., van Nieuwkerk, C. M., and Mulder, C. J. (2008). Nonalcoholic fatty liver disease: an overview of current insights in pathogenesis, diagnosis and treatment. *World J. Gastroenterol.* 14 (16), 2474–2486. doi:10.3748/wjg.14.2474

Schrieber, S. J., Hawke, R. L., Wen, Z., Smith, P. C., Reddy, K. R., Wahed, A. S., et al. (2011). Differences in the disposition of silymarin between patients with nonalcoholic fatty liver disease and chronic hepatitis C. *Drug Metab. Dispos.* 39 (12), 2182–2190. doi:10.1124/dmd.111.040212

Schweiger, M., Schreiber, R., Haemmerle, G., Lass, A., Fledelius, C., Jacobsen, P., et al. (2006). Adipose triglyceride lipase and hormone-sensitive lipase are the major enzymes in adipose tissue triacylglycerol catabolism. *J. Biol. Chem.* 281 (52), 40236–40241. doi:10.1074/jbc.M608048200

Seino, Y., Fukushima, M., and Yabe, D. (2010). GIP and GLP-1, the two incretin hormones: similarities and differences. *J. Diabetes Investig.* 1 (1-2), 8–23. doi:10.1111/j.2040-1124.2010.00022.x

Serviddio, G., Bellanti, F., and Vendemiale, G. (2013). Free radical biology for medicine: learning from nonalcoholic fatty liver disease. *Free Radic. Biol. Med.* 65, 952–968. doi:10.1016/j.freeradbiomed.2013.08.174

Shang, Z., Gao, Y., Xue, Y., Zhang, C., Qiu, J., Qian, Y., et al. (2024). Shenge Formula attenuates high-fat diet-induced obesity and fatty liver via inhibiting ACOX1. *Phytomedicine* 123, 155183. doi:10.1016/j.phymed.2023.155183

Shao, G., Liu, Y., Lu, L., Zhang, G., Zhou, W., Wu, T., et al. (2022). The pathogenesis of HCC driven by NASH and the preventive and therapeutic effects of natural products. *Front. Pharmacol.* 13, 944088. doi:10.3389/fphar.2022.944088

Shen, S., Wang, K., Zhi, Y., Shen, W., and Huang, L. (2020). Gypenosides improves nonalcoholic fatty liver disease induced by high-fat diet induced through regulating LPS/TLR4 signaling pathway. *Cell Cycle* 19 (22), 3042–3053. doi:10.1080/15384101.2020.1829800

Sheng, X., Wang, M., Lu, M., Xi, B., Sheng, H., and Zang, Y. Q. (2011). Rhein ameliorates fatty liver disease through negative energy balance, hepatic lipogenic regulation, and immunomodulation in diet-induced obese mice. *Am. J. Physiol. Endocrinol. Metab.* 300 (5), E886–E893. doi:10.1152/ajpendo.00332.2010

Shi, H., Qiao, F., Huang, K., Lu, W., Zhang, X., Ke, Z., et al. (2022). Exploring therapeutic mechanisms of San-Huang-Tang in nonalcoholic fatty liver disease through network pharmacology and experimental validation. *J. Ethnopharmacol.* 296, 115477. doi:10.1016/j.jep.2022.115477

Shi, M. J., Dong, B. S., Yang, W. N., Su, S. B., and Zhang, H. (2019). Preventive and therapeutic role of Tanshinone ⅡA in hepatology. *Biomed. Pharmacother.* 112, 108676. doi:10.1016/j.biopha.2019.108676

Shi, T., Wu, L., Ma, W., Ju, L., Bai, M., Chen, X., et al. (2020). Nonalcoholic fatty liver disease: pathogenesis and treatment in traditional Chinese medicine and western medicine. *Evid. Based Complement. Altern. Med.* 2020, 8749564. doi:10.1155/2020/8749564

Song, D., Yin, L., Wang, C., and Wen, X. (2020). Zhenqing recipe attenuates non-alcoholic fatty liver disease by regulating the SIK1/CRTC2 signaling in experimental diabetic rats. *BMC Complement. Med. Ther.* 20 (1), 27. doi:10.1186/s12906-019-2811-2

Stefan, N., Kantartzis, K., and Häring, H. U. (2008). Causes and metabolic consequences of Fatty liver. *Endocr. Rev.* 29 (7), 939–960. doi:10.1210/er.2008-0009

Stofan, M., and Guo, G. L. (2020). Bile acids and FXR: novel targets for liver diseases. *Front. Med. (Lausanne)* 7, 544. doi:10.3389/fmed.2020.00544

Tadić, V. M., Dobrić, S., Marković, G. M., Dordević, S. M., Arsić, I. A., Menković, N. R., et al. (2008). Anti-inflammatory, gastroprotective, free-radical-scavenging, and antimicrobial activities of hawthorn berries ethanol extract. *J. Agric. Food Chem.* 56 (17), 7700–7709. doi:10.1021/jf801668c

Tan, Y., Huang, Z., Liu, Y., Li, X., Stalin, A., Fan, X., et al. (2023). Integrated serum pharmacochemistry, 16S rRNA sequencing and metabolomics to reveal the material basis and mechanism of Yinzhihuang granule against non-alcoholic fatty liver disease. *J. Ethnopharmacol.* 310, 116418. doi:10.1016/j.jep.2023.116418

Tang, N., Ji, L., Shi, X., Xiong, Y., Xiong, X., Zhao, H., et al. (2024). Effects of ganjianglingzhu decoction on lean non-alcoholic fatty liver disease in mice based on untargeted metabolomics. *Pharm. (Basel)* 17 (4), 502. doi:10.3390/ph17040502

Teng, M. L., Ng, C. H., Huang, D. Q., Chan, K. E., Tan, D. J., Lim, W. H., et al. (2023). Global incidence and prevalence of nonalcoholic fatty liver disease. *Clin. Mol. Hepatol.* 29 (Suppl. l), S32–s42. doi:10.3350/cmh.2022.0365

Ter Horst, K. W., Gilijamse, P. W., Versteeg, R. I., Ackermans, M. T., Nederveen, A. J., la Fleur, S. E., et al. (2017). Hepatic diacylglycerol-associated protein kinase cε translocation links hepatic steatosis to hepatic insulin resistance in humans. *Cell Rep.* 19 (10), 1997–2004. doi:10.1016/j.celrep.2017.05.035

Tian, H., Fang, Y., Liu, W., Wang, J., Zhao, J., Tang, H., et al. (2023). Inhibition on XBP1s-driven lipogenesis by Qushi Huayu Decoction contributes to amelioration of hepatic steatosis induced by fructose. *J. Ethnopharmacol.* 301, 115806. doi:10.1016/j.jep.2022.115806

Tilg, H., and Moschen, A. R. (2010). Evolution of inflammation in nonalcoholic fatty liver disease: the multiple parallel hits hypothesis. *Hepatology* 52 (5), 1836–1846. doi:10.1002/hep.24001

van Stee, M. F., de Graaf, A. A., and Groen, A. K. (2018). Actions of metformin and statins on lipid and glucose metabolism and possible benefit of combination therapy. *Cardiovasc Diabetol.* 17 (1), 94. doi:10.1186/s12933-018-0738-4

Wang, H., Xu, Z., Wang, Q., and Shu, S. (2022). Danshao Shugan Granule therapy for non-alcoholic fatty liver disease. *Lipids Health Dis.* 21 (1), 76. doi:10.1186/s12944-022-01689-9

Wang, M., Xie, T., Chang, Z., Wang, L., Xie, X., Kou, Y., et al. (2015). A new type of liquid silymarin proliposome containing bile salts: its preparation and improved hepatoprotective effects. *PLoS One* 10 (12), e0143625. doi:10.1371/journal.pone.0143625

Wang, Y. C., Kong, W. Z., Jin, Q. M., Chen, J., and Dong, L. (2015). Effects of salvianolic acid B on liver mitochondria of rats with nonalcoholic steatohepatitis. *World J. Gastroenterol.* 21 (35), 10104–10112. doi:10.3748/wjg.v21.i35.10104

Winnay, J. N., Boucher, J., Mori, M. A., Ueki, K., and Kahn, C. R. (2010). A regulatory subunit of phosphoinositide 3-kinase increases the nuclear accumulation of X-box-binding protein-1 to modulate the unfolded protein response. *Nat. Med.* 16 (4), 438–445. doi:10.1038/nm.2121

Wu, C., Jing, M., Yang, L., Jin, L., Ding, Y., Lu, J., et al. (2018). Alisol A 24-acetate ameliorates nonalcoholic steatohepatitis by inhibiting oxidative stress and stimulating autophagy through the AMPK/mTOR pathway. *Chem. Biol. Interact.* 291, 111–119. doi:10.1016/j.cbi.2018.06.005

Wu, Y. L., Wu, J. X., Shen, T. T., Chai, H. S., Chen, H. F., and Zhang, Q. (2022). Quzhi formula alleviates nonalcoholic steatohepatitis by impairing hepatocyte lipid accumulation and inflammation via bip/eIF2α signaling. *J. Clin. Transl. Hepatol.* 10 (6), 1050–1058. doi:10.14218/JCTH.2021.00458

MEIm, X. D., Cao, Y. F., Che, Y. Y., Li, J., Shang, Z. P., Zhao, W. J., et al. (2019). Danshen: a phytochemical and pharmacological overview. *Chin. J. Nat. Med.* 17 (1), 59–80. doi:10.1016/s1875-5364(19)30010-x

Xiaoling, L., Fengxia, S., Zimeng, S., Yingxue, Z., Jie, L., and Qiuxiang, Z. (2022). Effect of Dangfei Liganning capsule on liver X receptor α/steroid regulatory element binding protein-1/fatty acid synthase signal pathway in rats with metabolic-associated fatty liver disease. *J. Traditional Chin. Med.* 42 (06), 940–947. doi:10.19852/j.cnki.jtcm.2022.06.007

Xu, J., Jin, Y., Song, C., Chen, G., Li, Q., Yuan, H., et al. (2023). Comparative analysis of the synergetic effects of Diwuyanggan prescription on high fat diet-induced non-alcoholic fatty liver disease using untargeted metabolomics. *Heliyon* 9 (11), e22151. doi:10.1016/j.heliyon.2023.e22151

Xu, L., and Cui, H. (2023). Yinchenhao Tang alleviates high fat diet induced NAFLD by increasing NR1H4 and APOA1 expression. *J. Tradit. Complement. Med.* 13 (4), 325–336. doi:10.1016/j.jtcme.2023.02.010

Yan, B. F., Wang, Y., Wang, W. B., Ding, X. J., Wei, B., Liu, S. J., et al. (2023). Huangqin decoction mitigates hepatic inflammation in high-fat diet-challenged rats by inhibiting TLR4/NF-κB/NLRP3 pathway. *J. Ethnopharmacol.* 303, 115999. doi:10.1016/j.jep.2022.115999

Yang, G. L., Jia, L. Q., Wu, J., Ma, Y. X., Cao, H. M., Song, N., et al. (2017). Effect of tanshinone IIA on oxidative stress and apoptosis in a rat model of fatty liver. *Exp. Ther. Med.* 14 (5), 4639–4646. doi:10.3892/etm.2017.5162

Yang, H., Wei, D., Zhang, Y., and Jian, W. (2024). Huangqin-huanglian decoction protects liver against non-alcoholic fatty liver disease in high fat-diet mice. *Endocr. Metab. Immune Disord. Drug Targets* 24 (6), 691–708. doi:10.2174/0118715303257018230927182802

Yang, H., Yang, T., Heng, C., Zhou, Y., Jiang, Z., Qian, X., et al. (2019). Quercetin improves nonalcoholic fatty liver by ameliorating inflammation, oxidative stress, and lipid metabolism in db/db mice. *Phytother. Res.* 33 (12), 3140–3152. doi:10.1002/ptr.6486

Yang, J. M., Sun, Y., Wang, M., Zhang, X. L., Zhang, S. J., Gao, Y. S., et al. (2019). Regulatory effect of a Chinese herbal medicine formula on non-alcoholic fatty liver disease. *World J. Gastroenterol.* 25 (34), 5105–5119. doi:10.3748/wjg.v25.i34.5105

Yin, J., Luo, Y., Deng, H., Qin, S., Tang, W., Zeng, L., et al. (2014). Hugan Qingzhi medication ameliorates hepatic steatosis by activating AMPK and PPARα pathways in L02 cells and HepG2 cells. *J. Ethnopharmacol.* 154 (1), 229–239. doi:10.1016/j.jep.2014.04.011

Yoo, J. H., Liu, Y., and Kim, H. S. (2016). Hawthorn fruit extract elevates expression of Nrf2/HO-1 and improves lipid profiles in ovariectomized rats. *Nutrients* 8 (5), 283. doi:10.3390/nu8050283

You, L., Wang, T., Li, W., Zhang, J., Zheng, C., Zheng, Y., et al. (2024). Xiaozhi formula attenuates non-alcoholic fatty liver disease by regulating lipid metabolism via activation of AMPK and PPAR pathways. *J. Ethnopharmacol.* 329, 118165. doi:10.1016/j.jep.2024.118165

Younossi, Z. M., Koenig, A. B., Abdelatif, D., Fazel, Y., Henry, L., and Wymer, M. (2016). Global epidemiology of nonalcoholic fatty liver disease-Meta-analytic assessment of prevalence, incidence, and outcomes. *Hepatology* 64 (1), 73–84. doi:10.1002/hep.28431

Younossi, Z. M., Wong, G., Anstee, Q. M., and Henry, L. (2023). The global burden of liver disease. *Clin. Gastroenterol. Hepatol.* 21 (8), 1978–1991. doi:10.1016/j.cgh.2023.04.015

Yu, X., Hao, M., Liu, Y., Ma, X., Lin, W., Xu, Q., et al. (2019). Liraglutide ameliorates non-alcoholic steatohepatitis by inhibiting NLRP3 inflammasome and pyroptosis activation via mitophagy. *Eur. J. Pharmacol.* 864, 172715. doi:10.1016/j.ejphar.2019.172715

Zeng, L., Lu, M., Mori, K., Luo, S., Lee, A. S., Zhu, Y., et al. (2004). ATF6 modulates SREBP2-mediated lipogenesis. *Embo J.* 23 (4), 950–958. doi:10.1038/sj.emboj.7600106

Zeng, W., Shan, W., Gao, L., Gao, D., Hu, Y., Wang, G., et al. (2015). Inhibition of HMGB1 release via salvianolic acid B-mediated SIRT1 up-regulation protects rats against non-alcoholic fatty liver disease. *Sci. Rep.* 5, 16013. doi:10.1038/srep16013

Zhang, B., Ni, M., Li, X., Liu, Q., Hu, Y., and Zhao, Y. (2021). QSHY granules promote white adipose tissue browning and correct BCAAs metabolic disorder in NAFLD mice. *Diabetes Metab. Syndr. Obes.* 14, 4241–4251. doi:10.2147/DMSO.S332659

Zhang, J., Du, H., Shen, M., Zhao, Z., and Ye, X. (2020). Kangtaizhi granule alleviated nonalcoholic fatty liver disease in high-fat diet-fed rats and HepG2 cells via AMPK/mTOR signaling pathway. *J. Immunol. Res.* 2020, 3413186. doi:10.1155/2020/3413186

Zhang, J., Zhao, Y., Xu, C., Hong, Y., Lu, H., Wu, J., et al. (2014). Association between serum free fatty acid levels and nonalcoholic fatty liver disease: a cross-sectional study. *Sci. Rep.* 4, 5832. doi:10.1038/srep05832

Zhang, L., Wang, X., Cueto, R., Effi, C., Zhang, Y., Tan, H., et al. (2019). Biochemical basis and metabolic interplay of redox regulation. *Redox Biol.* 26, 101284. doi:10.1016/j.redox.2019.101284

Zhang, L. L., Xu, W., Xu, Y. L., Chen, X., Huang, M., and Lu, J. J. (2017). Therapeutic potential of Rhizoma Alismatis: a review on ethnomedicinal application, phytochemistry, pharmacology, and toxicology. *Ann. N. Y. Acad. Sci.* 1401 (1), 90–101. doi:10.1111/nyas.13381

Zhang, M., Yuan, Y., Wang, Q., Li, X., Men, J., and Lin, M. (2018). The Chinese medicine Chai Hu Li Zhong Tang protects against non-alcoholic fatty liver disease by activating AMPKα. *Biosci. Rep.* 38 (6). doi:10.1042/BSR20180644

Zhang, P., Cao, J., Liang, X., Su, Z., Zhang, B., Wang, Z., et al. (2024). Lian-Mei-Yin formula alleviates diet-induced hepatic steatosis by suppressing Yap1/FOXM1 pathway-dependent lipid synthesis. *Acta Biochim. Biophys. Sin. (Shanghai)* 56 (4), 621–633. doi:10.3724/abbs.2024025

Zhang, S. S., and Li, J. X. (2017). Expert consensus on TCM diagnosis and treatment of nonalcoholic fatty liver disease (2017). *J. Clin. Hepatobiliary Dis.* 33 (12), 2270–2274. doi:10.3969/j.issn.1001-5256.2017.12.002

Zhang, Z., Chang, Q., Zhu, M., Huang, Y., Ho, W. K., and Chen, Z. (2001). Characterization of antioxidants present in hawthorn fruits. *J. Nutr. Biochem.* 12 (3), 144–152. doi:10.1016/s0955-2863(00)00137-6

Zhang, Z., Huang, Y., Fan, Y., and Liu, M. (2018). Effect of Xuezhikang on hepatitis and oxidative stress in rats with nonalcoholic fatty liver disease. *Clin. J. Med. Officers* 46 (6), 605–609. doi:10.16680/j.1671-3826.2018.06.01

Zhao, W., Yu, Y., Liu, L., and Wang, Y. (2014). Experimental study of Kezhi capsule on PPAR-γand IR expression in non-alcoholic steatohepatitis rats. *Chin. J. Integr. Traditional West. Med. Dig.* 22 (9), 501–505. doi:10.3969/j.issn.1671-038X.2014.09.04

Zhao, Z., Deng, Z. T., Huang, S., Ning, M., Feng, Y., Shen, Y., et al. (2022). Alisol B alleviates hepatocyte lipid accumulation and lipotoxicity via regulating rarα-pparγ-CD36 cascade and attenuates non-alcoholic steatohepatitis in mice. *Nutrients* 14 (12), 2411. doi:10.3390/nu14122411

Zhao, Z. Y., Liu, D., Cao, W. J., Sun, M., Song, M. S., Wang, W., et al. (2018). Association between IgG N-glycans and nonalcoholic fatty liver disease in han Chinese. *Biomed. Environ. Sci.* 31 (6), 454–458. doi:10.3967/bes2018.059

Zheng, C., Nie, H., Pan, M., Fan, W., Pi, D., Liang, Z., et al. (2024). Chaihu Shugan powder influences nonalcoholic fatty liver disease in rats in remodeling microRNAome and decreasing fatty acid synthesis. *J. Ethnopharmacol.* 318, 116967. doi:10.1016/j.jep.2023.116967

frontiers | Frontiers in Pharmacology

TYPE Original Research
PUBLISHED 30 January 2025
DOI 10.3389/fphar.2024.1487738

OPEN ACCESS

EDITED BY
Rongrui Wei,
Jiangxi University of Traditional Chinese Medicine, China

REVIEWED BY
Luca Rastrelli,
University of Salerno, Italy
Lihui Zhu,
Shanghai Academy of Agricultural Sciences, China
Ian James Martins,
University of Western Australia, Australia

*CORRESPONDENCE
Xia Li,
lixiawo@163.com
Zheng Li,
lizheng@zmu.edu.cn

†These authors have contributed equally to this work

RECEIVED 28 August 2024
ACCEPTED 20 December 2024
PUBLISHED 30 January 2025

CITATION
Chen D, Shen Y, Huang F, Huang B, Xu S, Li L, Liu J, Li Z and Li X (2025) Ethanol extract of *Polygonatum cyrtonema* Hua mitigates non-alcoholic steatohepatitis in mice. *Front. Pharmacol.* 15:1487738. doi: 10.3389/fphar.2024.1487738

Ethanol extract of *Polygonatum cyrtonema* Hua mitigates non-alcoholic steatohepatitis in mice

Dongliang Chen[1†], Yue Shen[1,2†], Fang Huang[1], Bo Huang[1], Shangfu Xu[1,3], Lisheng Li[1,4], Jie Liu[1], Zheng Li[1*] and Xia Li[1*]

[1]Key Laboratory of Basic Pharmacology of Ministry of Education and Joint International Research Laboratory of Ethnomedicine of Ministry of Education, Zunyi Medical University, Zunyi, China, [2]Department of Pharmacy, Bijie City Qixingguan District Hospital of Traditional Chinese Medicine, Bijie, Guizhou, China, [3]Key Laboratory of Cell Engineering of Guizhou Province, Affiliated Hospital of Zunyi Medical University, Zunyi, China, [4]Department of Pharmacology, Key Laboratory of Basic Pharmacology of Guizhou Province and School of Pharmacy, Zunyi Medical University, Zunyi, Guizhou, China

Background: *Polygonum cyrtonema* Hua is a kind of traditional Chinese botanic drug. Modern pharmacological research has confirmed that *Polygonum cyrtonema* Hua is able to alleviate nonalcoholic fatty liver disease, but the precise mechanism requires further investigation. This study investigated the protective effects and underlying mechanisms of *Polygonatum cyrtonema* ethanol extract (PCE) against Non-alcoholic steatohepatitis (NASH) in mice.

Methods: UHPLC-MS/MS was utilized to analyze the metabolites of PCE. The NASH mouse model was establishment in C57BL/6J mice via high-fat diet (HFD) feeding for 12 weeks, and from the 9th week, mice were gavaged with PCE (100, 300, and 900 mg/kg/day), simvastatin (4 mg/kg) or saline. One hand, liver injury was assessed by serum enzymes, biochemistry, and histopathology; On the other hand, RNA-seq, qPCR, and Western blot were employed to investigate the related molecular mechanisms.

Results: 211 metabolites were identified through UHPLC-MS/MS analysis. PCE ameliorated HFD induced liver injury and improved hepatocellular degeneration and steatosis in a dose-dependent way. PCE restored the expression of AMPK, SIRT1, SREBP1 and PPAR-α both in mRNA and protein levels. RNAseq identified unique gene expression profiles in response to high-fat diet (HFD) compared to the PCE treatments. HFD-induced DEGs were attenuated or abolished following PCE treatments. Ingenuity pathway analysis of RNA-seq data revealed key canonical pathways and upstream molecules regulated by PCE.

Conclusion: Our findings confirm the ability of PCE in alleviating NASH and underscores AMPK/SIRT1 pathway as a potential theraputic target for NASH treatment.

KEYWORDS

***Polygonatum cyrtonema* Hua, NASH, AMPK, SIRT1, NF-κ B, PPAR-α, RNA-Seq**

Introduction

Non-alcoholic fatty liver disease (NAFLD) is a metabolic syndrome marked by excessive fat accumulation in liver cells. NAFLD may initially present as simple steatosis, namely, Non-alcohol-associated fatty liver (NAFL), but can progressively develop into non-alcoholic steatohepatitis (NASH), liver fibrosis, cirrhosis, and potentially liver cancer (Friedman et al., 2018). NASH, an advanced form of NAFL, is more susceptible to develop into fibrosis, cirrhosis and hepatocellular carcinoma and is associated with need for liver transplantation (Geier et al., 2021). Nowadays, approximately 30% of the global population suffers from NAFLD (Younossi et al., 2023). Notably, about 20% of patients with NAFL progress to NASH, and over 40% of patients with NASH progress to fibrosis (Sheka et al., 2020). Therefore, the treatment of NASH can effectively prevent the progression of NAFLD.

Despite advancements in pathological research of NASH, its clinical treatment mainly relies on lifestyle changes at present. Although Rezdiffra was approved by the U.S. Food and Drug Administration in March 2024 to treat patients with NASH, its long-term surveillance is essential to identify potential risks related to thyroid, gonadal, or bone diseases (Petta et al., 2024). Meanwhile, as the global burden of NASH continues to grow, effective NAFLD treatment drugs are still lacking in clinical practice.

Traditional Chinese medicine employs a multi-target, multi-pathway strategy for disease treatment and has been widely utilized in the prevention and management of disease. *Polygonatum cyrtonema* Hua is a perennial plant with a long history for both medicinal and edible use. Containing a variety of bioactive metabolites, *Polygonatum cyrtonema* Hua has shown therapeutic effects in osteoporotic, fatigue and respiratory problems (Cui et al., 2018). In addition, the role of *Polygonatum cyrtonema* Hua in NAFLD has been discovered recently (Liu et al., 2022), however the specific mechanism remains nebulous.

AMP-activated kinase (AMPK) is a vital metabolic sensor in mammals and is activated when ATP levels decreased (Wang Q et al., 2018). The silent information regulator sirtuin 1 (SIRT1) protein is a highly conserved NAD^+-dependent deacetylase, and regulates fundamental biological functions such as genomic stability, energy metabolism, inflammation and tumorigenesis (You and Liang, 2023). It has been confirmed that activation of AMPK increases intracellular NAD^+ concentration and triggers activation of SIRT1 (Han et al., 2016). Meanwhile the inhibition of SIRT1 activity induced decreased AMPK activation (Zhang et al., 2024). AMPK and SIRT1 are important players in the coordinating network of cell homeostasis and are largely interdependent to function optimally (Wang L. et al., 2018). The current work was aim to determined the effect of *Polygonatum cyrtonema* Hua in alleviating NASH and whether its effect is related to the activation of AMPK/SIRT1 pathway. Additionally, the metabolites in PCE were systematically analyzed by UHPLC-MS/MS and the gene expression was comprehensively analyzed by RNA-seq.

Materials and methods

Preparation of PCE

Dry powder of *Polygonatum cyrtonema* Hua purchased from Guizhou Hengfenghao Agricultural Development Co., Ltd. (Guizhou, China) was soaked in 75% ethanol and extracted by ultrasonic at 40°C. Then the extraction liquid was filtered and concentrated by rotary evaporator. The residue was dried and was extracted again by the method above to obtained the secondary residue and concentrated solution. The secondary residue was soaked in distilled water and then concentrated at 60°C, combined the above concentrated solution and freeze dried the extraction. The PCE yield was around 40% and contained amino acids, flavonoids, polysaccharides, saponins, alkaloids, lectin, and others using UHPLC-ESI-MS/MS analysis by Sanshu Biotechnology (Shanghai, China).

UHPLC-MS/MS analysis PCE chemical constituents

Take an appropriate volume of sample (0.5–1 mL), add 1 mL water: acetonitrile: isopropanol (1:1:1, v/v) solution for metabolite extraction. The solution underwent 30 min of sonication at 4°C. Following centrifugation (20 min, 12,000 rpm, 4°C), the supernatant was transferred to clean microtubes. Until analysis, samples were freeze-dried and stored at −20°C. For UHPLC-ESI-MS/MS analysis, samples were dissolved in 200 μL of 30% ACN (v/v) and transferred to insert-equipped vials. The analysis was conducted using Thermo Xcalibur 4.0.

Experimental animals

Male C57BL/6J mice, weighing between 18 and 22 g and of SPF grade, were obtained from Specific Biotechnology Co. Ltd. (Certificate No: SCXK 2019-0010, Beijing, China). All mice were housed in an SPF-grade facility with unrestricted access to food and water. The environment was maintained at 25°C ± 2°C and 50% ± 5% humidity. A 12-h light/dark cycle was maintained. All procedures received approval from the Experimental Animal Ethics Committee of Zunyi Medical University (No. 2020-2-060, Zunyi Medical Lun Audit).

Animals treatments

Following a 7 days of adaptive feeding, mice were randomly assigned to six groups (n = 6): control, HFD model, HFD + PCE low-dose (100 mg/kg), HFD + PCE medium-dose (300 mg/kg), HFD + PCE high-dose (900 mg/kg), and positive control (simvastatin, 4 mg/kg). Mice in normal control group were fed on a normal chow diet, meanwhile, mice in other groups were fed on a high-fat diet for 12 weeks. From the ninth week, mice in PCE and simvastatin groups were correspondingly administered low-dose PCE, medium-dose PCE, high-dose PCE, or simvastatin via gavage for 4 weeks, mice in control group and HFD group were administered equal volumes of saline. After 12 weeks of high-fat diet feeding, all mice were anesthetized.

Chemicals and reagents

The high-fat diet was obtained from Ready Dietech in Shenzhen, China. Assay kits for alanine transaminase (ALT, C009-2-1), aspartate transaminase (AST, C010-2-1), triacylglycerol (TG, A110-1), total cholesterol (TC, A111-1), high-density lipoprotein cholesterol (HDL-

C, A112-1), and low-density lipoprotein cholesterol (LDL-C, A113-1) were procured from Nanjing Jiancheng Bioengineering Institute (Nanjing, China). All HPLC-grade solvents were obtained from ANPEL Laboratory Technologies (Shanghai, China).

Biochemical parameter detection

Blood samples were centrifuged to collect serum supernatants. Serum biochemical indicators were tested by commercial kits from Nanjing Jianjian Bioengineering Institute, following the manufacturer's instructions.

H&E staining

The same part of mouse liver were fixed in 10% neutral buffered formalin for 48 h and then embedded in paraffin and sliced into 5 μm-thick slides. After dewaxing and dehydration, slides were stained with hematoxylin. Then after differentiation and bluing, slides were stain with eosin. Using a series of gradient alcohol solutions for dehydration, slides were sealed with neutral resin. The pathological changes of mouse liver tissue were observed under an optical microscope.

Oil red O staining

The frozen liver tissue slides were rewarmed at room temperature, and washed with distilled water firstly to wash off the embedding agent and then washed with 60% isopropyl alcohol for 2 min. All sections are stained with staining solution for 25 min 60% isopropyl alcohol was used to adjust the color. Slides were restained with hematoxylin for 10–20 s and returned to blue with PBS. Glycerol gelatin was used to seal the slides. After drying at room temperature, slides were observed under the light microscope.

RNA isolation and sequencing

Total RNA was extracted using Trizol reagent (Takara, Japan). Fragmented mRNA samples were reverse transcribed into cDNA using random Oligo dT primers and M-MuLV. Double-stranded cDNA was synthesized using the generated first-strand cDNA, RNase H enzyme, DNA polymerase I, and dNTPs. Purified double-stranded cDNA underwent end repair, A-tailing, and adaptor addition. Screen 250-300bp cDNA using AMPure XP beads, followed by PCR amplification and subsequent purification with AMPure XP beads. The library concentration was measured using Qubit 2.0 and diluted to 1.5 ng/μL. The Agilent 2100 detected the inserted library (420–650 bp, tail <1 Kb), and qPCR confirmed an effective library concentration >3 nM. RNA sequencing was performed using the Illumina NovaSeq PE150 platform. Chongqing Knorigene Technologies (Chongqing, China) conducted the sequencing and bioinformatics analyses following successful library construction. DESeq2 was employed for RNA-seq data analysis, with comparisons made to the Control group. Differentially expressed genes (DEGs) were determined using a significance threshold of $p < 0.05$.

Reverse transcription-quantitative polymerase chain reaction

After quantifying at 260/280 nm, the total RNA were reverse transcribed by Prime Script TM RT Kit (Takara Biotechnology Co., Ltd., China). Primers were designed using Primer 3 and synthesized by Sangon Biotech and were listed in Table 1. The PCR reaction mixture consisted of 7.5 μL SYBR Super Mix, 0.5 μL of each 10 μM primer, 3 μL cDNA, and 3.5 μL DEPC water, making a total volume of 15 μL. The cycling conditions were set at 95°C for 10 min (1 cycle), 95°C for 10 s and 60°C for 1 min (40 cycles), followed by 95°C for 1 min, 55°C for 1 min, and 55°C for 10 s (80 cycles) for the melting curve. Gene expression levels were measured using quantification cycle (Cq) values. Glyceraldehyde-3-phosphate dehydrogenase (GAPDH) gene expression levels served as the internal control. Each group was normalized to the Control group.

Western blot analysis

Livers were homogenized with RIPA buffer containing PMSF and phosphatase inhibitor. The total protein concentrations

TABLE 1 Main experimental primers.

Gene	Forward primer	Reverse primer
SREBP-1c	GCTAGCTAGATGACCCTGCAC	GCAGCAGCAAGATTTGCCTA
PPAR-α	ACTGGTAGTCTGCAAAACCAAA	AGAGCCCCATCTGTCCTCTC
MTTP	ATGATCCTCTTGGCAGTGCTT	TGAGAGGCCAGTTGTGTGAC
TNF-α	GGCCTCCCTCTCATCAGTTC	CACTTGGTGGTTTGCTACGA
GAPDH	TGTGTCCGTCGTGGATCTGA	CCTGCTTCACCACCTTCTTGA
IL-1β	TGTGAAATGCCACCTTTTGA	GGTCAAAGGTTTGGAAGCAG
ApoB	TGAATGCACGGGCAATGA	GGCATTACTTGTTCCATGGTTCT
SIRT1	GTTGTGTGCCTTCGTTTTTGGA	AGGCCGGTTTGGCTTATACA
AMPK	ATGGCGCGACCCGGGCTTCTTCT-3	TACCGCGCTGGGCCCGAAGAAGA

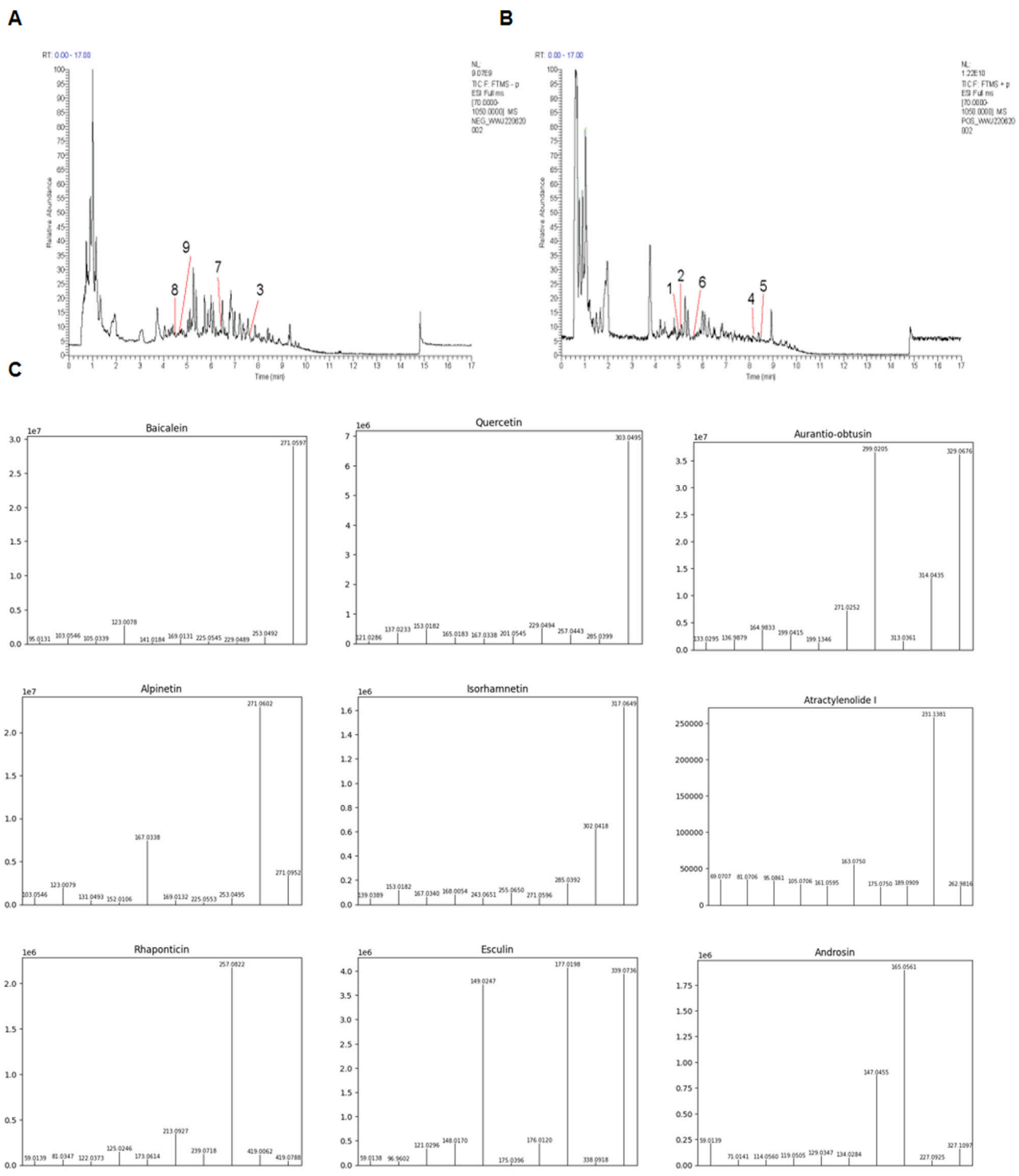

FIGURE 1
Total ion chromatograms of PCE. **(A)** Representative chromatography of PCE using the negative mode; **(B)** Representative chromatography of PCE using the positive mode; **(C)** UHPLC-ESI-MS/MS spectra of the identified 9 lipid - lowering metabolites from PCE.

were determined by BCA protein assay kit (General Biotech. Co., Shanghai, China). 30 μg of protein was separated using SDS-PAGE and transferred to a PVDF membrane for immunoblotting. After blocking with 5% skimmed milk, membranes were incubated with primary antibodies MTTP (Santa, #C2218), SREBP-1c (Abbkin, #ABP53239), PPAR-α (Abbkin, #ABP55667), ApoB (Proteintech, #20578-1-AP), SIRT1 (Abcam, #ab110304), P-AMPK (CST, #5759), AMPK (CST, #2603), P-ACC (CST, #50081), and ACC (CST, #3662) overnight at 4°C.Membranes were incubated with secondary antibody at room temperature for 1 h, followed by washing. Chemiluminescence ECL developed the color, and protein bands

were quantified using the ChemiDoc MP imaging system (Bio-Rad, United States).

Ingenuity pathway analysis

Canonical pathway and upstream regulator analyses were performed using the Ingenuity pathway analysis (IPA) server (Qiagen, Redwood City, CA). The IPA software determines significance using a right-tailed Fisher's Exact test, with the P-value indicating the probability of overlap between the treatment groups and the IPA pathway gene list. Additionally, upstream analysis employed differentially expressed genes to identify regulatory factors, with variations across treatment groups assessed using the Z-score.

Statistical analysis

The experimental data were statistically analyzed by GraphPad Prism 8.0 software. Quantitative data were presented as mean ± SEM. A t-test compared two groups, while one-way ANOVA with LSD *post hoc* test was used for multiple group comparisons. $p < 0.05$ signifies statistical significance.

Results

Identification of the constituents of PCE

UHPLC-ESI-MS/MS analysis was adopted to determine metabolites in PCE. The mass spectral total ion chromatogram of PCE was analyzed by UHPLC-ESI-MS/MS in positive and negative ion modes, as shown in Figures 1A, B. By comparing it with the database, a total of 211 metabolites were identified in PCE and 9 of which were reported to exhibit lipid-lowering effect. These 9 metabolites include baicalin (Guo et al., 2023), quercetin (Yang H. et al., 2019; Yang J. et al., 2019), and aurantio-obtusin (Li HY et al., 2023), atractylenolide (Li et al., 2022), alpinetin (Zhou et al., 2018), isorhamnetin (Ganbold et al., 2019), rhaponticin (Chen et al., 2009), esculin (Yang et al., 2021), and androsin (Singh et al., 2024). The main information of the 9 lipid-lowering metabolites is shown in Table 2 and their MS/MS fragment ions spectrum are displayed in Figure 1C.

TABLE 2 Identification of main metabolites in PCE by UHPLC-ESI-MS/MS analysis.

	Name	Formula	Mode	Remain time (min)
1	Baicalein	$C_{15}H_{10}O_5$	POS	4.98
2	Quercetin	$C_{15}H_{10}O_7$	POS	4.99
3	Aurantio-obtusin	$C_{17}H_{14}O_7$	NEG	7.38
4	Atractylenolide	$C_{15}H_{20}O_3$	POS	8.20
5	Alpinetin	$C_{16}H_{14}O_4$	POS	8.47
6	Isorhamnetin	$C_{16}H_{12}O_7$	POS	5.50
7	Rhaponticin	$C_{21}H_{24}O_9$	NEG	6.37
8	Esculin	$C_{15}H_{16}O_9$	NEG	4.39
9	Androsin	$C_{15}H_{20}O_8$	NEG	4.24

Protective effect of PCE on HFD-Induced nonalcoholic fatty liver in mice

For establishing a NASH mouse model, C57BL/6 mice were fed with HFD for 12 weeks, and the detailed experimental timeline is shown in Figure 2A. NAFLD begins with hepatic fat accumulation, and after 12 weeks HFD feeding, mice exhibited yellowish livers due to lipid deposition. In addition, the livers' volume were obviously increased and accompanied by significant enlarger gallbladders (Figure 2A).

In PCE groups, mice were gavaged different dose of PCE continuously for 4 weeks, which reversed HFD-induced increasing weight gain and liver index as shown in Figures 2B, C. Additionally, the color and volume of mice livers gradually approached normal in a dose-dependent manner (Figure 2D). Simvastatin is effective in reducing blood lipid levels and could be used as an appropriate positive control group for NAFLD (Yang et al., 2024). Our results indicated that simvastatin effectively reduced the increase of body weight and liver index in mice induced by HFD feeding. High doses of PCE and simvastatin showed almost the same improvement in lowering mice body weight and liver index.

PCE ameliorated HFD-induced histological changes and lipid metabolism disorder

H&E staining and Oil red O staining were adopted to observe the effect of PCE on histological changes and hepatic steatosis. Liver tissue of HFD mice exhibited obvious wide distribution of fatty vacuolation in H&E staining and red lipid droplets in Oil red O staining. Meanwhile, hepatocytic ballooning, a unique form of hepatocyte injury emerged in liver tissue of HFD group. Similarly, PCE treatment significantly ameliorated these histopathological changes in a dose-dependent manner (Figure 3A). The relative area of fat vacuoles in H&E staining and relative area of lipid droplets in Oil red O staining showed the same trend with staining results (Supplementary Figure S1).

To quantitative analysis the impact of PCE on alleviating HFD-induced liver injury, the levels of alanine aminotransferase (ALT) and aspartate aminotransferase (AST) were measured. HFD feeding significantly elevated serum levels of ALT and AST. Consistantly, both the high dose of PCE and simvastatin, effectively reduced the serum levels of AST and ALT (Figures 3B, C). PCE's lipid-lowering effect was further certificated by the reduced serum triglyceride (TG) and total cholestrol (TC) levels (Figures 3D, E). HFD induced NAFLD is often accompanied by cholesterol metabolism disorders (Li et al., 2021). Fortunately, PCE showed the ability to restore the balance of cholesterol metabolism (Figures 3F, G), and surprisingly, PCE upregulated plasma concentration of HDL-C (Figure 3G), which is is negatively associated with the

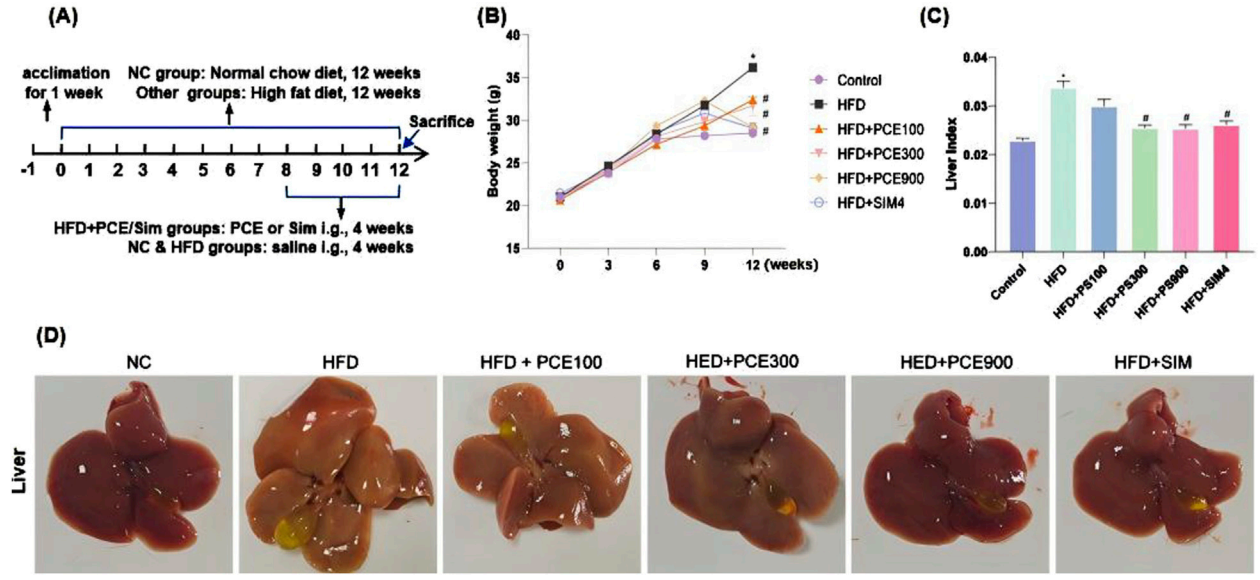

FIGURE 2
PCE alleviated the HFD-induced increases of body weight and liver index in mice. **(A)** The time modeling process of HFD-induced NASH mouse model, **(B)** Representative picture of liver morphology; **(C)** Weekly weight measurement curve; **(D)** Liver index (liver/body weight, g/g). Data are shown as mean ± SEM (n = 6).*$p < 0.05$ compared to Control; #$p < 0.05$ compared to Model.

development of cardiovascular disease (Deprince et al., 2020). These results highlight the remarkable potential of PCE in regulating lipid metabolism.

PCE reversed HFD-induced hepatic steatosis through regulating lipid synthesis and fatty acid oxidation

Given the excellent performance of PCE in reversing HFD-induced hepatic steatosis, we further determined the expression level of AMPK/SIRT1 in the liver tissue of each group by Western blot and qPCR. Activity of AMPK reduced by obesity, diabetes as well as NAFLD (Smith et al., 2016), which was confirmed by our data again. HFD feeding decreased the ratio of phosphorylated AMPK to total AMPK. PCE administration restore the expression of AMPK and phosphorylated AMPK. Similarly, numerous studies have point out that SIRT1 harnesses multiple pathways to hinder NAFLD (Tian et al., 2024). Consistent with this, HFD-induced decline in SIRT1 expression was restored after PCE administration (Figures 4A–C).

Enhanced *de novo* lipogenesis in hepatocytes plays an important role in the process of NAFLD. Sterol regulatory element-binding proteins (SREBPs) are key transcriptional factors for genes in the *de novo* lipogenesis pathway, such as acetyl CoA carboxylase (ACC), which is responsible for catalyzing the rate-limiting step of fatty acid synthesis (Zeng et al., 2022). Additionally, AMPK is involved in mitochondrial fatty acid β oxidation via activating peroxisome proliferation-activated receptor α (PPAR-α). Through regulating SREBP1 pathway and PPAR-α pathway, AMPK takes parts in the process of lipid metabolism (Li et al., 2011). Therefore, to further confirm the effects of PCE on activating AMPK/SIRT1, we determined the expression of SREBP1, ACC and PPAR-α by Western blot and qPCR. As show in Figures 4A–F, HFD-induced protein or mRNA level changes of these molecular were restored by PCE.

Dyslipidemia is often observed in NAFLD patients (Deprince et al., 2020), as well as in our mouse model. Therefore we also evaluated the expression of apolipoprotein B (ApoB) and microsomal triglyceride transfer protein (MTTP), which are crucial for very low-density lipoprotein (VLDL) secretion and lipid homeostasis in the liver (Peng et al., 2021). After a high-fat diet feeding, the amount of apoB and MTTP in the liver decreased, and which were reversed by PCE treatment.

PCE reversed HFD-induced hepatic inflammatory response

NASH is an inflammatory subtype of NAFLD. Besides fat accumulation, another significant feature of NASH is inflammation. Anti-inflammatory is adopt as therapy for NASH (Xu et al., 2022). Besides energy-sensing, the vital role of AMPK/SIRT1 in inflammation is emerging (Saravia et al., 2020). In view of the activation effect of PCE on AMPK/SIRT1 and to full evaluated the effect of PCE in alleviate NASH, the levels of interleukin-1β (IL-1β), IL-6, p65 and tumor necrosis factor-α (TNF-α) in mice liver tissue were tested by Western blot and qPCR. The representative images of Western blot are shown in Figure 5A. The findings indicate that PCE reduced HFD-induced overexpression of these proteins. Consistently, as show in Figures 5B–E, HFD increased mRNA levels of these four inflammatory factors obviously, and which were reversed by PCE treatment.

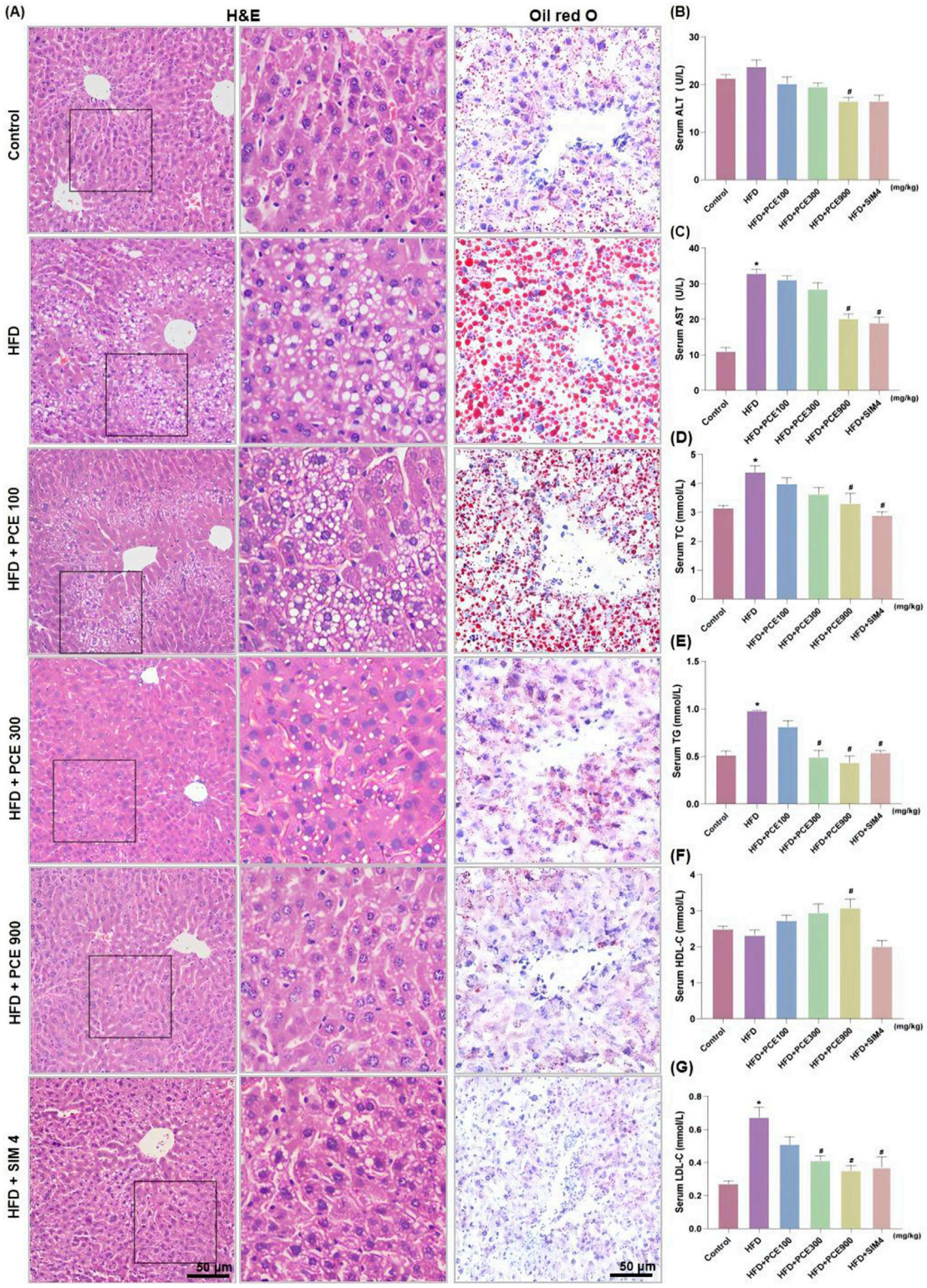

FIGURE 3
PCE treatment relieved HFD-induced liver injury and hepatosteatosis. **(A)** Representative H&E staining images and Oil red O staining images (×200, the middle panel is partly magnification of H&E staining images); **(B)** Serum ALT; **(C)** Serum AST; **(D)** Serun TC; **(E)** Serum TG; **(F)** Serum Serum high-density lipoprotein (HDL-C); **(G)** Serum low density lipoprotein (LDL-C). Data are presented as mean ± SEM (n = 6). *$p < 0.05$ compared to Control; #P< 0.05 compared to HFD group.

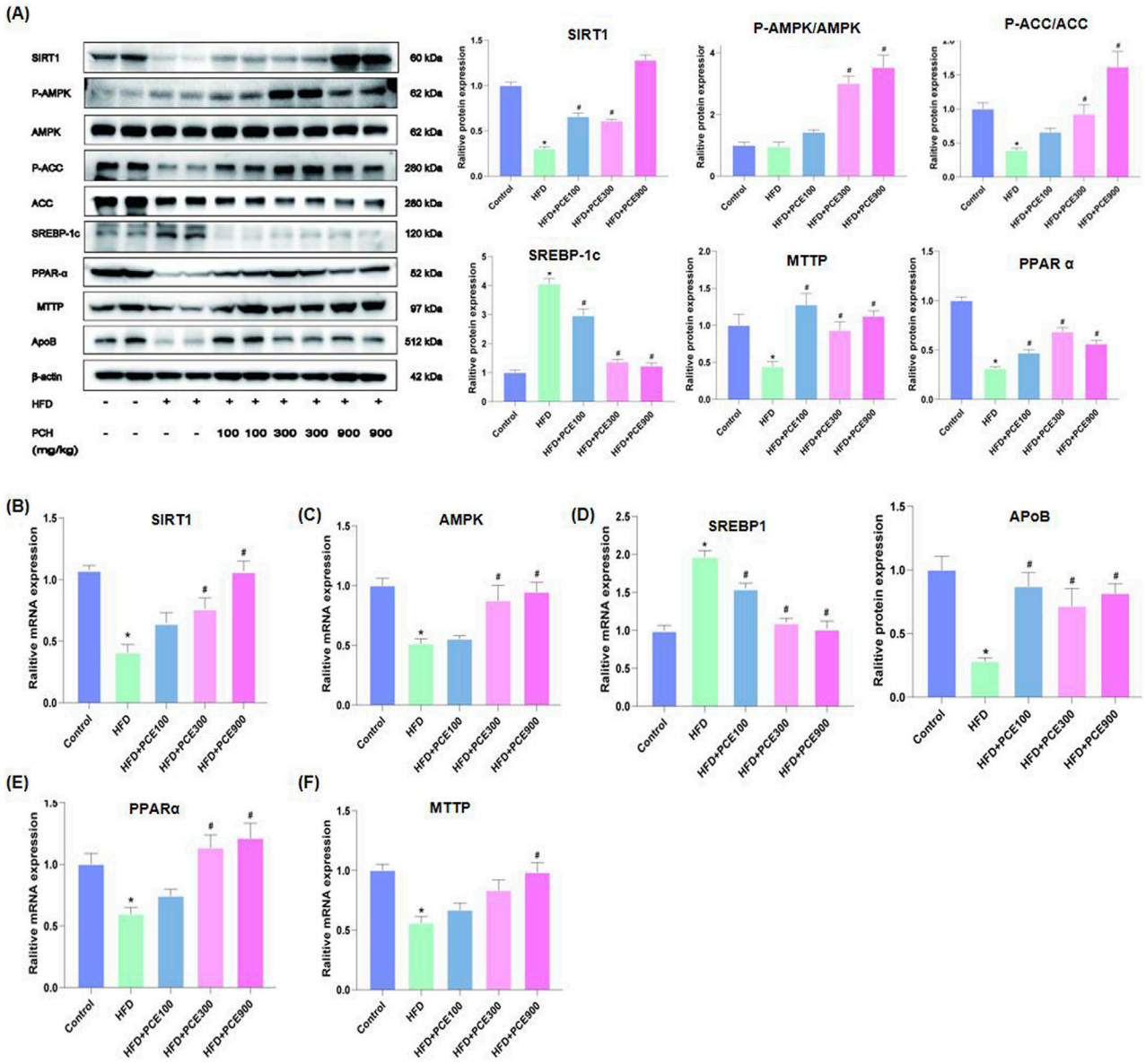

FIGURE 4
PCE treatment activated the AMPK/SITR1 signalling pathway. **(A)** Representative Western bolt results of SIRT1, AMPK, ACC, SREBP-1c, PPAR-α, MTTP, and ApoB and quantification results. **(B)** mRNA relative expression level of SIRT1; **(C)** mRNA relative expression level of AMPK; **(D)** mRNA relative expression level of SREBP1; **(E)** The mRNA relative expression level of PPAR-α; **(F)** The mRNA relative expression level of MTTP. Data are presented as mean ± SEM (n = 6). $^{*}p < 0.05$ compared to Control; $^{\#}p < 0.05$ compared to HFD group.

PCE attenuated HFD-induced DEGs and the related canonical pathways and upstream regulators were revealed

Given the diversity of metabolites in PCE, we hypothesize that the mechanisms by which PCE alleviates NASH are diverse. Therefore to fully elucidate the protective mechanism of PCE against HFD-induced NASH, we performed RNA-seq analysis. Under criteria of $p < 0.05$, HFD produced 232 (184 up, 48 down) differentially expressed genes (DEGs) as compared to control group (Supplementary Figure S2), which were attenuated or abolished following PCE treatment (PCE100, 275 up and 38 down; PCE300, 201 up and 21 down; PCE900, 172 up and 143 down). When the data were filtered by HFD, it is apparent that PCE treatment attenuated or abolished HFD-induced aberrant gene expressions (Supplementary Figure S3).

All DEGs ($p < 0.05$, HFD_vs._Cont, 232; HFD + PCE100_vs._Cont, 313; HFD + PCE300_vs._Cont, 222; HFD + PCE900_vs._Cont, 317) were loaded into Ingenuity Pathway Analysis server for core analysis, followed by comparative analysis. The 15selected canonical pathways is listed in Figure 6A. HFD increased "Neutrophil degradation, cachexia signaling pathway, acute phase response signaling, post-translational protein phosphorylation, activation of SREBP, IL-4 and IL-13 signaling, cholesterol biosynthesis, response to elevated Ca2+, circadian gene expression", etc. and PCE treatment attenuated or abolished such

10.3389/fphar.2024.1487738

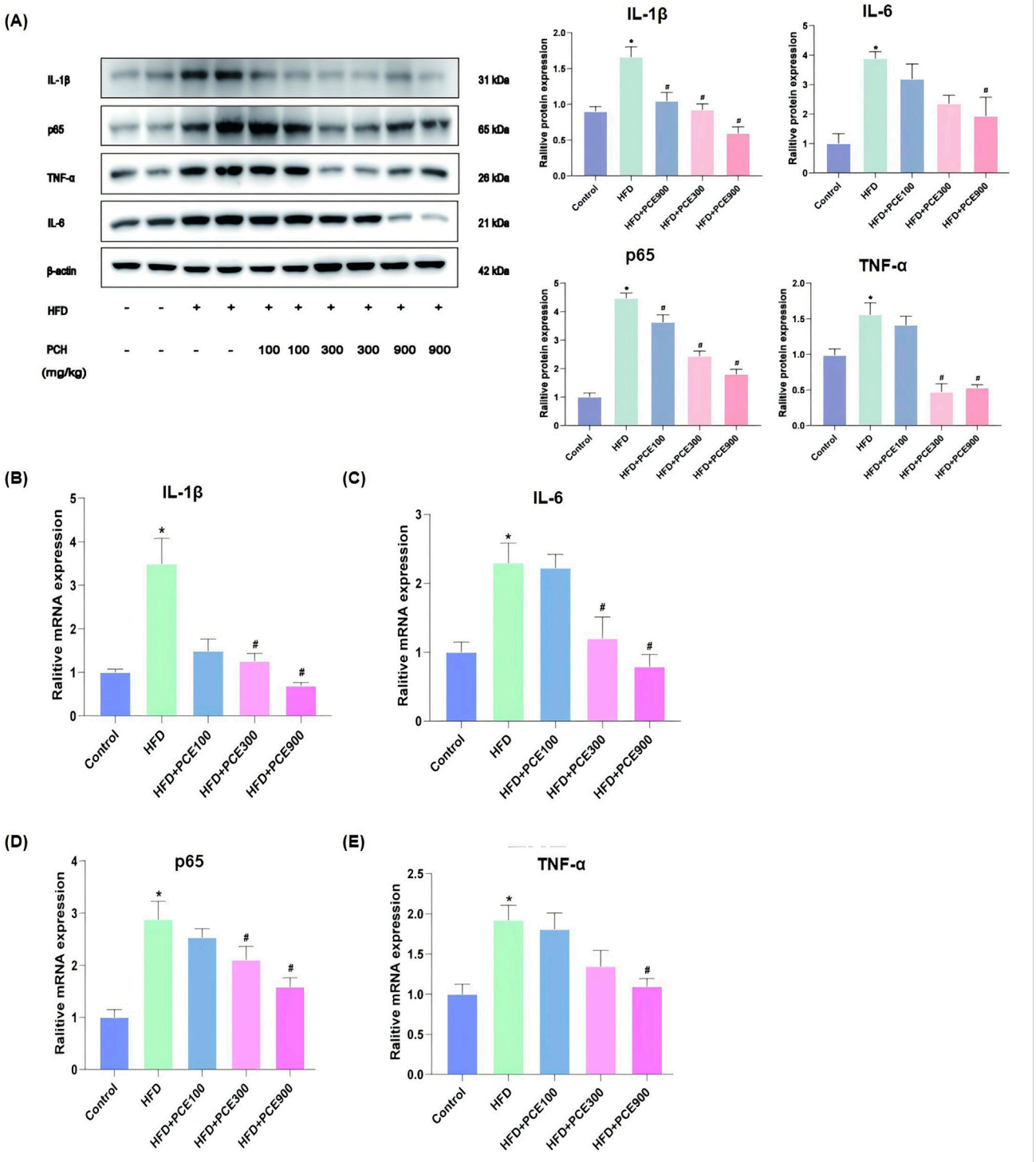

FIGURE 5
PCE treatment decreased HFD-induced high expression of inflammatory factors. **(A)** Representative Western bolt results of IL-1β, p65, TNF-α and IL-6 and quantification results. **(B)** mRNA relative expression level of IL-1β; **(C)** mRNA relative expression level of IL-6; **(D)** mRNA relative expression level of p65; **(E)** mRNA relative expression level of TNF-α. Data are presented as mean ± SEM (n = 6). *$p < 0.05$ compared to Control; $^{\#}p < 0.05$ compared to HFD group.

pathways. On the other hand. HFD decreased "FXR/RXR activation, IL-12 signaling, JAK2 signaling and Gap junction signaling" etc., and PCE treatment alleviated these changes.

Figure 6B shows the 20 selected upstream regulators. HFD increased "TNF, TNFRSF1A, IL6, IL6R, IL1B, IL1A, NFκB, NFκB1", confirming the findings above, and PCE treatment

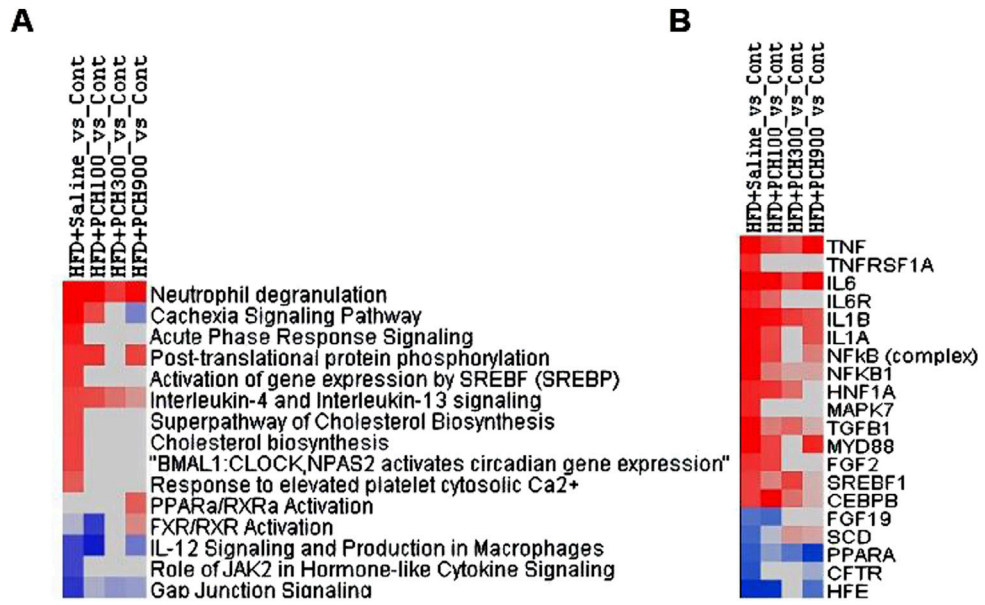

FIGURE 6
Differentially expressed genes were conducted Ingenuity Pathway Analysis. **(A)**. Top Canonical pathways; **(B)**. Top Upstream regulators.

attenuated or abolished these upregulations. In addition, HFD also increased "HNF1A, MAPK7, TGFB1, MTD88, FGF2, SREBP1, CEBPB" corresponding to HFD-induced NAFLD phenotype, which was ameliorated by PCE treatment. On the other hand, HFD decreased "FGF19, SCD, CFTR, and HFE" which was reversed by PCE to various extent.

Discussion

This study demonstrated the protective effect against NASH in mice of PCE. Through UPLC-MS/MS, 211 metabolites were identified in PCE and 9 of which were reported to exhibit lipid-lowering effect. After searching literature, we found that the lipid-lowering effects of baicalin (Yang H. et al., 2019; Xiang J. et al., 2019), quercetin (Zhang et al., 2019), atractylenolide (Li, et al., 2022), isorhamnetin (Huang et al., 2016), rhapontin (Wei et al., 2017) and ecsulin (Cheng et al., 2024) are related to the activating of AMPK/SIRT signaling pathway, which provides a basis for PCE to alleviate NASH by activating AMPK/SIRT1 pathway.

C57BL/6J mice underwent significant changes in their general health and biochemical indices following 12-week intake of high-fat chow. These changes included the increased liver indices, mild increases in serum AST and ALT activities, and elevated serum and liver TG levels, in agreement of the literature (Li YJ et al., 2023; Nie et al., 2023; Wang et al., 2020), which demonstrates the effective modeling of NAFLD. PCE effectively inhibited NAFLD development and improved liver function biochemical indices, demonstrating a clear dose-effect relationship.

SIRT1 activates AMPK through deacetylation and AMPK concurrently boosts SIRT1 activity by elevating intracellular NAD^+ levels (Cantó et al., 2009; Chen et al., 2019; Day et al., 2017). The interaction between SIRT1 and AMPK is essential for regulating molecules related to lipid metabolism and inflammation, significantly influencing NAFLD progression. SREBP-1 is the key transcriptional factors for genes related with the *de novo* lipogenesis pathway. PPAR-α is another AMPK downstream target and is crucial for hepatic lipid oxidation and export (Silva and Peixoto, 2018), its activation leads to the improvement of liver steatosis, inflammation and fibrosis in rodent model (Staels et al., 2013). In current study, PCE elevated the expression levels of AMPK, SIRT1 and PPAR-α, while decreasing SREBP1 levels. Therefore, activating of AMPK/SIRT1 pathway by PCE intake, on the one hand reduced *de novo* synthesis of fat through SREBP1 inhibition, and on the other hand increased fatty acid oxidation through upregulation of PPAR-α activity, and finally improved hepatosteatosis.

Inflammation, closely linked to high-fat diet-induced liver injury and steatohepatitis, is partly driven by the activation of the NF-κB pathway (Ding et al., 2017). SIRT1 deficiency triggers the activation of the NF-κB pathway, leading to increased expression of inflammatory factors like IL-1β, IL-6, and TNF-α, accelerating the progression of NAFLD from simple steatosis to steatohepatitis (Schug et al., 2010). SIRT1 agonists have been shown to exert anti-inflammatory effects by reducing the transcriptional activity of NF-κB p65. Our study demonstrated that PCE attenuated HFD-induced increases in IL-1β, IL-6, TNF-α, and NF-κB p65 at both mRNA and protein levels accompanied by upregulated SIRT1 expression, suggesting its anti-inflammatory effects may be related to SIRT1 activation.

The above two categories, lipid metabolism and inflammation were further supported by IPA analysis of DEGs from RNA-seq. Notably, HFD increased "Neutrophil degradation", "Cachexia Signaling Pathways" and "Acute Phase Response Signaling" pathways, along with increased upstream markers "TNF, TNFRSF1A, IL6, IL6R, IL1B, IL1A, NFκB, and NFκB1". This aligns with previous findings (Lian et al., 2020), indicating that anti-inflammation is a key mechanism through which PCE exerts its beneficial effects.

Similarly, HFD increased "post-translational protein phosphorylation" "Cholesterol biosynthesis" "Response to elevated $Ca2^+$". HFD also

increased "HNF1A, MAPK7, TGFB1, MTD88, FGF2, CEBPB", which were ameliorated by PCE treatment. On the other hand, HFD decreased "FXR/RXR activation" and "FGF19, SCD, CFTR, and HFE", which was reversed by PCE. Most of these molecules are targets for NAHLD (Parlati et al., 2021), supporting the beneficial effects of PCE in lipid metabolism.

PCE treatment also produced other beneficial effects, such as genes for maintaining circadian rhythm, and genes for TGF-β1 signaling, etc., which warrants further investigation.

Conclusion

In conclusion, the current study demonstrates the effects of PCE in alleviating NASH at least in part by activating the AMPK/SIRT1 pathway.

Data availability statement

The original contributions presented in the study are publicly available. This data can be found here: https://doi.org/10.5281/zenodo.14371978, version 1.

Ethics statement

The animal study was approved by the Ethics Committee of Zunyi Medical University No: (2020) 2 - 060. The study was conducted in accordance with the local legislation and institutional requirements.

Author contributions

DC: Investigation, Formal Analysis, Writing–original draft. YS: Validation, Formal Analysis, Writing–original draft. FH: Methodology, Writing–original draft. BH: Supervision, Writing–review and editing. SX: Methodology, Supervision, Writing–review and editing. LL: Methodology, Project administration, Writing–review and editing. JL: Data curation, Writing–review and editing. ZL: Funding acquisition, Conceptualization, Writing–original draft. XL: Funding acquisition, Conceptualization, Writing–review and editing.

Funding

The author(s) declare financial support was received for the research, authorship, and/or publication of this article. This research was funded by the Science and Technology Program of Guizhou Province (Grant No. [2021]118), College Students' Innovative Entrepreneurial Training Plan Program (ZYDC202202304, ZYDC2021004, ZYDC2020129), Science and Technology Program of Guizhou Province (Grant No. ZK2022 - General 595) and Guizhou Province Science and Technology Plan Project (Grant No. [2018]5772-073).

Conflict of interest

The authors declare that the research was conducted in the absence of any commercial or financial relationships that could be construed as a potential conflict of interest.

Publisher's note

Supplementary material

The Supplementary Material for this article can be found online at: https://www.frontiersin.org/articles/10.3389/fphar.2024.1487738/full#supplementary-material

References

Cantó, C., Gerhart-Hines, Z., Feige, J. N., Lagouge, M., Noriega, L., Milne, J. C., et al. (2009). AMPK regulates energy expenditure by modulating NAD+ metabolism and SIRT1 activity. *Nature* 458, 1056–1060. doi:10.1038/nature07813

Chen, J., Ma, M., Lu, Y., Wang, L., Wu, C., and Duan, H. (2009). Rhaponticin from rhubarb rhizomes alleviates liver steatosis and improves blood glucose and lipid profiles in KK/Ay diabetic mice. *Planta Med. Apr* 75, 472–477. doi:10.1055/s-0029-1185304

Chen, X. Y., Cai, C. Z., Yu, M. L., Feng, Z. M., Zhang, Y. W., Liu, P. H., et al. (2019). LB100 ameliorates nonalcoholic fatty liver disease via the AMPK/Sirt1 pathway. *World J. Gastroenterol.* 25 (25), 6607–6618. doi:10.3748/wjg.v25.i45.6607

Cheng, Z., Liu, Z., Liu, C., Yang, A., Miao, H., and Bai, X. (2024). Esculin suppresses the PERK-eIF2α-CHOP pathway by enhancing SIRT1 expression in oxidative stress-induced rat chondrocytes, mitigating osteoarthritis progression in a rat model. *Int. Immunopharmacol.* 132 (132), 112061. doi:10.1016/j.intimp.2024.112061

Cui, X., Wang, S., Cao, H., Guo, H., Li, Y., Xu, F., et al. (2018). A review: the bioactivities and pharmacological applications of Polygonatum sibiricum polysaccharides. *Mol. May* 14, 23. doi:10.3390/molecules23051170

Day, E. A., Ford, R. J., and Steinberg, G. R. (2017). AMPK as a therapeutic target for treating metabolic diseases. *Trends Endocrinol. Metab.* 28, 545–560. doi:10.1016/j.tem.2017.05.004

Deprince, A., Haas, J. T., and Staels, B. (2020). Dysregulated lipid metabolism links NAFLD to cardiovascular disease. *Mol. Metab.* 42, 101092. doi:10.1016/j.molmet.2020.101092

Ding, R. B., Bao, J., and Deng, C. X. (2017). Emerging roles of SIRT1 in fatty liver diseases. *Int. J. Biol. Sci.* 13, 852–867. doi:10.7150/ijbs.19370

Friedman, S. L., Neuschwander-Tetri, B. A., Rinella, M., and Sanyal, A. J. (2018). Mechanisms of NAFLD development and therapeutic strategies. *Nat. Med.* 24, 908–922. doi:10.1038/s41591-018-0104-9

Ganbold, M., Owada, Y., Ozawa, Y., Shimamoto, Y., Ferdousi, F., Tominaga, K., et al. (2019). Isorhamnetin alleviates steatosis and fibrosis in mice with nonalcoholic steatohepatitis. *Sci. Rep.* 9 (9), 16210. doi:10.1038/s41598-019-52736-y

Geier, A., Tiniakos, D., Denk, H., and Trauner, M. (2021). From the origin of NASH to the future of metabolic fatty liver disease. *Gut* 70, 1570–1579. doi:10.1136/gutjnl-2020-323202

Guo, C., Li, Q., Chen, R., Fan, W., Zhang, X., Zhang, Y., et al. (2023). Baicalein alleviates non-alcoholic fatty liver disease in mice by ameliorating intestinal barrier dysfunction. *Food Funct.* 14, 2138–2148. doi:10.1039/d2fo03015b

Han, X., Tai, H., Wang, X., Wang, Z., Zhou, J., Wei, X., et al. (2016). AMPK activation protects cells from oxidative stress-induced senescence via autophagic flux restoration and intracellular NAD(+) elevation. *Aging Cell* 15, 416–427. doi:10.1111/acel.12446

Huang, L., He, H., Liu, Z., Liu, D., Yin, D., and He, M. (2016). Protective effects of isorhamnetin on cardiomyocytes against anoxia/reoxygenation-induced injury is mediated by SIRT1. *J. Cardiovasc Pharmacol.* 67, 526–537. doi:10.1097/FJC.0000000000000376

Li, H., Yu, X. H., Ou, X., Ouyang, X. P., and Tang, C. K. (2021). Hepatic cholesterol transport and its role in non-alcoholic fatty liver disease and atherosclerosis. *Prog. Lipid Res.* 83, 101109. doi:10.1016/j.plipres.2021.101109

Li, H. Y., Huang, S. Y., Zhou, D. D., Xiong, R. G., Luo, M., Saimaiti, A., et al. (2023). Theabrownin inhibits obesity and non-alcoholic fatty liver disease in mice via serotonin-related signaling pathways and gut-liver axis. *J. Adv. Res.* 52, 59–72. doi:10.1016/j.jare.2023.01.008

Li, Q., Tan, J. X., He, Y., Bai, F., Li, S. W., Hou, Y. W., et al. (2022). Atractylenolide III ameliorates non-alcoholic fatty liver disease by activating hepatic adiponectin receptor 1-mediated AMPK pathway. *Int. J. Biol. Sci.* 18, 1594–1611. doi:10.7150/ijbs.68873

Li, Y., Xu, S., Mihaylova, M. M., Zheng, B., Hou, X., Jiang, B., et al. (2011). AMPK phosphorylates and inhibits SREBP activity to attenuate hepatic steatosis and atherosclerosis in diet-induced insulin-resistant mice. *Cell Metab.* 13 (13), 376–388. doi:10.1016/j.cmet.2011.03.009

Li, Y. J., Wu, R. Y., Liu, R. P., Wu, K. Y., Ding, M. N., Sun, R., et al. (2023). Aurantio-obtusin ameliorates obesity by activating PPARα-dependent mitochondrial thermogenesis in brown adipose tissues. *Acta Pharmacol. Sin.* 44, 1826–1840. doi:10.1038/s41401-023-01089-4

Lian, C. Y., Zhai, Z. Z., Li, Z. F., and Wang, L. (2020). High fat diet-triggered non-alcoholic fatty liver disease: a review of proposed mechanisms. *Chem. Biol. Interact.* 330, 109199. doi:10.1016/j.cbi.2020.109199

Liu, W., Shao, T., Tian, L., Ren, Z., Gao, L., Tang, Z., et al. (2022). Structural elucidation and anti-nonalcoholic fatty liver disease activity of Polygonatum cyrtonema Hua polysaccharide. *Food Funct. Dec* 13 (13), 12883–12895. doi:10.1039/d2fo03384d

Nie, K., Gao, Y., Chen, S., Wang, Z., Wang, H., Tang, Y., et al. (2023). Diosgenin attenuates non-alcoholic fatty liver disease in type 2 diabetes through regulating SIRT6-related fatty acid uptake. *Phytomedicine. Mar.* 111, 154661. doi:10.1016/j.phymed.2023.154661

Parlati, L., Régnier, M., Guillou, H., and Postic, C. (2021). New targets for NAFLD. *JHEP Rep.* 3, 100346. doi:10.1016/j.jhepr.2021.100346

Peng, H., Chiu, T. Y., Liang, Y. J., Lee, C. J., Liu, C. S., Suen, C. S., et al. (2021). PRAP1 is a novel lipid-binding protein that promotes lipid absorption by facilitating MTTP-mediated lipid transport. *J. Biol. Chem.* 296, 100052. doi:10.1074/jbc.RA120.015002

Petta, S., Targher, G., Romeo, S., Pajvani, U. B., Zheng, M. H., Aghemo, A., et al. (2024). The first MASH drug therapy on the horizon: current perspectives of resmetirom. *Liver Int.* 44, 1526–1536. doi:10.1111/liv.15930

Saravia, J., Raynor, J. L., Chapman, N. M., Lim, S. A., and Chi, H. (2020). Signaling networks in immunometabolism. *Cell Res. Apr* 30, 328–342. doi:10.1038/s41422-020-0301-1

Schug, T. T., Xu, Q., Gao, H., Peres-da-Silva, A., Draper, D. W., Fessler, M. B., et al. (2010). Myeloid deletion of SIRT1 induces inflammatory signaling in response to environmental stress. *Mol. Cell Biol.* 30, 4712–4721. doi:10.1128/MCB.00657-10

Sheka, A. C., Adeyi, O., Thompson, J., Hameed, B., Crawford, P. A., and Ikramuddin, S. (2020). Nonalcoholic steatohepatitis: a review. *Jama* 323 (323), 1175–1183. doi:10.1001/jama.2020.2298

Silva, A. K. S., and Peixoto, C. A. (2018). Role of peroxisome proliferator-activated receptors in non-alcoholic fatty liver disease inflammation. *Cell Mol. Life Sci. Aug* 75, 2951–2961. doi:10.1007/s00018-018-2838-4

Singh, A., Ansari, A., Gupta, J., Singh, H., Jagavelu, K., and Sashidhara, K. V. (2024). Androsin alleviates non-alcoholic fatty liver disease by activating autophagy and attenuating *de novo* lipogenesis. *Phytomedicine. Jul* 129, 155702. doi:10.1016/j.phymed.2024.155702

Smith, B. K., Marcinko, K., Desjardins, E. M., Lally, J. S., Ford, R. J., and Steinberg, G. R. (2016). Treatment of nonalcoholic fatty liver disease: role of AMPK. *Am. J. Physiol. Endocrinol. Metab.* 311, E730-E740–e740. doi:10.1152/ajpendo.00225.2016

Staels, B., Rubenstrunk, A., Noel, B., Rigou, G., Delataille, P., Millatt, L. J., et al. (2013). Hepatoprotective effects of the dual peroxisome proliferator-activated receptor alpha/delta agonist, GFT505, in rodent models of nonalcoholic fatty liver disease/nonalcoholic steatohepatitis. *Hepatology* 58, 1941–1952. doi:10.1002/hep.26461

Tian, C., Huang, R., and Xiang, M. (2024). SIRT1: harnessing multiple pathways to hinder NAFLD. *Pharmacol. Res. May* 203, 107155. doi:10.1016/j.phrs.2024.107155

Wang, L., Quan, N., Sun, W., Chen, X., Cates, C., Rousselle, T., et al. (2018). Cardiomyocyte-specific deletion of Sirt1 gene sensitizes myocardium to ischaemia and reperfusion injury. *Cardiovasc Res.* 114, 805–821. doi:10.1093/cvr/cvy033

Wang, Q., Liu, S., Zhai, A., Zhang, B., and Tian, G. (2018). AMPK-mediated regulation of lipid metabolism by phosphorylation. *Biol. Pharm. Bull.* 41 (41), 985–993. doi:10.1248/bpb.b17-00724

Wang, W., Xu, A. L., Li, Z. C., Li, Y., Xu, S. F., Sang, H. C., et al. (2020). Combination of probiotics and salvia miltiorrhiza polysaccharide alleviates hepatic steatosis via gut microbiota modulation and insulin resistance improvement in high fat-induced NAFLD mice. *Diabetes Metab. J. Apr* 44, 336–348. doi:10.4093/dmj.2019.0042

Wei, W., Wang, L., Zhou, K., Xie, H., Zhang, M., and Zhang, C. (2017). Rhapontin ameliorates colonic epithelial dysfunction in experimental colitis through SIRT1 signaling. *Int. Immunopharmacol.* 42, 185–194. doi:10.1016/j.intimp.2016.11.024

Xu, X., Poulsen, K. L., Wu, L., Liu, S., Miyata, T., Song, Q., et al. (2022). Targeted therapeutics and novel signaling pathways in non-alcohol-associated fatty liver/steatohepatitis (NAFL/NASH). *Signal Transduct. Target Ther. Aug* 13 (7), 287. doi:10.1038/s41392-022-01119-3

Yang, H., Yang, T., Heng, C., Zhou, Y., Jiang, Z., Qian, X., et al. (2019). Quercetin improves nonalcoholic fatty liver by ameliorating inflammation, oxidative stress, and lipid metabolism in db/db mice. *Phytother. Res.* 33, 3140–3152. doi:10.1002/ptr.6486

Yang, J., Xiang, D., Xiang, D., He, W., Liu, Y., Lan, L., et al. (2019). Baicalin protects against 17α-ethinylestradiol-induced cholestasis via the sirtuin 1/hepatic nuclear receptor-1α/farnesoid X receptor pathway. *Front. Pharmacol.* 10, 1685. doi:10.3389/fphar.2019.01685

Yang, S., Wei, Z., Luo, J., Wang, X., Chen, G., Guan, X., et al. (2024). Integrated bioinformatics and multiomics reveal Liupao tea extract alleviating NAFLD via regulating hepatic lipid metabolism and gut microbiota. *Phytomedicine* 132, 155834. doi:10.1016/j.phymed.2024.155834

Yang, X. D., Chen, Z., Ye, L., Chen, J., and Yang, Y. Y. (2021). Esculin protects against methionine choline-deficient diet-induced non-alcoholic steatohepatitis by regulating the Sirt1/NF-κB p65 pathway. *Pharm. Biol.* 59, 922–932. doi:10.1080/13880209.2021.1945112

You, Y., and Liang, W. (2023). SIRT1 and SIRT6: the role in aging-related diseases. *Biochim. Biophys. Acta Mol. Basis Dis. Oct.* 1869, 166815. doi:10.1016/j.bbadis.2023.166815

Younossi, Z. M., Golabi, P., Paik, J. M., Henry, A., Van Dongen, C., and Henry, L. (2023). The global epidemiology of nonalcoholic fatty liver disease (NAFLD) and nonalcoholic steatohepatitis (NASH): a systematic review. *Hepatology* 77, 1335–1347. doi:10.1097/HEP.0000000000000004

Zeng, H., Qin, H., Liao, M., Zheng, E., Luo, X., Xiao, A., et al. (2022). CD36 promotes *de novo* lipogenesis in hepatocytes through INSIG2-dependent SREBP1 processing. *Mol. Metab.* 57, 101428. doi:10.1016/j.molmet.2021.101428

Zhang, T., Xu, L., Guo, X., Tao, H., Liu, Y., Liu, X., et al. (2024). The potential of herbal drugs to treat heart failure: the roles of Sirt1/AMPK. *J. Pharm. Anal.* 14, 157–176. doi:10.1016/j.jpha.2023.09.001

Zhang, Y., Zhang, W., Tao, L., Zhai, J., Gao, H., Song, Y., et al. (2019). Quercetin protected against isoniazide-induced HepG2 cell apoptosis by activating the SIRT1/ERK pathway. *J. Biochem. Mol. Toxicol.* 33, e22369. doi:10.1002/jbt.22369

Zhou, Y., Ding, Y. L., Zhang, J. L., Zhang, P., Wang, J. Q., and Li, Z. H. (2018). Alpinetin improved high fat diet-induced non-alcoholic fatty liver disease (NAFLD) through improving oxidative stress, inflammatory response and lipid metabolism. *Biomed. Pharmacother.* 97, 1397–1408. doi:10.1016/j.biopha.2017.10.035

frontiers | Frontiers in Pharmacology

TYPE Systematic Review
PUBLISHED 03 February 2025
DOI 10.3389/fphar.2025.1523713

OPEN ACCESS

EDITED BY
Rongrui Wei,
Jiangxi University of Traditional Chinese Medicine, China

REVIEWED BY
Li-Long Jiang,
China Pharmaceutical University, China
Paola Ingaramo,
Universidad Nacional del Litoral, Argentina

*CORRESPONDENCE
Jinhao Zeng,
zengjinhao@cdutcm.edu.cn
Yaoguang Guo,
guoyaoguang@cdutcm.edu.cn
Xiao Ma,
tobymaxiao@cdutcm.edu.cn

†These authors have contributed equally to this work and share first authorship

RECEIVED 06 November 2024
ACCEPTED 03 January 2025
PUBLISHED 03 February 2025

CITATION
Jiang J, Wang Q, Wu Q, Deng B, Guo C, Chen J, Zeng J, Guo Y and Ma X (2025) Angel or devil: the dual roles of 2,3,5,4′-tetrahydroxystilbene-2-O-β-D-glucopyranoside in the development of liver injury based on integrating pharmacological techniques: a systematic review.
Front. Pharmacol. 16:1523713.
doi: 10.3389/fphar.2025.1523713

Angel or devil: the dual roles of 2,3,5,4′-tetrahydroxystilbene-2-O-β-D-glucopyranoside in the development of liver injury based on integrating pharmacological techniques: a systematic review

Jiajie Jiang[1,2†], Qixiu Wang[3†], Qiang Wu[4†], Bobin Deng[5], Cui Guo[1], Jie Chen[1], Jinhao Zeng[1*], Yaoguang Guo[1*] and Xiao Ma[2*]

[1]TCM Regulating Metabolic Diseases Key Laboratory of Sichuan Province, Hospital of Chengdu University of Traditional Chinese Medicine, Chengdu, China, [2]State Key Laboratory of Southwestern Chinese Medicine Resources, Chengdu University of Traditional Chinese Medicine, Chengdu, China, [3]Affiliated Hospital of Liaoning University of Traditional Chinese Medicine, Shenyang, China, [4]Chengdu Shuangliu Hospital of Traditional Chinese Medicine, Chengdu, China, [5]School of Pharmacy, Xian Medical University, Xi'an, China

Background and purpose: 2,3,5,4′-tetrahydroxystilbene-2-O-β-D-glucoside (TSG) exhibits a dualistic pharmacological profile, acting as both a hepatoprotective and hepatotoxic agent, which is intricately linked to its interaction with multiple signaling pathways and its stereoisomeric forms, namely, cis-SG and trans-SG. The purpose of this study is to evaluate both the hepatoprotective and hepatotoxic effects of TSG and give therapeutic guidance.

Methods: This study performed a systematic search of eight databases to identify preclinical literature up until March 2024. The CAMARADES system evaluated evidence quality and bias. STATA and Python were used for statistical analysis, including dose-effect maps, 3D maps and radar charts to show the dose-time-effect relationship of TSG on hepatoprotection and hepatotoxicity.

Results: After a rigorous screening process, a total of 24 studies encompassing 564 rodents were selected for inclusion in this study. The findings revealed that TSG exhibited bidirectional effects on the levels of ALT and AST, while also regulating the levels of ALT, AST, TNF-α, IL-6, serum TG, serum TC, SOD, MDA, IFN-γ, and apoptosis rate. The histological analysis of liver tissue confirmed the regulatory effects of TSG, and a comprehensive analysis revealed the optimal protective dosage range was 27.27–38.81 mg/kg/d and the optimal toxic dosage range was 51.93–76.07 mg/kg/d. TSG exerts the dual effects on liver injury (LI) through the network of Keap1/Nrf2/HO-1/NQO1, NF-κB, PPAR, PI3K/Akt, JAK/STAT and TGF-β pathways.

Conclusion: TSG could mediate the pathways of oxidation, inflammation, and metabolism to result in hepatoprotection (27.27–38.81 mg/kg/d) and hepatotoxicity (51.93–76.07 mg/kg/d).

KEYWORDS

2,3,5,4′-tetrahydroxystilbene-2-O-β-D-glucoside, hepatotoxicity, hepatoprotection, liver injury, systematic review

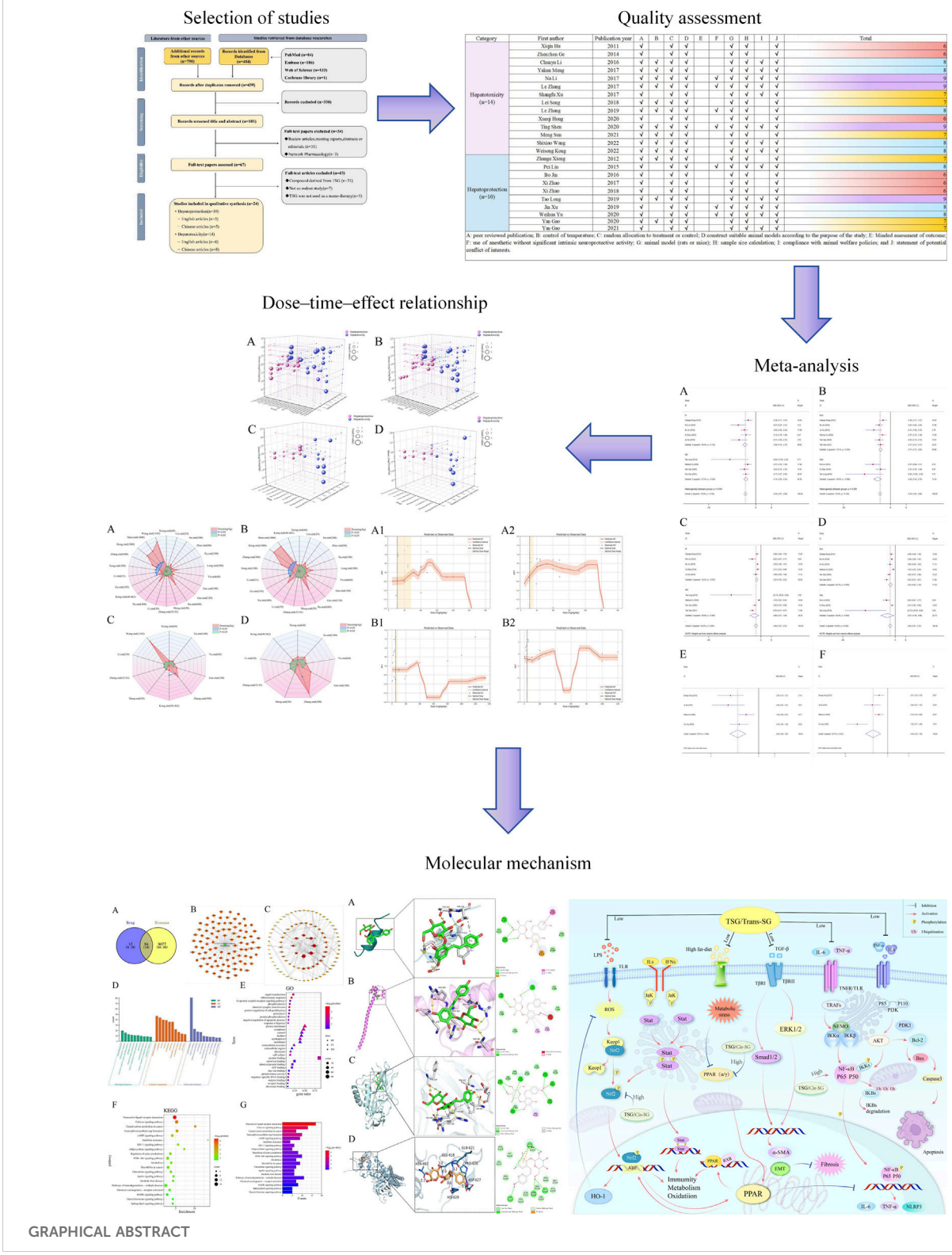

GRAPHICAL ABSTRACT

1 Introduction

The dynamic equilibrium between the toxic and therapeutic effects of pharmaceuticals used in the management of liver diseases presents a significant challenge that warrants meticulous examination. With the rising incidence of liver disease, it has become a significant public health concern, leading to 170,000 deaths each year in Europe (Acevedo, 2015). Liver injury (LI), often an early indicator of liver disease, can arise from various etiological factors, including alcohol consumption, infectious agents,

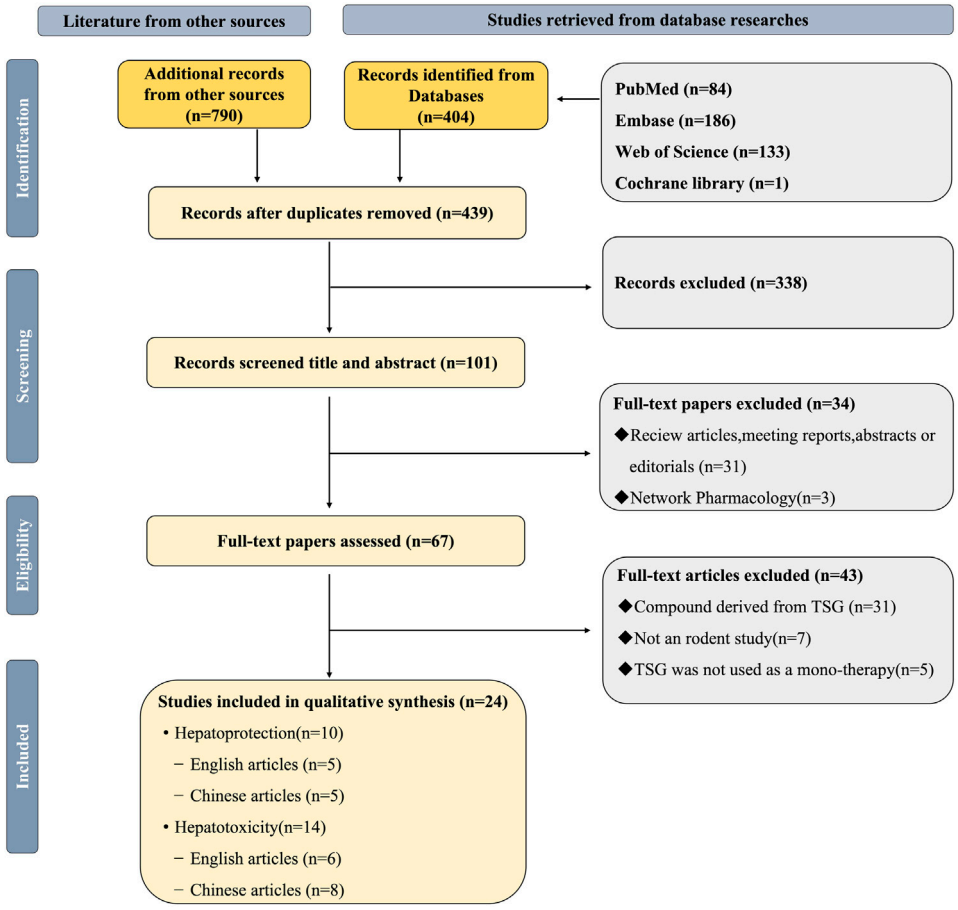

FIGURE 1
Selection of studies for this study.

immune dysregulation, and adverse drug reactions (Breit et al., 2023; Kirpich and McClain, 2012; Younossi et al., 2023). The pathological features of LI encompass inflammatory cell infiltration, steatosis, and ballooning degeneration of hepatocytes (Zhang et al., 2024b). Clinical presentations of LI encompass abnormal liver function test results, fever, nausea, vomiting, jaundice, and right upper quadrant pain (EASL et al., 2019; Knight, 2005). In the absence of timely intervention, LI may progress to liver failure, ultimately leading to mortality (Niewiński et al., 2020). Current standard therapeutic approaches for LI predominantly include antiviral medications, hepatoprotective strategies, and immunosuppressive agents such as corticosteroids, pioglitazone, and cholestyramine (Devarbhavi et al., 2023). However, these treatments can paradoxically induce drug-induced liver injury (DILI) due to their intrinsic hepatotoxic properties (Katarey and Verma, 2016). This highlights the urgent need to explore more effective and safer alternatives for the management of LI.

2,3,5,4′-tetrahydroxystilbene-2-O-β-D-glucoside (TSG; C20H22O9; MW = 406.38) is a bioactive compound extracted from the dried root of *Polygonum multiflorum* Thunb., which is a traditional herbal medicine and has garnered significant interest due to its complex nature regarding liver health (Lin et al., 2015a; Liu et al., 2022; Ma et al., 2015). TSG exhibits a dualistic pharmacological profile, acting as both a hepatoprotective and hepatotoxic agent, which is intricately linked to its interaction with multiple signaling pathways and its stereoisomeric forms, namely, cis-SG and trans-SG (Kong et al., 2022; Liu et al., 2022). The hepatoprotective effects of TSG are multifaceted, with its ability to activate the nuclear factor erythroid 2-related factor 2 (Nrf2)/heme oxygenase-1 (HO-1) pathway, a critical cellular defense mechanism against oxidative stress, being paramount (Gao et al., 2020; Yu W. et al., 2020). This activation bolsters the cell's antioxidant capacity, thereby mitigating liver damage induced by reactive oxygen species (ROS) (Liu et al., 2022; Yu W. et al., 2020). Additionally, TSG is known to modulate the nuclear factor kappa-B(NF-κB) pathway to protect liver tissues, which interacts with phosphatidylinositol 3-kinase (PI3K)/protein kinase B (Akt) and Nrf2 pathways (Elbaset et al., 2024; Lawrence, 2009; Lin et al., 2015b). TSG could potentially counteract LI through the suppression of the NF-κB signaling cascade, which in turn stimulates the Nrf2–HO-1 signaling axis, and dampens the PI3K/Akt/NF-κB pathway (Gao et al., 2020; Lawrence, 2009; Lin et al., 2015b; Wang et al., 2020b; Xiong et al., 2012). However, TSG's potential to cause liver damage has also been noted, particularly in relation to the peroxisome proliferator-activated receptor (PPAR) pathway, which has complex interactions with Janus kinase (JAK)/

TABLE 1 The key characteristics of all 24 studies.

Author(s)/ Year	Model category	Species	Gender (M/F)	Weight of the animal	Sample size (n) TSG/ model	Drug dosage	Treatment courses	Main outcome indicators
Xiong 2012	NBI	Kunming mice	Male	18–22 g	8/8	TSG: Chinese liquor (56% vol), 12 mL/kg + TSG, 60 mg/kg Mod: Chinese liquor (56% vol), 12 mL/kg	6 days	ALT, AST, TNF-α, IL-6
LIn 2015	BI	Sprague Dawley rats	Male	347–461 g	7/7	TSG: High-fat diet + TSG, 24 mg/kg Mod: High-fat diet	12 weeks	ALT, AST, Serum TG Serum TC
Jin 2016	NBI	C57BL/ 6 mice	Male	18–22 g	15/15	TSG: 50% ethanol, 6 g/kg BW + TSG, 200 mg/kg Mod: 50% ethanol, 6 g/kg BW	3 days	ALT, AST, SOD
Zhao 2017	BI	Sprague Dawley rats	Male	180–220 g	7/7	TSG: Fat milk + TSG, 80 mg/kg Mod: Fat milk	6 weeks	GSH, MDA, Serum TG Serum TC, SOD
Zhao 2018	BI	Sprague Dawley rats	Male	160–200 g	7/7	TSG: High-fat emulsion + TSG, 80 mg/kg Mod: High-fat emulsion	6 weeks	ALT, AST, Serum TG Serum TC
Xu 2019	BI	C57BL/ 6 mice	Male	26–32 g	6/6	TSG: High-fat diet + TSG, 100 mg/kg Mod: High-fat diet	12 weeks	ALT, AST, GSH, IL-6 Serum TG, Serum TC TNF-α, MDA, SOD
Long 2019	NBI	Sprague Dawley rats	Female	200–250 g	3/3	TSG: CCl4 + TSG, 300 mg/kg Mod: CCl4	8 weeks	ALT, AST, GSH, MDA SOD
Yu 2020	NBI	C57BL/ 6 mice	Male	NM	10/10	TSG: Diethylnitrosamine, 100 mg/kg + TSG, 60 mg/kg Mod: Diethylnitrosamine, 100 mg/kg	5 days	ALT, AST, GSH, IL-6, TNF-α, MDA
Gao 2020	NBI	C57BL/ 6 mice	NM	NM	10/10	TSG: Acetaminophen, 350 mg/kg + TSG 180 mg/kg Mod: Acetaminophen, 350 mg/kg	3 days	ALT, AST, GSH, IL-6, TNF-α, SOD
Gao 2021	NBI	C57BL/ 6 mice	NM	20–30 g	15/15	TSG: Acetaminophen, 350 mg/kg + TSG, 120 mg/kg Mod: Acetaminophen, 350 mg/kg	7 days	ALT, AST, MDA, SOD
Hu 2011	N	Sprague Dawley rats	Male and Female	NM	10/10	TSG: Distilled water, 1 mL/100 g + TSG, 1,200 mg/kg Mod: Distilled water, 1 mL/100 g	90 days	ALT, AST,TP
Ge 2014	N	ICR mice	Male and Female	18–22 g	10/10	TSG:Constant volume of 0.5% sodium carboxymethylcellulose + TSG, 185 mg/kg Mod: Constant volume of 0.5% sodium carboxymethylcellulose	10 days	ALT,AST
Meng 2017	LI	Sprague Dawley rats	Male	160–190 g	8/8/8/8 8/8	TSG 1. LPS, 2.8 mg/kg + Cis-SG, 50 mg/kg 2. LPS,2.8 mg/kg + Trans-SG, 50 mg/kg 3. Normal diet + Cis-SG,	3 days	ALT, AST, IL-6, TNF-α IFN-γ

(Continued on following page)

TABLE 1 (*Continued*) The key characteristics of all 24 studies.

Author(s)/ Year	Model category	Species	Gender (M/F)	Weight of the animal	Sample size (n) TSG/ model	Drug dosage	Treatment courses	Main outcome indicators
						50 mg/kg 4. Normal diet + Trans-SG, 50 mg/kg Mod 1. LPS, 2.8 mg/kg 2. Normal diet		
Li 2017	LI	Sprague Dawley rats	Male	160–180 g	10/10 10/10	TSG 1. LPS, 2.8 mg/kg + Trans-SG, 31 mg/kg 2. Normal diet + Trans-SG, 31 mg/kg Mod 1. LPS, 2.8 mg/kg 2. Normal diet	5 days	ALT,AST
Zhang 2017	LI	Sprague Dawley rats	Male	180–200 g	8/8/8/8/8/8 8/8	TSG 1. LPS, 2.8 mg/kg + Cis-SG,7.56 mg/kg 2. LPS, 2.8 mg/kg + Cis-SG, 26.46 mg/kg 3. LPS, 2.8 mg/kg + Cis-SG, 52.92 mg/kg 4. Normal diet + Cis-SG, 7.56 mg/kg 5. Normal diet + Cis-SG, 26.46 mg/kg 6. Normal diet + Cis-SG, 52.92 mg/kg Mod 1. LPS, 2.8 mg/kg 2. Normal diet	10 h	ALT, AST, IL-6, TNF-α
Li 2017	LI	Sprague Dawley rats	Male	190–210 g	9/9/9/9 9/9	TSG 1. LPS, 2.8 mg/kg + Cis-SG, 30 mg/kg 2. LPS, 2.8 mg/kg + Trans-SG, 200 mg/kg 3. Normal saline + Cis-SG, 30 mg/kg 4. Normal saline + Trans-SG, 200 mg/kg Mod 1. LPS, 2.8 mg/kg 2. Normal saline	10 h	ALT, AST, IL-6, TNF-α IFN-γ
Xu 2017	LI	C57BL/ 6 mice	Male	18–22 g	10/10	TSG: Acetaminophen, 200 mg/kg + TSG, 400 mg/kg Mod: Acetaminophen, 200 mg/kg	12 h	ALT,AST
Song 2018	N	ICR mice	Male and Female	18–22 g	10/10	TSG: Constant volume of normal saline + TSG, 100 mg/kg Mod: Constant volume of normal saline	14 days	ALT,AST,ALP,ALB,TP
Zhang 2019	N	Sprague Dawley rats	Male	180–200 g	8/8	TSG: Normal saline + TSG, 500 mg/kg Mod: Normal saline	7 h	ALT, AST, IL-6, TNF-α IFN-γ
Hong 2020	N	Sprague Dawley rats	Male	150–180 g	6/6	TSG: Normal saline + TSG, 1,000 g/kg Mod: Normal saline	28 days	ALT,AST,ALP
Shen 2020	N	Sprague Dawley rats	Male and Female	80–100 g	10/10	TSG: Distilled water, 1 mL/100 g + TSG, 1,000 mg/kg	90 days	ALT,AST,ALP

(Continued on following page)

TABLE 1 (*Continued*) The key characteristics of all 24 studies.

Author(s)/ Year	Model category	Species	Gender (M/F)	Weight of the animal	Sample size (n) TSG/ model	Drug dosage	Treatment courses	Main outcome indicators
						Mod: Distilled water, 1 mL/100 g		
Sun 2021	N	C57BL/ 6 mice	NM	NM	6/6	TSG: Normal saline + TSG, 400 mg/kg Mod: Normal saline	15 days	ALP,TNF-α
Wang 2022	N	ICR mice	Male	18–20 g	6/6	TSG: Normal saline + TSG, 1,345 mg/kg Mod: Normal saline	28 days	ALT,ALP,TPALB
Kong 2022	LI	Balb/c mice	Female	NM	6/6/6/6 6	TSG 1. LPS, 0.5 mg/kg + Cis-SG, 0.18 mg/kg + Trans-SG, 4.8 mg/kg 2. LPS, 0.5 mg/kg + Cis-SG, 0.45 mg/kg + Trans-SG, 18 mg/kg 3. LPS, 0.5 mg/kg + Cis-SG, 0.45 mg/kg + Trans-SG, 18 mg/kg Mod: LPS, 0.5 mg/kg	14 days	ALT, AST, IL-6, TNF-a

Abbreviations: Green area represents the subject of TSG's hepatoprotection (n = 8); Blue area represents the subject of TSG's hepatotoxicity (n = 13). NBI, non-biomacromaolecule induced; BI, biomacromaolecule induced; Mod, model; N, normal; NM, not mentioned; LI, liver injury; ICR, institute of cancer research; ALT, alanine aminotransferase; AST, aspartate aminotransferase; SOD, superoxide dismutase; TNF-α, tumor necrosis factor alpha; MDA, malondialdehyde; GSH, glutathione; IL-6, interleukin 6; ALP, alkaline phosphatase; ALB, albumin; TP, total protein; IFN-γ, interferon gamma.

signal transducer and activator of transcription (STAT), Nrf2/HO-1, and NF-κB signaling pathways (Christofides et al., 2021; Zhang, 2017). TSG may inhibit Nrf2 activity by suppressing the PPAR/JAK/STAT/Nrf2 axis, while activating NF-κB, leading to LI (Meng et al., 2017; Shao et al., 2024; Zhang, 2017). Several studies suggested that TSG and its isomers, specifically the cis-form and trans-form, may exhibit differential effects on liver health. The cis-isomer, in particular, has been associated with an increased risk of LI, possibly through the inhibition of the peroxisome proliferator-activated receptor γ (PPARγ) pathway, which can exacerbate inflammation and immune responses (Kong et al., 2022; Meng et al., 2017). The trans-isomer, on the other hand, might have a more protective role under certain conditions, although the exact mechanisms are still under investigation (Liu et al., 2022). Furthermore, the duration and dosage of TSG medication are pivotal factors influencing its toxicity and therapeutic efficacy. However, there is a noticeable gap in the literature regarding the precise delineation of the toxic dose range for TSG. Despite the importance of understanding the safe dosage limits, current research has not yet provided a definitive framework for distinguishing the toxic dose thresholds of this medication.

It is crucial to recognize that the hepatoprotective and hepatotoxic effects of TSG may be interrelated and influenced by on various factors, including dosage, duration of exposure, and individual susceptibility. Further research is needed to fully elucidate the mechanisms by which TSG and its isomers influence liver health and to determine the safe therapeutic window for its use in treating liver diseases. Consequently, the objective of this study is to integrate pharmacological techniques to assess the influence of TSG in the development of LI and elucidate the dynamic processes through which TSG exerts its hepatoprotective and hepatotoxic effects.

2 Methods

2.1 Data sources and search strategy

This study accessed data from eight distinct repositories, which included four English-language databases and an equal number of Chinese-language databases: PubMed, Web of Science, the Cochrane Library, and Embase, alongside the China National Knowledge Infrastructure, Wanfang Medicine Online, the Chinese Science and Technology Journal Database, and the Chinese Biomedical Database (Ju et al., 2018; Liu et al., 2021; Luo et al., 2021; Xiong et al., 2019; Zheng et al., 2021). Up to March 2024, all eligible literatures were searched. The keywords were "2,3,5,4′-tetrahydroxystilbene-2-O-β-D-glucoside," "liver injury," "hepatoprotection," and "hepatotoxicity." (Figure 1; Supplementary Table 1).

2.2 Included criteria

2.2.1 Studies on hepatoprotection

(1) Population: Studies must involve rats or mice. (2) Experimental design: At least one pair of intervention and control groups must be established, both consisting of liver injury models. (3) Intervention: The intervention groups should receive TSG monotherapy exclusively. (4) Control: Control groups must receive no treatment or a non-functional intervention. (5) Indicators: Alanine aminotransferase (ALT) and aspartate aminotransferase (AST) are essential experimental indicators. Tumor necrosis factor alpha (TNF-α), interleukin 6 (IL-6), serum triglyceride (TG), serum total cholesterol (TC), glutathione (GSH), malondialdehyde (MDA), and superoxide dismutase (SOD) are selective experimental indicators. (6)

Category	First author	Publication year	A	B	C	D	E	F	G	H	I	J	Total
Hepatotoxicity (n=14)	Xiqin Hu	2011	√		√	√			√	√		√	6
	Zhenzhen Ge	2014	√		√	√			√	√		√	6
	Chunyu Li	2016	√	√	√	√			√	√	√	√	8
	Yakun Meng	2017	√	√	√	√			√	√	√	√	8
	Na Li	2017	√	√	√	√		√	√	√	√	√	9
	Le Zhang	2017	√	√	√	√		√	√	√	√	√	9
	Shangfu Xu	2017	√		√	√			√	√	√	√	7
	Lei Song	2018	√	√	√	√			√	√		√	7
	Le Zhang	2019	√	√	√	√		√	√	√		√	8
	Xueqi Hong	2020	√		√	√			√	√		√	6
	Ting Shen	2020	√	√	√	√		√	√	√	√	√	9
	Meng Sun	2021	√	√	√	√			√	√		√	7
	Shixiao Wang	2022	√	√	√	√			√	√	√	√	8
	Weisong Kong	2022	√	√	√	√			√	√	√	√	8
Hepatoprotection (n=10)	Zhange Xiong	2012	√	√	√	√			√	√		√	7
	Pei Lin	2015	√		√	√		√	√	√	√	√	8
	Bo Jin	2016	√		√	√			√	√		√	6
	Xi Zhao	2017	√		√	√			√	√		√	6
	Xi Zhao	2018	√		√	√			√	√		√	6
	Tao Long	2019	√	√	√	√			√	√	√	√	9
	Jin Xu	2019	√		√	√		√	√	√	√	√	8
	Weihua Yu	2020	√		√	√		√	√	√	√	√	8
	Yan Gao	2020	√	√	√	√			√	√		√	7
	Yan Gao	2021	√		√	√			√	√	√	√	7

A: peer reviewed publication; B: control of temperature; C: random allocation to treatment or control; D:construct suitable animal models according to the purpose of the study; E: blinded assessment of outcome; F: use of anesthetic without significant intrinsic neuroprotective activity; G: animal model (rats or mice); H: sample size calculation; I: compliance with animal welfare policies; and J: statement of potential conflict of interests.

FIGURE 2
Risk of bias and quality assessment scores for included study.

Quality evaluation: The quality assessment score must not be less than 5 points on the CAMARADES 10-point scale.

2.2.2 Studies on hepatotoxicity

(1) Population: Studies must involve rats or mice. (2) Experimental design: At least one pair of intervention and control groups must be established. (3) Intervention: The intervention groups should receive TSG monotherapy exclusively. (4) Control: Control groups must receive no treatment or a non-functional intervention. (5) Indicators: ALT and AST are essential experimental indicators. TNF-α, IL-6, interferon gamma (IFN-γ), apoptosis rate, alkaline phosphatase (ALP), albumin (ALB), and total protein (TP) are selective experimental indicators. (6) Quality evaluation: The quality assessment score must be equal to or higher than 5 points on the CAMARADES 10-point scale.

2.3 Excluded criteria

(1) The animal subjects were not rats or mice. (2) No appropriate LI or normal animal models were selected for the study. (3) Lack of control group formation. (4) Intervention groups receiving interventions other than TSG monotherapy (e.g., Western medicine, traditional Chinese medicine, integrated medicine). (5) There are no necessary experimental indicators. (6) The quality evaluation result was less than 5 points.

2.4 Data extraction

Data extraction was performed by two independent researchers. The mean and standard deviation (SD) of continuous variables were estimated based on the collected experimental data using the Universal Desktop Ruler. The following information was extracted: (1) First author's name and publication year; (2) Number, species (mice or rats), strain, sex, and weight of experimental animals; (3) Methodology for modeling and criteria for successful modeling; (4) Name, dosage, and frequency of drug administration; (5) Outcome indicators. Graphics were prioritized over digital text for reporting results (Table 1).

2.5 Risk of bias and quality of evidence

The methodological quality of the included studies was independently assessed by two researchers using the CAMARADES (Collaborative Approach to Meta-Analysis and Review of Animal Data from Experimental Studies) 10-point scale (Macleod et al., 2004). Due to the specific nature of the study, the evaluation criteria were optimized by the researchers. In case of disagreements, the corresponding author acted as an arbitrator. The detailed method is presented in Figure 2.

2.6 Quantitative synthesis and statistical analyses

The study utilized STATA 16.0 software for conducting statistical analyses. Statistical significance was defined as p values less than 0.05 ($p < 0.05$). The results were assessed using the standardised mean difference (SMD) and the corresponding 95% confidence interval (95% CI). Heterogeneity between studies was evaluated using the I-squared (I^2) test, with a random-effects model applied for $I^2 > 50\%$ and a fixed-effects model for $I^2 \leq 50\%$. Results with an I^2 of less than 50% were considered to have insignificant heterogeneity. Subgroup analysis

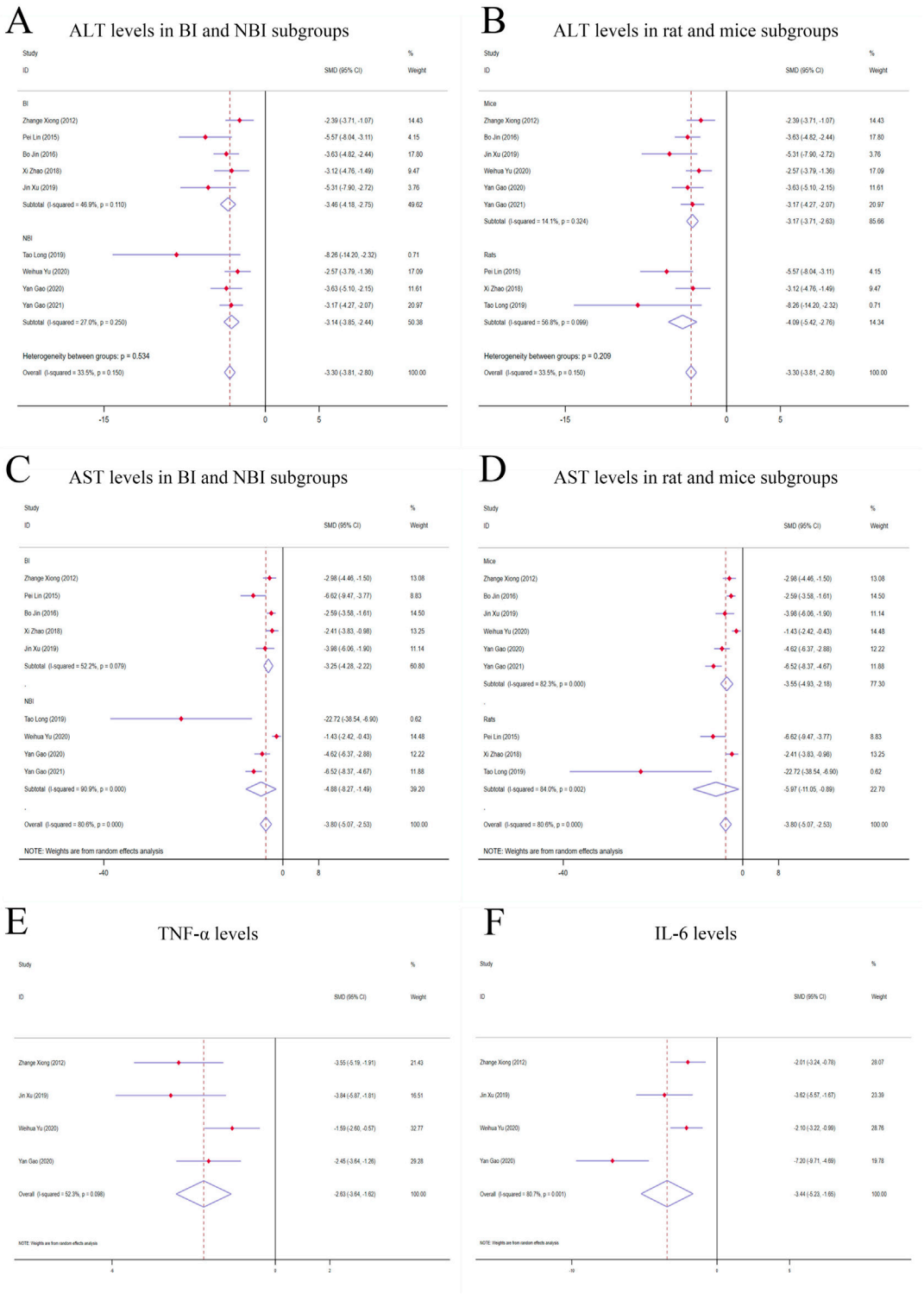

FIGURE 3
Forest plot (effect size and 95% CI) of TSG's hepatoprotective roles on ALT, AST, TNF-α and IL-6. **(A)** ALT levels in BI and NBI subgroups; **(B)** ALT levels in rat and mice subgroups; **(C)** AST levels in BI and NBI subgroups; **(D)** AST levels in rat and mice subgroups; **(E)** TNF-α levels; **(F)** IL-6 levels. Abbreviations: 95% CI, 95% confidence interval; ALT, alanine aminotransferase; AST, aspartate aminotransferase; TNF-α, tumor necrosis factor alpha; IL-6, interleukin 6; BI, biomacromolecule induced; NBI, non-biomacromolecule induced.

was conducted for exploring whether the hepatoprotective effect of TSG would be affected by differences in species and modeling methods, including animal species subgroups (rats, mice) and modeling methods subgroups [non-biomacromolecule induced (NBI), biomacromolecule induced (BI)]. Additionally, subgroup analysis was performed for exploring whether the hepatotoxicity of

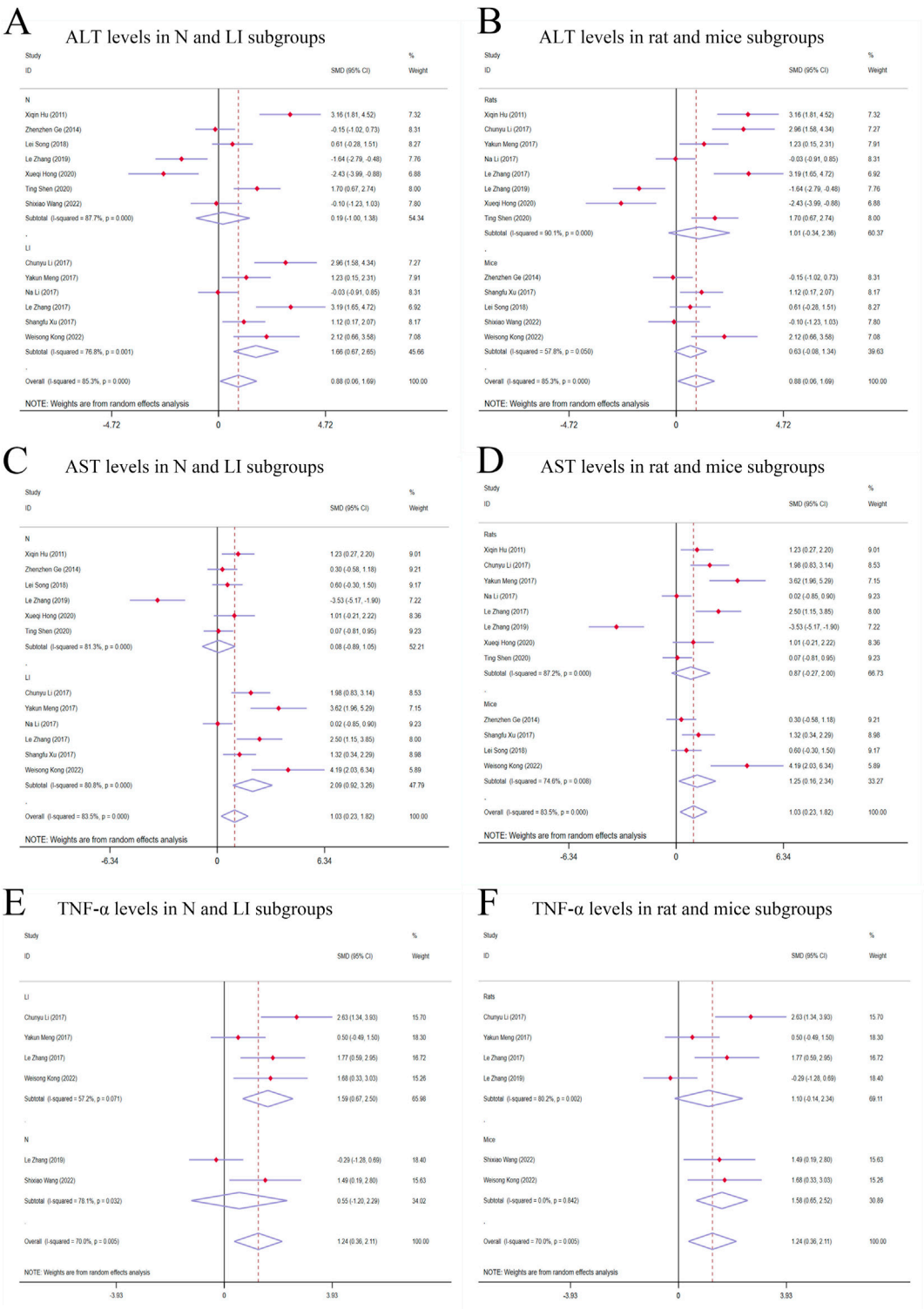

FIGURE 4
Forest plot (effect size and 95% CI) of TSG's hepatotoxic roles on ALT, AST and TNF-α. **(A)** ALT levels in N and LI subgroups; **(B)** ALT levels in rat and mice subgroups; **(C)** AST levels in N and LI subgroups; **(D)** AST levels in rat and mice subgroups; **(E)** TNF-α levels in N and LI subgroups; **(F)** TNF-α levels in rat and mice subgroups. Abbreviations: 95% CI, 95% confidence interval; ALT, alanine aminotransferase; AST, aspartate aminotransferase; TNF-α, tumor necrosis factor alpha; N, normal; LI, liver injury.

TSG is related to species, modeling methods, and isomers, including animal models subgroups [normal(N) rodents, LI rodents], animal species subgroups (rats, mice), and isomers subgroups (cis-SG, trans-SG, as well as cis-SG and trans-SG). A sensitivity analysis and Egger's test were carried out to ensure the credibility of the results for drawing inferences.

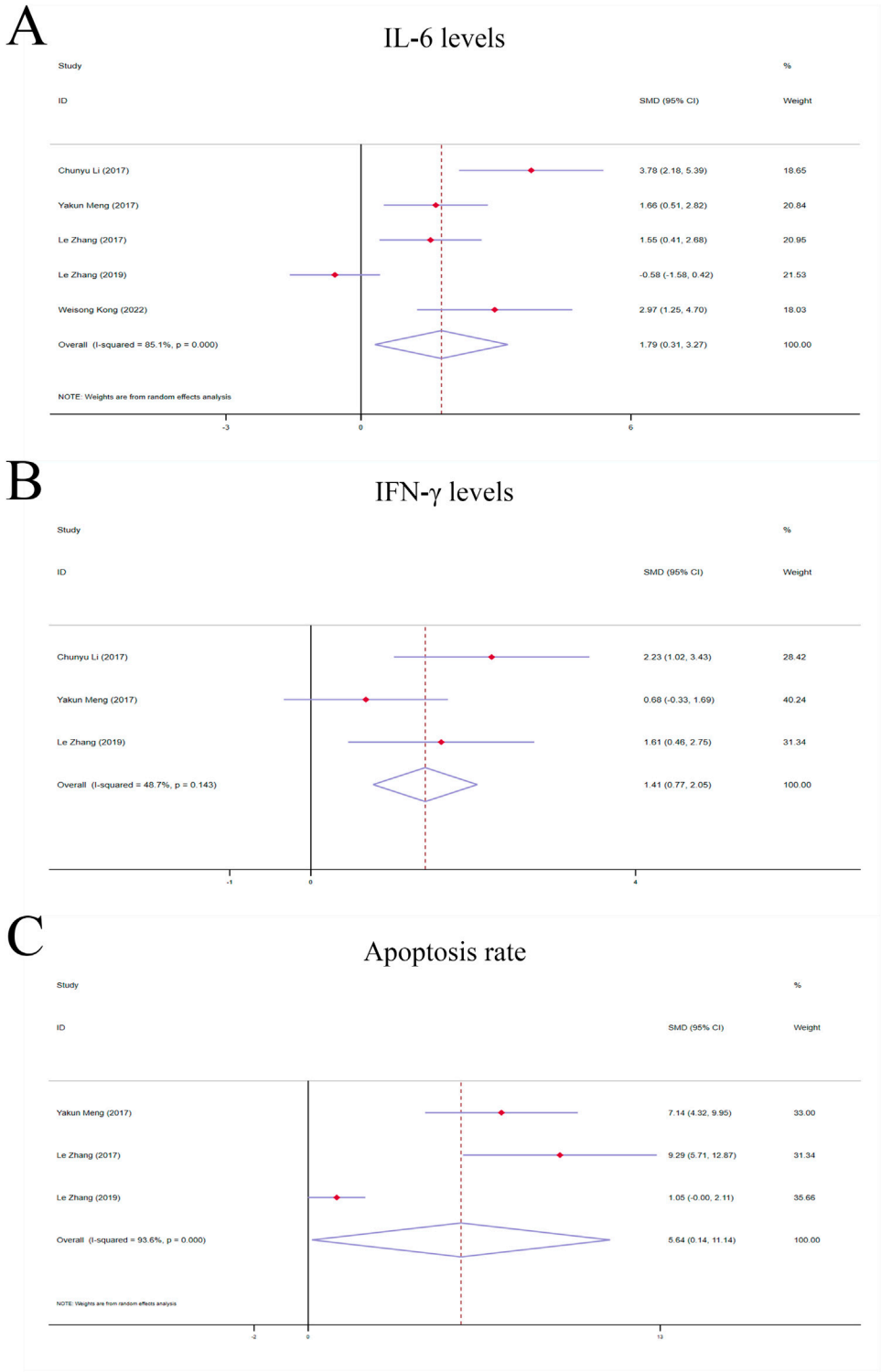

FIGURE 5
Forest plot (effect size and 95% CI) of TSG's hepatoprotective roles on IL-6, IFN-γ and apoptosis rate. **(A)** IL-6 levels; **(B)** IFN-γ levels; **(C)** Apoptosis rate. Abbreviations: 95% CI, 95% confidence interval; IL-6, interleukin 6; IFN-γ, interferon gamma.

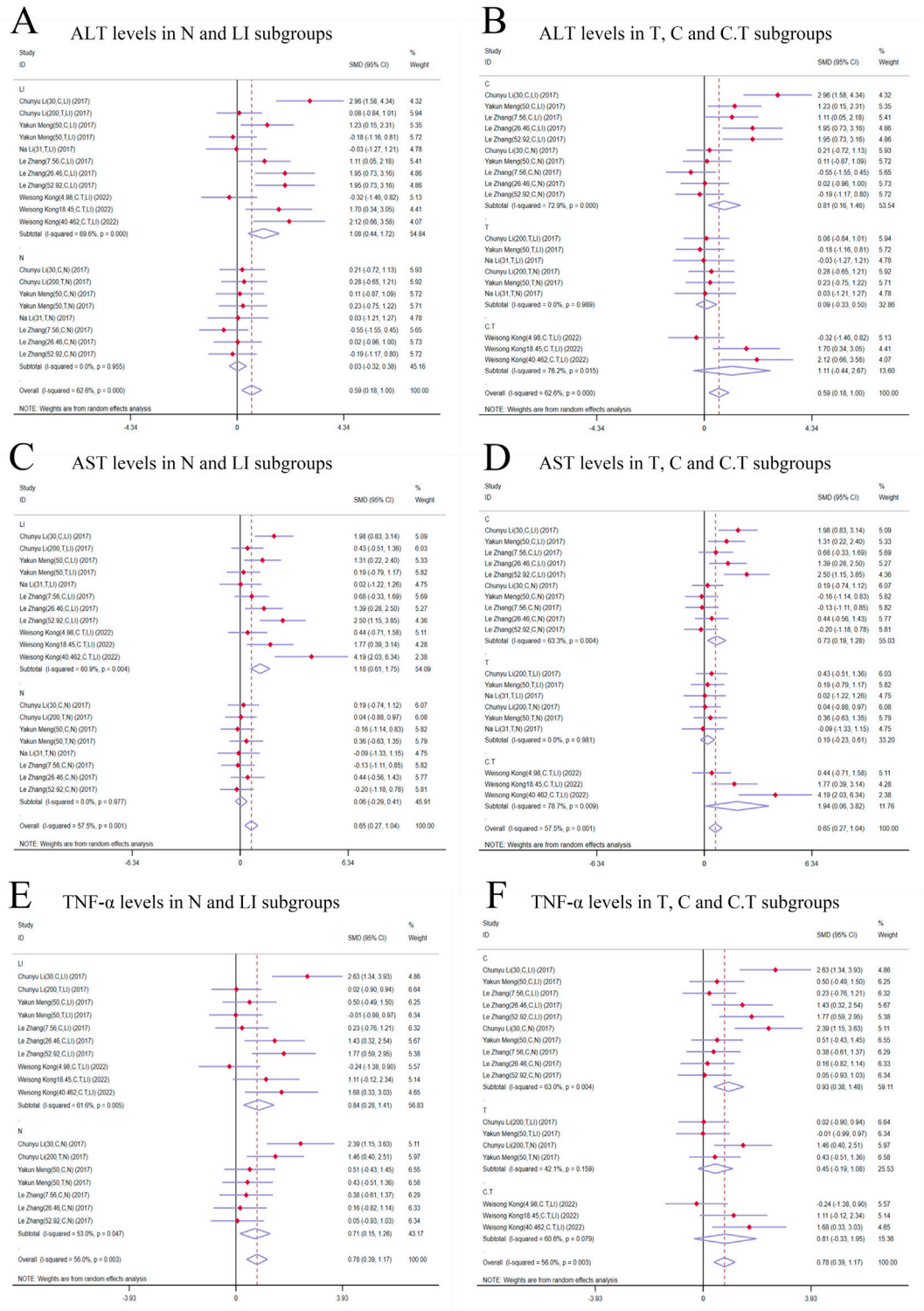

FIGURE 6
Forest plot (effect size and 95% CI) of cis/trans-SG's hepatotoxic roles on ALT, AST and TNF-α. **(A)** ALT levels in N and LI subgroups; **(B)** ALT levels in T, C and C.T subgroups; **(C)** AST levels in N and LI subgroups; **(D)** AST levels in T, C and C.T subgroups; **(E)** TNF-α levels in N and LI subgroups; **(F)** TNF-α levels in T, C and C.T subgroups. Abbreviations: 95% CI, 95% confidence interval; ALT, alanine aminotransferase; AST, aspartate aminotransferase; TNF-α, tumor necrosis factor alpha; N, normal; LI, liver injury; T subgroup, trans-SG subgourp; C subgroup, cis-SG subgroup; C.T subgroup, cis-SG and trans-SG subgroup.

2.7 The dose-time-effect relationship and machine learning

In this study, the time unit for all included experiments was standardized to weeks (W). The dose-time-effect/toxicity relationship of TSG on the liver was visualized using 3D maps and radar charts. Four datasets with 81 diverse samples was collected to analyze the impact of intervention dosage on ALT and AST levels, a measure of TSG's dual effects. The data underwent standardization using z-scores for consistency, enhancing model training efficiency and interpretability. A gradient boosting regression model was employed for precise prediction, with the data split into 8: 2 training and test sets. The Radial Basis Function (RBF) kernel captured nonlinear relationships, and mean squared error (MSE) served as the metric for model evaluation, guiding dosage optimization to maximize ALT and AST level intervention. The LOWESS method was utilized for visualizing the relationship between dosage and variable effects, with confidence intervals plotted for clarity. Model performance was gauged by MSE, with lower values indicating better fit. Python (3.12.3) and Stata (16.0) were the analytical tools of choice. This study demonstrates a systematic approach to optimizing dosage through data-driven modeling and analysis.

2.8 Network pharmacology-based analysis

2.8.1 Acquisition of TSG-related targets

Utilizing the SuperPred (https://prediction.charite.de/) and the BATMAN database (http://bionet.ncpsb.org.cn/batman-tcm/#/home), we conducted a comprehensive search to identify all potential targets of TSG. Subsequently, we refined the list of targets by aligning them with the UniProt database (https://www.uniprot.org/) to standardize the gene nomenclature. This process involved the exclusion of human-specific genes and the elimination of any invalid or redundant targets, ensuring a curated and standardized set of gene names.

2.8.2 Acquisition of LI-related targets

To identify LI-related targets, we conducted searches in the GeneCards (https://www.genecards.org/) and OMIM (https://www.omim.org/) databases using the keyword "liver injury." The resulting disease-associated targets were then compiled into a single Excel spreadsheet. We eliminated any duplicate genes and cross-referenced the list with the Uniprot database to refine and validate the gene information for the disease targets.

2.8.3 Assembly of a shared PPI network for TSG and LI targets

A Venn diagram approach was employed to pinpoint the overlapping targets between TSG and LI. Subsequently, these shared targets were examined using the STRING database to gather data on protein-protein interactions (PPIs), with an emphasis on human proteins. The PPI network for the common targets was then graphically represented using Cytoscape 3.8.2, where the size and color of the nodes were adjusted to reflect their connectivity within the network.

2.8.4 Go analysis and KEGG pathway enrichment analysis

The overlapping genes identified for TSG and LI were submitted to the DAVID database (https://david.ncifcrf.gov/summary.jsp) for comprehensive functional annotation. This resource is adept at evaluating the biological process (BP), cellular component (CC), and molecular function (MF) associated with the genes. The GO analysis elucidates the roles, pathways, and cellular contexts in which these genes are enriched. Additionally, the KEGG database (https://www.genome.jp/kegg/) serves as a repository for the systematic analysis of gene functions. The synthesis of GO and KEGG enrichment analyses facilitates a deeper understanding of the genes' functional profiles and the potential pathways that link drugs to diseases. The visualization of the data was achieved by selecting the top 10 GO categories and the top 20 KEGG pathways based on the lowest P-values, which were then depicted using bar and bubble charts for a clear presentation.

2.9 Molecular docking

Two distinct databases served as repositories for the chemical compounds and molecular ligands: the PubChem database (https://pubchem.ncbi.nlm.nih.gov) and the RCSB Protein Data Bank (https://www.rcsb.org/structure). For the molecular docking procedures, AutoDockTools version 1.5.6 and AutoDock Vina version 4.2 were the chosen software tools. The detailed docking workflow is as follows.

1. The molecular framework of TSG was retrieved from the PubChem database and subsequently transformed into a three-dimensional configuration using ChemDraw, which also optimized the molecular energy. This 3D model was processed through AutoDockTools 1.5.6, and the output was stored in pdbqt format.
2. The ligands were sourced from the RCSB protein repository. After importing them into PyMOL, they underwent dehydration and hydrogenation processes, preparing them for subsequent separation into individual ligands. AutoDockTools 1.5.6 was then utilized to create a docking grid box centered on the active site of the target proteins, with the configuration saved in pdbqt format.
3. AutoDock Vina, specifically version 1.1.2, was deployed for docking the potential targets with the active compounds and for assessing the free binding energies.
4. For the visualization and analysis of molecular interactions, PyMOL version 2.6 and Discovery Studio 2019 were the software applications utilized.

3 Result

3.1 Comprehensive literature selection and study quality

A total of 1,184 articles were initially identified using specific keywords, comprising 404 articles from English databases and 790 articles from Chinese databases. After eliminating

745 duplicate articles, the researchers proceeded with evaluating the remaining 439 articles. Following a thorough review of titles and abstracts based on inclusion and exclusion criteria, 101 articles were excluded. Subsequently, 34 articles, including those related to TSG reviews, conference reports, abstracts, editorials, and web pharmacology, were further eliminated. Finally, after full-text reviews, 43 articles were excluded, resulting in a meta-analysis comprising 24 publications (Bo, 2016; Gao et al., 2020; Kong et al., 2022; Song et al., 2018; Li C. et al., 2017; Lin et al., 2015b; Long et al., 2019; Meng, 2021; Meng et al., 2017; Li N. et al., 2017; Shen et al., 2020; Wang et al., 2022; Xi, 2017; Xi, 2018; Hu et al., 2011; Xu et al., 2019; Xu et al., 2017; Xueqi, 2020; Gao, 2021; Yu W. et al., 2020; Zhang, 2017; Zhang et al., 2019; Xiong et al., 2012; Zhenzhen et al., 2014) (Figure 1).

To evaluate the quality of the research methodology, a revised CAMARADES checklist was applied, consisting of 10 distinct criteria. The inclusion criteria included publication in peer-reviewed journals, maintenance of appropriate temperature conditions, the use of relevant rodent models that matched the research goals, random assignment of subjects in the experiments, unbiased evaluation of outcomes, clear documentation of anesthesia protocols without significant inherent neuroprotective properties, calculation of sample sizes, compliance with ethical guidelines for animal research, and the revelation of any potential conflicts of interest.

Out of the 24 reviewed papers, each employed suitable rodent models with well-defined experimental groupings, along with thorough reporting on sample sizes and the declaration of potential conflicts of interest. However, only seven papers specifically addressed the use of anesthesia without neuroprotective effects, eleven papers omitted references to animal welfare guidelines, and none reported on blinded outcome assessments. The quality scores varied from 6 to 9, with six papers receiving a score of 6 (25.00%), another six scoring 7 (25.00%), eight papers scoring 8 (33.33%), and four papers achieving a score of 9 (16.67%). A graphical representation of the methodological quality for each study is depicted in Figure 2.

3.2 Basic information and features of the articles included

Sufficient information was available in the 24 papers to conduct a meta-analysis. These trials involved a total of 564 rodents, with 324 assigned to the treatment group and the remaining rodents serving as the control group (Table 1).

The animals' weights in the studies ranged from 18 g to 250 g, categorized into five groups based on species distribution: Kunming mice (2.84%, 16/564), ICR mice (9.22%, 52/564), C57BL/6 mice (25.53%, 144/564), Balb/c mice (5.32%, 30/564), and Sprague Dawley Rats (57.09%, 322/564). Rats constituted 57.09% (322/564) of the total rodents, with mice comprising 42.91% (242/564).

Furthermore, all experiments on hepatoprotection were divided into rats (27.27%, 48/176) and mice (72.73%, 128/176) subgroups, with non-biomacromolecule-induced (NBI) (43.81%, 76/176) and biomacromolecule-induced (BI) (56.82%, 100/176) subgroups. Hepatotoxicity studies were categorized into rats (58.97%, 138/234) and mice (41.03%, 96/234) subgroups, as well as normal (N) (56.41%, 132/234) and liver injury (LI) (43.59%, 102/234) subgroups.

The daily TSG dosage ranged from 4.98 mg/kg to 1,345 mg/kg, administered for up to 90 days. For the two TSG isomers, 38 experiments involving 288 rodents examined the hepatotoxic effects of cis and trans isomers. Among the 288 mice, subgroups were based on animal modeling methods and TSG isomers: normal (N) (43.75%, 126/288) and liver injury (LI) (56.25%, 162/288); cis-SG (C) (56.94%, 164/288), trans-SG (T) (30.56%, 88/288), as well as cis-SG and trans-SG (C.T) (12.50%, 36/288) subgroups.

3.3 Protective effects of TSG on LI

The impact of TSG therapy on LI was evaluated by measuring the levels of ALT, AST, TNF-α, and IL-6, which were the primary outcomes. Additionally, the levels of GSH, MDA, SOD, serum TG and serum TC were also affected by TSG treatment (Supplementary Tables 2, 3). Histological analysis of 10 included articles of liver tissues from LI animals showed significant signs of inflammation, hepatocyte swelling, and hepatocellular necrosis (Bo, 2016; Gao et al., 2020; Lin et al., 2015b; Long et al., 2019; Xi, 2017; Xi, 2018; Xu et al., 2019; Gao, 2021; Yu W. et al., 2020; Xiong et al., 2012). Further analysis of this study to find out the optimal protective dosage range was 27.27–38.81 mg/kg/d.

3.3.1 TSG improves the primary outcomes of LI

3.3.1.1 ALT levels

Given the low degree of variability (I^2 < 50%), a fixed-effects model was applied for the analysis. The findings indicated a substantial decrease in ALT levels for the TSG-intervention groups when contrasted with the LI model groups [n = 162, *95% CI* (-3.81,-2.80), *SMD* = |-3.30|, I^2 = 33.5%, *P-value* <0.0001] (Figures 3A, B; Supplementary Table 2).

3.3.1.2 AST levels

Due to considerable variability among the studies (I^2 > 50%), a random-effects model was implemented for the analysis. The findings demonstrated a noteworthy divergence in the levels of AST between the TSG and LI model groups, favoring the TSG groups with lower AST levels [n = 162, *95% CI* (-5.07,-2.53), *SMD* = |-3.80|, I^2 = 80.6%, *P-value* <0.0001] (Figures 3C, D; Supplementary Table 2).

3.3.1.3 TNF-α levels

A considerable degree of heterogeneity (I^2 > 50%) was observed, prompting the use of a random-effects model for the analysis. The data analysis revealed that the TSG group exhibited significantly lower TNF-α levels compared to the LI model groups [n = 68, *95% CI* (-3.64, −1.62), *SMD* = |-2.63|, I^2 = 52.3%, *P-value* <0.0001] (Figure 3E; Supplementary Table 2).

3.3.1.4 IL-6 levels

Random-effects analyses showed variations in IL-6 levels among the rodent models in the study. The IL-6 levels in the TSG groups were notably lower than those in the control groups [n = 68, *95% CI* (-5.23,-1.65), *SMD* = |-3.44|, I^2 = 80.7%, *P-value* <0.0001] (Figure 3F; Supplementary Table 2).

3.3.2 TSG effects on secondary outcomes of LI

3.3.2.1 GSH levels

The random-effects model analysis indicated pronounced disparities in the levels of GSH between the TSG and LI model groups. It was found that the TSG groups had considerably elevated GSH levels in contrast to the LI model groups [n = 75, *95% CI* (1.97,5.26), *SMD* = |3.61|, I^2 = 75.1%, *P-value* <0.0001], as depicted in Supplementary Figure 1A; Supplementary Table 2.

3.3.2.2 MDA levels

The random-effects model analysis exposed significant variations in the levels of MDA between the TSG and LI model groups. The TSG groups displayed substantially reduced MDA levels relative to the LI model groups [n = 82, *95% CI* (-3.89,-1.44), *SMD* = |-2.66|, I^2 = 66.7%, *P-value* <0.0001], as illustrated in Supplementary Figure 1B; Supplementary Table 2.

3.3.2.3 SOD levels

Given the considerable heterogeneity (I^2 > 50%), a random-effects model was utilized for a more in-depth analysis. The results demonstrated a marked difference in SOD levels between the TSG and LI model groups, with the TSG groups showing an increase in SOD activity [n = 112, *95% CI* (1.64,4.09), *SMD* = |2.87|, I^2 = 74.6%, *P-value* <0.0001], which is detailed in Supplementary Figure 1C; Supplementary Table 2.

3.3.2.4 Serum TG levels

Based on the random-effects analysis, there were observed differences in serum TG levels among the animal models in the study. The TSG groups exhibited lower serum TG levels in comparison to the LI groups [n = 54, *95% CI* (-7.15,-1.13), *SMD* = |-4.14|, I^2 = 86.6%, *P-value* = 0.007], as represented in Supplementary Figure 1D; Supplementary Table 2.

3.3.2.5 Serum TC levels

The random-effects model analysis indicated significant variations in serum TC levels between the TSG and LI model groups. The TSG groups had significantly decreased serum TC levels compared to the LI model groups [n = 54, *95% CI* (-9.19,-1.61), *SMD* = |-5.40|, I^2 = 87.0%, *P-value* = 0.005], as depicted in Supplementary Figure 1E; Supplementary Table 2.

3.3.3 Subgroup analysis of hepatoprotection studies

3.3.3.1 Analysis of ALT levels in distinct subgroups

When analyzing the liver enzyme levels, it was found that the TSG groups had markedly lower levels of ALT compared to the LI model groups. The most notable decrease in ALT levels was observed in the BI subgroups [n = 86, 95% *CI* (-4.18, −2.75), *SMD* = |-3.46|, I^2 = 46.9%, *P-value* <0.0001], surpassing the reduction observed in the NBI subgroup [n = 76, 95% *CI* (-3.85,-2.44), *SMD* = |-3.14|, I^2 = 27.0%, *P-value* <0.0001] (Figure 3A; Supplementary Table 3). The TSG intervention proved to be effective in both mice [n = 128, 95% *CI* (-3.71,-2.63), *SMD* = |-3.17|, I^2 = 14.1%, *P-value* <0.0001] and rats [n = 34, 95% *CI* (-5.42,-2.76), *SMD* = |-4.09|, I^2 = 56.8%, *P-value* <0.0001] subgroups, with a more pronounced reduction in the latter (Figure 3B; Supplementary Table 3). The variability in results was primarily attributed to the rats and BI subgroups. The TSG intervention consistently reduced ALT levels across all analyzed subgroups, without any significant differences in its effectiveness.

3.3.3.2 Analysis of AST levels in distinct subgroups

In the evaluation of AST levels, the TSG groups also demonstrated a significant reduction compared to the LI model groups. The TSG intervention was particularly effective in reducing AST levels in mice [n = 128, 95% *CI* (-4.93,-2.18), *SMD* = |-3.55|, I^2 = 82.3%, *P-value* <0.0001] and rats [n = 34, 95% *CI* (-11.05,-0.89), *SMD* = |-5.97|, I^2 = 84.0%, *P-value* = 0.021] subgroups (Figure 3C; Supplementary Table 3). The BI subgroup [n = 86, 95% *CI* (-4.25,-2.22), *SMD* = |-3.25|, I^2 = 52.2%, *P-value* <0.0001] and the NBI subgroup [n = 76, 95% *CI* (-8.27,-1.49), I^2 = 90.9%, *SMD* = |-4.88|, *P-value* = 0.005] both responded positively to TSG, with the NBI and rats subgroups showing a more significant reduction in AST levels (Figure 3D; Supplementary Table 3). TSG demonstrated greater efficacy in lowering AST levels within the NBI and rat subgroups. Heterogeneity was more pronounced in the mice, rat, and NBI subgroups, contrasting with the comparatively lower heterogeneity observed in the BI subgroups.

3.4 Hepatotoxic effects of TSG

The hepatotoxic potential of TSG was assessed by examining four critical biomarkers in a comprehensive review of 14 research studies: ALT, AST, TNF-α, and IL-6. In contrast to the N groups, where no substantial changes were noted, a marked elevation in these biomarkers was observed in the LI groups. The findings suggest that TSG may intensify liver damage, particularly influencing the levels of ALT and AST in the LI groups. The histological examination of 9 included articles showed significant hepatotoxic effects in liver tissue, including inflammatory cell infiltration, cell edema, and vacuolar cytoplasmic degeneration (Kong et al., 2022; Li C. et al., 2017; Meng, 2021; Meng et al., 2017; Wang et al., 2022; Xu et al., 2017; Xueqi, 2020; Zhang, 2017; Zhang et al., 2019). Further analysis of this study to find out the optimal toxic dosage range was 51.93–76.07 mg/kg/d (Supplementary Tables 4, 5).

3.4.1 Primary indicators of TSG's hepatotoxic effects

3.4.1.1 ALT levels

Given the significant variability across studies (I^2 > 50%), a random-effects model was applied for the statistical analysis. The findings indicated that the treatment of TSG resulted in a significant increase in ALT levels when compared with the control groups [n = 222, *95% CI* (0.06,1.69), *SMD* = |0.88|, I^2 = 85.3%, *P-value* = 0.034] (Figures 4A, B).

3.4.1.2 AST levels

The random-effects model analysis highlighted a significant difference in AST levels between the groups treated with TSG and those in the control groups. The data suggested that TSG was linked to an increase in AST levels [n = 210, 95% *CI* (0.23,1.82), *SMD* = |1.03|, I^2 = 83.5%, *P-value* = 0.011] (Figures 4C, D).

3.4.1.3 TNF-α levels

The presence of considerable heterogeneity (I^2 > 50%) in the study data led to the application of a random-effects model. The analysis demonstrated that TSG-treated groups exhibited increased TNF-α levels compared to the control groups [n = 90, *95% CI* (0.36,2.11), *SMD* = |1.24|, I^2 = 70.0%, *P-value* = 0.006] (Figures 4E, F).

3.4.1.4 IL-6 levels

The random-effects model analyses revealed a notable variation in IL-6 levels among the rodent models under investigation. The IL-6 levels in the TSG groups were found to be markedly higher compared to the control groups [n = 78, *95% CI* (0.31,3.27), *SMD* = |1.79|, I^2 = 85.1%, *P-value* = 0.018] (Figure 5A).

3.4.2 Secondary indicators of TSG's hepatotoxic effects

3.4.2.1 IFN-γ levels

A fixed-effects model analysis revealed significant variations in IFN-γ levels between the TSG groups and the control groups. The TSG groups demonstrated notably elevated the levels of IFN-γ relative to the control groups [n = 50, *95% CI* (0.77,2.05), *SMD* = |1.41|, I^2 = 48.7%, *P-value* <0.0001] (Figure 5B).

3.4.2.2 Apoptosis rate

Due to the substantial heterogeneity observed (I^2 > 50%), a random-effects model was utilized for the analysis. The findings showed that the TSG groups experienced a significantly increased rate of apoptotic cell death when compared to the control groups [n = 48, *95% CI* (0.14,11.14), *SMD* = |5.64|, I^2 = 93.6%, *P-value* = 0.044] (Figure 5C).

3.4.3 Subgroup analysis of studies on hepatotoxicity

3.4.3.1 Subgroup analysis of ALT levels

The subgroup analysis showed that TSG notably increased ALT levels in the LI subgroups [n = 102, *95% CI* (0.67,2.65), *SMD* = |1.66|, I^2 = 76.8%, *P-value* = 0.001], whereas no significant changes were detected in the N subgroups [n = 120, *95% CI* (-1.00,1.38), *SMD* = |0.19|, I^2 = 87.7%, *P-value* = 0.755] (Figure 4A). Toxic effects of TSG were observed in both mice [n = 84, 95% CI (-0.08, 1.34), SMD = |0.63|, I^2 = 57.8%, *P-value* = 0.083] and rats [n = 138, 95% CI (-0.34, 2.36), SMD = |1.01|, I^2 = 90.1%, *P-value* = 0.144] subgroups, with a more pronounced increase in ALT levels in the rats subgroups compared to the mice subgroups (Figure 4B). Rats models and N models were identified as the main sources of increased heterogeneity in the subgroup analysis.

3.4.3.2 Subgroup analysis of AST levels

In the subgroup analysis based on modeling methods, AST levels were found to be elevated in the LI subgroups in response to TSG [n = 102, *95% CI* (0.92,3.26), *SMD* = |2.09|, I^2 = 80.8%, *P-value* < 0.001], whereas no significant differences were observed between the N subgroups and the control groups [n = 108, *95% CI* (-0.89,1.05), *SMD* = |0.08|, I^2 = 81.3%, *P-value* = 0.867] (Figure 4C). Both the N and LI subgroups contributed to the increased heterogeneity. Additionally, a trend of increasing AST levels was observed in the mice subgroups [n = 72, *95% CI* (0.16,2.34), *SMD* = |1.25|, I^2 = 74.6%, *P-value* = 0.025], whereas the rats subgroups did not exhibit statistically significant changes [n = 138, *95% CI* (-0.27,2.00), *SMD* = |0.87|, I^2 = 87.2%, *P-value* = 0.142] (Figure 4D).

3.4.3.3 Subgroup analysis of TNF-α levels

The subgroup analysis based on modeling methods indicated a significant increase in TNF-α levels in the LI subgroups due to TSG [n = 62, *95% CI* (0.67,2.50), *SMD* = |1.59|, I^2 = 57.2%, *P-value* = 0.001], while no significant differences were noted in the N subgroups when compared to the control groups [n = 28, *95% CI* (-1.20,2.29), *SMD* = |0.55|, I^2 = 78.1%, *P-value* = 0.541] (Figure 4E). An increase in TNF-α levels was observed in both mice [n = 24, *95% CI* (0.65,2.52), *SMD* = |1.58|, I^2 = 0.0%, *P-value* = 0.001] and rats [n = 66, *95% CI* (-0.14,2.34), *SMD* = |1.10|, I^2 = 80.2%, *P-value* = 0.082] (Figure 4F). Rats models and N models were identified as the primary sources of increased heterogeneity in the subgroup analysis.

3.5 Analysis of the hepatotoxic effects of cis-SG and trans-SG

Cis-SG and trans-SG were two isomers of TSG. This study encompassed 38 experiments involving 288 rodents to explore the hepatotoxic effects of these two isomers. ALT, AST, TNF-α, and IL-6 levels were evaluated as primary indicators to assess the toxic effects of cis-SG and trans-SG. The levels of these indicators were elevated in the LI subgroups, C subgroups, and C.T subgroups, while there was no significant difference between T subgroups and N subgroup (Supplementary Tables 6, 7).

3.5.1 The primary indicators of the hepatotoxic effects of cis-SG and trans-SG

3.5.1.1 ALT levels

In terms of modeling methods subgroups, ALT levels significantly increased in the LI subgroups [n = 162, *95% CI* (0.44,1.72), *SMD* = |1.08|, I^2 = 69.6%, *P-value* = 0.001], while there was no difference in the N subgroups [n = 126, *95% CI* (-0.32,0.38), *SMD* = |0.03|, I^2 = 0.0%, *P-value* = 0.875] (Figure 6A). Both C and C.T subgroups showed toxic effects of TSG [C subgroups: n = 164, 95% *CI* (0.16,1.46), *SMD* = |0.81|, I^2 = 72.9%, *P-value* = 0.015; C.T subgroups: n = 36, 95% *CI* (-0.44,2.67), *SMD* = |1.11|, I^2 = 76.2%, *P-value* = 0.161], but no difference was observed in the T subgroups between trans-SG therapy groups and control groups [n = 88, 95% *CI* (-0.33,0.50), *SMD* = |0.09|, I^2 = 0.0%, *P-value* = 0.689] (Figure 6B). The heterogeneity predominantly originated from the LI subgroups, C subgroups and C.T subgroups.

3.5.1.2 AST levels

AST levels exhibited a higher trend in the TSG groups in comparison with the control groups. A meticulous subgroup analysis exposed a significant surge in AST levels within the LI [n = 162, 95% *CI* (0.61,1.75), *SMD* = |1.18|, I^2 = 60.9%, *P-value* < 0.0001], C [n = 164, 95% *CI* (0.19,1.28), *SMD* = |0.73|, I^2 = 63.3%, *P-value* = 0.009], and C.T [n = 36, 95% *CI* (0.06,3.82), *SMD* = |1.94|, I^2 = 78.7%, *P-value* = 0.043] subgroups. Conversely, no substantial distinction was unearthed in the remaining groups when the intervention groups were appraised against the control groups [N subgroups: n = 126, 95% *CI* (-0.29,0.41),

SMD = |0.06|, I^2 = 0.0%, *P-value* = 0.721; T subgroups: n = 88, 95% *CI* (-0.23,0.61), *SMD* = |0.19|, I^2 = 0.0%, *P-value* = 0.382] (Figures 6C, D). The LI, C, and C.T subgroups were identified as the primary sources of increased heterogeneity in the subgroup analysis.

3.5.1.3 TNF-α levels

In contrast to the control groups, TNF-α levels were increased by TSG in intervention groups. This increase was noted across both the LI [n = 152, 95% *CI* (0.28,1.41), *SMD* = |0.84|, I^2 = 61.6%, *P-value* = 0.003] and the N [n = 120, 95% *CI* (0.15,1.26), *SMD* = |0.71|, I^2 = 53.0%, *P-value* = 0.013] subgroups as illustrated in Figure 6D. A detailed examination of the isomer-based subgroups indicated a rise in TNF-α levels across all categories [C subgroups: n = 166, 95% *CI* (0.38,1.48), *SMD* = |0.93|, I^2 = 63.0%, *P-value* = 0.001; T subgroups: n = 70, 95% *CI* (-0.19,1.08), *SMD* = |0.45|, I^2 = 42.1%, *P-value* = 0.170; C.T subgroups: n = 36, 95% *CI* (-0.33,1.95), *SMD* = |0.81|, I^2 = 60.6%, *P-value* = 0.164], while T subgroups and C.T subgroups did not exhibit statistical significance (Figure 6E).

3.5.1.4 IL-6 levels

Subgroup analysis based on modeling methods and isomers revealed a significant increase in IL-6 levels in LI [n = 152, 95% *CI* (0.41,2.41), *SMD* = |1.27|, I^2 = 80.9%, *P-value* = 0.004], C [n = 164, 95% *CI* (0.23,1.41), *SMD* = |0.82|, I^2 = 67.5%, *P-value* = 0.006], and C.T [n = 36, 95% *CI* (1.20,2.91), *SMD* = |2.05|, I^2 = 1.1%, *P-value* < 0.0001] subgroups. IL-6 levels in N [n = 116, 95% *CI* (-0.03,0.72), *SMD* = |0.34|, I^2 = 0.0%, *P-value* = 0.069] and T [n = 68, 95% *CI* (-0.88,1.02), *SMD* = |0.07|, I^2 = 72.6%, *P-value* = 0.886] subgroups showed no significant difference compared to control groups (Figures 7A, B). Conversely, the N [n = 116, 95% *CI* (-0.03,0.72), *SMD* = |0.34|, I^2 = 0.0%, *P-value* = 0.069] and T [n = 68, 95% *CI* (-0.88,1.02), *SMD* = |0.07|, I^2 = 72.6%, *P-value* = 0.886] subgroups demonstrated no significant deviation in IL-6 levels when compared to their respective control groups (Figures 7A, B).

3.5.2 Secondary indicators of the hepatotoxic effects of cis-SG and trans-SG

3.5.2.1 IL-1β levels

In the subgroup analysis based on modeling methods, IL-1β levels in the LI subgroups were higher than those in the control groups [n = 68, *95% CI* (0.12,1.54), *SMD* = |0.83|, I^2 = 46.8%, *P-value* = 0.022], while no significant difference was found between N subgroups and control groups [n = 32, *95% CI* (-0.56,0.83), *SMD* = |0.13|, I^2 = 0.0%, *P-value* = 0.711] (Figure 7C). Additionally, IL-1β levels exhibited an increasing trend in the C.T subgroups [n = 36, *95% CI* (0.63,2.12), *SMD* = |1.38|, I^2 = 0.0%, *P-value* <0.0001]. The T [n = 32, *95% CI* (-0.72,0.67), *SMD* = |-0.03|, I^2 = 0.0%, *P-value* = 0.942] and C [n = 32, *95% CI* (-0.36,1.05), *SMD* = |0.34|, I^2 = 0.0%, *P-value* = 0.338] subgroups did not show statistical significance (Figure 7D).

3.5.2.2 Apoptosis rate

Apoptosis rate significantly was increased in the LI [n = 80, *95% CI* (2.39,9.40), *SMD* = |5.89|, I^2 = 93.1%, *P-value* = 0.001] and C [n = 128, *95% CI* (1.57,5.14), *SMD* = |3.35|, I^2 = 91.2%, *P-value* <0.0001] subgroups. In contrast, the N [n = 80, *95% CI* (-0.08,1.62), *SMD* = |0.77|, I^2 = 68.6%, *P-value* = 0.078] and T [n = 32, *95% CI* (-0.09,1.76), *SMD* = |0.84|, I^2 = 36.3%, *P-value* = 0.076] subgroups demonstrated no significant changes in apoptosis rates (Figures 7E, F).

3.6 Sensitivity analysis and publication bias of outcome indicators

The ability of ALT and AST levels to LI in rodent models was found to be comparably effective. In order to assess potential publication bias, we employed the absolute value of the t-statistic and performed Egger's test. The absolute t-values for both of these biomarkers did not suggest the presence of publication bias within the included studies (ALT in hepatoprotection, |t|-value = |-3.49|; AST in hepatoprotection, |t|-value = |-3.67|; ALT in hepatotoxicity, |t|-value = |1.07|; AST in hepatotoxicity, |t|-value = |1.2|) (Supplementary Tables 2, 3).

3.7 Dose–time–effect/toxicity relationship and machine learning

3.7.1 Effective dose and time length of TSG on ALT and AST levels

In the context of LI models, the therapeutic substance (TSG) has been observed to lower ALT and AST levels when administered at dosages between 30 mg/kg/day and 100 mg/kg/day, as determined by three-dimensional (3D) scatter plot analysis. By employing machine learning techniques, the precise effective dosage was refined to a narrower range of 27.27 mg/kg/day to 38.81 mg/kg/day, with an optimal dosage identified at 27.27 mg/kg/day. It is important to note that these beneficial effects are not present if the dosage falls below the threshold of 27.27 mg/kg/day. In terms of treatment duration, 3D mapping and radar chart analysis suggest that TSG's efficacy in reducing ALT and AST levels is observed within a window of 0.43 weeks–1 week. Further research is necessary to ascertain the precise dosage and effectiveness of TSG for treatment periods extending beyond 1 week, as depicted in Figures 8–10.

3.7.1.1 Toxic dose and time length of TSG on ALT and AST levels

In the case of toxic effects, TSG has been found to elevate ALT and AST levels in LI models when given at higher dosages, ranging from 50 mg/kg/day to 200 mg/kg/day, as per 3D scatter plot analysis. Machine learning algorithms have pinpointed a more precise toxic dosage range of 51.93 mg/kg/day to 76.07 mg/kg/day, with a maximum toxic effect at 51.93 mg/kg/day. Interestingly, no toxic effects were detected in normal (N) models even at much higher dosages, from 100 mg/kg/day to 1,345 mg/kg/day. In terms of treatment duration, the 3D mapping and radar chart analysis indicate that TSG's toxicity, as measured by increased ALT and AST levels, is evident within a timeframe of 0.06 weeks–0.43 weeks. The impact of TSG at treatment durations shorter than 0.04 weeks or longer than 12.86 weeks remains unclear and requires further investigation to determine the specific toxic dosage levels of TSG *in vivo*, as illustrated in Figures 8–10.

3.7.1.2 Effective dose and time length of TSG on TNF-α and IL-6 levels

In the context of LI models, the therapeutic substance (TSG) has demonstrated the ability to lower the inflammatory markers

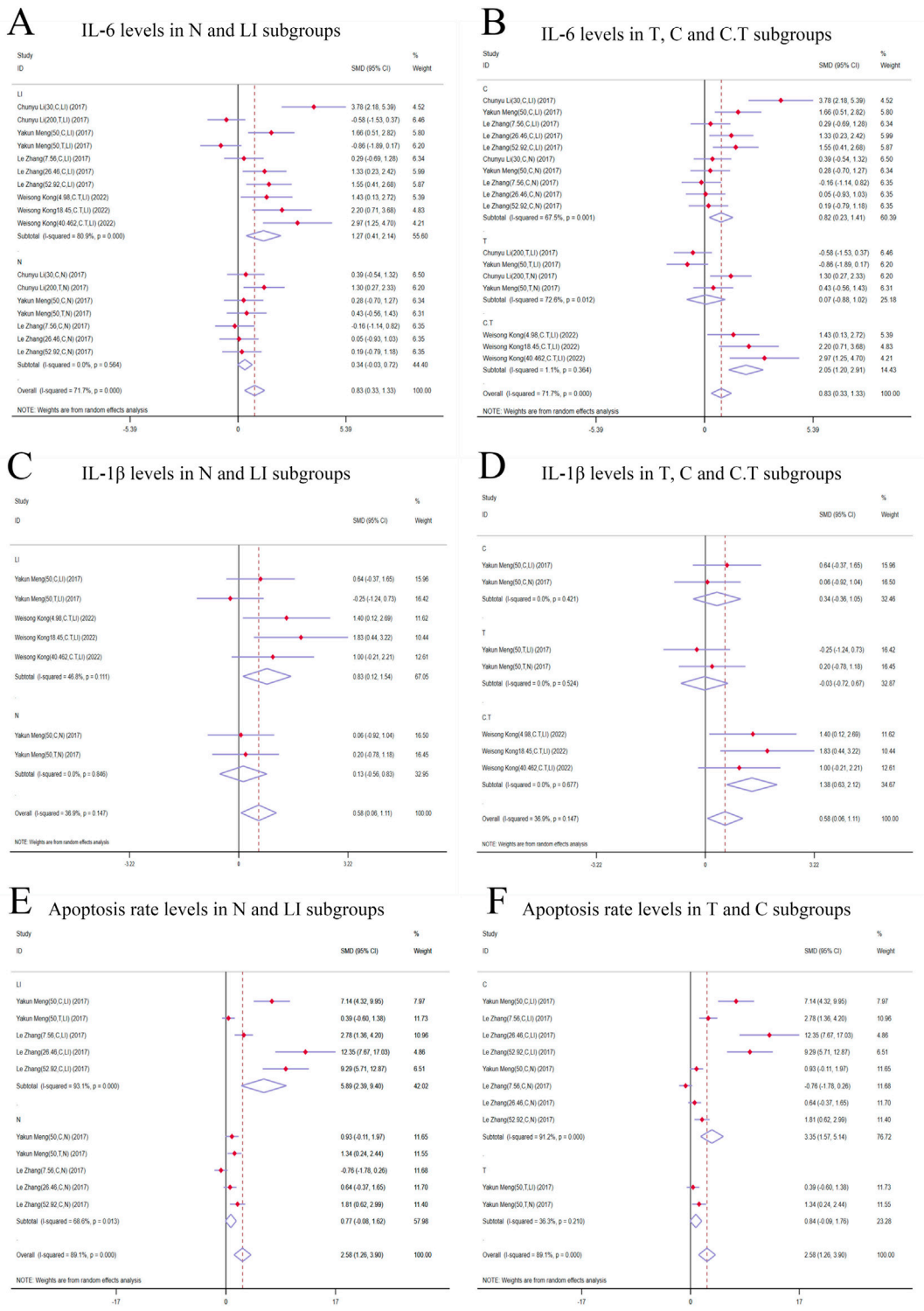

FIGURE 7
Forest plot (effect size and 95% CI) of cis/trans-SG's hepatotoxic roles on IL-6, IL-1β and apoptosis rate. **(A)** IL-6 levels in N and LI subgroups; **(B)** IL-6 levels in T, C and C.T subgroups; **(C)** IL-1β levels in N and LI subgroups; **(D)** IL-1β levels in T, C and C.T subgroups; **(E)** Apoptosis rate levels in N and LI subgroups; **(F)** Apoptosis rate levels in T and C subgroups. Abbreviations: 95% CI, 95% confidence interval; IL-6, interleukin 6; IL-1β, interleukin 1β; N, normal; LI, liver injury; T subgroup, trans-SG subgourp; C subgroup, cis-SG subgroup; C.T subgroup, cis-SG and trans-SG subgroup.

TNF-α and IL-6 when administered at daily doses spanning from 30 mg/kg to 60 mg/kg. This finding is contingent upon maintaining all other experimental parameters at their ideal states, with the exception of TSG's dosage. To pinpoint the precise dosage threshold for TSG's efficacy, further inquiry is warranted. It's important to highlight that the reduction in

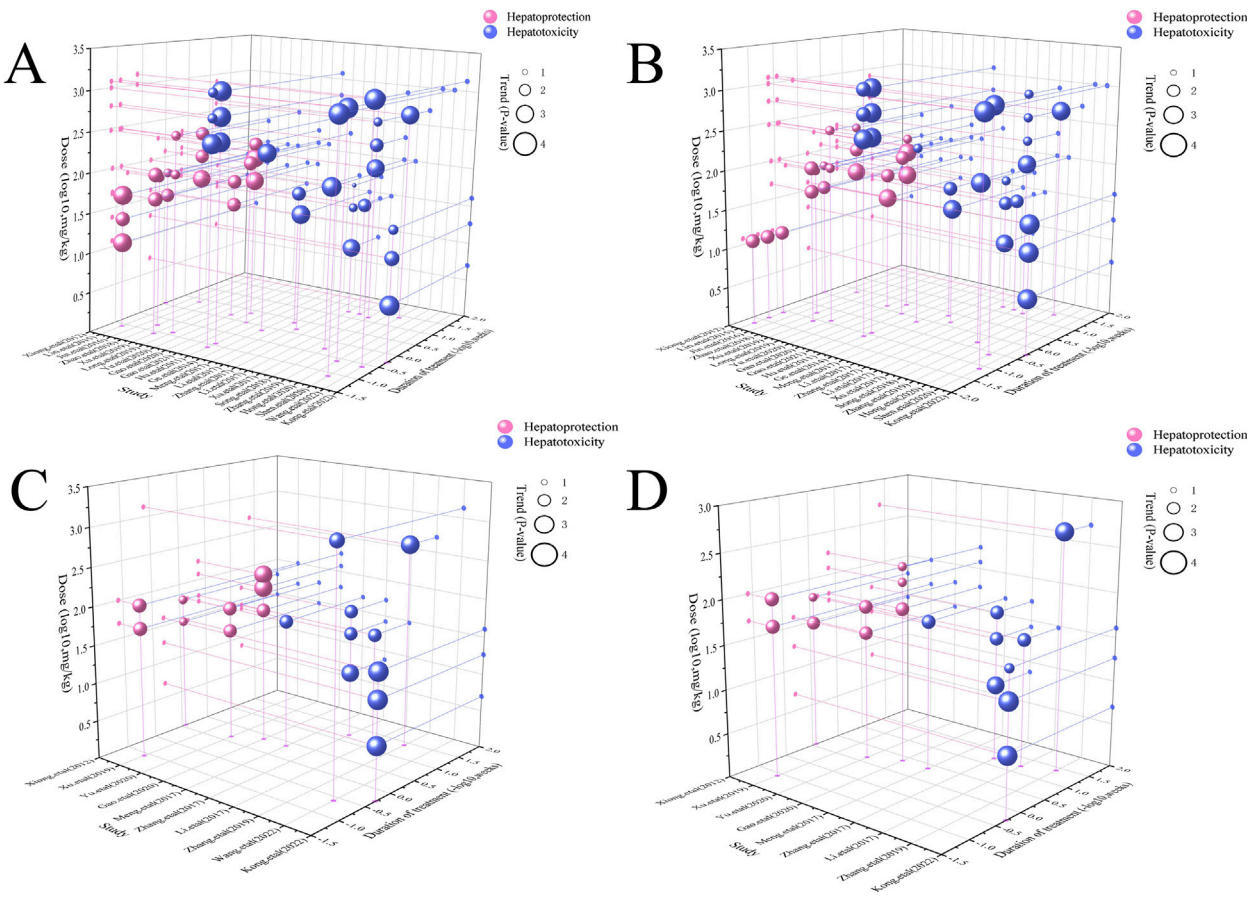

FIGURE 8
3D maps of dose–time–effect relationship. **(A)** ALT levels; **(B)** AST levels; **(C)** TNF-α levels; **(D)** IL-6 levels.

TNF-α and IL-6 levels is not observed at doses below the 30 mg/kg threshold. Regarding the temporal aspect of treatment, three-dimensional graphical representations and radar charts indicate that TSG's efficacy in modulating TNF-α and IL-6 levels is observed within a period of 0.4–0.86 weeks. Further research is necessary to delineate the optimal dosage of TSG and to assess its impact for treatment durations that surpass 0.86 weeks, as indicated in Figures 8–10.

3.7.1.3 Toxic dose and time length of TSG on TNF-α and IL-6 levels

In the realm of LI models, an increase in TNF-α and IL-6 levels is associated with TSG administration at higher doses, specifically at 50 mg/kg/day, 200 mg/kg/day, 400 mg/kg/day, and 800 mg/kg/day. However, in normal (N) models, no adverse effects of TSG were detected within the dosage range of 26.46 mg/kg/day to 52.92 mg/kg/day. When examining the time frame of treatment, three-dimensional mapping and radar charts reveal that TSG notably elevates TNF-α and IL-6 levels within a span of 0.06–0.43 weeks. Further exploration is essential to establish the exact toxic dosage levels of TSG and to understand its *in vivo* administration effects, as depicted in Figures 8–10.

3.8 Network pharmacology of TSG in LI

3.8.1 The common targets and TSG-LI network diagram

A total of 106 TSG targets were identified after the elimination of duplicates, sourced from the SuperPred and BATMAN databases. Concurrently, 9,700 and 101 LI-associated targets were extracted from the GeneCards and OMIM databases. Uniprot database was used to convert gene names into Symbol IDs. The commonality of active targets between the two conditions was graphically represented in a Venn diagram. The Venn diagram showed that there were 94 common targets between TSG and LI, accounting for 1% (Figure 11A). Following this, the active targets from TSG were incorporated into Cytoscape 3.7.2, resulting in the formation of a drug-ingredient-target network diagram, which consisted of 107 nodes and 106 edges. The CHRM2, HDAC2, ADAM10, NFE2L2, FPR1, PRCP, TOP2A, APP, TFPI and NFE2L2 emerged as central targets within this network (Figure 11B).

3.8.2 The PPI network diagram

After intersecting all TSG-related targets with the target genes of LI, 94 intersection target genes associated with LI and TSG were

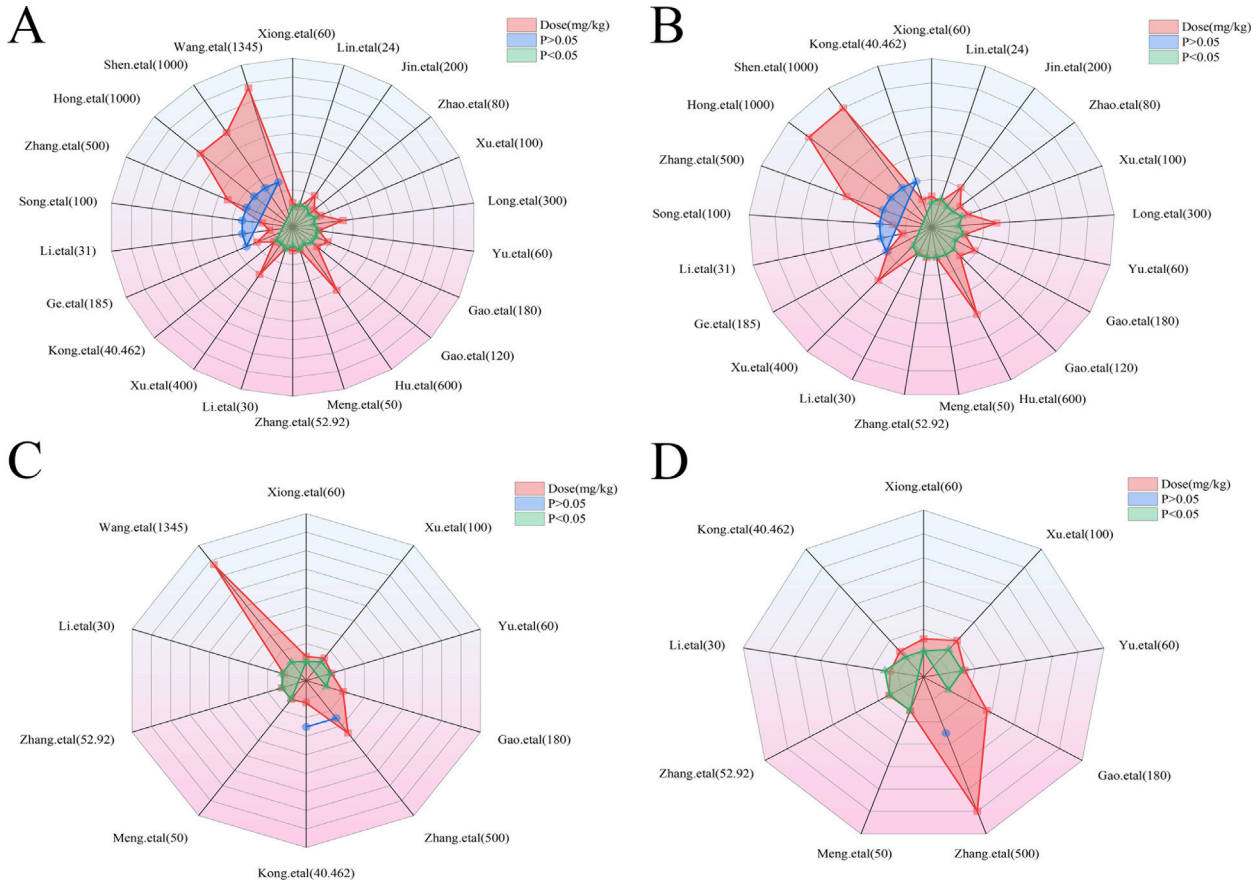

FIGURE 9
Radar charts of dose–time–effect relationship. **(A)** ALT levels; **(B)** AST levels; **(C)** TNF-α levels; **(D)** IL-6 levels.

obtained, representing the interactive target genes between the drug and LI. These 94 intersection target genes were imported into the String (https://string-db.org/) database for protein-protein interaction prediction, with the species set to: *Homo Sapiens* and the confidence level set to: 0.4. The network file was saved in TSV format, and the TSV file was imported into Cytoscape 3.8.2 to draw the protein interaction network, which includes 89 nodes and 460 edges. A topological analysis of the network was conducted, where the degree value was used to indicate the size and color of the targets, as well as the combined score determined the thickness of the edges, thus constructing the protein-protein interaction network as depicted in the illustration. Notably, the nodes with the highest degree of connectivity, ranking in the top 8, included APP, HDAC2, NFKB1, PPARGC1A, CXCR4, GRK5, PKM, and NFE2L2 (Figure 11C).

3.8.3 Go analysis and KEGG pathway enrichment analysis

Employing the DAVID database, we conducted a Gene Ontology (GO) analysis on the intersecting targets, revealing 103 BPs, 44 CCs, and 49 MFs with significant statistical enrichment ($P < 0.05$). The leading five BPs identified were signal transduction, inflammatory response, G-protein coupled receptor signaling pathways, phosphorylation, chemical synaptic transmission, positive regulation of cell proliferation, proteolysis, protein phosphory lation, negative regulation of apoptotic process, and response to hypoxia. In terms of CC, the most prominent were the plasma membrane, cytoplasm, cytosol, nucleus, nucleoplasm, membrane, extracellular exosome, extracellular region, chromatin, and cell surface. For MF, the top categories were protein binding, metal ion binding, identical protein binding, ATP binding, zinc ion binding, protein kinase activity, sequence-specific DNA binding, enzyme binding, receptor binding, and chromatin binding (Figures 11D, E).

For the enrichment of signaling pathways, the DAVID database was again utilized, identifying 40 pathways associated with TSG and LI. With a stringent P-value cutoff of <0.05, 32 pathways were selected as pertinent to the TSG-LI interaction. The top 20 of these pathways were neuroactive ligand-receptor interaction, calcium signaling pathway, central carbon metabolism in cancer, neutrophil extracellular trap formation, cAMP signaling pathway, antifolate resistance, HIF-1 signaling pathway, adipocytokine signaling pathway, regulation of actin cytoskeleton, PI3K-AKT signaling pathway, alcoholism, microRNAs in cancer, chemokine signaling pathway, apelin signaling pathway, alcoholic liver disease, pathways of neurodegeneration-multiple diseases, chemical carcinogenesis-receptor activation, MAPK signaling pathway, thyroid hormone signaling pathway, and sphingolipid signaling pathway (Figures 11F, G).

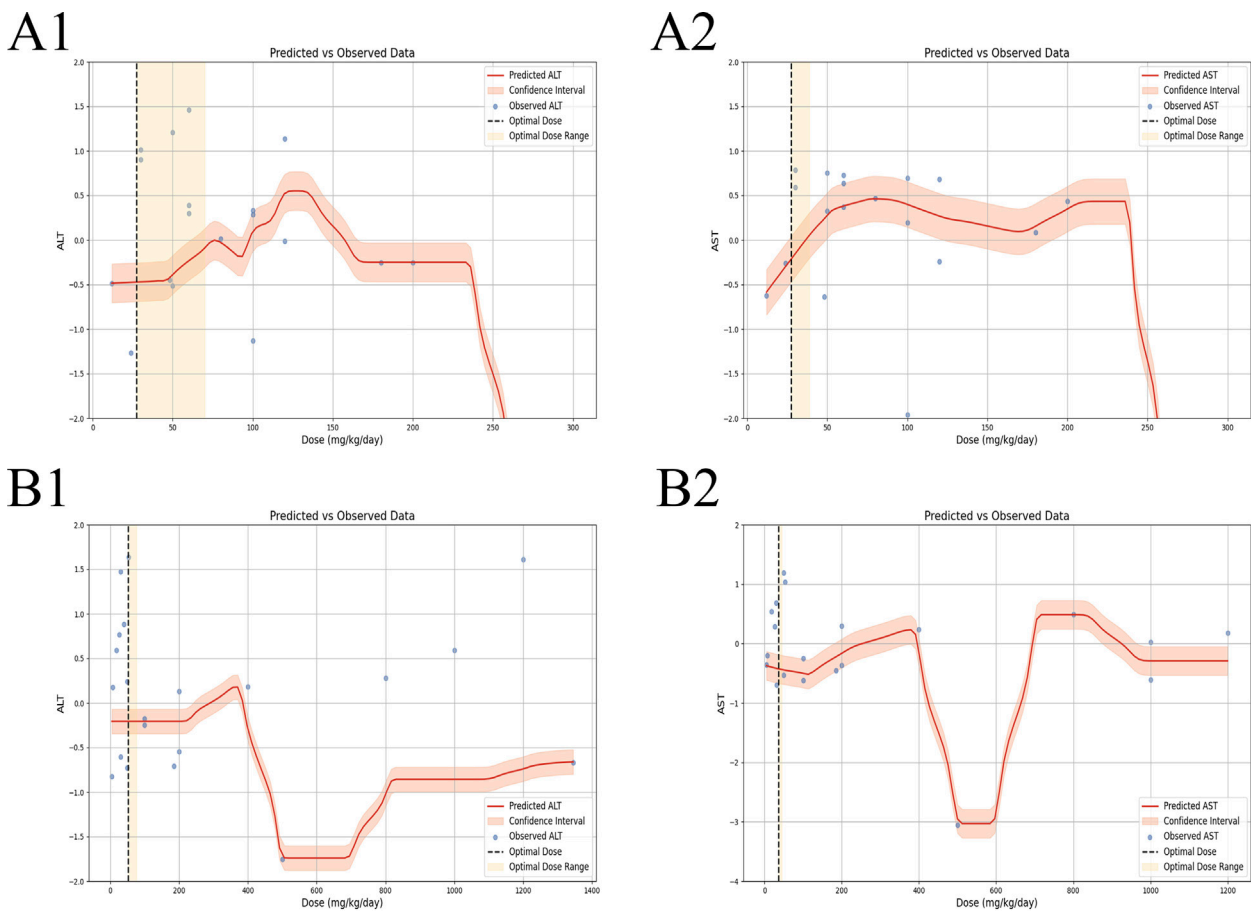

FIGURE 10
Machine learning of dose–time–effect relationship. **(A1)** ALT levels in hepatoprotection; **(A2)** AST levels in hepatoprotection; **(B1)** ALT levels in hepatotoxicity; **(B2)** AST levels in hepatotoxicity.

3.9 Potential mechanisms and molecular docking of key targets

The intricate and diverse mechanisms by which TSG influences the progression of LI are not straightforward. Supplementary Tables 8, 9 offers an assessment of the signaling transduction pathways that have been pinpointed, specifically Keap1/Nrf2/HO-1/NQO1, NF-κB, PPAR, as well as TGF-β pathways.

To substantiate the possible mechanisms through which TSG exerts its effects, we employed molecular docking techniques to evaluate the binding affinity of TSG with its principal targets. Our comprehensive molecular docking analysis has unveiled the intimate interactions of TSG with PPARGC1A, NFE2L2, NFKB1, and STAT, complemented by a meticulous examination of the thermodynamic data.

The calculated free energy of −5.1 kcal/mol indicates a strong interaction between TSG and key residues on the PPARGC1A protein, including THR215, THR216, TYR213, LYS212, and GLU209. Similarly, a free energy of −5.9 kcal/mol suggests robust binding of TSG to ARG503, ARG502, ARG499, LYS506, and ASN482 on the NFE2L2 protein. TSG also demonstrates substantial binding with NFKB1, highlighted by a free energy of −6.7 kcal/mol, involving residues such as PHE225, THR122, GLU117, ILE120, TYR163, ARG161, and GLY162. Additionally, TSG is shown to have significant interactions with the STAT protein, with an estimated free energy of −6.7 kcal/mol, engaging residues ASN662, GLU618, ASP627, HIS629, GLN621, and PRO626. These interactions are characterized by hydrogen bonding and hydrophobic contacts.

The visualization of the compound-target interactions was accomplished using PyMoL 2.6 and Discovery Studio 2019 (Figure 12). This study provides a comprehensive view of the molecular interactions that underpin the biological activity of TSG, offering insights into their potential therapeutic applications.

4 Discussion

TSG, a bioactive substance originating from the plant *P. multiflorum* Thunb., has garnered considerable attention for its dual influence on LI. Our study encompassed 24 scholarly articles that featured 564 rodent subjects, highlighting TSG's role in both liver protection and liver damage. We scrutinized a spectrum of biomarkers, such as ALT, AST, TNF-α, IL-6, serum TG, serum TC, SOD, MDA, IFN-γ, and the apoptosis rate, to assess the

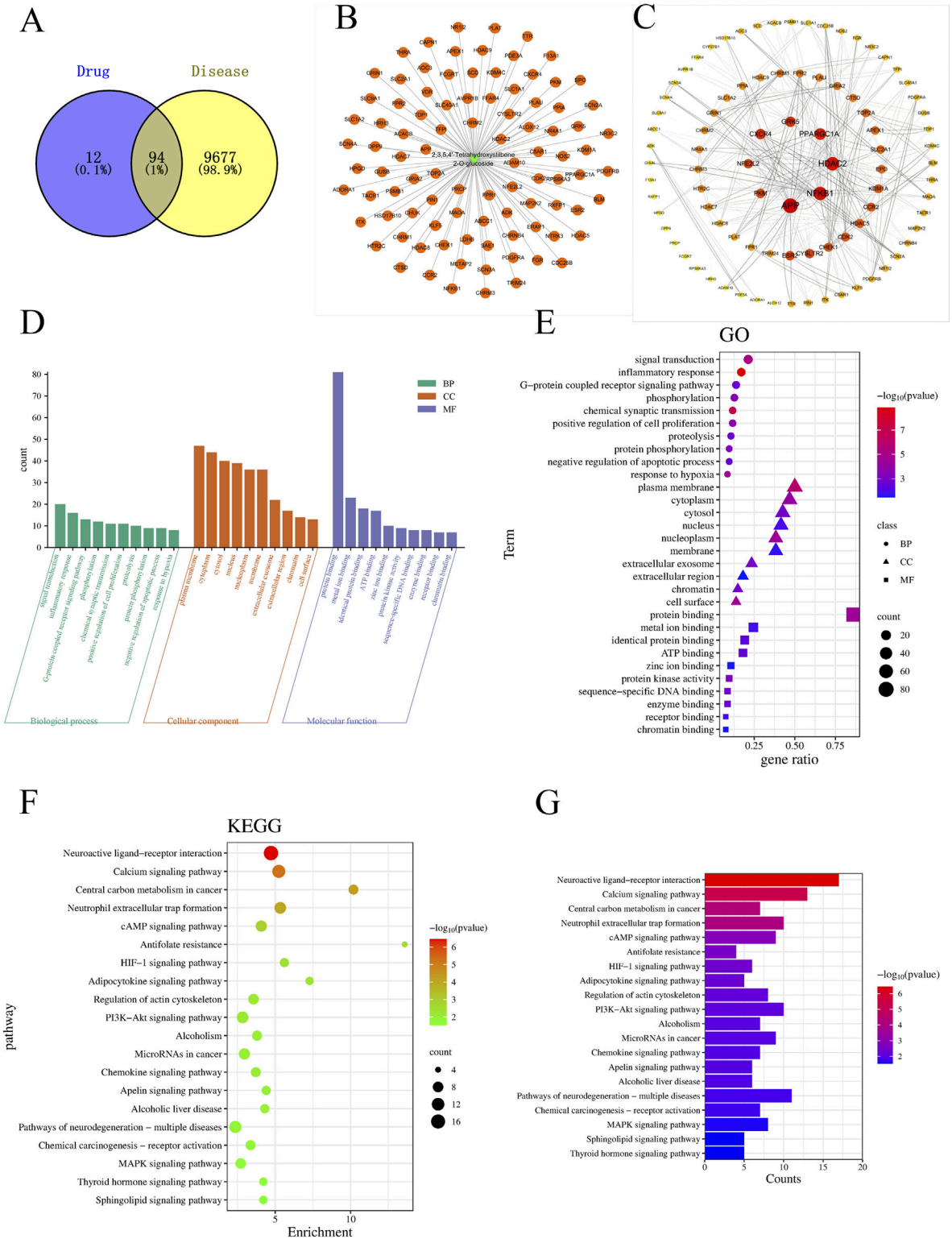

FIGURE 11
The charts of network pharmacology. **(A)** Venn diagram; **(B)** TSG-LI network diagram; **(C)** PPI network; **(D, E)** Go analysis; **(F, G)** KEGG analysis.

therapeutic efficacy and the dosage sensitivity of TSG in addressing both the reparative and harmful aspects of LI. Furthermore, we endeavored to elucidate the underlying mechanisms of TSG's protective and toxic effects by employing network pharmacology and molecular docking (Figure 13).

4.1 Protective mechanisms of TSG on LI

The protective effects of TSG on LI have been a focal point of research, given its multifaceted regulatory roles in various signaling pathways. As elucidated through literature and network

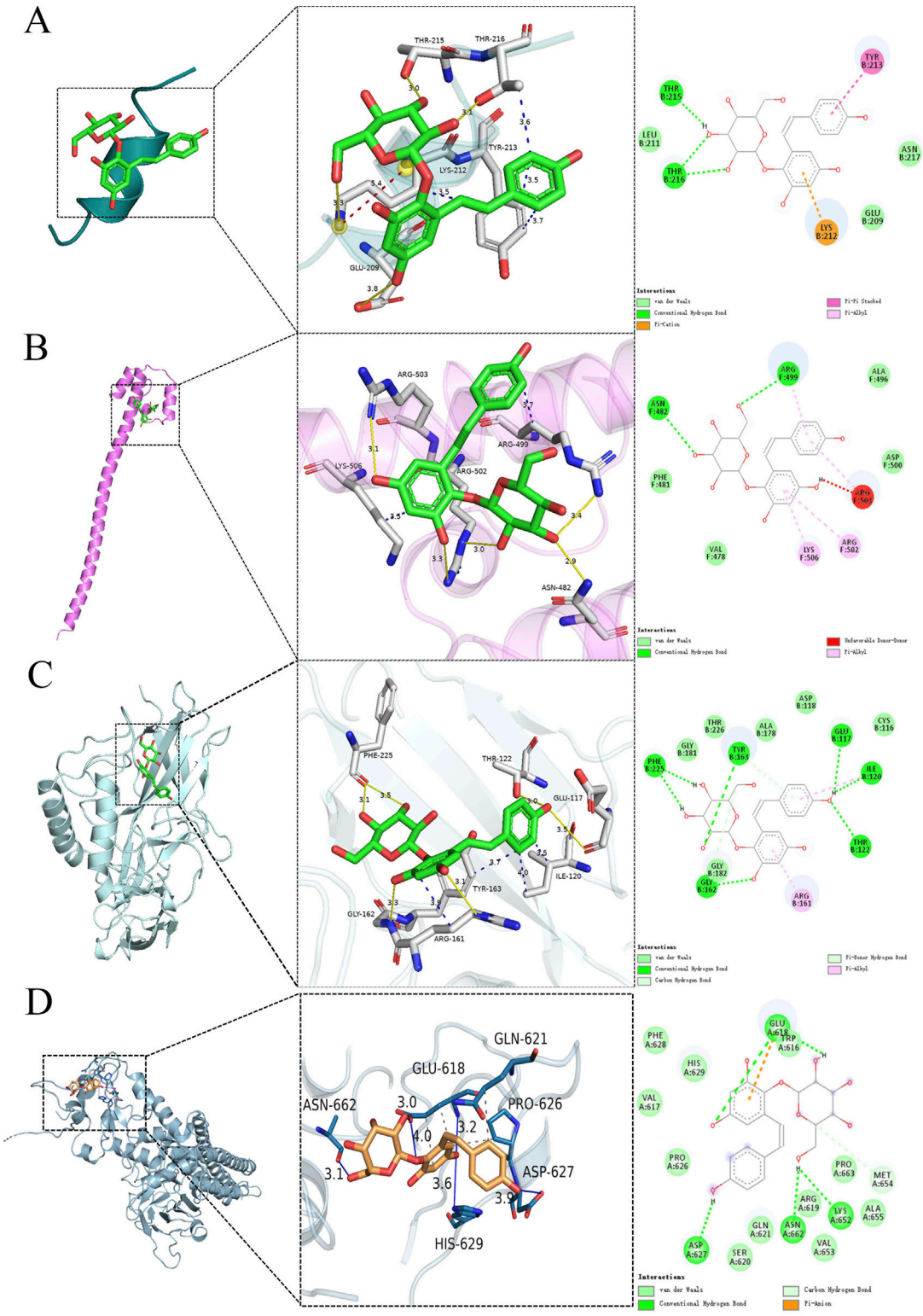

FIGURE 12
Molecular docking of TSG and key targets. **(A)** TSG binding to PPARGC1A; **(B)** TSG binding to NFE2L2; **(C)** TSG binding to NFKB1; **(D)** TSG binding to STAT.

pharmacology, TSG is posited to mediate its protective effects by intricately regulating a spectrum of pathways. These include the Keap1/Nrf2/HO-1/NQO1, NF-κB, PPAR, PI3K/Akt, transforming growth factor beta (TGF-β)/small mothers against decapentaplegic (Smad), as well as TGF-β/extracellular signal-regulated kinase (ERK) pathways. The modulation of these pathways is pivotal in

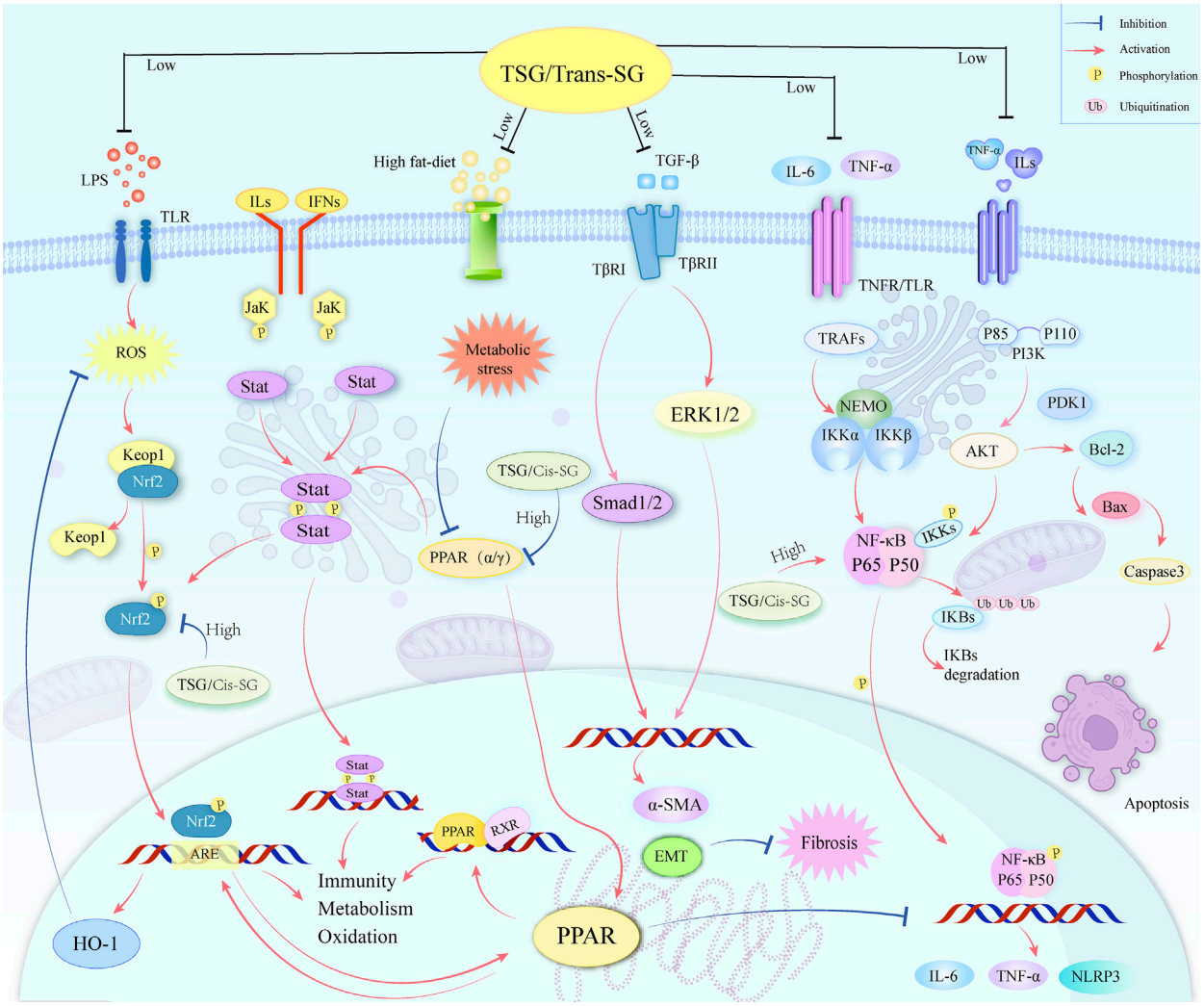

FIGURE 13
A graphical representation illustrates multiple molecular processes of TSG's protective and toxic in liver injury by modifying Keap1/Nrf2/HO-1/NQO1, NF-κB, PPAR, PI3K/Akt, TGF-β/Smad, TGF-β/ERK, as well as JAK/STAT signaling pathways.

mitigating the levels of liver enzymes, such as ALT and AST, which are indicative of LI. TSG's capacity to diminish these enzyme levels is instrumental in alleviating liver damage.

Furthermore, TSG has been observed to attenuate the levels of key inflammatory markers, including TNF-α and IL-6, which are associated with LI. It also modulates the rate of apoptosis by reducing the expression of pro-apoptotic factors and enhancing the expression of anti-apoptotic factors, thereby diminishing cell death in the liver (Wang et al., 2020a; Chen et al., 2020). This multifaceted action underscores TSG's potential as a therapeutic agent in the management of liver health.

The PI3K/Akt pathway, a critical signaling mechanism extensively studied for its role in cell survival and liver protection, is activated by TSG (Khezri et al., 2022; Li and Wang, 2014; Wang et al., 2020b). This activation leads to the phosphorylation of Akt, a serine/threonine kinase integral to fostering cell survival and averting apoptosis (Li and Wang, 2014; Lin et al., 2024). In the context of LI, TSG's activation of the PI3K/Akt pathway has been shown to bolster hepatocyte survival, thus contributing to liver repair and regeneration. Specifically, TSG treatment has been reported to activate the PI3K/Akt pathway, inducing autophagy in the liver, which serves a protective role against prediabetic injury by curbing inflammation and cell death while promoting cell proliferation (Qian et al., 2021; Wang et al., 2020b). In research conducted on human neuroblastoma cell lines (SH-SY5Y), it was discovered that the TSG enhances cell survival and reduces the likelihood of programmed cell death, or apoptosis, by increasing the levels of phosphatidylinositol 3-kinase (PI3K), protein kinase B (Akt), and the survival-promoting protein Bcl-2, while simultaneously decreasing the levels of the pro-apoptotic protein Bax (Kang et al., 2024). This indicates that TSG's protective effect against cell death may be mediated through the PI3K/Akt signaling pathway. TSG's influence on the expression levels of caspase 3, Bcl-2-associated X protein (Bax), and B-cell lymphoma-2 (Bcl-2) is significant, as these proteins play a pivotal role in the regulation of apoptosis. Bcl-2 is known for its anti-apoptotic properties, whereas Bax is associated with promoting cell death (Glick et al., 2010; Zhang et al., 2024a). The equilibrium

between these proteins is critical in the determination of whether cells live or die, and TSG's ability to modulate their expression suggests its potential to influence the cellular milieu towards a pro-survival state and against cell death by apoptosis (Atmaca et al., 2024; Wang et al., 2024a).

The PI3K/Akt signaling pathway interacts with the NF-κB signaling pathway, with the two pathways mutually regulating each other and jointly participating in a variety of biological processes, especially in cell survival, inflammatory responses, and immune responses (Aksoy et al., 2005; Li et al., 2024; Shafiek et al., 2024; Yu et al., 2024). The PI3K/Akt signaling pathway can activate the NF-κB signaling pathway by phosphorylating IκB kinase α (IKKα), thereby promoting the release of NF-κB from the IκB complex in the cytoplasm, and subsequently migrating to the nucleus to activate the expression of related genes (Agarwal et al., 2005; Aksoy et al., 2005; Bai et al., 2009; Oeckinghaus et al., 2011). In addition, Akt can activate the NF-κB pathway by phosphorylating IκB kinase (IKK), thereby affecting cell survival, proliferation, invasion, angiogenesis, and chemotherapy resistance (Agarwal et al., 2005; Bai et al., 2009). However, some studies have reported that the NF-κB pathway can be inhibited by upregulating the phosphorylation of PI3K and Akt while reducing the phosphorylation of IκBα and NF-κB, thereby inhibiting inflammatory responses (Agarwal et al., 2005; Misra et al., 2006). TSG may also have a similar pathway, inhibiting inflammatory responses by suppressing the PI3K/Akt/NF-κB pathway, which requires experimental validation.

Inflammation and immune response are critical components of LI (Jia et al., 2024; Wang et al., 2024b), and TSG modulates these through the inhibition of NFKB1. NF-κB is a vital transcription factor involved in immune responses, inflammation, cell growth, and stress responses (Hayden and Ghosh, 2011; Hoesel and Schmid, 2013; Lawrence, 2009; Yu H. et al., 2020). It is typically inactive in the cytoplasm due to interaction with IκB proteins. Upon receipt of pro-inflammatory signals, a signaling cascade is initiated that activates the IκB kinase (IKK) complex, leading to the degradation of IκB and the release of NF-κB into the nucleus to regulate gene expression (Lim et al., 2019). In LI, therapeutic substances like TSG may protect the liver by reducing the production of pro-inflammatory cytokines such as TNF-α and IL-6 and modulating NF-κB signaling (Lin et al., 2015b). They could potentially diminish NF-κB's nuclear translocation by inhibiting IκB phosphorylation and degradation, reducing inflammatory factor expression (Ma et al., 2016; Xiong et al., 2012). TSG might also regulate antioxidant stress response proteins to prevent NF-κB activation caused by oxidative stress. Understanding NF-κB's relationship with oxidative stress is crucial for developing treatments for diseases where oxidative stress is a factor (Deng et al., 2024; Ma et al., 2024; Yu H. et al., 2020).

Oxidative stress, a state caused by an imbalance between oxidation and antioxidation within the body, leads to the production of a plethora of oxidative intermediates that can damage cellular structures and affect their physiological functions (Filomeni et al., 2015; Sies, 2015; Thomas et al., 2024). The NF-κB pathway has both antioxidant and pro-oxidant roles in the context of oxidative stress. Reactive oxygen species (ROS) can activate or inhibit NF-κB signaling in a context-dependent manner (Morgan and Liu, 2011). There is a crosstalk between NF-κB and the Nrf2 signaling pathway, which is involved in the response to antioxidative stress (Oeckinghaus et al., 2011). During the oxidative stress response, electrophilic metabolites inhibit the activity of the BCR (Keap1) complex, promoting the formation of heterodimers between Nrf2 and small Maf proteins, which then accumulate in the nucleus (Bellezza et al., 2018). The activation of Nrf2 can regulate a series of genes involved in antioxidation and metabolic detoxification, and the activity of Nrf2 is also regulated by NF-κB (Oeckinghaus et al., 2011).

TSG exerts a multifaceted influence on LI, primarily through the modulation of oxidative stress and the antioxidant response. It triggers the activation of Nrf2, a key controller of cellular antioxidant processes, leading to an upregulation of genes responsible for detoxification and antioxidant production, such as those for heme oxygenase (HO-1) and quinone oxidoreductase-1 (NQO1) (Gao et al., 2020; Li et al., 2020; Loboda et al., 2016; Yu W. et al., 2020). This enhancement of the liver's ability to counteract reactive oxygen species (ROS) and preserve cellular redox equilibrium is crucial in reducing a primary cause of LI. Under normal physiological conditions, the activity of Nrf2 is controlled by Keap1, a protein rich in cysteine residues that marks Nrf2 for proteasomal degradation via the Cul3-dependent E3 ubiquitin ligase pathway (Baird and Yamamoto, 2020; Bellezza et al., 2018). However, under stress, Nrf2 is phosphorylated, enabling its release from Keap1, nuclear translocation, and subsequent binding to Maf proteins (Bellezza et al., 2018). This binding event initiates the activation of the antioxidant response element (ARE), which drives the transcription of genes that Nrf2 regulates, playing a central role in the cellular response to oxidative stress, including anti-inflammatory, antioxidant, and apoptotic activities (Jia et al., 2024; Katsuoka et al., 2005; Ulasov et al., 2022). TSG's involvement in the Nrf2/HO-1 signaling axis is particularly noteworthy in lessening the impact of acetaminophen (APAP)-induced LI (Gao et al., 2020), where it helps to alleviate lipid peroxidation and metabolic disturbances, underscoring its potential as a therapeutic agent for liver health.

TSG also plays a significant role in LI protection by modulating the TGF-β signaling pathway, central to the development of hepatic fibrosis (Long et al., 2019). By inhibiting the phosphorylation of key pathway components like ERK1/2 and Smad1/2 (Peng et al., 2022), TSG can attenuate the fibrotic response characterized by excessive extracellular matrix deposition and tissue scarring. This modulation is further supported by TSG's ability to suppress inflammation, promote liver regeneration, and reduce the activation of hepatic stellate cells, pivotal in fibrosis. Additionally, TSG's influence on immune responses could indirectly affect the TGF-β pathway, potentially protecting hepatocytes by curbing inflammation and oxidative stress. This may interfere with the TGF-β activation and its downstream signaling, including the Smad-dependent and Smad-independent pathways, which involve the activation of ERK and its role in cell survival and epithelial–mesenchymal transition (EMT) (Hata and Chen, 2016; Peng et al., 2022). Overall, TSG's intervention in the TGF-β/Smad and TGF-β/ERK pathways presents a promising therapeutic strategy for LI management (Long et al., 2019), aiming to regulate gene expression involved in cell proliferation, differentiation, and matrix production (Peng et al., 2022; Zhang et al., 2017).

The liver, as the metabolic command center for lipids, dutifully orchestrates the synthesis, secretion, and clearance of cholesterol and lipoproteins, which are the circulatory workhorses for lipids (Nguyen et al., 2008). TSG has been recognized for its ability to ignite the peroxisome proliferator-activated receptor alpha (PPARα) signaling pathway (Xu et al., 2019), a conductor of lipid metabolism and guardian of cellular homeostasis (Bougarne et al., 2018; Wang et al., 2020). Within the context of a meticulous study probing the effects of TSG on rats befallen by fatty liver disease, courtesy of a high-fat diet, the application of TSG was lauded for its capacity to significantly curtail the levels of total cholesterol, triglycerides, and free fatty acids in both serum and liver tissue (Xi, 2018; Xu et al., 2019). This salutary effect was found to be in tandem with an upregulation of PPARα and the autophagy-associated proteins LC3II and Beclin 1, while simultaneously orchestrating a retreat for p62 (Xi, 2018). The TSG-induced activation of autophagy is theorized to embolden the disintegration of lipid droplets, thereby refining the liver's lipid metabolic prowess and elevating its overall metabolic acumen.

In summary, TSG's intricate action on molecular targets results in a multifaceted response to LI, providing a comprehensive protective mechanism against liver damage. The precise mechanisms are still under investigation, but it is believed that TSG modulates various pathways, from the cell membrane to the nucleus, influencing the transcription of genes related to inflammation, fibrosis, and liver regeneration. This integrated approach, which enhances antioxidant defenses, regulates metabolism, curbs inflammation, and affects signal transduction, underscores TSG's potential as a therapeutic agent in liver disease management.

4.2 Hepatotoxic mechanisms of TSG on LI

TSG is a natural compound found in the dried root of *P. multiflorum* Thunb., and exhibits both hepatoprotection and hepatotoxicity. The molecular signaling pathways involved in TSG-induced hepatotoxicity are complex and multifaceted including proliferator-activated receptor (PPAR), JAK (Janus Kinase)/STAT (Signal Transducers and Activators of Transcription), Keap1/Nrf2/HO-1, and NF-κB signaling pathways.

The hepatotoxicity of TSG is deeply interwoven with its impact on energy metabolism and mitochondrial function, essential for liver health maintenance. TSG targets the PPARGC1A gene, which encodes the transcriptional coactivator PGC-1α, pivotal in regulating genes involved in energy metabolism (Liang and Ward, 2006; Tiraby and Langin, 2005). In synergy with PPARγ, this coactivator enhances mitochondrial gene expression, promoting energy production through fatty acid oxidation and oxidative phosphorylation, a critical mechanism for alleviating metabolic stress on the liver, especially during injury (Christofides et al., 2021; Wang et al., 2020). This process is also considered a key regulator of gluconeogenesis and adaptive thermogenesis (Hosseini et al., 2024; Tiraby and Langin, 2005).

However, TSG's hepatotoxic effects are manifested through the inhibition of PPARGC1A and PPARγ expression, thereby activating the NF-κB and STAT signaling pathways, commonly dysregulated in liver diseases and potentially leading to LI (Kong et al., 2022; Meng et al., 2017; Zhang, 2017). PPARs, a group of nuclear receptors, significantly regulate cellular processes such as differentiation, development, metabolism, and inflammatory responses (Berthier et al., 2021). Notably, PPAR-γ activation has demonstrated a protective role against LI, potentially through the inhibition of the NF-κB pathway (Shishodia et al., 2007; Zhang, 2017). In LI cases induced by Polygonum multiflorum Thunb., PPAR-γ expression levels have been negatively correlated with the extent of LI, suggesting that PPAR-γ agonists could counteract the LI caused by this traditional medicine (Meng et al., 2017).

The PPAR pathway is intricately involved with multiple pathways, and studies have observed that PPARγ activation can synergize with the Nrf2 pathway, promoting the expression of related genes and inhibiting ferroptosis (Reuter et al., 2010). The activation of the PPAR signaling pathway can also foster the anti-inflammatory differentiation of macrophages in a JAK2/STAT6 dependent manner, simultaneously activating both PPARγ and Nrf2 signals (Tu et al., 2023). This suggests a potential interaction between PPAR and Nrf2, highlighting their joint role in regulating inflammatory and antioxidant responses (Ghanim and Qinna, 2022; Tu et al., 2023). Furthermore, the PPAR pathway intersects with the NF-κB pathway, playing a significant role in modulating inflammatory responses and cellular metabolism (de Souza Basso et al., 2021; Reuter et al., 2010). These complex interactive networks may contribute to the hepatotoxicity induced by TSG.

The JAK/STAT pathway is a pivotal mechanism for intracellular communication, playing a role in numerous biological functions such as cellular proliferation, maturation, and immune system reactions (Hu et al., 2021; Xin et al., 2020). Dysfunctional activation of this pathway has been linked to a range of illnesses, including those affecting the liver (Owen et al., 2019; Xin et al., 2020). Research has shown that disruptions in the JAK/STAT signaling are prevalent in liver conditions associated with Hepatitis B Virus (HBV), influencing both the onset and progression of these diseases (Tang et al., 2023; Xu et al., 2022; Zhou et al., 2021). Moreover, an overactive JAK/STAT signaling pathway is a significant factor in the development and worsening of hepatocellular carcinoma, potentially serving as a key biomarker for assessing the severity and predicting the outcome of this type of liver cancer (Lokau et al., 2019; Zhao et al., 2021). Although these studies do not directly point out the mechanism by which TSG produces liver toxicity through the JAK/STAT pathway, they provide a connection between the JAK/STAT pathway and liver diseases. Additionally, a study based on an *in vitro* hepatotoxicity assessment system using liver organoids and high-content imaging technology has differentiated the hepatotoxic potential of TSG and its cis-isomer (cis-SG) in Polygonum multiflorum (Liu et al., 2022). It was found that the hepatotoxicity of cis-SG is related to mitochondrial damage, and this hepatotoxicity can be inhibited by mitochondrial protective agents. This suggests that some isomers of TSG may affect mitochondrial function, thereby affecting the JAK/STAT signaling pathway, leading to liver cell damage. Although there is currently no direct evidence to show the detailed mechanism by which TSG produces liver toxicity through the JAK/STAT pathway, we can speculate that TSG may affect the JAK/STAT pathway based on existing research and molecular docking results,

thereby affecting the function and survival of liver cells, ultimately leading to liver toxicity. Future research needs to further explore the specific mechanism of TSG's impact on the JAK/STAT pathway and how to mitigate or prevent LI caused by TSG by regulating this pathway.

TSG has garnered attention for its possible role in intensifying LI via the Keap1/Nrf2/HO-1 axis. This axis is a significant protective system against oxidative stress and plays a crucial role in both the prevention and mitigation of LI (Liu et al., 2022). Typically, Nrf2 is marked for degradation by the Keap1-CUL3 complex through ubiquitination, but when stress is present, Nrf2 detaches from Keap1, accumulates in the cytoplasm, and then moves to the nucleus to bind with specific genes, thereby triggering the transcription of genes that encode for antioxidant and detoxification enzymes (Ghanim and Qinna, 2022; Liu et al., 2022). In scenarios of TSG-induced hepatotoxicity, it has been noted that TSG can boost the expression and activity of CYP450 enzymes, which are key in the metabolism of drugs into potentially harmful reactive metabolites that can trigger LI (Manikandan and Nagini, 2018). Notably, TSG has been linked to the upregulation of CYP2E1, CYP3A4, and CYP1A2, which could lead to an increased metabolic conversion of hepatotoxic substances and a worsening of LI (Xu et al., 2017). Additionally, TSG has been observed to trigger the nuclear translocation of the aryl hydrocarbon receptor (AHR) and the pregnane X receptor (PXR), both of which are involved in the regulation of CYP1A2 and CYP3A4 expression (Meng, 2021; Xu et al., 2017). The suppression of AHR or PXR by specific inhibitors has been shown to lessen the exacerbating effect of TSG on acetaminophen-induced hepatotoxicity, suggesting that these transcription factors play a part in TSG's influence on LI (Meng, 2021). All in all, while TSG possesses various beneficial pharmacological properties, it also has the potential to induce hepatotoxicity by modulating the Keap1/Nrf2/HO-1 pathway and increasing the expression of CYP450 enzymes, which could enhance the metabolic activation of hepatotoxic compounds. The precise mechanisms of TSG's impact on the Keap1/Nrf2/HO-1 pathway and its role in LI require further investigation to fully understand its hepatotoxic potential and to develop strategies for the safe use of TSG-containing herbal remedies.

The NF-κB pathway is often activated in liver diseases and can contribute to LI when persistently activated (Liu et al., 2017). TSG has been reported to trigger the proliferation of $CD4^+$ T and $CD8^+$ T cells and the secretion of cytokines *in vivo*, suggesting its potential to initiate an immune response that may contribute to LI (Liu et al., 2024). The activation of T cells and the secretion of inflammatory cytokines such as TNF-α and IFN-γ can lead to the activation of the NF-κB pathway. Once activated, NF-κB can translocate to the nucleus and promote the transcription of genes involved in inflammation and cell survival (Lawrence, 2009). The exact mechanisms of TSG-induced hepatotoxicity through the NF-κB pathway are not fully understood. TSG may contribute to hepatotoxicity potentially through the NF-κB pathway by modulating the immune response and potentially interacting with other hepatotoxic compounds.

The PPAR, Nrf2, JAK/STAT, and NF-κB pathways are intricately linked and may all be implicated in LI induced by TSG. These pathways form an interactive network that is centered around the PPAR pathway. The PPAR/JAK/STAT/Nrf2 axis stands out as a crucial component of this network. Upon activation by their respective ligands, PPARs can modulate the expression of target genes, including those involved in the JAK/STAT pathway (Das et al., 2024). Once activated, JAKs phosphorylate STAT proteins, enabling them to dimerize and translocate to the nucleus, where they act as transcription factors regulating gene expression (Morris et al., 2018). Activated STAT proteins can then interact with Nrf2, which, when stabilized and activated, translocates to the nucleus and binds to antioxidant response elements (AREs), inducing the expression of detoxifying and antioxidant enzymes (Wang and He, 2022).

Furthermore, PPARs can interact with Nrf2 to produce synergistic effects, such as antioxidant actions (Reuter et al., 2010). The activation of PPARγ enhances the expression and activity of Nrf2, which in turn further stimulates the transcription of antioxidant and detoxifying enzymes (Abdelhamid et al., 2020; Zhang et al., 2018). This mutual promotion between PPAR and Nrf2 strengthens the cell's defense mechanisms against oxidative stress and other forms of cellular injury, highlighting their integral role in maintaining liver health and their potential as therapeutic targets for liver diseases (Zhang et al., 2018). TSG may inhibit Nrf2 activity by suppressing the PPAR/JAK/STAT/Nrf2 axis, while simultaneously activating NF-κB, contributing to LI. The crosstalk between these pathways and their combined impact on LI induced by TSG underscores the complexity of the hepatic response to this compound and suggests that interventions targeting this network could be beneficial in ameliorating liver damage.

In summary, the PPAR/JAK/STAT/Nrf2 axis, along with the NF-κB pathway, forms a complex regulatory network that plays a significant role in TSG-induced LI. TSG may cause LI through various mechanisms, including negative impacts on energy metabolism and mitochondrial function, activation of pathways related to inflammation and immune responses, and enhancement of oxidative stress. These findings emphasize the need for further research into the hepatotoxic mechanisms of TSG and the development of strategies to mitigate or prevent LI caused by TSG.

4.3 Hepatotoxic mechanisms of cis-SG/trans-SG on LI

Cis-SG and trans-SG are two isomers found in the dried root of *P. multiflorum* Thunb., commonly known as *Heshouwu*. They exhibit different mechanisms of hepatotoxicity. Cis-SG has demonstrated a stronger hepatotoxicity compared to trans-SG *in vivo* experiments. Studies indicate that cis-SG may cause liver damage by affecting multiple molecular signaling pathways. For instance, cis-SG may affect the function of mitochondria, leading to cellular energy metabolism disorders. Specifically, cis-SG may cause an increase in mitochondrial membrane permeability, leading to a decrease in mitochondrial membrane potential (MMP), thereby triggering mitochondrial dysfunction (Liu et al., 2022). Additionally, cis-SG can downregulate the expression of PPAR-γ, activate the NF-κB signaling pathway, and induce monocytes/macrophages to secrete pro-inflammatory cytokines such as TNF-α and IL-6, leading to liver damage (Zhang, 2017). In

contrast, trans-SG has not been observed to have significant hepatotoxic effects under normal administration conditions. However, if phase II metabolism is inhibited during the metabolic process, the risk of liver damage from trans-SG may increase. *In vitro* experiments have shown that trans-SG mainly undergoes phase II metabolism through UGT enzymes, and its metabolites are glucuronic acid conjugates (Li N. et al., 2017). When phase II metabolic enzymes are inhibited using ketoconazole, the degree of LI caused by trans-SG in LPS-sensitized rat models significantly increases, indicating that the metabolic state of trans-SG may significantly impact its risk of liver damage (Li N. et al., 2017).

It is worth noting that the hepatotoxicity of trans-SG and cis-SG in *Heshouwu* may have synergistic effects with other components, and LI caused by *Heshouwu* may involve various mechanisms, including immune stress, oxidative stress, and endoplasmic reticulum stress (Liang et al., 2024). Therefore, although cis-SG plays a major role in LI caused by *Heshouwu*, the metabolism and interactions of trans-SG and other components may also adversely affect the liver under certain conditions. To elaborate further, the hepatotoxicity mechanisms of trans-SG and cis-SG involve intricate cellular processes. Cis-SG, being more hepatotoxic, can disrupt cellular homeostasis by interacting with specific receptors and triggering a cascade of responses that lead to inflammation and cell death. On the other hand, trans-SG's impact is less pronounced unless metabolic pathways are compromised, leading to the accumulation of potentially toxic metabolites.

The dose-time-toxicity relationship is crucial in understanding the hepatotoxic potential of these compounds. The severity of LI is not only dependent on the concentration of these isomers but also on the duration of exposure. Continuous or high-dose exposure to cis-SG can lead to more significant liver damage, whereas trans-SG may only pose a risk under conditions that inhibit its metabolism.

The hepatotoxicity of trans-SG and cis-SG is a multifactorial process involving complex molecular signaling pathways and is influenced by dosage and exposure time. Further research is necessary to fully elucidate the mechanisms and identify potential therapeutic strategies to mitigate the hepatotoxic effects of these compounds in *Heshouwu*.

4.4 The dual effects of TSG depend on dosage and subgroups analysis

This study included 564 animals for meta-analysis, confirming the hepatotoxicity and hepatoprotective effects of TSG. In terms of hepatoprotective effects, TSG significantly reduced the levels of ALT, AST, TNF-α, IL-6, MDA, Serum TG, and Serum TC, while increasing the levels of SOD and GSH. The therapeutic effect of TSG on LI showed no significant differences across BI, NBI, Rats, and Mice subgroups, all significantly reducing the levels of main indicators. However, in terms of hepatotoxicity, TSG significantly increased the levels of ALT, AST, TNF-α, IL-6, IFN-γ, and Apoptosis rate. Due to the large differences in the levels of hepatotoxicity indicators across groups, we conducted further subgroup analyses. The results confirmed that TSG has obvious hepatotoxicity in the LI model subgroup and rat subgroup, while no obvious hepatotoxicity was found in the N model subgroup and mice. TSG also has two isomers (cis-SG and trans-SG), therefore we conducted subgroup analyses of the hepatotoxicity of the two isomers separately. The results showed that cis-SG could significantly increase the indicators and has obvious hepatotoxicity, while trans-SG showed no significant toxicity. Although trans-SG has not been found to exhibit significant hepatotoxicity, the levels of LI indicators are further increased when cis-SG is used in combination with trans-SG.

In order to develop and apply the drug, it is essential to reduce the toxic effects while ensuring the efficacy of the drug. We used machine learning, 3D scatter plots, and radar charts to divide the dose range of TSG that causes hepatotoxicity and hepatoprotection. The results show that the optimal dose range for TSG to treat LI is from 27.27 mg/kg/d to 38.81 mg/kg/d, with the best dose being 27.27 mg/kg/d. The optimal dose range for TSG to cause LI is from 51.93 mg/kg/d to 76.07 mg/kg/d, with the best dose being 51.93 mg/kg/d. Trans-SG, due to its therapeutic effect on LI and relatively low toxic side effects, may be the direction for drug development.

4.5 Limitations

The present article strictly followed the PRISMA guidelines, albeit with certain inherent limitations. Here are the refined points: 1. The study's scope was confined to a selection of four English and four Chinese databases, which inevitably introduced a degree of selectivity bias. Furthermore, it was not feasible to encompass the entire body of pertinent literature. 2. The diversity across the studies was challenging to fully reconcile, due to factors such as discrepancies in measurement tools, unit variances, and experimental design differences. 3. The study's corpus was limited to peer-reviewed articles, excluding reviews, correspondence, conference papers, and theses. 4. While articles with quality scores below the threshold of 5 were systematically excluded, the potential for result heterogeneity persists due to the variable quality of the included studies. 5. The lack of standardization in animal intervention protocols, dosages, treatment schedules, and model species across studies significantly contributed to the observed heterogeneity. 6. The research validated the potency and dependability of TSG in addressing liver impairment or hepatotoxic conditions by conducting a sensitivity analysis, applying Egger's test, and performing subgroup analyses, thereby bolstering the trustworthiness of the outcomes. 7. Although the study encapsulated the principal therapeutic mechanisms of TSG in safeguarding the liver and inducing hepatotoxic effects, a complete overview of every mechanism was not feasible due to the complexity inherent in the pathophysiological processes involved. 8. Ethical considerations have restricted the availability of literature on TSG's toxicological effects in humans, leading to an exclusive focus on animal model studies. The necessity for clinical trials to validate TSG's clinical utility in hepatoprotection and hepatotoxicity management is underscored. 9. Although molecular docking provided initial validation of TSG's interaction with key proteins, further experimental validation is essential for definitive conclusions. 10. TSG can cause various organ injuries, such as liver injury and kidney injury, but several articles reporting the toxicity of TSG mainly focus on its hepatotoxicity, with only a

small number of studies reporting its nephrotoxicity. Therefore, this article only focuses on the hepatotoxicity of TSG.

Despite these constraints, the study's findings have the potential to inform novel clinical strategies and contribute to the advancement of pharmaceutical development.

5 Conclusion

TSG's protective role against LI is attributed to its ability to decrease ALT and AST levels through multiple pathways, including Keap1/Nrf2/HO-1/NQO1, NF-κB, PPARα, PI3K/Akt, and TGF-β/Smad, as well as TGF-β/ERK pathways. These effects are observed at dosages ranging from 27.27 mg/kg/d to 38.81 mg/kg/d and over a period of 0.43 weeks–1 week. Conversely, at higher dosages between 51.93 mg/kg/d and 76.07 mg/kg/d and within the time of 0.06 weeks–0.43 weeks, TSG can increase ALT and AST levels through pathways associated with PPAR, JAK/STAT, Keap1/Nrf2/HO-1, and NF-κB, potentially leading to LI. It is important to note that hepatotoxicity induced by TSG is only evident in LI models and not observed in N models. In comparative *in vivo* studies, cis-SG has exhibited a more pronounced hepatotoxic effect compared to its isomer, trans-SG. Interestingly, trans-SG has shown negligible hepatotoxicity, indicating a significant difference in the biological activity of these isomers.

Data availability statement

The original contributions presented in the study are included in the article/Supplementary Material, further inquiries can be directed to the corresponding authors.

Author contributions

JJ: Data curation, Formal Analysis, Funding acquisition, Investigation, Methodology, Project administration, Software, Visualization, Writing–original draft. QxW: Data curation, Formal Analysis, Investigation, Methodology, Software, Visualization, Writing–original draft. QaW: Data curation, Formal Analysis, Investigation, Methodology, Software, Visualization, Writing–original draft. BD: Data curation, Software, Visualization, Writing–original draft. CG: Data curation, Software, Visualization, Writing–review and editing. JC: Formal Analysis, Methodology, Visualization, Writing–original draft. JZ: Conceptualization, Writing–review and editing. YG: Conceptualization, Writing–review and editing. XM: Conceptualization, Writing–review and editing.

Funding

The author(s) declare that financial support was received for the research, authorship, and/or publication of this article. This work was supported by Sichuan Science and Technology Program (2023NSFSC0687), Xinglin Scholar Research Promotion Project of Chengdu University of TCM (grant nos QJRC2022028 and QJJJ2022010), Major scientific research problems and key topics of medical technology problems of China Medical Education Association (2022KTZ016) and "The Hundred Talents Program" of the Hospital of the Chengdu University of Traditional Chinese Medicine (grant no. 22- B09).

Acknowledgments

This paper has been greatly improved by the advice of the reviewers and the authors of all references. The authors wish to thank the reviewers and the authors of all references.

Conflict of interest

The authors declare that the research was conducted in the absence of any commercial or financial relationships that could be construed as a potential conflict of interest.

Generative AI statement

The author(s) declare that no Generative AI was used in the creation of this manuscript.

Publisher's note

Supplementary material

The Supplementary Material for this article can be found online at: https://www.frontiersin.org/articles/10.3389/fphar.2025.1523713/full#supplementary-material

References

Abdelhamid, A. M., Elsheakh, A. R., Abdelaziz, R. R., and Suddek, G. M. (2020). Empagliflozin ameliorates ethanol-induced liver injury by modulating NF-κB/Nrf-2/PPAR-γ interplay in mice. *Life Sci.* 256, 117908. doi:10.1016/j.lfs.2020.117908

Acevedo, J. (2015). Multiresistant bacterial infections in liver cirrhosis: clinical impact and new empirical antibiotic treatment policies. *World J. Hepatol.* 7, 916–921. doi:10.4254/wjh.v7.i7.916

Agarwal, A., Das, K., Lerner, N., Sathe, S., Cicek, M., Casey, G., et al. (2005). The AKT/I kappa B kinase pathway promotes angiogenic/metastatic gene expression in colorectal cancer by activating nuclear factor-kappa B and beta-catenin. *Oncogene* 24, 1021–1031. doi:10.1038/sj.onc.1208296

Aksoy, E., Vanden Berghe, W., Detienne, S., Amraoui, Z., Fitzgerald, K. A., Haegeman, G., et al. (2005). Inhibition of phosphoinositide 3-kinase enhances

TRIF-dependent NF-kappa B activation and IFN-beta synthesis downstream of Toll-like receptor 3 and 4. *Eur. J. Immunol.* 35, 2200–2209. doi:10.1002/eji.200425801

Atmaca, H., Çamlı Pulat, Ç., Ilhan, S., and Kalyoncu, F. (2024). Hericium erinaceus extract induces apoptosis via PI3K/AKT and RAS/MAPK signaling pathways in prostate cancer cells. *Chem. Biodivers.* 21, e202400905. doi:10.1002/cbdv.202400905

Bai, D., Ueno, L., and Vogt, P. K. (2009). Akt-mediated regulation of NFkappaB and the essentialness of NFkappaB for the oncogenicity of PI3K and Akt. *Int. J. Cancer* 125, 2863–2870. doi:10.1002/ijc.24748

Baird, L., and Yamamoto, M. (2020). The molecular mechanisms regulating the KEAP1-NRF2 pathway. *Mol. Cell Biol.* 40, 000999-e120. doi:10.1128/MCB.00099-20

Bellezza, I., Giambanco, I., Minelli, A., and Donato, R. (2018). Nrf2-Keap1 signaling in oxidative and reductive stress. *Biochim. Biophys. Acta Mol. Cell Res.* 1865, 721–733. doi:10.1016/j.bbamcr.2018.02.010

Berthier, A., Johanns, M., Zummo, F. P., Lefebvre, P., and Staels, B. (2021). PPARs in liver physiology. *Biochim. Biophys. Acta Mol. Basis Dis.* 1867, 166097. doi:10.1016/j.bbadis.2021.166097

Bo, J (2016). Protection of TSG against acute alcoholic liver injury and the underlying mechanisms. *China J. Traditional Chin. Med. Pharm.*

Bougarne, N., Weyers, B., Desmet, S. J., Deckers, J., Ray, D. W., Staels, B., et al. (2018). Molecular actions of PPARα in lipid metabolism and inflammation. *Endocr. Rev.* 39, 760–802. doi:10.1210/er.2018-00064

Breit, H. C., Vosshenrich, J., Heye, T., Gehweiler, J., Winkel, D. J., Potthast, S., et al. (2023). Assessment of hepatic function employing hepatocyte specific contrast agent concentrations to multifactorially evaluate fibrotic remodeling. *Quant. Imaging Med. Surg.* 13, 4284–4294. doi:10.21037/qims-22-884

Chen, Z., Xu, Y., Zhao, J., Hai, C., and Yu, W. (2020). Antioxidant and anti inflammatory effects of 2,3,5,4'-tetrahydroxystilbene-2-O-β-D glucoside in macrophages.

Christofides, A., Konstantinidou, E., Jani, C., and Boussiotis, V. A. (2021). The role of peroxisome proliferator-activated receptors (PPAR) in immune responses. *Metabolism* 114, 154338. doi:10.1016/j.metabol.2020.154338

Das, D., Banerjee, A., Mukherjee, S., and Maji, B. K. (2024). Quercetin inhibits NF-kB and JAK/STAT signaling via modulating TLR in thymocytes and splenocytes during MSG-induced immunotoxicity: an *in vitro* approach. *Mol. Biol. Rep.* 51, 277. doi:10.1007/s11033-024-09245-7

de Souza Basso, B., Haute, G. V., Ortega-Ribera, M., Luft, C., Antunes, G. L., Bastos, M. S., et al. (2021). Methoxyeugenol deactivates hepatic stellate cells and attenuates liver fibrosis and inflammation through a PPAR-ɣ and NF-kB mechanism. *J. Ethnopharmacol.* 280, 114433. doi:10.1016/j.jep.2021.114433

Deng, X., Li, Y., Chen, Y., Hu, Q., Zhang, W., Chen, L., et al. (2024). Paeoniflorin protects hepatocytes from APAP-induced damage through launching autophagy via the MAPK/mTOR signaling pathway. *Cell Mol. Biol. Lett.* 29, 119. doi:10.1186/s11658-024-00631-4

Devarbhavi, H., Asrani, S. K., Arab, J. P., Nartey, Y. A., Pose, E., and Kamath, P. S. (2023). Global burden of liver disease: 2023 update. *J. Hepatol.* 79, 516–537. doi:10.1016/j.jhep.2023.03.017

EASLClinical Practice Guideline Panel: Chair:Panel membersEASL Governing Board representative: (2019). EASL clinical practice guidelines: drug-induced liver injury. *J. Hepatol.* 70, 1222–1261. doi:10.1016/j.jhep.2019.02.014

Elbaset, M. A., Mohamed, B., Hessin, A., Abd El-Rahman, S. S., Esatbeyoglu, T., Afifi, S. M., et al. (2024). Nrf2/HO-1, NF-κB and PI3K/Akt signalling pathways decipher the therapeutic mechanism of pitavastatin in early phase liver fibrosis in rats. *J. Cell Mol. Med.* 28, e18116. doi:10.1111/jcmm.18116

Filomeni, G., De Zio, D., and Cecconi, F. (2015). Oxidative stress and autophagy: the clash between damage and metabolic needs. *Cell Death Differ.* 22, 377–388. doi:10.1038/cdd.2014.150

Gao, Y., Li, J. T., Li, X., Li, X., Yang, S. W., Chen, N. H., et al. (2020). Tetrahydroxy stilbene glycoside attenuates acetaminophen-induced hepatotoxicity by UHPLC-Q-TOF/MS-based metabolomics and multivariate data analysis. *J. Cell. Physiology* 236, 3832–3862. doi:10.1002/jcp.30127

Gao, Y. (2021). Tetrahydroxy stilbene glycoside protects mice from acetaminophen-in duced liver injury: study based on metabonomics. *Chin. J. Clin. Pharmacol. Ther.* doi:10.12092/j.issn.1009-2501.2021.02.006

Ghanim, B. Y., and Qinna, N. A. (2022). Nrf2/ARE axis signalling in hepatocyte cellular death. *Mol. Biol. Rep.* 49, 4039–4053. doi:10.1007/s11033-022-07125-6

Glick, D., Barth, S., and Macleod, K. F. (2010). Autophagy: cellular and molecular mechanisms. *J. Pathol.* 221, 3–12. doi:10.1002/path.2697

Hata, A., and Chen, Y. G. (2016). TGF-B signaling from receptors to smads. *Cold Spring Harb. Perspect. Biol.* 8, a022061. doi:10.1101/cshperspect.a022061

Hayden, M. S., and Ghosh, S. (2011). NF-κB in immunobiology. *Cell Res.* 21, 223–244. doi:10.1038/cr.2011.13

Hoesel, B., and Schmid, J. A. (2013). The complexity of NF-κB signaling in inflammation and cancer. *Mol. Cancer* 12, 86. doi:10.1186/1476-4598-12-86

Hosseini, S. M., Tingzhu, Y., Zaohong, R., Ullah, F., Liang, A., Hua, G., et al. (2024). Regulatory impacts of PPARGC1A gene expression on milk production and cellular metabolism in buffalo mammary epithelial cells. *Anim. Biotechnol.* 35, 2344210. doi:10.1080/10495398.2024.2344210

Hu, X., Li, Y., and Wang, L. (2011). Effects of stilbene glucoside from Polygonum multiflorum Thunb. On hepatic enzymes and serum albumin of rats. *Liaoning J. Traditional Chin. Med.* doi:10.13192/j.ljtcm.2011.05.191.huxq.077

Hu, X., Li, J., Fu, M., Zhao, X., and Wang, W. (2021). The JAK/STAT signaling pathway: from bench to clinic. *Signal Transduct. Target Ther.* 6, 402. doi:10.1038/s41392-021-00791-1

Jia, R., Hou, Y., Zhang, L., Li, B., and Zhu, J. (2024). Effects of berberine on lipid metabolism, antioxidant status, and immune response in liver of Tilapia (*Oreochromis niloticus*) under a high-fat diet feeding. *Antioxidants (Basel)* 13, 548. doi:10.3390/antiox13050548

Ju, J., Li, J., Lin, Q., and Xu, H. (2018). Efficacy and safety of berberine for dyslipidaemias: a systematic review and meta-analysis of randomized clinical trials. *Phytomedicine* 50, 25–34. doi:10.1016/j.phymed.2018.09.212

Kang, B., Li, R., He, X., and Huang, Z. (2024). Mechanism of stilbene glycosides on apoptosis of SH-SY5Y cells via regulating PI3K/AKT signaling pathway. *J. Hainan Med. Univ.* doi:10.13210/j.cnki.jhmu.20231030.002

Katarey, D., and Verma, S. (2016). Drug-induced liver injury. *Clin. Med. (Lond)* 16, s104–s109. doi:10.7861/clinmedicine.16-6-s104

Katsuoka, F., Motohashi, H., Ishii, T., Aburatani, H., Engel, J. D., and Yamamoto, M. (2005). Genetic evidence that small maf proteins are essential for the activation of antioxidant response element-dependent genes. *Mol. Cell Biol.* 25, 8044–8051. doi:10.1128/MCB.25.18.8044-8051.2005

Khezri, M. R., Jafari, R., Yousefi, K., and Zolbanin, N. M. (2022). The PI3K/AKT signaling pathway in cancer: molecular mechanisms and possible therapeutic interventions. *Exp. Mol. Pathol.* 127, 104787. doi:10.1016/j.yexmp.2022.104787

Kirpich, I. A., and McClain, C. J. (2012). Probiotics in the treatment of the liver diseases. *J. Am. Coll. Nutr.* 31, 14–23. doi:10.1080/07315724.2012.10720004

Knight, J. A. (2005). Liver function tests: their role in the diagnosis of hepatobiliary diseases. *J. Infus. Nurs.* 28 (2), 108–117. doi:10.1097/00129804-200503000-00004

Kong, W. S., Zhou, G., Xu, L. W., Wang, K., Feng, Y. M., Tao, L. Y., et al. (2022). Beware of the potential risks for polygoni multiflori caulis-induced liver injury. *Front. Pharmacol.* 13, 868327. doi:10.3389/fphar.2022.868327

Lawrence, T. (2009). The nuclear factor NF-kappaB pathway in inflammation. *Cold Spring Harb. Perspect. Biol.* 1, a001651. doi:10.1101/cshperspect.a001651

Li, T., and Wang, G. (2014). Computer-aided targeting of the PI3K/Akt/mTOR pathway: toxicity reduction and therapeutic opportunities. *Int. J. Mol. Sci.* 15, 18856–18891. doi:10.3390/ijms151018856

Li C., C., Niu, M., Bai, Z., Zhang, C., Zhao, Y., Li, R., et al. (2017). Screening for main components associated with the idiosyncratic hepatotoxicity of a tonic herb, Polygonum multiflorum. *Front. Med.* 11, 253–265. doi:10.1007/s11684-017-0508-9

Li, B., Nasser, M. I., Masood, M., Adlat, S., Huang, Y., Yang, B., et al. (2020). Efficiency of Traditional Chinese medicine targeting the Nrf2/HO-1 signaling pathway. *Biomed. Pharmacother.* 126, 110074. doi:10.1016/j.biopha.2020.110074

Li, H., Xu, W., Hu, X., Tian, X., Li, B., Du, Y., et al. (2024). The surface protein GroEl of lactic acid bacteria mediates its modulation of the intestinal barrier in Penaeus vannamei. *Int. J. Biol. Macromol.* 278, 134624. doi:10.1016/j.ijbiomac.2024.134624

Li, N., Song, J., Li, X. I., and Jiabo, W. (2017). Influence of drug metabolizing enzyme inhibitors on liver injury susceptibility to trans-2,3,5,4'-tetrahydroxystilbene-2-O-β-D-glucoside. *Acta Pharm. Sin.* doi:10.16438/j.0513-4870.2017-0392

Liang, H., and Ward, W. F. (2006). PGC-1alpha: a key regulator of energy metabolism. *Adv. Physiol. Educ.* 30, 145–151. doi:10.1152/advan.00052.2006

Liang, Z., Li, J. I., and Wang, R. (2024). Mechanism of action of Polygonum multiflorum in inducing liver injury: a study based on signaling pathways. *J. Clin. Hepatology*. doi:10.12449/JCH240332

Lim, H. J., Jang, H. J., Kim, M. H., Lee, S., Lee, S. W., Lee, S. J., et al. (2019). Oleanolic acid acetate exerts anti-inflammatory activity via IKKα/β suppression in TLR3-mediated NF-κB activation. *Molecules* 24, 4002. doi:10.3390/molecules24214002

Lin, L., Ni, B., Lin, H., Zhang, M., Li, X., Yin, X., et al. (2015a). Traditional usages, botany, phytochemistry, pharmacology and toxicology of Polygonum multiflorum Thunb.: a review. *J. Ethnopharmacol.* 159, 158–183. doi:10.1016/j.jep.2014.11.009

Lin, P., Lu, J., Wang, Y., Gu, W., Yu, J., and Zhao, R. (2015b). Naturally occurring stilbenoid TSG reverses non-alcoholic fatty liver diseases via gut-liver Axis. *Plos One* 10, e0140346. doi:10.1371/journal.pone.0140346

Lin, Z., Wang, S., Cao, Y., Lin, J., Sun, A., Huang, W., et al. (2024). Bioinformatics and validation reveal the potential target of curcumin in the treatment of diabetic peripheral neuropathy. *Neuropharmacology* 260, 110131. doi:10.1016/j.neuropharm.2024.110131

Liu, T., Zhang, L., Joo, D., and Sun, S.-C. (2017). NF-κB signaling in inflammation. *Signal Transduct. Target. Ther.* 2, 17023. doi:10.1038/sigtrans.2017.23

Liu, M., Pu, Y., Gu, J., He, Q., Liu, Y., Zeng, Y., et al. (2021). Evaluation of Zhilong Huoxue Tongyu capsule in the treatment of acute cerebral infarction: a systematic review and meta-analysis of randomized controlled trials. *Phytomedicine* 86, 153566. doi:10.1016/j.phymed.2021.153566

Liu, J., Li, T., Li, R., Wang, J., Li, P., Niu, M., et al. (2022). Hepatic organoid-based high-content imaging boosts evaluation of stereoisomerism-dependent hepatotoxicity of stilbenes in herbal medicines. *Front. Pharmacol.* 13, 862830. doi:10.3389/fphar.2022.862830

Liu, W., Zeng, X., Wang, X., Hu, Y., Chen, L., Luo, N., et al. (2024). 2,3,5,4'-tetrahydroxystilbene-2-O-β-D- glucopyranoside (TSG)-Driven immune response in the hepatotoxicity of Polygonum multiflorum. *J. Ethnopharmacol.* 326, 117865. doi:10.1016/j.jep.2024.117865

Loboda, A., Damulewicz, M., Pyza, E., Jozkowicz, A., and Dulak, J. (2016). Role of Nrf2/HO-1 system in development, oxidative stress response and diseases: an evolutionarily conserved mechanism. *Cell Mol. Life Sci.* 73, 3221–3247. doi:10.1007/s00018-016-2223-0

Lokau, J., Schoeder, V., Haybaeck, J., and Garbers, C. (2019). Jak-stat signaling induced by interleukin-6 family cytokines in hepatocellular carcinoma. *Cancers (Basel)* 11, 1704. doi:10.3390/cancers11111704

Long, T., Wang, L., Yang, Y., Yuan, L., Zhao, H., Chang, C. C., et al. (2019). Protective effects of trans-2,3,5,4'-tetrahydroxystilbene 2-O-β-d-glucopyranoside on liver fibrosis and renal injury induced by CCl4via down-regulating p-ERK1/2 and p-Smad1/2. *Food and Funct.* 10, 5115–5123. doi:10.1039/c9fo01010f

Luo, X., Ni, X., Lin, J., Zhang, Y., Wu, L., Huang, D., et al. (2021). The add-on effect of Chinese herbal medicine on COVID-19: a systematic review and meta-analysis. *Phytomedicine* 85, 153282. doi:10.1016/j.phymed.2020.153282

Ma, J., Zheng, L., He, Y. S., and Li, H. J. (2015). Hepatotoxic assessment of Polygoni Multiflori Radix extract and toxicokinetic study of stilbene glucoside and anthraquinones in rats. *J. Ethnopharmacol.* 162, 61–68. doi:10.1016/j.jep.2014.12.045

Ma, J., Mi, C., Wang, K. S., Lee, J. J., and Jin, X. (2016). 4',6-Dihydroxy-4-methoxyisoaurone inhibits TNF-α-induced NF-κB activation and expressions of NF-κB-regulated target gene products. *J. Pharmacol. Sci.* 130, 43–50. doi:10.1016/j.jphs.2015.10.002

Ma, X., Zhang, W., Chen, Y., Hu, Q., Wang, Z., Jiang, T., et al. (2024). Paeoniflorin inhibited GSDMD to alleviate ANIT-induced cholestasis via pyroptosis signaling pathway. *Phytomedicine* 134, 156021. doi:10.1016/j.phymed.2024.156021

Macleod, M. R., O'Collins, T., Howells, D. W., and Donnan, G. A. (2004). Pooling of animal experimental data reveals influence of study design and publication bias. *Stroke* 35, 1203–1208. doi:10.1161/01.STR.0000125719.25853.20

Manikandan, P., and Nagini, S. (2018). Cytochrome P450 structure, function and clinical significance: a review. *Curr. Drug Targets* 19, 38–54. doi:10.2174/1389450118666170125144557

Meng, Y. K., Li, C. Y., Li, R. Y., He, L. Z., Cui, H. R., Yin, P., et al. (2017). Cis-stilbene glucoside in Polygonum multiflorum induces immunological idiosyncratic hepatotoxicity in LPS-treated rats by suppressing PPAR-γ. *Acta Pharmacol. Sin.* 38, 1340–1352. doi:10.1038/aps.2017.32

Meng, S. (2021). 2,3,5,4'-Tetrahydroxystibane-2-O-β-D-glucoside induces liver injury by disrupting bile acid homeostasis and phospholipids efflux. *China J. Chin. Materia Medica*. doi:10.19540/j.cnki.cjcmm.20200818.401

Misra, U. K., Deedwania, R., and Pizzo, S. V. (2006). Activation and cross-talk between Akt, NF-kappaB, and unfolded protein response signaling in 1-LN prostate cancer cells consequent to ligation of cell surface-associated GRP78. *J. Biol. Chem.* 281, 13694–13707. doi:10.1074/jbc.M511694200

Morgan, M. J., and Liu, Z. G. (2011). Crosstalk of reactive oxygen species and NF-κB signaling. *Cell Res.* 21, 103–115. doi:10.1038/cr.2010.178

Morris, R., Kershaw, N. J., and Babon, J. J. (2018). The molecular details of cytokine signaling via the JAK/STAT pathway. *Protein Sci.* 27, 1984–2009. doi:10.1002/pro.3519

Nguyen, P., Leray, V., Diez, M., Serisier, S., Le Bloc'h, J., Siliart, B., et al. (2008). Liver lipid metabolism. *J. Anim. Physiol. Anim. Nutr. Berl.* 92, 272–283. doi:10.1111/j.1439-0396.2007.00752.x

Niewiński, G., Morawiec, S., Janik, M. K., Grąt, M., Graczyńska, A., Zieniewicz, K., et al. (2020). Acute-on-chronic liver failure: the role of prognostic scores in a single-center experience. *Med. Sci. Monit.* 26, e922121. doi:10.12659/MSM.922121

Oeckinghaus, A., Hayden, M. S., and Ghosh, S. (2011). Crosstalk in NF-κB signaling pathways. *Nat. Immunol.* 12, 695–708. doi:10.1038/ni.2065

Owen, K. L., Brockwell, N. K., and Parker, B. S. (2019). JAK-STAT signaling: a double-edged sword of immune regulation and cancer progression. *Cancers (Basel)* 11, 2002. doi:10.3390/cancers11122002

Peng, D., Fu, M., Wang, M., Wei, Y., and Wei, X. (2022). Targeting TGF-β signal transduction for fibrosis and cancer therapy. *Mol. Cancer* 21, 104. doi:10.1186/s12943-022-01569-x

Qian, H., Chao, X., Williams, J., Fulte, S., Li, T., Yang, L., et al. (2021). Autophagy in liver diseases: a review. *Mol. Asp. Med.* 82, 100973. doi:10.1016/j.mam.2021.100973

Reuter, S., Gupta, S. C., Chaturvedi, M. M., and Aggarwal, B. B. (2010). Oxidative stress, inflammation, and cancer: how are they linked? *Free Radic. Biol. Med.* 49, 1603–1616. doi:10.1016/j.freeradbiomed.2010.09.006

Shafiek, M. S., Mekky, R. Y., Nassar, N. N., El-Yamany, M. F., and Rabie, M. A. (2024). Vortioxetine ameliorates experimental autoimmune encephalomyelitis model of multiple sclerosis in mice via activation of PI3K/Akt/CREB/BDNF cascade and modulation of serotonergic pathway signaling. *Eur. J. Pharmacol.* 982, 176929. doi:10.1016/j.ejphar.2024.176929

Shao, Y., Luo, Y., Sun, Y., Jiang, J., Li, Z., Wang, Z., et al. (2024). Leonurine exerts anti-inflammatory effects in lipopolysaccharide (LPS)-Induced endometritis by modulating mouse JAK-STAT/PI3K-Akt/PPAR signaling pathways. *Genes (Basel)* 15, 857. doi:10.3390/genes15070857

Shen, T., Wang, C., and Yang, H. (2020). Effect of anthraquinone and stilbene glycoside in polygonum multiflorum on liver function for rats. *J. Sichuan Traditional Chin. Med.*

Shishodia, S., Singh, T., and Chaturvedi, M. M. (2007). Modulation of transcription factors by curcumin. *Adv. Exp. Med. Biol.* 595, 127–148. doi:10.1007/978-0-387-46401-5_4

Sies, H. (2015). Oxidative stress: a concept in redox biology and medicine. *Redox Biol.* 4, 180–183. doi:10.1016/j.redox.2015.01.002

Song, L., Wang, Q., and Zhou, K. (2018). Study on liver and kidney toxicity of 4 components of polygoni multifori radix on mice after intragastric administration for 14 days. *Chin. J. Pharmacovigil.*

Tang, Q., Meng, C., Liu, Y., Cheng, Y., Liu, Y., Long, Y., et al. (2023). Silencing SIRT1 promotes the anti-HBV action of IFN-α by regulating Pol expression and activating the JAK-STAT signaling pathway. *Int. Immunopharmacol.* 124, 110939. doi:10.1016/j.intimp.2023.110939

Thomas, T. A., Francis, R. O., Zimring, J. C., Kao, J. P., Nemkov, T., and Spitalnik, S. L. (2024). The role of ergothioneine in red blood cell biology: a review and perspective. *Antioxidants (Basel)* 13, 717. doi:10.3390/antiox13060717

Tiraby, C., and Langin, D. (2005). PGC-1alpha, a transcriptional coactivator involved in metabolism. *Med. Sci. Paris.* 21, 49–54. doi:10.1051/medsci/200521149

Tu, Y., Liu, J., Kong, D., Guo, X., Li, J., Long, Z., et al. (2023). Irisin drives macrophage anti-inflammatory differentiation via JAK2-STAT6-dependent activation of PPARγ and Nrf2 signaling. *Free Radic. Biol. Med.* 201, 98–110. doi:10.1016/j.freeradbiomed.2023.03.014

Ulasov, A. V., Rosenkranz, A. A., Georgiev, G. P., and Sobolev, A. S. (2022). Nrf2/Keap1/ARE signaling: towards specific regulation. *Life Sci.* 291, 120111. doi:10.1016/j.lfs.2021.120111

Wang, L., and He, C. (2022). Nrf2-mediated anti-inflammatory polarization of macrophages as therapeutic targets for osteoarthritis. *Front. Immunol.* 13, 967193. doi:10.3389/fimmu.2022.967193

Wang, Y., Nakajima, T., Gonzalez, F. J., and Tanaka, N. (2020). PPARs as metabolic regulators in the liver: lessons from liver-specific PPAR-null mice. *Int. J. Mol. Sci.* 21, 2061. doi:10.3390/ijms21062061

Wang, M., Zhang, M., Fu, L., Lin, J., Zhou, X., Zhou, P., et al. (2020a). Liver-targeted delivery of TSG-6 by calcium phosphate nanoparticles for the management of liver fibrosis. *Theranostics* 10, 36–49. doi:10.7150/thno.37301

Wang, X., Zeng, J., Wang, X., Li, J., Chen, J., Wang, N., et al. (2020b). 2,3,5,4'-tetrahydroxystilbene-2-O-β-D-glucoside induces autophagy of liver by activating PI3K/Akt and Erk pathway in prediabetic rats. *BMC Complement. Med. Ther.* 20, 177. doi:10.1186/s12906-020-02949-w

Wang, S., Kong, X., Chen, N., Hu, P., Boucetta, H., Hu, Z., et al. (2022). Hepatotoxic metabolites in polygoni multiflori radix— comparative toxicology in mice. *Front. Pharmacol.* 13, 1007284. doi:10.3389/fphar.2022.1007284

Wang, J., Ma, H., Guo, H., Chen, Y., and Liu, Y. (2024a). Clinical applications of phosphocreatine and related mechanisms. *Life Sci.* 123012. doi:10.1016/j.lfs.2024.123012

Wang, S., Xiao, G., Tang, M., Bi, X., Xing, C., Liu, A., et al. (2024b). FKBP38 deletion exacerbates ConA-induced hepatitis by promoting the immune response through the MCP-1/p38 pathway. *Int. Immunopharmacol.* 138, 112659. doi:10.1016/j.intimp.2024.112659

Xi, Z. (2017). Therapeutic effect of 2,3,4',5-tetrahydroxystilbene-2-O-β-D-glucoside on hyperlipidemic fatty liver in rats. *Med. J. Commun.*

Xi, Z. (2018). Therapeutic effect of 2,3,4',5-tetrahydroxystilbene-2-O-β-D-glucoside on hyperlipidemic fatty liver in rats by activating PPAR α pathway of autophagy. *J. Nanjing Medicial Univ.* doi:10.7655/NYDXBNS20181203

Xin, P., Xu, X., Deng, C., Liu, S., Wang, Y., Zhou, X., et al. (2020). The role of JAK/STAT signaling pathway and its inhibitors in diseases. *Int. Immunopharmacol.* 80, 106210. doi:10.1016/j.intimp.2020.106210

Xiong, Z., Tong, Q. Y., Zheng, S. H., Li, Z. Y., and Wang, T. (2012). Tetrahydroxystilbene glucoside protects against ethanol induced liver injury in mice by inhibition of expression of inflammation-related factors. *World Chin. J. Dig.* 20, 3649. doi:10.11569/wcjd.v20.i36.3649

Xiong, X., Wang, P., Duan, L., Liu, W., Chu, F., Li, S., et al. (2019). Efficacy and safety of Chinese herbal medicine Xiao Yao San in hypertension: a systematic review and meta-analysis. *Phytomedicine* 61, 152849. doi:10.1016/j.phymed.2019.152849

Xu, S., Liu, J., Shi, J., Wang, Z., and Ji, L. (2017). 2,3,4',5-tetrahydroxystilbene-2-O-β-D-glucoside exacerbates acetaminophen-induced hepatotoxicity by inducing hepatic expression of CYP2E1, CYP3A4 and CYP1A2. *Sci. Rep.* 7, 16511. doi:10.1038/s41598-017-16688-5

Xu, J., Peng, Y., Zeng, Y., Hua, Y.-q., and Xu, X.-l. (2019). 2, 3, 4', 5-tetrahydroxystilbene-2-0-β-d glycoside attenuates age- and diet-associated non-alcoholic steatohepatitis and atherosclerosis in LDL receptor knockout mice and its possible mechanisms. *Int. J. Mol. Sci.* 20, 1617. doi:10.3390/ijms20071617

Xu, S., Huang, J., Xun, Z., Li, S., Fu, Y., Lin, N., et al. (2022). IFIT3 is increased in serum from patients with chronic hepatitis B Virus (HBV) infection and promotes the anti-HBV effect of interferon alpha via JAK-STAT2 *in vitro*. *Microbiol. Spectr.* 10, e0155722. doi:10.1128/spectrum.01557-22

Xueqi, H. (2020). The study of monomer components of Polygonum multiflorum on liver tissue and cell damages. *Chin. J. Geriatrics*. doi:10.3760/cma.j.issn.0254-9026.2020.07.024

Younossi, Z. M., Wong, G., Anstee, Q. M., and Henry, L. (2023). The global burden of liver disease. *Clin. Gastroenterology Hepatology* 21, 1978–1991. doi:10.1016/j.cgh.2023.04.015

Yu, P., Peng, X., Sun, H., Xin, Q., Kang, H., Wang, P., et al. (2024). Inspired by lubricin: a tailored cartilage-armor with durable lubricity and autophagy-activated antioxidation for targeted therapy of osteoarthritis. *Mater Horiz.* 11, 5352–5365. doi:10.1039/d4mh00812j

Yu H., H., Lin, L., Zhang, Z., Zhang, H., and Hu, H. (2020). Targeting NF-κB pathway for the therapy of diseases: mechanism and clinical study. *Signal Transduct. Target Ther.* 5, 209. doi:10.1038/s41392-020-00312-6

Yu W., W., Zhao, J., Li, W., Zheng, Y., Zhu, J., Liu, J., et al. (2020). 2,3,5,4'-Tetrahydroxystilbene-2-O-β-d-glucoside alleviated the acute hepatotoxicity and DNA damage in diethylnitrosamine-contaminated mice. *Life Sci.* 243, 117274. doi:10.1016/j.lfs.2020.117274

Zhang, Y., Alexander, P. B., and Wang, X. F. (2017). TGF-B family signaling in the control of cell proliferation and survival. *Cold Spring Harb. Perspect. Biol.* 9, a022145. doi:10.1101/cshperspect.a022145

Zhang, X., Ji, R., Sun, H., Peng, J., Ma, X., Wang, C., et al. (2018). Scutellarin ameliorates nonalcoholic fatty liver disease through the PPARγ/PGC-1α-Nrf2 pathway. *Free Radic. Res.* 52, 198–211. doi:10.1080/10715762.2017.1422602

Zhang, L., Liu, X., Tu, C., Li, C., Song, D., Zhu, J., et al. (2019). Components synergy between stilbenes and emodin derivatives contributes to hepatotoxicity induced by Polygonum multiflorum. *Xenobiotica* 50, 515–525. doi:10.1080/00498254.2019.1658138

Zhang, A., Wang, X., Fan, M., Guan, Y., Jiang, Y., Jin, S., et al. (2024a). Lycopene alleviates zearalenone-induced oxidative stress, apoptosis, and NLRP3 inflammasome activation in mice kidneys. *Toxicon* 249, 108078. doi:10.1016/j.toxicon.2024.108078

Zhang, K., Jia, R., Zhang, Q., Xiang, S., Wang, N., and Xu, L. (2024b). Metabolic dysregulation-triggered neutrophil extracellular traps exacerbate acute liver failure. *FEBS Lett.* 598, 2450–2462. doi:10.1002/1873-3468.14971

Zhang, L. (2017). Study on idiosyncratic liver injury and content of cis-2,3,5,4'-tetrahydroxystilbene-2-O-β-D-glucoside in radix Polygoni multiflori Preparata Acta Pharmaceutica Sinica.

Zhao, J., Qi, Y. F., and Yu, Y. R. (2021). STAT3: a key regulator in liver fibrosis. *Ann. Hepatol.* 21, 100224. doi:10.1016/j.aohep.2020.06.010

Zheng, Y., Ding, Q., Wei, Y., Gou, X., Tian, J., Li, M., et al. (2021). Effect of traditional Chinese medicine on gut microbiota in adults with type 2 diabetes: a systematic review and meta-analysis. *Phytomedicine* 88, 153455. doi:10.1016/j.phymed.2020.153455

Zhenzhen, G., Chao, Z., and Zhenxiao, S. (2014). Study on acute hepatotoxicity of Polygonum multiflorum extract in normal and hepatocarcinoma-bearing mice. *CHINA Pharm.* doi:10.6039/j.issn.1001-0408.2014.15.05

Zhou, H., Jia, X., Hu, K., Mo, Z., Xu, W., Peng, L., et al. (2021). TMEM2 binds to CSNK2A3 to inhibit HBV infection via activation of the JAK/STAT pathway. *Exp. Cell Res.* 400, 112517. doi:10.1016/j.yexcr.2021.112517

Glossary

ALT	Alanine aminotransferase
AST	Aspartate aminotransferase
ALP	Alkaline phosphatase
ALB	Albumin
Akt	Protein kinase B
ARE	Antioxidant-responsive elements
APAP	Acetaminophen
BI	Biomacromolecule induced
Bax	Bcl-2-associated X protein
Bcl-2	B-cell lymphoma-2
C subgroup	Cis-SG subgroup
CC	Cellular component
Cul3	Cullin3
CYP450	Cytochrome p450
C.T subgroup	Cis-SG and trans-SG subgroup
DILI	Drug-induced liver injury
ERK	Extracellular signal-regulated kinase
EASL	European Association for the Study of the Liver
GSH	Glutathione
HFD	High-fat die
HO-1	Heme oxygenase-1
I	Intervention
I^2	I-squared
IFN-γ	Interferon gamma
IL-6	Interleukin 6
IL-1β	Interleukin 1β
IKKα	IκB kinase α
ICR mice	Institute of Cancer Research mice
JAK	Janus kinase
Keap1	kelch-like ECH-associated protein 1
LI	Liver injury
MF	Molecular function
MSE	Mean squared error
MDA	Malondialdehyde
MMP	Mitochondrial membrane potential
N	Normal
NBI	Non-biomacromolecule induced
Nrf2	Nuclear factor erythroid 2-related factor 2
NF-κB	Nuclear factor kappa-B
NQO-1	Quinone oxidoreductase-1
PPI	Protein-protein interaction
PI3K	Phosphatidylinositol 3-kinase
PPAR	Peroxisome proliferator-activated receptor
BP	Biological process
ROS	Reactive oxygen species
RBF	Radial Basis Function
SD	Standard deviation
SOD	Superoxide dismutase
SMD	Standardised mean difference
Smad	Small mothers against decapentaplegic
STAT	Signal transducer and activator of transcription
T subgroup	Trans-SG subgroup
TP	Total protein
TC	Total cholesterol
TCM	Traditional Chinese medicine
TG	Triglyceride
TSG	2,3,5,4′-tetrahydroxystilbene-2-O-β-D-glucopyranoside
TGF-β	Transforming growth factor beta
TNF-α	Tumor necrosis factor alpha
W	Week(s)
95%CI	95% confidence interval

Frontiers in Pharmacology

Explores the interactions between chemicals and living beings

The most cited journal in its field, which advances access to pharmacological discoveries to prevent and treat human disease.

Discover the latest Research Topics

See more →

Frontiers

Avenue du Tribunal-Fédéral 34
1005 Lausanne, Switzerland
frontiersin.org

Contact us

+41 (0)21 510 17 00
frontiersin.org/about/contact